Methods in Molecular Biology 2565

Springer Protocols

Ricardo Borges *Editor*

Chromaffin Cells

Methods and Protocols

Humana Press

METHODS IN MOLECULAR BIOLOGY

Series Editor
John M. Walker
School of Life and Medical Sciences
University of Hertfordshire
Hatfield, Hertfordshire, UK

For further volumes:
http://www.springer.com/series/7651

For over 35 years, biological scientists have come to rely on the research protocols and methodologies in the critically acclaimed *Methods in Molecular Biology series*. The series was the first to introduce the step-by-step protocols approach that has become the standard in all biomedical protocol publishing. Each protocol is provided in readily-reproducible step-by step fashion, opening with an introductory overview, a list of the materials and reagents needed to complete the experiment, and followed by a detailed procedure that is supported with a helpful notes section offering tips and tricks of the trade as well as troubleshooting advice. These hallmark features were introduced by series editor Dr. John Walker and constitute the key ingredient in each and every volume of the Methods in *Molecular Biology series*. Tested and trusted, comprehensive and reliable, all protocols from the series are indexed in PubMed.

Chromaffin Cells

Methods and Protocols

Edited by

Ricardo Borges

Department of Physical Medicine and Pharmacology, Universidad de La Laguna, La Laguna, Spain

Humana Press

Editor
Ricardo Borges
Department of Physical Medicine
and Pharmacology
Universidad de La Laguna
La Laguna, Spain

ISSN 1064-3745 ISSN 1940-6029 (electronic)
Methods in Molecular Biology
ISBN 978-1-0716-2670-2 ISBN 978-1-0716-2671-9 (eBook)
https://doi.org/10.1007/978-1-0716-2671-9

Cover illustration: Imagen of human adrenal medulla stained with haematoxylin-eosin method. Inserted is the celebrated chromaffin cell cartoon (created by Harvey Pollard for the *III International Symposium on Chromaffin Cell Biology*, Coolfont, WV, USA, 1986). The cover composition was created by José Luis Carrasco Juan, Universidad de La Laguna. Tenerife. Spain.

This Humana imprint is published by the registered company Springer Science+Business Media, LLC, part of Springer Nature.
The registered company address is: 1 New York Plaza, New York, NY 10004, U.S.A.

Preface

In mammals, the adrenal glands are endocrine organs located on top of the kidney. The inner part of the gland is the medulla, a tissue derived from the neural crest. Early in the twentieth century, Alfred Kohn stained the adrenal medulla with chromium; hence, the name of chromaffin cells. In the beginning of the twentieth century, Jokichi Takamine isolated pure adrenaline from an extract of adrenal glands. Its dramatic effects on practically all cells of the body during violent stress led Walter Cannon to coin this reaction as the fight-or-flight response. From the 1950s onward, the so-called chromaffin granules storing the catecholamines, various proteins and ATP were isolated in large quantities from bovine adrenals. This contributed to our understanding of the life cycle of secretory vesicles, their synthesis and sorting, their cargo constituents such as chromogranins, the synthesis and storage in such vesicles of catecholamines, and their life cycle and reuse of vesicles for new rounds of exocytosis.

Another significant step in our understanding of the chromaffin cell physiology was the demonstration in the 1960s by William Douglas of the absolute requirement of calcium to trigger the exocytotic release of catecholamines, coining the concept of the *stimulus-secretion coupling*.

When in the 1980s the patch-clamp techniques were developed and refined by Erwin Neher and Bert Sakmann, an explosive interest arose on those parameters as chromaffin cells of various mammalian species served to clarify basic aspects of cell excitability, ion channels, impulse generation, regulated neurotransmitter release through calcium-dependent exocytosis, and the action of drugs that regulate brain functions. This was of no surprise, given the fact that as nerve tissues, chromaffin cells derive from the neural crest. In fact, in the late 1970s, Rita Levi-Montalcini and Klaus Unsicker demonstrated that chromaffin cells could transdifferentiate into sympathetic-like neurons when exposed to nerve growth factor.

In the mid-1970s, Lloyd Green and Arthur Perlman developed a chromaffin-derived cell line—the PC12—that largely complemented the research performed on primary cell cultures.

The concept of exocytosis also arose from research in chromaffin cells. It was grounded on the observation of the release with the catecholamines of high-molecular weight proteins such as chromogranins and dopamine beta-hydroxylase, implying the formation of a membrane pore. The membrane fusion pore underlying exocytosis could be finely studied when, at the beginning of the 1990s, R.M. Wightman developed the amperometric technique to record single-spike secretory events from an isolated chromaffin cell. The combination of patch-clamp with amperometry, fluorescent calcium probes, and confocal microscopy allowed the simultaneous recording of calcium currents, cytosolic calcium, and exocytosis monitoring. Using a combination of membrane capacitance and amperometry in the same cell, Manfred Lindau and Guillermo Álvarez de Toledo invented the patch-amperometry technique, which demonstrated the diverse modes of exocytosis and directly measured the concentration of adrenaline inside a single chromaffin granule.

The application of these high-resolution techniques facilitated the study and characterization in chromaffin cells of mice carrying specific gene mutations, of most SNARE proteins of the exocytotic machinery as well as their interaction, to end with the vesicle and plasmalemmal membrane fusion, the formation of the fusion pore, and its expansion to

get full exocytosis of vesicle contents. This was achieved in the 1990s and the first two decades of the twenty-first century by Erwin Neher, Reinhard Jahn, Thomas C. Südhof, and several other scientists.

This book gathers a collection of chapters on most techniques and methodological advances that have been fundamental to our present understanding of chromaffin cell biology and pharmacology, both in health and disease. I hope the contents of this book will contribute to draw the pathway for further exploration of chromaffin cells biology, which, on its own, draws physiological, pathophysiological, and pharmacological interest. And most importantly, chromaffin cells will continue to serve as a model to explore basic and molecular mechanisms in deciphering the electrochemical language of neurons to communicate with practically all cells of the body.

Looking back to all the important discoveries performed chromaffin cell we could considered them as the *E. coli* of neurobiology.

La Laguna, Spain ***Ricardo Borges***

Contents

Part IV Miscellanea

Contributors

Carolina Aguado • *Synaptic Structure Laboratory, Instituto de Investigación en Discapacidades Neurológicas (IDINE), Departamento de Ciencias Médicas, Facultad de Medicina, Universidad Castilla-La Mancha, Albacete, Spain*

Tzitzitlini Alejandre-García • *Department of Biological Sciences, Columbia University, New York, NY, USA*

Rocío Alfaro-Ruiz • *Synaptic Structure Laboratory, Instituto de Investigación en Discapacidades Neurológicas (IDINE), Departamento de Ciencias Médicas, Facultad de Medicina, Universidad Castilla-La Mancha, Albacete, Spain*

Javier Álvarez • *Departamento de Bioquímica y Biología Molecular y Fisiología, Facultad de Medicina, Unidad de Excelencia Instituto de Biología y Genética Molecular (IBGM), Universidad de Valladolid and CSIC, Valladolid, Spain*

Pilar Álvarez-Illera • *Departamento de Bioquímica y Biología Molecular y Fisiología, Facultad de Medicina, Unidad de Excelencia Instituto de Biología y Genética Molecular (IBGM), Universidad de Valladolid and CSIC, Valladolid, Spain*

Adekunle T. Bademosi • *Clem Jones Centre for Ageing Dementia Research (CJCADR), Queensland Brain Institute (QBI), The University of Queensland, St Lucia Campus, Brisbane, QLD, Australia*

Sebastian Barg • *Medical Cell Biology, Uppsala University, Uppsala, Sweden*

Ricardo Borges • *Department of Physical Medicine and Pharmacology, Universidad de La Laguna, La Laguna, Spain*

Alejandra Boronat-Garcia • *Section on Sensory Coding and Neural Ensembles, Eunice Kennedy Shriver National Institute of Child Health and Human Development, NIH, Bethesda, MD, USA*

María F. Cano-Abad • *Instituto Teófilo Hernando. Departamento de Farmacología. Facultad de Medicina. Universidad Autónoma de Madrid and Instituto de investigación Sanitaria Hospital de la Princesa, Madrid, Spain*

Ann-Sofie Cans • *Department of Chemistry and Chemical Engineering, Chalmers University of Technology, Gothenburg, Sweden*

Anna Capaldo • *Department of Biology, University of Naples Federico II, Naples, Italy; Center for Studies on Bioinspired Agro-environmental Technology (BAT Center), Portici, Italy*

Valentina Carabelli • *Department of Drug Science and Technology and "NIS" Inter-departmental Centre, University of Torino, Turin, Italy*

Emilio Carbone • *Department of Drug Science and Technology and "NIS" Inter-departmental Centre, University of Torino, Turin, Italy*

Ana María Cárdenas • *Centro Interdisciplinario de Neurociencia de Valparaíso, Facultad de Ciencias, Universidad de Valparaíso, Valparaíso, Chile*

Chung Yu Chan • *National Institute of Neurological Disorders and Stroke, Bethesda, MD, USA*

Pin-Chun Chen • *Institute of Molecular and Cellular Biology, National Taiwan University, Taipei, Taiwan*

Barbara Colombo • *Division of Experimental Oncology, IRCCS San Raffaele Scientific Institute, Milan, Italy*

Angelo Corti • *Division of Experimental Oncology, IRCCS San Raffaele Scientific Institute and Vita-Salute San Raffaele University, Milan, Italy*
Flavio Curnis • *Division of Experimental Oncology, IRCCS San Raffaele Scientific Institute, Milan, Italy*
Ana De la Iglesia • *Pharmacology Unit, Department of Physical Medicine and Pharmacology, Medical School, Universidad de La Laguna, Tenerife, Spain*
Natalia Domínguez • *Dpto. Bioquímica, Microbiología, Biología Celular y Genética, Facultad de Ciencias, Sección Biología, Universidad de La Laguna, Tenerife, Spain*
Santiago Echeverry • *Medical Cell Biology, Uppsala University, Uppsala, Sweden*
Maria De Falco • *Department of Biology, University of Naples Federico II, Naples, Italy; Center for Studies on Bioinspired Agro-environmental Technology (BAT Center), Portici, Italy; National Institute of Biostructures and Biosystems (INBB), Rome, Italy*
Ricardo de Pascual • *Instituto Fundación Teófilo Hernando, Departamento de Farmacología y Terapéutica, Facultad de Medicina, Universidad Autónoma de Madrid, Madrid, Spain*
Andrew G. Ewing • *Department of Chemistry and Molecular Biology, University of Gothenburg, Gothenburg, Sweden*
Rosalba I. Fonteriz • *Departamento de Bioquímica y Biología Molecular y Fisiología, Facultad de Medicina, Unidad de Excelencia Instituto de Biología y Genética Molecular (IBGM), Universidad de Valladolid and CSIC, Valladolid, Spain*
Claudio Franchino • *Department of Drug Science and Technology, University of Torino, Turin, Italy*
Luis Gandía • *Instituto Fundación Teófilo Hernando, Departamento de Farmacología y Terapéutica, Facultad de Medicina, Universidad Autónoma de Madrid, Madrid, Spain*
Antonio G. García • *Instituto Fundación Teófilo Hernando, Departamento de Farmacología y Terapéutica, and Instituto de Investigación Sanitaria de La Princesa, Facultad de Medicina, Universidad Autónoma de Madrid, Madrid, Spain*
Yolanda Giménez-Molina • *Instituto de Neurociencias, Centro Mixto CSIC-Universidad Miguel Hernández, Alicante, Spain*
Arlek González-Jamett • *Centro Interdisciplinario de Neurociencia de Valparaíso, Facultad de Ciencias, Universidad de Valparaíso, Valparaíso, Chile; Escuela de Química y Farmacia, Facultad de Farmacia, Universidad de Valparaíso, Valparaíso, Chile*
Nathalie C. Guérineau • *Institute of Functional Genomics, University of Montpellier, CNRS, INSERM, Montpellier, France*
Magdalena Guerra-Crespo • *Instituto de Fisiología Celular, División de Neurociencias, Universidad Nacional Autónoma de México and Laboratorio de Medicina Regenerativa, Departamento de Cirugía, Facultad de Medicina, Universidad Nacional Autónoma de México, Mexico City, Mexico*
Xiaoli Guo • *National Institute of Neurological Disorders and Stroke, Bethesda, MD, USA*
Luis M. Gutiérrez • *Instituto de Neurociencias, Centro Mixto CSIC-Universidad Miguel Hernández, Alicante, Spain*
Sue Han • *National Institute of Neurological Disorders and Stroke, Bethesda, MD, USA*
Keita Harada • *Department of Cell and Systems Physiology, University of Occupational and Environmental Health School of Medicine, Kitakyushu, Japan*
Arturo Hernández-Cruz • *Departamento Neurociencia Cognitiva, Instituto de Fisiología Celular, Universidad Nacional Autónoma de México, México City, Mexico*
Masumi Inoue • *University of Occupational and Environmental Health School of Medicine, Kitakyushu, Japan*

Vincenza Laforgia • *Department of Biology, University of Naples Federico II, Naples, Italy; National Institute of Biostructures and Biosystems (INBB), Rome, Italy*
Alex S. Lima • *Department of Chemistry and Molecular Biology, University of Gothenburg, Gothenburg, Sweden*
Manfred Lindau • *Department of Physiology and Biophysics, University of Miami, Miller School of Medicine, Miami, FL, USA*
Liangwen Liu • *Medical Cell Biology, Uppsala University, Uppsala, Sweden*
Manuela G. López • *Instituto Teófilo Hernando. Departamento de Farmacología. Facultad de Medicina. Universidad Autónoma de Madrid and Instituto de investigación Sanitaria Hospital de la Princesa, Madrid, Spain*
Rafael Luján • *Synaptic Structure Laboratory, Instituto de Investigación en Discapacidades Neurológicas (IDINE), Departamento de Ciencias Médicas, Facultad de Medicina, Universidad Castilla-La Mancha, Albacete, Spain*
José David Machado • *Dpto. Medicina Física y Farmacología, Facultad de Ciencias de la Salud, Medicina, Universidad de La Laguna, La Laguna, Tenerife, Spain*
Sushil K. Mahata • *VA San Diego Healthcare System, San Diego, CA, USA; Department of Medicine, University of California San Diego, La Jolla, CA, USA*
Soodabeh Majdi • *Department of Chemistry and Molecular Biology, University of Gothenburg, Gothenburg, Sweden*
María Constanza Maldifassi • *Centro Interdisciplinario de Neurociencia de Valparaíso, Facultad de Ciencias, Universidad de Valparaíso, Valparaíso, Chile*
Andrea Marcantoni • *Department of Drug Science and Technology and "NIS" Inter-departmental Centre, University of Torino, Turin, Italy*
Hidetada Matsuoka • *Yokohama University of Pharmacy, Yokohama, Japan*
Frédéric A. Meunier • *Clem Jones Centre for Ageing Dementia Research (CJCADR), Queensland Brain Institute (QBI), The University of Queensland, St Lucia Campus, Brisbane, QLD, Australia*
Diana Millán-Aldaco • *Departamento Neurociencia Cognitiva, Instituto de Fisiología Celular, Universidad Nacional Autónoma de México, México City, Mexico*
Pablo Montenegro • *Pharmacology Unit, Department of Physical Medicine and Pharmacology, Medical School, Universidad de La Laguna, Tenerife, Spain*
Mayte Montero • *Departamento de Bioquímica y Biología Molecular y Fisiología, Facultad de Medicina, Unidad de Excelencia Instituto de Biología y Genética Molecular (IBGM), Universidad de Valladolid and CSIC, Valladolid, Spain*
Eugene V. Mosharov • *Departments of Psychiatry and Neurology, Columbia University Medical Center, New York State Psychiatric Institute, New York, NY, USA*
Alicia Muñoz-Montero • *Instituto Fundación Teófilo Hernando, Departamento de Farmacología y Terapéutica, Facultad de Medicina, Universidad Autónoma de Madrid, Madrid, Spain*
Muhmmad Omar-Hmeadi • *Medical Cell Biology, Uppsala University, Uppsala, Sweden*
Marcela Palomero-Rivero • *Instituto de Fisiología Celular, División de Neurociencias, Universidad Nacional Autónoma de México, Mexico City, Mexico*
Oscar Javier Parada-Parra • *Departamento Neurociencia Cognitiva, Instituto de Fisiología Celular, Universidad Nacional Autónoma de México, México City, Mexico*
Alberto Pasquarelli • *Institute of Electron Devices and Circuits, University of Ulm, Ulm, Germany*
Federico Picollo • *Department of Physics and "NIS" Inter-departmental Centre, University of Torino, Istituto Nazionale di Fisica Nucleare – Sezione di Torino, Turin, Italy*

Luigi Rosati • *Department of Biology, University of Naples Federico II, Naples, Italy; Center for Studies on Bioinspired Agro-environmental Technology (BAT Center), Portici, Italy*
Jaime Santo-Domingo • *Departamento de Bioquímica y Biología Molecular y Fisiología, Facultad de Medicina, Unidad de Excelencia Instituto de Biología y Genética Molecular (IBGM), Universidad de Valladolid and CSIC, Valladolid, Spain*
Pedro Segura-Chama • *Cátedras CONACyT, Laboratorio de Fisiología Celular, Instituto Nacional de Psiquiatría Ramón de La Fuente Muniz, México City, Mexico*
Elizabeth P. Seward • *School of Biosciences, University of Sheffield, Sheffield, UK*
Kechun Tang • *VA San Diego Healthcare System, San Diego, CA, USA*
Giulia Tomagra • *Department of Drug Science and Technology and "NIS" Inter-departmental Centre, University of Torino, Turin, Italy*
José Villanueva • *Instituto de Neurociencias, Centro Mixto CSIC-Universidad Miguel Hernández, Alicante, Spain*
Chih-Tien Wang • *Institute of Molecular and Cellular Biology, National Taiwan University, Taipei, Taiwan*
Xin Wang • *National Institute of Neurological Disorders and Stroke, Bethesda, MD, USA*
Yuanmo Wang • *National Institute of Neurological Disorders and Stroke, Bethesda, MD, USA*
Ling-Gang Wu • *National Institute of Neurological Disorders and Stroke, Bethesda, MD, USA*
Robert C. Wykes • *Department of Clinical and Experimental Epilepsy, Queen Square Institute of Neurology, University College London, London, UK; Nanomedicine Lab, Faculty of Biology Medicine & Health, University of Manchester, Manchester, UK*

Part I

Culturing and Morphology

Chapter 1

Rat Pheochromocytoma PC12 Cells in Culture

Pin-Chun Chen and Chih-Tien Wang

Abstract

PC12 cells serve as a secretory cell model, especially suitable for studying the molecular mechanisms underlying fusion pore kinetics in regulated exocytosis of dense-core vesicles (DCVs). In this chapter, we describe a series of PC12 cell culture procedures optimized for real-time functional assays such as single-vesicle amperometry. In addition, these conditions have been widely used for single-cell biochemical assays such as the proximity ligation assay with immunostaining.

Key word Rat pheochromocytoma, PC12 cell culture, Regulated exocytosis, Dense-core vesicle, Fusion pore kinetics, Norepinephrine, Single-vesicle amperometry, Single-cell biochemistry assay, Proximity ligation assay with immunostaining

1 Introduction

Two types of vesicles, synaptic vesicles (SVs) and dense-core vesicles (DCVs), have been found in many neurons and neuroendocrine cells. Unlike SVs that mediate secretion of fast neurotransmitters (e.g., acetylcholine), DCVs are the key organelles for secretion of hormones, neuropeptides, and slow neurotransmitters such as monoamines that include catecholamines (dopamine, epinephrine, and norepinephrine) and indolamines (serotonin and histamine) [1]. Although both types of vesicles share common fusion machinery that mediates Ca^{2+}-regulated exocytosis for cargo secretion, DCVs possess certain unique molecular mechanisms that confer their differences in biogenesis, positions relative to the plasma membrane, and secretion rate [2]. Here we focus on a good secretory cell model to study the DCV exocytosis, i.e., PC12 cells.

Clonal PC12 cells are derived from rat pheochromocytoma, a type of neuroendocrine tumor growing from chromaffin cells of adrenal medulla [3]. Following nerve growth factor treatment, PC12 cells differentiate into neuronal morphology and mainly secrete acetylcholine from the SVs at neurite varicosities [3]. By contrast, undifferentiated PC12 cells mainly secrete catecholamines

Ricardo Borges (ed.), *Chromaffin Cells: Methods and Protocols*,
Methods in Molecular Biology, vol. 2565, https://doi.org/10.1007/978-1-0716-2671-9_1,

from the DCVs at somata. Indeed, undifferentiated PC12 cells possess many characteristics of neuroendocrine cells and are well-characterized model system for Ca^{2+}-regulated exocytosis for approximately four decades [4–6]. To determine the essential intracellular components for the DCV exocytosis, scientists have performed membrane permeabilization to "crack" undifferentiated PC12 cells [7]. Even after permeabilization, these undifferentiated PC12 cells still can undergo Ca^{2+}-regulated exocytosis, thus allowing practical manipulation of intracellular components [7–9]. Moreover, transfection of undifferentiated PC12 cells is relatively easy for molecular perturbation, suitable for studying the detailed molecular structure–functional relation for the proteins of interest. Furthermore, the relatively slow rate of exocytosis makes the secretory events discernible in undifferentiated PC12 cells, allowing high-resolution electrical measurements to resolve the dynamics of fusion pore, which represents a pivotal intermediate in Ca^{2+}-regulated exocytosis [10–12]. Based on the reasons above, undifferentiated PC12 cells have been widely used for studying the molecular–functional bases in the DCV exocytosis [8, 9, 13–21], even for identifying the structural components of the fusion pore [22, 23]. Here, we describe a series of PC12 cell culture procedures (*see* Fig. 1), including maintenance, transfection (*see* Fig. 2), seeding single cells, loading of norepinephrine, and permeabilization, which are specifically optimized for single-vesicle amperometry (*see* Fig. 3) and single-cell biochemical assays such as the proximity ligation assay with immunostaining (*see* Fig. 4).

2 Materials

2.1 Maintenance of Cell Culture

Undifferentiated PC12 cells [7] are used for the following experiments. Prepare all solutions using analytical grade reagents and ultra-pure water (deionized water; purified to attain a sensitivity of 18 MΩ cm at 25 °C). All the materials must be sterilized prior to use. Ensure to follow all water disposal regulations upon disposing waste materials. To disperse and anchor undifferentiated PC12 cells on the dish bottom without complete attachment, 10-cm culture dishes are previously coated with poly-d-lysine (PDL) before seeding cells.

2.1.1 Coating Dishes for Cell Culture

1. PDL coating solution: 50 μg/mL in serum-free medium; store at −20 °C. Prepared from 2.5 mg/mL PDL stock solution in water.
2. 10-cm culture dishes.
3. Serum-free medium: Dulbecco's modified Eagle's medium (DMEM) containing 4.5-g/L glucose and L-glutamine without pyruvate, supplemented with 3.7-g/L $NaHCO_3$, pH 7.2 (pH risen to 7.4 after sterile filtered).

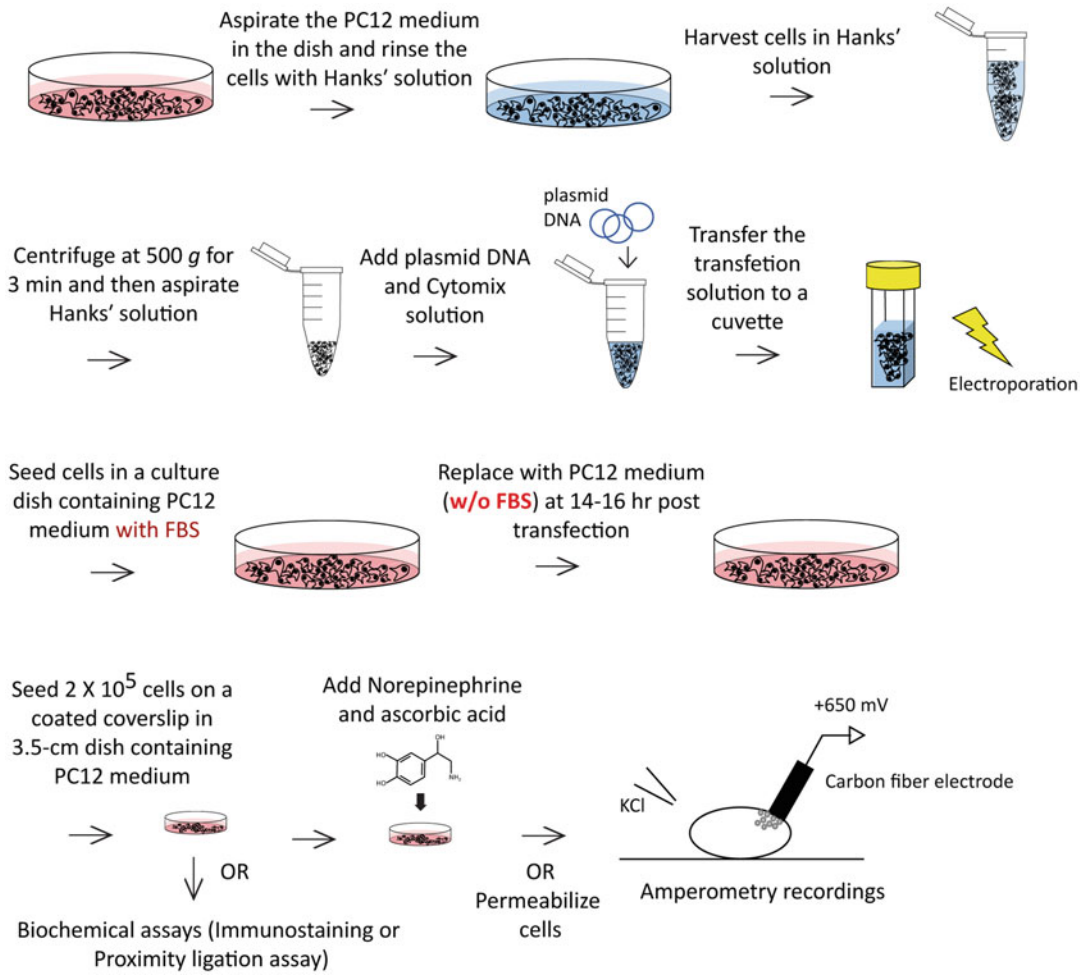

Fig. 1 Schematic illustration of the protocols described in this chapter

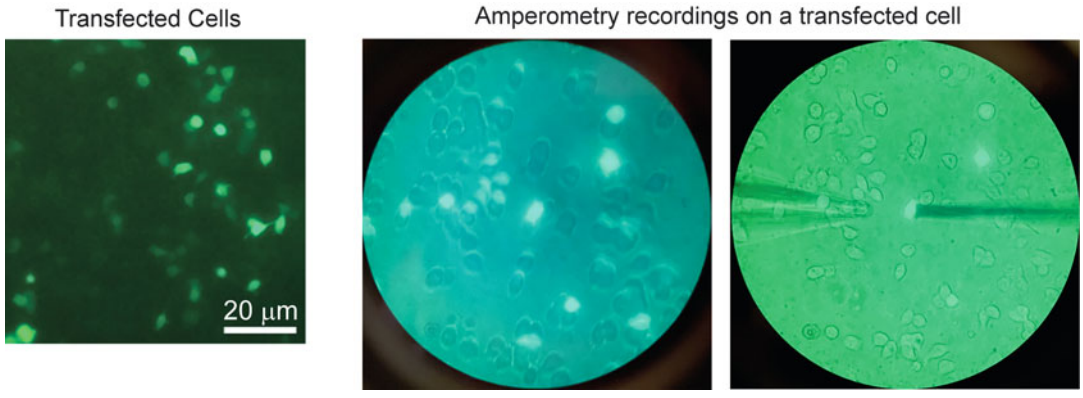

Fig. 2 Examples of transfected PC12 cells. (*Left*) Cells transfected with the DNA plasmid expressing green fluorescence protein (GFP) as a transfection marker. (*Right*) Amperometry recordings are performed on a transfected cell under a fluorescent microscope. The carbon fiber electrode is placed on the right to gently touch the cell, and a glass pipette is placed on the left to puff the high-KCl solution

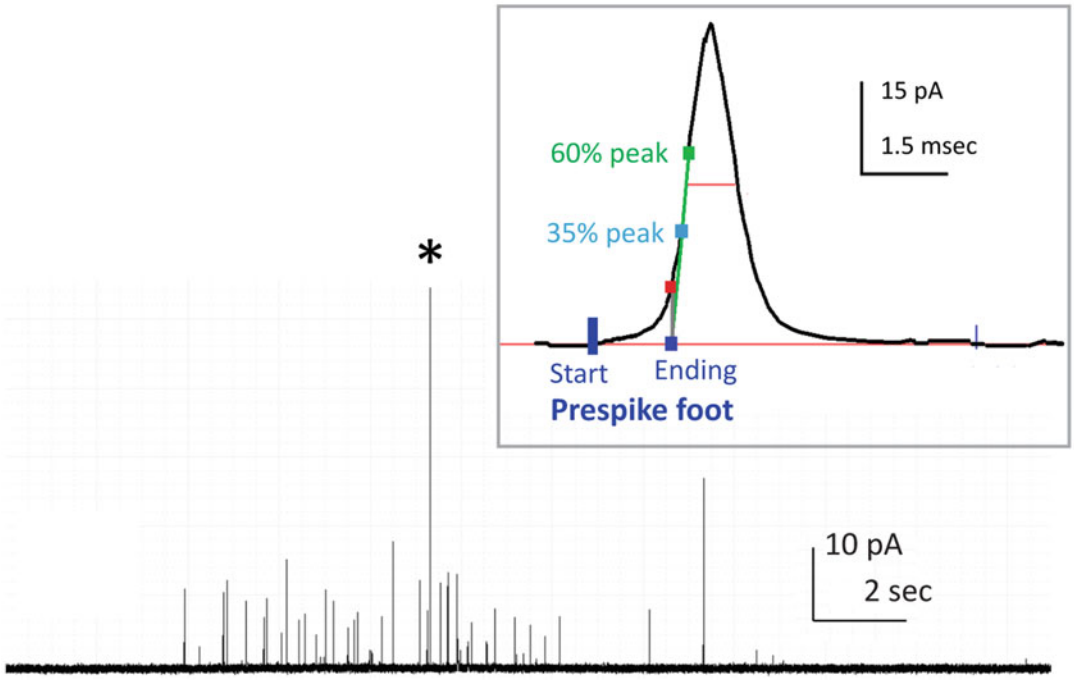

Fig. 3 Successful recordings in single-vesicle amperometry. (*Inset*) A representative spike (denotation * in the recording trace) displays a prespike foot. The start point of a prespike foot is defined by the current trace rising to 1× root-mean-square (RMS) noise above the baseline. The ending point of a prespike foot is defined by the intersection between the baseline and the green line going through the rise phase from 35% to 60% of the peak

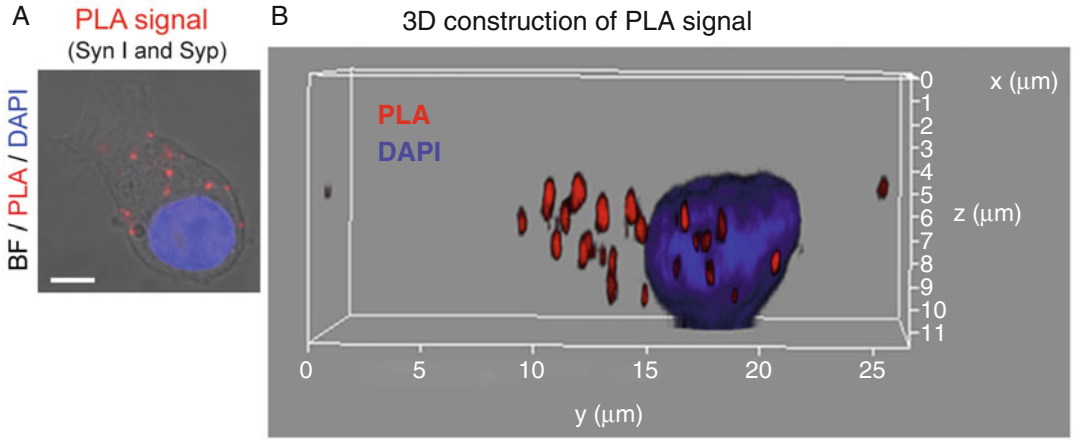

Fig. 4 The proximity ligation assay (PLA) displays in situ protein–protein interactions in a PC12 cell. (**a**) Individual fluorescent spots (red) represent in situ interactions between Synapsin I (Syn I) and Synaptophysin (Syp) detected by the PLA. BF, bright field; DAPI, blue. Scale bar: 5 μm. The fluorescence image (1.5-μm z-thickness) is from Fig. 9-A6 in [21] with authorization. (**b**) The 3D construction of PLA signals for the cell in (**a**) by laser scanning confocal microscopy (Leica TCS SP8 Spectral)

2.1.2 Pass Cells

1. Culture cells: Maintain the cells at 37 °C in the 10% CO_2 humidified incubator.
2. PC12 culture medium: Serum-free medium, supplemented with 5% donor equine serum and 5% iron-supplemented bovine calf serum.
3. Hanks' solution: Hanks' balanced salt modified powder, supplemented with 0.35-g/L $NaHCO_3$, pH 7.2 (pH risen to 7.4 after sterile filtered). Prior to use, add 5 mL of 100-mM ethylenediaminetetraacetic acid disodium salt dehydrate (EDTA) stock solution in water, yielding the final [EDTA] as 1 mM in 500-mL Hanks' solution.
4. 10-mL syringes with 22-gauge needles.
5. 10-cm coated dishes from Subheading 2.1.1.

2.1.3 Freeze and Thaw Cell Stocks

1. 90% confluent cells in 10-cm dishes (*see* **Note 1**).
2. PC12 culture medium, Hanks' solution, and 10-mL syringes with 22-gauge needles Subheading 2.1.2.
3. Sterile dimethylsulfoxide (DMSO), Eppendorf, cryogenic tubes, and the cryogenic freezing container with isopropanol.

2.2 Transfection

1. Plasmid preparation: DNAs are subcloned into a bicistronic vector. Subclone the genes of interest under the control of cytomegalovirus (CMV) promoter, followed by the internal ribosome entry site (IRES) that allows the expression of the transfection marker such as green fluorescent protein (GFP) (*see* Fig. 2) (*see* **Note 2**). All of the DNA plasmids were confirmed by automated sequencing and further amplified, attaining the final DNA purity (A_{260}/A_{280}) as 1.8–1.9. Plasmid DNA is stored in Tris buffer, pH 7.6, and prepared at 1 μg/μL concentration prior to transfection (*see* **Note 3**).
2. 80% confluent (1×10^7 cells/mL) cells (*see* **Note 1**) in a 10-cm dish: for transfection of one gene.
3. Transfection medium—Cytomix (*see* **Note 4**): 120-mM KCl, 0.15-mM $CaCl_2$, 10-mM KH_2PO_4, 2.5-mM HEPES, 2-mM EGTA, and 5-mM $MgCl_2$, pH 7.6.
4. Electroporation: A square-wave electroporator (square pulse electroporator, Harvard Apparatus, USA) and one 4-mm cuvette for transfection of one gene of interest (*see* **Note 5**).
5. Recovery medium: PC12 culture medium supplemented with 10% fetal bovine serum (FBS).

2.3 Seeding Single Cells

2.3.1 Coating Coverslips or 3.5-cm Culture Dishes (See **Note 6**)

1. PDL coating solution: from Subheading 2.1.1.
2. Collagen I coating solution: 50 μg/mL in 0.02-N acetic acid; store at −20 °C.
3. 3.5-cm culture dishes with 2 × 2 mm coverslips.
4. Serum-free medium.

2.3.2 Disperse and Replate Cells

1. Transfected cells in 10-cm dishes.
2. PC12 culture medium, Hanks' solution, and 10-mL syringes with 22-gauge needles Subheading 2.1.2.
3. Hemacytometer.

2.4 Loading of Norepinephrine

1. Freshly prepare 100-mM norepinephrine bitartrate (NE) in 20-mM HEPES, pH 7.5.
2. Freshly prepare 100-mM Na-ascorbate in water.
3. PC12 culture medium.

2.5 Cell Permeabilization (Optional)

1. Transfected cells in 3.5-cm coated dishes.
2. Permeabilization medium—K-Glu buffer with 2-mM EGTA (*see* **Note 7**): 120-mM K-glutamate, 20-mM K-acetate, 20-mM HEPES, 2-mM EGTA, pH 7.2.
3. Liquid N_2 in the storage container, a 50-mL tube with the stand, parafilm, a 250-mL beaker, a pencil, and timer.

2.6 Single-Vesicle Amperometry

1. Transfected cells in 3.5-cm coated dishes.
2. Bathing solution for intact cells—PC12 incubation buffer: 150-mM NaCl, 4.2-mM KCl, 1-mM NaH_2PO_4, 0.7-mM $MgCl_2$, 2-mM $CaCl_2$, and 10-mM HEPES, pH 7.4.
3. Stimulating solution for intact cells—High-K buffer: 140-mM KCl, 14.2-mM NaCl, 1-mM NaH_2PO_4, 0.7-mM $MgCl_2$, 2-mM $CaCl_2$, and 10-mM HEPES, pH 7.4.
4. Bathing solution for permeabilized cells—K-Glu buffer with 0.2-mM EGTA (*see* **Note 7**): 120.9-mM K-glutamate, 20-mM K-acetate, 20-mM HEPES, 0.2-mM EGTA, pH 7.2.
5. Stimulating solution for permeabilized cells—$CaCl_2$ buffer: Use 0.01-mM and 1-mM $CaCl_2$ (in water) to titrate K-Glu buffer with 0.2-mM EGTA until the concentrations of free $[Ca^{2+}]$ as 1, 2, 5, 10, 20, or 50 μM and pH are still 7.2. Free $[Ca^{2+}]$ is measured by calcium electrode.
6. Carbon fiber electrodes (CFE) (*see* **Note 8**): 5-μm carbon fiber electrode (CFE-2, ALA Scientific Instruments, USA).
7. Pipettes for puffing (*see* **Note 9**): Glass pipettes with 2-μm opening.
8. Amperometry setup and data analysis software (*see* **Note 10**): We use the amplifier (ALA Scientific Instruments, USA) at a polarized potential of 650 mV to record NE release from DCVs as an oxidative current. These amplified signals were sent to the Digidata 1440A interface (MDS Analytical Technologies, USA) and processed with pClamp10 software (Axon Instruments, USA). The green fluorescence of transfected cells can be observed under the 40× or 63× objective of the fluorescent microscope. A picospritzer (General Valve Corp., USA) is used

for puffing the stimulating solution. Amperometry data are analyzed using a written computer program to identify the prespike foot preceding a spike (*see* Fig. 3) [8, 9, 13–21].

2.7 Single-Cell Biochemical Assays: The Proximity Ligation Assay with Immunostaining

1. Transfected cells in 3.5-cm coated dishes.
2. Primary antibodies (*see* **Note 11**) and PLA reagents (Duolink® PLA Kit, Sigma, USA).
3. Secondary antibodies (optional) and general reagents for immunostaining.
4. Confocal microscopy and data analysis software: We acquire fluorescence images (1.5-μm z-thickness) by laser scanning confocal microscopy (Leica TCS SP5 or SP8 spectral laser scanning confocal microscope). PLA signals are analyzed with MetaMorph software (Molecular Devices, USA) (*see* Fig. 4).

3 Methods

3.1 Maintenance of Cell Culture

3.1.1 Coating Dishes for Cell Culture

1. Freshly prepare the low-concentration PDL solution (2.5 μg/5 mL in water) from the PDL coating solution (50 μg/mL in serum-free medium).
2. Add 5 mL of the low-concentration PDL solution into one 10-cm dish (a 10-cm dish has a surface area of 55 cm^2, yielding the coating concentration of PDL as 0.045 μg/cm^2) (*see* **Note 1**).
3. Incubate the dishes with PDL at room temperature for 1 h in the laminar hood.
4. Carefully aspirate the remaining solution without scraping the bottom surface of dishes.
5. Rinse dishes with serum-free medium to remove unbound PDL. Aspirate all the solution in dishes. Coated dishes are ready for use. Alternatively, coated dishes can be sealed by parafilm and stored at 4 °C for 1 week.

3.1.2 Pass Cells

1. PC12 cells are cultured in 10-cm dishes with the PC12 culture medium in a humidified atmosphere of 10% CO_2 at 37 °C. When the density of cells reaches to 90% confluence (1.5×10^7 cells/mL), the cells need to be passed to a new dish (*see* **Note 1**).
2. Aspirate the culture medium in the dish. Add 3 mL of Hanks' solution to rinse cells and then aspirate the solution.
3. Add 1 mL of Hanks' solution and incubate for 30 s, followed by gently patting the dish, allowing the cells detaching from the bottom of the dish.

4. Add 3 mL the culture medium into the dish. Collect all (~4 mL) cell suspension by a syringe with the 22-gauge needle.
5. Add 9-mL culture medium into four new coated dishes, followed by adding 1/4 cell suspension into a dish. Normally, one 90% confluent dish can be subdivided into four dishes of cells.
6. Replace with fresh culture medium every other day. Cells would reach 90% confluent after 4–5 days (*see* **Note 1**).

3.1.3 Freeze and Thaw Cell Stocks

1. Add 3-mL Hanks' solution to rinse 90% confluent cells in 10-cm dishes. Suck of all traces of rinse solution.
2. Add 1 mL of Hanks' solution to detach cells from the dish by shaking lightly. Put 1-mL cell suspension into a sterile Eppendorf.
3. Centrifuge cell suspension with 500 × *g* for 5 min at 4 °C. Discard the supernatant.
4. Make the anti-freezing medium containing 90% culture medium and 10% DMSO. Add 1 mL of the anti-freezing medium into the Eppendorf containing the cell pellet. Resuspend the cells by vortex.
5. Transfer the cell suspension into cryogenic tubes. Put the cryogenic tubes in the Nalgene cryogenic freezing container with isopropanol and store in the −80 °C deep freezer. After 4 h, transfer the cell frozen stocks in the box in the −80 °C deep freezer.
6. To resume the culture from a cell frozen stock, thaw a cryogenic tube at room temperature in the hood. Spin down the cell suspension and recover the pellet with the culture medium (*see* **Note 12**).

3.2 Transfection

1. Add 3-mL Hanks' solution to rinse 80% confluent cells in 10-cm dishes. Suck of all traces of rinse solution.
2. Harvest cell by 1 mL of Hanks' solution. Transfer cells into an Eppendorf, followed by centrifugation at 500 × *g* for 3 min. Discard the supernatant.
3. Add 500-μL Cytomix to resuspend the pellets. Transfer the cell suspension into a cuvette. Add 50-μL plasmid DNA (i.e., 50 μg) into the cuvette.
4. Apply a 230-V square pulse for 5 ms to the cuvette containing cell suspension and DNA.
5. Following electroporation, the cell suspension is immediately transferred into a 10-cm dish containing recovery medium (*see* **Note 13**). The recovery medium is replaced with fresh PC12 culture medium after 14–16 h.

3.3 Seeding Single Cells

3.3.1 Coating Coverslips or 3.5-cm Culture Dishes

1. Add 1-mL Collagen I (50 μg) and 1-mL PDL (50 μg) into one 3.5-cm dish together (a 3.5-cm dish has a surface area of 10 cm^2, so the concentration for each coating material would be 5 $\mu g/cm^2$).
2. Incubate at room temperature for 1 h in the hood until the color of culture medium turns from yellow to pink.
3. Carefully aspirate remaining solution without scraping bottom surface. Rinse well with serum-free medium to remove acid or unbound PDL.
4. Aspirate all the solution. Plates are ready for use and can be stored at 2–8 °C for up to 1 week under sterile conditions.

3.3.2 Disperse and Replate Cells

1. Harvest transfected cells by 1-mL Hanks' solution, followed by adding 3-mL culture medium as described in Subheading 3.1.2. To obtain single cells, the cell suspension is passed through a 22-gauge needle connected with a 10-mL syringe by three to five times (*see* **Note 14**).
2. Take 10 μL of cell suspension to calculate the density of cells using a hemacytometer (cell density = the number of cells in one of 0.1 × 0.1 cm-squares × 10^4/mL).
3. Replate cells with the density of 2 × 10^5 cells/mL on 3.5-cm coated dishes. Incubate cells on the coated dishes for at least 16 h before performing the following experiments.

3.4 Loading of Norepinephrine

1. For each 3.5-cm coated dish (containing 2 × 10^5 cells), add 1 mL of PC12 culture medium containing 1.5-mM norepinephrine (NE) and 0.5-mM ascorbic acid (*see* **Note 15**) from freshly prepared 100-mM NE and 100-mM ascorbate acid.
2. Replace with PC12 culture medium after 14–16 h.

3.5 Cell Permeabilization (Optional)

1. Rinse the cells on the 3.5-cm coated dish with K-Glu buffer with 2-mM EGTA for three times.
2. To crack the cells, add about 1 mL of K-Glu buffer with 2-mM EGTA, seal the dish with parafilm, place the whole dish into a 250-mL beaker, pour about 30-mL liquid N_2 into a 50-mL tube, and use a pencil to press the dish down to the bottom of the beaker. Take the dish out of the beaker after 10 s (*see* **Note 16**).
3. Thaw the cells at the CO_2 incubator at 37 °C for 30 min (*see* **Note 17**).
4. Rinse cells with K-Glu buffer with 0.2 mM EGTA. Add 1 mL of the same buffer into the dish.

3.6 Single-Vesicle Amperometry

At 60–96 h after transfection, transfected cells are used for the following experiments. We use the freshly cut CFE to gently touch the cell (*see* **Note 18**), and Ca^{2+}-dependent exocytosis is induced by puffing the high-KCl solution from a glass pipette for 20 s with pressure (10–20 p.s.i.) gated by a picospritzer during each trial of recordings. Each cell was recorded for five consecutive trials. The signal was digitized at 4 kHz and low-pass-filtered by eight-pole Bessel at 1 kHz.

1. For amperometry recordings on intact transfected cells: choose the cells displaying the intermediate level of green fluorescence.
2. For amperometry recordings on permeabilized transfected cells: choose well-cracked cells with green fluorescence. The nuclei can be seen clearly if the cells are well cracked. Prior to puffing Ca^{2+}, both nuclei and cytosol are green, but the nuclei are especially bright. After puffing Ca^{2+}, the green fluorescence in the cytosol disappears, and only the nuclei are green. Around 25% cells are well cracked by this method. Notably, upon CFE touching, a non-exocytotic current would be found. The baseline would go back within 1 min. Active secretion can be detected by puffin Ca^{2+} to the cracked cells, even after 2.5 h following liquid N_2 permeabilization.

3.7 Single-Cell Biochemical Assays: The Proximity Ligation Assay with Immunostaining

1. Transfected cells on coated coverslips are washed, incubated with the high-KCl solution for 1 min, fixed, and then permeabilized with 0.1% Triton X-100.
2. The cell-containing coverslips are transferred onto a parafilm sheet and quickly washed with water to remove salts. After blocking, cells were incubated with two primary antibodies in the antibody diluent from the PLA kit. According to the protocol of the Duolink® PLA Kit, we add two PLA probes, the ligation–ligase solution and finally the amplification–polymerase solution.
3. (Optional) To counterstain the DCV marker, after the PLA, cells are washed, blocked, and incubated with primary antibody (against chromogranin B) and then secondary antibody. Finally, the coverslips were mounted onto glass slides with mounting medium with 4′,6-diamidino-2-phenylindole (DAPI).

4 Notes

1. Keep the cells grow as monolayer in the dishes. Avoid to reach 100% confluence for the culture. The growth rate is about 4–5 days to 90% confluence in a 10-cm coated dish. When

the slow growth rate is found in culture, check the contamination of mycoplasma by quantitative polymerase chain reactions (qPCR).

2. Avoid to choose very bright cells for functional assays. The GFP fluorescence from the IRES2 would not be so bright. In addition, the pCMV-IRES vector allows the protein of interest and GFP to be translated separately. Thus, GFP only serves as a transfection marker, without being fused with the protein of interest. The function of proteins of interest could be altered by the N- or C-terminal fused GFP.
3. The volume of plasmid DNA should be less than 1/10 volume of Cytomix. Keeping the same concentration of plasmid DNA can make the consistent efficiency among different transfection groups.
4. Cytomix contains the high concentration of KCl. Do not incubate or rinse cells by Cytomix.
5. After electroporation, cuvettes are washed by detergent, water, and 75% ethanol, followed by sterilization with UV light. Cuvettes can be reused by three times.
6. Coating is very important for the following functional assays. Use Collagen I and PDL before the expiry date. Keep 1-mL stocks to avoid extra freeze–thaw cycles.
7. Adding 5-mM KCl in the permeabilization medium may inhibit the exocytosis in permeabilized cells. Avoid adding KCl in the permeabilization medium or any solutions for permeabilized cells.
8. Cut CFE prior to use. Reused CFE may lose good sensitivity.
9. At the end of recordings, check successful puffing of KCl by observing the changes in the levels of pipette solution.
10. Grounding of the amperometry setup is essential and similar to the setup of single-channel recordings. Briefly, connect all the instrumental grounding with the iron shield for covering the recording chamber to the floating table, except for the fluorescence light source, the computer, and the monitor. Choose a single cell for recording, but not a cell within a colony or exhibiting two nuclei.
11. Select the primary antibodies with different hosts.
12. After thawing the cell stock, add 1-mL culture medium for centrifugation.
13. Incubation with FBS would inhibit Ca^{2+} current in whole-cell voltage clamp recordings. Avoid doing recordings after 24 h following incubation with the FBS-containing medium.
14. The needle size of 21G or 22G can disperse PC12 cells without "cracking" cells.

15. These ratios of loading concentrations and cell density can be altered proportionally. Add 1.5-mM NE and 0.5-mM ascorbic acid into the 3.5-cm dish, which contains 1-mL medium and cells with the density of 2×10^5/mL. Note that ascorbic acid is an antioxidant and is also the co-factor for the enzyme (dopamine-β-hydroxylase) that converts dopamine into NE.
16. Avoid using liquid N_2 for more than 10 s since the GFP fluorescence may be lost.
17. Do not leave the cracked cells in a CO_2 incubator for more than 1 h. The permeabilized cells would become round shape and lose their secretion activity.
18. By gently touching the cell, the CFE may detect the secretory events at near distance.

Acknowledgments

We thank Dr. Thomas F. J. Martin (University of Wisconsin-Madison) for advice in PC12 cell culture and permeabilization; Dr. Meyer B. Jackson (University of Wisconsin-Madison) for technical support in single-vesicle amperometry; Dr. Payne Y. Chang for the amperometry analysis software; the staff of Technology Commons, College of Life Science, NTU, for help with confocal microscopy; and Dr. Juu-Chin Lu and members of the Wang lab for help and discussion. This work was supported by NTU (NTU-CC-111 L891102) and the Ministry of Science and Technology (MOST-109-2311-B-002-008-MY3) to CTW. PCC is the recipient of NTU fellowship direct to advanced study for the doctoral program.

References

1. Levitan IB, Kaczmarek LK (2015) The neuron. Oxford University Press, New York
2. Wassenberg JJ, Martin TF (2002) Role of CAPS in dense-core vesicle exocytosis. Ann N Y Acad Sci 971:201–209
3. Greene LA, Tischler AS (1976) Establishment of a noradrenergic clonal line of rat adrenal pheochromocytoma cells which respond to nerve growth factor. Proc Natl Acad Sci U S A 73:2424–2428
4. Martin TFJ (1994) Identification of proteins required for Ca2+–activated secretion. Ann N Y Acad Sci 710:328–332
5. Kasai H, Takagi H, Ninomiya Y et al (1996) Two components of exocytosis and endocytosis in phaeochromocytoma cells studied using caged Ca2+ compounds. J Physiol 494:53–65
6. Westerink RH, Ewing AG (2008) The PC12 cell as model for neurosecretion. Acta Physiol (Oxf) 192:273–285
7. Hay JC, Martin TF (1992) Resolution of regulated secretion into sequential MgATP-dependent and calcium-dependent stages mediated by distinct cytosolic proteins. J Cell Biol 119:139–151
8. Wang CT, Lu JC, Bai J et al (2003) Different domains of synaptotagmin control the choice between kiss-and-run and full fusion. Nature 424:943–947
9. Wang CT, Bai J, Chang PY et al (2006) Synaptotagmin-Ca2+ triggers two sequential steps in regulated exocytosis in rat PC12 cells: fusion pore opening and fusion pore dilation. J Physiol 570:295–307

10. Chow RH, Von Ruden L (1995) Electrochemical detection of secretion from single cells. In: Sakman B, Neher E (eds) Single-channel recording. Plenum Press, New York, pp 245–275
11. Albillos A, Dernick G, Horstmann H et al (1997) The exocytotic event in chromaffin cells revealed by patch amperometry. Nature 389:509–512
12. Jackson MB (2007) In search of the fusion pore of exocytosis. Biophys Chem 126:201–208
13. Wang CT, Grishanin R, Earles CA et al (2001) Synaptotagmin modulation of fusion pore kinetics in regulated exocytosis of dense-core vesicles. Science (New York, N.Y.) 294:1111–1115
14. Zhang Z, Jackson MB (2008) Temperature dependence of fusion kinetics and fusion pores in Ca2+−triggered exocytosis from PC12 cells. J Gen Physiol 131:117–124
15. Zhang Z, Hui E, Chapman ER et al (2009) Phosphatidylserine regulation of Ca2+−triggered exocytosis and fusion pores in PC12 cells. Mol Biol Cell 20:5086–5095
16. Zhang Z, Hui E, Chapman ER et al (2010) Regulation of exocytosis and fusion pores by synaptotagmin-effector interactions. Mol Biol Cell 21:2821–2831
17. Zhang Z, Jackson MB (2010) Membrane bending energy and fusion pore kinetics in ca (2+)-triggered exocytosis. Biophys J 98:2524–2534
18. Zhang Z, Zhang Z, Jackson MB (2010) Synaptotagmin IV modulation of vesicle size and fusion pores in PC12 cells. Biophys J 98:968–978
19. Zhang Z, Wu Y, Wang Z et al (2011) Release mode of large and small dense-core vesicles specified by different synaptotagmin isoforms in PC12 cells. Mol Biol Cell 22:2324–2336
20. Chiang N, Hsiao YT, Yang HJ et al (2014) Phosphomimetic mutation of cysteine string protein-α increases the rate of regulated exocytosis by modulating fusion pore dynamics in PC12 cells. PLoS One 9:e99180
21. Yang HJ, Chen PC, Huang CT et al (2021) The phosphoprotein synapsin Ia regulates the kinetics of dense-core vesicle release. J Neurosci 41:2828–2841
22. Han X, Wang CT, Bai J et al (2004) Transmembrane segments of syntaxin line the fusion pore of Ca2+−triggered exocytosis. Science (New York, N.Y.) 304:289–292
23. Han X, Jackson MB (2006) Structural transitions in the synaptic SNARE complex during Ca2+−triggered exocytosis. J Cell Biol 172: 281–293

Chapter 2

Adrenal Grafts in the Central Nervous System: Chromaffin and Chromaffin Progenitor Cell Transplantation

Alejandra Boronat-Garcia, Marcela Palomero-Rivero, and Magdalena Guerra-Crespo

Abstract

Chromaffin cells are neuroendocrine cells that synthesize and release catecholamines and neuroactive molecules. They have been used experimentally in animal models and preclinical studies as a source for cell replacement therapy in Parkinson's disease. The long-term cell survival of these cells in the nervous system is limited, and the observed motor improvements are highly variable. An alternative source for transplantation is chromaffin progenitor cells. These cells have the capacity of self-renewal and to form spheres under low attachment conditions. They release higher quantities of dopamine than chromaffin cells and can differentiate into dopaminergic-like neurons in vitro. The transplantation of these cells into Parkinson's disease animal models has shown to induce stronger motor improvements and better survival rates than chromaffin cells. However, several aspects of chromaffin progenitor cell transplantation remain to be elucidated. Here, we describe methods to isolate and culture chromaffin and chromaffin progenitor cells from the adult cattle adrenal glands. We also describe the procedure for their transplantation into the nervous system and give recommendations for their histological analysis.

Key words Chromaffin, Chromaffin progenitor cell, Adrenal glands, Transplant, Brain

1 Introduction

Chromaffin cells are neuroendocrine cells that synthesize and release catecholamines, such as dopamine and adrenaline, in response to sympathetic stimulation. Located in the medulla of the adrenal gland, chromaffin cells, together with sympathetic neurons and the intermediate small intensely fluorescent cells, constitute a major lineage of the neural crest cells—the sympathoadrenal lineage [1].

Due to their ability to release dopamine and neuroactive molecules such as opioids, and their potential as an autologous source for transplantation, chromaffin cells have been used experimentally in animal models and preclinical studies as a source for cell

Ricardo Borges (ed.), *Chromaffin Cells: Methods and Protocols*,
Methods in Molecular Biology, vol. 2565, https://doi.org/10.1007/978-1-0716-2671-9_2,

replacement therapy in Parkinson's disease (PD) [2] and chronic pain [3–5]. In PD, motor impairments are associated with the loss of dopaminergic neurons in the substantia nigra pars compacta, leading to a reduction of dopamine in its target region, the striatum. This feature is mimicked in animal models by selectively damaging the dopaminergic pathway which, in turn, induces motor alterations. To test the capacity of chromaffin cells to act as a cell source in PD, they have been transplanted into the striatum of animal models. The degree of the motor alterations before and after transplantation has served as a measure of the grafts' effectiveness. Additional measures, such as the survival of the cells over time and the ability to release dopamine in vivo, have been employed. Although chromaffin cell transplantation has offered some level of motor improvement, their long-term cell survival and the observed behavioral effects are highly variable and range from low to moderate [2].

Chromaffin progenitor cells have been another source for transplantation since the technique for isolating and culturing them was described [6]. These cells can be obtained from adult adrenal glands of different donors, including bovine [6], murine [7], and human [8]. They propagate under low-attachment conditions, which induce their aggregation and growth as spheres that, by analogy with neurospheres, are named chromospheres [6]. Like neural stem cells, these cells show self-renewal capacity and the ability to form clonal secondary spheres [6]. Additionally, they can release higher quantities of dopamine than chromaffin cells [2] and are able to differentiate into dopaminergic-like neurons in vitro [9]. To study their potential as a source of cell replacement therapy in PD, chromospheres have been transplanted into the striatum of rat models of PD [2, 10]. These grafted cells showed a higher survival rate and better motor improvements compared to chromaffin cell grafts when evaluated for at least 3 months [2]. Chromosphere grafts have also been shown to produce antinociceptive effects that may be mediated by dopamine and opioid receptors [10]. These studies show that chromaffin progenitor cells engrafted into the brain can survive and induce behavioral changes. However, further studies are necessary to assess the long-term behavioral effects of transplantation, the mechanisms involved in the behavioral changes, the capacity of the cells to respond to the microenvironment, and their survival.

In recent years, dopaminergic progenitor cells derived from human pluripotent stem cells have gained prominence: clinical trials have started, and more are on their way [11]. Induced pluripotent stem cells offer the advantage that they can be obtained from the same patient, as is the case for chromaffin and chromaffin progenitor cells. In a recent preclinical study, dopaminergic progenitor cells derived from human pluripotent stem cells were transplanted into the striatum of PD animal models, including rodents and monkeys,

to test their efficacy [12]. These cells were transplanted as 30 days spheres and became dopaminergic neurons that induced motor improvement and extended processes into the striatum of the host. Similarly, chromaffin progenitor cells have been transplanted as spheres (8 days), resulting in a higher survival rate than dissociated cells. However, contrary to the dopaminergic progenitor cells derived from pluripotent stem cells grafts, the capacity of chromaffin progenitor cells to become dopaminergic-like neurons after transplantation has not been studied.

In this chapter, we first describe the methods to isolate and culture chromaffin and chromaffin progenitor cells from the adult cattle adrenal glands as previously described in [6]. Next, we explain the procedure for their transplantation into the striatum of the brain and provide recommendations for their histological analysis [2, 10]. These methods provide researchers with the necessary techniques to perform their studies on chromaffin and/or chromaffin progenitor cell transplantation into the nervous system.

2 Materials

2.1 Chromaffin and Chromaffin Progenitor Cell Isolation

1. Antibiotic and antimycotic 100× solution: Mix 10,000 units of penicillin, 10-mg streptomycin, and 25 μg of amphotericin B per mL of culture grade water. Filter with a 0.1-μm pore size filter.
2. Antibiotic 100× solution: Mix 10,000 units of penicillin and 10 mg of streptomycin per mL of culture grade water. Filter with a 0.1-μm pore size filter.
3. Dulbecco's phosphate-buffered saline (dPBS) 20× solution: Mix 160 g of NaCl, 4 g of KCl, 4 g of KH_2PO_4, and 23 g of Na_2HPO_4. Add deionized water to the volume of ~900 mL. Adjust the pH to 7.4 and complete to obtain 1 L of dPBS. Filter through a 0.22-μm filter.
4. dPBS-a solution: 1× dPBS supplemented with 1:100 antibiotic/antimycotic 100× solution.
5. dPBS-b solution: 1× dPBS supplemented with 1:100 antibiotic 100× solution.
6. dPBS-c solution: 1× dPBS supplemented with 0.3% type II collagenase and 30 units/mL DNase I.
7. Culture medium A: Supplement Dulbecco's Modified Eagle's Medium/Nutrient Mixture F12 (DMEM/F12) with 10% steroid-free fetal bovine serum (FBS, *see* **Note 1**) and 1:100 penicillin-streptomycin solution.
8. 70% ethanol: Mix 350 mL of ethanol 100% and 150 mL of distilled water.
9. 50% bleach: Mix 250 mL of bleach and 250 mL of distilled water.

2.2 Chromosphere Formation and Expansion

1. Culture medium B: Supplement Neurobasal medium with 2% serum-free B-27 supplement, 2 mM L-glutamine, 20 ng/mL basic fibroblast growth factor, and 1:100 penicillin/streptomycin solution.

2.3 Cell Transplantation

1. Cyclosporine A.
2. Trypsin-EDTA 0.25%.
3. Trypan blue.

2.4 Perfusion and Brain Tissue Processing

1. 0.2-M and 0.1-M phosphate buffer: Mix 920 mL of deionized water with 58 g of NaH_2PO_4 and 5.24 g of Na_2HPO_4. Adjust the pH to 7.3 and complete to obtain 1 L of phosphate buffer 0.2 M. Dilute 500 mL of this solution in deionized water to 1:2 to obtain phosphate buffer 0.1 M.
2. 4% PFA: To prepare 1 L of PFA, take ~400 mL of deionized water and heat it in the microwave to 65 °C. Add 40 g of PFA and ~1 mL of NaOH and mix well. Once the PFA is dissolved, fill up with deionized water to the volume of 500 mL and add the 500 mL of the remaining 0.2-M phosphate buffer previously prepared. Adjust the pH to 7.4, and filter through a 0.22-μm filter. Allow the solution to cool down and refrigerate.
3. 10% Sucrose: Mix 10 g of sucrose in 100 mL of 0.1-M phosphate buffer.
4. 20% Sucrose: Mix 20 g of sucrose in 100 mL of 0.1-M phosphate buffer.
5. 30% Sucrose: Mix 30 g of sucrose in 100 mL of 0.1-M phosphate buffer.
6. Antifreeze: Mix 50% 0.1 M phosphate buffer, 25% glycerol, and 25% ethylene glycol.

3 Methods

3.1 Preculture Procedures: Isolation of Chromaffin and Chromaffin Progenitor Cells from Adult Cattle Adrenal Glands (See Fig. 1c)

3.1.1 Collection and Cleaning of Adrenal Glands

1. Add 500 mL of dPBS-a to a 1-L glass flask with a lid. Place the flask in a cooler box with ice packs. This flask is used to collect ~9 adult cattle adrenal glands at the slaughterhouse and transport them to the laboratory (*see* **Note 2**).
2. Once the adrenal glands are in the laboratory, clean the glass flask with a disposable paper towel and 70% ethanol and place it on a sterile table (*see* **Note 3**).
3. Add ~350 mL of the cold dPBS-a solution to a 500-mL beaker. This solution is used to wash the exterior of the glands to avoid microbial contamination.
4. Using Adson's forceps, pick up the adrenal glands and place them in the beaker with the cold dPBS-a solution.

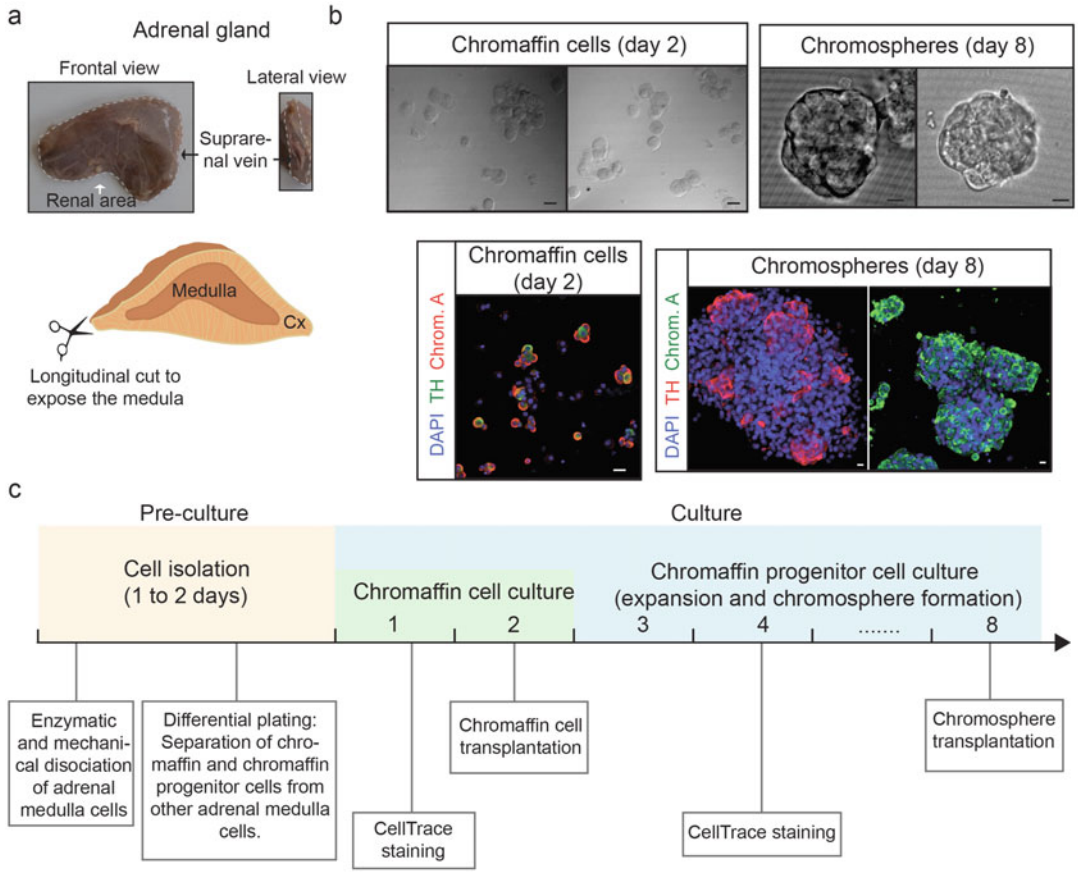

Fig. 1 (**a**) *Up*: Image of an adrenal gland from adult bovine. Frontal and lateral views show the location of the suprarenal vein indicated by the black arrows. The renal area is indicated by a white arrow. *Bottom*: Schematic representation of a longitudinal cut made to expose the medulla of the gland. (**b**) *Up*: Transmitted light images of chromaffin cells during the second day of culture (left) and of chromospheres during the eighth day of culture (right). *Bottom*: Fluorescence images of chromaffin cells during the second day of culture (left) and of chromospheres during the eighth day of culture (right). The cells were stained against tyrosine hydroxylase (TH, green) and chromogranin A (Chrom. A, red). The cell nuclei were stained with DAPI (4′,6-diamidino-2-phenylindole, blue). (**c**) Timeline of the preculture and culture procedures highlighting the main steps. The purpose of the preculture is to isolate chromaffin and chromaffin progenitor cells from the adrenal gland. This could take 1–2 days. It involves the enzymatic and mechanical dissociation of all the cells from the adrenal medulla and the separation of chromaffin cells and chromaffin progenitor cells from other adrenal medulla cells thru differential plating. During the culture stage, chromaffin and chromaffin progenitor cells are cultivated in optimal conditions. The chromaffin progenitor cell culture allows the expansion of progenitor cells and the formation of chromospheres. Chromaffin and chromaffin progenitor cells can be stained during this stage—this allows to track them in the brain after their transplantation. Scale bar: 12 μm. Cx Cortex

A potential source of contamination during these procedures is spilling on the table. Thus, it is important to clean up any spills immediately and keep the workspace sterile. To this end, use a disposable paper towel with 70% ethanol.

5. Prepare the workspace for cleaning the glands. Place a pair of tissue scissors and a pair of Adson's forceps in a 250-mL beaker. To keep the tools sterile, add enough benzalkonium chloride solution to cover half of the flask.
6. Add ~350 mL of 70% ethanol to a 500-mL beaker and cover it with aluminum foil. This solution is used in **step 12** to help remove connective tissue from the glands.
7. Place an empty 250-mL beaker on the table—it will be used to discard the connective and fatty tissues in **step 15**.
8. Add ~350 mL of dPBS-a solution to two 500-mL backer flasks and cover with aluminum foil. These flasks will be used to place the cleaned gland.
9. Turn on a shaking water bath and set it to 37 °C.
10. Place an empty 1-L beaker on the table—it will be used to discard the blood in **step 23**.
11. Add 250 mL of dPBS-c solution into a glass flask with a lid and large opening and place it in the water bath with agitation. This solution is used for the enzymatic digestion of the medulla in **step 1** in Subheading 3.1.2.
12. To remove the connective tissue surrounding the gland, first transfer the adrenal glands into the flask containing 70% ethanol (*see* **step 6**) using the tissue forceps. Proceed immediately to the next step.
13. Take one gland and place it in a Petri dish (100 mm × 21 mm).
14. Use the tissue forceps to gently grasp the gland.
15. Use the sharp tissue scissors and cut away the connective tissue surrounding the gland. Discard the tissue in the empty beaker (from **step 7**).
16. Place the cleaned gland in the 500-mL beaker with dPBS-a solution (from **step 8**).
17. Repeat **steps 13–16** for all adrenal glands.
18. Discard used beakers, flasks, and Petri dishes: Place the flask used to transport the glands and the two beakers (with ethanol and dPBS-a) in an autoclave safe tray and add 5 mL of 50% bleach solution. Place the beaker with the connective and fatty tissues in the tray and add 5 mL of 50% bleach solution. Set the tray aside.
19. Clean the working area with 70% ethanol.
20. To remove traces of blood from the glands, first place four Petri dishes (100 mm × 21 mm) on the table and add one gland to each dish.

21. Add ~400 mL of dPBS-b solution into a 500-mL beaker. This solution is used to wash off the blood debris from the glands.
22. Fill a 40-mL syringe (no needle) with the dPBS-b solution.
23. Inject around 20 mL of the solution into the central vein (*see* Fig. 1a). Place the glands back into the Petri dishes (100 mm × 21 mm) and wait for the solution to drain out of the tissue. Discard the blood into the empty 1-L beaker (from **step 10**).
24. Repeat **steps 22** and **23** until no more blood comes out of the glands. Between five and ten injections may be necessary depending on the size of the glands.
25. Add ~350 mL of dPBS-a solution into a beaker and place the cleaned glands into the solution.
26. Repeat **steps 22–25** for the rest of the glands.

3.1.2 Enzymatic and Mechanical Dissociation of Adrenal Medulla Cells

1. Remove the glass flask with the dPBS-c solution from the water bath (from **step 11**, Subheading 3.1.1) and fill a 40-mL syringe with the heated solution.
2. Inject the glands into the central vein once with ~10 mL of the solution and place them in a new glass flask with a lid.
3. Add some of the heated solution to the flask with the glands—add just enough to cover one third of the glands. Close the flask and place it in the shaking water bath for 40 min.
4. To improve the digestion of the medulla, repeat **steps 2** and **3** with a new prewarmed dPBS-c solution. This time leave the glands in the shaking water bath for 20 min.

Sterile procedures: The following steps should be performed in a sterilized biosafety cabinet.

5. Take the flask containing the glands and wipe it with a disposable paper towel and 70% ethanol.
6. Place a pair of clean tissue/dressing forceps and scissors in a 250-mL beaker and add enough benzalkonium chloride solution to cover half of the flask.
7. Pick up a gland with the forceps and place it in a Petri dish (100 mm × 21 mm).
8. To expose the digested medulla, use the dressing forceps to grasp the gland and the scissors to make a longitudinal cut in the gland (*see* Fig. 1a).
9. Using a spatula, detach the digested medulla and place it in a new Petri dish (100 mm × 21 mm). Avoid contamination from the cortex layer.
10. Add ~5 mL of dPBS-b solution in the Petri dish containing the digested medulla. This will facilitate mechanical dissociation in the following steps.

11. To mechanically dissociate any poorly digested medulla, first use the tissue scissors to cut any piece of medulla into very small pieces.
12. Pipette the cell mixture up and down several times with a 25-mL serological pipette to obtain a homogenous mixture.
13. Repeat the **step 12** with a 10-mL serological pipette.
14. Transfer the mixture to a 50-mL Falcon tube.
15. Repeat **steps 7–14** for the remaining glands. The dissociated mixture can be combined in the same Falcon tube.
16. For the next part of the mechanical dissociation, place a piece of sterile chiffon in a stainless steel strainer and place the strainer over a 250-mL polypropylene beaker (*see* **Notes 4** and **5**).
17. Filter the mixture through the chiffon/strainer and collect it in the polypropylene beaker.
18. Repeat **steps 16** and **17** using a new clean sterile chiffon over a clean strainer.
19. Filter the mixture through a sterile 100-μm cell strainer and collect the solution in a 50-mL Falcon tube. Collect a maximum of 30 mL per tube. Use as many 50-mL Falcon tubes as necessary.
20. Repeat **step 19**.
21. Filter the mixture through a sterile 70-μm cell strainer and collect the solution in a 50-mL Falcon tube. Change the strainer in case of clogging and/or add more dPBS-b.
22. Repeat the **step 21**.
23. Wash the cell mixture by adding dPBS-b solution to fill the tubes to the 50-mL line.
24. Pipette up and down to create a homogenous solution using a 50-mL serological pipette.
25. Centrifuge for 8 min at ~150 × *g*.
26. Carefully remove the supernatant.
27. Repeat washing **steps 23–26** twice.
28. Resuspend the pellets in 25 mL of culture medium A by pipetting up and down with a 25-mL pipette several times. This culture medium allows for proper growth and cell viability of primary cells without promoting the expansion of chromaffin progenitor cells. To separate chromaffin and chromaffin progenitor cells from the other adrenal medulla-isolated cells, such as fibroblasts and endothelial cells, proceed to Subheading 3.1.3.

Pause point Transfer 25 mL of the mixture to a 175-cm adherent culture flask and add 25 mL of medium A. Use as many flasks as needed. The adherent conditions do not facilitate aggregation of chromaffin progenitor cells and other types of cells. The isolated cells can be incubated overnight in a humidified atmosphere (95% air, 5% CO_2) at 37 °C. The cell culture is always maintained under these atmosphere and temperature conditions. If the protocol is paused here, proceed the next day to **step 1** in Subheading 3.1.3; otherwise, go directly to **step 8** in Subheading 3.1.1.

3.1.3 Differential Plating for Separation of Chromaffin and Chromaffin Progenitor Cells from Other Adrenal Medulla Cell Types (~4.5 h)

1. Detach the cells from the walls of the culture flasks by pipetting up and down and flushing the cells against the wall several times.
2. Transfer the contents to 50-mL Falcon tubes.
3. Centrifuge for 8 min at ~150 × *g*.
4. Remove the supernatant.
5. Resuspend the cells in 5 mL of medium A and combine all pellets in a 50-mL Falcon tube.
6. Add medium A to fill the tubes to 50 mL.
7. Transfer the mixture to a new adherent flask.
8. Incubate the cells for 2 h at 37 °C.
9. Transfer the supernatant (this contains mostly chromaffin and chromaffin progenitor-like cells) to a new adherent flask and incubate for 1 h.
10. Repeat the previous step one more time.
11. Transfer the supernatant to a 50-mL Falcon tube(s).
12. Centrifuge for 8 min at ~150 × *g*.
13. Remove the supernatant and proceed to Subheading 3.2.1 to continue with chromaffin cell culture or to Subheading 3.2.2 to continue with chromaffin progenitor cell culture.

3.2 Chromaffin and Chromaffin Progenitor Cells Culture (See Fig. 1c)

3.2.1 Chromaffin Cell Culture

1. Resuspend the pellet in 30-mL culture medium A. As mentioned above, this medium allows for proper growth and viability of the chromaffin cells.
2. Divide the cell suspension into three and transfer them to three adherent Petri dishes (100 mm × 21 mm).
3. Add ~2 mL of medium A to each dish.
4. Incubate the cells at 37 °C for 2 days.

To track the cells after transplantation, follow **steps 5–12**; otherwise, skip this part and go to **steps 13–15**.

5. On the second day, detach the cells from the walls of the culture dishes by pipetting up and down against the wall dish several times.

6. Transfer the contents to 50-mL Falcon tubes.
7. Centrifuge for 8 min at ~150 × *g*.
8. Remove the supernatant.
9. Use CellTrace CFSE (excitation, 498; emission, 518) or CellTrace Far Red (excitation, 630; emission, 661) Cell Proliferation kits to stain the cells. Follow the manufacturer's instructions for cells in suspension.
10. After staining, centrifuge the cells for 8 min at ~150 × *g*.
11. Resuspend the cells in culture medium A following the **steps 1–3**.
12. Proceed to **step 16**.
13. If cells are not to be stained for tracking: Remove the medium from the Petri dishes using a 15-mL pipette.
14. Add 12.5 mL of medium A to the culture plates.
15. Proceed to **step 16**.
16. Incubate the cells at 37 °C for an additional day.
17. Proceed to Subheading 3.3 to continue with the transplantation.

3.2.2 Chromaffin Progenitor Cell Culture (Chromospheres Formation and Expansion)

1. Resuspend the pellet in 25 mL of culture medium B. This medium allows for proper growth and expansion of the chromaffin progenitor cells.
2. Divide the mixture in three and transfer it to three ultra-low attachment culture flasks (75 cm) and add enough medium B to fill the flasks to the 20-mL line. The ultra-low attachment conditions allow aggregation of the chromaffin progenitor cells and chromosphere formation.
3. Incubate the cells at 37 °C for 5 days by changing the medium every 2 days. To change the medium, follow **steps 4–9**.
4. Equilibrate culture medium B to room temperature for at least 1 h.
5. Transfer the cells into a 50-mL Falcon tube(s).
6. Centrifuge for 8 min at ~150 × *g*.
7. Remove the supernatant.
8. Resuspend the pellet in ~25-mL culture medium B.
9. Divide the mixture into three and transfer it to three new ultra-low attachment culture flasks and add enough medium B to fill the flasks to the 20-mL line.

To track the cells after transplantation, follow **steps 10–15**; otherwise, skip this part and go to **steps 16–17**.

10. On the fifth day, transfer the cells to 50-mL Falcon tubes.
11. Centrifuge for 8 min at ~150 × *g*.

12. Remove the supernatant carefully to avoid sucking up the pellet.
13. Use CellTrace CFSE or CellTrace Far Red and follow the manufacturer instructions for cells in suspension.
14. After staining, centrifuge the cells for 8 min at ~150 × *g*.
15. Resuspend the cells in culture medium B following **steps 4–9**.
16. Incubate the cells at 37 °C in culture medium B for 4 more days. Change medium every 2 days following the **steps 4–9**.
17. Proceed to Subheading 3.3 to continue with the transplantation.

3.3 Preparation of the Cells for Transplantation into the CNS

3.3.1 Chromaffin Cells Preparation

1. Detach the cells from the walls of the Petri dishes by pipetting up and down against the walls several times. Use a 10-mL serological pipette.
2. the cells to 15-mL Falcon tubes.
3. Centrifuge for 8 min at ~150 × *g*.
4. Remove the supernatant.
5. To disaggregate and quantify the cells, add 2 mL of trypsin-EDTA 0.25% (previously warmed up to room temperature) to each tube and incubate for 15 min at room temperature.
6. Gently shake the tubes every 5 min.
7. Inactivate the trypsin-EDTA 0.25% by adding 3 mL of medium A supplemented with FBS (10%). Pipette up and down with a 1000-μL pipette to mechanically disaggregate any clusters of cells.
8. Centrifuge for 3 min at ~150 × *g*.
9. Remove the supernatant and resuspend the pellets in 5–10-μL Opti-MEM medium.
10. Place the tubes on ice.

Quantify the cells in each tube following **steps 11–19**.

11. Take 0.5 μL of the cell suspension and place it in a 0.2-mL microcentrifuge tube.
12. Add 0.5-μL trypan blue strain to the microcentrifuge tube and pipette up and down to mix the contents.
13. Place a glass lid in the central area of a Neubauer chamber.
14. Take 0.5 μL of the cell mixture with a micropipette and place the tip right in the center of the chamber (between the chamber and the glass lid).
15. Release the content slowly in the Neubauer chamber. The solution should enter the chamber uniformly avoiding the formation of bubbles.

16. Place the Neubauer chamber under an upright microscope stage. The cells should be disaggregated and in small clusters of a few cells. However, if there are large clusters of cells, repeat the digestion with trypsin-EDTA 0.25%.
17. Use a cell counting device to count the live cells (blue negative cells) in the four large grid squares (corner areas). Note that the 4 large squares are made of 16 smaller squares each. Count the number of cells within each of the 16 small squares and note the number of cells counted per each large square. Sum the number of cells counted in the four large squares to obtain the final number of cells.
18. Apply the formula Concentration (cells/mL) = Final number of cells/Volume (in mL).
19. Divide the concentration by the dilution factor Concentration = Number of cells × 10,000/Number of squares (4) × dilution. In this case, 0.01 (1:100).
20. Add the necessary volume of Opti-MEM medium to each tube to get a density of ~7.5×10^4 cells/μL. Keep the cells on ice (*see* **Note 6**).
21. Proceed to Subheading 3.3.3.

3.3.2 Chromaffin Progenitor Cells Preparation

1. Transfer the cells from the three flasks to three 50-mL Falcon tubes.
2. Centrifuge for 8 min at ~150 × *g*.
3. Remove the supernatant carefully to avoid sucking up the pellets.
4. Resuspend the cells in 2 mL of medium B and transfer the three tubes (~6 mL) to a 15-mL Falcon tube.

   To disaggregate and quantify the cells, follow **steps 5–14**.
5. Take 1 mL of the cell suspension and transfer it to a 15-mL Falcon tube.
6. Centrifuge for 8 min at ~150 × *g*.
7. Remove the supernatant.
8. Add 2 mL of trypsin-EDTA 0.25% (previously tempered at room temperature) to each tube and incubate for 15 min at room temperature.
9. Gently shake the tubes every 5 min.
10. Inactivate the trypsin-EDTA 0.25% by adding 3 mL of medium B. Pipette up and down with a 1000-μL pipette to mechanically disaggregate any clusters of cells.
11. Centrifuge for 3 min at ~150 × *g*.
12. Remove the supernatant and resuspend the pellets in 5–10-μL Opti-MEM medium.

13. Place the tubes on ice.
14. To quantify the cells, follow the **steps 11–19** in Subheading 3.3.1.
15. Centrifuge the 15-mL Falcon tube from **step 4** for 8 min at ~150 × *g*.
16. Remove the supernatant and add the necessary volume of Opti-MEM medium to each tube to obtain a density of ~7.5 × 10^4 cells *per* μL. Keep the cells on ice (*see* **Note 6**).
17. To identify that the cells to transplant are expressing the markers of interest, perform immunohistochemistry (e.g., tyrosine hydroxylase, chromogranin A) (*see* Fig. 1b) as indicated in Subheading 3.4.
18. Proceed to Subheading 3.3.3.

3.3.3 Transplantation into the Central Nervous System of Adult Wistar Rats

1. To avoid the rejection of transplanted cells, 24–48 h before transplantation, treat rats (~250 g) with cyclosporine A (100 mg/kg/day) orally. Continue the immunosuppression treatment until the animals are euthanized.
2. Take 4 μL of the cell suspension (~300,000 chromaffin cells or chromaffin progenitor cells) with a 5-μL Hamilton syringe.
3. Anesthetize the animals by intraperitoneal injection of a mixture of xylazine (8 mg/kg) and ketamine (10 mg/kg).
4. Perform stereotaxic surgery to inject the cells into the region of interest (*see* **Note 7**). Inject the cells at a rate of 0.5 μL per minute by lowering the plunger of the Hamilton syringe manually. Example grafts provided in Fig. 2 are from cells injected into the left striatum of rats lesioned with 6-hydroxydopamine (+1.0 mm AP, ±3.0 mm ML, −5.3 (2 μL of cell suspension), and −5.0 (the remaining 2 μL) DV, with respect to Bregma 0).
5. After injecting the cells, leave the cannula in place for 5 min to prevent backflow.
6. Thoroughly clean the needle well with distilled H_2O between injections.

3.4 Analysis of the Transplanted Cells in the Brain Tissue

1. Cells can be analyzed at different times after transplantation (*see* **Note 8**). To do this, euthanize the animals by an intraperitoneal injection of an overdose of sodium pentobarbital (*see* **Note 9**).
2. Perform intracardial perfusion (*see* **Note 9**) with ~200 mL of 0.1-M phosphate buffer followed by ~200 mL of 4% PFA. The temperature of the solutions should be ~4 °C; keep them on the ice during the procedure.
3. After perfusion, use the dissection tools to collect the brain tissue.

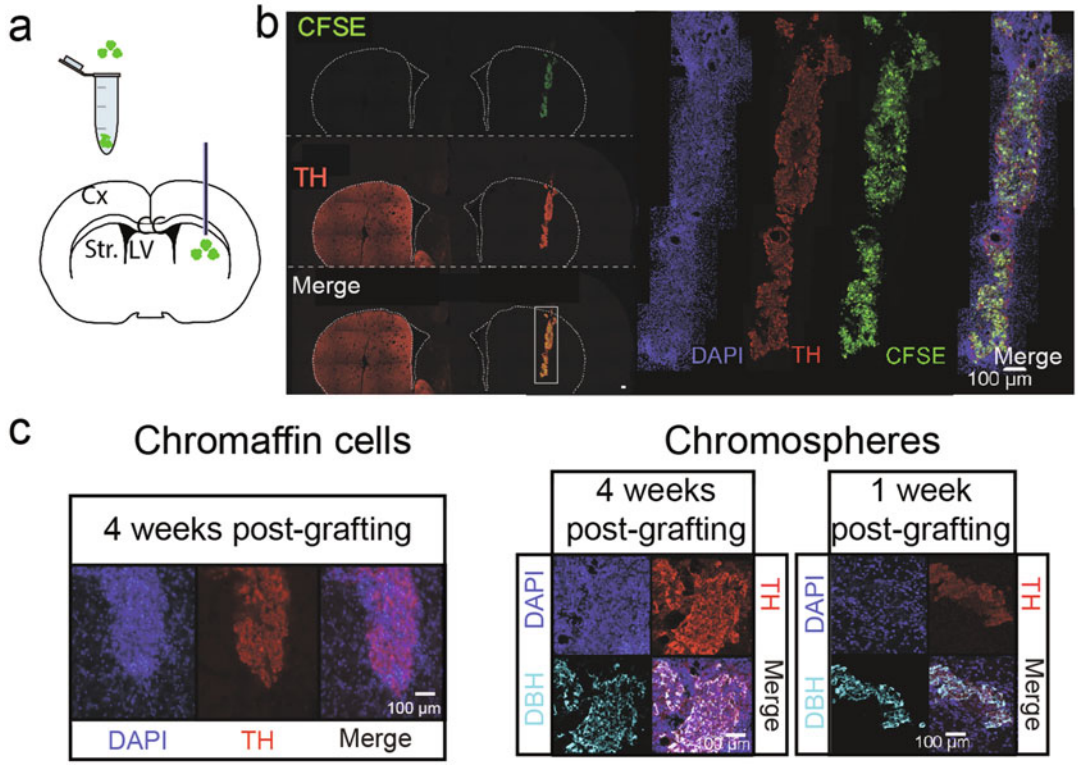

Fig. 2 (**a**) Schematic representation of the site of transplantation, the striatum. (**b**, **c**) Fluorescence images of cells (green) transplanted into the striatum. The cells were stained with CFSE (green) during the culture stage and transplanted into the lesioned striatum of rats treated with 6-OHDA. One and four weeks after transplantation, the brains were fixed, cryoprotected, and processed to collect coronal sections of the transplantation site. The coronal sections containing the grafted cells were selected to perform immunofluorescence against tyrosine hydroxylase (TH, red) and dopamine-b-hydroxylase (DBH, cyan). Cell nuclei were stained with DAPI (4′,6-diamidino-2-phenylindole, blue). Scale bar: 100 µm. Cx cortex, Str striatum, LV lateral ventricles, CC corpus callosum, CFSE carboxyfluorescein succinimidyl ester, 6-OHDA 6-hydroxydopamine. (A, B, and C taken and adapted from ref. 2)

4. Postfix the brains overnight with 4% PFA at 4 °C.
5. To cryoprotect the brains, incubate them for 24 h in 10%, 20%, and 30% sucrose in 0.1-M phosphate buffer.
6. Embed the brains in tissue optimal cutting temperature compound and collect cryosections of ~40 µm thickness using a cryostat. If the samples are not to be processed immediately, fill a 96-well plate with antifreeze solution and store it at −20 °C; otherwise, use phosphate-buffered saline (PBS) and collect serial sections of the area of interest by placing one section per well.
7. For short-term analysis (less than ~14 days after engraftment): if cells were pre-stained with a cell tracker (Subheading 2.2), the engraftment can be visualized immediately under an

epifluorescence microscope. Otherwise, all sections must be processed by immunohistochemistry against any of the markers of interest that are expressed by the engrafted cells (e.g., tyrosine hydroxylase, dopamine beta-hydroxylase) (*see* Fig. 2b, c, **Note 8**).

8. For mid- and long-term analysis (more than ~14 days after engraftment): all sections containing the region of interest should be processed by immunohistochemistry against any of the markers of interest that are expressed by the engrafted cells (e.g., tyrosine hydroxylase, dopamine beta-hydroxylase) (*see* Fig. 2b, c, **Note 8**).

4 Notes

1. We recommend making ~10-mL aliquots of the steroid-free fetal bovine serum to avoid repeated cycles of thawing and freezing.
2. Adrenal glands should be freshly collected from local slaughterhouse.
3. The material and tools used for the dissection and handling of the glands should be autoclaved. This includes scissors, forceps, stainless steel strainers, beakers, and glass containers.
4. The stainless steel strainer should be large enough to fit into the 250-polypropylene beaker.
5. The chiffon fabric used during the cell isolation procedure should be sterile. To this end, cut pieces of ~15 × 15 cm and place them in individual bags made with kraft paper. Put the paper bags with the chiffon squares in a glass flask to autoclave them.
6. We recommend preparing the cells in small batches—prepare enough to transplant ~3 animals at a time. This will keep the remaining cells in optimal culture conditions until before transplantation.
7. To become familiar with stereotactic surgery, several resources may be visited (e.g., [13, 14]).
8. Depending on the experimental design, engrafted cells can be identified by the presence of one of the dyes used during culture (CellTrace CFSE or CellTrace Far Red Cell Proliferation Kit) or by immunohistochemistry against specific markers expressed by the cells. Cell tracing dyes are a great tool because they allow easy identification of grafts in cryosections and selection of sections with grafts for further analysis (*see* Fig. 2b). To identify cells with specific markers and for further cell analysis, immunohistochemistry or immunofluorescence

techniques can be used. The use of specific antibodies against tyrosine hydroxylase, dopamine-β-hydroxylase, and chromogranin A may allow visualization of cells in the brain. However, although these markers have shown to be expressed in cells during culture and after transplantation into the striatum (*see* Fig. 2b, c), the proportion of cells expressing each of these markers after transplantation is unknown and may be affected by the transplantation microenvironment.

9. There are several resources available regarding transcranial perfusion that may be visited (e.g., [15]). Additionally, follow your federal, state, and local guidelines.

Acknowledgments

This work was supported by IN211419 DGAPA-PAPIIT and CONACYT No. A1-S-10064. We are grateful to Francisco Pérez Eugenio and Omar Collazo Navarrete for their critical comments.

References

1. Huber K (2006) The sympathoadrenal cell lineage: specification, diversification, and new perspectives. Dev Biol 298(2):335–343. https://doi.org/10.1016/j.ydbio.2006.07.010
2. Boronat-García A, Palomero-Rivero M, Guerra-Crespo M et al (2016) Intrastriatal grafting of chromospheres: survival and functional effects in the 6-OHDA rat model of Parkinson's disease. PLoS One 11(8):e0160854. https://doi.org/10.1371/journal.pone.0160854
3. Winnie AP, Pappas GD, Das Gupta TK et al (1993) Subarachnoid adrenal medullary transplants for terminal cancer pain. A report of preliminary studies. Anesthesiology 79(4):644–653. https://doi.org/10.1097/00000542-199310000-00004
4. Jeon Y, Baek WY, Chung SH et al (2011) Cultured human chromaffin cells grafted in spinal subarachnoid space relieves allodynia in a pain rat model. Korean J Anesthesiol 60(5):357–361. https://doi.org/10.4097/kjae.2011.60.5.357
5. Ambriz-Tututi M, Sanchez-Gonzalez V, Drucker-Colin R (2011) Chromaffin cell transplant in spinal cord reduces secondary allodynia induced by formalin in the rat. Role of opioid receptors and α2-adrenoreceptors. Eur J Pharmacol 668(1–2):147–154. https://doi.org/10.1016/j.ejphar.2011.06.030
6. Chung K-F, Sicard F, Vukicevic V et al (2009) Isolation of neural crest derived chromaffin progenitors from adult adrenal medulla. Stem Cells 27(10):2602–2613. https://doi.org/10.1002/stem.180
7. Saxena S, Wahl J, Huber-Lang MS et al (2013) Generation of murine sympathoadrenergic progenitor-like cells from embryonic stem cells and postnatal adrenal glands. PLoS One 8(5):e64454. https://doi.org/10.1371/journal.pone.0064454
8. Santana MM, Chung K-F, Vukicevic V et al (2012) Isolation, characterization, and differentiation of progenitor cells from human adult adrenal medulla. Stem Cells Transl Med 1(11):783–791. https://doi.org/10.5966/sctm.2012-0022
9. Vukicevic V, Schmid J, Hermann A et al (2012) Differentiation of chromaffin progenitor cells to dopaminergic neurons. Cell Transplant 21(11):2471–2486. https://doi.org/10.3727/096368912X638874
10. Gomez-Paz A, Drucker-Colin R, Milan-Aldaco D et al (2018) Intrastriatal chromospheres' transplant reduces nociception in hemiparkinsonian rats. Neuroscience 387:123–134. https://doi.org/10.1016/j.neuroscience.2017.08.052
11. Barker R, Parmar M, Studer L et al (2017) Human trials of stem cell-derived dopamine

neurons for Parkinson's disease: dawn of a new era. Cell Stem Cell 21(5):569–573. https://doi.org/10.1016/j.stem.2017.09.014

12. Doi D, Magotani H, Kikuchi T et al (2020) Pre-clinical study of induced pluripotent stem cell-derived dopaminergic progenitor cells for Parkinson's disease. Nat Commun 11:3369. https://doi.org/10.1038/s41467-020-17165-w
13. JoVE Science Education Database (2021) Neuroscience. Rodent stereotaxic surgery. JoVE, Cambridge, MA. https://www.jove.com/es/v/5205/rodent-stereotaxic-surgery. Accessed 6 Jun 2021
14. Paxinos G, Watson C (2013) The rat brain in stereotaxic coordinates. Academic Press, London
15. Gage GJ, Kipke DR, Shain W (2012) Whole animal perfusion fixation for rodents. J Vis Exp 65:3564. https://doi.org/10.3791/3564

Chapter 3

Immunocytochemistry of Acutely Isolated Adrenal Medullary Chromaffin Cells

Keita Harada, Hidetada Matsuoka, and Masumi Inoue

Abstract

Immunocytochemistry enables the detection and localization of proteins in cells that are acutely dissociated or in culture. There are advantages and disadvantages to the use of cultured cells for immunocytochemistry. One of the advantages is that cultured cells can be used for one or more weeks after the dissociation of cells, whereas one of the disadvantages is that the properties of cells in culture might change under artificial conditions. On the other hand, acutely dissociated cells are expected to have the original properties of cells because almost all procedures before fixation, except for enzymatic digestion, are carried out at low temperatures. Here, we describe how adrenal medullary cells of small animals are acutely dissociated for immunostaining.

Key words Immunocytochemistry, Immunofluorescence, Acutely isolated cell, Adrenal medullary chromaffin cell, Confocal microscopy

1 Introduction

Identification of the proteins involved in signal transduction is an inevitable step for the clarification of molecular mechanisms. To express a protein, the transcription of its gene first occurs in the nucleus with the consequent generation of mRNAs; then, protein production results from translation on the ribosome based on the genetic information encoded by the mRNA. Subsequently, the protein is subjected to posttranslational modifications in the endoplasmic reticulum [1] before being transported to a specific site where the protein functions. Therefore, it is true that when a protein is produced, the corresponding mRNA should be generated. Thus, which proteins are expressed in cells can be explored at the mRNA level by molecular biological approaches, such as RT-PCR. The probes used for RT-PCR are specific and relatively easy to generate at a low cost. On the other hand, analysis at the protein level with immunoblotting and/or immunocytochemistry

Ricardo Borges (ed.), *Chromaffin Cells: Methods and Protocols*,
Methods in Molecular Biology, vol. 2565, https://doi.org/10.1007/978-1-0716-2671-9_3,

requires a specific antibody, which is sometimes difficult to make and costs more. Expression at the mRNA level, however, does not always mean expression at the protein level [2, 3]. There are regulatory mechanisms for translation based on mRNA producing a protein [4]. In addition, turnover rates for mRNAs differ [5]. Therefore, exploring expression at the protein level is indispensable for the elucidation of what proteins are expressed in cells. In addition, proteins function at the site where they are delivered via a membrane transport mechanism, so it is important to clarify where the proteins are located inside the cell. Thus, determining the expression and location of proteins by using immunocytochemistry and/or immunoelectron microscopy is crucial for the elucidation of their functions in cells.

Immunocytochemistry of adrenal medullary chromaffin (AMC) cells has mainly been performed in culture [6, 7], as many AMC cells are obtained from animals and maintained for a certain period of time under artificial conditions. AMC cells in situ, however, are exposed to high concentrations of adrenal cortical hormones because of the development of the intra-adrenal portal vascular system [8]. Namely, some of the arteries become capillaries in the adrenal cortex before entering the adrenal medulla. Therefore, AMC cells are exposed to adrenal cortical hormones at concentrations which are 7–80 times higher than those in the general circulation [9]. This high concentration of hormones has been shown to play a critical role in the expression of certain proteins in AMC cells, such as chromogranin A [10]. In addition, AMC cells are innervated by sympathetic preganglionic nerve fibers, and synaptic transmission is known to regulate the expression of certain proteins in AMC cells [11]. Thus, it is important to functionally and morphologically study AMC cells that are continuously receiving hormonal and neuronal inputs. To circumvent the lack of humoral and neuronal influence on AMC cells in culture, acutely dissociated AMC cells are used for the analysis of protein expression and functional studies [11–13]. This chapter aims to describe the detail of immunocytochemical analysis in acutely dissociated AMC cells from small experimental animals.

2 Materials

1. Balanced salt solution: 137-mM NaCl, 5.4-mM KCl, 1.8-mM $CaCl_2$, 0.5-mM $MgCl_2$, 0.53-mM NaH_2PO_4, and 5-mM D-glucose; the pH is adjusted to 7.4 with 4-mM NaOH. Ca^{2+}-free balanced salt solution lacks the $CaCl_2$ in balanced salt solution.
2. Phosphate buffer saline (PBS): 137-mM NaCl, 2.7-mM KCl, 10-mM Na_2HPO_4, and 2-mM KH_2PO_4.

3. 0.2-M phosphate buffer (PB): 0.2-M NaH_2PO_4-containing and 0.2-M Na_2HPO_4-containing solutions are mixed so that the pH of the combined solutions is 7.4.
4. 4% paraformaldehyde (PFA) in 0.1 M PB: 8 g of PFA is put into about 60 mL of distilled water, and the pH is adjusted to 7.4 with 2-N NaOH while being stirred at 60 °C. Then, the total volume of the solution is measured up to 100 mL with distilled water. The same volumes of 8% PFA solution and 0.2 M PB are mixed to obtain 4% PFA in PB.
5. 0.3% Triton X-100 in 5% fetal bovine serum-containing PBS: Triton X-100, 15 μL; fetal bovine serum, 0.25 mL; PBS, 5 mL.
6. Collagenase is available from several commercial sources, and its potency should be titrated by researchers.
7. Glass-bottomed dishes (P35GC-O-14-C) is available from MatTek Corporation (Ashland, MA, USA).
8. Anti-fade fluorescence mounting medium is available from Abcam plc (Cambridge, UK).
9. Many antibodies are commercially available. Otherwise, they need be made by researchers themselves.

3 Methods

1. A rat or guinea pig is killed by cervical dislocation, and the adrenal glands are removed and put into an ice-cold Ca^{2+}-free balanced salt solution. The microscissors and forceps are used to remove the adrenal cortex from the adrenal gland under microscopic observations (*see* **Note 1**).
2. After rough removal of the adrenal cortex, the preparation is cut into half by microscissors. The adrenal medulla looks more whitish than the adrenal cortex in the cutting plane. Accordingly, the adrenal cortex is excised from the adrenal medulla as much as possible (*see* Fig. 1) (*see* **Note 2**).
3. Four pieces of the adrenal medullae obtained from one animal (*see* **Note 3**) are put into a centrifuge tube containing 1.5 mL of Ca^{2+}-free balanced salt solution with the addition of 10 mg of collagenase (*see* **Note 4**). The centrifuge tube is warmed at 36 °C in a water bath while the solutions are gently stirred by O_2 gas. The flow rate of O_2 gas is adjusted for the preparations to fluctuate 5–10 times per second in the solution (*see* Fig. 2).
4. The preparations are treated with collagenase for 15 min, and the treatment is repeated twice with a fresh collagenase solution (*see* **Note 5**). After the enzyme treatment, the preparations are put into a Ca^{2+}-free balanced salt solution at 5 °C.

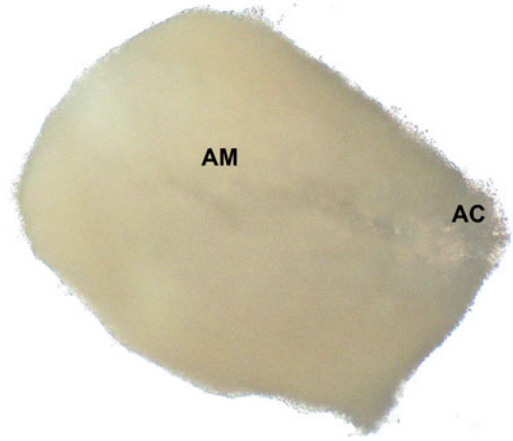

Fig. 1 Photograph of the cut section of adrenal medulla. The adrenal cortex was removed from the adrenal gland with microscissors and forceps under microscopic observations. Then, the adrenal medulla preparation was cut into two with microscissors. The preparation contained predominantly adrenal medulla (AM) and minimally adrenal cortex (AC), which is evident as less transparent tissue on part of periphery

5. A glass-bottomed dish is placed on an inverted microscope, and about 150 μL of the Ca^{2+}-free solution is placed onto the glass in the dish, and then one piece of the digested adrenal medullary preparation is placed into the solution. Next, AMC cells are mechanically dissociated using needles (27 G with 13 mm in length) attached to 1-mL syringes. After dissociation, the dish is left for 30 min to facilitate attachment of the cells to the glass.
6. The cells are fixed with 4% PFA in PB for 1 h. After fixation, the cells are washed three times in PBS and then treated with 0.3% triton-X 100 in 5% fetal bovine serum-containing PBS to permeabilize the cell membrane and reduce nonspecific binding by antibodies. The cells are washed three times in PBS (*see* **Note 6**).
7. The cells are treated overnight with an antibody (*see* **Notes 7–10**) which is appropriately diluted in PBS to obtain specific immunostaining. After being washed three times in PBS, the cells are treated with a secondary antibody conjugated with Alexa Fluor 488 or 546 at room temperature for 1 h.
8. After being washed three times in PBS, an anti-fade reagent, such as anti-fade fluorescence mounting medium, is placed on the cells, and then the tissue is covered using a glass cover slip. The edges of the cover slip are sealed with nail polish (*see* **Note 11**).

Fig. 2 Instruments and arrangements for the dissociation of adrenal medullary cells. The adrenal cortex is removed from the adrenal gland under microscopic observations in a Petri dish whose bottom is covered with silicone mixed with carbon powder. O_2 gas is delivered through a polyethylene tube from an O_2 gas cylinder to the bottom of a centrifuge tube that is filled with 1.5 mL of collagenase-containing Ca^{2+}-free balanced salt solution

4 Notes

1. Hamster AMC cells are obtained in the same manner as for a rat or guinea pig. However, mouse adrenal glands are small, so the mouse adrenal gland is first cut in half. The adrenal cortex is recognized as a less whitish tissue in the section, and adrenal cortical cells are removed. Two or three mice are used for the dissociation of AMC cells.
2. To obtain a dish containing many AMC cells, it is important to remove as many adrenal cortical cells as possible from the adrenal medullary preparations. The presence of adrenal cortical tissue in them hinders efficient enzymatic digestion. In addition, the adrenal cortical tissue contains relatively more red blood cells and connective tissue. Thus, when the digested preparation is mechanically dissociated with needles, red blood cells and strings of connective tissue first settle on the glass before AMC cells, thereby preventing AMC cells from attaching to the glass.

3. The age of animals is also crucial for effective digestion. As animals age, the connective tissue in the adrenal medulla develops further, thus preventing efficient digestion. Three months old or younger show good dissociation of AMC cells.
4. The enzyme activity of collagenase produced by the same maker can change depending on the rot number. Thus, the optimal condition must be searched for a new enzyme. Generally speaking, the concentration of collagenase and/or the duration of enzyme treatment may be modified to achieve an appropriate digestion.
5. Appropriate digestion of the adrenal medulla preparation results in the easy dissociation of AMC cells with needles. On the other hand, when the preparation is excessively digested, AMC cells are isolated by shaking of the preparation. In this case, AMC cells do not stick to the glass and are easily washed off when solutions are exchanged.
6. If fixed cells are not subjected to immunostaining immediately after dissociation, 0.1% azide must be added to the dishes, thereby preventing the proliferation of bacteria. However, even azide-treated dishes should be used within 1 or 2 weeks for successful immunostaining.
7. A specific antibody is critical for successful immunocytochemical analysis. If the antibody has been used for immunostaining, its specificity can be evaluated based on the reference. Generally speaking, when the number of references where the antibody was used is large, it would be more reliable. However, because the experimental conditions for immunostaining differ between experiments, researchers have to evaluate the specificity of an antibody in immunostaining.
8. The specificity of an antibody in our experiments has been assessed by the double immunostaining of a target protein, which is exogenously expressed in PC12 cells originating from rat AMC cells. The expression vector for a fusion protein is created so that a tag is inserted somewhere in the target protein without the hindrance of the protein function. The cells expressing the fusion protein are subjected to double immunostaining with anti-tag and anti-target protein antibodies. The specificity of the anti-target protein antibody is assessed by measuring the extent of coincidence of the two immunostains. It would be worth noting that the tag should be inserted at a site that is sufficiently away from an epitope site in the three-dimensional structure, which is used to produce the antibody. Otherwise, the anti-tag antibody binding could hinder the anti-target protein antibody from binding to the epitope.

9. When a fluorescent protein, such as green fluorescent protein (GFP), is used as a tag, the addition of the fluorescent protein, whose molecular weight is about 27 kDa, might affect the vesicular transport of the target protein [14]. In that case, the intracellular distribution of a fusion protein differs from that of a native protein.
10. Another point to be noted is a difference in the expression level between exogenous and endogenous proteins. The finding that AMC cells are not immunostained under conditions where exogenously expressed proteins are immunocytochemically detected in a cell line generally means that the target protein is not expressed in AMC cells. This conclusion, however, is based only on the assumption that the expression level of the endogenous protein in AMC cells is similar to that of the protein exogenously expressed in the cell line. If the expression level of endogenous proteins in AMC cells is relatively low, they might not be detected by a low affinity antibody. In compact cells, such as AMC cells, a small amount of protein may be sufficient to exert a function. For example, the activation of a single nicotinic receptor results in depolarization in a bovine AMC cell [15].
11. After being sealed with nail polish, the dish can be kept in a refrigerator for at least 1 week before observation with a confocal laser microscope.

References

1. Aebi M (2013) N-linked protein glycosylation in the ER. Biochim Biophys Acta 1833:2430–3437
2. Barry DM, Trimmer JS, Merlie JP, Nerbonne JM (1995) Differential expression of voltage-gated K^+ channel subunits in adult rat heart. Relation to functional K^+ channels? Circ Res 77:361–369
3. Inoue M, Harada K, Matsuoka H, Sata T, Warashina A (2008) Inhibition of TASK1-like channels by muscarinic receptor stimulation in rat adrenal medullary cells. J Neurochem 106: 1804–1814
4. Roux P, Topisirovic I (2018) Signaling pathways involved in the regulation of mRNA translation. Mol Cell Biol 38:e00070–e00018
5. Roy B, Jacobson A (2013) The intimate relationships of mRNA decay and translation. Trends Genet 29:691–699
6. Fenwick EM, Fajdiga PB, Howe NBS, Livett BG (1978) Functional and morphological characterization of isolated bovine adrenal medullary cells. J Cell Biol 76:12–30
7. O'Connor DT, Mahata SK, Mahata M, Jiang Q, Hook VY, Taupenot L (2007) Primary culture of bovine chromaffin cells. Nat Protoc 2:1248–1253
8. Coupland RE, Selby JE (1976) The blood supply of the mammalian adrenal medulla: a comparative study. J Anat 122:539–551
9. Mailhot J-P, Traistaru M, Soulez G, Ladouceur M, Giroux M-F, Gilbert P, Zhu PS, Bourdeau I, Oliva VL, Lacroix A, Therasse E (2015) Adrenal vein sampling in primary aldosteronism: sensitivity and specificity of basal adrenal vein to peripheral vein cortisol and aldosterone ratios to confirm catheterization of the adrenal vein. Radiology 277:887–894
10. Rozansky DJ, Wu H, Tang K, Parmer RJ, O'Connor DT (1994) Glucocorticoid activation of chromogranin a gene expression. Identification and characterization of a novel

glucocorticoid response element. J Clin Invest 94:2357–2368

11. Harada K, Matsuoka H, Toyohira Y, Yanagawa Y, Inoue M (2021) Mechanisms for the establishment of GABA signaling in adrenal medullary chromaffin cells. J Neurochem 158: 153–168
12. Inoue M, Kuriyama H (1991) Muscarinic receptor is coupled with a cation channel through a GTP binding protein in guinea-pig chromaffin cells. J Physiol 436:511–529
13. Matsuoka H, Harada K, Endo Y, Warashina A, Doi Y, Nakamura J, Inoue M (2008) Molecular mechanisms supporting a paracrine role of GABA in rat adrenal medullary cells. J Physiol 586:4825–4842
14. Madziva MT, Edwardson JM (2001) Trafficking of green fluorescent protein-tagged muscarinic M_4 receptors in NG108-15 cells. Eur J Pharmacol 428:9–18
15. Fenwick EM, Marty A, Neher E (1982) A patch-clamp study of bovine chromaffin cells and of their sensitivity to acetylcholine. J Physiol 231:577–597

Chapter 4

Transmission Electron Microscopy: A Method for Studying the Adrenal Chromaffin Cells

Anna Capaldo, Maria De Falco, Luigi Rosati, and Vincenza Laforgia

Abstract

Transmission electron microscopy and the use of glutaraldehyde-osmium fixation allow to distinguish norepinephrine from epinephrine granules in the adrenochromaffin cells, a difficult distinction with histochemical methods if both types of granules are present in the same cell. Here we describe all the steps necessary to process the adrenochromaffin tissue for the transmission electron microscopy; this protocol is suitable for any kind of adrenal tissue, and personally we used it in mammals, reptiles, and amphibians.

Key words Transmission electron microscopy, Chromaffin granules, Norepinephrine, Epinephrine, Glutaraldehyde-osmium fixation

1 Introduction

Adrenochromaffin cells, mainly producing epinephrine (E) and norepinephrine (NE), in addition to biogenic amines and regulatory peptides, are present in vertebrates, though their localization and topographical relationships with steroidogenic cells are different. Indeed, the degree of separation between steroidogenic and chromaffin tissues decreases progressively passing from cyclostomes to mammals, in which the chromaffin tissue forms the medullary part of the suprarenal gland [1]. The progressive approximation of both tissues increases E synthesis, since the corticosteroids produced from the steroidogenic tissue activate the enzyme N-phenylethanolamine-N-methyltransferase (PNMT), converting NE into E [2–4]. The presence of chromaffin granules is the main feature of chromaffin cells. In most vertebrates, there are two types of chromaffin cells, one of which contains E granules and the other NE granules; instead, in many species, only E cells have been observed, whereas in other species, chromaffin cells contain both E and NE granules [1]. Therefore, in addition to histological

Ricardo Borges (ed.), *Chromaffin Cells: Methods and Protocols*,
Methods in Molecular Biology, vol. 2565, https://doi.org/10.1007/978-1-0716-2671-9_4,

and histochemical methods [5], the transmission electron microscopy technique is particularly useful for detecting the content of the cells, since glutaraldehyde-osmium fixation makes it possible to distinguish between NE and E granules. In this technique, a first fixation with glutaraldehyde is followed by a post-fixation with osmium tetroxide. Indeed, NE forms with glutaraldehyde an insoluble complex, responsible for the subsequent staining with osmium tetroxide; E, instead, does not form this complex, and it is largely lost during the fixation and dehydration, so that E granules show only a light electron density [6]. Osmium tetroxide, on the other hand, is an excellent fixative but little penetrating; since it has a great affinity for unsaturated fatty acids of cell membranes phospholipids, it gives them a high electron density, acting also like a stain. Here, we describe the method we used to observe the chromaffin cells to the transmission electron microscope (TEM); this method allowed us to observe the presence of both NE and E cells [7], as well as chromaffin cells containing both types of granules [8].

2 Materials

Prepare the buffer and the fixatives with analytical grade reagents. In electron microscopy, cleaning is one of the determining factors for the success of the samples, so always use very clean laboratory glassware, tweezers, and scissors. The fixatives and many of the reagents used in electron microscopy are extremely hazardous and must be used in a fume hood, avoiding any contact with them (skin, eyes) or inhaling them, because they are volatile and can fix every tissue they contact. Therefore, you need to protect yourself using gloves and face masks. The buffer and the osmium tetroxide must be prepared in advance, the day before use, whereas glutaraldehyde must be prepared on the same day to be used. All these chemicals must be placed in the refrigerator to reach the operating temperature of 4 °C. Do not forget to label all containers of reagents.

2.1 Removal of the Adrenal Glands and Fixation

1. Stereomicroscope equipped with a fiber-optic light source.
2. pH meter.
3. Fume hood.
4. Petri dish, better if glass, with a diameter of at least 100 mm.
5. Dental wax or Parafilm®.
6. Small scissors and high precision tweezers, with very fine, straight tips.
7. Pasteur pipettes.
8. Small, very clean transparent, glass vials with cap, of a volume of 2–5 mL, to put tissue samples. Label all vials.

9. Crushed ice container.
10. Crushed ice.
11. A little dark glass bottle, of a volume of about 50 mL with narrow mouth and cap, for osmium tetroxide preparation.
12. Laboratory eyeglasses and gloves.
13. Millonig's buffer, pH 7.3–7.4. For buffer preparation, you must prepare four solutions:

    Solution A, sodium phosphate monobasic monohydrate $NaH_2PO_4 \cdot H_2O$ 2.26%. In a 500-mL graduated cylinder, add 300 mL of distilled water and 6.78 g of sodium phosphate monobasic monohydrate. Close the cylinder with Parafilm® and shake it well repeatedly.

    Solution B, sodium hydroxide NaOH 2.52%. Add 63 mL of 1-N NaOH to a 100-mL graduated cylinder and add distilled water to a volume of 100 mL. Close the container with Parafilm® and shake it well repeatedly.

    Solution C, glucose 5.4%. Add 5.4 grs of glucose to 100 mL of distilled water. Close the cylinder with Parafilm® and shake well repeatedly.

    Solution D. Mix 207.5 mL of solution A with 42.5 mL of solution B to a volume of 250 mL. Close the cylinder with Parafilm® and shake well repeatedly.

    Millonig's buffer. Mix 225 mL solution D with 25 mL of solution C. Close the cylinder with Parafilm® and shake well repeatedly. Check pH, which must be 7.3–7.4, and then transfer the buffer to a glass bottle of a volume of 250–300 mL, close the bottle and seal with the Parafilm®, and put the bottle in the refrigerator (*see* **Note 1**).
14. Fixation: 2.5% glutaraldehyde in Millonig's phosphate buffer pH 7.3–7.4. Add 9-mL Millonig's buffer to a 10-mL graduated cylinder; with an insulin syringe, withdraw 1 mL of 25% glutaraldehyde directly through the bottle cap and add to the cylinder. Close the cylinder with Parafilm® and shake well repeatedly. Put the fixative in a container of a volume of 10 mL and plug and put it in the refrigerator.
15. Post-fixation: 1% osmium tetroxide (OsO_4) in Millonig's buffer pH 7.3–7.4. Generally, the osmium tetroxide is sold in dark glass 100 mg vials, with a glued label. First, carefully wash the vial in cold water removing the label and label glue totally (*see* **Note 2**). Dry the vial well externally. Osmium tetroxide is highly harmful to the retina, so preparation must be carried under a fume hood and wearing glasses and gloves. Take a clean 100-mg vial and put it in a dark clean glass bottle, perfectly dry; if the vial is not pre-cut, make a slight incision with a razor

blade. Close the bottle tight and shake it until the vial breaks. Add 10 mL of Millonig's buffer in the dark bottle, close it with cap and Parafilm®, and shake it until the osmium tetroxide dissolves completely in the buffer (*see* **Note 3**). Put the osmium solution in the refrigerator.

2.2 Dehydration and Embedding

1. Fume hood.
2. Natural air convection oven dedicated exclusively to the electron microscopy.
3. Freezer.
4. High precision tweezers with very fine, straight tips.
5. Small, very clean transparent, glass vials, of a volume of 2–5 mL, to put tissue samples. Label all vials.
6. Plastic curved tip squeeze bottle (*see* Fig. 1a), of a volume of about 500 mL.

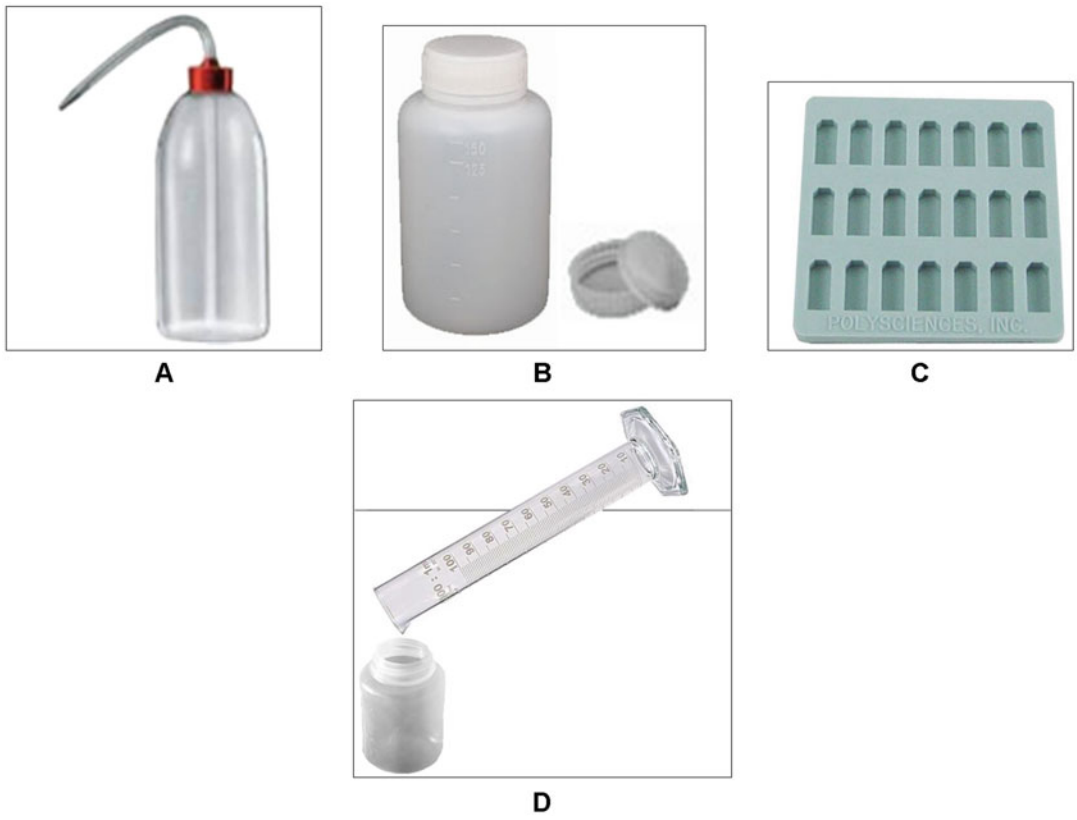

Fig. 1 Some of the materials used during the preparation of samples for electron microscopy. (**a**) Curved plastic tip squeeze bottle. (**b**) Plastic wide-mouth bottle, with a double cap. (**c**) Flexible silicon rubber mold. (**d**) Schematic drawing of the cylinder position with respect to the bottle, during the preparation of Epoxy resin

7. Plastic wide mouth bottles, with a double cap (*see* Fig. 1b), of a volume of 50 and 100 mL, to contain Epoxy resin. Generally, 100 mL of Epoxy resin are prepared; however, to protect the resin from moisture, and avoid repeated freezing and defrosting, it is convenient to divide the resin into smaller bottles, of a volume of 50 mL.
8. Flexible silicon rubber molds (*see* Fig. 1c), which release up to 21 blocks by flexing.
9. Color-indicating silica gel.
10. Sealed container for Epoxy resin embedded samples.
11. 0.5% NaCl. Dissolve 0.5 g of NaCl in 100 mL of distilled water. This solution must be prepared in advance and refrigerated.
12. Ethyl alcohol 50° in 0.5% NaCl. Mix 90 mL of 0.5% NaCl with 100 mL of ethyl alcohol 95° (alternatively, mix 92 mL of 0.5% NaCl with 100 mL of ethyl alcohol 96°). Close the cylinder with Parafilm® and shake to mix the solution well. Transfer the solution to a curved plastic tip squeeze bottle (*see* Fig. 1a) and put it in the refrigerator. This solution must be prepared in advance.
13. Epoxy resin. This resin must be prepared in a single, graduated 100-mL cylinder. The different components must be added to the cylinder exactly in the following order: (1) 48.5-mL Epon 812; (2) 18.5-mL dodecenylsuccinic anhydride (DDSA); and (3) 33-mL methyl nadic anhydride (MNA) (*see* **Note 4**). When the three components have been added, without shaking, pour the content of the cylinder in a plastic wide-mouth bottle, with a double cap (*see* Fig. 1b), at least twice the volume of the resin. When all the resin has fallen into the bottle (*see* Fig.1d), close the bottle and shake vigorously until the resin has become whitish. Then take 2 mL of benzyldimethylamine (BDMA) with a syringe, put it quickly in the bottle, close quickly, and shake vigorously the resin to mix well. Finally, freeze the resin (*see* **Note 5**).
14. Propylene oxide–Epoxy resin mixture, in equal parts. Pour into a container first the Epoxy resin (denser) and then an equal amount of propylene oxide. Close the container and shake well. Distribute the mixture in glass vials, as many as there are the samples to prepare for embedding.

2.3 Slicing

1. Ultramicrotome.
2. Razor blades.
3. Glass or diamond knives.
4. Petri dish, better if glass, with a diameter of at least 100 mm.
5. Pasteur pipettes.

6. High precision tweezers with very fine, curved tips.
7. Microscope slides.
8. 200 mesh copper grids coated with formvar. As electrons cannot pass through the glass, the electron microscopy sections are placed on grids (tiny circular disks with openings), generally copper grids, of 3 mm of diameter. These grids are coated with a transparent membrane, usually formvar, which serves to support the sections (mesh is a measure of how close the grid bars are; generally, 200 mesh copper grids are used).
9. Filter paper.
10. 1% toluidine blue in 2.5% Na_2CO_3, pH 11. Weigh 2.5 g of anhydrous Na_2CO_3 and pour it in 100 mL of distilled water. Add to the solution 1 g of toluidine blue. Shake well and then filter the solution with filter paper and store in the refrigerator.

2.4 Staining

1. Parafilm®.
2. Petri dish.
3. Filter paper.
4. Pasteur pipettes.
5. High precision tweezers with very fine, curved tips.
6. Scissors.
7. Wash bottle.
8. Face mask.
9. 2% Uranyl acetate. You must wear a mask to avoid inhaling uranyl dust, since it is not only radioactive but also very toxic. Weigh 2 g of uranyl acetate and pour it in 100 mL of bidistilled water. Shake well and then filter the solution with filter paper. Put the solution in a flask coated with aluminum paper, close the flask with Parafilm®, and then put the flask in the refrigerator.
10. 2.66% Lead citrate. Pour in a 50-mL graduated cylinder 1.33 g of lead citrate, 30-mL bidistilled water, and 8-mL 1-N NaOH. Close the cylinder with Parafilm®, shake well, and then add bidistilled water to a volume of 50 mL. Shake again. Do not filter the solution to avoid the contact with CO_2 that causes lead carbonate precipitates. Put the solution in a flask coated with aluminum paper, close the flask with Parafilm®, and then put the flask in the refrigerator.

3 Methods

Carry out all procedures at 4 °C unless otherwise specified. Remember to label the samples. Use glass Petri dish with a diameter of at least 100 mm.

3.1 Removal of the Adrenal Glands and Fixation

1. Put a Petri dish under a stereomicroscope. Put a piece of dental wax or Parafilm® in the Petri dish and put a drop of cold fixative (2.5% glutaraldehyde in Millonig's phosphate buffer at pH 7.3–7.4) on the dental wax (or Parafilm®).
2. The removal of the adrenal glands must be fast to prevent tissue degradation. During removal, wet the tissue with few drops of cold Millonig's buffer phosphate, pH 7.3–7.4, to prevent dehydration of the tissue.
3. Put the tissue in the drop of fixative on the Petri dish. The sample size shall be a few mm; if the sample is too large, it can be cut to smaller fragments on the Petri dish.

3.2 Fixation

The following steps must be carried out in very clean glass vials with cap, placed in trays full of crushed ice. At each step, the vials must be emptied of the liquid contained without dropping the tissue and must be filled quickly with the next liquid. Close always the vials.

1. Put the cold fixative (2.5% glutaraldehyde in Millonig's phosphate buffer at pH 7.3–7.4) in the vials; close and place them in trays full of crushed ice.
2. Put the tissue in the vials with fixative and close them; move the trays with the vials in the refrigerator. The tissue must remain in the fixative for 1 h.
3. Remove the trays with the vials from the refrigerator. Remove the fixative from the vials without dropping the tissue. Pour into the vials cold Millonig's phosphate buffer at pH 7.3–7.4 and leave it for 1–2 h. You can also leave the tissues in the buffer overnight in the refrigerator.
4. Remove the buffer from the vials without dropping the tissue. Pour into the vials cold 1% OsO_4 in Millonig's phosphate buffer at pH 7.3–7.4 for 2 h (*see* **Note 6**). Move the trays with osmium tetroxide in the refrigerator.

3.3 Dehydration and Embedding

1. Remove the osmium tetroxide from the vials without dropping the tissue. Pour into the vials cold 0.5% NaCl for 5 min.
2. Rinse the tissue in cold ethyl alcohol 50° in 0.5% NaCl for 5 min (*see* **Note 7**).
3. Remove the previous solution from the vials without dropping the tissue. Pour cold ethyl alcohol 50° into the vials for 10 min.

4. Remove the ethyl alcohol 50° from the vials without dropping the tissue. Pour cold ethyl alcohol 75° into the vials for 10 min.
5. Remove the ethyl alcohol 75° from the vials without dropping the tissue. Pour cold ethyl alcohol 95° into the vials for 10 min.

   Carry out all the following procedures at room temperature. The embedding resin and its components, and propylene oxide, are very hazardous and need to be handled carefully.
6. Remove the ethyl alcohol 95° from the vials without dropping the tissue. Pour ethyl alcohol 100° into the vials for 1 h, changing the ethyl alcohol every10 min (*see* **Note 8**).
7. Remove the ethyl alcohol 100° from the vials without dropping the tissue. Pour into the vials propylene oxide and change it every 5 min three times; this time (15 min) cannot be exceeded.
8. Take the samples of tissue with tweezers and put them in the vials containing the mixture propylene oxide–Epoxy resin until the propylene oxide evaporates (*see* **Note 9**).
9. Put the Epoxy resin in the embedding molds. Take the samples of tissue with tweezers and put them in the Epoxy resin; place the embedding molds into a natural air convection oven set to 60 °C for 3 days to make polymerization of Epoxy resin takes place.
10. The blocks embedded in Epoxy resin, and removed from the embedding molds, must be stored in a sealed container, with silica gel to absorb humidity. The silica gel must be replaced periodically.

3.4 Slicing

1. Trim the face of the block into a trapezoid with sloping sides (a flat pyramid), by using a razor blade, and then put the block into the arm of the ultramicrotome and make sections of 3 μm with a glass knife. To find the region of the tissue where the chromaffin cells are present, stain 1 section out of 10–20 sections with 1% toluidine blue in 2.5% Na_2CO_3, pH 11, that stains the section of blue and the chromaffin cells of brown (*see* Fig. 2a). Leave the dye on the section for about a minute and then rinse by spraying on the slide a gentle jet of distilled water from a curved plastic tip squeeze bottle (*see* Fig. 1a). Dry in air and observe under a light microscope.
2. Take thin (30–60 nm) sections, white, light gray in color, and collect the sections on 200-mesh copper grids coated with formvar. It is very important that the sections have the right thickness since the electrons have a very low penetration capacity.
3. Place the grids, sections side up, on a clean piece of filter paper inside a glass Petri dish and cover.

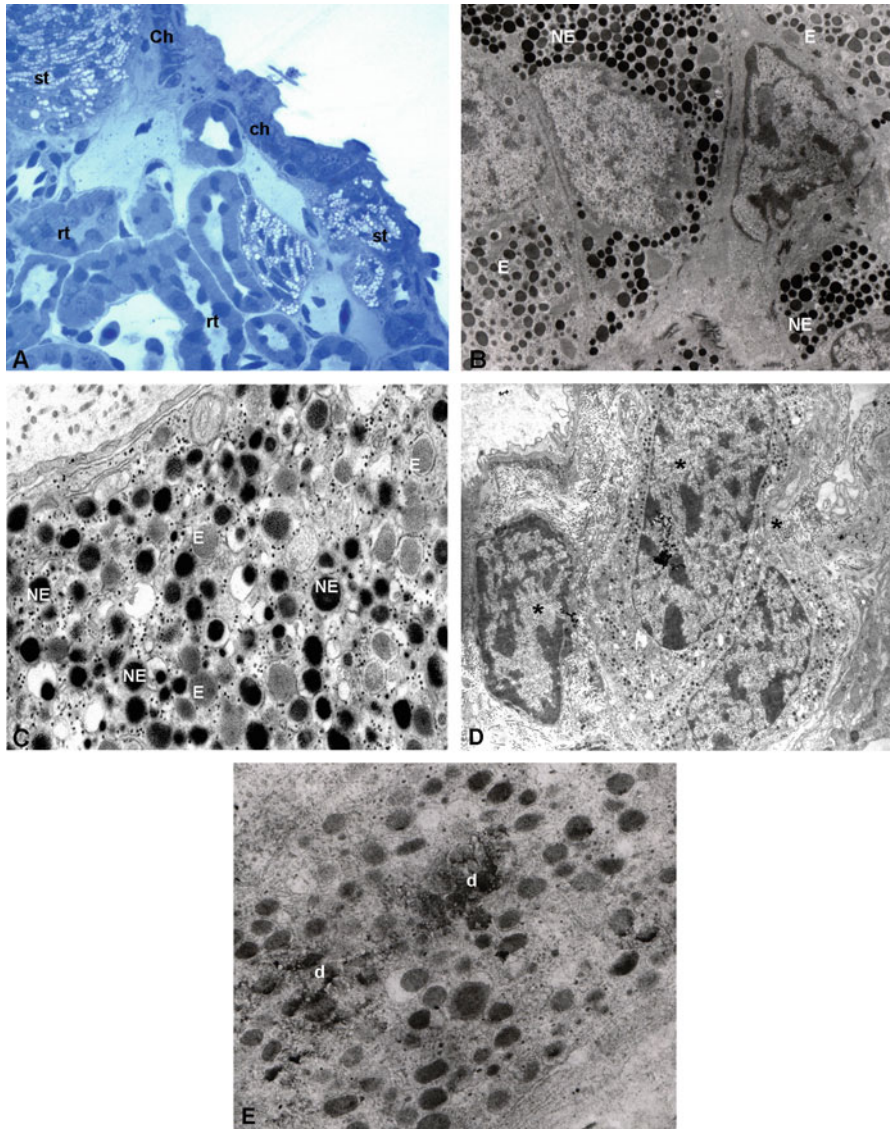

Fig. 2 Light and electron micrographs of chromaffin cells. (**a**) Semithin section, stained with toluidine blue, of the adrenochromaffin cells of *Triturus carnifex* (Amphibia, Urodela). Chromaffin cells (ch) appear brown in color, whereas the section is colored blue. Islets of steroidogenic (st) tissue and renal tubules (rt) are also observed. (**b**) Electron micrograph of NE and E cells of *Algyroides fitzingeri* (Reptilia, Lacertidae). In this species the adrenal gland shows NE and E cells, well distinguishable from each other. NE cells have granules with a variable shape and a strong electron density, whereas E cells have round granules, with a fine granular core of medium electron density and a clear halo between the core of the granule and the limiting membrane. (**c**) Electron micrograph of the adrenochromaffin cells of *Triturus carnifex* (Amphibia, Urodela). In this species, the chromaffin cells contain both NE and E granules, in variable proportions according to a functional cycle related to the reproductive cycle [8, 9]. In the cells, NE granules, strongly electron dense, and E granules, of medium electron density, are evident. (**d**) Electron micrograph of the adrenochromaffin cells of *Triturus carnifex* (Amphibia, Urodela). In this case, imperfections of the glass knife used to slice caused a series of stripes (asterisk) in the section. (**e**) Electron micrograph of the adrenochromaffin cells of *Triturus carnifex* (Amphibia, Urodela). Sections are contaminated by dirt (**d**). (**a**) 400×; (**b**) 5700×; (**c**) 20,000×; (**d**) 5000×; (**e**) 25,000×

3.5 Staining

The stains used are very hazardous and need to be handled carefully. Uranyl acetate is both a chemical and a radiological hazard and is decomposed by light, so it should be used in the dark.

1. Centrifuge uranyl acetate and lead citrate for 5 min at 1000 *g* and then cover the lead citrate tube with Parafilm® and put it in the refrigerator.
2. Clean the tweezers well with ether, alcohol 100°, and distilled water.
3. Cut a piece of Parafilm® and put it on a Petri dish, spreading it well on the glass.
4. Pipette as many drops of 2% uranyl acetate in bidistilled water as there are grids to stain.
5. Insert a grid in each drop, sections side up, and cover the Petri dish. Wait 5 min.
6. Wash every grid with a jet of bidistilled water from a curved plastic tip squeeze bottle (*see* Fig. 1a). If the jet is too violent, it can break the formvar membrane of the grid and destroy the sections (*see* **Note 10**).
7. Dry the water between the tips of the tweezers with a piece of filter paper.
8. Put the grids on a clean piece of filter paper, in a Petri dish, and cover. Wait for the grids to dry.
9. Cut a piece of Parafilm® and put it on a Petri dish, spreading it well on the glass.
10. Pipette as many drops of 2.66% lead citrate in bidistilled water as there are grids to stain (*see* **Note 11**).
11. Insert a dry grid in each drop, sections side up, and cover the Petri dish. Wait 11–12 min.
12. Wash every grid with a light jet of bidistilled water from a curved plastic tip squeeze bottle (*see* Fig. 1a) (*see* **Note 10**).
13. Dry the water between the tips of the tweezers with a piece of filter paper.
14. Put the grids on a clean piece of filter paper, in a Petri dish, and cover. Wait for the grids to dry.
15. Observe the grids at the transmission electron microscopy (TEM). This microscope visualizes specimens using a high-voltage electron beam and generates a highly magnified image, because the electron beam has a smaller wavelength which creates images of higher resolution. An electron gun at the top of a TEM emits electrons that travel through the microscope's vacuum tube; the electrons are deflected by electromagnetic lenses which focus the electrons into a very fine beam. This beam then passes through the specimen, which is

very thin, and the electrons either scatter or hit a fluorescent screen at the bottom of the microscope. On the screen, an image of the specimen can be seen, with its assorted parts shown in different shades according to its density. This image can be then studied directly within the TEM or photographed; currently, this image can be captured by a camera attached to a computer, running an image analysis system, allowing to analyze the images.

When all stages of the preparation of the sample have been carried out correctly, you can observe an image like Fig. 2b, c. The main feature of chromaffin cells is the chromaffin granules that occupy most of the cytoplasm and that are surrounded by a limiting membrane. NE granules appear of variable shape and show a very electron dense core, which is sometimes not separated from the limiting membrane, whereas E granules are rounded and show a fine granular core of medium electron density separated from the limiting membrane by a narrow space. As can be observed, this technique allows to distinguish both the two types of chromaffin cells (*see* Fig. 2b) and the two types of granules in the same cell (*see* Fig. 2c).

However, during the preparation of the samples, different errors can be made at different stages, affecting the good observation of the sample. For example, there is an insufficient fixation of the sample, due to the excessive sample size or the poor quality of reagents. In this case, the outer part of the sample is fixed well, while the inner part is not fixed; therefore, during the slicing of the sample at the ultramicrotome, sections crumble, and it will be impossible to slice the sample. Again, if Epoxy resin is too hard, compared to the sample, during the slicing at the ultramicrotome, the sections can be vibrated or serrated, and the observation at the TEM is impossible. Another problem may arise from the fact that the glass knife is worn or not perfectly smooth; in this case, in the image, a series of stripes will be visible (*see* Fig. 2d). Especially, during preparation of the samples, it is necessary to avoid contamination of the sections with any form of dirt. Indeed, in this case, the dirt will settle on the sections making very difficult to observe and acquire images under TEM (*see* Fig. 2e).

4 Notes

1. The buffer must be stored at 4 °C; always check the pH before using it. The buffer tends to form molds; if this happens, you must throw it out.
2. Washing the vial in hot water causes the osmium to dissolve.
3. The osmium can be contaminated by the glue of the label, so it is necessary to wash accurately the vial. The solution must be prepared in advance and must be completely transparent; if the

solution appears colored (straw yellow or yellow), it is not very effective and must be changed.

4. The three components are dense and sticky, so it is important to drop them exactly in the center of the cylinder, without sliding them on the walls.
5. Before you freeze the resin, you must remove the air bubbles. You can leave the resin at room temperature for one night and then freeze. If prepared well, the resin can be stored for a very long time, as long as it does not take moisture. Divide the resin into two bottles, one to be used for inclusion and the other for the propylene oxide–Epoxy resin.
6. The samples of tissue must be wetted by just a layer of OsO_4, so take a few drops with a pipette for each bottle. OsO_4 is toxic and colors the skin, so always wear gloves.
7. This step must be carried out without removing the 0.5% NaCl. Ethyl alcohol 50° in NaCl must be poured into the vial, containing both the tissue and 0.5% NaCl, from a curved plastic tip squeeze bottle (*see* Fig. 1a) with a gentle jet. Wait a short time.
8. Ethyl alcohol 100° must be taken from a new bottle. If you do not have new alcohol, change the alcohol every 5 min.
9. Leave the vials open, under a fume hood, all night, until to the evaporation of propylene oxide. After use, the vials can be washed with acetone.
10. During the washing, direct the jet of water from the curved plastic tip squeeze bottle only on the grid, and not on the tweezers. To do this, first let out a jet of water from the squeeze bottle and then insert the grid into the jet holding the grid vertically and not horizontally. The water that settles between the tips of the tweezers is always dirty, so it must not end up on the grid. This water can be dried with a filter paper disc placed between the tips of the tweezers.
11. As Pb precipitates are induced by CO_2, use a large Petri dish to insert NaOH beads (a maximum of ten beads) in addition to lead citrate drops. Also add a few drops of lead citrate on soda beads. Then cover the Petri dish.

References

1. Perry FS, Capaldo A (2011) The autonomic nervous system and chromaffin tissue: neuroendocrine regulation of catecholamine secretion in non-mammalian vertebrates. Auton Neurosci 165:54–66
2. Mazzocchi G, Gottardo G, Nussdorfer GG (1998) Paracrine control of steroid hormone secretion by chromaffin cells in the adrenal gland of lower vertebrates. Histol Histopathol 13:209–220
3. Capaldo A, Laforgia V, Sciarrillo R, Valiante S, Gay L, Varano L (2003) Localization and role of serotonin in the adrenal gland of *Podarcis sicula* (Reptilia, Lacertidae). Gen Comp Endocrinol 132:66–76
4. Laforgia V, Varano L, Capaldo A, Putti R, Cavagnuolo A (1991) Comparative morphology of the adrenal gland in selected species of the genus *Podarcis*. Amphibia-Reptilia 12(2): 153–160

5. Wood JG (1963) Identification of and observations on epinephrine and norepinephrine containing cells in the adrenal medulla. Am J Anat 112:285–304
6. Tramezzani JH, Chiocchio S, Wasserman GF (1964) A technique for light and electron microscopic identification of adrenaline and noradrenaline storing cells. J Histochem Cytochem 12: 890–899
7. Capaldo A, Laforgia V, Sciarrillo R, De Falco A, Valiante S, Gay F, Virgilio F, Varano L (2003) Effects of dopamine on the adrenal gland of *Podarcis sicula* (Reptilia, Lacertidae). Gen Comp Endocrinol 135:17–24
8. Gay F, Laforgia V, Capaldo A (2012) Human follicle-stimulating hormone modulation of adrenal gland activity in the Italian crested newt, *Triturus carnifex* (Amphibia, Urodela). Comp Biochem Physiol C 155:352–358
9. Laforgia V, Capaldo A (1991) Annual cycle of the chromaffin cells of *Triturus cristatus*. J Morphol 208:83–90

Chapter 5

Immunogold for Protein Location in Chromaffin Cells

Rafael Luján, Rocío Alfaro-Ruiz, and Carolina Aguado

Abstract

The localization and density of any plasma membrane or intracellular protein in chromaffin cells are prerequisites for those studies designed to elucidate their contribution to cellular function within the adrenal gland and can be achieved only by immunoelectron microscopy. The most popular immunoelectron microscopic techniques involved gold particles conjugated to secondary antibodies, leading to electron-dense markers and the so-called immunogold EM method. Two main immunogold electron microscopic techniques exist: the pre-embedding immunogold, whereby the immunolabeling steps take place before samples are embedded, and the post-embedding immunogold, where the immunolabeling steps take place on embedded and sectioned samples. Pre-embedding immunogold is a very sensitive technique useful for simultaneous observation of labeled tissue at the light and electron microscopic levels. Post-embedding immunogold enables the simultaneous localization of different molecules in the cell using secondary antibodies conjugated with gold particles of different size. In this chapter, we introduce pre-embedding and post-embedding immunogold procedures used for the identification of quantitative changes in a wide range of signaling molecules in different tissues and also discuss the limitations inherent to these approaches.

Key words Electron microscopy, Freeze-substitution, High-resolution techniques, Immunohistochemistry, Pre-embedding immunogold, Post-embedding immunogold, Protocols, Adrenal gland

1 Introduction

Electron microscopy (EM) continues to be an essential tool in biological research. The combination of EM with detection methods for biomolecules gives rise to immunoEM techniques, which provides the appropriate resolution to localize molecules to any cellular compartment. The most popular way to reveal the localization and distribution of specific antigens in various tissues, including the adrenal gland, is by using electron-dense markers such as colloidal gold coupled to secondary antibodies, leading to the so-called immunogold EM method. Immunogold EM involves many technical challenges, of which the most critical is to achieve

Ricardo Borges (ed.), *Chromaffin Cells: Methods and Protocols*,
Methods in Molecular Biology, vol. 2565, https://doi.org/10.1007/978-1-0716-2671-9_5,

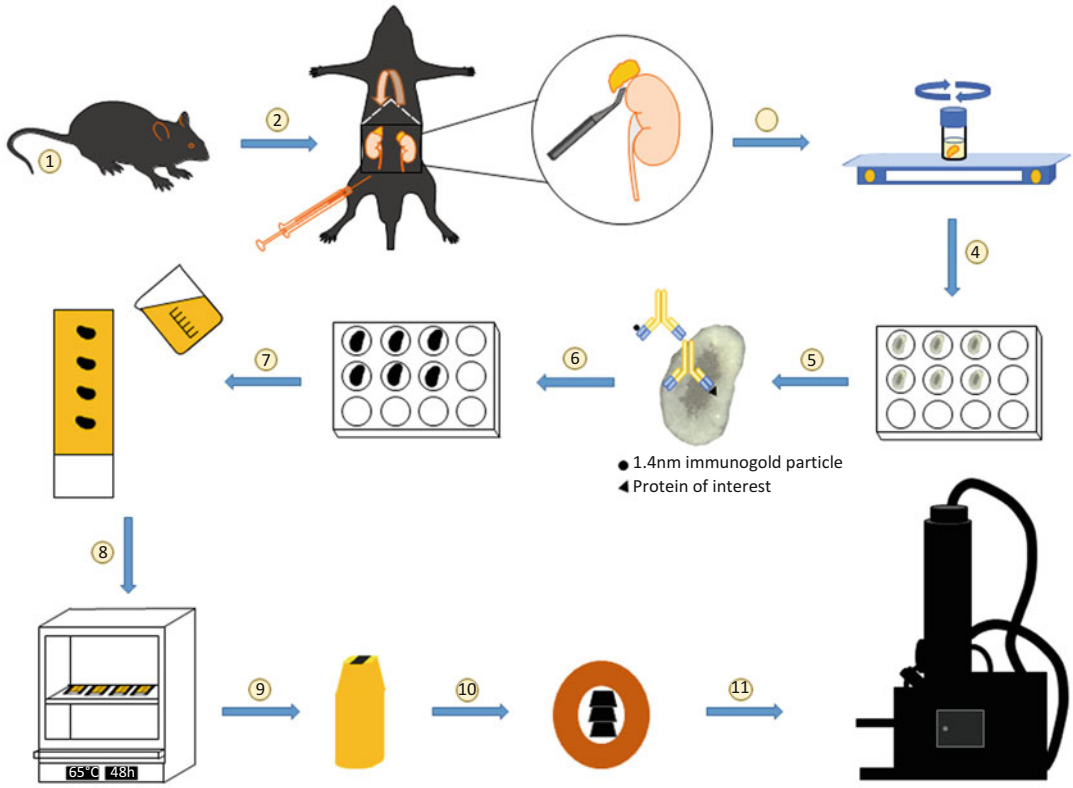

Fig. 1 Flowchart of the pre-embedding immunogold technique. Schematic drawing of the various procedural steps of the pre-embedding immunogold method from fixation of samples to visualization at the TEM. (1) Experimental animal; (2) perfusion fixation and dissection of adrenal gland; (3) washing in 0.1-M PB; (4) selection of adrenal gland sections and placement in a multi-well plate; (5) incubation in primary antibody, wash in TBS and incubation in secondary antibody; (6) incubation in osmium tetroxide; (7) preparation of epoxy resin and flat-embedding on slides; (8) polymerization of epoxy resin in oven at 60° for 48 h; (9) selection of the adrenal gland region of interest stuck on a blank block of resin; (10) ultrathin sectioning (70–80 nm) using an ultramicrotome and collection on single slot pioloform-coated copper grids; (11) visualization of section and analysis using a TEM

the right balance between the detection of antigen with enough sensitivity and the optimal information on the cell ultrastructure [1].

At the electron microscopic level, immunogold techniques can be divided into two groups: pre-embedding methods (*see* Figs. 1 and 2), whereby the immunolabeling steps take place before samples are embedded in resin, and post-embedding methods (*see* Fig. 3), where the immunolabeling steps take place on resin embedded and sectioned samples [1–3]. On one hand, the pre-embedding immunogold method produces a non-diffusible label, so the precise site of the reaction can be determined (*see* Fig. 2). Furthermore, this method is reliable for the localization of antigens along biological membranes in single and serial sections and has been successfully used to quantify different antigens along

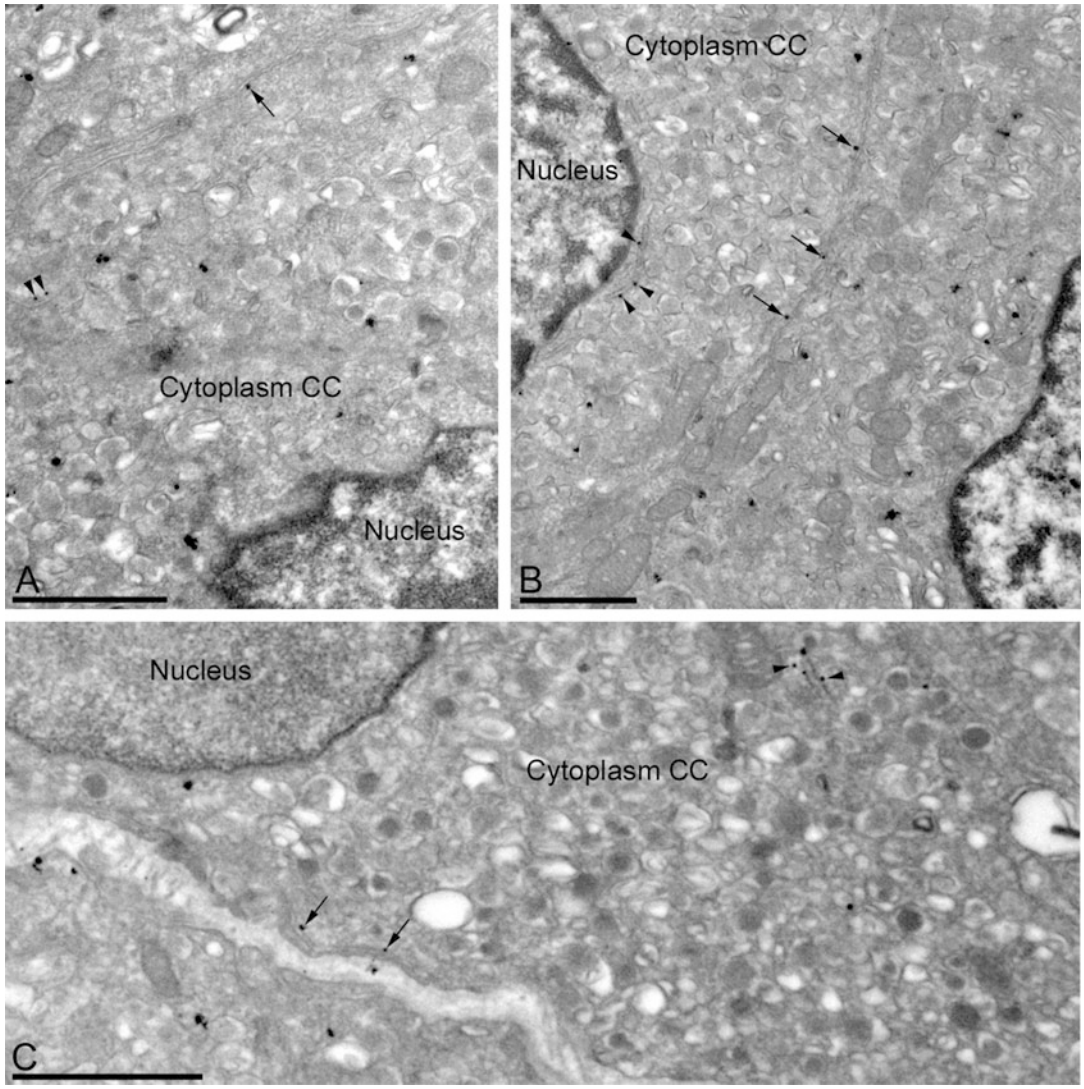

Fig. 2 Electron micrographs showing immunoreactivity for the SK2 subunit of the small-conductance K^+ channel, as demonstrated by a pre-embedding immunogold method in the adrenal gland of the mouse. (**a–c**) Immunoparticles for SK2 are localized along the plasma membrane (*arrows*) of chromaffin cells (CC) and associated with the rough endoplasmic reticulum (*arrowheads*) in the cytoplasm of chromaffin cells (CC). The nucleus of CC is devoid of any immunolabeling. *Scale bars*: (**a–c**) 1 μm

the plasma membrane and cytoplasmic sites [4–6]. In addition, pre-embedding methods are generally very sensitive and provide denser labeling than post-embedding methods [3, 5]. However, antigens located in compartments with high density of proteins such as the postsynaptic density of excitatory synapses in the brain are not generally detected using this method [1, 2, 5, 6]. On the other hand, the post-embedding immunogold method has a lower sensitivity than pre-embedding methods because primary and secondary antibodies only detect antigens present on the surface of the ultrathin section [5, 6]. For instance, a much lower density of

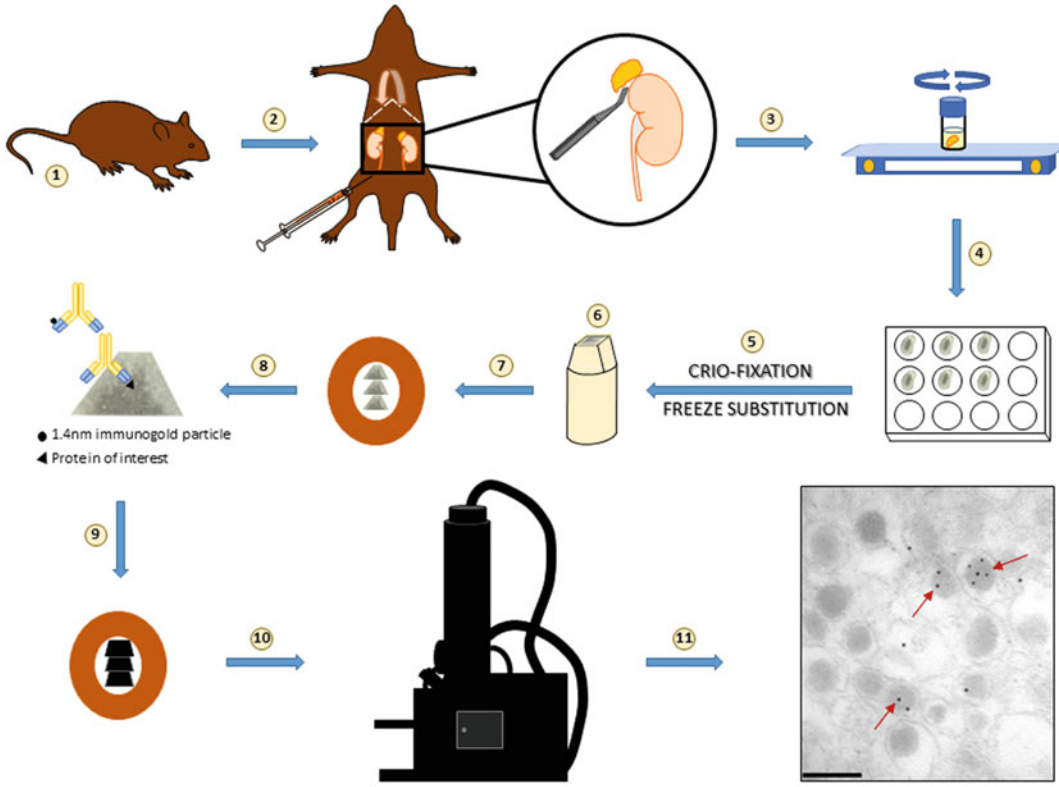

Fig. 3 Flowchart of the post-embedding immunogold technique. Schematic drawing of the various procedural steps of the post-embedding immunogold method from fixation of samples to visualization at the TEM. (1) Experimental animal; (2) perfusion fixation and dissection of adrenal gland; (3) washing in 0.1-M PB and cryoprotection in 2-M sucrose; (4) adrenal gland sectioning in 300-μm think sections; (5) cryofixation in Leica EM CPC machine and freeze-substitution in Leica AFS machine; (6) ultrathin sectioning (80–000 nm) of Lowicryl HM20 resin blocks using an ultramicrotome; (7) collection of adrenal gland ultrathin sections on single slot pioloform-coated nickel grids; (8) incubation in primary antibody, wash in TBS and incubation in secondary antibody; (9) counterstaining with uranyl acetate and lead citrate; (10) visualization of immunolabeled sections and analysis using a TEM; and (11) immunolabeling using post-embedding immunogold. Mouse adrenal medullary chromaffin cells immunolabeled for chromogranin A (20 nm gold) with monoclonal anti-mouse CGA antibody. CGA immunoreactivity is localized in the central region of the secretory granules. *Scale bar*: 200 nm

signaling molecules has revealed with the post-embedding method than under pre-embedding conditions [1]. However, this is the only reliable method to localize antigens present at cellular compartments with high density of proteins (*see* Fig. 3) because the entire cut length of biological membranes is uniformly exposed to the antibodies [1, 3, 6]. In addition, the post-embedding immunogold offers the opportunity to co-label multiple proteins in the same sections using secondary antibodies conjugated with gold particles of different sizes and offers a more accurate quantification [4, 6]. In conclusion, these two methods have advantages and

disadvantages but can provide complementary information about the subcellular localization of any specific antigen in the adrenal gland.

We describe here two protocols. One protocol involves a pre-embedding immunogold procedure on vibratome sections of fixed tissue. A second protocol involves a post-embedding immunogold procedure on vibratome sections of fixed tissue, but labeling step is performed on ultrathin sections. We have previously used these protocols to characterize the subcellular localization of several proteins in different organs and tissues. The procedures described here can be used to any biological molecule involved in adrenal functions.

2 Materials

Always use ultrapure deionized water to prepare solutions. Prepare and store reagents at room temperature, unless otherwise indicated. Always wear protective clothing and gloves. Follow waste disposal regulations when disposing waste materials.

2.1 Buffers

We used four buffers: 0.1-M phosphate (PB) and 0.05-M Tris (TB) buffers and their saline version, PBS and TBS, respectively.

1. *0.1-M phosphate buffer, pH 7.4.* Phosphate buffer consists of monobasic sodium phosphate (NaH_2PO_4) and dibasic sodium phosphate (Na_2HPO_4). The weight of each component will vary depending on the waters of hydration. The pH can be adjusted to 7.4 by mixing the two components in the appropriate amounts.

   Stock solution of 0.2-M sodium phosphate buffer (PB), pH 7.4. To prepare 1 L, combine 35.6 g of $Na_2HPO_4{\cdot}2H_2O$ and 31.2 g $NaH_2PO_4{\cdot}2H_2O$, each at 0.2 M, in the ratio 4:1. Add few drops of 1-M sodium hydroxide (NaOH) in distilled water to adjust pH. This stock solution can be stored at 4 °C for several weeks. Dilute equal volumes of the 0.2-M PB stock solution with distilled water to prepare 0.1-M PB (pH 7.4).
2. *0.1-M phosphate-buffered saline, pH 7.4.* PBS is prepared by mixing 0.9% NaCl with 0.1-M PB.
3. *0.05-M Tris buffer, pH 7.4.* Weight 6.61-g Trizma HCl and 0.97-g Trizma Base and dissolve them in 1000 mL of distilled water.
4. *0.05-M Tris-buffered saline, pH 7.4.* TBS is prepared by mixing 0.9% NaCl with the stock solution of 0.05 M TB. TBS can be stored at 4 °C for several weeks.

2.2 Tissue and Fixation

Adrenal gland requires fixation before performing pre-embedding immunohistochemistry. This fixation step is necessary to preserve antigenicity and ultrastructure of the gland. The choice of fixative, whose function is cross-linking the macromolecules to lock the tissue structures in place, affects both structural preservation and antigenicity. Because good preservation of antigenicity differs from optimal conditions for good ultrastructural preservation, the degree of fixation requires a compromise between obtaining the best possible immunolabeling and minimal disruption of ultrastructure. For this purpose, a mixture of paraformaldehyde (4%) and a low concentration of glutaraldehyde (0.05–0.5%) are recommended for immunogold electron microscopy in adrenal glands.

1. Anesthesia of animals (Nembutal or ketamine–xylazine 1:1, 0.1 mL/kg b.w.). Diligently follow the protocols approved by your local Animal Care and Use Committee. The care and handling of animals prior to and during the experimental procedures should be in accordance with national and international regulations.
2. Buffers: (a) 0.2-M PB, pH 7.4, and (b) 0.1-M PB, pH 7.4.
3. Paraformaldehyde (PFA). PFA is supplied as powder and is very toxic in contact with skin, by inhalation, and if it is swallowed.
4. Glutaraldehyde (EM grade). Glutaraldehyde supplied as a 25% aqueous solution is also very toxic. Store at 4 °C in a separate drawer from other reagents.
5. Fixative solution: 4% paraformaldehyde and 0.05% glutaraldehyde in 0.1-M PB, pH 7.4. Freshly prepared is needed.

   Dissolve 40 g of paraformaldehyde in 300 mL of distilled water, make up to 500 mL with distilled water, filter, and add 500-mL 0.2-M PB and 2 mL of 25% glutaraldehyde. Adjust pH to 7.4. Safety note: all these steps should be carried out in a fume hood. If the amount of glutaraldehyde in this fixative solution needs to be higher than 0.05%, add the right amount of 25% glutaraldehyde accordingly. Always wear protective clothing and gloves and handle in a fume hood.
6. Peristaltic pump.
7. Needle (20 gauge).
8. Small scissors, fine scissors, clamps, and tweezers.

2.3 Sectioning of the Adrenal Gland

There are several procedures to cut the adrenal gland. However, some of them require cryoprotection and freezing of the adrenal gland for sectioning, and they are not recommended for immunoelectron microscopy due to the formation of very large ice crystals. The most appropriate procedure is cutting at room temperature or 4 °C immediately after fixation using a vibrating microtome. Thus, the immunohistochemical techniques will be performed using free-floating sections (around 50–70 μm thickness).

1. Vibrating microtome.
2. Double-edge stainless steel razor blades.
3. Instant glue.
4. Buffer: 0.1-M PB, pH 7.4.
5. 24-well culture plate.
6. Paintbrush (size 0–1) to transfer sections.

2.4 Membrane Permeabilization

To enhance the penetration of immunoreagents and favor accessibility to antigens after fixation, the partial disruption of plasma membrane is recommended by incubating the sections with the detergent Triton X-100, which dissolves part of the lipid bilayer of membranes, or using freeze-thawing, which produces small ice crystals that mechanically disrupts the plasma membranes.

1. Buffers: (a) 0.05-M TBS, pH 7.4, and (b) 0.1-M PB, pH 7.4.
2. Blocking solution: 10% normal goat serum in TBS containing 0.05% Triton X-100.
3. Sucrose. Prepare cryoprotectant solutions: (1) 10% sucrose in 0.1-M PB; (2) 30% sucrose in 0.1-M PB.
4. Liquid nitrogen, stored in Dewar flask.

2.5 Cryofixation

This step could be carried out in unfixed brain as an alternative or in combination with chemical fixation. Major aims of cryofixation are to immobilize molecules and stop metabolic activities in the cell (*see* **Note 1**).

1. Freezing apparatus (Leica EM CPC or a similar equipment).
2. Buffer: 0.1-M PB, pH 7.4.
3. Cryoprotectant solutions: 1-M and 2-M sucrose in 0.1-M PB.
4. Liquid nitrogen.
5. Paintbrush (size 0–1) to transfer sections.

2.6 Freeze-Substitution

Following cryofixation, samples of adrenal gland must be transferred to the freeze-substitution unit. During freeze-substitution, water within the frozen samples is gradually substituted with pure methanol at −80 °C, and then brain sections are gradually warmed and embedded in acrylic resin (*see* **Note 2**). Even though adrenal gland may have been previously chemically fixed by perfusion, the freeze-substitution step reduces the harmful effects that the dehydration and embedding reagents have on antigenicity preservation.

1. Automatic freeze-substitution machine (AFS Leica or a similar equipment).
2. Dry absolute methanol.
3. Liquid nitrogen.

4. 0.5% uranyl acetate in dry absolute methanol.

   Prepare at least 30 min before use and enwrapped the bottle of flask with aluminum foil during preparation to avoid precipitation produced by light. Filter before use. This is a very toxic solution, so always wear protective clothing and gloves and handle in a fume hood.

5. Lowicryl HM20 resin.

   Lowicryl HM20 resin has three components: cross-linker-D, monomer E, and initiator C. The resin is prepared by weighing 2.98 g of cross-linker D and 17.02 g of monomer E and mixing gently by bubbling a continuous stream of dry nitrogen gas into the mixture with a disposable glass pipette. Add 0.1 g of initiator C to the final solution and mix again gently in the same way. Humidity will interfere with the polymerization of the resin. All are toxic reagents, so avoid inhaling the vapors from the Lowicryl resin, wear protective clothing and gloves, and use a well-ventilated fume hood when missing the three components of the resin.

2.7 Pre-Embedding Immunohistochemistry

1. Buffers: (a) 0.1-M PB, pH 7.4; (b) 0.1-M PBS, pH 7.4; (c) 0.05-M TB, pH 7.4; (d) 0.05-M TBS, pH 7.4.
2. Shaker.
3. Refrigerator.
4. Primary antibodies (*see* **Note 3**).
5. Blocking solution: Normal serum (*see* **Note 4**).
6. Biotinylated secondary antibodies: working dilution of 1:200 in TBS.
7. Secondary antibodies conjugated to 1.4-nm gold particles: working dilution of 1:100 in TBS.
8. Avidin–biotin–peroxidase complex (ABC).
9. 3.3′-Diaminobenzidine tetrahydrochloride (DAB): 0.05% in TB. Maintain in darkness because this solution is light sensitive.
10. Hydrogen peroxide: working solution of 1% in distilled water to give a final concentration of 0.01%.
11. Glutaraldehyde: 1% in 0.1 M PB. This is a very toxic solution, so always wear protective clothing and gloves and handle in a fume hood.
12. HQ Silver intensification kit. Store the HQ silver kit, composed of three solutions, in the freezer at −20 °C. To allow melting of the different solutions in this kit, take it out of the freezer 2 h before use and maintain at room temperature in a dark place.

2.8 Post-Embedding Immunohistochemistry

All immunohistochemical reactions are performed on ultrathin sections (70–100 nm-thick) from Lowicryl resin-embedded tissue blocks, collected on pioloform-coated single slot nickel grids.

1. Buffers: (a) 0.05-M TBS, pH 7.4; (b) TBS containing 0.1% Triton X-100 (TBST).
2. Blocking solution: Human serum albumin (HSA; supplied as powder). Working solution of 2% HSA in TBST. Can be stored at 4 °C.
3. Monoclonal or polyclonal primary antibodies.
4. Secondary antibodies conjugated to 10-nm colloidal gold particles (*see* **Note 5**).
5. Uranyl acetate: 40–60 μL of a saturated solution in distilled water. Filter before use.

2.9 Processing for Electron Microscopy in Pre-Embedding Immunohistochemistry

1. Buffer: 0.1-M PB, pH 7.4.
2. Osmium tetroxide (OsO_4): 1% in 0.1-M PB, pH 7.4 (*see* **Note 6**). Very toxic and volatile, so always wear protective clothing and gloves and handle in a fume hood.
3. 1% Uranyl acetate in ultrapure deionized water. The incubation of sections from adrenal gland with uranyl acetate improves contrast when ultrathin sections are examined at the transmission electron microscope. Protect from light to prevent the formation of uranyl acetate precipitates during incubation. This is a very toxic solution, so always wear protective clothing and gloves and handle in a fume hood.
4. Graded series of ethanol in water (50%, 70%, 90%, 95%, and 100%) for dehydration.
5. Dry absolute ethanol: absolute ethanol with anhydrous cupric sulfate.
6. Propylene oxide. It is very toxic in contact with skin, by inhalation, and if swallowed. Volatile and flammable. Do not wear protective gloves, as this substance will dissolve them, and handle in a fume hood.
7. Epoxy resin: Durcupan ACM.

   This resin type facilitates flat-embedding (*see* below) of the samples on slides. Durcupan consists of four components: component A (epoxy resin), component B (hardener), component C (accelerator), and component D. *The four components have a long shelf life if bottles are properly closed and stored in a dry place.*

   Weight 10 g of component A, 10 g of component B, 0.3 g of component D, and 0.3 g of component C in a disposable plastic beaker. Always follow the sequence of A:B:D:C. Mix thoroughly with a disposable plastic pipette. Bubbles will form during the mixing step, but they will rise to the surface in a few

minutes and will disappear. If large amount of epoxy resin is required, follow the ratio 10:10:0.3:0.3 g of A:B:D:C, respectively. Resin waste should be collected in a disposable beaker and allowed to polymerize at 60 °C for 24 h, before disposal. Always wear protective clothing and gloves and handle in a fume hood.

8. Oven (temperature range up to 200 °C) to polymerize the epoxy resin.
9. Adhesive labels.
10. Paintbrush or toothpick.
11. Glass slides and coverslips.
12. Polyethylene molds for embedding samples for electron microscopy.

2.10 Ultrathin Sectioning

Tissue blocks of epoxy resins and Lowicryl resins will section easily. However, if the Lowicryl resin is not properly polymerized, sectioning becomes difficult, and the resulting sections can break up during the immunohistochemical steps.

1. Ultramicrotome.
2. Diamond knife.
3. Glass knifemaker.
4. Glass knives.
5. Pioloform-coated single slot copper grids.
6. Forceps to handle grids.
7. Grid storage box.

2.11 Staining of Ultrathin Sections

Ultrathin sections usually need to be counterstained using heavy metal solutions to improve their contrast. This is particularly important for the tissue processed by cryofixation and freeze-substitution and embedded in Lowicryl HM20, which exhibit low contrast when visualized using the transmission electron microscope. The most commonly used stain is Reynold's lead citrate.

1. Lead citrate. Weight 0.133-g lead nitrate and 0.176-g tri-sodium citrate, add 4.8 mL of double distilled water, and shake vigorously to dissolve. Next, add the tri-sodium citrate, shake gently until a milky suspension is formed, and add 0.2-mL 4-M NaOH and mix well until the solution becomes totally clear. Sodium carbonate is formed when the lead citrate solution is exposed to air. Therefore, transfer the solution to a 10-mL glass bottle with a screw cap for storage, and wrap it with aluminum foil. Lead citrate solution. Store at 4 °C. Wear protective gloves.
2. Sodium hydroxide pellets.
3. Laboratory film (e.g., Parafilm).

3 Methods

3.1 Tissue and Fixation

1. Fix the adrenal gland by perfusion fixation of the animal (*see* **Note 7**).
2. Set up peristaltic pump. Place open end of tubing into the beaker of saline and fixative solution (in ice). Avoid air bubbles in the tubes. The volume of fixative solution should be scaled to size of animal.
3. Perform deep anesthesia of the animal by intraperitoneal injection of ketamine-xylazine 1:1 (0.1 mL/kg b.w.). Wait a few minutes for anesthesia to produce effect, indicated by the loss of reflex responses. Pinch the toes of the animal to judge the level of response to painful stimuli.
4. Place the animal on its back on a Styrofoam board and pin out all four limbs at the feet using small needles.
5. Cut the skin just below the diaphragm with small scissors to expose the liver. Cut the ribs laterally, bend the chest backward, and fix it with a clamp to allow easy access to the heart. Once the chest is opened, the animal can no longer breathe, and lack of oxygen (anoxia) causes poor preservation of the ultrastructure and may compromise antigenicity. Therefore, all following steps should be carried out as quickly as possible.
6. Remove any excess adipose or connective tissue from the heart. Separate the thymus with a small spatula and make sure the ascending aorta is visible.
7. Make a small cut in the left ventricle using fine scissors.
8. Insert a blunt needle connected to the end of the tubing into the left ventricle. Secure needle by clamping in place near the point of entry into the heart and turn on the peristaltic pump. Then immediately cut the right atrium using fine scissors.
9. Perfuse the animal with saline for 1 min. At this point, switch to the fixative solution and continue perfusion for 15 min. Check tail and neck flexibility as good indicators of how well the animal is being fixed; a well-fixed animal should have a stiff tail and neck.
10. Turn off the peristaltic pump. The animal should be stiff at this point. Cut the adrenal gland and wash in 0.1-M PB, pH 7.4.
11. After perfusion is completed, the animal carcass should be wrapped and placed in a plastic bag in a freezer, until properly disposed of in the animal housing facility.
12. Wash the adrenal gland thoroughly in 0.1-M PB, for 2 h, before sectioning.

3.2 Sectioning of the Adrenal Gland

1. Mount and stick the adrenal gland on the vibratome's specimen holder, using fast glue.
2. Fill the vibratome reservoir with 0.1-M PB and cut 50- to 70-μm thick sections (*see* **Note 8**).
3. Collect the sections with a brush and place each section in a well of the 24-well plate containing PB.
4. Store sections in 0.1-M PB, at 4 °C.

3.3 Membrane Permeabilization

3.3.1 Freeze-Thaw

1. Once tissue blocks containing brain areas of interest have been obtained after perfusion-fixation, place them in 10% sucrose in 0.1-M PB and shake gently until tissue blocks sink.
2. Place tissue blocks in 30% sucrose in 0.1-M PB and shake gently until they sink.
3. Drain off the excess sucrose and place the tissue blocks in an empty plastic beaker.
4. Drop the beaker quickly into liquid nitrogen without full submersion, so the tissue blocks are in contact with the liquid nitrogen through the wall of the beaker. Allow the tissue blocks to freeze completely, and immediately let the blocks thaw in 0.1-M PB, at room temperature.
5. Wash the tissue blocks twice with 0.1-M PB, for 15 min each.
6. Section tissue blocks in a vibrating microtome (*see* Subheading 3.2).

3.3.2 Detergent Treatment: Triton X-100

1. Blocking solution.
2. Incubate sections and shake gently for 1 h, at room temperature.
3. Wash the sections four times with TBS, for 15 min each.

3.4 Cryofixation

1. Wash freshly fixed tissue four times for 15 min each in 0.1-M PB, pH 7.4.
2. Place sections (400 μm thickness, cut with a vibratome) in cryoprotectant solutions of 1-M sucrose, until they sink, and then in 2-M sucrose, overnight at 4 °C (*see* **Note 9**).
3. Switch on Leica EM CPC and fill dewars with liquid N_2. Carry out the slam freezing of the sections, following manufacturer's instructions.

3.5 Freeze-Substitution

1. Fill the freeze-substitution machine with liquid nitrogen.
2. Choose the appropriate settings (time and temperature) for the different steps. In order to program and to operate the machine, follow the manufacturer's instructions.

3. Place all the holders and substitution media into the machine to reach the working temperature and wait until the machine has equilibrated −80 °C.
4. Place frozen sections in the chamber of the freeze-substitution machine. All following steps are carried out in this machine.
5. Place sections in 0.5% uranyl acetate in dry absolute methanol at −80 °C overnight.
6. Wash four times for 2 h each with dry absolute methanol at −80 °C.
7. Warm from −80 °C to −50 °C at 10 °C/h in the AFS machine in the evening.
8. Resin infiltration: infiltrate with a mixture of dry methanol/Lowicryl HM20 (1:1) for 2 h.
9. Change to a mixture of dry methanol/Lowicryl HM20 (1:2) for 2 h.
10. Infiltrate in pure Lowicryl HM20 for 2 h. Leave in pure Lowicryl HM20 overnight at −50 °C.
11. Embedding process: transfer the sections into freshly prepared Lowicryl HM20 resin in embedding molds at −50 °C.
12. Start UV light polymerization for 48 h at −50 °C.
13. Warm from −50 °C to 18 °C at 10 °C/h under continuous UV irradiation and continue UV polymerization at 18 °C for 24 h.
14. Remove the tissue blocks from molds, label blocks, and store them at room temperature.

3.6 Pre-Embedding Immunogold

1. Wash sections three times with 0.1-M PB, for 15 min each, to remove any excess of fixative and once with TBS, for 30 min.
2. Block nonspecific binding by incubating sections with blocking solution consisting of TBS containing 10% normal serum, for 1 h.
3. Remove the blocking solution and replace it with primary antibody diluted in TBS containing 1% normal serum, at 4 °C, for 12–24 h.
4. Wash the sections four times with TBS, for 15 min each.
5. Incubate the sections with 1.4-nm gold compound-conjugated secondary antibody (use at 1:100 dilution) in TBS containing 1% normal serum, at room temperature, for 2 h.
6. Wash the sections four times with TBS, for 15 min each, and once with PB, for 15 min.
7. Postfix the sections with 1% (w/v) glutaraldehyde in PB, at room temperature, for 10 min.

8. Remove the glutaraldehyde solution and wash the sections three times with PB, for 10 min each, followed by two washes in Milli-Q water, for 10 min each.
9. Prepare the silver intensification solution immediately before use by mixing equal volumes of the three reagents (components A, B, and C) from the HQ Silver enhancement kit, in a dark room, at room temperature.
10. Place the sections in silver intensification solution at room temperature, for 6–8 min, in the dark (*see* **Note 10**).
11. Remove the silver intensification solution and stop reaction with Milli-Q water.
12. Wash the sections four times in Milli-Q water, for 5 min each, in the dark. Although reaction stops with washing, the silver-enhanced slices may continue to darken during washing and storage. Therefore, do not store, and process sections for electron microscopy as soon as possible.

3.7 Post-Embedding Immunogold

1. Place grids, sections down, on drops of filtered blocking solution (2% HSA in TBST) for 30 min at room temperature.
2. Place grids in drops of primary antibody in filtered TBST with 2% HSA at 27 °C overnight (*see* **Note 11**).
3. Wash grids three times for 15 min each with TBST. To do the first wash, pick up each grid with forceps and dip it in three small vials of filtered TBST. Excess buffer is dried off the forceps and grids with filter paper. The second and third washes are performed on drops of filtered TBST.
4. Place grids in drops of 2% HSA in TBST for 10 min at room temperature.
5. Place grids in drops of 10-nm gold-conjugated secondary antibody (*see* **Note 12**) diluted 1:10 in TBST with 2% HSA for 2 h at room temperature.
6. Wash grids four times for 10 min each in TBS. For the first wash, pick up each grid and dip it in three small vials of filtered TBS. The second, third, and fourth washes are performed on drops of filtered TBS.
7. Let grids dry at room temperature.

3.8 Processing Sections for Electron Microscopy

1. Wash the sections three times with 0.1-M PB, for 15 min each.
2. Postfix the sections with 1% osmium tetroxide in 0.1-M PB, for 30 min (*see* **Note 13**).
3. Wash the sections five times with 0.1-M PB, for 8–10 min each, to remove all traces of osmium and then wash once with distilled water, for 8–10 min.
4. Stain with 1% uranyl acetate solution in distilled water, for 30 min.

5. Dehydrate the sections with 50%, 70%, 90%, 95%, and 100% ethanol, for 10–15 min each, and then 100% dry ethanol, for 10–15 min.
6. Incubate with propylene oxide twice, for 10–15 min each. Use glass pipettes, as propylene oxide dissolves plastic pipettes.
7. Infiltrate in epoxy resin (e.g., Durcupan) for 4 h and then proceed with flat-embedding (*see* **Note 14**).
8. Polymerize the resin by heating in an oven, at 60 °C, for 48 h.
9. With the unused epoxy resin, fill the polyethylene molds (capsules) up to the top and place in an oven for polymerization, at 60 °C, for 24 h.

3.9 Ultrathin Sectioning of Pre-Embedding Reactions

1. Remove the coverslip. Observe the sections with a stereomicroscope and choose the brain region of interest.
2. Trim the area of interest by making four small cuts in the section using a scalpel. The small sample will detach from the slide.
3. Take one block of resin polymerized in the polyethylene capsules. Stick the small sample on the tip of the resin block with fast glue, and let dry for 10–15 min.
4. In an ultramicrotome, trim the sample on the resin block with a single-edge razor blade.
5. Fit the block into the ultramicrotome and align the block face with a glass knife.
6. Remove the empty resin from the top of the sample using a glass knife. Then change to a diamond knife.
7. Cut ultrathin sections (60–80 nm thickness) with the ultramicrotome.
8. Collect short ribbons of sections on pioloform-coated slot grids and let dry. Store the grids in a grid box.

3.10 Staining of Ultrathin Sections

1. Prepare the lead citrate solution (*see* Subheading 2.8).
2. Take a plastic or glass Petri dish with a piece of laboratory film and place a few sodium hydroxide pellets in one of the sides.
3. Draw up the lead citrate solution into a Pasteur pipette, placing individual drops on the laboratory film.
4. Place grids with ultrathin sections onto the drops of the lead citrate solution. Leave for 1.5–3 min.
5. Wash the grids three times in double distilled water, for several seconds each.
6. Blot the bottom of the grid with filter paper and then allow grids to dry at room temperature. Place grids in a grid box.
7. Examine sections with a transmission electron microscope.

4 Notes

1. Several cryofixation techniques can be used: slam freezing, plunge freezing, propane jet freezing, and high-pressure freezing. In all procedures, the freezing must achieve very rapid cooling rates to minimize damage to the sample caused by ice crystal formation. To ensure high-quality preservation of adrenal gland tissue, we recommend cryofixation with slam freezing in combination with freeze-substitution and Lowicryl resin embedding. Currently, high-pressure freezing is considered as the most reliable method of cryofixation and can also be combined with freeze-substitution.
2. The most widely used resins to detect most antigens using post-embedding immunogold techniques are acrylic resins, particularly Lowicryls; epoxy resins are not often used for these approaches because heating is required for resin polymerization, thus compromising the detection of the epitopes. Lowicryl resin is a hydrophilic acryl resin having a low viscosity that is an advantage to infiltrate into the tissue. It is a low-temperature cured resin that can be polymerized at −50 °C under UV irradiation, thus minimizing the loss of antigenicity during embedding. There are four variants of Lowicryl resins (K4M, HM20, K11M, and HM23) that differ in their hydrophobic and hydrophilic properties and the temperature at which they freeze.
3. Using a primary antibody that is specific and works with good efficiency for immunogold electron microscopic techniques is maybe the most critical step. Many primary antibodies work well when used for immunoblotting or immunocytochemistry at the light microscopic level. However, this may not be the case when using the same antibody on tissue prepared for electron microscopy. When testing out primary antibodies for the first time for immunoelectron microscopy, suitable positive and negative control tests should be performed. Positive controls involve the use of tissue known to contain the antigen of interest, while negative controls use tissue, tissues or cell types that do not to contain a given antigen.
4. The purpose of blocking solution is to prevent the secondary antibody from cross-reacting with endogenous immunoglobulins in the tissue. Many types of blocking solutions can be used, but the most widely used contain normal serum, which should be from the species in which the secondary antibody is raised.
5. When single labeling experiments are used for post-embedding immunogold, we recommend secondary antibodies conjugated to 10-nm colloidal gold particles. When double labeling

is required, also use secondary antibodies conjugated to either 5-nm or 15-nm colloidal gold particles. Please note that secondary antibodies conjugated to smaller gold particles yield higher immunogold labeling, and the higher the size of the gold particle, the lower the spatial resolution and efficiency. Therefore, be aware of this bias when performing double or triple labeling.

6. Osmium tetroxide is used as a secondary fixative following aldehyde fixation. The rate of penetration of osmium solution through the tissue is very slow to prevent artefacts; hence, it is used after aldehyde solution. For convenience and safety in the laboratory, aqueous solutions of osmium tetroxide in sealed 2-mL glass ampoules can be purchased. Osmium solutions should be disposed of properly. Post-embedding immunohistochemistry is an osmium-free protocol. The absence of osmium tetroxide treatment in the processing of the tissue embedded in acrylic resins results in poor preservation of membranes and low contrast for all the neuronal organelles.
7. The recommended fixation procedure for the adrenal gland is by perfusion fixation of animals because it yields very good morphology preservation. If this procedure cannot be carried out, fixation can be carried out by immersion placing the adrenal gland in a chemical bath that includes fixatives.
8. Sections thinner than 40 μm are difficult to handle with a paintbrush, and there is an increased risk that the tissue will break. Sections thicker than 100 μm are easy to handle but turn very dark after osmification, making it impossible to observe gross structure of the section in the light microscope. In our experience, a section of 50–70 μm is a good thickness, affording easy handling.
9. Cryoprotection step for freeze-substitution could be performed using either 2-M sucrose or by placing sections in 10%, 20%, or 30% glycerol in 0.1-M Tris-maleate buffer, pH 7.4, overnight. To use one or the other depends on the nature of the antigen. Therefore, we recommend doing trials to choose the best procedure.
10. Although there are several protocols for silver intensification, the HQ Silver intensification kit (Nanoprobes, Inc.; www.nanoprobes.com/) is one of the most widely used. It produces small silver particles that are approximately 20–40 nm in diameter. It is easy to use and prepared by thoroughly mixing equal volumes of three components (initiator, moderator, and activator). However, this kit is light sensitive, and all steps should be carried out in the dark. In addition, the silver intensification

reaction does not work efficiently at temperatures below 20 °C. At room temperature, the intensification process is quite fast, and it normally takes 6–8 min to achieve silver particles of good size. Longer periods of incubation yield very large silver particles, increasing the possibility of two or more independent silver particles fusing into a single larger particle. A series of different intensification times should be tested to determine the optimum size of the immunoparticles.

11. If double labeling is required, prepare a cocktail of the two primary antibodies raised in different species in filtered TBST with 2% HAS and place grids in drops of antibodies' solution at 27 °C overnight.
12. For double-labeling experiments, prepare a cocktail of the two secondary antibodies conjugated with 10-nm and 15-nm colloidal gold, both diluted 1:10 in TBST with 2% HSA for 2 h at room temperature. Adding polyethylene glycol (5 mg/mL), which dissolves lipids, to the final solution may facilitate the penetration of the colloidal gold secondary antibodies, thus improving immunolabeling in our ultrathin sections.
13. Avoid vigorous agitation because osmium tetroxide rapidly turns black sections and turns them rigid and fragile. Strong osmification and high OsO_4 concentrations may dissolve the silver deposited on the immunogold particles. To solve this problem, reduce osmification to 0.5% for 10–15 min, or prepare a new stock solution of 4% osmium tetroxide in distilled water.
14. To perform infiltration with epoxy resin, transfer the sections to aluminum boats using a paintbrush, add freshly prepared resin to each aluminum boat, and ensure that the sections remain fully immersed and do not float on the resin. For flat-embedding, use a toothpick to remove the sections very carefully from the aluminum boats and place them on a slide. Add a few drops of resin to the sections and ensure that they remain completely covered. Place a coverslip over the sections and remove any excess resin with filter paper.

Acknowledgments

This work was supported by the grants Spanish Ministerio de Economía y Competitividad (RTI2018-095812-B-I00) and the Junta de Comunidades de Castilla-La Mancha (SBPLY/17/180501/000229).

References

1. Luján R, Nusser Z, Roberts JDB, Shigemoto R, Somogyi P (1996) Perisynaptic location of metabotropic glutamate receptors mGluR1 and mGluR5 on dendrites and dendritic spines in the rat hippocampus. Eur J Neurosci 8:1488–1500
2. Luján R, Roberts JDB, Shigemoto R, Somogyi P (1997) Differential plasma membrane distribution of metabotropic glutamate receptors mGluR1α, mGluR2 and mGluR5, relative to neurotransmitter release sites. J Chem Neurochem 13:219–241
3. Luján R (2010) Organisation of potassium channels on the neuronal surface. J Chem Neuroanat 40:1–20
4. Polishchuk EV, Polishchuk RS (2019) Pre-embedding labeling for subcellular detection of molecules with electron microscopy. Tissue Cell 57:103–110
5. Luján R (2021) Pre-embedding methods for the localization of receptors and ion channels. In: Lujan R, Ciruela F (eds) Receptor and ion channel detection in the brain. Springer, New York, pp 223–242
6. Luján R, Watanabe M (2021) Post-embedding immunohistochemistry in the localization of receptors and ion channels. In: Lujan R, Ciruela F (eds) Receptor and ion channel detection in the brain. Springer, New York, pp 243–265

Chapter 6

Visualization of Exo- and Endocytosis Membrane Dynamics with Super-Resolution STED Microscopy

Chung Yu Chan, Sue Han, Xin Wang, Xiaoli Guo, and Ling-Gang Wu

Abstract

Recent advances in stimulated emission depletion (STED) microscopy offer an unparalleled avenue to study membrane dynamics of exo- and endocytosis, such as fusion pore opening, pore expansion, constriction, and closure, as well as the membrane transformation from flat-shaped to round-shaped vesicles in real time. Here we depict a method of using the state-of-the-art STED microscopy to image these membrane dynamics in bovine chromaffin cells. This method can potentially be applied to study other membrane structure dynamics in other cell model system.

Key words STED microscopy, Exocytosis, Endocytosis, Fusion pore

1 Introduction

Adrenal chromaffin cells are neuroendocrine cells containing catecholamine-laden large dense-core vesicles (LDCVs) in the medulla of adrenal glands in mammals. They release catecholamines and mediate fight or flight response, a sympathetic nervous system response [1–3]. Upon arrival of the sympathetic nerve firing, LDCVs fuse with the plasma membrane in a process called exocytosis. This synchronized process contains multiple steps (docking, priming, and fusion) and is tightly mediated and regulated by factors such as calcium, SNARE complex, and other exocytotic molecules [4–10]. After exocytosis, the vesicles are retrieved and recycled in a process termed endocytosis [11–14]. Therefore, real-time visualization of the membrane dynamics of exo- and endocytosis in chromaffin cells will provide valuable insights into these two fundamental processes.

One of the methods that allow direct visualization of the processes would be through light microscopy. For the past decade, many super-resolution imaging techniques have emerged which are able to break the diffraction limit of light established by Ernst Abbé

Ricardo Borges (ed.), *Chromaffin Cells: Methods and Protocols*,
Methods in Molecular Biology, vol. 2565, https://doi.org/10.1007/978-1-0716-2671-9_6,

more than 100 years ago. These technological advancements provide an opportunity for researchers to real-time monitor biological objects of size <100 nm and hence better understand chromaffin cell function [15, 16]. Among those super-resolution techniques, stimulated emission depletion (STED) microscopy is well suited to study the membrane dynamics of exo-endocytosis in chromaffin cells owing to its high spatiotemporal resolution and multicolor capabilities [15–18]. STED microscopy employs specific optics to generate a donut-shaped depletion laser beam and overlaps this onto the excitation laser beam. The center of the donut (non-depleted region) is usually 20–50 nm in diameter [15, 19]. Hence, the fluorophores at donut-shaped area of the excitation region will be depleted, while the fluorophores in the center of the donut can still emit light, allowing features closer than the diffraction limit to be separated [17, 18, 20]. Recently, STED lateral resolution has improved to ~30 nm while the axial resolution is ~100 nm [20]. Nowadays, many studies related to exo-endocytosis have been carried out in STED microscopy [4, 21–26].

In this book chapter, a detailed protocol will be provided to guide individual to visualize exo- and endocytosis in chromaffin cells with STED microscopy in a reproducible manner.

2 Materials

All solutions are prepared using ultrapure deionized water (18 MΩ-cm at 25 °C, Millipore) and are stored at room temperature unless mentioned otherwise. Prepare all solutions fresh.

2.1 Primary Culture of Bovine Adrenal Chromaffin Cells

1. Locke's solution at pH 7.3 (*see* Table 1): Weigh 8.465-g NaCl, 0.403-g KCl, 0.305-g Na_2HPO_4, 0.102-g NaH_2PO_4, 1.008-g glucose, and 2.382-g HEPES and transfer them to a 5-L glass beaker. Add water to a volume of 900 mL. Add magnetic bar and mix them on magnetic stirrer. Adjust pH with 5-N NaOH. Make up to 1-L final solution with water (*see* **Note 1**). Filter the solution with 0.22 μm pore vacuum filter system into a 500-mL sterile storage bottle (*see* **Note 2**). Store at 4 °C.
2. Collagenase solution (*see* Table 2): Weigh 45-mg collagenase P, 150-mg Bovine serum albumin, and 9.75-mg trypsin inhibitor and transfer them to a 50-mL conical tube. Add Locke's solution to a total volume of 30 mL (*see* **Note 3**).
3. Cell culture medium: Add 50 mL of Fetal bovine serum (FBS) to 450 mL of DMEM to make 10% FBS in DMEM solution. Aliquot in a 50-mL conical tube and pre-warm the amount that is needed for the cell culture at 37 °C water bath. Store the remaining tubes at 4 °C (*see* **Note 4**).

Table 1
Final concentrations of chemical compounds in Locke's solution

Chemical	Final concentration (mM)
NaCl	145
KCl	5.4
Na_2HPO_4	2.2
NaH_2PO_4	0.9
Glucose	5.6
HEPES	10

Table 2
Final concentrations of chemical compounds in collagenase solution

Chemical	Final concentration (mg/mL)
Collagenase P	1.5
Bovine serum albumin	5
Trypsin inhibitor	0.325

4. Fresh bovine adrenal glands from 21- to 27-month-old adult bovine (*see* Subheading 3.1 for more details).

2.2 Bovine Chromaffin Cells Transfection

1. DNA plasmids of interest: Maxi-prep the plasmids of interest with high quality (*see* **Note 5**).
2. Nucleofector transfection solution (commercially available, Lonza).
3. 10% FBS in DMEM solution (as described above).
4. 25-mm diameter, #1.5 thickness, sterilized poly-D-Lysine and laminin-coated coverslips in 35-mm cell culture dishes.

2.3 Stimulated Emission Depletion (STED) Microscopy

1. Bath solution at pH 7.2 (*see* Table 3): Weigh 1.826-g NaCl, 0.084-g KCl, 0.826-g TEA, 0.45-g glucose, and 0.596-g HEPES and transfer them to a 1-L beaker. Add 1 mL of $MgCl_2$ (2 M) and 5 mL of $CaCl_2$ (2 M) solutions to the beaker. Add water to a total volume of 250 mL. Adjust the pH to 7.2 with 5-N NaOH. Filter the solution with 0.22 μm pore vacuum filter system into a 500-mL sterile storage bottle. Store the solution at 4 °C until use (*see* **Note 6**).
2. A532 solution (30 μM): Dissolve Atto 532 (Atto-tec) in DMSO to make a 1-mM stock solution according to the manufacturer suggestion. Dilute the 1-mM Atto 532 solution to 30 μM by adding 18 μL of 1-mM Atto 532 solution to 600 μL of bath solution.

Table 3
Final concentrations of chemical compounds in Locke's solution

Chemical	Final concentration (mM)
NaCl	125
KCl	4.5
Tetraethylammonium chloride (TEA)	20
Glucose	10
HEPES	10
$MgCl_2$ (2 M)	1
$CaCl_2$ (2 M)	5

3 Methods

Perform all the following procedures in a tissue culture hood unless otherwise specified. All the solutions are loaded from a syringe passes through a 0.22-μm syringe filter before reaching the glands.

3.1 Primary Culture of Bovine Adrenal Chromaffin Cells

1. Obtain at least four fresh bovine adrenal glands from a nearby slaughterhouse. Transport the glands back to the lab in pre-chilled Locke's solution on ice (*see* **Note 7**).
2. Pick complete and intact adrenal glands for the culture. Trim the surrounding tissue and fat of the glands (*see* Fig. 1a).
3. Clean the glands by perfusing with Locke's solution to remove the blood inside the glands (*see* Fig. 1b) (*see* **Note 8**).
4. After the blood is removed, inject the glands with collagenase solution and incubate them at 37 °C water bath in a glass container for 10 min (*see* **Note 9**).
5. Repeat **step 4** with fresh collagenase solution.
6. Dissect the glands longitudinally with a sterile scissor. Collect the digested medulla (cream color) in 50-mL Locke's solution (*see* Fig. 1c). Any other material (red or purple) that contains cortical cells are discarded.
7. Mince the medulla materials in Locke's solution with a small scissor (*see* Fig. 1d). Pipette the materials up and down ten times with a 50-mL serological pipette.
8. Filter the materials through a 100-μm nylon mesh.

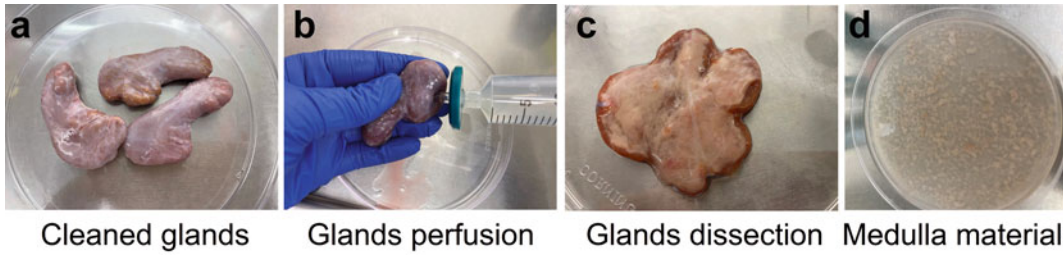

Fig. 1 Work flow for primary culture of bovine adrenal chromaffin cells. (**a**) Clean and intact bovine adrenal glands after fat and connecting tissues removed. (**b**) Procedure to perfuse the glands with Locke's solution or collagenase solution. (**c**) Longitudinally dissected glands after digestion showing the medulla materials. (**d**) Minced medulla materials in Locke's solution

9. Collect the filtrate in a 50-mL conical tube and then centrifuge at 50 × *g* for 5 min with supernatant discarded. Resuspend the cell pellet in 20-mL Locke's solution (*see* **Note 10**).
10. Repeat **step 9** until the supernatant is clear. Flow the cell suspension through a 100-μm cell strainer and add fresh Locke's solution to a final volume of 40 mL.
11. Centrifuge at 50 × *g* for 5 min with supernatant discarded. Resuspend the cell pellet in 20-mL 10% FBS in DMEM solution.
12. Count the cell number in a hemocytometer.

3.2 Bovine Chromaffin Cells Transfection

To fluorescently labeled protein of interest for STED microscopy, chromaffin cells are transiently transfected by electroporation. As an example, we describe below the transfection of phospholipase Cδ1 PH domain tagged with mNeonGreen (mNG) (PH–mNG) [22], which binds specifically to phosphatidylinositol-4,5-bisphosphate (PIP2) that labels the plasma membrane. Other plasmids can also be transfected using the same method. For illustration purpose, the procedures of using the Basic Primary Neurons Nucleofector Kit from Lonza are described. Other equivalent electroporation system can also be used according to the manufacturer's protocol.

1. For a 100-μL reaction, around 3×10^6 cells are used per each reaction.
2. Centrifuge 3×10^6 bovine chromaffin cells prepared from the previous section at 50 × *g* for 2 min and discard the supernatant.
3. Resuspend the cell pellet carefully in 100-μL Nucleofector transfection solution.
4. Add 3 μg of PH–mNG plasmid to the cell suspension. The amount of different plasmids can be varied depending on the experimental condition.

5. Transfer the cell suspension into the Nucleofector cuvette and put the cuvette into the Nucleofector™ 2b device or equivalent equipment (*see* **Note 11**).
6. Choose program O-005 from the list and electroporate the cells.
7. Add 1.8 mL 10% FBS in DMEM solution (pre-warmed at 37 °C water bath) immediately to the cuvette. Gently mix the cell suspension with the medium.
8. Transfer 300 μL of cell suspension onto each 25-mm diameter, #1.5 thickness, sterilized poly-D-Lysine and laminin-coated coverslips in 35-mm cell culture dishes (*see* **Note 12**).
9. Incubate the cells at 37 °C with 9% CO_2 for 1 h. Add 2 mL pre-warmed 10% FBS in DMEM to each dish (*see* **Note 13**). Continue to incubate the cells at 37 °C with 9% CO_2.
10. Image the cells within 5 days.

3.3 Stimulated Emission Depletion (STED) Microscopy

The protocol described below is specifically for Leica TCS SP8 STED 3X microscope. Procedures for other commercially available STED microscope are varied. In general, the Leica system has a 100 × 1.4 N.A. HC PL APO CS2 oil immersion objective, white light laser source (WLL), and 592-nm and 775-nm STED depletion lasers. For simplicity, the protocol for imaging PH–mNG and A532 in 592 nm STED depletion is described.

1. Switch on the computer, controller, and the Leica TCS SP8 STED 3X microscope.
2. Open the Leica Application Suite X (LAS X) software.
3. Turn on the WLL and set to 80% laser power. Turn on 592 nm laser and set to 70% laser power. Allow for 30 min warmup time.
4. Use the "align STED beams" function in the LAS X software.
5. Get one dish of transfected chromaffin cells out from the incubator. Remove the coverslip from the dish with forceps and gently rinse it with bath solution.
6. Mount the coverslip onto a magnetic imaging chamber. Add 600 μL of 30-μM A532 bath solution to the coverslip.
7. Focus the cells on z direction with the microscope.
8. General settings for imaging parameters (*see* Table 4).
9. Specific settings for mNG/A532 combination in the software control: Excite mNG at 485 nm (5–10% of WLL) and the gain of the HyD detector (490–530 nm) is 20. Excite A532 at 540 nm (30% of WLL) and the gain of HyD detector (545–582 nm) is 100 (*see* **Note 14**). The gain for both

Table 4
Parameters settings in Leica TCS SP8 STED 3X microscope

Parameters	Settings
Scan mode	Many modes (e.g., xzy and xzt)
Scan direction	Uni- or bidirectional
Scan speed	8000 Hz
Image resolution	1248 × 1248 (xyt scanning) and 1248 × 150 (xzt scanning)
Pixel size	16 nm
Zoom	6.0×
Pinhole	0.5 AU (75.8 μm)
Filter	NF 445/594
HyD detector gating	1.0–6.5 ns

detectors can be adjusted based on the brightness of the fluorophores.

10. Set the 592 nm STED depletion laser power to 10% and 5% for mNG and A532, respectively.
11. Use the microscope to scan through the coverslip and find a healthy transfected chromaffin cell under bright-field with high fluorescence in epifluorescence (*see* **Note 15**).
12. Click "Live" in the software to focus to the area of interest. Click "Capture image" for a single image.
13. Click "Start" to acquire the image sequences series (xzy or xzt) (*see* Fig. 2).

3.4 STED Image Deconvolution

Huygens Professional is used because it contains software wizards that can allow users to restore images without being a specialist on image restoration and optical theory. It supports many file formats, and it can link to the LAS X software for file conversion thus facilitating the imaging processing [27].

1. Install Huygens Professional on a workstation computer.
2. Run Leica LAS X software and load the experimental data (file with *.lif).
3. Run Huygens Professional software and Export the data from LAS X to it.
4. Match the microscopic parameters (**step 8**, Subheading 3.3) from LAS X to the Huygens Professional.
5. Run "Deconvolution wizard" and choose the deconvolution parameters of each channel. Deconvolution can be done by

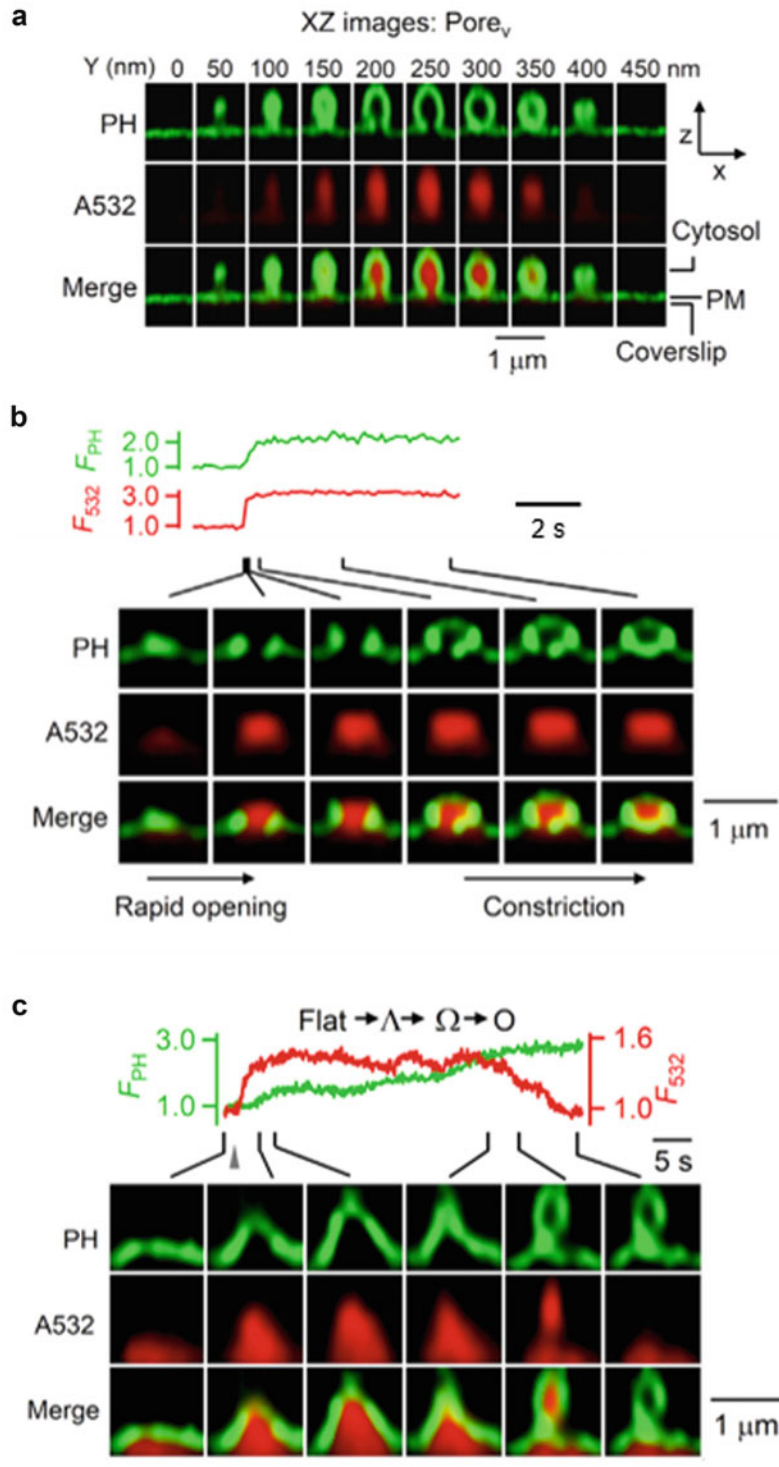

Fig. 2 STED images of vesicle structure, fusion pore closure, and endocytic transition. (**a**) STED images of PH–mNG and A532 showing a Ω-shape membrane profile with a visible pore at the XZ-plane at various Y-axis location as labeled. The Ω-profile was generated by vesicle fusion at the plasma membrane. Cytosol, plasma membrane (PM), and coverslip location are shown in the figure. (**b**) PH–mNG fluorescence (F_{PH}, normalized to baseline), A532 fluorescence (F_{532}, normalized to baseline), and sampled STED images showing fusion pore

using the preset parameters, but different parameters should be optimized until the deconvoluted images cannot be improved further. More tutorial details can be found on Huygens Professional website: (https://svi.nl/Huygens-Professional) [27].

6. After deconvolution, export the file back to LAS X. The deconvoluted images can now be further analyzed in LAS X or ImageJ.

4 Notes

1. Around 1 mL of 5-N NaOH is needed to increase the pH of the solution to 7.3. Add concentrated NaOH slowly during the pH measurement.
2. This filtering step is very critical to remove the contaminant and sterilize the solution.
3. Collagenase solution should be prepared fresh in a 50-mL conical tube immediately before starting dissection, as the enzymatic properties would deteriorate across the time.
4. The pH of the medium is important for cell culture. After preparation, immediately aliquot the medium into 50-mL conical tubes and seal the tube with parafilm, as it is often changed when it is in contact with air. Make fresh medium every week or every 2 weeks.
5. The concentration of the plasmids should be >1 μg/μL to avoid changing too much the total volume of the cell suspension, which in turn will affect the electroporation.
6. This filtering step is very critical to remove the contaminant and sterilize the solution. Check the osmolarity of the solution after adjusting pH to 7.2 with 5-N NaOH. It should be 300 ± 10 mOsm. If not, adjust the osmolarity using osmometer.
7. Transport the Locke's solution in a container topped with ice. This ensures the glands are kept on ice to minimize degradation.
8. The glands should swell a bit when the Locke's solution is being injected. Try not to use strong force as it may rupture the glands.

Fig. 2 (continued) opening and subsequent constriction. STED images were acquired every ~26–100 ms at the XZ-plane with Y-axis location fixed. (**c**) PH–mNG fluorescence (F_{PH}, normalized to baseline), A532 fluorescence (F_{532}, normalized to baseline), and sampled STED images showing an endocytic transition from flat shape to oval/round shape. STED images were acquired every ~26–100 ms at the XZ-plane with Y-axis location fixed. (Reproduced from refs. [24, 26] with permission from Elsevier)

9. Water bath instead of metallic bead thermal bath should be used as it can transfer heat to the glands more efficiently in a shorter time. The water level in the water bath is around half of the height of the container to avoid contamination.
10. Slow acceleration and deceleration should be used in centrifugation to prevent cell damage.
11. Avoid air bubbles when mixing or transferring cells to avoid cell damage.
12. Use only #1.5 thickness coverslips for STED imaging. Thinner coverslips would result in strong reflection.
13. Add culture medium drop by drop to avoid disturbance on seeded cells.
14. The detection range for the HyD detector close to the 592 nm depletion laser should be at least 10 nm from it to avoid the damage of the detector.
15. Lowest level of white light and epifluorescence should be used for cell searching to minimize fluorescence bleaching and phototoxicity to the cells.

Acknowledgments

This work was supported by the National Institute of Neurological Disorders and Stroke Intramural Research Program (ZIA NS003009-18 and ZIA NS003105-13 to L.G.W.).

References

1. Becherer U, Rettig J (2006) Vesicle pools, docking, priming, and release. Cell Tissue Res 326:393–407. https://doi.org/10.1007/s00441-006-0243-z
2. Stevens D, Schirra C, Becherer U, Rettig J (2011) Vesicle pools: lessons from adrenal chromaffin cells. Front Synaptic Neurosci 3:2. https://doi.org/10.3389/fnsyn.2011.00002
3. Kasai H, Takahashi N, Tokumaru H (2012) Distinct initial SNARE configurations underlying the diversity of exocytosis. Physiol Rev 92:1915–1964. https://doi.org/10.1152/physrev.00007.2012
4. López I, Ortiz JA, Villanueva J et al (2009) Vesicle motion and fusion are altered in chromaffin cells with increased SNARE cluster dynamics. Traffic 10:172–185. https://doi.org/10.1111/j.1600-0854.2008.00861.x
5. Südhof TC (2012) Calcium control of neurotransmitter release. Cold Spring Harb Perspect Biol 4:a011353. https://doi.org/10.1101/cshperspect.a011353
6. Rizo J, Südhof TC (2012) The membrane fusion enigma: SNAREs, Sec1/Munc18 proteins, and their accomplices—guilty as charged? Annu Rev Cell Dev Biol 28:279–308. https://doi.org/10.1146/annurev-cellbio-101011-155818
7. Villanueva J, Torregrosa-Hetland CJ, García-Martínez V et al (2012) The F-actin cortex in chromaffin granule dynamics and fusion: a minireview. J Mol Neurosci 48:323–327. https://doi.org/10.1007/s12031-012-9718-4
8. Abbineni PS, Axelrod D, Holz RW (2018) Visualization of expanding fusion pores in secretory cells. J Gen Physiol 150:1640–1646. https://doi.org/10.1085/jgp.201812186
9. Majdi S, Larsson A, Najafinobar N et al (2019) Extracellular ATP regulates the vesicular pore

opening in chromaffin cells and increases the fraction released during individual exocytosis events. ACS Chem Neurosci 10:2459–2466. https://doi.org/10.1021/acschemneuro.8b00722

10. Prasai B, Haber GJ, Strub M-P et al (2021) The nanoscale molecular morphology of docked exocytic dense-core vesicles in neuroendocrine cells. Nat Commun 12:3970. https://doi.org/10.1038/s41467-021-24167-9
11. Wu L-G, Hamid E, Shin W, Chiang H-C (2014) Exocytosis and endocytosis: modes, functions, and coupling mechanisms. Annu Rev Physiol 76:301–331. https://doi.org/10.1146/annurev-physiol-021113-170305
12. Kononenko NL, Haucke V (2015) Molecular mechanisms of presynaptic membrane retrieval and synaptic vesicle reformation. Neuron 85:484–496. https://doi.org/10.1016/j.neuron.2014.12.016
13. Gan Q, Watanabe S (2018) Synaptic vesicle endocytosis in different model systems. Front Cell Neurosci 12:171. https://doi.org/10.3389/fncel.2018.00171
14. Ferreira APA, Boucrot E (2018) Mechanisms of carrier formation during clathrin-independent endocytosis. Trends Cell Biol 28:188–200. https://doi.org/10.1016/j.tcb.2017.11.004
15. Bost A, Pasche M, Schirra C, Becherer U (2013) Super-resolution microscopy in studying neuroendocrine cell function. Front Neurosci 7:222. https://doi.org/10.3389/fnins.2013.00222
16. Riachy L, Ferrand T, Chasserot-Golaz S et al (2021) Advanced imaging approaches to reveal molecular mechanisms governing neuroendocrine secretion. Neuroendocrinology. https://doi.org/10.1159/000521457
17. Vicidomini G, Bianchini P, Diaspro A (2018) STED super-resolved microscopy. Nat Methods 15:173–182. https://doi.org/10.1038/nmeth.4593
18. Egner A, Geisler C, Siegmund R (2020) STED Nanoscopy. In: Salditt T, Egner A, Luke DR (eds) Nanoscale Photonic Imaging. Topics in Applied Physics, vol 134. Springer, Cham. https://doi.org/10.1007/978-3-030-34413-9_1
19. Rittweger E, Wildanger D, Hell SW (2009) Far-field fluorescence nanoscopy of diamond color centers by ground state depletion. EPL 86:14001. https://doi.org/10.1209/0295-5075/86/14001
20. Müller T, Schumann C, Kraegeloh A (2012) STED microscopy and its applications: new insights into cellular processes on the nanoscale. ChemPhysChem 13:1986–2000. https://doi.org/10.1002/cphc.201100986
21. Chiang H-C, Shin W, Zhao W-D et al (2014) Post-fusion structural changes and their roles in exocytosis and endocytosis of dense-core vesicles. Nat Commun 5:3356. https://doi.org/10.1038/ncomms4356
22. Zhao W-D, Hamid E, Shin W et al (2016) Hemi-fused structure mediates and controls fusion and fission in live cells. Nature 534:548–552. https://doi.org/10.1038/nature18598
23. Wen PJ, Grenklo S, Arpino G et al (2016) Actin dynamics provides membrane tension to merge fusing vesicles into the plasma membrane. Nat Commun 7:12604. https://doi.org/10.1038/ncomms12604
24. Shin W, Ge L, Arpino G et al (2018) Visualization of membrane pore in live cells reveals a dynamic-pore theory governing fusion and endocytosis. Cell 173:934–945. https://doi.org/10.1016/j.cell.2018.02.062
25. Shin W, Arpino G, Thiyagarajan S et al (2020) Vesicle shrinking and enlargement play opposing roles in the release of exocytotic contents. Cell Rep 30:421–431.e7. https://doi.org/10.1016/j.celrep.2019.12.044
26. Shin W, Wei L, Arpino G et al (2021) Preformed Ω-profile closure and kiss-and-run mediate endocytosis and diverse endocytic modes in neuroendocrine chromaffin cells. Neuron 109:3119–3134. https://doi.org/10.1016/j.neuron.2021.07.019
27. Huygens Professional | Scientific Volume Imaging. https://svi.nl/Huygens-Professional. Accessed 15 Jan 2022

Part II

Stimulus-Secretion Coupling

Chapter 7

Online Detection of Catecholamine Release from the Perfused Rat Adrenal Gland

Ricardo Borges, Ana De la Iglesia, and Antonio G. García

Abstract

Retrogradely perfused adrenal glands have historically served for establishing many of our current knowledge on the stimulus-secretion coupling process. Although the use of intact adrenals has largely been switched to isolated chromaffin cells, adrenal glands are still a very valuable tool to characterize physiological and pharmacological questions. Even more, this is an excellent preparation for studying the splanchnic nerve/chromaffin cell interaction. In this chapter, we will provide the ways to (i) perform retrograde perfusion of isolated rat adrenals, (ii) the method to apply electrical splanchnic nerve stimulation, and (iii) the preparation of adrenals to conduct online electrochemical detection of catecholamine release.

Key words Perfused adrenal gland, Catecholamine release, Electrochemical detection

1 Introduction

Adrenal medulla constitutes the inner portion of the adrenal gland. Its parenchyma is constituted mostly by chromaffin cells, which secrete catecholamines and other species to the blood stream in response to splanchnic nerve activation (which releases acetylcholine, PACAP, SP, VIP) or to stimulation with blood-carried secretagogues (histamine, bradykinin, angiotensin II, endothelins). Although secretion studies have been largely moved from intact glands to cultured chromaffin cells along the last decades, there are intrinsic advantages in the use of intact adrenals that cannot be studied in dissociated cells. Cultured cells are non-innervated and have lost their original polarity and are out from their physiological environment, thereby loosing paracrine interactions between chromaffin cells and their relationship with the cortex [1].

Perfused adrenals (cow, cat, rabbit, guinea pig, rat, and mouse) have been largely used since the early 1960s to clarify the basic mechanisms involved in the stimulus-secretion coupling process

Ricardo Borges (ed.), *Chromaffin Cells: Methods and Protocols*,
Methods in Molecular Biology, vol. 2565, https://doi.org/10.1007/978-1-0716-2671-9_7,

[2, 3], its regulation, and the contribution of receptors in the triggering and modulation of secretory responses [4–6].

The arrival of electrochemical detection allowed the online quantification of the secreted catecholamines thus increasing the time resolution over the tedious way of collecting samples and the poorer time resolution of biochemical analyses.

2 Materials

2.1 Rats

No special requirements are needed for strain, sex, or weight, although younger animals (200–250 g) are preferable, especially if electrical stimulation is required because they have less surrounding fat.

Animals are anaesthetized by intraperitoneal injection of 50-mg/kg sodium pentobarbital, dissolved in 1:5 ethanol: water.

2.2 Surgical Material

Please *see* Fig. 1.

1. Large scissors for cutting abdominal skin.
2. Large forceps with teeth for abdominal skin.
3. Hemostatic forceps.
4. Two 10-cm curved forceps.

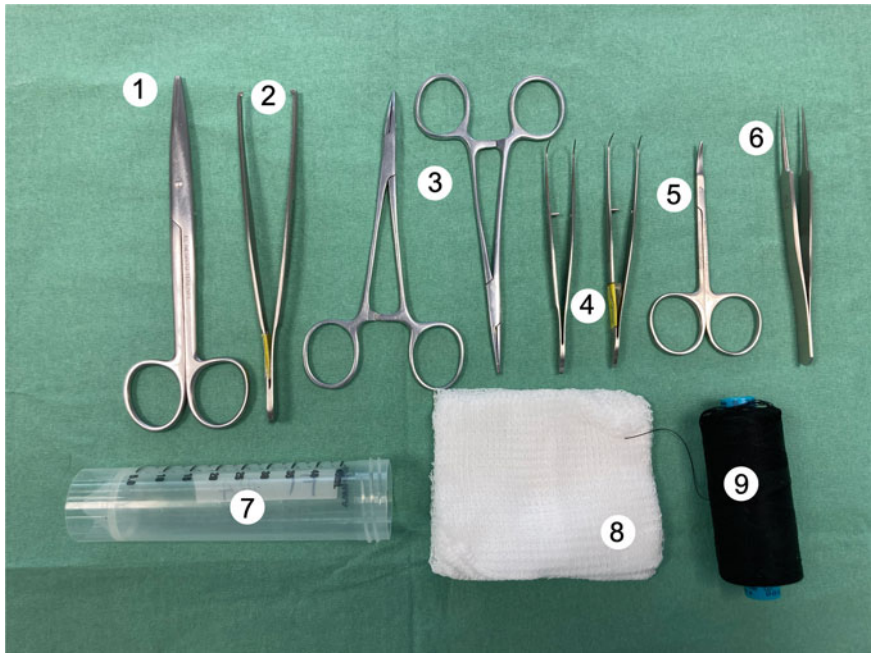

Fig. 1 Surgical material needed. (1) Large scissors for cutting abdominal skin. (2) Large forceps with teeth for abdominal skin. (3) Hemostatic forceps. (4) Two 10-cm curved forceps. (5) Surgical precision scissors (curved). (6) Fine tip forceps. (7) 50-mL Falcon-like tube. (8) Cotton gauzes. (9) Silk thread 4/0

5. Surgical precision scissors (curved).
6. Fine tip forceps.
7. 50-mL Falcon-like tube.
8. Cotton gauzes.
9. Silk thread 4/0.

2.3 Other Materials

1. Surgical table to fix the rat limbs with pins.
2. 2× 32G needle.
3. 2 × (4 cm) PE100 polyethylene tubing.
4. Oxygen or O_2 95%/CO_2 5% (carbogen) system for solutions bubbling.
5. Peristaltic (roller) pump and tubing (*see* **Note 1**).
6. Electrical stimulator (*see* **Note 2**).
7. Electronic valves (*see* **Note 3**).

2.4 Krebs-Bicarbonate Solution

Prepare 1 L of Krebs-bicarbonate solution: 119-mM NaCl, 5-mM KCl, 1-mM KPO_4H_2, 1.2-mM $MgSO_4$, 2-mM $CaCl_2$, 11-mM glucose, 25-mM $NaCO_3H$. The pH is stabilized by continuous bubbling with O_2 95%/CO_2 5% mixture (*see* **Note 4**).

3 Methods

3.1 General Setup

Set the peristaltic pump to 0.2 mL/min for the first minute of initial perfusion and then increase it to 1 mL/min during the stabilization and along the experiment. The full general setup (including electrochemical detection and sample collection) is described in Fig. 5.

3.2 Surgical Procedure

Anaesthetize the rat. Once it becomes asleep and the righting reflex is lost, test the deep of anesthesia by a limb punction. For the surgical procedure, please *see* Fig. 2.

1. Fix the animal to a surgical table.
2. Cut the abdomen skin along to the midline from the ilium bone to the xiphoid terminal of breastbone and expose the abdominal muscles.
3. Make an incision along the *linea albicans*.
4. Make two lateral excisions and, using both hemostatic forceps, open the abdomen exposing the intestines.
5. Place a 50-mL Falcon-like test tube behind the rat back to force lordosis.
6. Using the fingers move the intestines to your left and localize the left kidney.

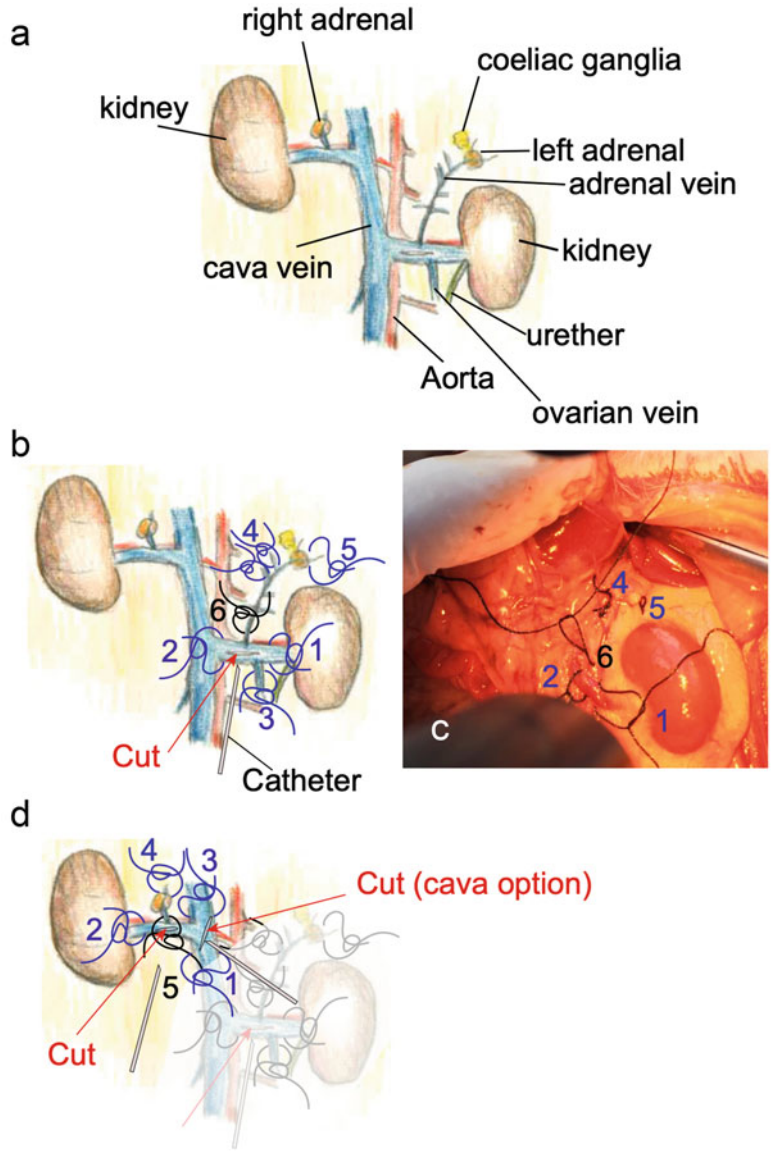

Fig. 2 Surgical procedure. (**a**) Anatomical description of adrenals and main vessels. (**b**) Thread locations for isolating the left adrenal. (**c**) Picture showing the location of thread ties. (**d**) Thread locations for isolating the right adrenal. Note the two options for placing the cuts depending on whether the right adrenal vein origin. Adrenal vein is subsidiary to the renal vein or directly onto the cava vein. For description see the text

7. *Left adrenal.* Using the curved forceps, carefully remove the retroperitoneal membrane over the renal vein and place ≈10 cm silk threads as indicated in Fig. 2b, c sequentially: proximal and distal renal vein and, if necessary, the ovarian/spermatic vein (1–3, do not tie these vessels yet). Pass threads

and tie the collaterals to adrenal vein (4) and the fat surrounding distal part of the adrenal gland. Carefully, pass a thread to the adrenal vein (5). Initiate the isolation procedure:

8. Tie the renal vein distal and proximal and, if necessary, the ovarian/spermatic vein.
9. With the curved scissors and fine tip forceps, make a 5-mm incision in the renal vein opposite to the point of adrenal vein arrival.
10. Carefully, dilate the adrenal vein by introducing one tip of the curved forceps.
11. Introduce the catheter along the adrenal vein to 2–3 mm of the adrenal; blood should flow through it.
12. Tie with two knots the thread to fix the catheter and extract the adrenal avoiding pulling the cannula.
13. Connect the gland to the perfusion system.
14. *Right adrenal*. The procedure is like that described for the left gland (*see* Fig. 2), even though right adrenal is more complex to perfuse as it is hidden under a liver lobule. The tricky procedure is to place a cotton gauze under the liver to create a wide surgical field. Sometimes, the adrenal vein goes directly to the ascending cava vein. In these occasions, the threads and incision have to be performed in the cava vein (cava option in Fig. 2d).

3.3 Perfusion

Set the peristaltic (roller) pump to 0.2 mL/min and connect the cannula (*see* **Note 1**). The gland should swell. Make two to three punches on the gland surface to facilitate the perfusate flow. Take care and avoid punching the adrenal vein; the color of the gland should change from red to light pink indicating good perfusion. Clean the surrounding fat and allow 20–30 min of stabilization.

The usual flow for a standard experiment is 1 mL/min although we have increased this to 3 mL without any apparent tissue damage.

In our hands, glands can still produce healthy secretory responses for over 6–8 h. It is crucial to avoid bubbles that may damage the tissue and promote artifact on electrochemical detection.

The secretory responses of glands can be analyzed by fluorescence or HPLC methods by collecting the effluent in test tubes. However, the use of electrochemical (amperometrical) detection offers several advantages mainly due to its high time-course resolution, which allows applying short and repetitive pulses of secretagogues [5].

3.4 Splanchnic Nerve Stimulation

Two major methods have been developed to stimulate the splanchnic branches, direct nerve stimulation of the major splanchnic nerve, or field (transmural) stimulation. Wakade's method was developed for collecting samples from an adrenal gland placed onto one of the electrodes and applying square pulses through an electrode in contact with the upper part of the gland [7].

As we use an electrochemical device for the online recording of catecholamine secretion, we have to place the glands in a perfusion hermetic chamber to use the silver spring electrodes for applying field electrical stimuli [8]; see below.

When electrical stimulation is intended to be coupled to electrochemical detection, the use of a stimulus isolated unit becomes mandatory in order to avoid passing current to the electrochemical cell. This equipment is inserted between the stimulator and the stimulating electrodes; its role is to provide a quasi-infinite resistance to ground (*see* **Note 5**). If you do not have this device, an alternative is intercalating an electrical isolation gap between the glands and the electrochemical cell (see a simple design in the inset of Fig. 5).

3.4.1 Electrical Stimulation Parameters

Electrical stimulation pulses can be directly applied to the splanchnic nerve by placing a bipolar electrode between the coeliac ganglia and the adrenal gland (*see* Fig. 2a). However, it becomes easier using the silver springs of the perfusion chamber (*see* Fig. 3) (*see* **Note 6**).

We can either perform stimulus–response curves by doubling the frequency or applying repetitive stimuli at a fixed frequency [8, 9].

The usual parameters are:

- Pulse duration 0.5–1 ms
- Frequency: 10–20 Hz
- Train duration: 1–10 s
- Train frequency: 1 every 5–10 min
- Voltage: supramaximal 30 (*see* **Note 7**)

3.5 Online Recording of Secretion

The system is an adaptation of the one initially developed for cat adrenals [10]. However, our current perfusion chamber for rat adrenals was designed to also warm the tissues [9]. Similar systems were also implemented in the labs of K. Kumakura [11] and A. Warashina [12].

In principle, any commercial electrochemical detector for HPLC can be used. We started employing the LC-4B from Bioanalytical Systems (West Lafayette, IN, USA) although those from Metrohm (791 VA or IC; Metrohm, Herisau, Switzerland) offers a large gain range. Currently, we have designed our own four-

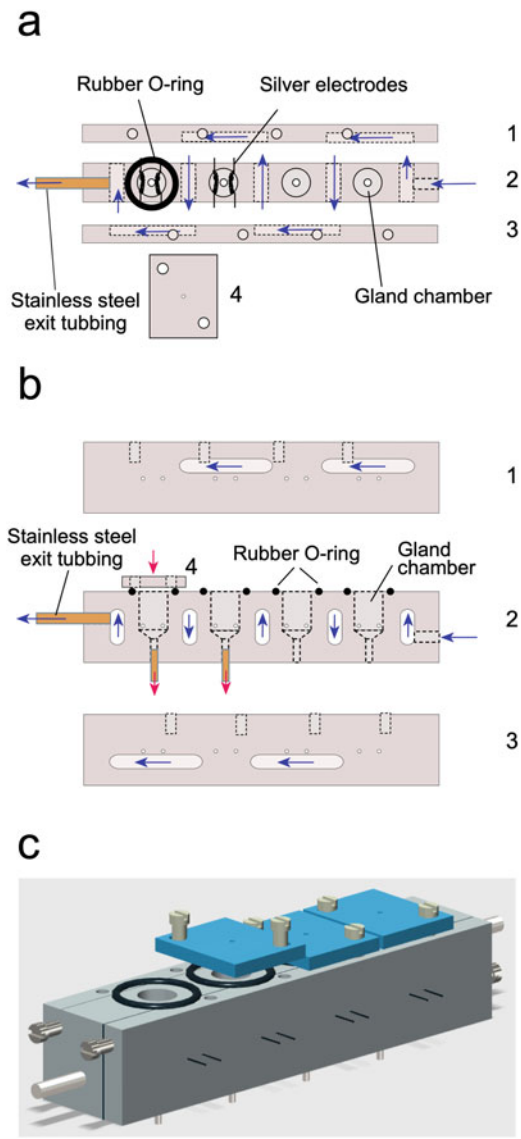

Fig. 3 Perfusion chamber for parallel online recording of secretory responses from rat adrenals. The chamber is built by drilling three methacrylate pieces (1, 2, and 3) that lately are glued to allow circulation of warm water (blue arrows). (**a**) *Upper view*. Each chamber incorporates a pair of spring silver wires to serve as bipolar field electrodes. Rubber O-rings are accommodated to circular grooves for hermetic seal of each chamber with the caps (4). Warm water enters (not shown) and leaves through stainless steel tubing placed at both ends. (**b**) *Side view*. The perfusion buffer is pumped through the chamber caps exiting from the bottom (red arrows). (**c**) *Perspective view*. Three-dimensional representation of the chamber. The chamber caps are fixed with two nylon screws. Notice the electrode connectors and the metal screws used for holding the chamber to brackets. For clarity reasons, not all elements are displayed

channel system (CANSTAT-4, Universidad de La Laguna, Spain) [13].

Analogical signal (voltage) is recorded using any commercial analogic/digital converter. We use a PowerLab (ADInstruments, Bella Vista, NSW, Australia) that, in addition to the analogical inputs, incorporates digital programmable outputs for triggering electronic valves or the fraction collector.

3.6 Perfusion Chamber Design

Figure 3 shows the construction of a four-channel perfusion chamber, which includes electrodes for transmural electrical stimulation and temperature control by circulating water. The chamber is built in methacrylate to allow the simultaneous perfusion of four adrenals in hermetic compartments.

The perfusion cannula of each gland is passed through the chamber cap (number 4 in Fig. 3) and sealed with nail varnish. Then the cannulas are connected to the perfusion system and the effluent drained to the electrochemical cells (*see* Fig. 4).

Application of secretagogues can be performed by different ways. For pulses of 20–30 s duration or over, the simplest system is to place a three-way valve (either manual or electronic) at the fluid entering in the peristaltic pump. However, because of drug dilution, this way is not desirably when shorter pulses are required. We can opt for a six-way valve with calibrated loop placed after the pump or implementing an electronic valve system, whose flow circuity is described in Fig. 4a, b. Figure 4c describes the electrical circuitry to manage and synchronize the valves from an external trigger (i.e., a TTL signal from a computer). This simple electronic circuitry can be implemented in a local electronic workshop. Indeed, any person with some abilities would be able to make it.

The advantage of using this system for delivering short pulses of secretagogues is somehow mimicking the physiological stimuli resulting from splanchnic nerve stimulation. We can apply highly concentrated drugs (i.e., acetylcholine 100 μM) for 3–5 s every 2 min. Fluid samples emanating from the glands are directed to electrochemical cells for online recordings and then can be also collected using a fraction collector with parallel collection capabilities. In our lab, we have designed a fraction collector coupled to the perfusion system. This equipment can be made in any lab as we provided all the STL files and parts description; its cost is of less than 100 $/€ [14]. In Fig. 5 we show the general view of the complete system.

In summary, the perfused isolated adrenal gland is still a very useful preparation for the study of the stimulus-secretion coupling in an environment that resembles the physiological conditions by preserving the cell-to-cell interactions and intact innervation. In the gland, chromaffins are distributed in acini of adrenergic and in acini of noradrenergic cells, which preserve electrical coupling through gap junctions. Also, cells maintain the polarity and their original collection of receptors, channels, and membrane transporters distributed along the cell. Also, the finely regulated

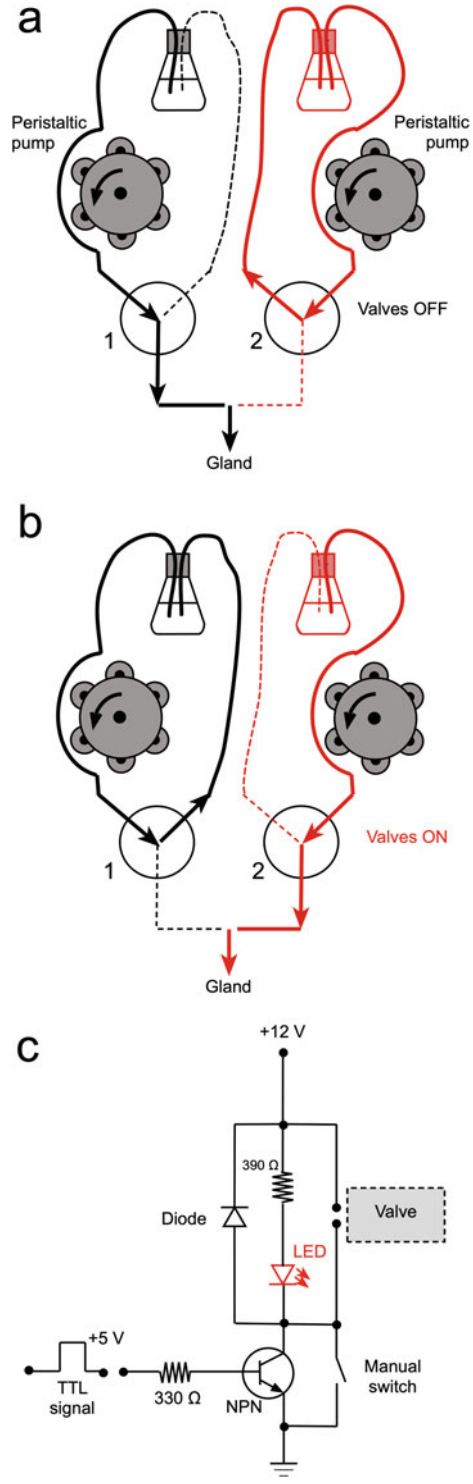

Fig. 4 Using three-way electronic valves for applying short chemical stimuli. Scheme shows the system for a single adrenal. Two channel of the peristaltic pump, two electronic valves, and one T connection are required. (**a**) Valve 1 delivers Krebs' solution (black arrows) to the gland when valve is OFF,

transduction mechanisms and enzymes expression have not been altered by isolation and cultured procedures.

4 Notes

1. Peristaltic (roller) pump. There are several commercially available eight-channel pumps. We use two four-channel pumps for perfusing four glands when the low-dead space system is required (*see* Fig. 4). Otherwise, a single four-channel roller pump is enough when this system is not necessary. It is advisable having at hand tubing and connectors:
   - Silicone tubing 3 × 1 mm (OD × ID) for roller pump and for connecting polyethylene tubing.
   - Barber fitting polypropylene connectors.
   - Polyethylene tubing. Any tubbing trademark can be used. As a guide, we use for liquid delivery (800/100/340/100) and (800/100/100) for gland cannulation both from Portex™ (Thermo Fisher Scientific).
2. Because of the salts present in the perfusion buffer, the tissue impedance (electrical resistance) is usually low. For this reason, it is important to use an electrical stimulator that can provide enough current to maintain the voltage, according to the Ohm's law. We should test it with an oscilloscope to assure voltage is maintained when the gland is present. There are several commercially available electrical stimulators. We use Grass stimulators although they are currently discontinued. We have developed our own digital eight-channel electrical stimulator for low impedance purposes.
3. Electronic valves (three-way). Any small- and low-volume valves can be used. As a guide, we use valves from Lee Co. (HDA1231115H) or its former equivalent version (LFA-A1201610H) (The Lee Company, Westbrook, CT, USA).

Fig. 4 (continued) whereas valve 2 returns the stimulating drug (red arrows) to reservoir. (**b**) When valves are *on*, the Krebs' solution is returned to the drug reservoir, whereas the secretagogue stimuli are directed to the gland. This system, created by Dr. Pedro Michelena (†), permits to apply short stimulation pulses (even of 1 s) allowing very reproducible repetitive responses as desensitization is drastically reduced. (**c**) Electronic circuit for manual or computer-driven stimuli. The NPN transistor is BD135; as protection diode, we use either 1N4148 or 1N4007; the red LED is placed in series with a 390 resistor. TTL (+5 V) is applied directly from an ADDA card

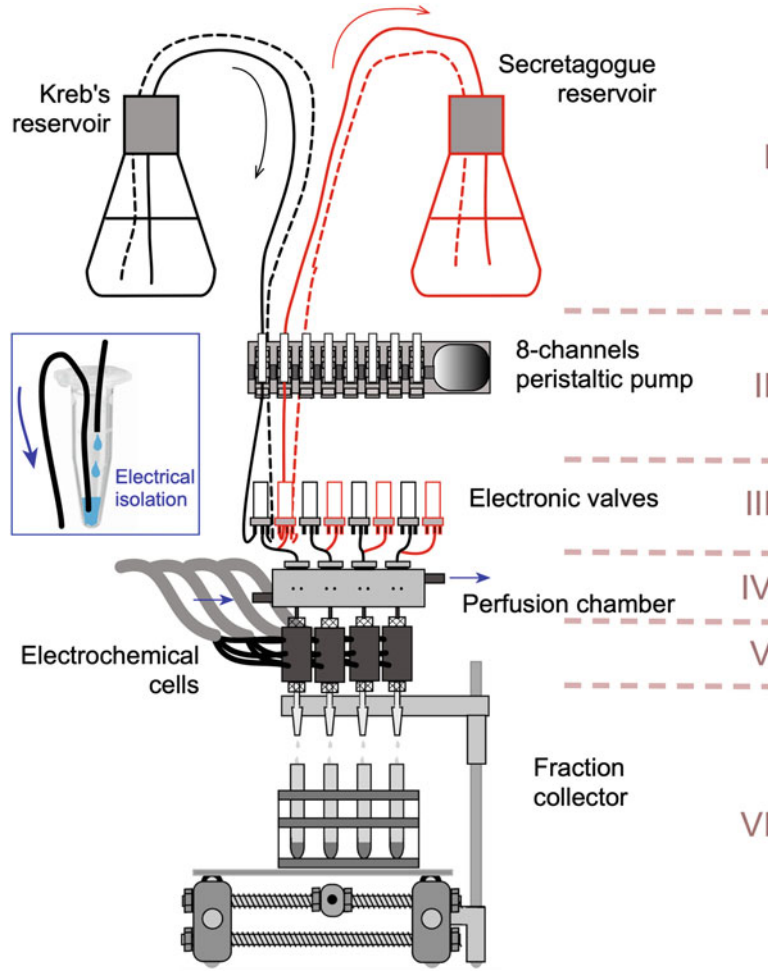

Fig. 5 General setup of our system for rat adrenals perfusion. The system comprises six stages: (**I**) buffer reservoirs for saline buffer (Krebs-bicarbonate solution and secretagogue); (**II**) peristaltic (roller) pump, eight channels are necessary for four glands; (**III**) eight electronic valves whose circuitry is described in Fig. 4—for clarity the tubing are only displayed for one gland; (**IV**) the perfusion chamber, as described in Fig. 3; (**V**) the electrochemical cells; and (**VI**) the fraction collector for parallel dripper. *Inset*, simple trick for providing electrical isolation to avoid passing current from stimulant electrodes to the electrochemical cell. This consists in placing two drills in a 5-mL Eppendorf-like tube and placing two tubing for allowing free dropping; it is important to seal the tubing entries through the cap to maintain the tube hermetic for keeping the dead volume to a minimum ≈100 μL

4. If for any reason bicarbonate/phosphate/sulfates cannot be used, the alternative is using Krebs-HEPES: 144-mM NaCl, 5-mM KCl, 1.2-mM $MgCl_2$, 2-mM $CaCl_2$, 11-mM glucose, 10-mM HEPES, pH 7.2–7.4 (NaOH).
5. A stimulus isolation unit is fairly simple. An analog input voltage is used to control a regulated current output. The current

output is uncoupled from the system ground. Therefore, current flows only between the two outputs of it and does not flow to ground or through the electrochemical detector. There are some commercially available devices also; these devices can also be made by a local electronic technician.

6. At least the moment when the system is implemented, it is important to test whether the electrical stimuli are promoting catecholamine release through splanchnic branches activation and not by direct chromaffin cell depolarization. This can be assessed by a cocktail of antagonist consisting in of 100 nM of atropine, mecamylamine, and naloxone. This cocktail should almost abolish the secretory responses, indicating that the secretory responses are truly due to stimulation of splanchnic nerve terminals.
7. To determine the supramaximal 30% voltage, we should perform some preliminary experiments by applying 5-s pulses at 10 Hz starting every minute from 10 V and then increasing by 10 V steps until no further increase in the release is observed; this is the maximal voltage; then increase it by 30%. This maneuver permits to obtain reproducible results without the problems caused by any drop in the impedance across the gland.

Acknowledgments

We are grateful to Mr. Barry Taylor (Formerly in King's College London) for designing and building the perfusion chamber described and also to the late Dr. Pedro Michelena for conceiving the valve system. Authors are grateful to all our researchers who have been working and bringing their experience with this technique. This work was supported in part by the Spanish Ministry of Science and Innovation (grants BFU2017-82618-P and PID2020-116589GB-100 to RB).

References

1. Borges R (1997) The rat adrenal gland in the study of the control of catecholamine secretion. Semin Cell Dev Biol 8:113–120
2. Douglas WW, Rubin RP (1961) The role of calcium in the secretory response of the adrenal medulla to acetylcholine. J Physiol 159:40–57
3. Garcia AG, Kirpekar SM, Prat JC (1975) A calcium ionophore stimulating the secretion of catecholamines from the cat adrenal. J Physiol 244:253–262. https://doi.org/10.1113/jphysiol.1975.sp010795
4. Borges R, Ballesta JJ, Garcia AG (1987) M2 muscarinoceptor-associated ionophore at the cat adrenal medulla. Biochem Biophys Res Commun 144:965–972
5. Borges R (1994) Histamine H1 receptor activation mediates the preferential release of adrenaline in the rat adrenal gland. Life Sci 54:631–640
6. Alvarez C, Lorenzo C, Santana F, Borges R (1997) Interaction between G protein-operated receptors eliciting secretion in rat adrenals. A possible role of protein kinase C. Biochem Pharmacol 53:317–325
7. Wakade AR (1981) Studies on secretion of catecholamines evoked by acetylcholine or

transmural stimulation of the rat adrenal gland. J Physiol 313:463–480

8. Alamo L, Garcìa AG, Borges R (1991) Electrically-evoked catecholamine release from cat adrenals. Role of cholinergic receptors. Biochem Pharmacol 42. https://doi.org/10.1016/0006-2952(91)90277-C
9. Santana F, Michelena P, Jaen R, Garcia AG, Borges R (1999) Calcium channel subtypes and exocytosis in chromaffin cells: a different view from the intact rat adrenal. Naunyn Schmiedeberg's Arch Pharmacol 360:33–37
10. Borges R, Sala F, Garcia AG (1986) Continuous monitoring of catecholamine release from perfused cat adrenals. J Neurosci Methods 16. https://doi.org/10.1016/0165-0270(86)90054-3
11. Kumakura K, Sato A, Suzuki H (1988) Direct recording of total catecholamine secretion from the adrenal gland in response to splanchnic nerve stimulation in rats. J Neurosci Methods 24:39–43
12. Warashina A, Fujiwara N (1991) Differential effects of protein kinase C activation on catecholamine secretions evoked by stimulations of various receptors in the rat adrenal medulla. Neurosci Lett 129:181–184
13. Gomez JF, Brioso MA, Delgado G, Borges R (2003) CANSTAT-4: a four channels potentiostat for the on-line monitoring of catecholamine secretion. In: Borges R, Gandia L (eds) Cell biology of chromaffin cell. Instituto Teófilo Hernando, La Laguna and Madrid, pp 281–285
14. Diaz D, De la Iglesia A, Barreto F, Borges R (2021) A DIY universal fraction collector. Anal Chem 93:9314–9318. https://doi.org/10.1021/acs.analchem.1c01519

Chapter 8

Real Time Recording of Perifused Chromaffin Cells

Ricardo de Pascual, Alicia Muñoz-Montero, and Luis Gandía

Abstract

Amperometry is an electrochemical method based on the oxidation or reduction of molecules. Many secretion products, including catecholamines, contain in their molecule chemical groups with the ability to yield (oxidize) or capture (reduce) electrons upon its exposure to an electrical field. In order to measure the secretion of catecholamines, they are oxidized at +650 mV with a carbon electrode, releasing every molecule of catecholamine that is oxidized two electrons (e^-) that are recorded as an electrical current. Amperometry is an easy-to-use and noninvasive technique for cells (unlike patch-clamp techniques for measuring membrane capacitance) and has been widely used to monitor online catecholamine release from perifused bovine chromaffin cell populations.

Key words Catecholamine release, Online amperometry recordings, Chromaffin cell

1 Introduction

During the decade of the 1960s, Aaron H. Anton and David F. Sayre devised an oxidation method for the analysis of catecholamines in biological fluids. In this method, collected samples were acidified with perchloric acid (PCA; 0.05 N), and then a daily-made solution containing ascorbic acid (0.11 M), ferrocyanide (76 mM), and a phosphate buffer at pH 7.3 was added. The entire procedure had to be performed in the dark in a cold environment. For the quantification of catecholamine content, samples were measured with a spectrofluorometer at an excitation wavelength of 395 and 505 nm of emission [1].

A decade later, Shellenberger and Gordon devised an alternative procedure for the oxidation and measurement of catecholamines in previously collected samples acidified with PCA 0.05 N. In this case, instead of oxidizing the samples with the ferrocyanide solution, they were oxidized with a 0.1 N iodine solution. Then fluorescence was measured at the 380 nm for excitation and 595 nm for emission [2]. This method was widely used to measure catecholamine release from intact adrenal glands (mouse, rat, cat,

Ricardo Borges (ed.), *Chromaffin Cells: Methods and Protocols*,
Methods in Molecular Biology, vol. 2565, https://doi.org/10.1007/978-1-0716-2671-9_8,

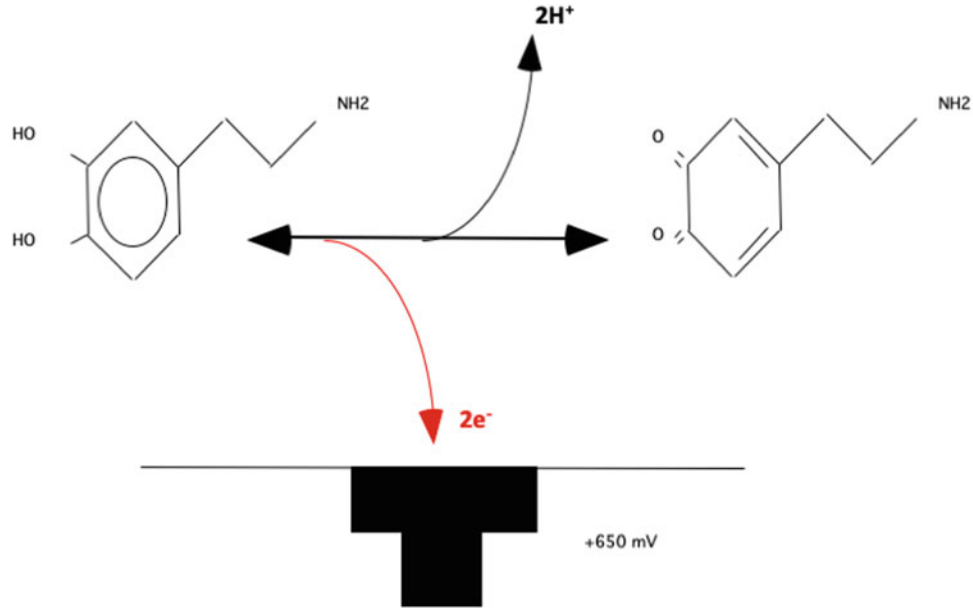

Fig. 1 Oxidation of catecholamines. Diagram of the oxidation of an adrenaline molecule (note how what is oxidized is the catechol ring of the molecule)

or bovine) superfused with the aid of a peristaltic pump and receiving different secretory stimulus [3–10].

In the 1980s, the amperometric technique was introduced to measure the secretion of catecholamines from superfused adrenal glands in real time [11–14]. In this method, catecholamines are oxidized at +650 mV with a carbon electrode, releasing two electrons (e^-) every oxidized molecule of catecholamine that are recorded as electrical current (*see* Fig. 1). This method has allowed the recording of the release of catecholamines on real time, increasing the time resolution and with a high sensitivity, thus facilitating the study of the exocytotic process and/or its modulation under different physiological or pharmacological conditions.

This method has been widely used within the last 30 years for the study of the exocytotic process of catecholamines either from intact adrenal glands (*see* Chapter 7 of this book) or from populations of isolated bovine chromaffin cells. One of the main advantages of this perifusion method is the possibility of applying repetitive pulses at short intervals minimizing the occurrence of desensitization of the secretory response, thanks to the possibility of applying brief stimuli (even as short as 1 s) to a cell population. In this chapter we will briefly describe the use of the amperometric technique to this aim.

2 Materials

2.1 General SetUp

The general setup of our system for the online amperometric recording of catecholamines secretion from perifused chromaffin cells is described in Fig. 2.

2.2 Krebs HEPES (KH) Solution

All solutions are prepared using ultrapure water (prepared by purifying deionized water, to attain a sensitivity of 18 MΩ-cm at 25 °C) and analytical grade reagents.

We usually prepare a KH(10×) stock solution without Ca^{2+}: 1440-mM NaCl, 12-mM $MgCl_2$, 59-mM KCl, 100-mM HEPES; pH 7.4 (NaOH).

For running experiments, we prepare KH(1×) solution, adding 11-mM glucose, and the desired amount of Ca^{2+} needed (usually 2 mM) for the specific experiment (we add Ca^{2+} using a 1-M stock solution of $CaCl_2$).

2.3 KH-35 mM K^+ (35K-KH)

We usually prepare a 35K-KH solution without Ca^{2+}: 114.9-mM NaCl, 1.2-mM $MgCl_2$, 35-mM KCl, 10-mM HEPES; pH 7.4 (NaOH).

For running experiments: add 11-mM glucose and the desired amount of Ca^{2+} needed (usually 2 mM) for the specific experiment (we add Ca^{2+} using a 1-M stock solution of $CaCl_2$).

2.4 KH-59 mM K^+ (59K-KH)

We usually prepare a 59K-KH solution without Ca^{2+}: 90.9-mM NaCl, 1.2-mM $MgCl_2$, 59-mM KCl, 10-mM HEPES; pH 7.4 (NaOH).

For running experiments: add 11-mM glucose and the desired amount of Ca^{2+} needed (usually 2 mM) for the specific experiment (we add Ca^{2+} using a 1-M stock solution of $CaCl_2$).

2.5 KH-70 mM K^+ (70K-KH)

We usually prepare a 70K-KH solution without Ca^{2+}: 79.9-mM NaCl, 1.2-mM $MgCl_2$, 70-mM KCl, 10-mM HEPES; pH 7.4 (NaOH).

For running experiments: add 11-mM glucose and the desired amount of Ca^{2+} needed (usually 2 mM) for the specific experiment (we add Ca^{2+} using a 1 M stock solution of $CaCl_2$) (i.e., 2 mL/L of a 1-M stock solution of $CaCl_2$ (110.98 g/L)).

2.6 KH-ACh

For the preparation of ACh containing solutions, we use KH(1×) solution, supplemented with 11-mM glucose, and the desired concentration of Ca^{2+} and ACh (30–100 μM; we add ACh from a 10^{-2}-M stock solution of acetylcholine).

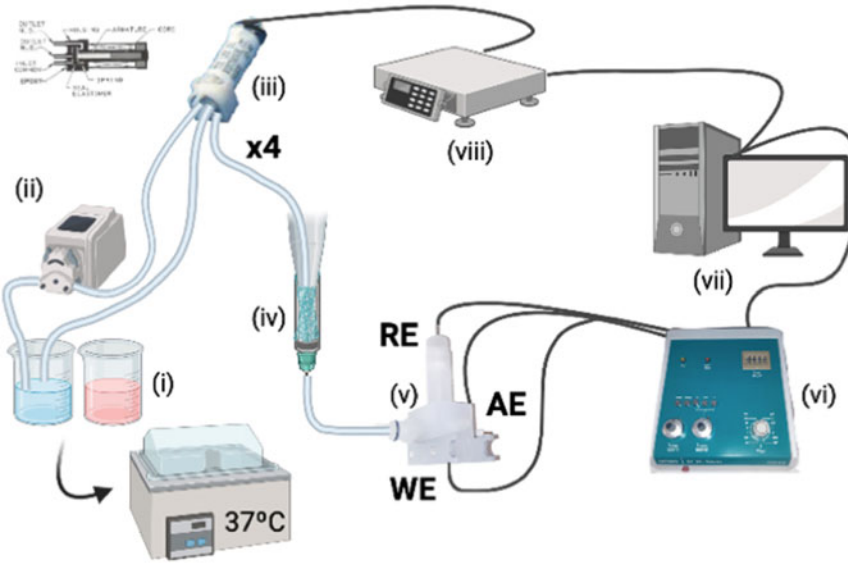

Fig. 2 Diagram of the general setup of our system for chromaffin cells perifusion (created with Biorender.com). The general setup of our system for the online amperometric recording of catecholamines secretion from perifused chromaffin cells comprises the following elements: (i) Reservoirs for saline buffer (Krebs–HEPES solution, experimental drugs and secretagogues). (ii) Peristaltic (roller) pump (four channels): Set the peristaltic pump to 2 mL/min. (iii) Electronic miniature solenoid valves (three-way): Because of the continuous flowing of the experimental solutions, we need to use three-way valves to direct the pumped solution to the cells or back to the reservoirs. Thus, when valves are not being activated, the pumped solution enters the valve through the "common inlet" and returns through the "normal close outlet" to the reservoirs. When activated (i.e., to deliver control KH or the stimuli to the cells), the pumped solution will exit through the "normal open outlet" of the valve and will reach the microchamber containing the cells. A homemade device with four polyethylene tubing is connected to the four valves and inserted into the microchamber with the cells leaving a death space as minimum as possible. (iv) Microchamber (200-μL volume): We use a homemade microchamber build with a 1-mL syringe (insulin type), cut by the 0.3-mL mark. Chamber must be filled with glass wool mesh to create a "filter" that will serve to trap the cells. (v) Electrochemical cell: Solutions emanating from the cell microchamber are directed to the electrochemical cell where the oxidation voltage (+650 mV) is applied between a working electrode (in our case carbon electrode) and the reference electrode to oxidize the released catecholamines. (vi) Electrochemical detector. In principle, any commercial electrochemical detector for HPLC can be used. We use a Metrohm (641VA, Metrohm, Herisau, Switzerland) that offers a large gain range. This electrochemical detector generates the oxidation voltage applied to the oxidation chamber and recording the oxidation current. (vii) Computer: It serves both for the generation of the stimulation protocols and/or the recording of amperometric signals. To that purpose, analogical signals (voltage) from the electrochemical detector are digitalized using any commercial analogic/digital converter. Analogical signal (voltage) is recorded using any commercial analogic/digital converter. We use a PowerLab (ADInstruments, Bella Vista, NSW, Australia) that, in addition to the analogical inputs, incorporates TTL programmable outputs for triggering electronic valves. (viii) Electronic valves controller: We use a homemade valve controller that provides 12 V signals to open the miniature valves. The controller includes an electronic device to permit the opening of a single valve simultaneously. Thus, only one type of solution (control KH, drug treatments, or stimuli) will reach the cells

3 Methods

3.1 Online Amperometric Recordings of Catecholamine Release from Cell Populations

In our experiments of real time recording of perifused chromaffin cells, we use bovine chromaffin cells isolated from adrenal glands obtained from a local slaughterhouse. Cells are isolated by enzymatic digestion of the adrenal medulla with collagenase following standard methods [15] with some modifications [16]. After isolation, the chromaffin cells are suspended in Dulbecco's Modified Eagle's Medium (DMEM) supplemented with 5% fetal bovine serum. For catecholamine release measurements in chromaffin cell populations, cells were plated on 5 cm diameter Petri dishes at 5×10^6 cells per dish. Cultures were maintained in an incubator at 37 °C in a water-saturated atmosphere with 5% CO_2. Cells were used 1–3 days after plating.

In our experiments, catecholamine secretion will be elicited by the application of brief (1–5 s) pulses of a secretagogue solution. We use two types of stimuli:

1. K^+-enriched KH solutions (with isosmotic reduction of NaCl). These solutions will induce the depolarization of chromaffin cells, thus inducing the direct opening of voltage-gated calcium channels. Calcium entering the cells though the different subtypes of calcium channels will induce the exocytotic process [17, 18].
2. Acetylcholine (ACh), the physiological neurotransmitter released at the splanchnic nerve–chromaffin cell synapse, that upon binding to nicotinic receptors in chromaffin cells induces a rapid membrane depolarization. This triggers action potentials that allow Ca^{2+} influx calcium channels.

To perform these experiments, we use the following protocol:

1. Carefully scrape off the cells (about 5×10^6 cells/dish) from the bottom of the Petri dish with a rubber policeman.

   Our experiments of amperometry in cell populations of bovine chromaffin cells are performed at physiological temperature (37 °C). We use cells from 1 to 3 days after culture.
2. Centrifuge at $120 \times g$ for 10 min.
3. Resuspend the cell pellet in 200 μL of KH solution.
4. Place the resuspended cells in a microchamber with glass wool (*see* **Note 1**).
5. Connect the microchamber to a perfusion pump with a flow rate of 2 mL/min, connected to a reservoir with KH solution (*see* **Notes 2** and **3**).
6. The liquid flowing from the perfusion microchamber has to be directed to the electrochemical detector placed just at the outlet of the microchamber.

The electrochemical detector monitors online the amount of catecholamines secreted under the amperometric mode, and the oxidation current is recorded on a PC computer at a sampling rate of 2 Hz.

7. Stimulate the cells to secrete catecholamines.

   To stimulate the cells, we use brief pulses of depolarizing solutions (i.e., KH solution containing 35, 59, or 70 mM K^+) or the physiological agonist ACh (i.e., KH solution containing 30 or 100 μM ACh).

   Stimulation solutions are applied through a homemade device with four perfusion tubes connected to three-way electronic valves that are electronically controlled to allow the opening of a single valve (i.e., control KH solution or stimulus solution).

   Duration (1–10 s) and frequency of secretory pulses (every 1, 3, or 5 min) are controlled by the recording software.

   This amperometric strategy allows the recording of reproducible catecholamine release responses during long time periods of 30–60 min. See, for instance, a representative example of a record obtained in an experiment of amperometric detection of catecholamines released by a population of bovine chromaffin cells in response to repeated 3 s pulses of ACh (100 μM) applied at 1 min intervals (*see* Fig. 3).

   Representative recordings of the experiments are pictured by importing the data in into the Origin 8.0 (MicroCal) or similar software.

In summary, the perifusion of chromaffin cell populations is a very useful preparation for the study of the stimulus-secretion coupling when using amperometric techniques to measure real time the exocytotic process.

4 Notes

1. Cells microchamber: we use a homemade microchamber of about 200 μL volume. To build this microchamber, we use a 1-mL syringe (insulin type) that is cut by the 0.3-mL mark (we use the tip part, to easily connect to the perfusion circuit). Chamber has to be filled with glass wool mesh (introduce an enough amount of glass wool in the syringe tip) and slightly press it with forceps to build a "filter" that will serve to trap the cells.

   As an alternative to glass wool, we use cigarette slim filters made of pure cellulose. These filters have a diameter of 6 mm and a length of 15 mm. We use a 5-mm piece inserted in the syringe tip.

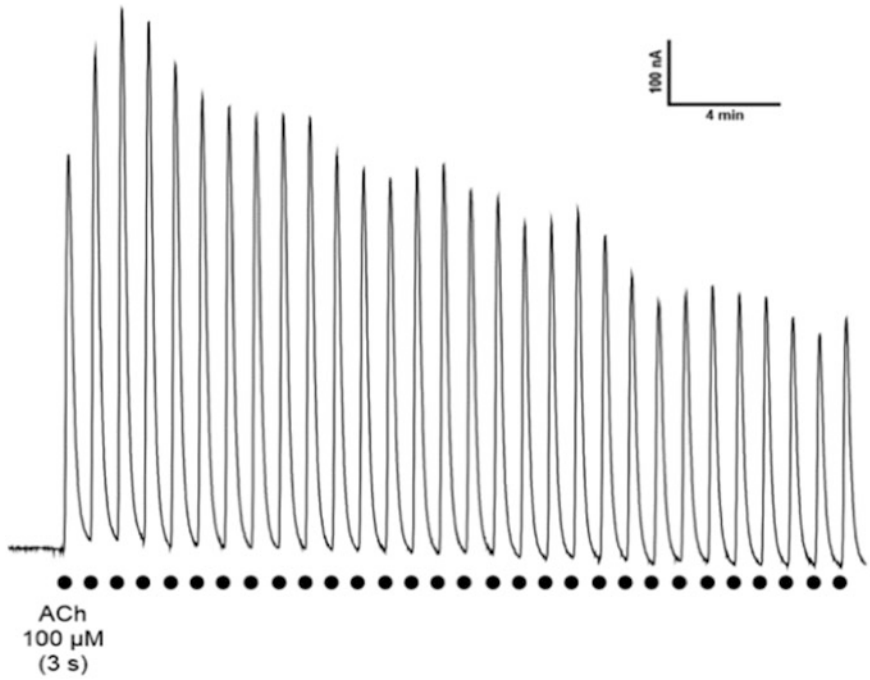

Fig. 3 Representative example of online detection of catecholamine release perifusion cells. In this experiment, bovine chromaffin cells (5×10^6 cells) were continuously perifused with a solution of KH containing 2 mM of Ca^{2+}. Catecholamine exocytosis was elicited by the application of repetitive 3 s pulses with a KH solution containing ACh (100 µM) applied at 1 min intervals

2. Peristaltic (roller) pump. There are several types of commercial pumps. We use one four-channel pump for perfusing up to four different solutions in our experiments (i.e., control KH, stimulus, drug treatments). Such solutions are continuously being pumped, and only one of them is directed to the microchamber containing the cells. This is done with the aid of three-way solenoid valves electronically controlled that can be activated to drive the solution flowing through the valve either to the microchamber or drive it back the solution reservoir. The opening of the corresponding valve is controlled by the recording software that permits that only one valve will be open.
3. Electronic valves (three-way). Any small- and low-volume valves can be used. As a guide, we use valves from Lee Co. (LFAA-A1201618H; The Lee Company, Westbrook, CT, USA).

Acknowledgments

This work was supported by Spanish Ministerio de Economía y Competitividad (MINECO), grant number SAF2017-78892-R. We also thank Instituto Fundación Teófilo Hernando for its continued support.

References

1. Anton AH, Sayre DF (1962) A study of the factors affecting the aluminum oxide-trihydroxyindole procedure for the analysis of catecholamines. J Pharmacol Exp Ther 138: 360–375
2. Shellenberger MK, Gordon JH (1971) A rapid, simplified procedure for simultaneous assay of norepinephrine, dopamine, and 5-hydroxytryptamine from discrete brain areas. Anal Biochem 39:356–372. https://doi.org/10.1016/0003-2697(71)90426-x
3. Garcia AG, Garcia-Lopez E, Horga JF, Kirpekar SM, Montiel C, Sanchez-Garcia P (1981) Potentiation of K^+-evoked catecholamine release in the cat adrenal gland treated with ouabain. Br J Pharmacol 74:673–680. https://doi.org/10.1111/j.1476-5381.1981.tb10478.x
4. Garcia AG, Sala F, Reig JA, Viniegra S, Frias J, Fonteriz R, Gandia L (1984) Dihydropyridine BAY-K-8644 activates chromaffin cell calcium channels. Nature 309:69–71. https://doi.org/10.1038/309069a0
5. Artalejo AR, Montiel C, Sanchez-Garcia P, Uceda G, Guantes JM, Garcia AG (1990) Alamethicin-evoked catecholamine release from cat adrenal glands. Biochem Biophys Res Commun 169:1204–1210. https://doi.org/10.1016/0006-291x(90)92024-t
6. Artalejo CR, Lopez MG, Moro MA, Castillo CF, de Pascual R, Garcia AG (1988) Voltage-dependence of nitrendipine provides direct evidence for dihydropyridine receptor coupling to calcium channels in intact cat adrenals. Biochem Biophys Res Commun 153:912–918. https://doi.org/10.1016/s0006-291x(88)81314-7
7. Gandia L, Michelena P, de Pascual R, Lopez MG, Garcia AG (1990) Different sensitivities to dihydropyridines of catecholamine release from cat and ox adrenals. Neuroreport 1:119–122. https://doi.org/10.1097/00001756-199010000-00009
8. Garrido B, Lopez MG, Moro MA, de Pascual R, Garcia AG (1990) Voltage-dependent inactivation of catecholamine secretion evoked by brief calcium pulses in the cat adrenal medulla. J Physiol 428:615–637. https://doi.org/10.1113/jphysiol.1990.sp018231
9. Dixon WR, Garcia AG, Kirpekar SM (1975) Release of catecholamines and dopamine beta-hydroxylase from the perfused adrenal gland of the cat. J Physiol 244:805–824. https://doi.org/10.1113/jphysiol.1975.sp010827
10. Schiavone MT, Kirpekar SM (1982) Inactivation of secretory responses to potassium and nicotine in the cat adrenal medulla. J Pharmacol Exp Ther 223:743–749
11. Borges R (1997) The rat adrenal gland in the study of the control of catecholamine secretion. Semin Cell Dev Biol 8:113–120. https://doi.org/10.1006/scdb.1996.0130
12. Borges R, Sala F, Garcia AG (1986) Continuous monitoring of catecholamine release from perfused cat adrenals. J Neurosci Methods 16: 289–300. https://doi.org/10.1016/0165-0270(86)90054-3
13. Herrera M, Kao LS, Curran DJ, Westhead EW (1985) Flow-injection analysis of catecholamine secretion from bovine adrenal medulla cells on microbeads. Anal Biochem 144:218–227. https://doi.org/10.1016/0003-2697(85)90109-5
14. Green DJ, Perlman RL (1981) On-line measurement of catecholamine secretion. Anal Biochem 110:270–276. https://doi.org/10.1016/0003-2697(81)90191-3
15. Livett BG (1984) Adrenal medullary chromaffin cells in vitro. Physiol Rev 64:1103–1161
16. Moro MA, Lopez MG, Gandia L, Michelena P, Garcia AG (1990) Separation and culture of living adrenaline- and noradrenaline-containing cells from bovine adrenal medullae. Anal Biochem 185:243–248. https://doi.org/10.1016/0003-2697(90)90287-j
17. Garcia AG, Garcia-De-Diego AM, Gandia L, Borges R, Garcia-Sancho J (2006) Calcium signaling and exocytosis in adrenal chromaffin cells. Physiol Rev 86:1093–1131. https://doi.org/10.1152/physrev.00039.2005
18. Carbone E, Borges R, Eiden LE, Garcia AG, Hernandez-Cruz A (2019) Chromaffin cells of the adrenal medulla: physiology, pharmacology, and disease. Compr Physiol 9:1443–1502. https://doi.org/10.1002/cphy.c190003

Chapter 9

Recording of Chromaffin Cell Electrical Activity In Situ in Acute Adrenal Slices

Nathalie C. Guérineau

Abstract

Because catecholamines secretion mainly relies on the excitable nature of adrenal chromaffin cells, monitoring their electrical activity is an essential step in assessing the adrenal medullary tissue function. The difficult access to the gland in vivo allows only population activity to be recorded in this condition. In vitro preparations allow recordings of spontaneous or evoked activity from single or multiple cells, depending on the biological samples used (dissociated chromaffin cells versus adrenal tissue preparations). In this chapter, I provide a detailed description of the techniques used for electrophysiological recordings in rodent chromaffin cells in acute adrenal slices, using the patch-clamp technique. This methodology allows preservation of the tissue integrity and detection of action potentials, synaptic activity, and secretory events; it is thus suitable for the study of adrenomedullary activity-secretion coupling.

Key words Chromaffin cell, Acute adrenal slice, Excitability, Action potential, Synaptic activity, Stimulus-secretion coupling, Rat, Mouse

1 Introduction

Adrenal chromaffin cells are the main drivers of catecholamine release, and as such they critically contribute to the adaptive response to stress. To efficiently cope with stressful life events, the organism needs to adapt the amounts of catecholamines (epinephrine and norepinephrine) released in the blood circulation. Catecholamine secretion is a finely regulated process, through the continuous remodeling of the adrenomedullary stimulus-secretion coupling [1–3]. Among the "intra-adrenal" parameters undergoing dynamic changes during stress, the electrical activity of chromaffin cells is undoubtedly one of the most critical [4], as it chiefly patterns the release of catecholamines [5, 6]. To study the physiological/pathological functions that occur in vivo, it is necessary to work on biological preparations that maintain, as much as possible, the structural integrity of the adrenal gland (i.e. including cortical

Ricardo Borges (ed.), *Chromaffin Cells: Methods and Protocols*,
Methods in Molecular Biology, vol. 2565, https://doi.org/10.1007/978-1-0716-2671-9_9,

and medullary tissues). Such a level of tissular organization is attainable in ex vivo preparations, and especially in acute slices, in which the cellular composition and tissular architecture are maintained and the exchange of biological signals between cells is preserved [7]. While recordings of the electrical activity from single isolated chromaffin cell have been described in the literature for many decades, the use of acute adrenal slices is comparatively more recent.

The procedures reported here describe both the preparation of rodent acute adrenal gland slices and the electrophysiological recordings from chromaffin cells in these slices. Additional information on other experiments that can be carried out with this methodology is also provided.

2 Materials

2.1 Dissection of the Adrenal Glands

1. Fine scissor to remove the adrenal glands from the animal.
2. Two fine forceps to unsheathe each gland from the surrounding fat tissue.
3. A carbogen gas cylinder (95% O_2/5% CO_2).
4. Ringer's saline: 125-mM NaCl, 2.5-mM KCl, 2-mM $CaCl_2$, 1-mM $MgCl_2$, 1.25-mM NaH_2PO_4, 26-mM $NaHCO_3$, 12-mM glucose. The saline is continuously bubbled with carbogen (95% O_2/5% CO_2) and buffered to pH 7.4 (pH adjusted with NaOH). The osmolarity is adjusted to 310–320 mOsm. Milli-Q water is used for preparing solutions. The extracellular solution is used on the day of the experiment. However, a stock solution (e.g., Ringer 10X) can be prepared in advance and stored at 4 °C for 4–5 days. $CaCl_2$, $MgCl_2$, and glucose are added on the day of the experiment and only when the pH is adjusted (to prevent divalent ions from precipitation). Fill a glass beaker with Ringer's saline (100 mL). To reach the Ringer's saline optimal temperature (0–3 °C) required for adrenal gland survival during slicing, the beaker is placed in a mixture of crushed ice and salt (NaCl) in a polystyrene box.
5. Filter paper Grade 1 (circles, 90 mm diameter).

2.2 Adrenal Slice Preparation

1. Extracellular medium for slicing: cooled Ringer's saline bubbled with carbogen.
2. A vibratome (many models are commercially available). To maintain the optimal temperature of the Ringer's saline during slicing (0–3 °C), the vibratome chamber must be cooled, either by an automatic cooling unit included in the vibratome or by enclosing the chamber in a mixture of ice and salt.

3. A razor blade (no need for a special blade, use a simple blade commonly used for shaving, Fig. 1c). Before use, clean the razor blade with alcohol (70%) to remove traces of grease.
4. A tube of rapid glue. The use of surgical glue is not mandatory. Prefer using gel glue which is easier to manipulate rather than liquid glue.
5. An agarose block. Prepare 100 mL of an agarose solution (6% in Milli-Q water) and pour the whole solution into a Petri dish (100-mm diameter) to obtain a final thickness of about 1 cm. After cooling, cut a 1-cm cube and hemisection it. The half-cube shape is optimal for stabilizing the adrenal gland during slicing without affecting free floating of slices in the chamber (*see* Fig. 1d).
6. A plastic Pasteur pipette used to manipulate the slices. Cut the pipette tip with a scissor and fire polish it to a diameter slightly larger than the slice size.

2.3 Slice Storage After Cutting

1. A storage chamber maintained at 35–37 °C (*see* Fig. 1e), filled with Ringer's saline and continuously bubbled with carbogen to maintain a constant pH of 7.4.
2. A nylon sieve on which the adrenal slices are deposited. For an optimal preservation of the slices, control carefully that they lie flat on the sieve and do not stick to it or to each other. Under these conditions, adrenal slices can be used up to 6–8 h after slicing.

2.4 Electrophysiological Recordings (Patch-Clamp)

1. Extracellular solution: 125-mM NaCl, 2.5-mM KCl, 2-mM $CaCl_2$, 1-mM $MgCl_2$, 1.25-mM NaH_2PO_4, 26-mM $NaHCO_3$, 12-mM glucose. The saline is continuously bubbled with carbogen (95% O_2/5% CO_2) and buffered to pH 7.4 (pH adjusted with NaOH). The osmolarity is adjusted to 310–320 mOsm with sucrose. Milli-Q water is used for preparing solution. Prepare a 1-L solution. The composition indicated here corresponds to a standard solution, which can be modified with pharmacological drugs to assess the contribution of specific components to the electrical activity recorded (Na^+ currents, Ca^{2+} currents, K^+ currents, excitatory/inhibitory synaptic currents, gap junction currents, etc.).
2. Borosilicate glass for the patch pipettes (thin wall with filament, 1.5 mm outer diameter, 1.17 mm inner diameter).
3. A glass puller (many models are commercially available). For recordings in the whole-cell configuration, patch pipettes are pulled to have a resistance of 5–7 MΩ when filled with the intracellular solution of K-gluconate (see below). For perforated patch-clamp recordings, the resistance of the pipettes is 2–5 MΩ. For loose patch-clamp recordings, increase the

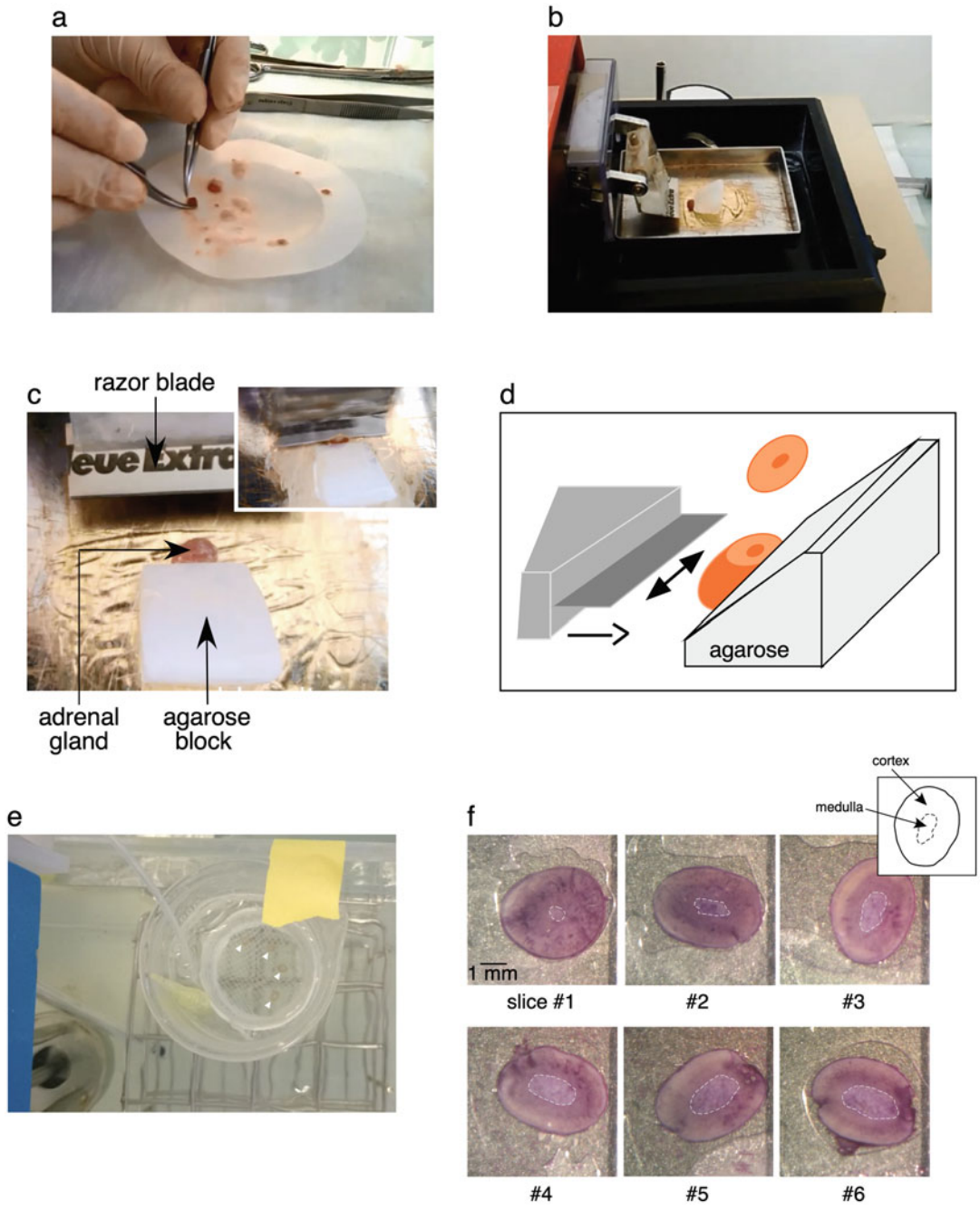

Fig. 1 Protocol for acute adrenal slice preparation. (**a**) Dissection of an adrenal gland and fat removal. (**b**) Illustration of a vibratome chamber. (**c**) Positioning of an adrenal gland in the chamber with the agarose block and the razor blade. Inset: a slice in progress. (**d**) Schematic representation of the agarose block (note its half-cube shape) placed behind the adrenal gland. (**e**) Top view of the storage chamber. Note the nylon sieve on which slices (see arrow heads) are stored before use. (**f**) Photographs of six serial slices from a rat adrenal gland. Each slice was labeled with hematoxylin (1 g/L, 2 min), as such the cortical and medullary tissues can be distinguished by differential staining intensity (the dashed line delimits the surface of the medullary tissue). The inset illustrates a schematic representation of the two (neuro)endocrine tissues (cortex and medulla) of an adrenal gland

pipette resistance to 5–10 MΩ when filled with extracellular medium. Except for recordings in perforated patch [8–10], there is no specific need to polish the pipette tips after pulling. Also, since the signals recorded are not very small, there is no need for further electrical isolation.

4. An upright microscope equipped with differential interference contrast optics and with low-magnification ×5 (or ×4) and high-magnification (×60, water immersion) objective lenses. Notice that the magnification value can slightly differ between microscope's manufacturers.
5. An electrophysiology setup (patch-clamp amplifier + one or two three-axis micromanipulators + an anti-vibration air table and a Faraday cage).
6. A recording chamber equipped with perfusion and temperature control systems. A peristaltic pump can be used for perfusing the recording chamber (perfusion rate of about 2 mL/min).
7. Intra-pipette solutions. All solutions are prepared in Milli-Q water. The composition of solutions differs between the recording configurations (conventional whole-cell recording versus perforated whole-cell recording, patch-clamp versus loose patch), the recording modes (current-clamp versus voltage-clamp), and the ion current recorded (Na^+, Ca^{2+}, K^+ currents). Three examples of intra-pipette solutions are listed below:
   (a). Intra-pipette milieu for whole-cell conventional patch-clamp recordings: 140-mM K-gluconate, 2-mM $MgCl_2$, 1.1-mM EGTA, 5-mM HEPES, 3-mM Mg-ATP, 0.5-mM Na-GTP. The solution is titrated to pH 7.2 with KOH. Osmolarity is adjusted at 285–295 mOsm with K-gluconate [11].
   (b). Intra-pipette milieu for perforated patch-clamp recordings: Differing from the standard internal solution used for conventional patch-clamp recording is the presence of a pore-forming antibiotic (typically amphotericin B, nystatin or gramicidin). The most commonly used agent in rat/mouse adrenal slices is amphotericin B (0.1–1 mg/mL prepared in dimethyl sulfoxide) [7, 8, 12]. See [13] for a detailed description of the methodology using amphotericin B. When deciding which permeant agent to use, it is important to take into consideration the ion selectivity of the pores formed. Indeed, most antibiotics create an anion-selective channel when incorporating the cell membrane, and chloride ions will equilibrate between intra- and extracellular compartments.
   (c). Intra-pipette milieu for loose patch recordings: 125-mM NaCl, 2.5-mM KCl, 2-mM $CaCl_2$, 1-mM $MgCl_2$,

10-mM HEPES, 10-mM glucose and buffered to pH 7.4 with NaOH. Osmolarity is adjusted at 285–295 mOsm with NaCl [11].

All internal solutions are maintained at 4 °C before use. Solution containing the permeabilizing agent is prepared on the day of the experiment and stored at 4 °C. Patch pipettes are filled using a fine catheter from a 1-mL plastic syringe (or a yellow pipette tip), for which the tip has been pulled with a flame. For perforated patch-clamp, pipettes are tip-filled with standard internal solution and then back-filled with the solution containing the pore-forming agent.

3 Methods

3.1 Acute Slice Preparation

1. After removal, keep the adrenal glands in ice-cold saline for 2 min. Before slicing, the glands have to be unsheathed from the surrounding adipose tissue (*see* Fig. 1a). Transfer one gland on filter paper and remove the fat engulfing the adrenal with two fine forceps. A well-dissected gland will facilitate the slicing procedure, as the slices will themselves release from the gland. During the dissection process, be careful to maintain the integrity of the capsule. This then helps to generate healthy slices, with cortex and medulla.
2. Transfer the dissected gland to the stage of the vibratome (*see* Fig. 1b). Apply a small amount of glue on the stage and glue the gland first and then the agarose block. Position the agarose cube just behind the gland to stabilize it during slicing (*see* Fig. 1c, d). As they are generated, handle the slices with a plastic Pasteur pipette and gently release them on the nylon sieve in the storage chamber (maintained at 35–37 °C and bubbled with carbogen). The acute adrenal slices obtained using the above protocol are suitable for electrophysiological recording immediately after cutting and for 6–8 h after cutting (*see* **Note 1**). Figure 1f illustrates an example of six serial slices prepared from the same adrenal gland (adult male rat). As expected from the tissular organization of the adrenal gland, the first slices are exclusively composed of the cortex, and the medullary tissue gradually appears with the next slices. With a little knowledge of the adrenal gland, it is easy to recognize the two tissues by eye. The labeling of living slices with a dye can help a novice person to be trained (*see* **Note 2**).

Note that acute adrenal slices can be used to investigate the amount of catecholamines released from the entire medullary tissue, as reported in rat [14].

3.2 Electrophysiological Recordings (Patch-Clamp)

The reader can find a detailed description of the patch-clamp technique in the pioneer article authored by Hamill and colleagues [15]. Regarding chromaffin cells, electrophysiological recordings in acute slices have been successfully performed on both rat and mouse, male and female, adult and newborn animals [11, 16–20].

1. Collect a slice with a plastic Pasteur pipette from the storage chamber and carefully transfer it to the recording chamber attached to the stage of the upright microscope. Ensure that the perfusion is switched off during the transfer procedure to avoid aspiration of the slice in the vacuum.
2. Once the slice is positioned into the chamber, place a nylon mesh on the edge of the slice (*see* **Note 3**) to keep it flat in the bottom of the chamber. Restart the perfusion system and check that the temperature of the extracellular saline is maintained at 30-32°C. Importantly, make sure that the slice is well positioned on the bottom of the chamber and does not drift during perfusion. Electrophysiological recordings will not be stable with submerged slices not secured to the bottom of the chamber.
3. Locate the adrenal medullary tissue as a whole using the low magnification objective lens. To observe chromaffin cells, switch to the water immersion objective lens. Choose a cell for recording and move the stage of the microscope to position it at the center of the optic field (*see* **Notes 4** and **5**).
4. Switch again to the low magnification objective and mount a patch pipette (filled with the internal solution) in the holder of a patch-clamp amplifier. Apply a small amount of positive pressure to the patch electrode as approaching the target cell (*see* **Note 6**). This allows i) keeping the tip of the pipette clean and ii) facilitating high resistance seal.
5. Use the micromanipulator ('macro-travel' mode) to move the pipette down to reach the surface of the adrenal medulla (without touching the tissue).
6. Switch to the high magnification objective. Locate the patch pipette above the slice surface and use the 'micro-travel' mode of the micromanipulator to carefully position the patch electrode above the chosen cell. Move slowly the pipette down to delicately touch the cell. Note that a light halo can sometimes be viewed on the cell surface. Stop to move down. From this position, several recording configurations are possible (*see* Fig. 2)
   (a) Conventional patch-clamp recording: As soon as the patch electrode touches the cell, apply a continuous but slight negative pressure (suction) until the formation of a high-resistance (> GΩ) electrical seal, known as a gigaseal,

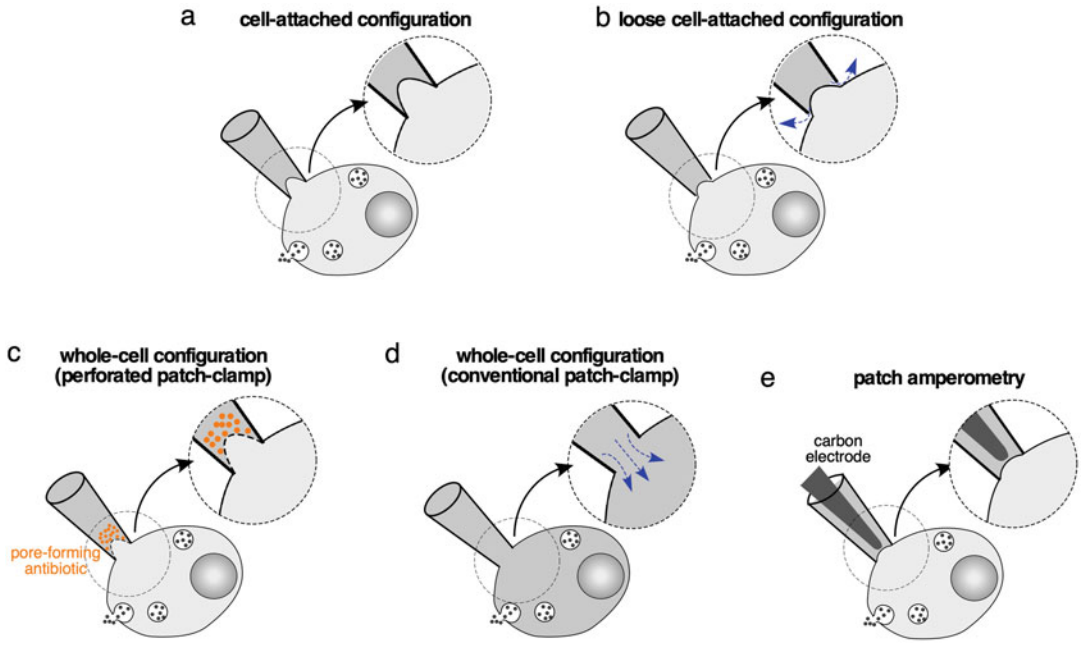

Fig. 2 Schematic representations of some patch-clamp configurations. (**a**) Cell-attached configuration with the gigaseal. (**b**) Loose cell-attached configuration. Note the formation of a loose seal rather than the tight gigaseal. Blue arrows indicate the weak contact between the electrode tip and the cell membrane. (**c**) Whole-cell configuration in perforated patch-clamp. The presence of a pore-forming antibiotic in the intra-pipette solution (orange circles) allows to permeabilize the cell membrane, allowing electrical access between the cell and the patch pipette. (**d**) Whole-cell configuration in conventional patch-clamp. Under this experimental condition, the membrane fragment under the patch pipette is broken, which leads to a gradual dialysis of the cytosol by the intra-pipette solution (blue arrows). (**e**) Cell-attached configuration for patch amperometry. This technique combines amperometric detection of secretory events and capacitance measurement. Note the carbon fiber electrode inserted into the patch pipette

between the pipette and the cell (*see* Fig. 2a). From this configuration (cell-attached configuration) and to switch to the whole-cell configuration, apply an additional suction pressure, shorter but stronger (*see* **Notes 6** and **7**, Fig. 2d). Breaking of the cell membrane fragment under the pipette leads to a gradual "washout" of the cytoplasm by the intra-pipette solution. Depending on the experiment conducted, this can be seen as an advantage (possibility to load the recorded cell with an extrinsic agent (pharmacological drug, calcium/voltage-sensitive dyes, fluorescent tracer; *see* Fig. 4d)) or a disadvantage when considering the dialysis-induced loss of internal compounds which are crucial for cell function.

Signals are sampled at 10 kHz and filtered at 3 kHz. In the current-clamp mode of the whole-cell configuration, changes in membrane potential are monitored, and spontaneous discharges of action potentials can be

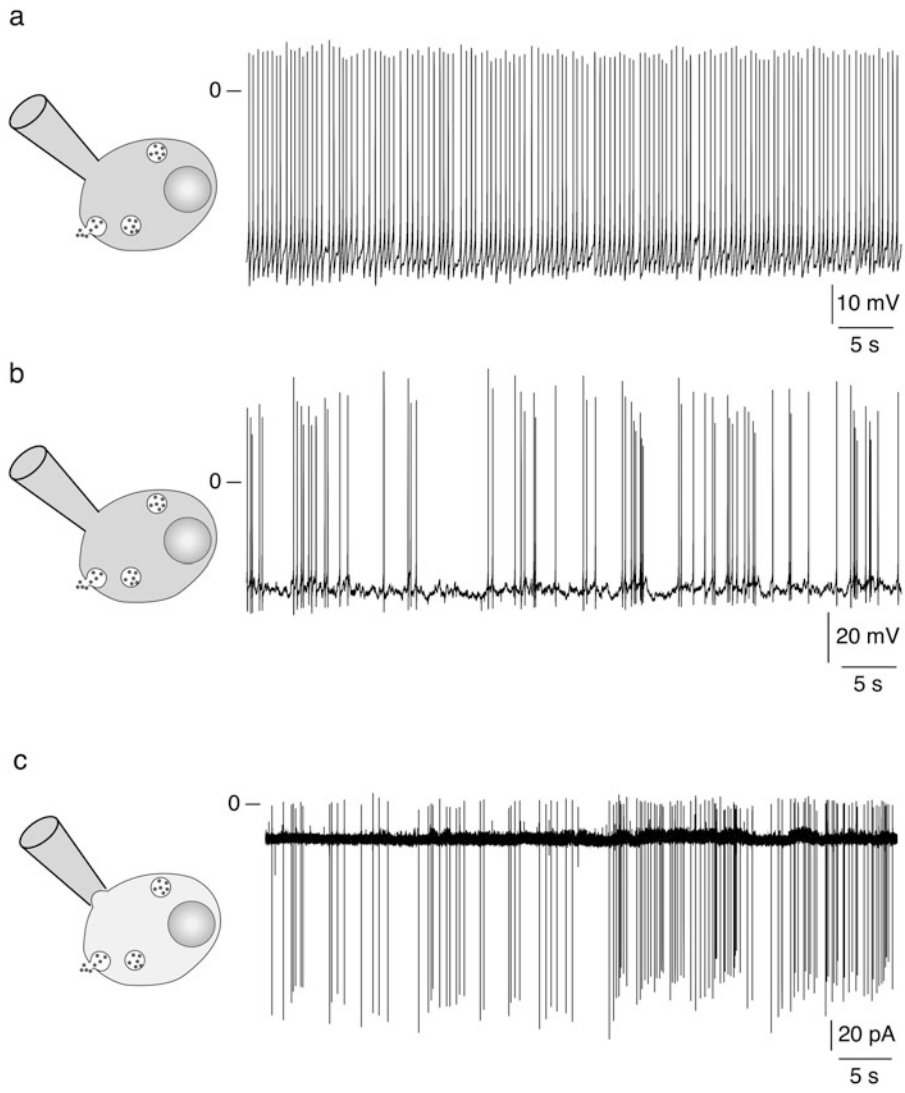

Fig. 3 Representative examples of spontaneous electrical activity in chromaffin cells recorded in mouse adrenal slices. Regular discharge (**a**) and discharge in bursts (**b**) of action potentials recorded in conventional whole-cell patch-clamp condition. (**c**) Discharge of action potential currents recorded in loose patch-clamp configuration (holding potential = 0 mV). The detailed methodology is available in [11]

recorded (*see* Fig. 3a, b). In the voltage-clamp mode, the membrane potential is maintained at a holding value (−50 mV, e.g., corresponding to chromaffin cell resting membrane potential), and changes in membrane currents (Na^+, Ca^{2+}, K^+ currents) can be monitored (with appropriate composition of both extracellular and internal recording solutions).

(b) Perforated patch-clamp recording (*see* Fig. 2c): The first steps until obtaining the gigaseal are identical to those

described above for conventional patch-clamp recording. From the cell-attached configuration, the access resistance gradually decreases upon the action of the permeabilizing agent to reach a stable value within a couple of minutes to about 20 min [7]. A low access resistance (<20 MΩ) is required before starting recording. The time to reach this resistance value depends on many parameters, such as the extent to which the tip of the pipette is filled with amphotericin-free solution, the quality of the gigaseal (resistance), or the accessibility of the cell surface. While the use of a cleaning pipette to remove loose material from the cell surface is not necessary required for conventional patch-clamp, this can improve the quality of recording in the perforated conditions [8]. Typical chart recordings of membrane potential/current changes can be found in [7–10, 12, 21, 22]. Electrophysiological recordings in this configuration have been successfully performed on both adult rat and mouse, male and female.

(c) Dual patch-clamp recording: The maintenance of the tissular architecture in adrenal slices allows recording of electrical events occurring in chromaffin cell pairs, such as junctional currents flowing through gap junction channels [23]. The procedure is roughly similar to that described for "single" patch-clamp recordings. The following sequence is recommended: gigaseal in cell #1, gigaseal in cell #2, whole-cell in cell #1, and whole-cell in cell #2. Like for "single" patch-clamp, both membrane potential and membrane current changes can be monitored. The principle of dual patch-clamp to record junctional currents is to clamp the two cells engaged in the pair at the same potential and then change the potential (depolarization/hyperpolarization) in only one cell. If the two cells are electrically coupled, the current in cell #1 results from the addition of the membrane current evoked in response to depolarizing/hyperpolarizing voltage steps and the junctional current. The current in cell #2 corresponds to the junctional current (same amplitude as recorded in cell #1 but opposite direction). Representative chart recordings of junctional currents in chromaffin cell pairs in rodent adrenal slices can be found in [17–19, 24].

The whole-cell configuration of the patch-clamp technique offers the possibility to record various classes of electrical signals (*see* Fig. 4 and **Note 8**). The most common ones are membrane potential changes driven by action potential firing and membrane current changes in response to activation/inhibition of ion channels (*see* Fig. 4a). In chromaffin cells, the synaptic activity induced

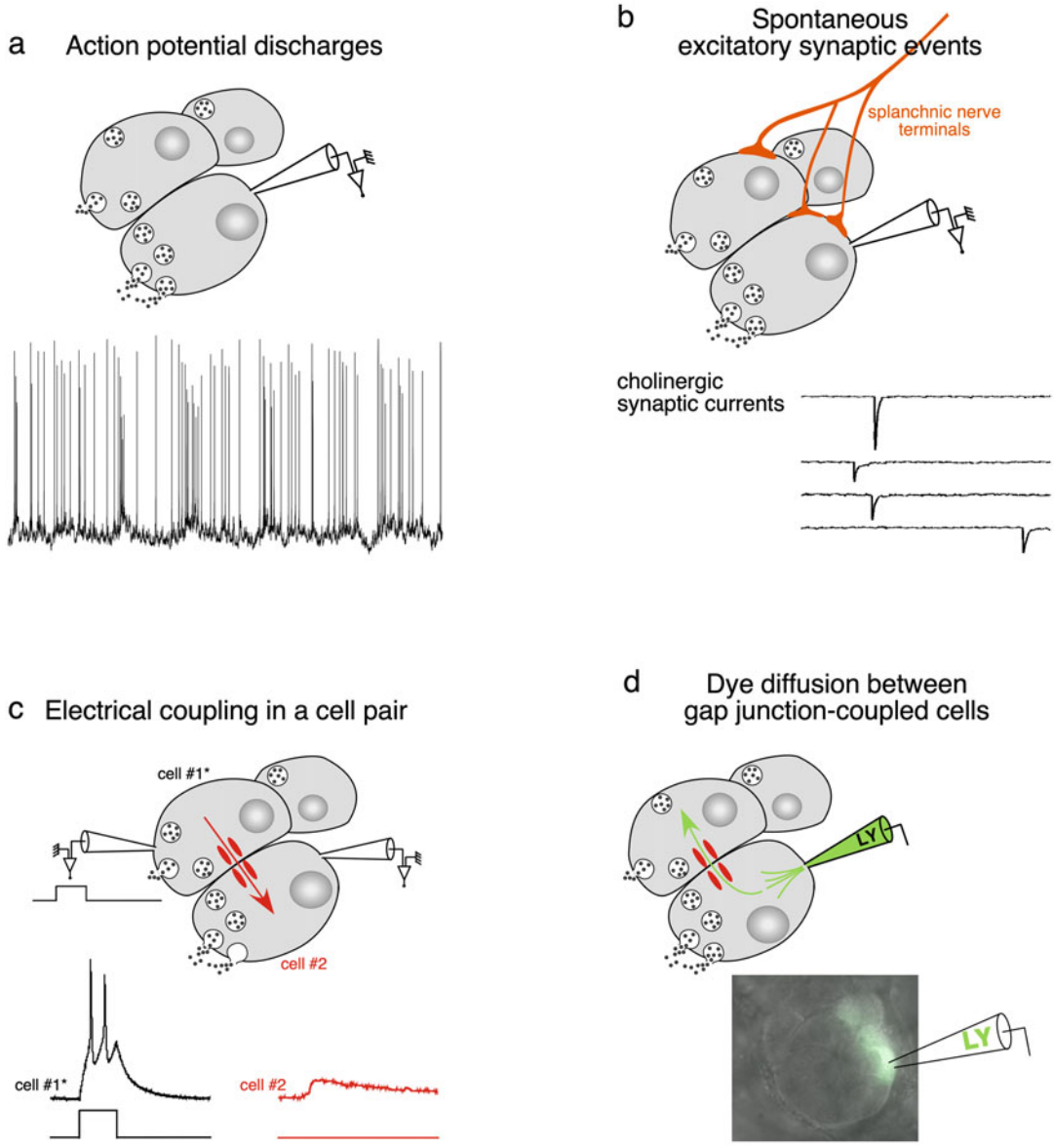

Fig. 4 Whole-cell configuration of the patch-clamp: a versatile technique for recording many parameters. The different possibilities are illustrated on a schematic cluster of three chromaffin cells releasing catecholamines. (**a**) Recording of action potential firing discharges in a mouse adrenal slice (current-clamp mode, conventional patch clamp). To assess the electrical activity at resting membrane potential, the injected current by the amplifier is held at 0 pA. (**b**) Recording of synaptic activity. Example of excitatory postsynaptic cholinergic currents recorded in a rat adrenal slice (voltage-clamp mode, holding potential $= -60$ mV, conventional patch-clamp). (**c**) Recording of junctional coupling in a pair of electrically coupled chromaffin cells in a rat adrenal slice. Cell #1* is the stimulated cell. The depolarizing injected current triggers action potentials in cell#1* (black traces). In the unstepped cell (#2), a small depolarization resulting from gap junctional communication between cell #1 and cell#2 is elicited (red traces). (**d**) Monitoring of the dye diffusion between gap junction-coupled chromaffin cells. Example of Lucifer yellow (LY) diffusion between a chromaffin cell triplet within a lobule. The patch pipette is filled with Lucifer yellow, and the passage in the whole-cell configuration (i.e., disruption of the membrane fragment under the patch pipette) allows the passive diffusion of the dye into the patched cell and neighboring gap junction-coupled cells

by innervating axons (excitatory/inhibitory postsynaptic potentials/currents) can be easily recorded (*see* Fig. 4b). The electrical coupling in a cell pair can also be investigated through patch-clamp recording (*see* Fig. 4c). One can assess the intercellular communication through passive diffusion of fluorescent tracers (*see* Fig. 4d).

(d) Loose cell-attached patch recording (*see* Fig. 2b): This method allows investigating of membrane excitability under physiological conditions since there is no rupture of the cell membrane. In the absence of intracellular milieu dialysis by the intra-pipette medium, long-lasting recordings (>10 min) are possible. Position the tip of a patch electrode at the surface of a chromaffin cell and apply a minimal suction pressure to get a "weak" seal resistance (<500 MΩ.) This configuration using a loose seal is well appropriate for recording cell spiking activity. Under the voltage-clamp mode, the electrical activity is viewed as action potential currents. To record the electrical firing occurring at the resting membrane potential (a condition for which no current is injected by the patch amplifier), adjust the holding potential of the recording pipette to get a holding current equal to zero. Note that a gigaseal seal (resistance >GΩ as describe above) is required for triggering action potentials in the patched cell and for recording resting and synaptic potentials. The theory and the experimental applications of this technique are detailed in [25]. A representative example of action potential currents recorded in chromaffin cells in acute adrenal slices is illustrated in Fig. 3c.

4 Notes

1. The adjustment of the cutting parameters depends on the equipment used. The following values are given as a guide: slicing speed approximately 0.05–0.1 mm/s, vibration amplitude 1.2 mm, and vibration frequency 30–100 Hz. Slices can be generated at various thickness (from 100 to 250 μm), depending, at least in part, on the species and the age of animals. The small size of adrenal glands in neonates is a limiting factor for the number of slices containing medulla. In our hand, slices of 100-μm thickness appear the best compromise in rat neonates, taking into account the two parameters (adrenal size and number of slices) [17, 18].
2. To distinguish between the cortical and the medullary tissues in a living slice, a labeling with hematoxylin (1 g/L for 2 min) can be helpful.

3. Mesh of nylon threads used to maintain the slices in the recording chamber are commercially available as grids. Choose an appropriate size and format to allow the recording pipettes to fully access the recording area. It is possible to use homemade grids with a nylon sock. The main advantage, if we except the cost, is the possibility to stretch the sock to adjust the spacing between threads to the size of the slice.
4. The use of a microscope eyepiece equipped with an ocular micrometer can be useful to precisely locate the cell of interest.
5. For some reasons (tissue structure, cell composition, etc.), the access via the patch pipette to chromaffin cells located deeply in the tissue is tricky or even impossible. As such, most of the electrical signals recorded in chromaffin cells come from cells one or two layers deep into the slice.
6. All pressures (positive when approaching the cell of interest, or negative to induce the cell-attached and whole-cell configurations) can be generated either from the mouth of the experimenter or using plastic syringes (1–10 mL).
7. Coating and fire polishing of the patch electrode tips are generally not required for recording in the conventional patch-clamp condition.
8. Secretory events such as hormone release (= catecholamine release in the case of chromaffin cells) can be monitored by an electrochemical approach based on amperometry. The technique uses a carbon fiber electrode to detect ion currents generated by the oxidizing reaction of catecholamines (dopamine, norepinephrine, epinephrine). The instrumentation usually found on an electrophysiological setup (microscope, electrode holder, micromanipulators, patch-clamp amplifier, etc.) is quite suitable for the amperometric detection of secretory events. The carbon fiber used for amperometry is placed in close vicinity of the cell (use a micromanipulator to precisely position the electrode). The exocytotic currents generated by oxidation of catecholamines at the surface of the carbon fiber are measured at a constant potential of +800 mV and recorded by a patch-clamp amplifier (voltage-clamp mode). Note that the detection of catecholamine exocytosis by amperometry does not discriminate between dopamine, norepinephrine, and epinephrine secretion. Examples of exocytotic events recorded in chromaffin cells in rat adrenal slices are illustrated elsewhere [7, 16]. A variant of this technique, called "patch amperometry," combines, as its name suggests the two techniques of patch-clamp and amperometry. The insertion of a carbon fiber electrode into a patch pipette (*see* Fig. 2e) allows monitoring of exocytotic events of individual chromaffin granules by using capacitance measurements (a cell surface-related

electrophysiological parameter) combined with electrochemical detection of catecholamines. This technique has been first described in isolated bovine chromaffin cells using the cell-attached configuration of the patch-clamp technique [26] and then extended to cell-free membrane patches in the inside-out configuration [27]. To learn more, step-by-step instructions for the application of this method are described in [28]. To my knowledge, the use of patch amperometry in adrenal slices has not yet been reported.

Acknowledgments

The author thanks Dr. Alexandre Milman for providing recordings in mouse acute adrenal slices and Dr. Philippe Lory, Dr. Michel Desarménien, and Claire Bernat for the critical reading of the manuscript. I also acknowledge the Centre National de la Recherche Scientifique, Institut National de la Santé et de la Recherche Médicale, the Laboratory of Excellence "Ion Channel Science and Therapeutics" (LabEx ICST, grant ANR-11-LABX-0015-01), and the Fondation pour la Recherche Médicale for supporting our research.

References

1. Guerineau NC, Desarmenien MG, Carabelli V, Carbone E (2012) Functional chromaffin cell plasticity in response to stress: focus on nicotinic, gap junction, and voltage-gated Ca^{2+} channels. J Mol Neurosci 48:368–386
2. Desarmenien MG, Jourdan C, Toutain B, Vessieres E, Hormuzdi SG, Guerineau NC (2013) Gap junction signalling is a stress-regulated component of adrenal neuroendocrine stimulus-secretion coupling in vivo. Nat Commun 4:2938
3. Guerineau NC (2020) Cholinergic and peptidergic neurotransmission in the adrenal medulla: a dynamic control of stimulus-secretion coupling. IUBMB Life 72:553–567
4. Colomer C, Lafont C, Guerineau NC (2008) Stress-induced intercellular communication remodeling in the rat adrenal medulla. Ann N Y Acad Sci 1148:106–111
5. Kidokoro Y, Ritchie AK (1980) Chromaffin cell action potentials and their possible role in adrenaline secretion from rat adrenal medulla. J Physiol 307:199–216
6. Zhou Z, Misler S (1995) Action potential-induced quantal secretion of catecholamines from rat adrenal chromaffin cells. J Biol Chem 270:3498–3505
7. Barbara JG, Poncer JC, McKinney RA, Takeda K (1998) An adrenal slice preparation for the study of chromaffin cells and their cholinergic innervation. J Neurosci Methods 80:181–189
8. Albillos A, Neher E, Moser T (2000) R-type Ca^{2+} channels are coupled to the rapid component of secretion in mouse adrenal slice chromaffin cells. J Neurosci 20:8323–8330
9. Hernandez A, Segura-Chama P, Jimenez N, Garcia AG, Hernandez-Guijo JM, Hernandez-Cruz A (2011) Modulation by endogenously released ATP and opioids of chromaffin cell calcium channels in mouse adrenal slices. Am J Physiol Cell Physiol 300: C610–C623
10. Hill J, Chan SA, Kuri B, Smith C (2011) Pituitary adenylate cyclase-activating peptide (PACAP) recruits low voltage-activated T-type calcium influx under acute sympathetic stimulation in mouse adrenal chromaffin cells. J Biol Chem 286:42459–42469
11. Milman A, Venteo S, Bossu JL, Fontanaud P, Monteil A, Lory P, Guerineau NC (2021) A sodium background conductance controls the spiking pattern of mouse adrenal chromaffin cells in situ. J Physiol 599:1855–1883

12. Chan SA, Polo-Parada L, Smith C (2005) Action potential stimulation reveals an increased role for P/Q-calcium channel-dependent exocytosis in mouse adrenal tissue slices. Arch Biochem Biophys 435:65–73
13. Rae J, Cooper K, Gates P, Watsky M (1991) Low access resistance perforated patch recordings using amphotericin B. J Neurosci Methods 37:15–26
14. De Nardi F, Lefort C, Breard D, Richomme P, Legros C, Guerineau NC (2017) Monitoring the secretory behavior of the rat adrenal medulla by high-performance liquid chromatography-based catecholamine assay from slice supernatants. Front Endocrinol (Lausanne) 8:248
15. Hamill OP, Marty A, Neher E, Sakmann B, Sigworth FJ (1981) Improved patch-clamp techniques for high-resolution current recording from cells and cell-free membrane patches. Pflugers Arch 391:85–100
16. Martin AO, Mathieu MN, Chevillard C, Guerineau NC (2001) Gap junctions mediate electrical signaling and ensuing cytosolic Ca^{2+} increases between chromaffin cells in adrenal slices: a role in catecholamine release. J Neurosci 21:5397–5405
17. Martin AO, Mathieu MN, Guerineau NC (2003) Evidence for long-lasting cholinergic control of gap junctional communication between adrenal chromaffin cells. J Neurosci 23:3669–3678
18. Martin AO, Alonso G, Guerineau NC (2005) Agrin mediates a rapid switch from electrical coupling to chemical neurotransmission during synaptogenesis. J Cell Biol 169:503–514
19. Colomer C, Olivos Ore LA, Coutry N, Mathieu MN, Arthaud S, Fontanaud P, Iankova I, Macari F, Thouennon E, Yon L, Anouar Y, Guerineau NC (2008) Functional remodeling of gap junction-mediated electrical communication between adrenal chromaffin cells in stressed rats. J Neurosci 28:6616–6626
20. Guerineau NC, Monteil A, Lory P (2021) Sodium background currents in endocrine/neuroendocrine cells: towards unraveling channel identity and contribution in hormone secretion. Front Neuroendocrinol 63:100947
21. Kuri BA, Chan SA, Smith CB (2009) PACAP regulates immediate catecholamine release from adrenal chromaffin cells in an activity-dependent manner through a protein kinase C-dependent pathway. J Neurochem 110: 1214–1225
22. Albinana E, Segura-Chama P, Baraibar AM, Hernandez-Cruz A, Hernandez-Guijo JM (2015) Different contributions of calcium channel subtypes to electrical excitability of chromaffin cells in rat adrenal slices. J Neurochem 133:511–521
23. Neyton J, Trautmann A (1985) Single-channel currents of an intercellular junction. Nature 317:331–335
24. Hill J, Lee SK, Samasilp P, Smith C (2012) Pituitary adenylate cyclase-activating peptide enhances electrical coupling in the mouse adrenal medulla. Am J Physiol Cell Physiol 303: C257–C266
25. Perkins KL (2006) Cell-attached voltage-clamp and current-clamp recording and stimulation techniques in brain slices. J Neurosci Methods 154:1–18
26. Albillos A, Dernick G, Horstmann H, Almers W, Alvarez de Toledo G, Lindau M (1997) The exocytotic event in chromaffin cells revealed by patch amperometry. Nature 389:509–512
27. Dernick G, Alvarez de Toledo G, Lindau M (2003) Exocytosis of single chromaffin granules in cell-free inside-out membrane patches. Nat Cell Biol 5:358–362
28. Dernick G, Gong LW, Tabares L, Alvarez de Toledo G, Lindau M (2005) Patch amperometry: high-resolution measurements of single-vesicle fusion and release. Nat Methods 2: 699–708

Chapter 10

Calcium Imaging and Amperometric Recording in Cultured Chromaffin Cells and Adrenal Slices from Normotensive, Wistar Kyoto Rats and Spontaneously Hypertensive Rats

Tzitzitlini Alejandre-García, Pedro Segura-Chama, Oscar Javier Parada-Parra, Diana Millán-Aldaco, and Arturo Hernández-Cruz

Abstract

The spontaneously hypertensive rat (SHR) is a model widely used to investigate the causal mechanisms of essential hypertension. The enhanced catecholamine (CA) release reported in adrenal glands from adult SHRs raised considerable interest for its possible implication in the genesis of hypertension. The use of powerful techniques such as calcium imaging, electrophysiology, and single-cell amperometry to monitor in real time the key steps in CA secretion has allowed a better understanding of the role of chromaffin cells (CC) in the pathophysiology of hypertension, although several questions remain. Additionally, the implementation of these techniques in preparations in situ, such as the acute adrenal gland slice, which maintains the microenvironment, cell-to-cell communication, and anatomical structure similar to that of the intact adrenal gland, yields data that may have even greater physiological relevance. Here, we describe the procedures to measure the blood pressure of rats in a noninvasive manner, how to obtain primary cultures of adrenal chromaffin cells and acute adrenal slices, and how to perform amperometric recordings and intracellular calcium imaging in these preparations.

Key words Chromaffin cells, Adrenal slices, Calcium imaging, Electrophysiology, Amperometry, Hypertension

1 Introduction

The spontaneously hypertensive rat (SHR), an inbred from the Wistar strain, has been widely used to investigate the causal mechanisms of essential hypertension [1–9]. Normotensive descendants of the same colony, the Wistar Kyoto rats (WKY), are often used as controls [2–7].

Since cultured chromaffin cells (CCs) are robust and easy to obtain, abundant morphological and functional information can be obtained from them. This chapter describes how to obtain cultures

Ricardo Borges (ed.), *Chromaffin Cells: Methods and Protocols*,
Methods in Molecular Biology, vol. 2565, https://doi.org/10.1007/978-1-0716-2671-9_10,

of rat CC that can be used for electrophysiological and calcium imaging recordings. Using single-cell carbon fiber amperometry and calcium imaging in cultured CCs, we showed that stimulus elicited intracellular calcium ($[Ca^{2+}]i$) elevations are approximately threefold larger and catecholamine (CA) secretion approximately twofold greater in SHR CCs than in WKY CCs [6].

Nonetheless, CCs in culture differ in several ways from their counterparts in the intact adrenal gland. On one hand, the physiological environment is not maintained in culture [10], and the expression of voltage-gated ion channels involved in the secretory process is altered with time [11, 12]. Moreover, synaptic cholinergic input [13, 14] and cell-to-cell communications are missing [15, 16].

As showed by Iijima [17], CCs in the adrenal medulla are organized into functional unit "clusters" of ~50–100 cells, where each cell cluster receives innervation of ~4 splanchnic nerve fibers [17]. This anatomical arrangement is well preserved in adrenal slices. Also, in the adrenal gland slice preparation, the correlation of neuronal input and CA secretion can be examined [11, 13, 18]. Several electrophysiological studies like patch-clamp and amperometry indicate that CCs in slices preserve better their native properties. For instance, it has been shown that voltage-gated calcium channels of CCs are tonically downregulated by endogenous molecules present in the microenvironment, like ATP and opioids [19–21]. Also, in adrenal medulla slices, the activity of many individual CCs under different physiological and pathological conditions can be simultaneously monitored using calcium imaging. Using this technique, the dual effect of GABA (inhibitory and excitatory) in different subpopulations of CCs in slices has been demonstrated [22].

Thus, patch-clamp electrophysiology with real-time measurement of CA secretion using amperometry and intracellular calcium recordings in both cultured cells and adrenal slices are excellent complementary models to investigate the physiology of these cells and their role in hypertension. In this chapter, we explain the methods used to measure the blood pressure of rats in a noninvasive manner and how to obtain cultures of CCs and acute adrenal slices. We also describe how to perform calcium imaging and amperometric recordings from CCs of normotensive and hypertensive rats in these two preparations.

2 Materials

2.1 Animals

Normotensive Wistar Kyoto (WKY) rats and the spontaneously hypertensive rats (SHR) are used [23]. The methodology describes how to perform noninvasive blood pressure measurements, amperometric and calcium imaging recordings from primary cultures, and

adrenal slices from young (3–5 weeks), juvenile (6–10 weeks), and adult (12 or more postnatal weeks) rats.

The reproduction of colonies of SHR and WKY strains withstands significant challenges. Compared to WKY rats, female SHRs display several reproductive disorders: the first estrus is delayed; there is a lower number of oocytes released, a delay in the vaginal opening, a decrease in the percentage of successful pregnancies, a longer duration of gestation, and smaller litter size (7.8 against 10.4 pups); they also have lower plasma concentrations of progesterone, LH, and FSH. Males have lower fertility and copulatory activity and produce abnormal sperm [24]. The main problems detected with the SHR and WKY strains in our animal facility are (a) cannibalism of the offspring, (b) abandonment of litter, (c) scattering of the offspring and their death from hypothermia, (d) low average prolificacy (number of total offspring born, alive, or dead per birth), (e) low milk production, and (f) low weeding weight [25–27].

1. *Environmental enrichment*. As reported by Rivera et al. [28], the animal environment can be improved by placing cotton in the cages of the mother to stimulate nesting behavior so that the litter stays together and conserves heat better. After weeding, two to three cardboard tubes are placed inside the cage. This simulates burrowing and helps the litter to maintain its temperature. These tubes can also serve to familiarize the rats with the holders used to measure blood pressure.
2. *Social enrichment*. After weaning, the offspring are not separated by sexes, as is usually done. Instead, they remain together longer; the separation by sexes is done a month and a half later. Also, the litter is not immediately passed to a clean cage, but it remains in the cage shared with the mother and the cotton nest, so that the familiar smell stays in the cage, reducing stress [28].

2.2 Materials for Noninvasive Blood Pressure and Heart Rate Measurements

The material details of any manufacturers provided in this article have the purpose to provide complete information about the experiments; we encourage you to use the manufacturers of your preference. Here, we describe the two methods that we use indistinctly to perform these measurements [29].

2.2.1 Materials for Blood Pressure and Heart Rate Measurements with Panlab (Harvard Apparatus) or Similar

1. Noninvasive plethysmograph device LE 5002 (Panlab Harvard Apparatus).
2. Pulse transducer and pressure cuff kit. Analogous to the sphygmomanometer used in humans.

   Use the kit LE5160R for juvenile or adult rats (>6 weeks postnatal).

   Use the kit LE5160M for young rats (3–5 weeks postnatal).

3. Rat holder (plexiglass restraining device) to keep the rat relatively immobilized during measurements.

   Use rat holder LE5022 for juvenile or adult rats (>6 weeks postnatal).

   Use rat holder LE5018 for young rats (3–5 weeks postnatal).
4. The rat holder is attached to the individual heater chamber LE5610A (*see* **Note 1**).
5. Plastic animal cage with a thin layer of sawdust bed.
6. Small thermal heating pad (Chattanooga Theratherm or similar) with temperature control to place under the rat's cage before its introduction into the rat holder (*see* **Note 1**).

2.2.2 Materials for Blood Pressure and Heart Rate Measurements with CODA (Kent Scientific Corporation) or Similar

1. CODA 2-Channel High Throughput Noninvasive Blood Pressure system which consists of:
2. Laptop computer with the CODA software installed.
3. CODA controller connected by USB to the computer.
4. Occlusion and VPR (volume pressure recording) cuffs, appropriately connected to the controller's output channels.
5. Plastic rodent holder. Small-sized rodent holder and small occlusion and VPR sensor cuffs for rats 8–80 g, medium-sized rodent holder and medium-sized occlusion and VPR sensor cuffs for rats 80–500 g, large-sized rodent holder and large occlusion and VPR sensor cuff for rats >500 g.
6. An animal warming platform.
7. An infrared thermometer.
8. A warming pad with temperature control to pre-heat rodents in their cage before measurements.

2.3 Materials for the Preparation of Primary Cultures of Chromaffin Cells

1. Ca^{2+}/Mg^{2+}-free Hank's solution (HS).
2. Collagenase type-1 and DNase type-1.
3. Dulbecco's Modified Eagle Medium.
4. Fetal bovine serum (FBS), insulin, penicillin-streptomycin, poly-L-lysine.
5. Cell strainer (40 μm).
6. Fire-polished siliconized glass Pasteur pipettes.
7. #1 round glass coverslips of 18 mm in diameter.
8. Sterile 12-well cell culture plates.
9. Standard culture room facilities (laminar flow hood and CO_2 incubator) with a stereomicroscope.

2.4 Materials for the Preparation of Adrenal Gland Slices

1. A 95% O_2/5% CO_2 outlet or tank with a pressure meter to connect silicone tubing outlets to oxygenate several solutions (two-three bubbles/s; *see* **Note 2**).
2. Use ultrapure deionized water (resistivity >18 MΩ/cm) and analytical grade reagents to prepare the solutions (*see* **Note 3**).
3. *Standard Krebs-Ringer Bicarbonate (KR-B)* solution: 125-mM NaCl, 2.5-mM KCl, 2-mM $CaCl_2$, 1-mM $MgCl_2$, 26-mM $NaHCO_3$, 1.25-mM NaH_2PO_4, and 10-mM of glucose (500 mL).
4. *Low* Ca^{2+} *KR-B* solution, replacing from the standard KR-B recipe, 2-mM $CaCl_2$ with 0.1-mM $CaCl_2$ and adding 3-mM $MgCl_2$. Both KR-B solutions must be continuously oxygenated with 95% O_2/5% CO_2 (100 mL, *see* **Note 2**).
5. Agarose solution 3%. Weigh 0.3 g of agarose and add 10 mL of KR-B solution, store at room temperature until its use.
6. Stereomicroscope.
7. Nunc cell culture 4-well plates or similar to pour the agarose solution.
8. Petri dish (35 mm), scalpel, spatula, forceps No. 5 (Dumont or similar), cyanoacrylate glue, thin razor blades.
9. Vibratome Leica VT1000S or similar.
10. Paintbrush (No.4) or fire-polished Pasteur pipettes to handle adrenal slices.
11. Slice incubation chamber (BSK-4 AutoMate Scientific) or custom designed. For custom-made, remove the bottom of a plastic beaker (50 mL) and replace it with a nylon mesh. Then, place it into another beaker (100 mL) filled with KR-B solution and bubble gently with 95% O_2/5% CO_2.

2.5 Materials for Amperometry

2.5.1 Materials for the manufacturing of Carbon Fiber Microelectrodes

1. Stereomicroscope.
2. Carbon fiber of 10 μm in diameter.
3. Polypropylene tube (pipette tips Z7440030, Sigma-Aldrich or similar).
4. Borosilicate glass capillary (1.2/1.0 mm OD/ID).
5. Micropipette Puller P-97 (Sutter Instrument or similar).
6. Micromanipulator (MPC-200, Sutter Instrument or similar).
7. Thin razor blade or scalpel blade.
8. Epoxy glue.
9. CD ROM coated with fine diamond sandpaper.

2.5.2 Materials for Amperometry in Cultured Cells and Adrenal Slices

1. *For slices*: An upright microscope with 20× and 40× long working distance water immersion objective. For cultured cells, an inverted microscope is more convenient.
2. EPC-10 HEKA amplifier or similar to control the carbon fiber microelectrode voltage in the range ±1 V, running under voltage-clamp mode with the PatchMaster software (HEKA Elektronik, Lambrecht, Germany) or similar.
3. Commercial carbon fiber microelectrodes (895162, 895163 HEKA; CF WPI) or custom-made. *See* Subheadings 3.5 and 3.6 construction of carbon-fiber microelectrodes.
4. Specific holder for commercial carbon fiber microelectrodes (895302 HEKA or similar).
5. Vacuum connection for suction of waste perfusate into a glass Erlenmeyer flask.
6. Micromanipulator.
7. Local perfusion pipette for the gravity-fed system positioned with a micromanipulator with coarse and fine movements.
8. *For cultured CCs*: Krebs/HEPES (K-H) solution: 135-mM NaCl, 4.7-mM KCl, 1.2-mM KH_2PO_4, 1.2-mM $MgCl_2$, 2.5-mM $CaCl_2$, 10-mM glucose, and 15-mM HEPES (500 mL, pH 7.3 adjusted with NaOH) (*see* **Note 3**).
9. *For adrenal slices*: Krebs-Ringer Bicarbonate (KR-B) solution: 125-mM NaCl, 2.5-mM KCl, 2-mM $CaCl_2$, 1-mM $MgCl_2$, 26-mM $NaHCO_3$, 1.25-mM NaH_2PO_4, and 10-mM of glucose (500 mL), continuously oxygenated with 95% O_2/5% CO_2 (*see* **Note 3**).
10. For brief cell depolarization, high-K^+ solution: 60-mM KCl, 85-mM NaCl, 2-mM $CaCl_2$, 1-mM $MgCl_2$, 10-mM HEPES, 10-mM glucose (50 mL, pH 7.3 adjusted with NaOH; *see* **Note 3**).
11. *3-M KCl solution* (10 mL) or mercury 5 mL to facilitate electrical contact between the carbon fiber microelectrode and the amplifier head-stage.

2.5.3 Materials for Intracellular Calcium Imaging

1. Cell-permeable fluorescent calcium indicator fluo-4 AM (1 mg; Invitrogen, or similar).
2. #1 Glass coverslips 18 mm in diameter coated with 0.3% poly-L-lysine.
3. Pluronic acid F-127 solution 0.5% in DMSO. Use an ultrasonic bath until dissolved (30 min to 1 h).
4. Fluo-4 AM *stock solution* at 10-mM concentration in DMSO. Keep in an ultrasonic bath (5–10 min) until dissolved. Split into 1 μL aliquots.

5. Fluo-4 AM *loading solution,* mix 1 μL of fluo-4 10 mM in 9 μL of Pluronic acid 0.5%, ultrasonicated for 5 min. Then complete to 1 mL with gassed KR-B (adrenal slice) or 2 mL of K-H (cultured cells) and ultrasonicate for 5 extra min. This gives a working concentration of 10 and 5 μM, respectively.
6. *High [K^+] solution*: 60-mM KCl, 80-mM NaCl, 2-mM $CaCl_2$, and 10-mM HEPES, pH = 7.4 (*see* **Note 3**).
7. *Caffeine solution*: 10-mM caffeine in K-H solution.
8. *For adrenal slices*: Open round bath imaging/recording chamber for tissue slice studies (Warner RC-27LD or custom-made) with Nylon mesh to hold adrenal slices in place, attached to the stage of an upright microscope equipped with a water immersion long working distance objective (20×, 40×, 0.8 NA) and a cooled digital CCD camera.
9. *For cultured cells*: Open round bath imaging/recording chamber (Warner Series 20 or custom-made) attached to the stage of an inverted microscope equipped with oil immersion objectives (20×, 40×, 1.2 NA) and a cooled digital CCD camera.
10. Argon laser or an alternative light source emitting at 480 nm (e.g., Xenon or Mercury lamp, LED).
11. Yokogawa spin-disk confocal scan head (CSU10B, Yokogawa Electronic, or similar).
12. Vacuum connection for liquid waste disposal from perfusion system.

3 Methods

3.1 Blood Pressure and Heart Rate Measurement Methods Using Panlab

1. Perform blood pressure (BP) measurements in a noiseless environment. The person who will perform the measurements must remain calm and tolerant to prevent unnecessary stress to the rats (*see* **Note 1**).
2. Restrict food and water for 2 h before BP measurements (*see* **Note 4**). Place the animal cage with the rat inside on the thermal heating pad set at 30 °C for 30 min before measurements. This maneuver favors vasodilation (*see* Fig. 1a).
3. Habituate animals to the restraining device, pressure cuff, and pulse transducer at least on three occasions before BP measurements (*see* **Note 5**). The restraining device must be adequate in size so that the rat remains straight and cannot curve its body. Rats should be introduced in this device 10–15 min before measurements to minimize stress.
4. BP should be measured at approximately the same time of day between 9 AM and 12 noon for 4–5 days and on the day of the animal's use for experimentation (*see* **Note 4**).

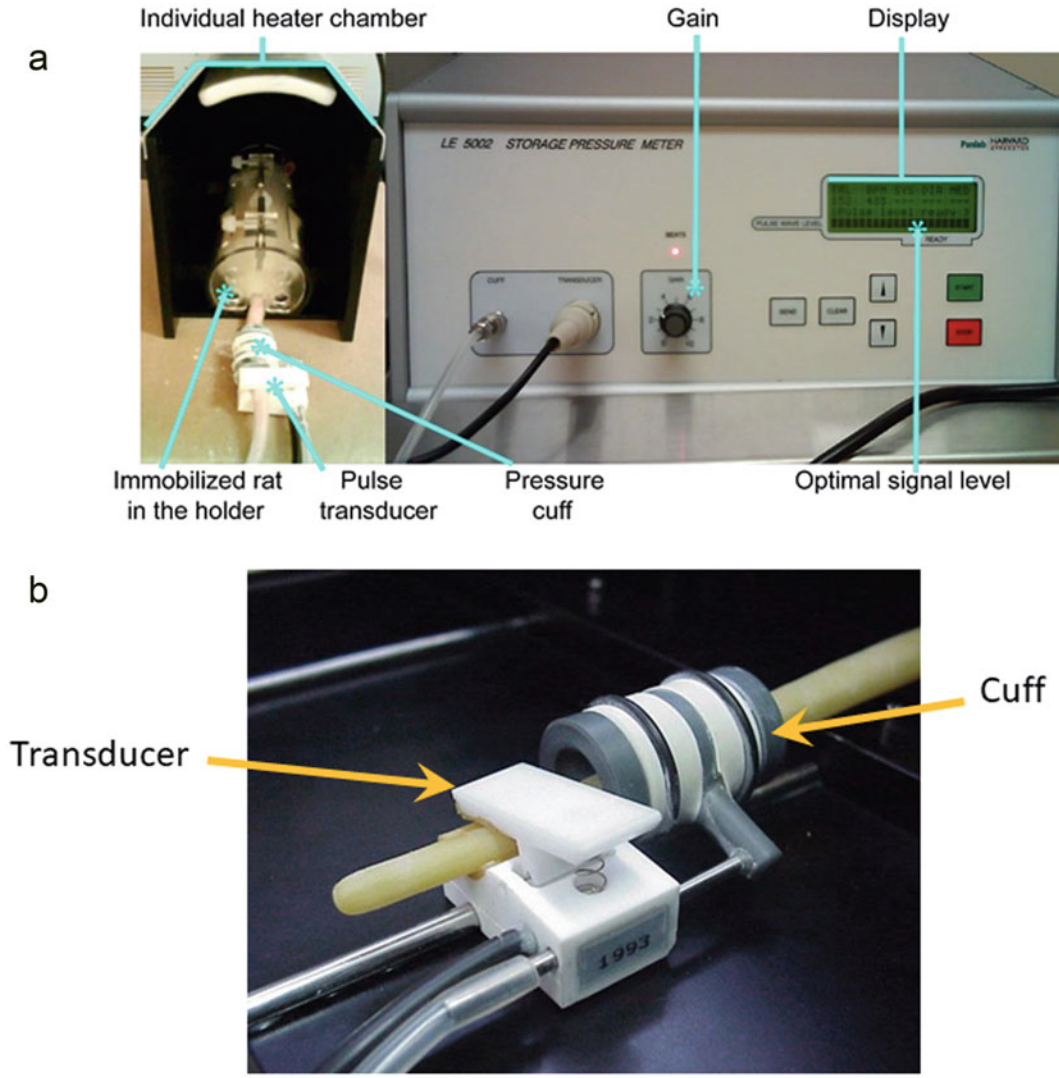

Fig. 1 (**a**) Noninvasive plethysmograph device LE 5002 (Panlab Harvard Apparatus) with a rat in the holder. (**b**) Pulse transducer and pressure cuff in place in the rat tail

5. Place the rat carefully inside the plexiglass restraining device; the tail should be free and clean to adjust the pressure cuff and pulse transducer. The restraining device with the rat inside is placed inside the heater chamber (LE5610A) set at 30 °C to maintain vasodilation.
6. Place the pulse transducer and the pressure cuff in the middle section of the tail. The distance between the pressure cuff and pulse transducer should not exceed 2 cm to avoid incorrect measurements (*see* Fig. 1b). The transducer and the pressure cuff operate over the caudal artery. To obtain a better signal, slightly rotate the pulse transducer on the tail.

7. Check the signal in the plethysmograph. The gain should be set between 2 and 5. When the pulse transducer is placed correctly, the "beats per minute" signal should be stable (*see* **Note 6**: Fig. 1a).
8. When the pulse wave amplitude is steady, a READY message appears on the display (*see* Fig. 1a). Press the start button of the plethysmograph to measure the BP (*see* **Note 7**).
9. The measurement, using the pressure cuff and pulse transducer, is analogous to the sphygmomanometer used in humans: the pressure cuff occludes the passage of blood in the rat's tail, and the transducer captures the BP pulses.
10. The plethysmograph displays the measurements obtained: BPM = beats per minute, SYS = systolic pressure, DIA = diastolic pressure, and MEAN = mean pressure; these values are stored in the internal memory of the instrument.
11. BP (systolic and diastolic) and heart rate should be measured three to four times with 5 min intervals, and values can be averaged.

3.2 Blood Pressure and Heart Rate Measurement Methods Using CODA

1. Follow **steps 1–4** of Subheading 3.1 (Panlab).
2. Verify that components of the CODA system are properly connected: CODA controller must be connected to the computer through a USB cable, and their output channels must be connected to the corresponding occlusion and VPR sensor cuffs (*see* Fig. 2a).
3. Check that the cuff bladder from the occlusion and VPR sensor cuffs are not cracked. From time to time, it is convenient to run the protocol of the CODA software to verify for possible leaks on the cuff bladders for replacement.
4. Turn on the animal warming platform and set it to level 2 (~35 °C). This temperature is needed to induce vasodilation in the rat, which enhances the blood flow to the tail.
5. Place a pre-warmed rat (*see* **step 4** of Subheading 3.1) into the corresponding plastic holder according to its weight. Adjust the plastic holder in such a way that the animal is comfortable inside and the animal's tail retains the warmth during recordings (*see* **Note 1**).
6. Place an occlusion cuff on the rat's tail, adjusting its position close to the tail base. Make sure that the cuff fits properly, i.e., it must slide freely, but fits closely when not pressurized (*see* Fig. 2b).
7. Repeat **step 6** using a VPR sensor cuff, positioning it just behind the occlusion cuff without touching it to avoid inappropriate measurements (*see* Fig. 2b).

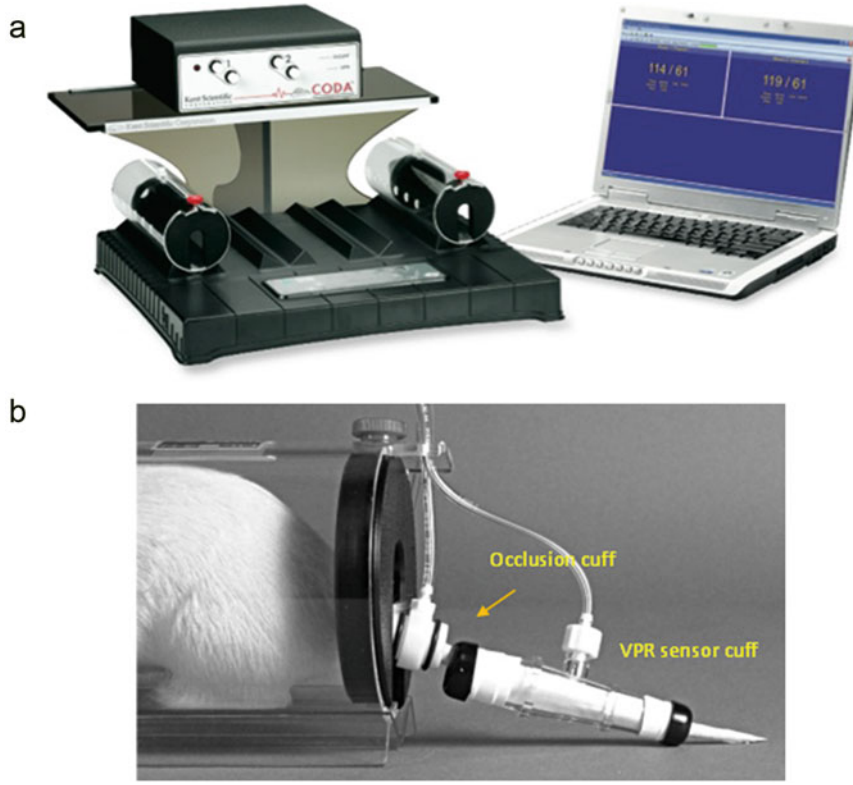

Fig. 2 (**a**) Noninvasive CODA 2-Channel High Throughput Noninvasive Blood Pressure system. (From CODA high-throughput manual. Kent Scientific Corp.) (**b**) Correct placement of the occlusion cuff and VPR sensor cuff in the rat tail. (From CODA high-throughput manual. Kent Scientific Corp)

8. Set up the CODA software to perform three acclimation cycles and ten regular cycles with a deflation time set to 20 s. It is highly recommended not to perform more than 10–13 recordings per experiment, to avoid unnecessary stress on the rat (*see* **Note 1**). The values from these recordings are averaged.
9. Just before starting recordings, be sure that the rat's tail is at an appropriate temperature by pointing the infrared thermometer at the tail base. It is critically important to start the recordings once the tail base temperature is between 32 and 35 °C to ensure proper blood flow to the tail.
10. Run recordings with the CODA software observing the display on the computer screen. The blue line drops gradually at the beginning of each cycle meaning that there are no leaks in the VPR sensor cuff. The same must be happening for the occlusion cuff (red line on the display). When there are leaks at the VPR sensor or occlusion cuffs, either the blue or red line drops precipitously. The faulty cuff or sensor should be replaced.

11. After each run, the CODA system will display six parameters: systolic pressure, diastolic pressure, mean pressure, heart rate, tail blood volume, and tail blood flow [29].

3.3 Preparation of Primary Cultures of Chromaffin Cells

1. Wash and sterilize glass coverslips and coat them with poly-L-lysine (0.01% solution during 15–20 min), wash three times with sterile pure water (*see* **Note 3**), and let them dry before use. Place coverslips on the bottom of 12-well cell culture plates.
2. Juvenile or adult rats are anesthetized by intraperitoneal administration of ketamine (80 mg/kg) and xylazine (10 mg/kg). Euthanize the animals by decapitation.
3. Remove adrenal glands under aseptic conditions and immerse them in sterile ice-cold Ca^{2+}/Mg^{2+}-free Hank's solution (HS). Under a stereomicroscope, trim glands of excessive fat and separate the adrenal medullas with scissors and needles.
4. In the laminar flow hood, incubate medullas in Ca^{2+}/Mg^{2+}-free HS pH = 7.4 with 2-mg/mL collagenase type-1 and 1.5-mg/mL DNase type-1 for 30–40 min at 37 °C. Every 10 min gently triturate the fragments with a fire-polished siliconized Pasteur pipette, until the larger fragments are dissociated.
5. After 30–40 min of incubation with the enzymes, gently triturate the remaining tissue fragments, centrifugate at 120 × *g* for 5 min, discard the supernatant, and resuspend pellet in fresh HS.
6. Filter the sample through a Falcon Cell Strainer. Centrifugate at 120 × *g* for 5 min, discard the supernatant, and resuspend the pellet in DMEM supplemented with 10% FBS, 5-μg/mL insulin, 10,000-U penicillin, and 10-mg/mL streptomycin.
7. Plate 10^3–10^4 cells per well. Allow cells to settle for 20 min and add 1 mL of supplemented DMEM at 37 °C in a humidified atmosphere (95% air, 5%CO_2).
8. CCs cultures can be used for recordings 24–48 h after plating.

3.4 Preparation of Adrenal Gland Slices

1. Animals are anesthetized by intraperitoneal administration of ketamine (80 mg/kg) and xylazine (10 mg/kg) and sacrificed by decapitation.
2. The rat body is placed in the prone position (ventral), and the kidneys are accessed through a flank incision, the kidney is lifted with forceps, and the adrenal glands surrounded by fatty tissue are removed under aseptic conditions and placed in a 35-mm Petri dish filled with sterile ice-cold low Ca^{2+} KR-B solution bubbled with 95% O_2/5% CO_2 (*see* **Note 2**).

3. Under a stereomicroscope, remove the excess fat from the adrenal glands using a straight tip of the forceps. Do not remove the connective tissue capsule that surrounds the gland, since it helps to maintain the agar attached to the adrenal slice (*see* **Note 8**).
4. Heat the 3% agarose solution until nearly boiling. Then, pour the mixture in two wells of a Nunc multi-well dish (four wells) or similar.
5. Remove the excess liquid by placing the glands on filter paper for about 5 s, and immediately immerse the glands into the agarose solution which should be at about 30 °C (*see* **Note 9**).
6. Place the wells with agarose and embedded glands on ice for about 5 min until the agarose solidifies.
7. Move a spatula or tip forceps along the edge of the well to detach the agarose blocks from the wells (*see* **Note 10**).
8. Place each agar block on parafilm, and with a scalpel, trim it as a cube of approximately 5 mm per side, keeping the glands embedded in the center of the block.
9. Put a drop of cyanoacrylate glue on the specimen holder of the vibratome and then place two agar blocks, each with an embedded gland, and pour ice-cold low Ca^{2+} KR-B solution into the cutting chamber. Cold KR-B solution maintains the agar block firmness while cutting (*see* **Note 11**).
10. For adult adrenal glands, set the thickness at 200 μm. For young rats, slices should be 150 μm thick. The vibration frequency should be set at 0.5 mm/s in 1-mm amplitude and the blade angle between 40° and 50°.
11. The slices can be handled with a brush or sucked into a glass Pasteur pipette and then placed gently into a slice holding chamber containing KR-B at room temperature (22–25 °C) continuously bubbled with 95% O_2/5% CO_2 (*see* **Note 12**). Slices should be allowed to recover for at least an hour before initiating electrophysiological recordings or calcium imaging.

3.5 Manufacture of Plastic-Encased Carbon Fiber Microelectrodes

1. Perform these steps under a stereomicroscope.
2. The carbon fiber of 10 μm in diameter should be cut to approximately 2–3 cm in length.
3. Insert the carbon fiber into a polypropylene tube (*see* Fig. 3a). Yellow pipette tips (Sigma Aldrich Z740030) or similar can be used. Fill the pipette tip with 2-propanol to reduce the static attraction between the fiber and the polypropylene, so the fiber can slip along the tube, preventing its fracture [30, 31].
4. Place the pipette tip with fiber inside on absorbent paper to eliminate 2-propanol.

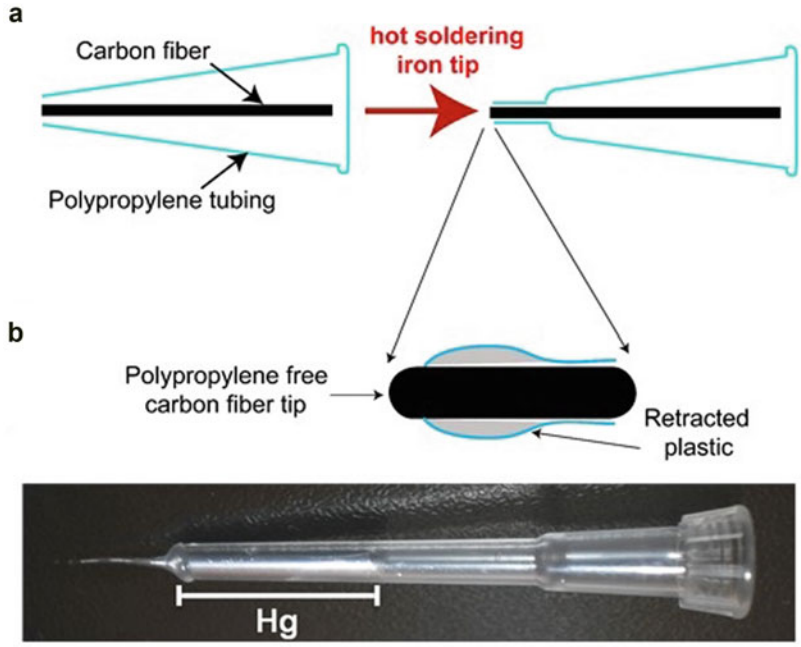

Fig. 3 Construction of polypropylene carbon fiber microelectrodes

5. Bring the pipette tip closer to a hot soldering iron tip. When the polypropylene melts, gently pull the ensemble, so that the melted polypropylene forms a tight seal around the carbon fiber.
6. In a narrowed part of the device, cut with a thin razor blade to expose the carbon fiber tip inside. Move the microelectrode tip close to the hot soldering iron tip to retract plastic debris from the carbon fiber tip (*see* Fig. 3a).
7. Seal the plastic tubing to the glass capillary using epoxy glue and allow it to harden.
8. Before the experiment, cut the carbon fiber electrode close to the plastic tip using a new scalpel blade.
9. The plastic electrodes are backfilled with mercury or 3-M KCl solution to allow the electrical connection to the Ag/AgCl filament of the head-stage (*See* Fig. 3b).
10. Plastic electrodes become insensitive with use and must be discarded.

3.6 Manufacture of Glass-Encased Carbon Fiber Microelectrodes

1. Glass microelectrodes are made as in [31] with some modifications.
2. Under a stereomicroscope, insert a carbon fiber of 10 μm in diameter along the capillary into a borosilicate glass capillary (1.2/1.0 mm OD/ID; *see* Fig. 4).

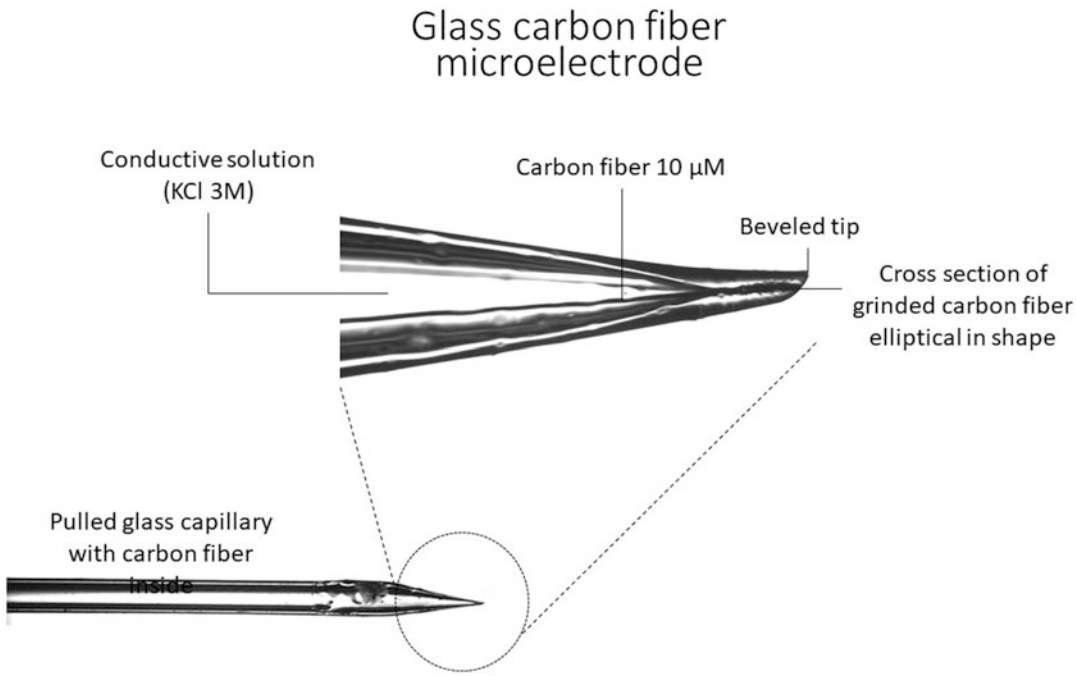

Fig. 4 Construction of glass carbon fiber microelectrodes

3. Heat the glass capillary at the center and pull it by using a puller. Cut the exposed carbon fiber at the level of pulled glass tip and then immerse the capillary in epoxy glue at ~80 °C for 5 min and curate it in a dry atmosphere set at ~100 °C for 24 h until complete sealing.
4. With a micromanipulator, press the glass capillary tip at an angle of 30–45° against the grinding surface of a spinning CD room coated with fine diamond sandpaper.
5. During this process, the surface contact should be constantly humidified with isopropanol as a lubricant. The final microelectrode tip should be elliptical in shape.
6. The electrodes are backfilled with a 3-M KCl solution to allow the electrical connection to the Ag/AgCl filament of the head-stage (*see* Fig. 4).
7. Unlike the plastic electrodes, glass microelectrodes can be reused after brief repolishing.

3.7 Single-Cell Amperometry Recordings

3.7.1 Amperometric Recordings

1. Connect the back end of the microelectrode to the patch-clamp amplifier. To ensure electrical contact between the carbon fiber and the Ag-Ag/Cl wire of the amplifier head-stage, fill the pipette with mercury or 3-M KCl solution.
2. Electrodes are tested and calibrated before their use for amperometry: For this purpose, set microelectrode voltage at

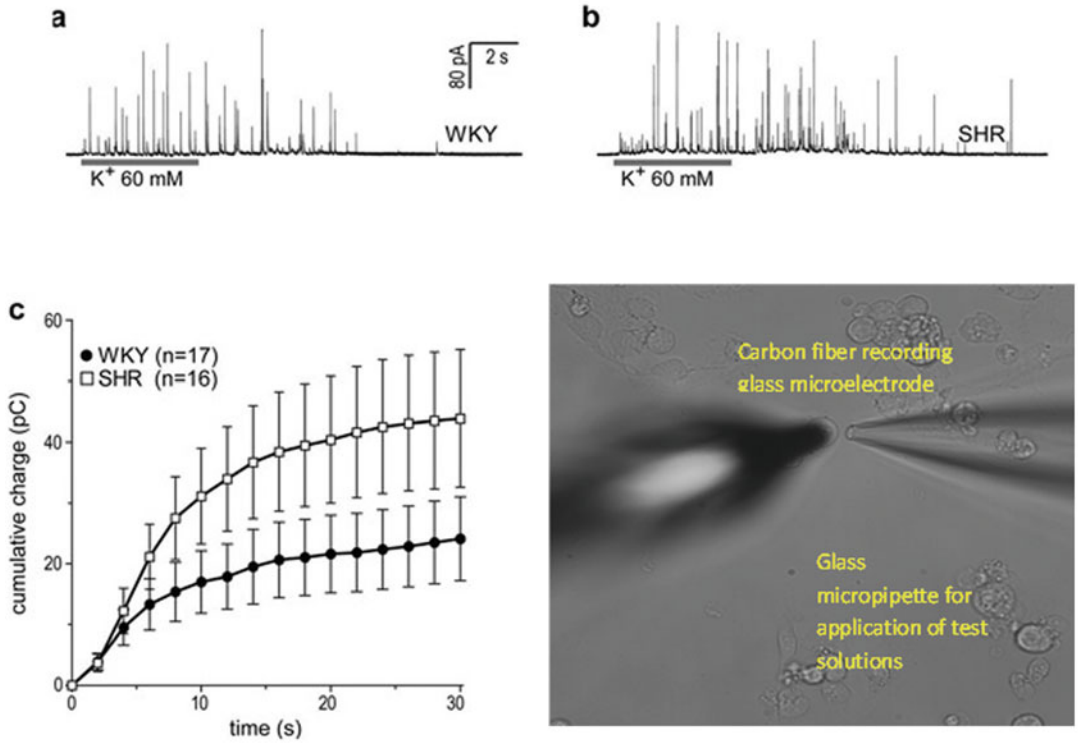

Fig. 5 Single-cell amperometric recordings. (**a**, **b**) Representative amperometric spikes elicited by a 5-s-long depolarizing pulse with high K^+ (**a**) WKY and (**b**) SHR CC. (**c**) Mean cumulative charge overtime of amperometric spikes for WKY (black circles) and SHR CCs (white squares). Membrane depolarization elicited a burst of spikes whose cumulative charge integral was approximately twofold higher in SHR than in WKY CCs (43.8 ± 11.2 pC vs. 24.1 ± 6.9 pC, respectively; mean $\pm$ SEM; $p < 0.001$). The number of cells examined is shown in parentheses. Single-cell amperometric recording with a glass carbon fiber microelectrode. (Taken from ref. 6, Fig. 1)

+700 mV and expose the tip to a puff of 50-μM adrenaline. Insensitive electrodes (i.e., adrenaline-induced amperometric current <200 pA) are discarded.

3. With the aid of a high-precision micromanipulator, place the tip of the microelectrode in close apposition to the cell membrane (*see* Fig. 5; *see* **Notes 13** and **14**).
4. Set the microelectrode voltage at +700 mV against an Ag/AgCl bath reference electrode while recording current continuously in voltage-clamp mode. Signal acquisition at 4 kHz or more is suggested to resolve the kinetics of real-time amperometric spikes which represent the oxidation of catecholamines released from exocytosis of single dense-core vesicles from the chromaffin cell surface.
5. Occasionally when the microelectrode touches the cell, it elicits a burst of amperometric spikes; in that case, we discontinue the recording because the ready-release pool of vesicles was altered and the stimulated release pool could be compromised.

6. Depending on the experimental protocol, it is advised to first obtain amperometric recordings from unstimulated cells for 5 min. Check if spontaneous catecholamine secretion events occur. Then evaluate the cell's response to test solutions contained in the micropipette perfusion system (high K^+, caffeine, nicotine, acetylcholine, etc.; *see* Fig. 5; *see* **Note 15**).
7. Test solutions are applied by gravity through an electronic valve-controlled puffer micropipette located near (~100 μm) the cells under study. Alternatively, a glass micropipette connected to a Picospritzer® or similar pressure injection device can be used to deliver test solutions (*see* Fig. 5).

3.7.2 Amperometric Recordings in Primary Cultures of Chromaffin Cells

1. Place a coverslip containing CCs in the bottom of a recording chamber on the stage of an upright microscope equipped with a long working distance water immersion 40× objective (*see* **Note 13**). An inverted microscope can also be used.
2. Cultures must be continuously perfused (2 mL/min) with K-H solution.
3. To monitor single-cell catecholamine release, select a healthy-looking chromaffin cell (*see* Fig. 5).

3.7.3 Amperometric Recordings in Chromaffin Cells of Adrenal Gland Slices

1. Place the adrenal slice in the bottom of a recording chamber on the stage of an upright microscope; put the nylon slice anchor over the slice. Make sure the medulla is not positioned underneath a nylon thread (*see* **Note 16**).
2. The slice should be perfused at 2 mL/min with KR-B solution oxygenated with 95% O_2/5% CO_2. Use the vacuum connection of the perfusion system to drain the waste solution into an Erlenmeyer flask.
3. Focus on the surface of the adrenal gland medulla with a long working distance water immersion objective (20×). With a manipulator, position the local perfusion pipette at ~100–150 μm from the cell under-recording to deliver the stimuli (*see* **Note 13**).
4. Select a healthy-looking chromaffin cell just beneath the surface of the slice.

3.8 Amperometric Spike Analysis

1. The oxidation product of CA released from a single secretory granule will be detected as amperometric spikes. The amperometric individual spike can be identified, measured, and analyzed to obtain a statistical analysis of frequency, amplitude, and kinetics parameters [32, 33].
2. For spike detection, use filters to remove high-frequency noise (Bessel or Gaussian) and filters that can remove 50/60 Hz noise from recordings.
3. Typically, the threshold to detect spikes is set at twice the standard deviation of the noise, calculated from a segment of recording without spikes.

4. Run the automatic spike detection. Only positive and monophasic spikes that returned to baseline are analyzed.
5. Verify each spike selected by the Quanta Analysis application [32]; it allows to add or delete spikes with a high magnification view.
6. Kinetic parameters of spikes include charge (picocoulombs), oxidized molecules, amplitude, half-width ($t^{1/2}$), rise time, rise slope, fall time, fall fit (single or double exponential fit), start, and end of the spike, among others; it also includes foot detection parameters: charge (picocoulombs), oxidized molecules, amplitude, and foot duration (*see* **Notes 15** and **17**).
7. Statistical analysis, frequency histograms, and Gaussian curve fitting can be performed using commercial statistics software or a costume-designed program. Results are expressed as mean ± S.E.M. Unpaired t-test is used, and in some cases, one-way ANOVA followed by Tukey's multiple comparison test is preferred. A p value <0.05 is taken as the limit of significance.

3.9 Single-Cell Intracellular Calcium Imaging

3.9.1 Intracellular Calcium Imaging in Primary Cultured Chromaffin Cells

1. See above: primary cultures of adrenal CCs.
2. Incubate a coverslip containing CCs for 30 min at room temperature with 2 μM of the cell-permeable Ca^{2+} indicator fluo-4 AM.
3. Wash twice the coverslip containing labeled CCs and place it in the bottom of the recording chamber attached to the stage of an upright or inverted microscope with continuous perfusion (2 mL/min) with K-H solution with a gravity-fed perfusion system.
4. All intracellular Ca^{2+} imaging experiments are performed at room temperature (22–24 °C).

3.9.2 Intracellular Calcium Imaging in Chromaffin Cells of Adrenal Gland Slices

1. See above for the preparation of rat adrenal slices.
2. In a 35-mm Petri dish, incubate the adrenal slice adhered to a glass coverslip with the fluo-4 *loading solution* (final dye concentration 20 μM, with 0.5% Pluronic acid) for 35 min at room temperature in the dark (*see* **Note 18**).
3. Wash at least three times with fresh Krebs-Ringer Bicarbonate (KR-B) saturated with 95% O_2/5% CO_2. During this manipulation, avoid slice flipping over under any circumstance (*see* **Note 19**).
4. Place the slice in the bottom of a plexiglass slice recording chamber on the stage of the microscope. Perfuse continuously (2 mL/min) with KR-B saturated with 95% O_2/5% CO_2 into the recording chamber by a gravity-fed system at room

temperature (22–25 °C). Use a slice anchor to hold the tissue in place (*see* **Note 20**).

5. View the adrenal slice with a long working distance water immersion objective (20×, 0.5 NA), centering the medullae in the field of view and focusing just below the surface, since cells at the surface are damaged by the cutting blade (*see* **Note 21**).

3.9.3 Intracellular Calcium Imaging

1. First, adjust illumination intensity and exposure. For excitation of fluo-4, light is band-passed at 488 nm, and emitted fluorescence is band-passed at 510 nm before its reflection into the camera port.
2. It is important to keep the illumination at a minimum to avoid photobleaching and photodamage. Use the acquisition live mode to focus. Illumination and image exposure should be synchronized during image acquisition to avoid overexposition and bleaching of the specimen. Also, it is best to do fluorescence imaging in complete darkness to avoid stray light contamination and improve the signal/noise ratio.
3. For fast confocal imaging of fluo-4 loaded in cells, a Yokogawa spin-disk confocal can be used (or a similar imaging system).
4. Fluorescence images should be acquired at 10–50 ms exposure and 100–500-m intervals with a cooled digital CCD camera. Acquire image sequences (movies) of about 2–5 min duration. An experimental run typically comprises several such episodes plus pauses. Total recording time per field should not exceed ~30 min to avoid bleaching and photodamage.
5. Save image sequences in multi-tiff format for analysis [34].
6. At the end of the experimental run, expose briefly (0.5–1 s) all cells in the field of view to a high $[K^+]$ solution, which depolarizes all healthy CCs, increasing their intracellular Ca^{2+} and therefore their fluorescence. Responsive cells are healthy CCs in the field of view (Fig. 6).

3.9.4 Recording Spontaneous and Evoked Intracellular Calcium Signals

1. Spontaneous calcium signals. Obtain image sequences (movies) of ~5 min in duration from unstimulated CCs from a field of view during perfusion with either normal K-H (culture) or KR-B (slice) solution.
2. Stimulus-induced Ca^{2+} signals. A stimulus (in our case either a 0.5 s long high $[K^+]$ or 2–5 s long caffeine solution) which increases intracellular Ca^{2+} is introduced into the bath or directly applied close to the imaging field of view with a local puffer pipette (Fig. 6).
3. Save fluorescence image sequences (movies) from all CCs in the field in multi-tiff format for subsequent analysis.

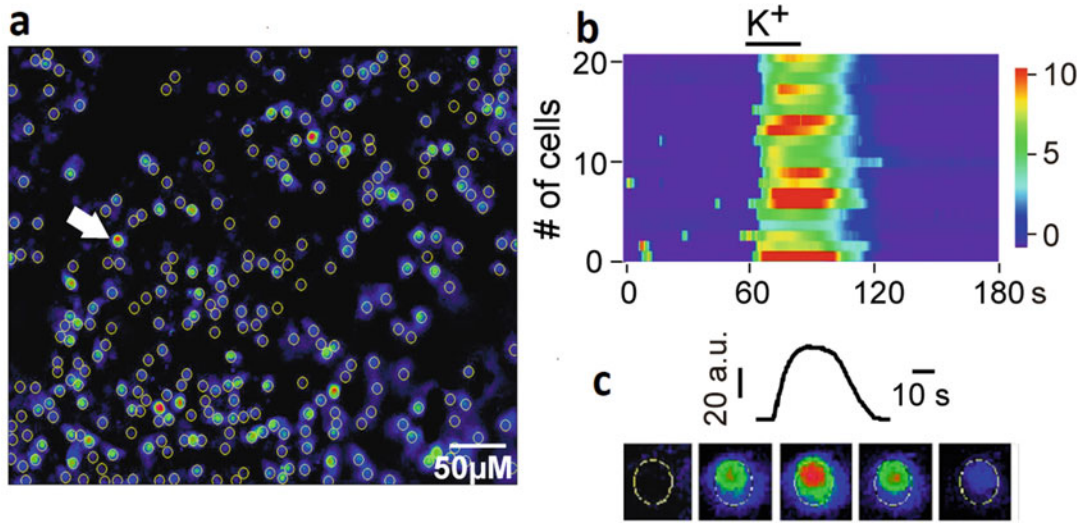

Fig. 6 Ca^{2+} imaging in adrenal medulla slices. (**a**) Standard deviation (SD) image from the adrenal medulla at the peak of the depolarization-induced Ca^{2+} entry. Yellow circles indicate regions of interest (ROIs) placed on cells that increased their fluorescence by >5 a.u. These ROIs were copied to the stack of ΔF (Fi − F0) images to obtain the ΔF over time values. (**b**) Twenty such ROIs were selected, and their K^+ responses are shown. Ordinate, cell number; abscissae, time. Fluorescence changes (ΔF) are displayed in pseudo-color. (**c**) Frames extracted from the movie of the CC indicated with a white arrow in (**a**), before, during, and after high-K^+ application. The depolarization-induced Ca^{2+} transient recorded from this cell is shown on top. (Taken from ref. 22, Fig. 1)

3.10 Data Analysis and Statistics

1. Fluo-4 is a single wavelength dye, and its fluorescence is a function of dye concentration, illumination pathway, and $[Ca^{2+}]i$. Our experiments are designed to maximize fluorescence changes associated with fluctuations of $[Ca^{2+}]i$.
2. Convert raw movies to ΔF movies: ΔF = Fi − Fo, where Fo is the average of the first five frames of the sequence and Fi represents each (i) fluorescence image of the set. ΔF values are expressed as arbitrary units (a.u.).
3. Regions of interest (ROIs) are drawn around each cell that responded to high K^+ with a fluorescence increase (SD > 5 ± 0.5) (Fig. 6). These ROIs are used for single-cell quantification of ΔF fluctuations throughout the entire experimental run [34].

4 Notes

1. External stimuli or stress can induce significant variations in BP in rodents. Precautions should be taken to avoid the stress or anxiety of the subject. Both the heater chamber and the

thermal pad are required to induce rat vasodilation with little or no stress so that measurements are more reliable.

2. KR-B solutions must be continuously oxygenated in separate reservoirs and connect silicone tubing outlets (1–2 mm internal diameter) from the pressure gauge of the 95% O_2/5% CO_2 tank. The number of silicone tubing outlets depends on the number of solutions needed (one for the cutting chamber solution, one for adrenal slices holding chamber, one or more for recording solutions, etc.). Bubbling should be approximately two to three bubbles per second.
3. Use ultrapure deionized water (resistivity 18 MΩ/cm) and analytical grade reagents to make extracellular bath recording solutions.
4. Take measurements at about the same hour of the day to avoid circadian variations. Restrict food and water 2 h before to minimize defecation and urination in the restraining device. The rat's tail must be kept clean and dry for better contact with the pressure cuff and pulse transducer.
5. For habituation, follow the same steps to measure BP while keeping the equipment turned off. The goal is to familiarize the rat with manipulation and to remain inside the rat holder with the pressure cuff and transducer in place.
6. When the pressure cuff is placed correctly (*see* Fig. 1b), it is not necessary to increase the gain of the plethysmograph. Gain settings greater than 5 can produce artifacts in the recordings from tail movements or muscular tremors due to anxiety or stress.
7. Check that the signal LEVEL of the plethysmograph reads READY before pressing the start button. If the signal level is too high, the measurement will automatically stop. If this happens, turn the gain potentiometer counterclockwise until the pulse level READY appears on the display.
8. If the connective capsular tissue is removed from the adrenal gland, it may not adhere sufficiently to the agarose, and the slices may peel and lose firmness during recording. To maintain the stability of the slice, it must be maintained firmly attached with agar.
9. Whisking gently a few times the glands once into the agarose solution allows a greater adherence of the gland with the agar.
10. To detach the agarose blocks with embedded glands, gently move the Dumont forceps or a spatula along the edge of the wells and then put the Nunc multidish upside down so that the blocks come out by gravity.

11. Place a 100-mL beaker with low Ca^{2+} KR-B solution in the freezer for 30 min before cutting to pour the cold solution into the cutting chamber.
12. To handle the freshly obtained slices, two methods can be used:
    - With a No. 4 paintbrush, recover the slices immediately after they are freed from the agarose block.
    - With the rear end of a siliconized glass Pasteur pipette, the slices can be recovered, immediately after cutting.
13. A long work distance (LWD) water immersion 20× objective should be used to have sufficient space to place and manipulate the microelectrode and approach the cell surface.
14. In the adrenal slice, CCs are arranged in clusters. If the electrode tip is placed on a cluster, and no amperometric spikes are observed, it means that cluster anatomy is preserved. Select a healthy-looking cell from an open cluster, where individual cells popping out can be distinguished.
15. During high K^+ application, the baseline of the amperometric recording can increase significantly, due to the massive release of catecholamines from stimulated cells contiguous to the recorded cell. This is observed more frequently in adrenal slice recordings.
16. When placing the slice anchor over the slice, leave the adrenal medulla area free of nylon threads, to have enough space to manipulate the carbon fiber microelectrode.
17. For more detailed information about the amperometric spike parameters, these articles can be consulted: Mosharov and Sulzer [32], Segura et al. [33].
18. Place a polyethylene tube with carbogen gas flowing near the surface of the fluo-4 *loading solution*. Do not allow the tube to touch the solution and produce gas bubbles that can be harmful to the slice.
19. During incubation with fluo-4 *loading solution*, oxygenation of the bottom of the slice is poor, and it is hard to find healthy cells in the bottom of the slice. Therefore, avoid flipping the slice over.
20. Holding the specimen steady during perfusion with a slice holder (e.g., Warner Instruments (SHD-40/2 WI 64-1415) or similar) is very important to avoid slice movement, motion artifacts, and defocusing that can affect the quality of the recordings.
21. Be advised that fluo-4 does not penetrate deeper than about 50 μm into the slice. Therefore, only two to three layers of fluo-4-loaded cells are visible underneath the surface.

References

1. Borkowski KR, Quinn P (1983) The effect of bilateral adrenal demedullation on vascular reactivity and blood pressure in spontaneously hypertensive rats. Br J Pharmacol 80:429–437. https://doi.org/10.1111/j.1476-5381.1983.tb10712.x
2. Lee RM, Borkowski KR, Leenen FH, Tsoporis J, Coughlin M (1991) Combined effect of neonatal sympathectomy and adrenal demedullation on blood pressure and vascular changes in spontaneously hypertensive rats. Circ Res 69:714–721. https://doi.org/10.1161/01.res.69.3.714
3. Lee RM, Borkowski KR, Leenen FH, Tsoporis J, Coughlin M (1991a) Interaction between sympathetic nervous system and adrenal medulla in the control of cardiovascular changes in hypertension. J Cardiovasc Pharmacol 17(suppl.2):S114–S116. https://doi.org/10.1097/00005344-199117002-00025
4. Lim DY, Jang SJ, Park DG (2002) Comparison of catecholamine release in the isolated adrenal glands of SHR and WKY rats. Auton Autacoid Pharmacol 22:225–232. https://doi.org/10.1046/j.1474-8673.2002.00264.x
5. Segura-Chama P, Hernández A, Jiménez-Pérez N, Alejandre-García T, Rivera-Cerecedo CV, Hernández-Guijo JM, Hernández-Cruz A (2010) Comparison of Ca^{2+} currents of chromaffin cells from normotensive Wistar Kyoto and spontaneously hypertensive rats. Cell Mol Neurobiol 30:1243–1250. https://doi.org/10.1007/s10571-010-9566-0
6. Segura-Chama P, López-Bistrain P, Pérez-Armendáriz EM, Jiménez-Pérez N, Millán-Aldaco D, Hernández-Cruz A (2015) Enhanced Ca(2+)-induced Ca(2+) release from intracellular stores contributes to catecholamine hypersecretion in adrenal chromaffin cells from spontaneously hypertensive rats. Pflugers Arch 467(11):2307–2323. https://doi.org/10.1007/s00424-015-1702-8. Epub 2015 Mar 21
7. Peña Del Castillo JG, Segura-Chama P, Rincón-Heredia R, Millán-Aldaco D, Giménez-Molina Y, Villanueva J, Gutiérrez LM, Hernández-Cruz A (2021) Development of the hypersecretory phenotype in the population of adrenal chromaffin cells from prehypertensive SHRs. Pflugers Arch 473:1775–1793. https://doi.org/10.1007/s00424-021-02614-2
8. Miranda-Ferrerira R, de Pascual R, de Diego AM, Caricati-Neto A, Gandía L, Jurkiewicz A, García AG (2008) Single-vesicle catecholamine release has greater quantal content and faster kinetics in chromaffin cells from hypertensive, as compared with normotensive, rats. J Pharmacol Exp Ther 324:685–693. https://doi.org/10.1124/jpet.107.128819
9. Miranda-Ferreira R, de Pascual R, Caricati-Neto A, Gandía L, Jurkiewicz A, García AG (2009) Role of the endoplasmic reticulum and mitochondria on quantal catecholamine release from chromaffin cells of control and hypertensive rats. J Pharmacol Exp Ther 329:231–240. https://doi.org/10.1124/jpet.108.147413
10. Borges R (1997) The rat adrenal gland in the study of the control of catecholamine secretion. Cell Dev Biol 8:113–120. https://doi.org/10.1006/scdb.1996.0130
11. Albillos A, Neher E, Moser T (2000) R-type Ca^{2+} channels are coupled to the rapid component of secretion in mouse adrenal slice chromaffin cells. J Neurosci 20:8323–8330. https://doi.org/10.1523/JNEUROSCI.20-22-08323.2000
12. Aldea M, Jun K, Shin HS, Andres-Mateos E, Solis-Garrido LM, Montiel C, García AG, Albillos A (2002) A perforated patch-clamp study of calcium currents and exocytosis in chromaffin cells of wild-type and alpha1A knockout mice. J Neurochem 81:911–921. https://doi.org/10.1046/j.1471-4159.2002.00845.x
13. Barbara JG, Takeda K (1996) Quantal release at a neuronal nicotinic synapse from rat adrenal gland. Proc Natl Acad Sci U S A 93:9905–9909. https://doi.org/10.1073/pnas.93.18.9905
14. Barbara JG, Poncer JC, McKinney RA, Takeda K (1998) An adrenal slice preparation for the study of chromaffin cells and their cholinergic innervation. J Neurosci Methods 80:181–189. https://doi.org/10.1016/s0165-0270(97)00200-813
15. Martin AO, Mathieu MN, Chevillard C, Guérineau NC (2001) Gap junctions mediate electrical signaling and ensuing cytosolic Ca^{2+} increases between chromaffin cells in adrenal slices: a role in catecholamine release. J Neurosci 21(15):5397–5405. https://doi.org/10.1523/JNEUROSCI.21-15-05397.2001
16. Martin AO, Mathieu MN, Guérineau NC (2003) Evidence for long-lasting cholinergic control of gap junctional communication between adrenal chromaffin cells. J Neurosci 23(9):3669–3678. https://doi.org/10.1523/JNEUROSCI.23-09-03669.2003
17. Iijima T, Matsumoto G, Kidokoro Y (1992) Synaptic activation of rat adrenal medulla

examined with a large photodiode array in combination with a voltage-sensitive dye. Neuroscience 51:211–219. https://doi.org/10.1016/0306-4522(92)90486-l

18. Voets T, Neher E (1999) Mechanisms underlying phasic and sustained secretion in chromaffin cells from mouse adrenal slices. Neuron 23: 607–615. https://doi.org/10.1016/s0896-6273(00)80812-0
19. Hernández-Guijo JM, Gandía L, Lara B, García AG (1998) Autocrine/paracrine modulation of calcium channels in bovine chromaffin cells. Pflugers Arch 437(1):104–113. https://doi.org/10.1007/s004240050754
20. Hernández-Guijo JM, Carabelli V, Gandía L, García AG, Carbone E (1999) Voltage-independent autocrine modulation of L-type channels mediated by ATP, opioids and catecholamines in rat chromaffin cells. Eur J Neurosci 11(10):3574–3584. https://doi.org/10.1046/j.1460-9568.1999.00775.x
21. Hernández A, Segura-Chama P, Jiménez N, García AG, Hernández-Guijo JM, Hernández-Cruz A (2011) Modulation by endogenously released ATP and opioids of chromaffin cell calcium channels in mouse adrenal slices. Am J Phys 300(3):C610–C623. https://doi.org/10.1152/ajpcell.00380.2010
22. Alejandre-García T, Segura-Chama P, Pérez-Armendáriz EM, Delgado-Lezama R, Hernández-Cruz A (2017) Modulation of spontaneous intracellular Ca^{2+} fluctuations and spontaneous cholinergic transmission in rat chromaffin cells in situ by endogenous GABA acting on $GABA_A$ receptors. Pflugers Arch - Eur J Physiol 469:1413. https://doi.org/10.1007/s00424-017-2041-8
23. Pinto YM, Paul M, Ganten D (1998) Lessons from rat models of hypertension: from Goldblatt to genetic engineering. Cardiovasc Res 39:77–88. https://doi.org/10.1016/S0008-6363(98)00077-7
24. Pinilla L, Rodriguez-Padilla ML, Sanchez-Criado J, Gaytan F, Aguilar E (1999) Mechanism of reproductive deficiency in spontaneously hypertensive rats. Physiol Behav 51(1): 99–104. https://doi.org/10.1016/0031-9384(92)90209-k
25. Cierpial MA, Shasby DE, Mc Carty R (1987) Patterns of maternal behavior in the spontaneously hypertensive rat. Physiol Behav 39(5): 633–637. https://doi.org/10.1016/0031-9384(87)90165-x
26. Myers MM, Brunelli SA, Squire JM, Shindeldecker RD, Hofer MA (1989) Maternal behavior of SHR rats and its relationship to offspring blood pressures. Dev Psychobiol 22(1):29–53. https://doi.org/10.1002/dev.420220104
27. Rose JL, Mc Carty R (1994) Maternal influence of milk intake in SHR and WKY pups. Physiol Behav 56(5):901–906. https://doi.org/10.1016/0031-9384(94)90321-2
28. Rivera C, Hernandez R, Marin H (2013) Reproductive management of colonies to spontaneously hypertensive rat (SHR) and normotensive Wistar Kyoto (WKY) in the Institute of Cellular Physiology, National Autonomous University of Mexico. Rev Electrón Vet 14(11B) http://www.veterinaria.org/revistas/redvet/n11113B.html
29. Daugherty A, Rateri D, Hong L, Balakrishnan A (2009) Measuring blood pressure in mice using volume pressure recording, a tail-cuff method. J Vis Exp 27:1291. https://doi.org/10.3791/1291
30. Machado DJ, Montesinos MS, Borges R (2008) Good practices in single-cell amperometry. Methods Mol Biol 440:297–313. https://doi.org/10.1007/978-1-59745-178-9_23
31. Kawagoe KT, Zimmerman JB, Wightman RM (1993) Principles of voltammetry and microelectrode surface states. J Neurosci Methods 48(3):225–240. https://doi.org/10.1016/0165-0270(93)90094-8
32. Mosharov EV, Sulzer D (2005) Analysis of exocytotic events recorded by amperometry. Nat Methods 2:651–658. https://doi.org/10.1038/nmeth782
33. Segura F, Brioso M, Gómez JF, Machado JD, Borges R (2000) Automatic analysis for amperometrical recordings of exocytosis. J Neurosci Methods 103(2):151–156. https://doi.org/10.1016/s0165-0270(00)00309-5
34. Patel TP, Man K, Firestein B, Meaney DF (2015) Automated quantification of neuronal networks and single-cell calcium dynamics using calcium imaging. J Neurosci Methods 243:26–38. https://doi.org/10.1016/j.jneumeth.2015.01.020

Chapter 11

Measurements of Calcium in Chromaffin Cell Organelles Using Targeted Aequorins

Jaime Santo-Domingo, Pilar Álvarez-Illera, Pablo Montenegro, Rosalba I. Fonteriz, Mayte Montero, and Javier Álvarez

Abstract

The molecular mechanisms that mediate and regulate calcium (Ca^{2+}) fluxes through the membranes of intracellular organelles play a key role in the generation and shaping of the local and global cytosolic Ca^{2+} signals triggering the process of regulated exocytosis in chromaffin cells. Beyond that role, intraorganellar Ca^{2+} homeostasis also regulates organelle-specific processes such as oxidative phosphorylation in mitochondria, maturation of secretory granules, or stress in the endoplasmic reticulum. In this chapter, we describe current methods to study mitochondrial, endoplasmic reticulum, and secretory vesicle calcium homeostasis in living chromaffin cells using engineered targeted aequorins.

Key words Aequorin, Calcium, Chromaffin cells, Organelles, Mitochondria, Endoplasmic reticulum, Secretory vesicles

1 Introduction

Historically, multiple tools and methods have been developed to assess Ca^{2+} fluxes in intracellular organelles. The methods range from initial approaches requiring the isolation of organelles combined with the use of Ca^{2+}-sensitive electrodes or radioactive labeling [1] to more modern luminescence and fluorescence-based targeted sensors that allow the study of organelle Ca^{2+} dynamics in its cellular context and even in whole body living organisms [2]. Fluorescence-based targeted sensors generally provide a good spatial resolution of the Ca^{2+} fluxes inside the cells using microscopy techniques and are suitable for continuous recording over long periods of time [3]. In contrast, aequorin-based sensors lack the spatial resolution provided by fluorescent Ca^{2+} sensors and display temporal constrictions given the irreversible nature of the photoreaction. Nevertheless, aequorin-based sensors generally provide better signal/noise ratio, display a broader dynamic range

Ricardo Borges (ed.), *Chromaffin Cells: Methods and Protocols*,
Methods in Molecular Biology, vol. 2565, https://doi.org/10.1007/978-1-0716-2671-9_11,

(allowing measurements in organelles with very different free Ca^{2+} levels with high accuracy), display less buffering capacity [4], and facilitate a simplest calibration method when compared with its fluorescent counterparts. These qualities have made the use of luminescent probes based on aequorin the tool of choice for many scientists trying to dig into the physiological relevance and the molecular mechanisms mediating Ca^{2+} fluxes in cellular organelles [5]. In particular, aequorins-based measurements significantly contributed to reveal new aspects of the mitochondrial [6], endoplasmic reticulum [7–9], and secretory vesicles [10, 11] Ca^{2+} homeostasis in chromaffin cells over the last 20 years.

Aequorin is a 21 kDa bioluminescent protein cloned from the jellyfish *Aequorea victoria* and belonging to the family of Ca^{2+}-activated photoproteins (Fig. 1a) [12]. These proteins are characterized for their ability to produce photons according to the level of Ca^{2+} in the nearby environment. At the molecular level, the Ca^{2+} sensitivity of the aequorin relies on the presence of three functional EF-hands (Fig. 1a). The ability to emit photons upon Ca^{2+} binding is fully dependent on its highly hydrophobic prosthetic group coelenterazine (Fig. 1a, in blue) and the presence of O_2. Ca^{2+} binding to the EF-hands triggers a conformational change that opens a hole into the hydrophobic core containing the coelenterazine binding site. The reaction proceeds as described in Fig. 1b. In the presence of O_2, coelenterazine cycles forming a dioxetanon ring, generating an extremely unstable compound that immediately breaks down generating CO_2, coelenteramide, and emitting one photon ($\lambda = 470$ nm). At this point, coelenteramide is discharged and bound Ca^{2+} is released. It is worth mentioning that reconstitution of aequorin is a very slow process; thus, in a regular experimental setting, we assume that aequorin molecules that already emitted a photon upon Ca^{2+} binding do not contribute more to light emission during the experiment. Aequorin molecules are therefore "consumed" as Ca^{2+} triggers the emission of light during the experiment.

Measurement of Ca^{2+} with the photoprotein aequorin requires a highly sensitive luminometer to quantify the number of photons emitted during the experiment. We describe the basic components of a custom-made luminometer and provide examples of commercially available plate readers suitable for aequorin measurements. Aequorin-based Ca^{2+} measurements also demand a robust mammalian expression vector. Efficient transduction or, alternatively, electroporation systems for effective expression of the photoprotein in primary chromaffin cells are thus necessary. Once aequorin is sufficiently expressed in the target organelle and just before initiating the photon recordings, organelle-localized aequorins are reconstituted with coelenterazine to generate the active form of the photoprotein. Depending on intracellular localization and the Ca^{2+} affinity of the aequorin variant used, several strategies of

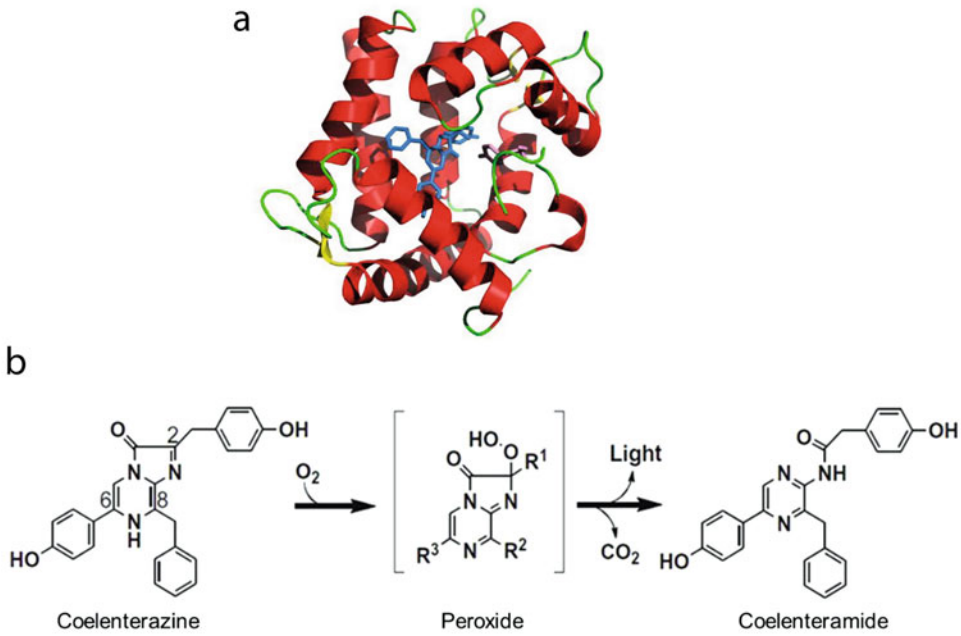

Fig. 1 Calcium sensitivity of the photoprotein aequorin. (**a**) Structural representation of aequorin highlighting the three EF-hand functional domains (helix-loop-helix motif) in red with turns in green and its prosthetic group, coelenterazine, in blue. (**b**) Representation of the reaction carried out by coelenterazine after oxidative decarboxylation

reconstitution will be described. The study of Ca^{2+} transport through the membranes of organelles usually require its perturbation. We describe common agonists, drugs, and approaches that can be efficiently used to perturb organelle Ca^{2+} fluxes in chromaffin cells. We finally show the procedure to transform photon recordings into Ca^{2+} concentration. In summary, in the next sections, we provide a detailed description of instrument, solutions, reagents, and protocols required to study organelle Ca^{2+} dynamics in chromaffin cells using organelle-targeted aequorins.

2 Materials

2.1 Instrument/ Luminometer

Here, we describe the basic components of a custom-made luminometer (Figs. 2 and 3) specially designed to optimize the capture of photons from cell populations expressing aequorins and seeded in 12- to 13-mm-diameter glass coverslips. It can be easily built by following the description provided by Cobbold and Lee, 1991 [13] (Fig. 2) (*see* **Note 1**).

Briefly, the instrument consists of a *perfusion chamber* (Fig. 3) maintained at the temperature of choice by a water jacket continuously renewed by a pump placed in an external temperature-controlled bath. The chamber contains an inlet and an outlet hole

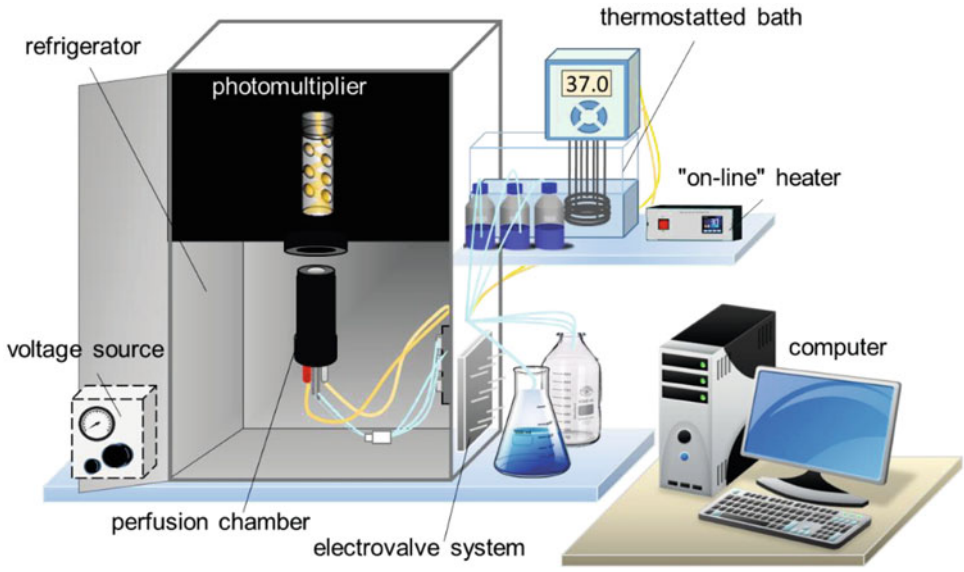

Fig. 2 Calcium measurement system. Diagram of a custom-made luminometer specially designed to optimize the capture of photons from cell populations seeded in glass coverslips and expressing aequorins. The diagram shows the main components of the instrument

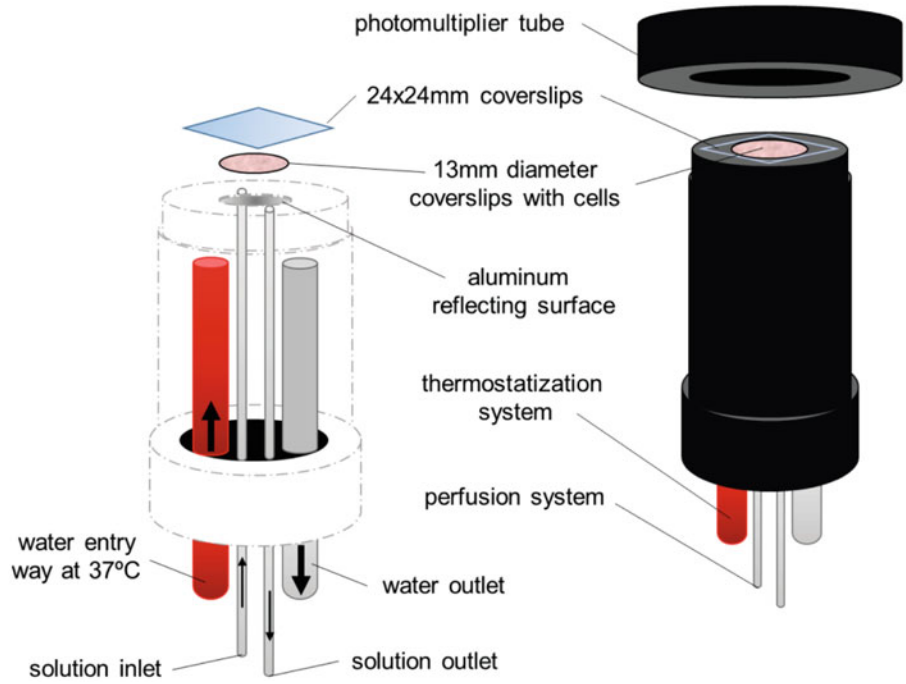

Fig. 3 Perfusion chamber of the calcium measurement system. The diagram shows the main components of the perfusion chamber

to perfuse different solutions throughout the experiment. Perfusing solutions are placed in a temperature-controlled bath, and the passage of the desired solution is controlled by an electro-valve system. The difference in height between the bath and the perfusion chamber generates a flow of approximately 1 mL/min. The 13-mm-diameter coverslips seeded with chromaffin cells expressing organelle-targeted aequorins are placed into the perfusion chamber sealed at the top using a square 24 × 24-mm coverslip adhered to it by a silicone grease thin film. The perfusion chamber is built entirely of black methacrylate to prevent photon loss and leaked photons from the outside. The base of the perfusion chamber is composed of a reflective aluminum surface that allows all the emitted photons to be directed toward the photomultiplier and thus improve photon collection efficiency.

The perfusion chamber is located immediately below a high-gain *photomultiplier* EMI 9789a from Electron Tubes, collecting the photons emitted by a 10-mm photocathode placed just above the perfusion chamber containing the adhered cells (Figs. 2 and 3). Both photomultiplier and perfusion chamber are placed inside a refrigerator at 4 °C to avoid the electron thermal emission from the photocathode and significantly reduce the basal noise of the sample (Fig. 2).

The difference in potential between the anode and the cathode of the photomultiplier is generated by a *high-voltage source*, Thorn EMI type and PM28B model (Fig. 2). The signal emitted by the photomultiplier is subsequently sent through an EMI AD2 *discriminator–amplifier* to a CT2 Counter Timer from Electron Tubes, from which the data were input to the computer (Fig. 2). The luminescence data were collected every second and displayed on the computer through the *Electron Tubes EM6 Counter/Timer software*. The stored data in form of txt. File can be then transformed into $[Ca^{2+}]$.

2.2 Solutions

1. Standard extracellular medium 1 mM Ca^{2+}: 145 mM NaCl, 5 mM KCl, 1 mM $MgCl_2$, 1 mM $CaCl_2$, 5 mM glucose, 10 mM HEPES; pH 7.4 (adjusted with NaOH).
2. Standard extracellular medium 0.5 mM EGTA: 145 mM NaCl, 5 mM KCl, 1 mM $MgCl_2$, 0.5 mM EGTA, 5 mM glucose, 10 mM HEPES; pH 7.4 (adjusted with NaOH). Essentially used to deplete the intracellular Ca^{2+} stores or to transiently remove the contribution of the extracellular Ca^{2+} influx to the event of Ca^{2+} signaling studied.
3. Standard intracellular medium for cell permeabilization: 10 mM NaCl, 130 mM KCl, 1 mM $MgCl_2$, 1 mM H_2KPO_4, 0.5 mM EGTA, 5 mM succinate, 5 mM glutamate, 5 mM malate, 20 mM HEPES, digitonin 20 μM; pH 7.0 (adjusted with KOH). The medium lacks adenine nucleotides to prevent

Table 1
Chemical composition of standard intracellular mediums

	Standard intracellular medium 0.5 mM EGTA	Standard intracellular medium 1 mM EGTA	Standard intracellular medium 1 mM EGTA/Ca^{2+}	Standard intracellular medium 5 mM HEDTA
KCl	130 mM	130 mM	130 mM	130 mM
NaCl	10 mM	10 mM	10 mM	10 mM
$MgCl_2$	1 mM	1 mM	1 mM	4.5 mM
H_2KPO_4	1 mM	1 mM	1 mM	1 mM
HEPES	20 mM	20 mM	20 mM	20 mM
Succinate	5 mM	5 mM	5 mM	5 mM
Malate	5 mM	5 mM	5 mM	5 mM
Glutamate	5 mM	5 mM	5 mM	5 mM
ATP-K^+	1 mM	1 mM	1 mM	1 mM
ADP	20 μM	20 μM	20 μM	20 μM
EGTA	0.5 mM	1 mM	1 mM	–
HEDTA	–	–	–	5 mM
$CaCl_2$	–	–	1 mM	–

Ca^{2+} signaling associated to the activation of purinergic receptors during the process of permeabilization (*see* **Note 18**).

4. Standard intracellular medium 0.5 mM EGTA: 10 mM NaCl, 130 mM KCl, 1 mM $MgCl_2$, 1 mM H_2KPO_4, 0.5 mM EGTA, 5 mM succinate, 5 mM glutamate, 5 mM malate, 1 mM ATP-K^+, 20 μM ADP, 20 mM HEPES; pH 7.0 (adjusted with KOH). See Table 1.
5. Standard intracellular medium 1 mM EGTA: 10 mM NaCl, 130 mM KCl, 1 mM $MgCl_2$, 1 mM H_2KPO_4, 1 mM EGTA, 5 mM succinate, 5 mM glutamate, 5 mM malate, 1 mM ATP-K^+, 20 μM ADP, 20 mM HEPES; pH 7.0 (adjusted with KOH). See Table 1.
6. Standard intracellular medium 1 mM EGTA/1 mM Ca^{2+}: 10 mM NaCl, 130 mM KCl, 1 mM $MgCl_2$, 1 mM H_2KPO_4, 1 mM EGTA, 1 mM $CaCl_2$, 5 mM succinate, 5 mM glutamate, 5 mM malate, 1 mM ATP-K^+, 20 μM ADP, 20 mM HEPES; pH 7.0 (adjusted with KOH). See Table 1.
7. Standard intracellular medium 5 mM HEDTA: 10 mM NaCl, 130 mM KCl, 4.5 mM $MgCl_2$, 1 mM H_2KPO_4, 5 mM HEDTA, 5 mM succinate, 5 mM glutamate, 5 mM malate, 1 mM ATP-K^+, 20 μM ADP, 20 mM HEPES; pH 7.0 (adjusted with KOH). See Table 1.

Table 2
Preparation of intracellular medium with defined free [Ca^{2+}] (37 °C) by mixing different volumes of intracellular medium 1 mM EGTA/1 mM Ca^{2+} and intracellular medium 1 mM EGTA (both defined in Table 1)

Ca^{2+} free	Intracellular medium 1 mM EGTA/1 mM Ca^{2+} (%)	Intracellular medium 1 mM EGTA (%)
100 nM [Ca^{2+}]	22.4	77.6
200 nM [Ca^{2+}]	36.4	63.6
300 nM [Ca^{2+}]	46.3	53.7
400 nM [Ca^{2+}]	53.5	46.5
500 nM [Ca^{2+}]	59	41
700 nM [Ca^{2+}]	66.8	33.2
1 μM [Ca^{2+}]	74.4	25.7
1.5 μM [Ca^{2+}]	81.2	18.8

Table 3
Intracellular medium containing free Ca^{2+} levels from 2 to 10 μM (37 °C)

Ca^{2+} free (μM)	$CaCl_2$ (μM)	$MgCl_2$ (mM)
2.5	80	1
3.5	110	1
4.5	138	1
5.5	165	1
7	215	0.9
10	303	0.82

Prepare intracellular medium 5 mM HEDTA and complete with $CaCl_2$ and $MgCl_2$ to reach the concentrations indicated in the table to obtain the desired Ca^{2+} free

8. Intracellular medium with Ca^{2+} free levels in the range of nanomolar: Intracellular solutions with different free Ca^{2+} concentrations can be easily arranged by mixing variable volumes of standard intracellular medium free of Ca^{2+}-1 mM EGTA and standard intracellular medium 1 mM EGTA/1 mM Ca^{2+}. The percentage of volumes required are summarized in Table 2.
9. Intracellular medium with Ca^{2+} free levels in the range of micromolar. Intracellular solutions with different free Ca^{2+} concentrations can be easily prepared from standard intracellular medium 5 mM HEDTA adjusting the concentrations of $CaCl_2$ and $MgCl_2$. Table 3 shows the concentrations of $CaCl_2$

and $MgCl_2$ required to obtain intracellular medium with the following free Ca^{2+} concentrations: 2.5, 3.5, 4.5, 5.5, 7, and 10 μM.

10. Lysis solution: 10 mM $CaCl_2$ and 100 μM digitonin in water. Transformation of luminescence data into $[Ca^{2+}]$ requires the estimation of the total amount of reconstituted/active aequorins in the sample. This is achieved with the lysis solution that is perfused/added at the end of the experimental procedure to trigger the emission of photons from the residual nonconsumed pool of aequorin molecules.
11. Coelenterazine stock solutions (100×). 200 μM native coelenterazine, 200 μM synthetic coelenterazine *n*, and 200 μM synthetic coelenterazine *i* stocks in methanol (*see* **Note 2**).
12. Digitonin stock solution: 100 mM digitonin in DMSO (1 mL). Store at −20 °C.
13. 2,5-di-tert-butyl-benzohydroquinone (BHQ) stock solution: 100 mM BHQ in DMSO (1 mL) and divide in aliquots. Store at −20 °C.
14. Ionomycin stock solution: 1 mM ionomycin in DMSO (1 mL) and divide in aliquots. Store at −20 °C.
15. Monensin stock solution: 1 mM monensin in DMSO (1 mL) and divide in aliquots. Store at −20 °C.
16. Poly-L-lysine-coated coverslips. Glass coverslips can be easily coated with poly-L-lysine by introducing autoclaved coverslips in a filtered sterile 0.01 mg/mL poly-L-lysine solution for 5 min, washing them 2 min in sterile water, and finally air-drying them completely under sterile conditions. Alternatively, they are also commercially available.

2.3 Transduction and Expression System

When measuring organelle Ca^{2+} dynamics in primary chromaffin cells, we advise the use of adenoviral vectors as they provide high efficiency of infection and a robust expression of the different aequorin variants combined with very low toxicity [14]. We have successfully used the Adeno X™ Expression System 1 (Clontech) to produce the adenoviral particles. Briefly, aequorin variants are cloned into the multicloning site of the vector pShuttle2. The aequorin-cloned pShuttle2 vector is subsequently digested with *PI-Sce I* and *I-Ceu I* restriction enzymes to clone the excised aequorin-containing fragment into the destination Adeno X–Viral vector. The new generated vector is further linearized for its efficient transfection into HEK293 viral packaging cells and later production of adenoviral infection particles. The whole workflow for adenoviral particles production can be easily completed in 10–14 days.

2.4 Adenoviral Particles

1. Adenoviral particles for expression of ER-targeted aequorins variants:
   Adeno-ER-mutAEQ, Adeno-ER-2mutAEQ
2. Adenoviral particles for expression of mitochondrial-targeted aequorins variants:
   Adeno-mit-AEQ, Adeno-mit-mutAEQ, Adeno-2mit-mutAEQ
3. Adenoviral particles for expression of secretory vesicles-targeted aequorin variants:
   VAMP-mut-AEQ, CgA-mutAEQ, NPY-mutAEQ.

Figure 4 shows a diagram of the different aequorin variants described here. Table 4 provides a guide to choose the configuration of aequorin variant, coelenterazine type, and experimental temperature required to achieve the desired Ca^{2+} affinity. For further discussion on ER-targeted aequorins, *see* **Note 3**; on mitochondrial-targeted aequorins, *see* **Note 4**; and on secretory vesicles-targeted aequorins, *see* **Note 5**.

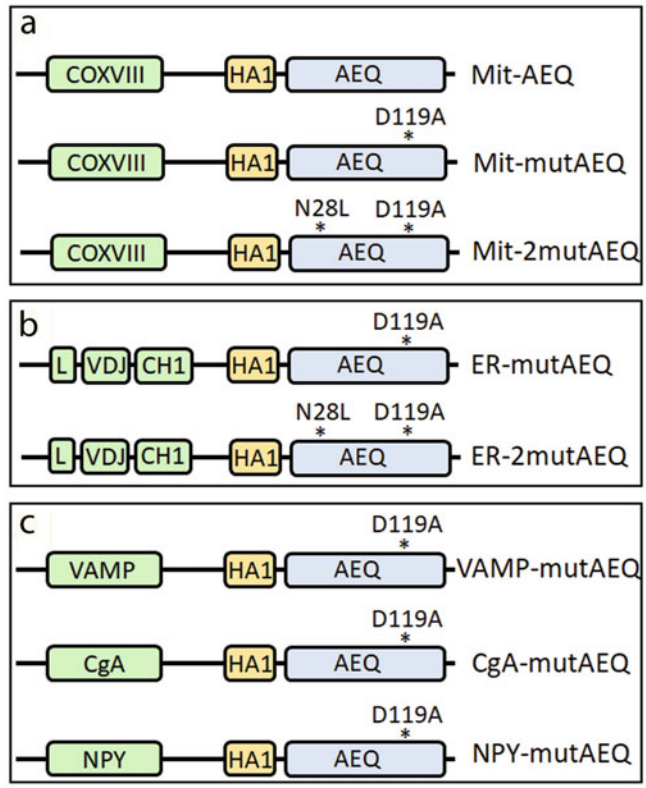

Fig. 4 Aequorin variants. (**a**) Aequorin variants targeted to mitochondria. (**b**) Aequorin variants targeted to the endoplasmic reticulum. (**c**) Aequorin variants targeted to the secretory vesicles. Further described in **Notes 2–4**. *Abbreviations*: AEQ aequorin

Table 4
[Ca^{2+}] ranges measured according to different aequorin variants, type of coelenterazine used for the reconstitution, and temperature of the experiment

Aequorin variant	Coelenterazine	*T* (°C)	[Ca^{2+}] range	Organelle
ER-mutAEQ	Synthetic: *n*	37	20 μM–500 μM	ER
ER-mutAEQ	Synthetic: *n*	22	50 μM–1 mM	ER
ER-2mutAEQ	Synthetic: *i*	37	100 μM–10 mM	ER
Mit-AEQ	Native	37	0.1–10 μM	Mit
Mit-AEQ	Synthetic: *n*	37	1–100 μM	Mit
Mit-mutAEQ	Native	37	1–100 μM	Mit
Mit-mutAEQ	Synthetic: *n*	37	100 μM–1 mM	Mit
Mit-2mutAEQ	Synthetic *i*	37	100 μM–10 mM	Mit
VAMP-mutAEQ	Native	37/22	20–500 μM/20 μM–1 mM	SV
CgA-mutAEQ	Native	37/22	20–500 μM/20 μM–1 mM	SV
NPY-mutAEQ	Native	37/22	20–500 μM/20 μM–1 mM	SV

3 Methods

3.1 Endoplasmic Reticulum Calcium Measurements

3.1.1 Recording ER Ca2+ Dynamics in Intact Cells

1. Bovine adrenal medulla chromaffin cells are isolated as described previously [15] and seeded at 70–80% confluence (0.25×10^6 cells) on 12- to 13-mm-diameter glass coverslips coated with poly-L-lysine and placed inside 24-well plates (*see* **Note 6**).
2. Cell cultures are infected 24 h later with the adenoviral particles with a MOI = 1–2 (*see* **Note 7**).
3. One day later (24 h post infection), chromaffin cells express significant amounts of aequorin into the ER and thus are suitable to record Ca^{2+} dynamics in the luminometer.
4. Reconstitution of ER-mutAEQ with the synthetic coelenterazine *n* requires prior Ca^{2+} depletion of the endoplasmic reticulum, but this mode of reconstitution is optional in case of using ER-2mutAEQ reconstituted with the synthetic coelenterazine *i* (Table 4). For experiments requiring the reconstitution of any ER-targeted aequorin in Ca^{2+}-depleted cells, move to **step 5**. For experiments requiring the reconstitution of ER-2mutAEQ with coelenterazine *i* in non-depleted cells move to **step 16**.

5. Extract the 24-well plate from the cell incubator, and transfer the cell-seeded coverslips growing in cell culture medium to a new well (24-well plate) containing 1 mL standard extracellular medium 0.5 mM EGTA at room temperature.
6. Wash once with 1 mL standard extracellular medium 0.5 mM EGTA to ensure elimination of the remaining traces of cell culture medium.
7. Add 0.4 mL of standard extracellular medium 0.5 mM EGTA supplemented with 10 μM BHQ (depletion solution). Incubate for 10 min at room temperature (*see* **Note 8**).
8. Remove depletion solution and add 0.2 mL of standard extracellular medium 0.5 mM EGTA.
9. Then add 1 μL of 100× synthetic coelenterazine *n* (*see* **Note 9**). Mix gently with a 200-μL micropipette to ensure effective distribution of coelenterazine, and incubate in the dark at room temperature for 1–2 h.
10. Transfer the coverslip to the perfusion chamber of the custom-made luminometer, and seal the chamber with silicone. Important: The perfusion chamber must be previously loaded with standard extracellular medium 0.5 mM EGTA (*see* **Note 10**).
11. Activate the perfusion of standard extracellular medium 0.5 mM EGTA, open the EM6 Counter/Timer software, and initiate photon recording.
12. In the beginning, perfuse the cells for 5 min with standard extracellular medium 0.5 mM EGTA to wash completely BHQ and release the inhibition of the ER-Ca^{2+}-ATPase.
13. Perfuse standard extracellular medium 1 mM Ca^{2+} to refill the ER.
14. Once $[Ca^{2+}]_{ER}$ reaches steady state, perfuse the perturbation agent to study the mechanism of choice (Table 5).
15. At the end of every experiment, perfuse lysis solution until signal (counts) back to background levels (*see* **Notes 11** and **12**).
16. In case of working with ER-2mutAEQ reconstituted with coelenterazine *i* in non-depleted cells, extract the 24-well plate from the cell incubator and transfer the cell-seeded coverslips growing in cell culture medium to a new well (24-well plate) containing 1 mL standard extracellular medium 1 mM Ca^{2+} at room temperature.
17. Wash once with 1 mL standard extracellular medium 0.5 mM EGTA to ensure elimination of the remaining traces of cell culture medium.
18. Add 0.2 mL of standard extracellular medium 1 mM Ca^{2+}.

Table 5
Most common agents to perturb endoplasmic reticulum Ca^{2+} fluxes in chromaffin cells

Agent	Concentration	Target	ER Ca^{2+} transport mechanism	Experimental configuration
ACh	100 μM	Muscarinic r.	Ca^{2+} release (IP3R)	Intact
Carbachol	100 μM	Muscarinic r.	Ca^{2+} release (IP3R)	Intact
ATP	100 μM	Purinergic r.	Ca^{2+} release (IP3R)	Intact
Histamine	100 μM	Histamine r.	Ca^{2+} release (IP3R)	Intact
KCl	35–70 mM	VOCCs	Ca^{2+} uptake (SERCA)	Intact
Caffeine	10–50 mM	Ryanodine r.	Ca^{2+} release (RyR)	Intact/perm.
IP3	2 μM	IP3R	Ca^{2+} release (IP3R)	Perm.
BHQ	10 μM	SERCA	Ca^{2+} uptake (SERCA)	Intact/perm.
CPA	10 μM	SERCA	Ca^{2+} uptake (SERCA)	Intact/perm.
Thapsigargin	0.1–1 μM	SERCA	Ca^{2+} uptake (SERCA)	Intact/perm.

R receptor, *VOOCs* voltage-operated Ca^{2+} channels, *IP_3R* inositol trisphosphate receptor, *SERCA* sarco-endoplasmic reticulum-Ca^{2+}-ATPase, *Ach* acetylcholine, *IP3* inositol trisphosphate, *CPA* cyclopiazonic acid, *BHQ* 2,5-di-tert-butyl-benzohydroquinone, *perm* permeabilized cells

19. Then add 1 μL of 100× synthetic coelenterazine *i*. Mix gently with a 200-μL micropipette to ensure effective distribution of coelenterazine, and incubate in the dark at room temperature for 1–2 h (*see* **Note 9**).
20. Transfer the coverslip to the perfusion chamber of the custom-made luminometer, and seal the chamber with silicone. Important: The perfusion chamber must be previously loaded with standard extracellular medium 1 mM Ca^{2+} (*see* **Note 10**).
21. Activate the perfusion of standard extracellular medium 1 mM Ca^{2+}, open the EM6 Counter/Timer software, and initiate photon recording.
22. Perfuse the perturbation agent to study the mechanism of choice (Table 5).
23. At the end of every experiment, perfuse lysis solution until signal (counts) back to background levels (*see* **Note 11**).

3.1.2 Recording ER Ca2+ Dynamics in Permeabilized Cells

1. Follow **steps 1–12** described in the previous Subheading 3.1.1 (*see* **Note 13**).
2. Perfuse standard intracellular medium for cell permeabilization for 1 min.

3. Perfuse standard intracellular medium 0.5 mM EGTA for 3 min to get rid of the detergent.
4. Perfuse intracellular medium containing 100 nM free Ca^{2+} (Table 2) to refill the ER.
5. Once $[Ca^{2+}]_{ER}$ reaches the new steady state, perfuse the perturbation agent to study the mechanism of choice (Table 5).
6. At the end of every experiment, perfuse lysis solution until photon emission (signal/counts) back to background levels (*see* **Note 11**).

3.2 Mitochondrial Calcium Measurements

3.2.1 Recording Mitochondrial Ca^{2+} Dynamics in Intact Cells

1. Bovine adrenal medulla chromaffin cells are isolated as described previously [15] and seeded at 70–80% confluence (0.25×10^6 cells) on 12- to 13-mm-diameter glass coverslips coated with poly-L-lysine and placed inside 24-well plates (*see* **Note 6**).
2. Cell cultures are infected 24 h later with the adenoviral particle of choice (Adeno-mit-AEQ, Adeno-mit-mutAEQ, Adeno-mit-2mutAEQ) with a MOI = 1–2 (*see* **Note 7**).
3. One day later (24 h post infection), chromaffin cells express significant amounts of aequorin into the mitochondria and thus are suitable to record Ca^{2+} in the luminometer.
4. Extract the 24-well plate from the cell incubator, and transfer the cell-seeded coverslips to a new well (24-well plate) containing 1 mL standard extracellular medium 1 mM Ca^{2+} at room temperature.
5. Wash once with 1 mL standard extracellular medium 1 mM Ca^{2+} to ensure elimination of the remaining traces of cell culture medium, and add 0.2 mL of standard extracellular medium 1 mM Ca^{2+}.
6. Then add 1 μL of 100× coelenterazine (see Table 6 for type of coelenterazine). Mix gently with a 200-μL micropipette to ensure effective distribution of coelenterazine, and incubate in the dark at room temperature for 1–2 h (*see* **Note 9**).
7. Transfer the coverslip to the perfusion chamber of the custom-made luminometer, and seal the chamber with silicone. The perfusion chamber must be previously loaded with standard extracellular medium 1 mM Ca^{2+} (*see* **Note 10**).
8. Activate the perfusion of standard extracellular medium 1 mM Ca^{2+}, open the EM6 Counter/Timer software, and initiate photon recording.
9. Perfuse the perturbation agent to study the mechanism of choice (Table 7).

Table 6
Values of constants for transformation of luminescence data into [Ca^{2+}] according to aequorin variant, type of coelenterazine used for reconstitution, and temperature of the experiment

Aequorin	Coelenterazine	T (°C)	K_R (M^{-1})	K_{TR}	n	λ
ER-mutAEQ	Synthetic: *n*	37	8.47×10^7	1.65×10^5	1.2038	0.138
ER-mutAEQ	Synthetic: *n*	22	5×10^7	1.60×10^5	1.271	0.025
ER-2mutAEQ	Synthetic: *i*	37	1.98×10^4	1.85×10^4	1.15	0.4
Mit-AEQ	Native	37	4.81×10^7	601	2.3	1
Mit-AEQ	Synthetic: *n*	37	2.23×10^7	348	2	0.129
Mit-mutAEQ	Native	37	2.28×10^7	2.2×10^5	1.43	1
Mit-mutAEQ	Synthetic: *n*	37	8.47×10^7	1.65×10^5	1.2038	0.138
Mit-2mutAEQ	Synthetic: *i*	37	5.67×10^4	3.15×10^4	1.089	0.4
VAMP-mutAEQ	Native	37	2.28×10^7	2.2×10^5	1.43	1
VAMP-mutAEQ	Native	22	1.61×10^7	2.2×10^5	1.43	1
CgA-mutAEQ	Native	37	2.28×10^7	2.2×10^5	1.43	1
CgA-mutAEQ	Native	22	1.61×10^7	2.2×10^5	1.43	1
NPY-mutAEQ	Native	37	2.28×10^7	2.2×10^5	1.43	1
NPY-mutAEQ	Native	22	1.61×10^7	2.2×10^5	1.43	1

10. At the end of every experiment, perfuse lysis solution until signal (counts) back to background levels (*see* **Notes 11** and **14**).

3.2.2 Recording Mitochondrial Ca^{2+} Dynamics in Permeabilized Cells

1. Follow **steps 1–7** described in the previous Subheading 3.2.1.
2. Perfuse standard extracellular medium 0.5 mM EGTA for 30 s.
3. Perfuse standard intracellular medium for cell permeabilization for 1 min.
4. Perfuse standard intracellular medium 0.5 mM EGTA for 3 min to get rid of the detergent.
5. To study the kinetics of mitochondrial Ca^{2+} uptake, perfuse intracellular medium containing the desired free [Ca^{2+}] (Table 3) to promote mitochondrial Ca^{2+} uptake until $[Ca^{2+}]_{mit}$ reaches new steady state. In case of interest in recording the mitochondrial release kinetics, go to **step 6**; if not, move directly to **step 7**.
6. Perfuse standard intracellular medium 0.5 mM EGTA until mitochondrial Ca^{2+} levels back to the previous basal state.
7. Perfuse lysis solution until photon emission (signal/counts) back to background levels (*see* **Notes 11** and **15**).

Table 7
Most common agents to perturb mitochondrial Ca^{2+} fluxes in chromaffin cells

Agent	Concentration	Target	Mitochondrial Ca^{2+} transport mechanism	Experimental configuration
ACh	100 μM	Cholinergic receptor	Uptake/release (MCU/NCLX)	Intact
Carbachol	100 μM	Muscarinic receptor	Uptake/release (MCU/NCLX)	Intact
ATP	100 μM	Muscarinic receptor	Uptake/release (MCU/NCLX)	Intact
Histamine	100 μM	Histamine receptor	Uptake/release (MCU/NCLX)	Intact
KCl	35–70 mM	Voltage-operated calcium channels	Uptake/release (MCU/NCLX)	Intact
Caffeine	10–50 mM	Ryanodine receptor	Uptake/release (MCU/NCLX)	Intact
Ca^{2+}	1–10 μM (*see* Table 3)	MCU	Uptake (MCU)	Permeabilized
EGTA	0.5 mM (*see* Table 2)	NCLX	Release (NCLX)	Permeabilized

Perfusion of intact chromaffin cells expressing mitochondrial-targeted aequorins with the agents described in the table generates a mitochondrial Ca^{2+} transient. The kinetics of the rise phase essentially reflect the activity of the Ca^{2+} uptake mechanisms (MCU), whereas the decay kinetics mainly reflects the activity of the Ca^{2+} release mechanisms (NCLX). For better isolation of mitochondrial Ca^{2+} uptake and release kinetics, we recommend the use of permeabilized cells. In this experimental configuration, perfusion of intracellular Ca^{2+} buffers in the range of micromolar promotes net mitochondrial Ca^{2+} uptake, letting the study of mitochondrial Ca^{2+} uptake mechanisms and kinetics. Subsequent perfusion of Ca^{2+}-loaded mitochondria with intracellular solutions devoid of Ca^{2+} prevents the activity of the uniporter and promote net Ca^{2+} release, allowing the isolation of the mitochondrial Ca^{2+} release mechanisms
Abbreviations: *Ach* acetylcholine, *MCU* mitochondrial Ca^{2+} uniporter, *NCLX* mitochondrial Na^+/Ca^{2+} exchanger

3.3 Secretory Vesicles Calcium Measurements

3.3.1 Recording Secretory Vesicle Ca^{2+} Dynamics in Intact Cells

1. Bovine adrenal medulla chromaffin cells are isolated as described previously [15] and seeded at 70–80% confluence (0.25×10^6 cells) on 12- to 13-mm-diameter glass coverslips coated with poly-L-lysine and placed inside 24-well plates (*see* **Note 6**).
2. Cell cultures are infected 24 h later by adding the adenoviral particle of choice (Adeno-VAMP-mutAEQ, Adeno-CgA-mutAEQ, or Adeno-NPY-mutAEQ) with a MOI = 1–2 (*see* **Note 7**).
3. At 48–72 h post infection, chromaffin cells express significant amounts of aequorin into the secretory vesicles and are suitable to record Ca^{2+} in the luminometer.
4. Reconstitution of SV-targeted aequorins with native coelenterazine requires prior Ca^{2+} depletion of the secretory vesicles.

Extract the 24-well plate from the cell incubator, and transfer the cell-seeded coverslips growing in cell culture medium to a new well (24-well plate) containing 1 mL standard extracellular medium 0.5 mM EGTA at room temperature.

5. Wash once with 1 mL standard extracellular medium 0.5 mM EGTA to ensure elimination of the remaining traces of cell culture medium.
6. Add 0.4 mL of standard extracellular medium 0.5 mM EGTA supplemented with 10 μM BHQ, 10 μM ionomycin, and 10 μM monensin (depletion solution). Incubate for 10 min at room temperature (*see* **Note 16**).
7. Wash twice with 1 mL standard extracellular medium 0.5 mM EGTA to ensure elimination of the remaining traces of the ionophores present in the depletion solution.
8. Add 0.2 mL of standard extracellular medium 0.5 mM EGTA.
9. Then add 1 μL of 100× native coelenterazine (*see* **Note 9**). Mix gently with a 200-μL micropipette to ensure effective distribution of coelenterazine, and incubate in the dark at 15 °C for 1–2 h.
10. Transfer the coverslip to the perfusion chamber of the custom-made luminometer, and seal the chamber with silicone. The perfusion chamber must be previously loaded with standard extracellular medium 0.5 mM EGTA (*see* **Note 10**).
11. Activate the perfusion of standard extracellular medium 0.5 mM EGTA, open the EM6 Counter/Timer software, and initiate photon recording. Perfuse at least for 5 min to wash completely the depletion solution.
12. Only in case of using VAMP-mutAEQ, perfuse for 5 min standard extracellular medium 0.5 mM EGTA supplemented with 500 μM $LaCl_3$ to release the photons of the pool of aequorin located at the outer side of the plasma membrane (*see* **Note 5**).
13. Only in case of using VAMP-mutAEQ, perfuse standard extracellular medium 0.5 mM EGTA for 3 min to wash the lanthanum.
14. Perfuse standard extracellular medium 1 mM Ca^{2+} to refill the secretory vesicles until $[Ca^{2+}]_{SV}$ reaches new steady state.
15. Perfuse the perturbation agent to study the mechanism of choice (Table 8).
16. Perfuse lysis solution until signal (counts) backs to background levels (*see* **Notes 11** and **17**).

Table 8
Most common agents to perturb secretory vesicle Ca^{2+} fluxes in chromaffin cells

Agent	Concentration	Target	SV Ca^{2+} transport mechanism	Cell format
ACh	100 μM	Muscarinic r.	Ca^{2+} release (IP3R)	Intact
Carbachol	100 μM	Muscarinic r.	Ca^{2+} release (IP3R)	Intact
ATP	100 μM	Purinergic r.	Ca^{2+} release (IP3R)	Intact
Histamine	100 μM	Histamine r.	Ca^{2+} release (IP3R)	Intact
KCl	35–70 mM	VOCCs	Ca^{2+} uptake (SERCA)	Intact
Caffeine	10–50 mM	Ryanodine r.	Ca^{2+} release (RyR)	Intact/perm.
IP3	2 μM	IP3R	Ca^{2+} release (IP3R)	Perm.
BHQ	10 μM	SERCA	Ca^{2+} uptake (SERCA)	Intact/perm.
CPA	10 μM	SERCA	Ca^{2+} uptake (SERCA)	Intact/perm.
Thapsigargin	0.1–1 μM	SERCA	Ca^{2+} uptake (SERCA)	Intact/perm.
Bafilomycin	100 nM	V-ATPase	Ca^{2+} uptake (CHX)	Intact/perm.
NH_4Cl	10 mM	Disruption ΔH^+	Ca^{2+} uptake (CHX)	Intact/perm.
FCCP	1 μM	Disruption ΔH^+	Ca^{2+} uptake (CHX)	Intact/perm.

R receptor, *VOOCs* voltage-operated Ca^{2+} channels, *IP3R* inositol trisphosphate receptor, *SERCA* sarco-endoplasmic reticulum-Ca^{2+}-ATPase, *CHX* Ca^{2+}/H^+ exchanger, *Ach* acetylcholine, *IP3* inositol trisphosphate, *CPA* cyclopiazonic acid, *BHQ* 2,5-di-tert-butyl-benzohydroquinone, *FCCP* carbonyl cyanide 4-(trifluoromethoxy)phenylhydrazone, *perm* permeabilized cells

3.3.2 Recording Secretory Vesicle Ca^{2+} Dynamics in Permeabilized Cells

1. Follow **steps 1–11** described in the previous Subheading 3.3.1. In case of using VAMP-mutAEQ, include **steps 12** and **13**.
2. Perfuse standard intracellular medium for cell permeabilization for 1 min.
3. Perfuse standard intracellular medium 0.5 mM EGTA for 3 min to get rid of the detergent.
4. Perfuse intracellular medium containing 100 nM free Ca^{2+} (Table 2) to refill the secretory vesicles until $[Ca^{2+}]_{SV}$ reaches new steady state.
5. Perfuse the perturbation agent to study the mechanism of choice (Table 8).
6. Perfuse lysis solution until photon emission (counts) backs to background levels (*see* **Notes 11** and **19**).

3.4 Transforming Luminescence in $[Ca^{2+}]$

1. Import luminescence data stored in txt. to an excel file. This file contains the luminescence value of every point along the experiment (L).
2. Subtract the background.
3. Calculate total light emitted during the experiment (L_T).
4. Calculate accumulated light emitted at every point of the experiment (L_{acc}).

5. Calculate L_{max}, which is the integral of luminescence (minus the background) from every temporal point to the end of the experiment. It is calculated as $L_T - L_{acc}$.
6. Transform data into $[Ca^{2+}]$ values using the following mathematical algorithm at every point along the experiment (*see* **Note 20**).

$$\left[Ca^{2+}\right] = \frac{\text{Ratio} + (\text{Ratio} \times K_{TR}) - 1}{K_R - (\text{Ratio} - K_R)}$$

$$\text{Ratio} = \left(\frac{L}{L_{max} \times \lambda}\right)^{\frac{1}{n}}$$

Table 6 provides constants (K_{TR}, K_R, n, and λ) for different experimental configurations according to the aequorin variant used, type of coelenterazine, and temperature of the experiment.

4 Notes

1. Commercially available luminescence plate readers including injection ports and suitable for aequorin-based measurements in cell populations are currently accessible through several providers. In our experience, the Cytation3/5 plate reader provided by Biotek constitutes a versatile and economic solution to explore mitochondrial and cytosolic Ca^{2+} dynamics. Importantly for plate readers, detection must occur from the bottom of the plate to allow continuous recording even during injection of stimuli. Furthermore, liquid injection in the well must be optimized to allow a rapid diffusion of the stimulus. For higher throughput, especially indicated in the context of high-content chemical screenings, some providers have developed instruments containing multiple readers. The MicroBeta2 LumiJET Microplate Counters (Perkin Elmer) is available in 12-detector configuration. This system supports up to 384 well plates. The FLIPR station (Molecular Devices) with the aequorin configuration allows the simultaneous detection of a whole plate and is also compatible with 384-well plate format.
2. Once resuspended in methanol, we recommend splitting the 100× coelenterazine stock solution into small aliquots (20 μL) in Eppendorf tubes previously gassed with N_2 to prevent oxidation. Methanol evaporates fast, so we recommend sealing the aliquots with Parafilm. Coelenterazine is also light-sensitive, so we recommend avoid light exposure by handling it in a low-light environment and wrapping each aliquot in aluminum foil. Once split in aliquots, store at −20 °C for short periods

(maximum 1 week) or store at −80 °C to maintain the dissolved stock of coelenterazine for long periods of time.

3. Aequorins have been guided to the endoplasmic reticulum (ER) by fusing on the N-terminus the leader sequence (L), followed by the VDJ and CH1 domains of an Igγ2b heavy chain. ER targeting relies on the leader sequence, recognized by the SRP system for peptide translocation to the ER, whereas retention on the ER depends on the presence of the CH1 domain [16] (Fig. 4b). Ca^{2+} levels in the ER often ranges from 100 to 500 μM, and thus, low-affinity aequorins are required for reliable assessment of ER Ca^{2+} dynamics (Fig. 4b). The combination of a low-affinity mutated aequorin containing a point mutation in the second EF-hand (Asp119 → Ala) [16] reconstituted with the synthetic coelenterazine *n*, ER-mutAEQ − *n*, has been widely used to measure ER Ca^{2+} in situ over the years [9]. ER-mutAEQ − *n* is still consumed at relatively high rates at the Ca^{2+} levels found in the ER lumen. Thus, measurement of ER Ca^{2+} levels and dynamics with ER-mutAEQ − *n* requires an initial step of Ca^{2+} depletion to allow the effective reconstitution of the aequorin with coelenterazine followed by a second step of Ca^{2+} refilling (procedure described in Subheading 3) [8]. It is worth mentioning that reduction of experimental temperature to 22 °C reduces the affinity of aequorin for Ca^{2+}, thus reducing consumption rates and expanding the dynamic range (Table 4). This approach allows repetitive stimulations without the temporal constrictions associated to aequorin consumption (Fig. 5) [9]. A more recent development consists of the combination of a double-mutated aequorin variant reconstituted with the synthetic coelenterazine *i*, *ER-2mutAEQ − i* [17]. This new aequorin variant contains an additional mutation (Asn28 → Leu) in the first EF-hand domain, rendering the probe around one order of magnitude less sensitive to Ca^{2+} when compared with ER-mutAEQ − *n*. Given its extremely low sensitivity, stepwise Ca^{2+} depletion of the ER is no longer required. Table 4 summarizes the different experimental configurations to measure Ca^{2+} with ER-targeted aequorins and their Ca^{2+} affinities.

4. Mitochondrial-targeted aequorins are efficiently directed to the mitochondrial matrix by fusing on the N-terminus of the photoprotein the 25 amino acid sequence of the mitochondrial targeting signal of the cytochrome-c oxidase subunit, COX-8 (Fig. 4a). Although mitochondrial Ca^{2+} levels under non-stimulatory conditions are close to those measured in the cytosol, these values can rapidly rise to a wide range of concentrations upon cell stimulation (10 μM to 1 mM) depending on the specific stimuli. For this reason, we generally

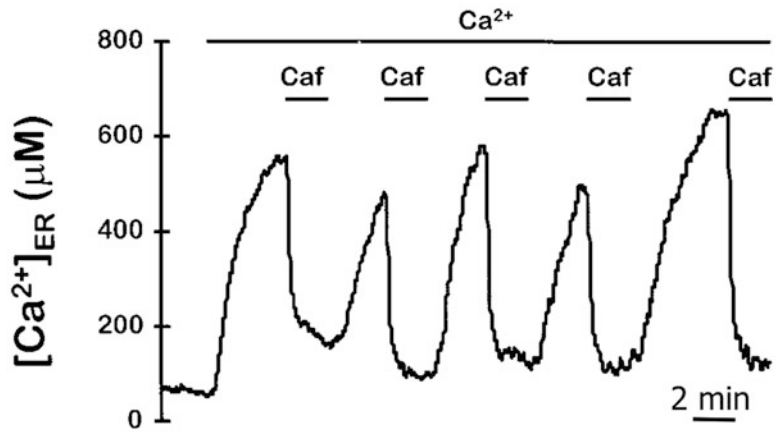

Fig. 5 ER calcium measurements in bovine chromaffin cells expressing ER-mutAEQ reconstituted with synthetic coelenterazine *n* at 22 °C. Example of an experiment in intact cells performed as described in Subheading 3.1.1. In this particular case, cells were infected with HSV-1 viral particles carrying the ER-targeted aequorin construct. As indicated, Ca^{2+}-depleted chromaffin cells were perfused with standard extracellular medium 1 mM Ca^{2+} to refill the secretory vesicle compartment. When indicated, cells were repeatedly stimulated with short pulses of 50 mM of caffeine to activate ER Ca^{2+} release through ryanodine receptors. (Reproduced from Alonso et al. [9]. With permission to reuse content from Rockefeller University Press)

recommend the use of low-affinity aequorins to record mitochondrial Ca^{2+} dynamics. According to the aequorin variant (Fig. 4a) and type of coelenterazine, mitochondrially targeted aequorin can be configurated for reliable $[Ca^{2+}]_M$ measurements at a wide range of concentrations with high accuracy, from the sub-micromolar to the millimolar (Table 4). Wild-type aequorin reconstituted with native coelenterazine (*mit-AEQ – native*) shows affinity for Ca^{2+} in the concentration range of 0.3–8 μM [6]; wild-type aequorin reconstituted with synthetic coelenterazine *n* (*mit-AEQ – n*) covers the range of 1 to 40 μM of Ca^{2+} [6]; mutated low Ca^{2+} affinity aequorin reconstituted with native coelenterazine (mit-mutAEQ – *native*) measures Ca^{2+} in the range of 1–100 μM; mutated low Ca^{2+} affinity aequorin reconstituted with synthetic coelenterazine *n* (*mit-mutAEQ – n*) can measure Ca^{2+} in the concentration range 20–500 μM [6]. Alternatively, the combination of a very low Ca^{2+} affinity aequorin variant (mit-2mutAEQ) reconstituted with the native coelenterazine (*mit-2mutAEQ – native*) displays similar Ca^{2+} affinity [18]. Finally, the reconstitution of the same very low-affinity aequorin variant (*mit-2mutAEQ*) with the synthetic coelenterazine *i* (*mit-2mutAEQ – i*) can be used for efficient estimation of mitochondrial Ca^{2+} up to 1–5 mM [18]. In intact cells, this

new configuration allows monitoring of agonist-induced increases of $[Ca^{2+}]_M$ for long periods of time without the problems derived from aequorin consumption. Table 4 summarizes the different experimental configurations to measure Ca^{2+} with mitochondrial-targeted aequorins and their Ca^{2+} affinities.

5. Secretory vesicle Ca^{2+} levels ($[Ca^{2+}]_{SV}$) in chromaffin cells reaches 20–30 μM [11]. Current strategies to measure $[Ca^{2+}]_{SV}$ with aequorins requires the use of low-affinity variants targeted to the secretory vesicles (*SV-mutAEQ*) reconstituted with native coelenterazine (*SV-mutAEQ − native*) and involves stepwise Ca^{2+} depletion of the secretory vesicle compartment to prevent premature consumption of the photoprotein. To our knowledge, aequorin has been successfully driven to the secretory vesicles following three different targeting strategies. First is fusing the vesicle-associated membrane protein (VAMP) 2/synaptobrevin on the N-terminus of the aequorin, *VAMP-mutAEQ* [11]. Second is fusing the secretory vesicle lumen protein Chromogranin A on the N-terminus of the photoprotein, *CgA-mutAEQ*. Third is fusing the N-terminus of the aequorin with the neuropeptide-Y, similarity localized in the lumen, *NPY-mutAEQ* (Fig. 4c). We noticed that chromaffin cells expressing VAMP-mutAEQ exhibit a fraction of the photoprotein localized at the plasma membrane, with its Ca^{2+}-sensitive domain facing the extracellular medium. Given that reconstitution of the photoprotein is performed in absence of extracellular Ca^{2+}, the exposure of chromaffin cells to 1 mM Ca^{2+} during the refilling step generates a pulse of light as the pool of photoproteins localized at the plasma membrane reacts with the extracellular Ca^{2+} present into the refilling solution. The extracellularly released photons add to the photons emitted by the aequorin localized at the SV, masking the real $[Ca^{2+}]_{SV}$ values and refilling dynamics, for the use of VAMP-targeted aequorins is thus necessary to inactivate the plasma membrane photoprotein pool, a procedure that requires the transient exposure of chromaffin cells to 1 mM lanthanum (procedure described in Subheading 3). We currently recommend the use of CgA- and NPY-targeted aequorins as they provide similar steady-state levels of Ca^{2+} and dynamics, and their localization remains essentially restricted to the secretory granule compartment (unpublished data by Pablo Montenegro). Table 4 summarizes the different experimental configurations to measure Ca^{2+} with SV-targeted aequorins and their Ca^{2+} affinities.

6. A good attachment of the chromaffin cells to the coverslip is critical as cells must be perfused with different solutions during the experiment.

7. Careful analysis on the ability of adenoviral particles to infect bovine chromaffin cells demonstrated that a Multiplicity of Infection (MOI) = 1–2 provides maximal efficiency of infection with minimal effects on cell toxicity and functionality [14]. To calculate the volume of viral stock necessary to inoculate viral particles with the MOI of choice, use:

$$\text{MOI} = \frac{\frac{\text{Infection units}}{\text{mL}} \times \text{Volume of viral stock in mL}}{\text{Number of cells}}$$

8. BHQ is a reversible inhibitor of the sarco-endoplasmic-Ca^{2+}-ATPase. This compound induces a rapid Ca^{2+} depletion of the ER with a halftime of 1–2 min.
9. We recommend to insert the 100× coelenterazine stock aliquots on ice and protect from light during handling.
10. Make sure the perfusion system does not contain any leaks and the perfusion chamber does not contain any air bubbles.
11. Reduction of counts to the initial basal levels upon lysis solution perfusion implies that the total amount of luminescence that can be emitted by the sample has been reached and thus the entire pool of active and reconstituted aequorin has been consumed.
12. Example of a calibrated Ca^{2+} recording in intact bovine chromaffin cells expressing ER-mutAEQ reconstituted with synthetic coelenterazine *n* at 22 °C is shown in Fig. 5.
13. In case of working with permeabilized cells to record ER Ca^{2+} dynamics in cells expressing ER-2mutAEQ reconstituted with the synthetic coelenterazine *i*, we recommend following the protocol described here including the step of Ca^{2+} depletion before reconstitution. The standard intracellular medium for cell permeabilization does not contain neither Ca^{2+} nor ATP, whereas the standard intracellular medium 0.5 mM EGTA does not contain Ca^{2+}. Therefore, these two solutions preclude the activity of the ER-Ca^{2+}-ATPases during permeabilization, triggering a transient depletion of ER Ca^{2+} and thus generating a recording artifact.
14. Example of a calibrated Ca^{2+} recording in intact bovine chromaffin cells expressing mit-mutAEQ reconstituted with synthetic coelenterazine *n* at 37 °C is shown in Fig. 6b.
15. Example of a calibrated Ca^{2+} recording in permeabilized bovine chromaffin cells expressing mit-mutAEQ reconstituted with synthetic coelenterazine *n* at 37 °C is shown in Fig. 6a.
16. Calcium depletion solution in secretory vesicles requires three different compounds: (a) BHQ, a reversible inhibitor of the sarco-endoplasmic-Ca^{2+}-ATPase; (b) ionomycin, a specific Ca^{2+} ionophore in membrane lipid bilayers; and

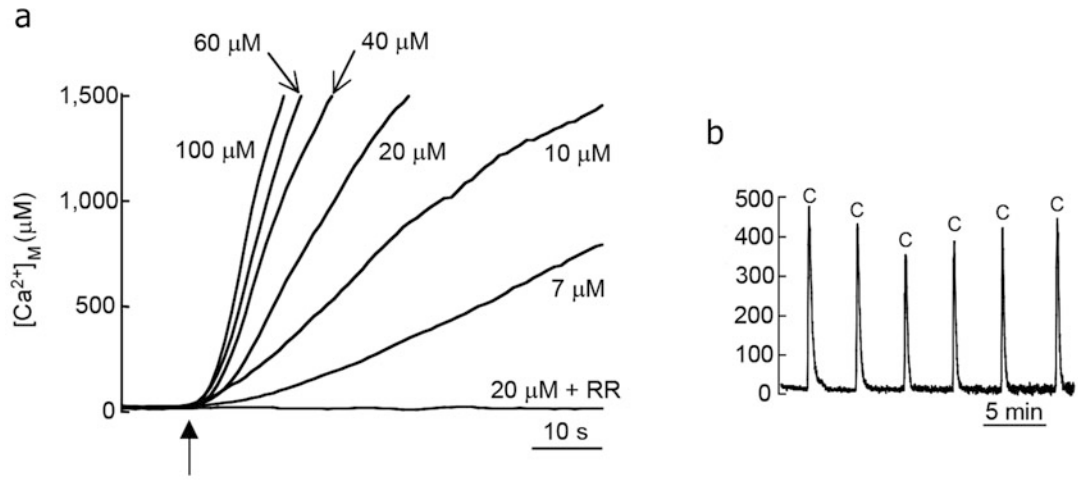

Fig. 6 Mitochondrial calcium measurements in bovine chromaffin cells expressing mit-mutAEQ reconstituted with synthetic coelenterazine *n* at 37 °C. (**a**) Example of an experiment in permeabilized cells performed as described in Subheading 3.2.2. After permeabilization and when indicated, chromaffin cells were perfused with a range of intracellular Ca^{2+} buffers (7–100 μM) to promote mitochondrial Ca^{2+} uptake. Perfusion of ruthenium red (RR), an inhibitor of the mitochondrial Ca^{2+} uniporter (MCU), prevented mitochondrial Ca^{2+} uptake. (**b**) Example of an experiment in intact cells performed as described in Subheading 3.2.1. Cells were repeatedly stimulated with short pulses (30 s) with 50 mM of caffeine (shown as **c**). (Reproduced from Montero et al. [6]. With permission to reuse content from Springer Nature)

(c) monensin, an ionophore that catalyzes the electroneutral exchange of Na^+/H^+ though membrane lipid bilayers.

17. Example of a calibrated Ca^{2+} recording in intact bovine chromaffin cells expressing VAMP-mutAEQ reconstituted with synthetic coelenterazine *n* at 22 °C is shown in Fig. 7a.
18. The digitonin concentration in the permeabilization solution must be adapted to the cell type used. Many usual culture cell lines, such as HeLa or HEK293 cell lines, require using 100 μM of digitonin for adequate permeabilization. However, 1-min permeabilization of chromaffin or PC12 cells with 100 μM of digitonin induces an important loss of aequorin luminescence from intracellular compartments, while 1-min permeabilization with 20 μM of digitonin allows the accessibility of the perfusion medium to the intracellular space without aequorin loss.
19. Example of a calibrated Ca^{2+} recording in permeabilized bovine chromaffin cells expressing VAMP-mutAEQ reconstituted with synthetic coelenterazine *n* at 22 °C is shown in Fig. 7b.
20. The algorithm derives from a mathematical model proposed to explain from a molecular point of view the light emission dependency on the $[Ca^{2+}]$ [19]. Here is used as a simple mathematical function that transforms luminescence data into $[Ca^{2+}]$.

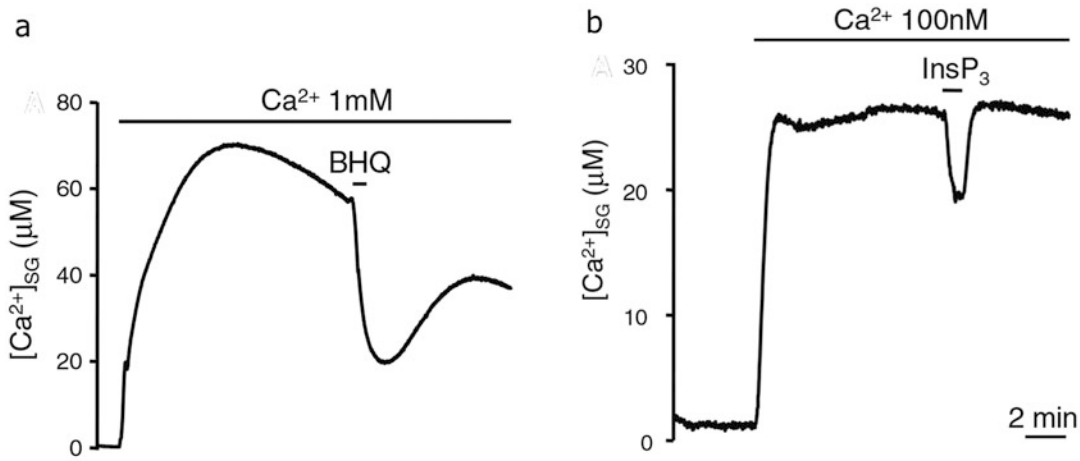

Fig. 7 Secretory vesicles calcium measurements in PC12 cells expressing mit-mutAEQ reconstituted with synthetic coelenterazine *n* at 37 °C. (**a**) Example of an experiment in intact cells performed as described in Subheading 3.3.1. As shown, Ca^{2+} depleted chromaffin cells were perfused with standard extracellular medium 1 mM Ca^{2+} to refill the secretory vesicle compartment. A 10 μM of BHQ was added when indicated to inhibit the SERCA pump. (**b**) Example of an experiment in permeabilized cells performed as described in Subheading 3.3.2. As shown, Ca^{2+}-depleted chromaffin cells were perfused with intracellular medium containing 100 nM Ca^{2+} free to refill the secretory vesicle compartment. A 2 μM of IP_3 was added when indicated to activate the IP_3-Receptors. (Reproduced from Santo-Domingo et al. [10]. With permission to reuse content from Springer)

References

1. Sparagna GC, Gunter KK, Sheu S-S et al (1995) Mitochondrial calcium uptake from physiological-type pulses of calcium. J Biol Chem 270:27510–27515
2. Zhao Y, Araki S, Wu J et al (2011) An expanded palette of genetically encoded Ca2+ indicators. Science 333:1888–1891
3. Suzuki J, Kanemaru K, Iino M (2016) Genetically encoded fluorescent indicators for organellar calcium imaging. Biophys J 111:1119–1131
4. Simpson USA, Brini AWM, Pozzan M et al (1995) Transfected aequorin in the measurement of cytosolic Ca 2 + concentration ([Ca 2 +]c). J Biol Chem 270:9896–9903
5. García AG, García-De-Diego AM, Gandía L et al (2006) Calcium signaling and exocytosis in adrenal chromaffin cells. Physiol Rev 86: 1093–1131
6. Montero M, Alonso MT, Carnicero E et al (2000) Chromaffin-cell stimulation triggers fast millimolar mitochondrial Ca2+ transients that modulate secretion. Nat Cell Biol 2:57–61
7. Rigual R, Montero M, Rico AJ et al (2002) Modulation of secretion by the endoplasmic reticulum in mouse chromaffin cells. Eur J Neurosci 16:1690–1696
8. Alonso MT, Barrero MJ, Carnicero E et al (1999) Functional measurements of Ca2+ in the endoplasmic reticulum using a herpes virus to deliver targeted aequorin. Cell Calcium 24:87–96
9. Alonso MT, Barrero MJ, Michelena P et al (1999) Ca2+-induced Ca2+ release in chromaffin cells seen from inside the ER with targeted aequorin. J Cell Biol 144:241–254
10. Santo-Domingo J, Fonteriz RI, Lobatón CD et al (2010) Ca2+ dynamics in the secretory vesicles of neurosecretory PC12 and INS1 cells. Cell Mol Neurobiol 30:1197–1199
11. Santo-Domingo J, Vay L, Camacho M et al (2008) Calcium dynamics in bovine adrenal medulla chromaffin cell secretory granules. Eur J Neurosci 28:1265–1274
12. Inouye S, Noguchi M, Sakaki Y et al (1985) Cloning and sequence analysis of cDNA for the luminescent protein aequorin. Proc Natl Acad Sci USA 82:3154–3158
13. Cobbold PH, Lee JAC (1991) Aequorin measurements of cytoplasmic free calcium. In:

Cellular calcium: a práctical approach. Oxford Press

14. Li X, Drakulich DA, Zhang P et al (2002) Transduction of bovine adrenal chromaffin cells using a recombinant adenovirus expressing GFP. J Neurosci Methods 122:91–96
15. Moro M, López M, Gandía L et al (1990) Separation and culture of living adrenaline- and noradrenaline-containing cells from bovine adrenal medullae. Anal Biochem 185: 234–238
16. Montero M, Brini M, Marsault R et al (1995) Monitoring dynamic changes in free Ca2+ concentration in the endoplasmic reticulum of intact cells. EMBO J 14:5467–5475
17. De la Fuente S, Fonteriz RI, Montero M et al (2013) Ca2+ homeostasis in the endoplasmic reticulum measured with a new low-Ca2+-−affinity targeted aequorin. Cell Calcium 54: 37–45
18. De la Fuente S, Fonteriz RI, de La Cruz PJ et al (2012) Mitochondrial free [Ca2+] dynamics measured with a novel low-Ca2+ − affinity aequorin probe. Biochem J 445:371–376
19. Allen DG, Blinks JR, Prendergast FG (1977) Aequorin luminescence: relation of light emission to calcium concentration-a calcium-independent component. Science 195:996–998

Chapter 12

Quantification of Secretory Granule Exocytosis by TIRF Imaging and Capacitance Measurements

Muhmmad Omar-Hmeadi, Liangwen Liu, Santiago Echeverry, and Sebastian Barg

Abstract

Hormones and neurotransmitters are released from (neuro)endocrine cells by regulated exocytosis of secretory granules. During exocytosis, the granule membrane fuses with the plasma membrane, which allows release of the stored content into the bloodstream or the surrounding tissue. Here, we give a detailed description of two complementary methods to observe and quantify exocytosis in single cells: high-resolution TIRF microscopy and patch-clamp capacitance recordings. Precise stimulation of exocytosis is achieved by local pressure application or voltage-clamp depolarizations. While the chapter is focused on insulin-secreting cells as an accessible and disease-relevant model system, the methodology is applicable to a wide variety of secretory cells including chromaffin and PC12 cells.

Key words Chromaffin cells, Insulin release, Patch-clamp, PC12, Secretory vesicles

1 Introduction

Insulin is secreted by regulated exocytosis in response to elevated blood glucose from β-cells in the islets of Langerhans, small clumps of cells that form the endocrine part of the pancreas [1]. Secretion of the hormone occurs by Ca^{2+}-dependent exocytosis of insulin containing granules and is often measured by traditional immunodetection (i.e., RIA or ELISA), but these assays have limited time resolution and do not give any direct information of insulin granule behavior or the exocytosis machinery. Here, we describe the application of two powerful (and complementary) single-cell techniques for studying exocytosis in individual pancreatic β-cells and other hormone-secreting cells: (1) patch-clamp cell-capacitance measurements [2] and (2) live-cell imaging by the total internal reflection fluorescence (TIRF) microscopy [3–5].

Ricardo Borges (ed.), *Chromaffin Cells: Methods and Protocols*,
Methods in Molecular Biology, vol. 2565, https://doi.org/10.1007/978-1-0716-2671-9_12,

2 Materials

2.1 Cells

1. Rat insulinoma INS1 cells are a popular model for β-cell insulin secretion and well suited for single-cell studies. Our lab uses INS1 832/13 cells ([6]; passage 79–100) maintained at 37 °C and 5% CO_2 in RPMI 1640 cell culture medium containing 10 mM glucose, supplemented with 10% fetal bovine serum, 100 μg/mL streptomycin, 100 U/mL penicillin, 1 mM sodium pyruvate, 10 mM HEPES, 2 mM L-glutamine, and 50 μM β-mercaptoethanol.
2. Human pancreatic β-cells prepared from isolated islets of human cadaveric donors (e.g., from the Nordic Network for Clinical Islet Transplantation Uppsala [7] or the ADI Isletcore at the University of Alberta; with ethical clearance from Uppsala Regional Ethics Board 2006/348 and Alberta Human Research Ethics Board, Pro00001754) [8]. Islets are maintained in CMRL 1066 culture medium containing 5.5 mM glucose, 10% fetal calf serum (FCS), 2 mM L-glutamine, 100 U/mL streptomycin, and 100 U/mL penicillin at 37 °C in an atmosphere of 5% CO_2.
3. Mouse β-cells isolated from dissected pancreas tissue by partial digestion with collagenase P (16 U/mL, Boehringer Mannheim) followed by manual isolation from exocrine tissue using a 200-mL pipette. Islets are maintained in RPMI-1640, 10% fetal calf serum, 100 U/mL penicillin, and 10 μg/mL streptomycin.

2.2 Labeling of Secretory Granules

Insulin granules are labeled by transient expression of marker proteins that combine a granule-localized protein with a fluorescent-protein tag, e.g., neuropeptide-Y-EGFP (NPY-EGFP). Both transient transfections with DNA plasmids using Lipofectamine 2000 or Lipofectamine 3000 (Life Technologies) in Opti-MEM (Life Technologies) and adenoviral vectors coding for the reporter constructs can be used. Cells should be imaged 24–30 h after transfection.

2.3 Solutions

1. Extracellular solution: 138 mM NaCl, 5.6 mM KCl, 1.2 mM $MgCl_2$, 2.6 mM $CaCl_2$, 3 or 10 mM D-glucose, and 5 mM HEPES, pH 7.4 adjusted with NaOH.
2. For imaging, add 200 μM diazoxide, a K^+-ATP-channel opener that prevents glucose-dependent depolarization.
3. For imaging, exocytosis is stimulated with high K^+ solution (75 mM KCl equimolarly replacing NaCl), which is pressure applied through a glass capillary (*see* Subheading 2.6).
4. For patch clamp: Intracellular solution: 125 mM Cs-glutamate, 10 mM CsCl, 10 mM NaCl, 1 mM $MgCl_2$, 0.05 mM EGTA,

3 mM Mg-ATP, 0.1 mM cAMP, and 5 mM HEPES, pH 7.2 adjusted using CsOH.

2.4 TIRF Microscope

Microscopy is performed on a custom-built or commercial "through the lens" total internal reflection (TIRF) microscope, based on a research grade upright microscope with high numeric aperture (NA > 1.42) objective. Our lab uses an Axio Observer Z1 (Zeiss) with a 100×/1.45 oil immersion objective. Excitation is from 3 DPSS lasers at 405, 491, and 561 nm passed through a cleanup quad-filter and controlled with an acousto-optical tunable filter. The emission light is split into two- or four-color channels (dual view, Teledyne) and projected onto a back-illuminated EMCCD or sCMOS camera.

2.5 Patch-Clamp Setup

Patch-clamp measurements are performed on an inverted research grade microscope equipped with a 40×/0.75 objective and optional fluorescence illumination and filters (for detecting fluorescently labeled cells). A commercial computer-controlled patch-clamp amplifier with appropriate software (e.g., HEKA EPC10 or Molecular Devices Axopatch) is used for recordings, and electrodes are maneuvered to individual cells using a commercial micromanipulator.

2.6 Pressure Application

Individual cells are stimulated during imaging by pressure ejection of a test solution (e.g., K^+ solution). The system consists of back-filled patch-clamp-type glass pipette seated in a patch-clamp-type holder that an be pressurized from an air pressure supply using a computer-controlled three-way valve (e.g., Lee Valves, LFAA1201618H the third port is left open to allow pressure release). The pipette is situated close to an individual cell using a micromanipulator.

3 Methods

3.1 Coverslip Preparation

1. Coat sterilized coverslip (#1.5, round 22 mm) with 100 μL poly-L-lysine in each 6-well plate. Incubate for 15–30 min at room temperature.
2. Wash three times with 2 mL PBS or ddH_2O and let dry.

3.2 Cell Preparation

1. For transfection, seed cells on poly-L-lysine-treated coverslips, transfect immediately with DNA plasmids using Lipofectamine 2000, and analyze 24–30 h later.
   (a) Opti-MEM and Lipofectamine 2000 are used for plasmid DNA transfection at a ratio of DNA (μg): Lipofectamine 2000 (μL) = 1: 0.8–1. Use 0.1–1 μg of plasmid per coverslip.

(b) Dilute plasmid DNA and Lipofectamine 2000 separately, each in 30 μL Opti-MEM per well, combine after 5 min, and incubate mixture for 20–25 min.

(c) Add 30 μL suspension of trypsinized INS1 cells or dispersed primary islet cells in Opti-MEM to the mixture.

(d) Seed the mixture (90 μL) into the center of coverslips placed in 6-well plates, and incubate at 37 °C/5% CO_2.

(e) After 2 h, remove the transfection mixture, and add 2 mL culture medium per well.

2. Seed dispersed human or primary mouse islets and infect with adenoviral vector.

(a) Disperse islets into single cells in 2 mL commercial Ca^{2+}-free cell dissociation buffer (e.g., PBS without Ca^{2+}/Mg^{2+}+EDTA) supplemented with trypsin (0.005%, e.g., Life Technologies) and gentle pipetting for 30 s.

(b) End trypsinization by adding 4 mL serum-containing medium and sediment cells for 5 min at 160 × *g*. Resuspend cells in 50–100 μL medium, and plate into the center of prepared coverslips.

(c) After 30 min, add 2 mL culture medium per well.

(d) Add adenovirus suspension after overnight culture of the cells.

3.3 TIRF Imaging of Single Granule Exocytosis

1. Mount the coverslip into a chamber suitable for microscopy, add the extracellular buffer, and maintain 37 °C by heating the chamber or perfusing with pre-warmed buffer. (Note: Prepare fresh extracellular buffer just before experiments.)

2. Find live and transfected cells and focus using minimal illumination (to minimize photodamage and bleaching of the granule marker).

3. A capillary filled with test solution (e.g., 75 mM K^+) is placed near the selected cell for computer-controlled application during an experiment. (1) Make sure the glass capillary is not leaking or broken after filling with K^+ solution. (2) Fill one-half to two-thirds of the capillary volume with no air bubbles at the tip of the capillary. (3) Test the computer-controlled flow is not too harsh to flow cells away. (4) Place the capillary perfectly near a single cell (too close will move or blow away the cell when pressure is applied, too far will not allow complete exchange of the solutions near the cell).

4. Acquire images at appropriate intervals; for exocytosis, we use 100 ms exposure at 10 s^{-1}; for slower processes, 1 s^{-1}. Stimulate cells by computer-controlled application of the stimulating solution. For exocytosis measurements, we apply K^+ solution

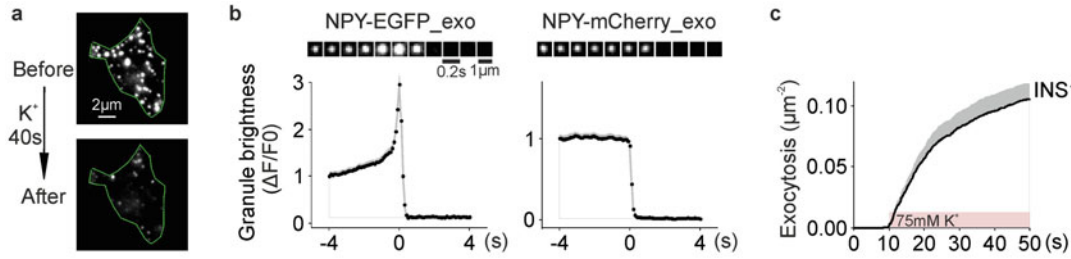

Fig. 1 (**a**) TIRF images of an INS1 cell expressing the granule marker NPY-EGFP before and after stimulation with elevated K^+ solution: Note loss of punctate granules by exocytosis. Scale bar: 2 μm. (**b**) Image sequences (0.2 s per frame) and time course of single granule exocytosis with the pH-sensitive marker NPY-EGFP (left) or the pH-insensitive marker NPY-mCherry. Traces quantify the fluorescence signal (ΔF), normalized to pre event average; the transient increase with NPY-EGFP is due the pH neutralization of the granule lumen during exocytosis that unquenches the marker fluorescence [4]. (**c**) Cumulative number of K^+ stimulated exocytosis events as function of time in NPY-EGFP expressing INS1 cells, normalized to cell footprint area ($n = 30$ cells). K^+ solution was applied during $t = 10$ to $t = 50$ s. Shaded areas represent SEM

for 40 s, starting 10 s into the recording, or 10 mM glucose for up to 20 min.

5. Save the acquired images.
6. Data analysis (example data are shown in **Note 1**).
   - Identify exocytosis events manually based on the characteristic rapid loss of the granule marker fluorescence (1–2 frames; *see* Fig. 1a, b); detecting is facilitated by rapidly playing the movie forward and back. Record position and time/frame of each event.
   - Measure cell footprint area (ImageJ-Analyze-area, circled by dash line with green color in Fig. 1a) for normalization.
   - Plot cumulative exocytosis events normalized by cell area versus time averaged for 30 cells each from at least three preparations (*see* Fig. 1c).

3.4 Patch-Clamp Measurements of Exocytosis and Ca^{2+} Currents

1. Configuration and protocols

   Exocytosis is measured as the change in the cell's membrane capacitance in the whole-cell or perforated whole-cell patch configurations. Capacitance is calculated from the current response to a sine wave voltage protocol during the repolarized segments of the stimulus protocol (−70 mV +/− 15 mV peak-to-peak at 1000 s^{-1}). Exocytosis is stimulated by brief depolarizations (e.g., −70 to 0 mV for 200 ms) or a train of depolarizations (e.g., 14 × 200 ms depolarizations at 2 s^{-1}).
2. Patch electrodes
   (a) Pull patch-clamp electrodes from glass capillaries (Hilgenberg, Germany; borosilicate glass 3.3, OD = 1.6 mm ID = 1.24 mm S = 0.18 mm) in two steps using a

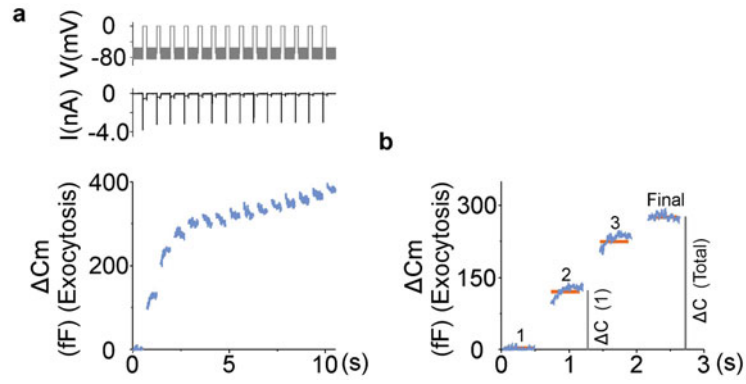

Fig. 2 (**a**) Depolarization evoked Ca^{2+} currents (black, middle) and exocytosis measured as capacitance increase (blue, lower) in response to a train depolarization protocol (upper) in INS1 cells. The increase in cell capacitance is due to exocytosis. (**b**) Illustration of the analysis. Every capacitance segment is averaged (red lines) and the difference between two segments (ΔC) if calculated. The sum of all ΔC is reported as total capacitance increase, which minimizes the influence of slow endocytosis

commercial micropipette puller (e.g., List-Medical D-6100 or Sutter P-77). The final resistance in the recording solution should be 2.8–4 MΩ.

(b) Coat the micropipettes tips with Sylgard 184 close to the tip without clogging; heat briefly to cure the Sylgard. Sylgard stock can be stored premixed with the curing agent at −20 C for several months.

(c) Fire-polish the tip of the micropipettes over a heated wire to smooth the edges. Store in a clean/dust-free environment and use the same day.

3. Seal formation and protocol acquisition

(a) Turn on the microscope, amplifier, and heating device 1 h before starting.

(b) Place the coverslip with the transfected cells into the preheated microscope chamber (37 °C), and fill it with an extracellular solution. Turn on the perfusion system with a low flow and constant bath level.

(c) Select a cell and center in the field of view. In our experience, cells with oval morphology are easy to patch. Avoid extremely flat cells or cells that are not well attached.

(d) Fill up a micropipette with the intracellular solution one-third, and shake to get rid of air bubbles that might clog the tip. Place the micropipette in the pipette holder of the headstage.

(e) While applying positive pressure in the micropipette, approach the cell using the micromanipulator controls. Zero the amplifier (zero current at zero voltage) before touching. Use the fine movements of the micromanipulator to let the electrode gently touch the cell, which increases resistance to ~0.3–0.5 MΩ (as determined using the square test-pulse function of the amplifier; 5 mV/5 ms). Apply low and constant negative pressure to induce the gigaseal formation >1 GΩ. Lower the holding potential to −70 mV.

(f) When a gigaseal is established, compensate the pipette capacitance (R_p), and then establish whole-cell mode with a brief pulse of suction. When in whole-cell mode, compensate the membrane capacitance (C_m) and the series resistance (R_s). The parameters for a good seal are seal resistance of >1 GΩ, $R_s < 10$ MΩ and leak ~30 pA for INS-1 cells.

4. Following the whole-cell formation, wait 1–2 min for the seal to stabilize, and then trigger the desired experimental protocol (Fig. 2a).

5. Data analysis (example data are shown in **Note 2**)

(a) Quantify average membrane capacitance for each segment of the train using the built-in capacitance function of the software, and report capacitance changes (ΔC_m) for each depolarization and the total (Fig. 2b).

(b) Ca^{2+} currents (ICa) are calculated as the average of 5–85% of the depolarization segment for the current segment. Na^+ currents (INa) are quantified as the negative peak current during the first 3% of the depolarization of the current segment.

4 Notes

1. Example of imaging of secretory granule exocytosis by TIRF microscopy Fig. 1.

2. Example of capacitance measurements of exocytosis Fig. 2.

References

1. Rorsman P, Ashcroft FM (2018) Pancreatic β-cell electrical activity and insulin secretion: of mice and men. Physiol Rev 98:117–214. https://doi.org/10.1152/PHYSREV.00008.2017

2. Lindau M, Neher E (1988) Patch-clamp techniques for time-resolved capacitance measurements in single cells. Pflugers Arch 411:137–146. https://doi.org/10.1007/BF00582306

3. Steyer JA, Almers W (2001) A real-time view of life within 100 nm of the plasma membrane. Nat Rev Mol Cell Biol 2:268–275. https://doi.org/10.1038/35067069

4. Barg S, Olofsson CS, Schriever-Abeln J et al (2002) Delay between fusion pore opening and peptide release from large dense-core vesicles in neuroendocrine cells. Neuron 33:287–299. https://doi.org/10.1016/S0896-6273(02)00563-9
5. Gandasi NR, Yin P, Omar-Hmeadi M et al (2018) Glucose-dependent granule docking limits insulin secretion and is decreased in human type 2 diabetes. Cell Metab 27:470–478.e4. https://doi.org/10.1016/J.CMET.2017.12.017
6. Hohmeier HE, Mulder H, Chen G et al (2000) Isolation of INS-1-derived cell lines with robust ATP-sensitive K+ channel-dependent and -independent glucose-stimulated insulin secretion. Diabetes 49:424–430
7. Goto M, Eich TM, Felldin M et al (2004) Refinement of the automated method for human islet isolation and presentation of a closed system for in vitro islet culture. Transplantation 78:1367–1375. https://doi.org/10.1097/01.TP.0000140882.53773.DC
8. Manning Fox JE, Lyon J, Dai XQ et al (2015) Human islet function following 20 years of cryogenic biobanking. Diabetologia 58:1503–1512. https://doi.org/10.1007/s00125-015-3598-4

Chapter 13

Membrane Capacitance Measurements of Stimulus-Evoked Exocytosis in Adrenal Chromaffin Cells

Elizabeth P. Seward and Robert C. Wykes

Abstract

Research using membrane capacitance (C_m) measurements in adrenal chromaffin cells has transformed our understanding of the molecular mechanisms controlling regulated exocytosis. This is in part due to the exquisite temporal resolution of the technique, and the possibility of combining quantification of exo-/endocytosis at the whole-cell level, with the ability to simultaneously monitor and control the calcium signals triggering vesicle fusion. In this regard, experiments performed with C_m measurements complement amperometry experiments that give a measure of secreted transmitter and the behavior of the fusion pore, and fluorescent microscopy studies used to monitor vesicle and protein dynamics in imaged regions of the cell. In this chapter, we provide a detailed account of the methodology used to perform whole-cell patch clamp measurements of C_m in combination with voltage-clamp recordings of voltage-gated calcium channels to quantify stimulus-secretion coupling in chromaffin cells. Stimulus protocols developed for investigation of functionally distinct releasable vesicle pools are also described.

Key words Exocytosis, Endocytosis, Chromaffin cells, Capacitance measurements, Calcium channels, RRP, IRP, SRP

1 Introduction

The ability to measure secretion has been an important advancement in our understanding of the mechanisms underlying stimulus-coupled exocytosis. Biochemical methods like spectrophotometric detection (a chemical reaction between the released product and an extracellularly applied molecule leading to formation of a colored or fluorescent signal) or radiochemical detection (radiolabeling of the released product) have been useful but offer poor time resolution and report secretion from a population of cells. Biophysical methods like amperometry (electrochemical detection) or membrane capacitance measurements (C_m) have much higher temporal resolution. These techniques allow the kinetics of release to be studied in detail at the single-cell level.

Ricardo Borges (ed.), *Chromaffin Cells: Methods and Protocols*,
Methods in Molecular Biology, vol. 2565, https://doi.org/10.1007/978-1-0716-2671-9_13,

Exocytosis involves the fusion of a secretory vesicle (a membrane-enclosed packet of neurotransmitter) with the cell plasma membrane to release its contents to the outside. The mixing of vesicle and cell membranes leads to an increase in the surface area of the plasma membrane. This increase in cell surface area can be measured by determining the cell membrane capacitance C_m since the value of a capacitor is directly proportional to its surface area [1].

The specific membrane capacitance of almost all biological membranes can be calculated (and experimentally measured using a modified Wheatstone bridge current balance) to be roughly 1 μF/cm^2:

$$C_m = (\varepsilon\varepsilon_0/d)A$$

(ε = dielectric constant, ε_0 = polarizability of free space, d = membrane thickness, A = area).

Therefore, a cell of 13 μm diameter will have a C_m of about 5.0 pF [2].

If the size of the vesicle can be calculated and a change in capacitance is measured, then it is possible to determine how many vesicles have fused in response to a given stimulus [3]. For adrenal chromaffin granules, the estimated increase in C_m resulting from fusion of single vesicle has been estimated to be in the range of 1.3 fF [4].

Measurements of C_m with whole-cell patch clamp recordings essentially apply a voltage and separate a capacitative current from a resistive current.

The current that flows across a capacitor is given by:

$$I_C = C \times dV/dt$$

Thus, if the voltage does not change, there is no capacitative current. Membranes also have resistive properties, and the current that flows across a resistor is given by Ohm's law:

$$I_R = V/R$$

Several distinct techniques have been developed for detecting C_m changes resulting from vesicle fusion. Time domain-based techniques involve applying square voltage pulses (at hyperpolarized voltages that will not activate nonlinear membrane conductances). The capacitive transients that charge the membrane capacitance are then canceled. Subsequent voltage steps to depolarized potentials evoke a nonlinear ionic current of interest. This current declines with an exponential time course. Fitting this exponential can be used to evaluate ΔC_m. A problem associated with this technique is that it relies on an instantaneous voltage step, which experimentally is difficult to achieve (pipette resistance can slow the voltage step, etc.), and the interval between

voltage steps must allow for complete charging/discharging of C_m. This therefore limits the resolution of this technique to estimate C_m to a frequency of 1 Hz (for further details, *see* refs. 2 and 5). The PRBS technique, similar to the time domain technique square-wave voltage pulses, is applied; however, the duration of the voltage step is now a random variable. The resulting stimulus spectrum approximates white noise. The spectrum of the resulting current signal is directly related to the admittance spectrum, from which C_m can be derived [6]. This method relies on fitting the admittance to theoretical algorithms to determine C_m; if these are not accurate, then the estimation of the cellular parameters will be inaccurate [7].

Sinusoidal excitation is the most commonly used technique and involves applying a sine wave about a hyperpolarized potential. If a sine wave is applied ($V_{Command}$) to a cell, then the resulting sinusoid current (I_m) will contain both a resistive and capacitative component. It is possible to split these components. When there is no change in voltage (peak of sine wave), there is no capacitative current. Therefore, all the current will be resistive and we know the voltage, allowing the determination of R_m. Likewise, when the voltage changes most (at the inflection point of the sine wave), there is no net applied voltage and thus no resistive current. At this point, all the current will be capacitative. As the voltage and current are known, it is possible to calculate membrane capacitance. Since the sinusoid current is shifted with respect to the voltage stimulus, the magnitude and degree of phase shift can be analyzed using a phase-sensitive detector to produce estimates of C_m. The first studies using a hardware-based phase-sensitive detector (lock-in amplifier) were developed by [1]. Since then, software-based phase detectors and C_m measurement techniques have been developed [8–10]. Exocytosis may be triggered by interrupting the sinusoidal stimulus and applying variable depolarizing steps to stimulate calcium influx through voltage-gated calcium channels [11–14], ligand-gated and receptor-operated channels [15, 16], or photolysis of caged Ca^{2+} [17, 18]. Combining measurements of the calcium signals controlling exocytosis with C_m measurements of vesicle fusion has transformed our understanding of the molecular mechanisms regulating exocytosis in chromaffin cells [19] and crucially allows the researcher to quantify and distinguish between effects mediated through the calcium signals and calcium-sensitive proteins that regulate vesicle priming and fusion and calcium-independent molecular interactions that also control stimulus-secretion coupling.

2 Materials

2.1 Solutions and Small Parts

All solutions should be prepared using ultrapure water and analytical grade reagents. For convenience, we recommend making a 10X stock of the "external" solution (without added glucose or HEPES) to inhibit bacterial growth; this solution can be stored at room temperature for several months. 1X "external" solution with added glucose and HEPES and pH adjusted are made fresh on the day of the experiment. The pipette filling solutions are filter sterilized (0.4-μm filter) and stored frozen in aliquots at −20 °C.

1X external solution: 150 mM NaCl; 2 mM KCl; 5 mM $NaHCO_3$; 1 mM $MgCl_2$; 2.5 mM $CaCl_2$; 10 mM glucose; 10 mM HEPES; pH adjusted to 7.3 with NaOH; osmolarity adjusted with 1 M sucrose to ~310 mOsm.

Whole-cell patch pipette solution: 145 mM D-Cs-glutamate; 10 mM HEPES; 8.5 mM NaCl; 2.0 mM ATP-Mg, 0.1 mM GTP, 0.3 mM BAPTA, adjusted to pH 7.3 with CsOH; osmolarity ~290 mOsm (*see* **Note 1**).

For perforated whole-cell patch recordings, ATP and GTP are omitted from the pipette solution (*see* **Note 2**).

Borosilicate glass capillaries (such as those available from Multichannel Systems or Warner Instruments) with external and internal diameters of 1.65 (or as required to fit the electrode holder supplied with headstage of patch clamp amplifier) and 1.3 mm, respectively.

Patch pipette filling needle, such as MicroFil™ (World Precision Instruments) nonmetallic syringe needle.

A 1-mL plastic syringes and 0.22-μm syringe filters.

Sylgard™ 184 Elastomer kit.

2.2 Equipment

Inverted microscope on a vibration-isolation table with micromanipulator.

Patch clamp amplifier such as HEKA EPC-10 or Sutter dPatch (*see* **Note 3**).

Pipette holder suitable for patch clamp headstage.

Computer for controlling amplifier and data recording.

Pipette puller (such as Narishige PC-100 or Sutter Instruments P1000).

Microforge for polishing pipette tip and curing Sylgard (such as MF2 from Narishige or CPM-2 from ALA Scientific).

Vortex and sonicator (if using perforated patch method; *see* **Note 2**).

3 Methods

3.1 Fabrication of Patch Pipettes

1. Custom-made capillary borosilicate glass microelectrodes are pulled in two stages on a commercial pipette puller, and the second heat setting is adjusted produce a pipette with a tip diameter of ~1–2 μm and resistances of 1.5–2.0 mΩ for perforated patch or 2–5 mΩ for whole cell recordings.
2. To reduce stray capacitance (*see* **Note 4**), coat the shank of the pipette up to the tip with a hydrophobic substance (wax or Sylgard) to prevent liquid from "climbing" up and wetting the pipette due to surface tension. Sylgard is prepared by mixing nine parts resin to one part catalyst oil. The mixture may be placed and stored in a small volume syringe and stored at −20 °C until needed. Sylgard is "painted" around the shank of each electrode up to the tip using a hypodermic needle (19-gauge needle) attached to the syringe. The Sylgard must be cured quickly by placing the electrode between the coils of a fine wire heater for ~30 s. Alternatively, pipettes may be dipped in Sticky Wax (Kerr Inc., Orange, CA, USA, or similar) [20].
3. Fire polishing is the final stage of pipette fabrication and used to remove any contaminants and smooth the edges of the pipette to aid "giga seal" formation with the membrane. A microforge is used to visualize and fire polish the pipette; a platinum filament lightly coated with melted electrode glass provides the heat source. A reduction in pipette tip diameter and a faint darkening of the tip indicate that polishing has occurred. Once fabricated, patch pipettes are stored on a layer of BluTack™ stuck on the base of large petri dish; keep the dish closed at all times to protect the pipettes from accidental damage and to avoid contamination with dust. We find pipettes work best if made on the same day of the experiment and fire polished shortly before the experiment. For further discussions on making patch electrodes, *see* [21].

3.2 Whole-Cell Patch Clamp Recording and C_m Measurements of Exocytosis

1. Set up the patch clamp amplifier as per manufacturer instructions, mount the headstage on a micromanipulator located near the recording chamber, and attach the manufacturer-recommended patch pipette holder with mounted Ag/AgCl wire to the headstage.
2. Set up voltage stimuli protocols on the data acquisition software, and activate the software-implemented lock-in amplifier (e.g., *see* Fig. 2). We routinely use the Sine + DC method available with Patchmaster software (HEKA). For whole-cell recordings of C_m in chromaffin cells, we add a 1-kHz sinusoidal voltage (30–35 mV amplitude; *see* Table 1) to the holding membrane potential, typically set at −80 mV. Estimates of

Table 1
Sine wave parameters used for software lock-in measurements of C_m

Peak amplitude (mV)	35
Frequency	1.0 kHz
Points per cycle	25
Cycles to skip	1
Cycles to average	1
Total cycles	250

C_m are generated at one point per cycle; for these settings, the time resolution will be 1 ms per point. Avoid setting the amplitude of the sinusoid in a range where activation of voltage-dependent channels may occur.

3. Set the gain of the patch clamp amplifier between 5 and 10 mV/pA, and adjust as needed to avoid saturation by current transients. Set the current Bessel filters: filter 1–10 kHz and filter 2–3 kHz.
4. Isolated chromaffin cells need to be plated in such a way that they are easily visualized on an (inverted) microscope and accessible with a patch electrode (*see* **Note 5**). Continuous or frequent perfusion of the cells with external solutions at 1–5 mL/min is recommended to avoid autocrine and paracrine regulation of calcium channels and exocytosis [22, 23]. Figure 1 illustrates a simple gravity-fed system that may be used to perfuse cells with external solution and apply drugs in a time- and concentration-dependent manner.
5. After placing the recording chamber and cells on the stage of the microscope, place a Ag/AgCl pellet, which is connected to the ground pin of the headstage, in the external solution perfusing the cells (*see* **Note 6**). Identify the cell you wish to record from before proceeding to fill the patch pipette.
6. Once a cell has been identified for patching, proceed with filling the patch pipette with solution. If using non-capillary glass or perforated patch methods, pipette tips are first dipped into filtered internal solution for a few seconds to induce uptake by capillary action and then backfilled using a Micro-Fil™ nonmetallic syringe needle. Gentle shaking and flicking of the pipette will remove any air bubbles. In perforated patch recordings, the same procedure is applied although the tips are dipped in amphotericin B-free internal for 10 s prior to backfilling with internal containing amphotericin B (*see* **Note 2**).
7. The filled pipette is attached to the headstage of the amplifier using the pipette holder supplied with the amplifier, making

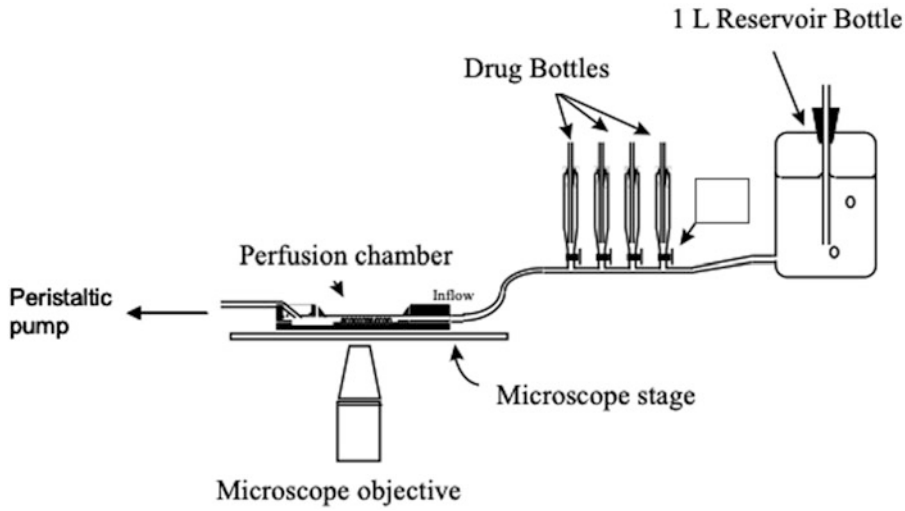

Fig. 1 A schematic representation of a gravity-controlled perfusion system. Cells were continually superfused (~1–2 mL/min) with external solution to remove effects of released endogenous modulators and remove traces of culture media and cell debris, which impede gigaohm seal formation. All solutions may be kept at room temperature or passed through an in-line controllable perfusion heating system placed in front of the inflow (such as the TC02 from MultiChannel Systems or Warner Instruments). Superfusion was obtained by use of gravity flow from a 1-liter reservoir bottle. Solutions containing drugs or altered external composition were stored in 10-, 20-, or 50-mL syringes connected in series with the main reservoir bottle. The solutions can be changed by switching a three-way stopcock/taps (such as those available through Cole-Parmer) connected to the bottom of the syringes; numerous stopcocks may be connected in series to allow easy switching between multiple different solutions. The height of the syringes is adjusted so that the flow rate from them is matched to the flow rate from the reservoir bottle. Additionally, stoppers containing a fixed length of plastic tubing are placed into the syringes to ensure a constant flow rate; aligning the bottom of the tubing in the bottle and syringes will ensure even flow rates. The addition of the stoppers and plastic tubing is important; otherwise, the flow rate will alter as the fluid levels in the syringes and bottles change. The outflow may be controlled by a peristaltic pump, vacuum, or gravity. A narrow bore metal tube, bent at 45° and beveled at one end, is attached to the outflow tubing (a low-gauge needle (e.g., 19 G) may be used for this purpose). This metal tube is placed in the superfusion chamber and held in place by either a small magnet or a piece of BluTack™. The tip of this metal tube is placed just below the meniscus of the desired bath volume. The outflow tube contained a small piece of silver wire and was passed through a bubble trap to reduce noise. A steady rate (inflow matching outflow) is achieved by optimizing the diameter of tubing flowing in and out of the system

sure that the Ag/AgCl wire in the holder is in contact with the solution in the pipette. Positive and negative pressure is applied to the pipette through tubing attached at one end to the holder and at the other end to a three-way stopcock and 1-mL syringe. With the aid of the micromanipulator, lower the pipette into the bath solution with positive pressure applied to prevent the tip being clogged before it reaches the cell membrane. Avoid applying much positive pressure when using the perforated patch experiments as the aim is to achieve giga seal formation

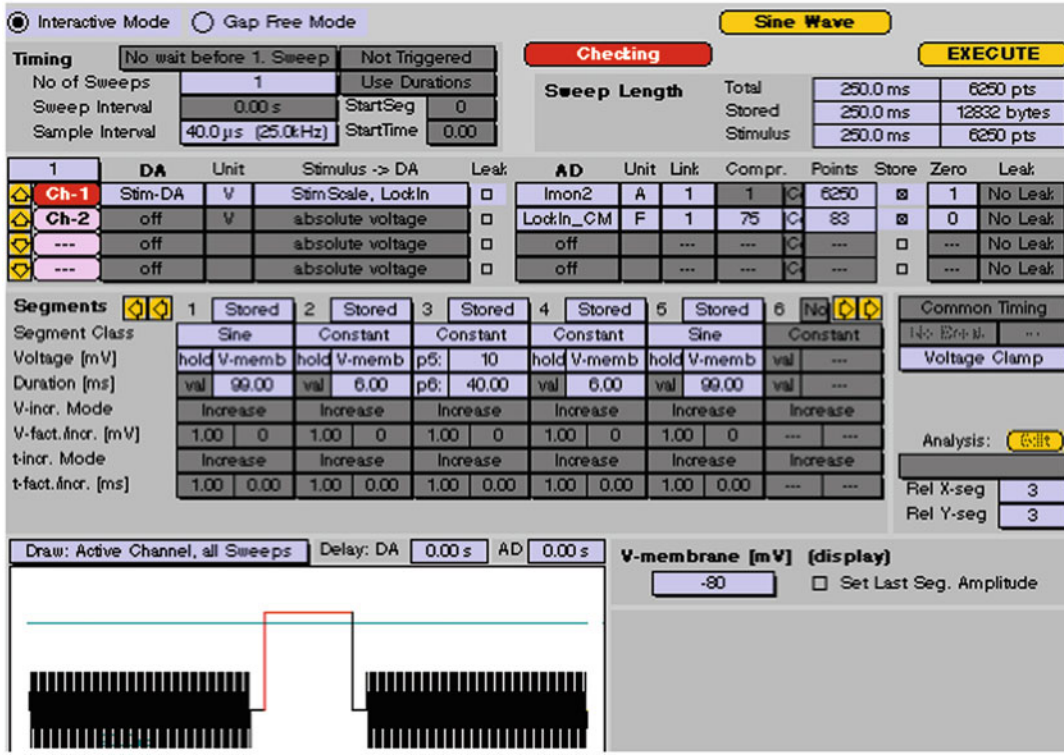

Fig. 2 Setting up a simple voltage-stimulus protocol for quantifying exocytosis using C_m measurements in response to a step depolarization. The image above shows a sample pulse generator file setup using Patchmaster software to perform C_m measurements with an EPC-10 amplifier. Activation of voltage-gated calcium channels and calcium influx to trigger exocytosis is accomplished through delivery of a single step in the membrane potential from a holding potential of −80 to +10 mV for the specified time, in the case shown here 40 ms. A sinusoidal voltage is added to membrane potential (100 ms duration in this case) before and after the step depolarization. A short segment of constant potential (6 ms in the example) at the holding potential is inserted between the step and sinusoidal segment to allow for measurements of the holding current and settling of any tail currents evoked by the step. A cartoon view of the stimulus can be seen at the bottom of the image. Currents recorded during the step depolarization are used to measure calcium influx across the membrane, while positive differences in C_m (ΔC_m) measured before and after the voltage step are used to quantify exocytosis. Parameters of the sine wave used can be seen in Table 1

before the perforant (amphotericin B) reaches the tip and perforation commences.

8. Once the electrode is in contact with the external solution, the command potential at the electrode is set to 0 mV and the current zeroed by canceling any junction potential differences using the offset on the amplifier (*see* **Note 7**). A small seal test voltage step (5–10 mV, 5 ms duration) is applied at high frequency (10 Hz) to monitor the electrode resistance. The electrode is then manipulated until its shadow can be seen under high magnification and then placed directly above a target cell; positive pressure is released. The electrode is then

slowly lowered onto the cell using the fine control on the micromanipulator; contact with the cell membrane can be observed by an increase in the input resistance. Before going whole cell, or obtaining electrical assess with the perforated patch method, it is necessary to obtain a giga seal (a seal whose electrical resistance is >1 GΩ) between the electrode tip and cell; this is achieved by application of gentle negative pressure on the pipette. Formation of the giga seal is monitored by observing a decrease the current evoked by the test seal voltage step as the resistance at the electrode tip increases. As the seal is forming and the resistance of the pipette is observed to be increasing, the holding potential may be hyperpolarized from 0 to −80 mV. A giga seal is usually obtained within seconds of touching a cell. Diagrammatic representations of the whole-cell and perforated patch recording configuration can be seen in Fig. 2 of Chapter 9 of this book.

9. Once a stable giga seal is established, use the fast capacitance compensation on the amplifier to eliminate the electrode current transients elicited by the test seal voltage steps.
10. To establish the whole-cell recording configuration, apply further gentle suction (negative pressure) to rupture the patch of membrane under the pipette; this leads to a sudden increase in capacitive transients; *see* ref. [24] for further details. This increase in current reflects the addition of the whole cell membrane to the pipette input capacitance. These transients at the start and end of a pulse should now be nulled by use of the patch amplifier capacitance compensation and series resistance compensation. For chromaffin cells, typically whole-cell capacitance is ~6 pF and series resistance <10 mΩ. If using the perforated patch recording method, do not apply any further pressure after establishing the giga seal, but wait for the perforant to enter the membrane and monitor perforation of the patch by observing changes in the transients evoked by the seal test voltage steps, the gradual appearance of the slow capacitance transients, and the series resistance to drop <15 mΩ. When stable (usually after ~20 min), use the patch amplifier slow capacitance compensation and series resistance compensation to null the transients (*see* **Note 8**).
11. Once voltage clamp of the cell has been established, the external solution may be exchanged for one in which the [NaCl] is reduced by 10 mM and replaced with 10 mM TEA-Cl. TEA will block calcium-dependent outward potassium currents that could contaminate calcium current traces elicited with long depolarizations. The solution should only be exchanged after establishing voltage clamp to avoid uncontrolled depolarization of the cell (due to block of potassium channels by TEA-Cl) stimulating secretion prior to the start of the experiment.

Tetrodotoxin (1 μM) may also be added to the external solution to block voltage-gated sodium current contamination of voltage-gated calcium current recordings.

12. After a suitable delay (~3 min) to allow the pipette solution to dialyze the cell, exocytosis may be triggered by application of a stimulus that causes sufficient rise in intracellular [Ca^{2+}]. Application of depolarizing voltage steps of varying amplitude and duration to stimulate Ca^{2+} influx through voltage-gated calcium channels is easily implemented. C_m is measured before and after each depolarization using the software lock-in and addition of a sinusoidal voltage to the holding potential (*see* Figs. 2, 3, 4, and 5 and **Note 9** for a description of commonly used stimulus protocols).

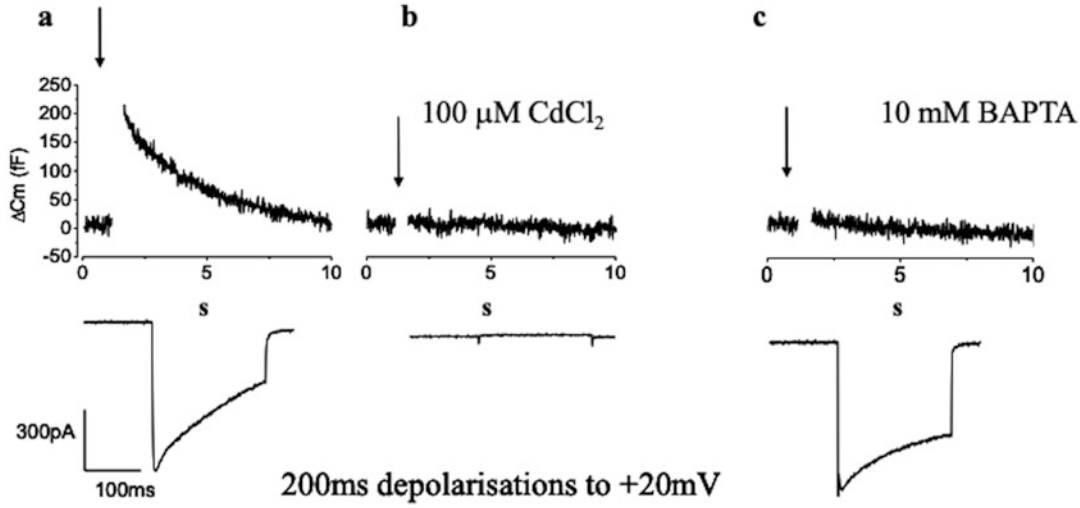

Fig. 3 C_m increases caused by exocytosis are triggered by a rise in intracellular Ca^{2+} in chromaffin cells. Exocytosis may be inhibited either by blocking calcium channels with 100 μM $CdCl_2$ or by addition of a high concentration (10 mM) of the fast calcium chelator BAPTA to the pipette solution. (**a**) Sample capacitance (top) and current (bottom) traces evoked by 200-ms depolarizations from −80 to +20 mV in bovine adrenal chromaffin cells. Arrows above the traces indicate when C_m measurements were interrupted (indicated by gaps) to apply the depolarizing voltage stimulus. Increases in C_m due to exocytosis can be clearly seen to occur on a much faster timescale than compensatory endocytosis, observed as a subsequence decline in C_m back to baseline. (**b**) Application of 100 μM $CdCl_2$ to the extracellular solution abolishes both ΔC_m and calcium entry in response to a 200-ms depolarization. (**c**) In whole-cell patch clamp experiments, increasing intracellular [BAPTA] from 0.3 to 10 mM increases calcium entry by inhibiting calcium channel inactivation [14], but exocytosis and ΔC_m increases are inhibited due to calcium chelation
Performing a simple experiment such as this is recommended for researchers setting up C_m measurements of exocytosis for the first time to validate their method

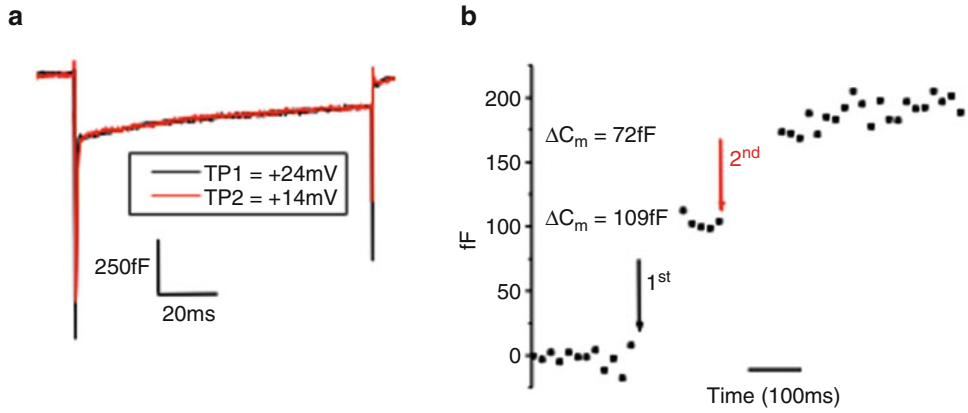

Fig. 4 Using C_m measurements to quantify the readily releasable pool of vesicles in chromaffin cells. (**a**) Sample current traces from a pair of 100-ms depolarizations given 100 ms apart to different membrane potentials to ensure identical calcium entry during the depolarization. (**b**) Sample capacitance points, displaying the ΔC_m in response to each depolarization. To determine the size of the RRP, a pair of 100-ms depolarizations are applied with a 400-ms interval, and the step potentials for the two pulses are adjusted to ensure that equivalent calcium influx is delivered in response, as shown. Using this protocol, we have estimated the RRP in bovine chromaffin cells using the perforated patch configuration at 193 ± 27 fF, $n = 9$. To measure the IRP, a similar approach is taken, but the step depolarizations are reduced to 10 ms duration and given with a 100-ms interval, giving an estimated pool size of 40 ± 10 fF, $n = 18$

3.3 Data Analysis

Calcium currents may be analyzed by determining the maximum "peak" current detected within predefined limits. Limits are usually set between 3 ms after the start of the step depolarization and 1 ms from the end to avoid contamination from sodium and tail currents, respectively (*see* **Note 10**). Additionally, calcium influx may also be quantified determined by integration of the voltage-gated calcium currents, again between the defined limits.

The total "synchronous" ΔC_m triggered by each voltage step in a protocol is calculated as the difference between an averaged value before depolarization and an averaged value after depolarization; typically, we average between 3 and 5 points. With trains of depolarizations, positive drifts in C_m between pulses, referred to as "asynchronous" exocytosis, are quantified by averaging the first 3–5 points acquired immediately after the voltage step and subtracting them from the average of 3–5 points taken immediately before the next voltage pulse. Summing the synchronous and asynchronous C_m increases provides a total measure of exocytosis evoked by a given protocol. Exocytotic efficiency may be determined by dividing the size of the C_m increase by the value obtained for integrating the corresponding calcium current.

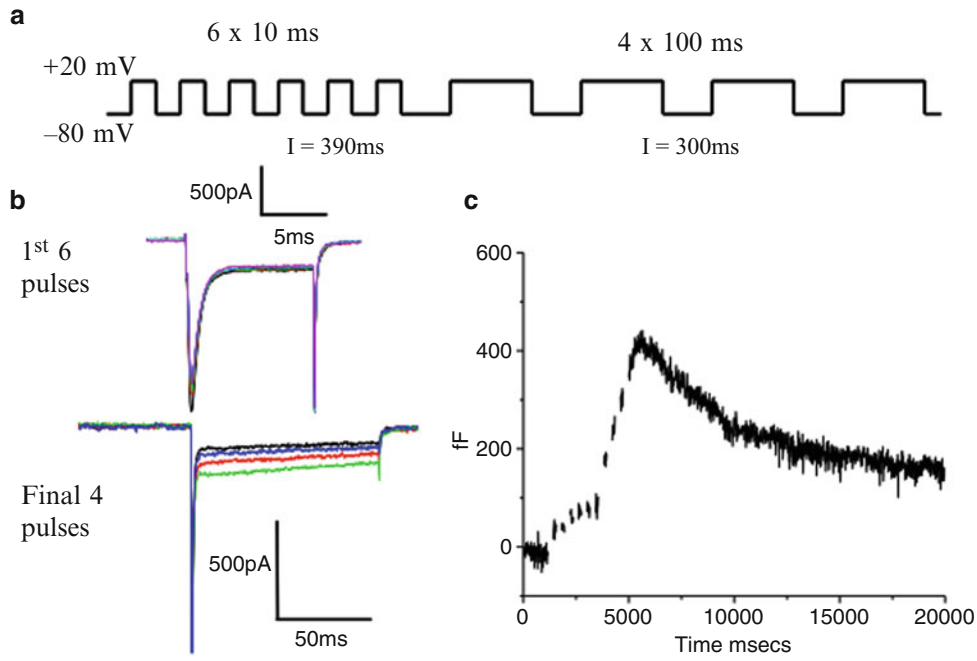

Fig. 5 Exocytosis evoked by a train of depolarizing voltage steps shows depletion of the immediately releasable pool of vesicles. (**a**) The protocol is shown schematically. Six 10-ms depolarizations with an interpulse interval of 390 ms are delivered immediately followed by four 100-ms depolarizations with an interpulse interval of 300 ms. (**b**) Representative calcium currents in response to this protocol, top (6 × 10 ms), bottom (4 × 100 ms). (**c**) Corresponding capacitance trace to the calcium currents shown in (**b**). The trace is biphasic with release in response to the first six short pulses becoming depressed as the IRP is depleted and then increasing again in response to the last four longer pulses as secretion from the RRP and SRP is triggered. Asynchronous release can be observed as a slow upward drift in the C_m after the last depolarization, and this is then followed by a slow decline as endocytosis takes over

4 Notes

1. Note the concentration of BAPTA or EGTA and free [Ca^{2+}] in the internal patch electrode solution impacts exocytosis when using the whole-cell configuration [11, 25, 26]. In perforated patch experiments [27], intracellular [Ca^{2+}] is not directly manipulated but controlled by endogenous buffering mechanisms [28].
2. For perforated whole-cell patch recordings, ATP and GTP are omitted from the pipette solution, and amphotericin B (Sigma, A4888) at a final concentration of 250 μg/mL (made freshly from a stock of 10 mg/mL in tissue culture grade DMSO, Sigma, D2650) is added to an aliquot of the pipette solution, vortexed (~30 s), sonicated (~30 s), and then vortexed again immediately before use. Stock is kept at room temperature in the dark and can be used for several days. The pipette solution

is made fresh on the day of the experiment and also stored in the dark; we find making fresh amphotericin pipette solution every few hours improves perforation.

The electrode tip is dipped for a few seconds into amphotericin-free internal and then backfilled with internal containing the perforation reagent. Internal solution is briefly vortexed before pipette filling. The 1-mL syringe used to backfill the pipette with the amphotericin-containing pipette solution must not be fitted with any filters. For further details on the perforated patch method for establishing whole-cell voltage-clamp, please *see* ref. 27.

3. Patch clamp amplifiers suggested both have facilities to combine whole-cell voltage-clamp recordings with the software-based sinusoidal excitation and C_m measurements described in this chapter.
4. It is essential when making capacitance recordings that there are no stray capacitance changes associated with the pipette. Most stray capacitance arises across the pipette wall between the pipette and bath [29]. Pipette capacitance can be reduced using the pipette capacitance cancellation circuitry on the patch clamp amplifier. It is possible (and necessary) to reduce stray capacitance further by using a small perfusion chamber, keeping the depth of the bathing solution to a minimum, and only filling the electrode with enough internal solution to make contact with the silver wire. Also, stray capacitance is attenuated further by coating the shank of the pipette up to the tip with a hydrophobic substance to prevent liquid from "climbing" up and wetting the pipette due to surface tension. To do this, we coat our electrodes with Sylgard, which also has the advantage of thickening the wall of the pipette, reducing capacitive coupling between the bath and pipette solutions.
5. Isolated chromaffin cells may be plated on 13- or 16-mm collagen type VII (rat tail), poly-D lysine or Matrigel-coated glass coverslips in 24- or 12-well plates at either 100,000 or 200,000 cells/well and covered with 1 or 2 mL of feeding media (10% fetal calf serum, 90% DMEM supplemented with 44 mM $NaHCO_3$, 15 mM HEPES, 0.1 mg/mL penicillin/streptomycin solution, 0.05 mg/mL gentamicin, 2.5 mg/mL 5′-fluorodeoxyuridine, 0.5 mg/mL cytosine-β-γ-arabinofuranoside, and 1% glutamine). Cells are kept in a humid incubator (5% CO_2 at 37 °C). At 24 h post preparation, ~ 70–80% of the feeding media is exchanged with fresh media. Cells are typically used 48–120 h post preparation.

   For each experiment, a coverslip with isolated adrenal chromaffin cells is transferred to a perfusion chamber (such as Warner instruments, model P3/P4), placed on the stage of an inverted microscope, and viewed under phase contrast optics at

320–400× magnification using a long-working distance objective.

6. In experiments where the ionic composition of the external solution is altered in such a way that a change in the liquid junction potential will occur [30], use of a salt bridge to connect the ground electrode/pellet to the recording chamber is recommended. *See* [31] and https://www.warneronline.com/tutorials-method for further details.
7. Since the external and patch pipette contain solutions of different ionic composition, a liquid junction potential will exist at the pipette tip. An error in membrane voltage measurement will arise because of this liquid junction potential of the pipette tip [29]. The voltage error induced by liquid junction potentials is fairly easy to measure. With the patch clamp amplifier set to current clamp, a pipette containing internal solution is placed into the bath, which also contains internal solution. Any tip potential should then be zeroed before exchanging the bath solution for external solution. A liquid junction potential between internal and external will be displayed on the amplifier, which can be noted. This potential difference can be applied to the voltage command when performing experiments or corrected for when analyzing results if desired. For the solutions given here, the liquid junction potential between the patch pipette solution and external solutions is +15 mV. If the bath solution is changed for one with a different ionic composition, a further liquid junction will develop between the new bath solution and the reference (ground) electrode. In this case, an agar or salt bridge should be employed to keep the reference electrode zero.
8. Exocytosis and endocytosis have been shown to run down in the whole-cell configuration [11, 32]; therefore, if the experiment requires prolonged recordings, for example, for testing the effects of pharmacological agents or activation of receptor signaling pathways [16, 33], then use of the perforated configuration is recommended as this prevents rundown, allowing reproducible responses for periods of several hours.
9. In chromaffin cells across species, capacitance jumps evoked in response to a train of brief (10–25 ms) depolarizations [17, 34] or photoreleased Ca^{2+} are biphasic [18], which are interpreted as representing fusion of vesicles from functionally distinct "releasable" pools. Vesicles in the immediately releasable pool (IRP) fuse in response to very brief depolarizations in which the required elevation of intracellular calcium for exocytosis is restricted to the immediate proximity of the calcium channels [35, 36], while vesicles in the readily releasable pool (RRP) fuse in response to longer depolarizations but are rapidly depleted.

It is possible to quantitate the size of the IRP and RRP using a dual-pulse protocol [17, 37] (*see* Fig. 4) and using the equation $B_{max} = S/(1 - R^2)$, where S represents the capacitance sum of the first (ΔC_{m1}) and second (ΔC_{m2}) and R is the ratio $\Delta C_{m2}/\Delta C_{m1}$. The upper limit of the pool size is assumed to be the value derived for B_{max}, and a lower pool size estimate is given by S.

An alternative protocol used to measure vesicle pools with C_m measurements is the "6 + 4" train of depolarizations (*see* Fig. 5). This protocol consists of a train of six 10-ms pulses followed by four 100-ms pulses. With this protocol, the 10-ms stimuli will result in a ΔC_m that reflects fusion of the IRP, and the further four longer pulses result in a second bout of secretion that reflects fusion of the remainder of the RRP and a fraction of the SRP [38].

10. It is not always necessary to block sodium currents in chromaffin cells if step depolarizations used to trigger calcium influx and exocytosis are to potentials greater than 0 mV. This is because sodium currents in adrenal chromaffin cells inactivate by 3 ms after a depolarizing pulse to potentials greater than 0 mV and may be easily distinguished from the slower activating voltage-gated calcium channels (*see* Fig. 4).

References

1. Neher E, Marty A (1982) Discrete changes of cell membrane capacitance observed under conditions of enhanced secretion in bovine adrenal chromaffin cells. Proc Natl Acad Sci U S A 79:6712–6716
2. Gillis K (1995) Techniques for membrane capacitance. In: Sakmann B, Neher E (eds) Single channel recording. Springer, pp 155–198
3. Penner R, Neher E (1989) The patch-clamp technique in the study of secretion. Trends Neurosci 12(4):159–163. https://doi.org/10.1016/0166-2236(89)90059-3
4. Moser T, Neher E (1997) Estimation of mean exocytic vesicle capacitance in mouse adrenal chromaffin cells. Proc Natl Acad Sci U S A 94:6735–6740
5. Lindau M, Neher E (1988) Patch-clamp techniques for time-resolved capacitance measurements in single cells. Pflugers Arch 411(2): 137–146
6. Fernandez JM, Bezanilla F, Taylor RE (1982) Effect of chloroform on charge movement in the nerve membrane. Nature 297(5862): 150–152
7. Neher E, Zucker RS (1993) Multiple calcium-dependent processes related to secretion in bovine chromaffin cells. Neuron 10(1):21–30
8. Joshi C, Fernandez J (1988) Capacitance measurements. An analysis of the phase detector technique used to study exocytosis and endocytosis. Biophys J 53:885–892
9. Filder N, Fernandez J (1989) Phase tracking: an improved phase detection technique for cell membrane capacitance measurements. Biophys J 56:1153–1162
10. Gillis KD (2000) Admittance-based measurement of membrane capacitance using the EPC-9 patch-clamp amplifier. Pflugers Arch 439(5):655–664. https://doi.org/10.1007/s004249900173
11. Seward EP, Nowycky MC (1996) Kinetics of stimulus-coupled secretion in dialyzed bovine chromaffin cells in response to trains of depolarizing pulses. J Neurosci 16(2):553–562
12. Moser T, Neher E (1997) Rapid exocytosis in single chromaffin cells recorded from mouse adrenal slices. J Neurosci 17:2314–2323
13. Lukyanetz EA, Neher E (1999) Different types of calcium channels and secretion from bovine chromaffin cells. Eur J Neurosci 11(8): 2865–2873
14. Wykes RC, Bauer CS, Khan SU et al (2007) Differential regulation of endogenous N- and P/Q-type Ca2+ channel inactivation by Ca2+/calmodulin impacts on their ability to support

exocytosis in chromaffin cells. J Neurosci 27(19):5236–5248
15. Mollard P, Seward EP, Nowycky MC (1995) Activation of nicotinic receptors triggers exocytosis from bovine chromaffin cells in the absence of membrane depolarization. Proc Natl Acad Sci U S A 92:3065–3069
16. Teschemacher AG, Seward EP (2000) Bidirectional modulation of exocytosis by angiotensin II involves multiple G-protein-regulated transduction pathways in adrenal chromaffin cells. J Neurosci 20:4776–4785
17. Voets T, Neher E, Moser T (1999) Mechanisms underlying phasic and sustained secretion in chromaffin cells from mouse adrenal slices. Neuron 23:607–615
18. Houy S, Martins JS, Mohrmann R et al (2021) Measurements of exocytosis by capacitance recordings and calcium uncaging in mouse adrenal chromaffin cells. Methods Mol Biol 2233:233–251. https://doi.org/10.1007/978-1-0716-1044-2_16
19. Marengo FD, Cárdenas AM (2018) How does the stimulus define exocytosis in adrenal chromaffin cells? Pflugers Arch 470(1):155–167. https://doi.org/10.1007/s00424-017-2052-5
20. Dernick G, de Toledo GA, Lindau M (2007) The patch amperometry technique: Design of a Method to study exocytosis of single vesicles. In: Michael AC, Borland LM (eds) Electrochemical methods for neuroscience, Frontiers in neuroengineering. CRC Press, Boca Raton
21. Ogden D, Stanfield P. (1994). Patch clamp techniques for single channel and whole-cell recording. In "Microelectrode Techniques: The Plymouth Workshop Handbook" editor David Ogden, published by The Company of Biologists, 2nd edition
22. Hernandez-Guijo JM, Gandia L, Lara B et al (1998) Autocrine/paracrine modulation of calcium channels in bovine chromaffin cells. Pflugers Arch 437:104–113
23. Powell AD, Teschemacher AG, Seward EP (2000) P2Y purinoceptors inhibit exocytosis in adrenal chromaffin cells via modulation of voltage-operated calcium channels. J Neurosci 20:606–616
24. Yawo H (2012) Whole-cell patch method. In: Okada Y (ed) Patch clamp techniques: from beginning to advanced protocols. Springer, Tokyo, pp 43–69
25. Augustine GJ, Neher E (1992) Calcium requirements for secretion in bovine chromaffin cells. J Physiol Lond 450(1):247–271. https://doi.org/10.1113/jphysiol.1992.sp019126
26. Smith C, Moser T, Xu T et al (1998) Cytosolic Ca2+ acts by two separate pathways to modulate the supply of release-competent vesicles in chromaffin cells. Neuron 20:1243–1253
27. Linley JE (2013) Perforated whole-cell patch-clamp recording. Humana Press, pp 149–157
28. Zhou Z, Neher E (1993) Mobile and immobile calcium buffers in bovine adrenal chromaffin cells. J Physiol (Lond) 469:245–273
29. Ogden D, Stanfield P (eds) (1994) Patch clamp techniques for single channel and whole cell recording, Microelectrode techniques, 2nd edn. The Company of Biologists, Cambridge
30. Neher E (1992) Correction for liquid junction potentials in patch clamp experiments. Methods Enzymol 207:123–131. https://doi.org/10.1016/0076-6879(92)07008-c
31. Barry PH, Lewis TM, Moorhouse AJ (2013) An optimised 3 M KCl salt-bridge technique used to measure and validate theoretical liquid junction potential values in patch-clamping and electrophysiology. Eur Biophys J 42(8):631–646. https://doi.org/10.1007/s00249-013-0911-3
32. Smith C, Neher E (1997) Multiple forms of endocytosis in bovine adrenal chromaffin cells. J Cell Biol 139:885–894
33. Bauer CS, Woolley RJ, Teschemacher AG et al (2007) Potentiation of exocytosis by phospholipase C-coupled G-protein-coupled receptors requires the priming protein Munc13-1. J Neurosci 27(1):212–219. https://doi.org/10.1523/JNEUROSCI.4201-06.2007
34. Horrigan FT, Bookman RJ (1994) Releasable pools and the kinetics of exocytosis in adrenal chromaffin cells. Neuron 13:1119–1129
35. Neher E (1998) Vesicle pools and Ca2+ microdomains: new tools for understanding their roles in neurotransmitter release. Neuron 20:389–399
36. Marengo FD, Monck JR (2000) Development and dissipation of Ca(2+) gradients in adrenal chromaffin cells. Biophys J 79(4):1800–1820
37. Gillis KD, Mossner R, Neher E (1996) Protein kinase C enhances exocytosis from chromaffin cells by increasing the size of the readily releasable pool of secretory granules. Neuron 16(6):1209–1220
38. Voets T, Moser T, Lund PE et al (2001) Intracellular calcium dependence of large dense-core vesicle exocytosis in the absence of synaptotagmin I. Proc Natl Acad Sci U S A 98(20):11680–11685

Chapter 14

Quantal Release Analysis of Electrochemically Active Molecules Using Single-Cell Amperometry

José David Machado, Pablo Montenegro, and Natalia Domínguez

Abstract

Single-cell amperometry is a powerful technique that permits the detection of electrochemically active transmitters, such as catecholamines, histamine, or serotonin, released by exocytosis from secretory cells.

Amperometry has two main characteristics that make it ideal for the study of exocytosis at the single-cell level with single-vesicle resolution quantal release. (i) *It is noninvasive*. The carbon fiber microelectrode can be carefully positioned on plasma membrane of a single cell, allowing the detection of the oxidation current of the secreted molecules. (ii) *High temporal resolution and sensitivity*. Exocytosis can be monitored with a real-time resolution that allows the determination of the kinetics release with an attomol detection sensitivity, which ensures an accurate calculation of the amount of transmitter released.

Here, we compile some recommendations and advices to perform amperometry quantal analysis.

Key words Chromaffin cell, Secretion, Exocytosis, Microelectrodes

1 Introduction

Single-cell amperometry was originally developed by Wightman [1] and is a noninvasive analytical technique with high sensitivity and temporal resolution timescale (sub-millisecond) that allows studying the main characteristics of exocytosis, providing quantitative information of single-vesicle transmitter release.

Amperometry detects substances that can be oxidized at the holding potential applied on carbon microelectrode placed in close contact to a secretory cell (usually chromaffin or PC12 cells). Upon exocytosis, dopamine and other amines (including noradrenaline, adrenaline, serotonin) are oxidized, generating an electrical current detectable by an electrode, which yields characteristic peaks when the current is plotted versus time (Fig. 1a).

In order to carry out experiments that lead to the analysis of the quantal size (*see* **Note 1**), we have structured the protocol in three steps:

Ricardo Borges (ed.), *Chromaffin Cells: Methods and Protocols*,
Methods in Molecular Biology, vol. 2565, https://doi.org/10.1007/978-1-0716-2671-9_14,

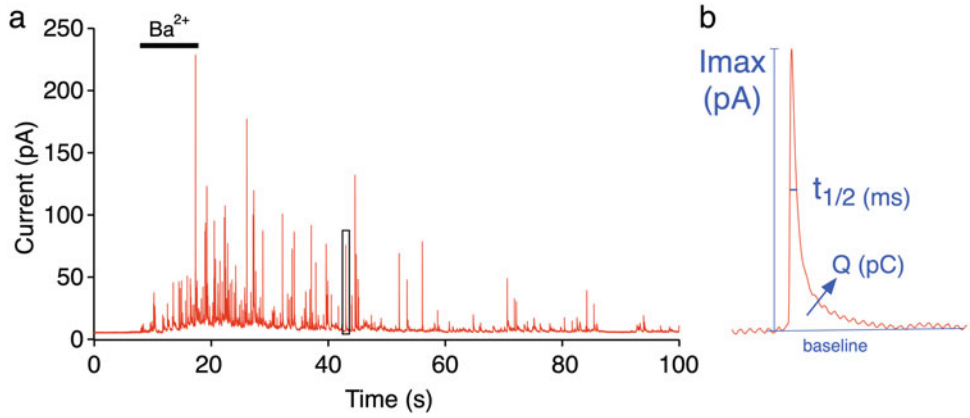

Fig. 1 (**a**) Typical amperometric recording from a chromaffin cell showing a characteristic firing pattern of exocytosis after $BaCl_2$ application. Each peak represents the release of catecholamines from a single vesicle. It is interpreted as a fast increase of current followed by a slow decay that corresponds with the release of the high concentration of catecholamines from the release site to the electrode surface. (**b**) Examples of single spike indicating the different amperometric parameters are I_{max}, maximum oxidation current, expressed in pA; $t_{1/2}$, the duration of the signal at half of height expressed in ms; and charge (Q), by integrating the current versus time for each recorded amperometric peak, expressed in pC. Quantal size is used to determine the number of neurotransmitters released from individual exocytosis events. The calculations follow the Faraday's law expressed as $Q = nNF$, where n is the number of electrons transferred in the redox reaction ($n = 2$ for oxidation of catecholamines), N is the number of neurotransmitter molecules detected, and F is the Faraday constant (96,485 C/mol)

- Chromaffin cells plating.
- Acquisition of amperometric recordings.
- Spike analysis and statistics.

2 Material

1. Computer.
2. Software for data analysis. The most popular for amperometry spikes analysis are:
   - IGOR-Pro (Wavemetrics, Lake Oswego, OR).
   - MATLAB (MATLAB, The MathWorks Inc., Natick, MA).
   - OriginLab (Origin, Northampton, MA).

   Macros or routines for automatic analysis of amperometric spikes. Almost all available for free upon request. The first macro was developed by Ricardo Borges' laboratory and was named "*Spikes*" [2]; the second one, most popular and used routinely, is named "*Quanta Analysis*" from David Sulzer' laboratory [3]. More recently, the use of new programs has been published "*Mini Analysis program*" (Synaptosoft Inc.,

Fort Lee, NJ) [4] or new routines for Igor-Pro [5, 6], MATLAB [7], or OriginLab [8] platform.

3. Software for statistical analysis and graphing:
   - SPSS Statistics (IBM, Chicago, IL).
   - Prism (GraphPad Software, San Diego, CA).
   - R (free software in source code form).

The main differences between the macros are given by the spike identification algorithms and the criteria on signal filtering. However, over time, they have been automated and the speed of processing and analysis has improved. All of them extract the following parameters from each spike: Q, spike net charge, expressed in pC; I_{max}, maximum oxidation current, expressed in pA; and $t_{1/2}$, the duration of the signal at half of height, expressed in ms. Also, these macros allow to estimate the foot duration in ms.

3 Methods

3.1 Chromaffin Cells Plating

Culture of chromaffin cells is out of the scope of this chapter. The procedures for isolation and culture of bovine, rat, or mouse chromaffin cells have been extensively described, including in this book, that provide exhaustive details from Harada et al., Chan et al., and Machado [9].

1. Seed cells on 12-mm Ø glass coverslips at an approximate density of 5×10^4 cells per well. For rat or mouse chromaffin cells, it is recommended to use 5-mm Ø glass coverslips coated with poly D-lysine or collagen to obtain the density of 5×10^4 cells per well.
2. Keep the cells at 37 °C in a humidified atmosphere with 5% CO_2 until used between 1 and 4 days after isolation. Cells that have been in culture longer tend to lose spherical volume, making amperometric recording more difficult, and a reduction in quantal size over time is also common, probably due to loss of catecholamines.

3.2 Amperometric Detection of Exocytosis

The procedures for the fabrication and calibration of carbon fiber electrode are out of the scope of this chapter. Electrodes can be also purchased from several companies or locally fabricated following any of the already described procedures [10–12].

1. Calibrate electrodes using a flow-injection system, and choose two of them with similar properties and sensitivity. The apparatus requires that the control buffer (usually Krebs-HEPES solution) can be easily exchanged to a freshly prepared buffer containing 50 μM of noradrenaline or other electrochemically

active substances. For more details, check [10]. Not all microelectrodes are suitable for amperometric recordings (*see* **Note 2**).

2. Choose the appropriate secretagogue. It should be a goal of the experimental design to get distinguishable individual spikes rather than secretory bursts (*see* **Note 3**).
3. Perform the electrochemical recordings using a potentiostat connected to a data acquisition system (*see* **Note 4**). The duration of each recording should be proportional to the expected secretory response, usually 2–3 min at 4 kHz.

3.3 Amperometry—Spike Analysis

Due to large variability on secretory spikes obtained upon cell stimulation, from a single cell, it becomes necessary to conduct statistical analysis on populations of several hundreds of events. All of them should be obtained from cells resulting from the same culture [13]. It is necessary to carry out replicate experiments to assess and isolate sources of variation when comparing chromaffin cells obtained from different cultures, for example, when they are obtained from knock-in or knockout mice.

1. Data should be analyzed by a second investigator, who must be blinded to the experimental conditions.

   Every amperometric recording represents the secretion from one cell.

   The number of exocytotic events can be highly variable between cells although the spike characteristics from single chromaffin cells are cell dependent [13]. For this reason, the number of spikes analyzed must be representative of the cellular response. In our hands, at least, 25 secretory spikes that satisfy all criteria per cell are necessary. The duration of each recording should be proportional to the expected secretory response, usually 2–3 min.
2. Use one of the available software for automatic spike analysis.
3. You must consider the previous analysis to perform (i) a digital filtering and (ii) set the threshold for identification of spikes. It is important to use a specific threshold of detection, above which exocytosis have occurred. The discrimination threshold typically is fixed at 2.5 times the standard deviation of the basal noise of the first derivative of each recording or 2.5 times the root-mean-squared noise of the signal baseline. In these conditions, spikes with an I_{max} over 2.5 pA are usually included in the data analysis.

   All software should detect the location of the initial, the maximum, and the final points of spikes and extract the quantal size (Q) and the kinetic parameters.
4. Check that all spikes identified satisfy the following criteria [14]:

- The I_{max} must be above the detection threshold.
- Spikes must not show overlapping. The beginning and end of each spike can be easily identified without interfering with neighboring spikes.
- None of the measured parameters are affected by any artifact that will affect the parameters extracted from amperometrical spikes.

3.4 Statistical Analysis

For a correct statistical analysis in single cell amperometry, it is crucial to have enough cells with representative secretory spikes for each experimental condition. The number and the parameters of amperometric spikes from chromaffin single cells are largely variable. Thus, an overrepresentation of data is probably coming from cells that are highly active [15–19]. To avoid bias caused by the different number of spikes produced by each cell, the mean or median values of spikes parameters from each cell must be considered as $n = 1$. The averages of mean or median from control cells are then used to compare each parameter with experimental cells, avoiding cell to cell variability [13]. It is also recommended for amperometric recordings obtained by Multi Electrode Arrays [16, 20–24].

The statistical analyses should include the following:

- Calculate the value for each parameter of each spike.
- Calculate the mean, median, and standard deviation of each spike parameter for each cell.
- Group the different records into categories (control and experimental conditions).
- Quantal size data follows a skewed distribution and should be evaluated for statistical significance using a nonparametric test, for example, Mann–Whitney *U* test.
- Define threshold P value for significance for the test.
- Specify whether tests were one- or two-tailed, and provide details of any corrections for multiple comparisons, as well as a justification if no corrections were applied.
- Describe and justify any data normalization, including whether this results in the need for nonparametric analysis.
- Plot the results. When representing data with an $n < 30$, preferably use box-plot representation. Box plots are a simple but powerful graphing tool that can be used in place of histograms, require a sample size of only five, and provide more detail in the tails of the distribution.

4 Notes

1. It is important to establish a priori that the expected quantal size change can be tested statistically with the number of cells that are going to be used in the experiment. Thus, before starting the experiment, we should consider answering the following questions:
   - What difference between the means of quantal size do I consider biologically significant?
   - How many cells (or recordings) are really needed to estimate the quantal size when two or more experimental conditions are compared?
   - How many spikes per cell are necessary to carry out an experiment of these characteristics?

   To calculate the sample size based on statistical power, you will need to know the standard deviation of the parameter Q (Fig. 1b) from preliminary data, the difference between means that are considered biologically relevant and the statistical confidence.
2. *Basal current level* $\leq$ *15 pA*. If the electrode has a high basal current level (>15 pA), it indicates large electrode surface, normally due to a bad electrical seal, electrode protrusion, or fissures. These electrodes usually record large oxidation currents, but they should be discarded for amperometric recordings because part of the exposed surface will be far from the cell and the electric noise will increase.

   An example of good electrode implies that oxidation current in flow conditions. For instance, 50 μM of noradrenaline should produce an oxidation current of approximately 150–200 pA under stopping flow conditions. After the stop flow, the oxidation current should not decay more than 30% of the current in flow condition. If the oxidation current is smaller, it means that the active surface is smaller than expected. Sometimes, this is caused by debris at the tip of the electrode. If after microscopic inspection the tip is narrow enough, an extra polish should be perform. This can be done and the calibration repeated. These values may change with the exposed surface of the electrode.

   The ascending slope should be fast; otherwise, a very slow ascending slope indicates a dirty surface. The electrode tip needs to be cleaned by repolishing, cutting, or soaking in pure 2-propanol. A useful trick consists of placing the tip of the electrode at approximately 0.5 mm over the surface of the spinning grinder wheel and then applying a few drops of 2-propanol over the surface of the grinder. The flow of the

2-propanol is usually enough to remove the debris deposited on the electrode surface.

The main concern comes from an electrode that rapidly loses its sensitivity. The causes are difficult to establish. To test how good my calibrated electrode is, the following protocol should be done. Leave the electrode in the calibration system and give repeated norepinephrine pulses for an hour. An electrode is considered suitable when the oxidation current in flow condition does not decay more than 15% at the end of protocol. It is crucial to use calibrated electrodes with similar sensitivity. Do not perform recordings using different electrodes without an appropriate calibration. It should be noticed that a re-cut electrode should be considered as a different one. It is possible that a microelectrode breaks during the experiment, so if you replace it, you must do it with one of similar characteristics in the calibration.

During several single-cell amperometric recordings, the carbon fiber microelectrode may change its sensitivity. This is the reason why we must recalibrate the electrode every six recordings. We need to ensure that there are no significant changes in its sensitivity. It is possible that a simple soaking in 2-propanol by 10 min is enough for recovering electrode sensitivity.

It is recommendable to reduce bias caused by the decaying sensitivity of an electrode over time, recording control and experimental cell conditions alternatively.

Caution should be taken when a new drug or substance, mainly negatively charged or highly lipophilic, is used. These substances can attach to the electrode surface reducing its sensitivity (varnishing effect).

3. The secretory response differs depending on the type, concentration, and application time of secretagogues.

   Usually, chromaffin cell secretion is stimulated by pressure perfusion of cholinergic agonists, high potassium, or $BaCl_2$ from a glass micropipette situated 30–50 μm from the cell. To see the effect on secretion of different secretagogues, *see* Fig. 1 by Baraibar et al. [25]. For the precise quantification of quantal content and kinetic parameters, it is desirable that secretory spikes are well distinguishable. The overlapping between spikes should be the minimum possible.

4. It is necessary to perform amperometric recordings from cells obtained under the same culture conditions. For statistical analysis, it is not adequate to include amperometric data for the same experimental group when cells are obtained from different cultures or from the same culture but recorded in different days. It is also important to know that procedures

such electroporation, nucleofection, or liposomes transfection can modify the quantal size.

Acknowledgment

This work was supported by Spanish Ministerio de Ciencia e Innovación (PID2020-116589GB-I00).

References

1. Wightman RM, Jankowski JA, Kennedy RT, Kawagoe KT, Schroeder TJ, Leszczyszyn DJ, Near JA, Diliberto EJ, Viveros OH (1991) Temporally resolved catecholamine spikes correspond to single vesicle release from individual chromaffin cells. Proc Natl Acad Sci U S A 88: 10754–10758
2. Segura F, Brioso MA, Gómez JF, Machado JD, Borges R (2000) Automatic analysis for amperometrical recordings of exocytosis. J Neurosci Methods 103:151–156
3. Mosharov EV, Sulzer D (2005) Analysis of exocytotic events recorded by amperometry. Nat Methods 2:651–658
4. Omiatek DM, Dong Y, Heien ML, Ewing AG (2010) Only a fraction of quantal content is released during exocytosis as revealed by electrochemical cytometry of secretory vesicles. ACS Chem Neurosci 1:234–245
5. Ramachandran SB, Gillis KD (2019) Estimating amperometric spike parameters resulting from quantal exocytosis using curve fitting seeded by a matched-filter algorithm. J Neurosci Methods 311:360
6. Ramachandran SB, Gillis KD (2018) A matched-filter algorithm to detect amperometric spikes resulting from quantal secretion. J Neurosci Methods 293:338
7. Friedrich R, Ashery U (2010) From spike to graph-a complete automated single-spike analysis. J Neurosci Methods 193:271–280
8. Jackson MB, Hsiao YT, Chang CW (2020) Fusion pore expansion and contraction during catecholamine release from endocrine cells. Biophys J 119:219
9. Domínguez N, Rodríguez M, MacHado JD, Borges R (2012) Preparation and culture of adrenal chromaffin cells. Methods Mol Biol 846:223–234
10. Machado JD, Montesinos MS, Borges R (2008) Good practices in single-cell amperometry. Methods Mol Biol 440:297–313
11. Mundorf ML, Wightman RM (2002) Amperometry and cyclic voltammetry with carbon fiber microelectrodes at single cells. Curr Protoc Neurosci 18:6.14.1–6.14.22
12. Kawagoe KT, Zimmerman JB, Wightman RM (1993) Principles of voltammetry and microelectrode surface states. J Neurosci Methods 48:225–240
13. Colliver TL, Hess EJ, Pothos EN, Sulzer D, Ewing AG (2000) Quantitative and statistical analysis of the shape of amperometric spikes recorded from two populations of cells. J Neurochem 74:1086–1097
14. Gómez JF, Brioso MA, Machado JD, Sánchez JL, Borges R (2002) New approaches for analysis of amperometrical recordings. Ann N Y Acad Sci 971:647–654
15. Westerink RHS, de Groot A, Vijverberg HP (2000) Heterogeneity of catecholamine-containing vesicles in PC12 cells. Biochem Biophys Res Commun, Elsevier 270(2):625–630
16. Huang M, Delacruz JB, Ruelas JC, Rathore SS, Lindau M (2018) Surface-modified CMOS IC electrochemical sensor array targeting single chromaffin cells for highly parallel amperometry measurements. Pflugers Arch Eur J Physiol 470:113–123
17. Dominguez N, Estevez-Herrera J, Borges R, Machado JD (2014) The interaction between chromogranin a and catecholamines governs exocytosis. FASEB J 28:4657–4667
18. Estévez-Herrera J, Domínguez N, Pardo MR, González-Santana A, Westhead EW, Borges R, Machado JD (2016) ATP: the crucial component of secretory vesicles. Proc Natl Acad Sci U S A 113:E4098–E4106
19. González-Santana A, Estévez-Herrera J, Seward EP, Borges R, Machado JD (2021) Glucagon-like peptide-1 receptor controls exocytosis in chromaffin cells by increasing full-fusion events. Cell Rep 36:109609
20. Ranjbari E, Taleat Z, Mapar M, Aref M, Dunevall J, Ewing A (2020) Direct measurement of Total vesicular catecholamine content with electrochemical microwell arrays. Anal Chem 92:11325–11331

21. Chen X, Gao Y, Hossain M, Gangopadhyay S, Gillis KD (2007) Controlled on-chip stimulation of quantal catecholamine release from chromaffin cells using photolysis of caged Ca2+ on transparent indium-tin-oxide microchip electrodes. Lab Chip 8:161–169
22. Gillis KD, Liu XA, Marcantoni A, Carabelli V (2018) Electrochemical measurement of quantal exocytosis using microchips. Pflugers Arch Eur J Physiol 470:97–112
23. Huang M, Delacruz JB, Ruelas JC, Rathore SS, Lindau M (2018) Surface-modified CMOS IC electrochemical sensor array targeting single chromaffin cells for highly parallel amperometry measurements. Pflugers Arch 470:113–123
24. Picollo F, Battiato A, Bernardi E, Plaitano M, Franchino C, Gosso S, Pasquarelli A, Carbone E, Olivero P, Carabelli V (2016) All-carbon multi-electrode array for real-time in vitro measurements of oxidizable neurotransmitters. Sci Rep 6:20682. https://doi.org/10.1038/srep20682
25. Baraibar AM, de Pascual R, Camacho M, Domínguez N, David Machado J, Gandía L, Borges R (2018) Distinct patterns of exocytosis elicited by Ca 2+, Sr 2+ and Ba 2+ in bovine chromaffin cells. Pflugers Arch Eur J Physiol 470:1459–1471

Chapter 15

Methodologies for Detecting Quantal Exocytosis in Adrenal Chromaffin Cells Through Diamond-Based MEAs

Giulia Tomagra, Claudio Franchino, Emilio Carbone, Andrea Marcantoni, Alberto Pasquarelli, Federico Picollo, and Valentina Carabelli

Abstract

Diamond-based multiarray sensors are suitable to detect in real-time exocytosis and action potentials from cultured, spontaneously firing chromaffin cells, primary hippocampal neurons, and midbrain dopaminergic neurons. Here, we focus on how amperometric measurements of catecholamine release are performed on micrographitic diamond multiarrays (μG-D-MEAs) with high temporal and spatial resolution by 16 electrodes simultaneously.

Key words Diamond microelectrode devices, Chromaffin cells, Exocytosis, Ion beam lithography

1 Introduction

Chromaffin cells of the adrenal gland have been extensively used as a model for investigating exocytosis as the process of catecholamine release shares with neurosecretion many molecular players [1–3]. The gold standard technique for monitoring the release of oxidizable molecules from single cells is the carbon fiber (CFE) amperometry, which allows to resolve single exocytotic events with sub-millisecond time resolution [4–7]. This approach, however, has a main drawback. It allows to carry out only one measurement at the time, whereas this limitation can be overcome by using multielectrode arrays [8–11]. Integrated multielectrode CMOS devices for amperometric measurements have been proposed as well [12, 13]. They appear suitable for recording exocytotic events with sufficient time resolution and amplitude sensitivity. However, the long-term reliability of these complex silicon-based complex devices is still an open question, especially regarding the stability of the silicon oxide passivation, which is known [14] to slowly hydrolyze when in contact with a water-based environment.

Ricardo Borges (ed.), *Chromaffin Cells: Methods and Protocols*,
Methods in Molecular Biology, vol. 2565, https://doi.org/10.1007/978-1-0716-2671-9_15,

Here, we describe the fabrication of multielectrode array sensor (μG-D-MEAs), the electronic chain, the maintenance protocol of the devices, and the procedure of interfacing μG-D-MEAs with isolated chromaffin cells. The main advantage of using cultured CCs is that they are spontaneously firing [15] and can be stimulated to secrete catecholamines (adrenaline and noradrenaline) by cell depolarization using KCl solutions [16, 17] or effective secretagogues (ACh, muscarine, PACAP, etc.) [18, 19]. We will show some representative examples of MEA real-time detection of quantal exocytosis from chromaffin cells, reminding that the same MEA prototypes can be used for monitoring quantal dopamine release and action potential firing from cultured midbrain dopaminergic neurons [20–22].

It is relevant to notice that μG-D-MEAs can reveal quantal amperometric spikes with the same sensitivity and time resolution of carbon fiber electrodes. Thus, comparable spike parameter values can be revealed by the two approaches. Furthermore, a tentative analysis of exocytosis modes has been performed and targeted to discriminate among different fusion events (large, small, stand-alone foot events) [23].

Because of their biocompatibility and extreme versatility, combined with the possibility of detecting quantal exocytosis and neuronal firing in real time, we have recently demonstrated that μG-D-MEAs behave as reliable multifunctional sensors [20, 22]. The monitoring of the functional properties of developing neuronal circuits together with neurotransmission makes μG-D-MEAs an unmatched tool targeted to cell physiology and neurodegenerative disorders.

2 Materials

2.1 Diamond Material

The substrates employed for the realization of the μG-D-MEAs are synthetic diamond that can be either polycrystalline or single crystal. The sample dimensions are typically $5 \times 5 \times 0.5$ mm^3 with large faces optically polished. The crystal has substitute nitrogen and boron, whose concentrations are less than 1 ppm and 0.05 ppm, respectively. These low concentrations of impurities ensure good optical transparency of substrates over the whole visible spectrum up to near UV [9, 24].

2.2 Solutions for Bovine Chromaffin Cells

All solutions are prepared using double distilled water. All reagents are prepared at room temperature and stored in the fridge at 6 °C.

1. Locke buffer: 154 mM NaCl, 5.6 mM KCl, 3.5 mM $NaHCO_3$, 5.6 mM glucose, and 10 mM HEPES (pH 7.3 with NaOH).
2. Locke solution: 0.2% collagenase, 1.7% hyaluronidase, 0.5% BSA, and 0.15% DNase I.

3. Culture medium: DMEM, fetal calf serum (15%), penicillin (50 IU/mL), and streptomycin (50 μg/mL).

3 Methods

3.1 μG-D-MEA Microfabrication

The diamond MEA device (Fig. 1) is composed by an artificial diamond in which graphitic tracks have been implanted using the MeV ion beam lithography technique [25]. The implantation is carried out using an ion beam typically employing light ion (He, C, etc.) with energy ranging from 0.5 MeV to 3 MeV that allows creating graphitic electrodes at few micron below the sample surface. The implantation ion current is of few hundreds of nA. The beam, opportunely collimated, is delivered on the diamond at a fluence high enough to induce a density of defects (mainly vacancies) overcoming a critical dose called graphitization threshold ($4–9 \times 10^{22}$ cm^{-3}). This condition allows to promote the complete amorphization of the material with high spatial resolution in all the three dimensions [9, 26, 27].

1. The damage profile induced by the ions into the diamond matrix is evaluated by using SRIM [28] Monte Carlo code. This approach considers the product between the linear damage density and the implantation fluence assuming a linear approximation that does not take into account effects such as self-annealing or defect–defect interactions. Nevertheless, the prediction on the depth and thickness of the sub-superficial modified layer is sufficiently accurate.
2. The three-dimensional geometry of the implanted structures is defined using a two-level masking system.
3. The first mask consists of a matrix of copper deposition with variable thickness placed directly on the sample surface whose purpose is the modulation of ion penetration depth, thus ensuring the connection of the amorphized subsurface structures with the sample surface at their endpoints [8].
4. The second mask is made of a 20- to 100-μm-thick metal sheet microfabricated with a high-ablation power laser. This mask is thick enough to completely block the MeV ion beam, thus allowing the definition of the lateral geometry of the amorphized regions.

   The two masking systems are suitably aligned simultaneously in order to define 16 microchannels of amorphous carbon with emerging endpoints in each sample.
5. After the implant, a high-temperature thermal annealing is performed at 950 °C for 2 h in high vacuum, inducing the permanent conversion of the amorphized regions into a graphite phase.

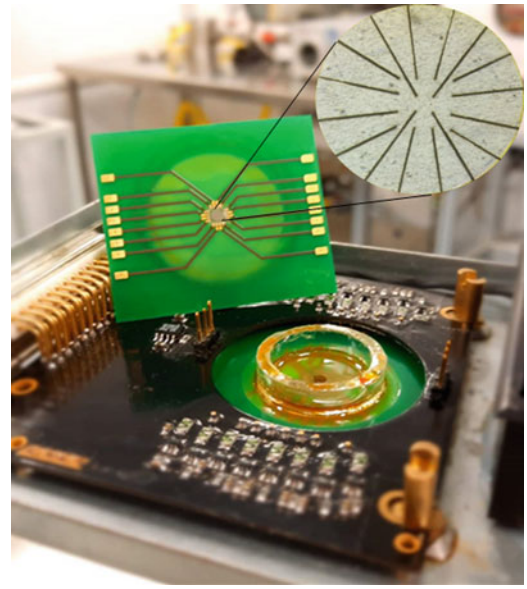

Fig. 1 Diamond chip plugged in electronic chain; an enlargement of diamond matrix with graphitic tracks

6. Typically, the 16 graphitic microchannels are obtained with ~20 μm width, 1.4–1.9 mm length, ~250 nm thickness, and ~2 μm depth in each substrate, with the endpoints (i.e., the sensing electrodes) emerging at the surface.

Each device consists of 16 graphite microchannels with a sensing area of ~20 × 3.5 μm^2. The 16 electrodes are arranged in a 4 × 4 array spaced by 200 μm and converge in a central region where their endpoints are exposed to the surface.

3.2 Characteristics of the Electronic Chain

The chip carrier is equipped with 1 mL culture chamber and an Ag/AgCl quasi-reference electrode. The chip is directly plugged into the front-end electronic. The electronic chain is characterized by:

1. A front-end stage, made of 16 low-noise trans-impedance amplifiers with an input bias current of 2 pA and a gain of 100 MΩ.
2. A biasing potential of +800 mV applied to the electrodes for the catecholamine oxidation.
3. Bessel low-pass filters of the sixth order with cut-off frequency of 5 kHz.
4. An analog to digital conversion using an A/DC module (National Instrument USB-6229) having 16-bit resolution with an input range of ±1 V and a sampling rate of 25 kHz per channel.

5. The bias applied to the channels is +800 mV that guarantees catecholamine oxidation.
6. Data acquisition through a hi-speed USB link and controlled by a program developed in LabView™ environment [9, 20, 29].

3.3 Bovine Chromaffin Cells Culturing on μ-D-MEAs

3.3.1 Isolation and Culture of Bovine Chromaffin Cells.

1. Rapidly place the adrenal glands from 6- to 18-month-old cows in Locke buffer (*see* Subheading 2; *see* **Note 1**).
2. After controlling the integrity of the gland (*see* **Note 2**), start the medulla digestion by injecting 3 mL of Locke solution (*see* Subheading 2). Repeat three times at 30 min intervals while glands are kept at 37 °C.
3. Separate manually the medulla from the cortex (*see* **Notes 3** and **4**).
4. Wash with the digestion solution, and filter the tissue suspension with a nylon mesh (217-μm pore). Centrifuge at 170 × *g* for 12 min at room temperature.
5. Remove the supernatant and the upper pellet of erythrocytes (*see* **Note 5**) while resuspending the pellet of chromaffin cells in DMEM. Filter with a nylon mesh (80-μm pore) (*see* **Note 6**).
6. Plate the cells at a density of 1.5×10^4 mL^{-1}.
7. The cells are incubated at 37 °C in an incubator with 5% CO_2 and used within 2–4 days after plating. To favor cell adhesion, the diamond devices are pretreated with poly-D-lysine (0.2%) or with poly-L-ornithine (1 mg/mL) and laminin (5 μg/mL in L-15 carbonate) [30, 31].

3.4 How to Carry Out the Measurement

The experiment procedure can be summarized in the following steps:

1. Connect the electronic chain, i.e., front end, A/DC unit, and PC (*see* **Notes 7** and **8**).
2. Plate the chromaffin cells onto the diamond MEA as described in the previous section.
3. Insert the diamond MEA into the dedicated connector and make sure the pins contact the pads (*see* **Note 9**).
4. Exchange the culture medium with the external bath solution containing 130 mM NaCl, 4 mM KCl, 2 mM $CaCl_2$, 2 mM $MgCl_2$, 10 mM glucose, and 10 mM HEPES; pH 7.4.
5. Immerse the Ag/AgCl reference electrode in the bath solution (*see* **Note 10**).
6. Start the control and acquisition program, and set the biasing potential to +800 mV.

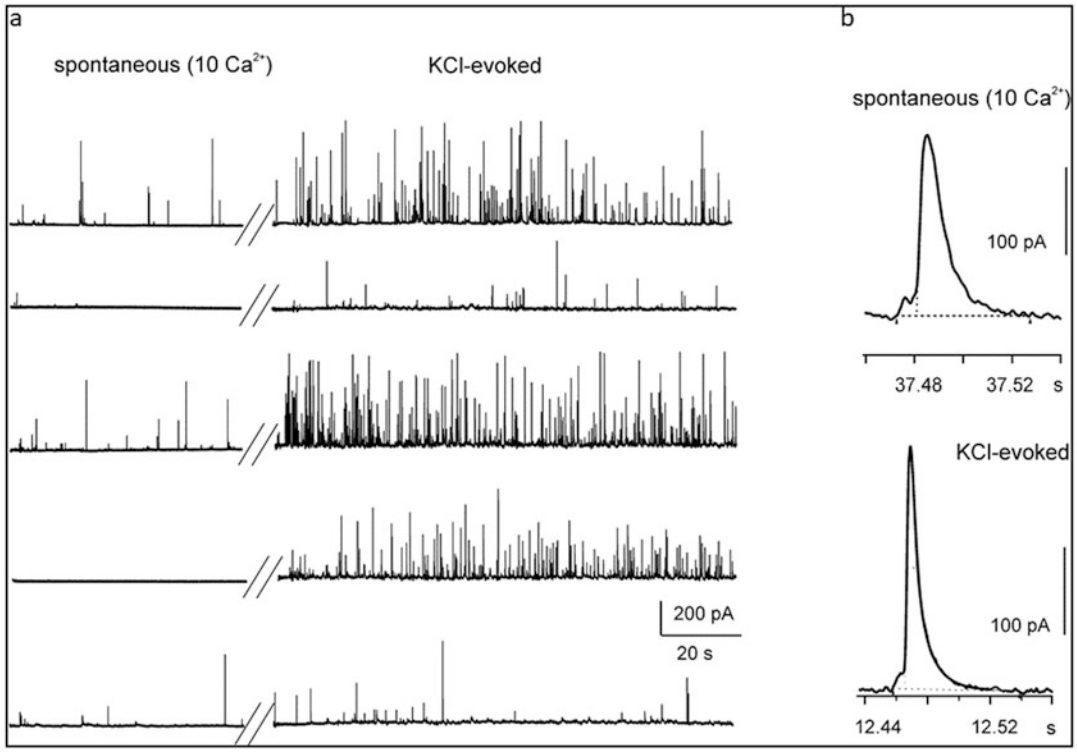

Fig. 2 (**a**) Representative traces of quantal release from chromaffin cells monitored by different electrodes. Exocytotic events detected during spontaneous release in 10-mM extracellular Ca^{2+} (left) and during stimulation with KCl-enriched solution. (**b**) Representative examples of single amperometric spikes under spontaneous release and after KCl perfusion. (Adapted with permission from ref. 23, Copyright © 2017, American Chemical Society)

7. Start signal recording. Usually, it is run a control recording of exocytosis on resting, spontaneously firing chromaffin cells followed by the recording of exocytosis during prolonged depolarization with a KCl solution as illustrated in Fig. 2.
8. Visually observe the exocytotic events on the computer screen during the running protocol and quick off-line data analysis to validate the success of the experiment.

3.5 Cleaning Procedure of MEA Devices

After each experiment, it is necessary to clean the device accurately to be able to reuse it multiple times and prolong its correct functioning over time. The adopted cleaning protocol consists of:

1. Wash the diamond MEA in Tergazyme 1 g/100 mL
   (a) Let stay 1 day in Tergazyme solution.
2. Rinse well with sterile water to remove traces of Tergazyme.
3. Remove the liquid with a vacuum-connected Pasteur pipette.
4. Wash in 70% alcohol/water solution, only 1–2 min.

5. Remove the liquid with a vacuum-connected Pasteur pipette, strictly under the hood to keep the environment sterile.
6. Wash the device two times with sterile water.
7. Remove the liquid with a vacuum-connected Pasteur pipette.
8. Dry under sterile conditions.

4 Notes

1. When you take the gland, clean it well. Remove all adipose tissue; if the layer of fat is not removed well, the gland will not swell properly.
2. Test by inflating with the solution to make sure there are no holes.
3. Open the gland where you made the pore, but be careful not to break it; you must open it in two parts like with a "book."
4. At the time of taking the medulla, if you have digested well, it will come away very easily. You can easily remove it using a bistoury like a spatula, gently without scraping.
5. After the centrifuge, you will see a dense dark red area. You suck it away taking care not to pick up the pellet below.
6. Some protocols do a second centrifuge, but I do not recommend it; you risk damaging the cells.
7. Always store the electronics under a correctly grounded Faraday cage during measurement.
8. Do not use mobile phone during the experiment; they could interfere with the measurement.
9. Be careful when positioning the device. If liquid escapes, you could create short circuit. Tip: Use a protective cap or parafilm when housing the device.
10. Do not touch the Ag/AgCl ground without gloves, you risk pulling off the chlorination of the electrode.

References

1. Neher E (2018) Neurosecretion: what can we learn from chromaffin cells. Pflugers Arch Eur J Physiol 470:7–11. https://doi.org/10.1007/S00424-017-2051-6
2. Neher E (2006) A comparison between exocytic control mechanisms in adrenal chromaffin cells and a glutamatergic synapse. Pflugers Arch Eur J Physiol 453:261–268. https://doi.org/10.1007/S00424-006-0143-9
3. Carbone E, Borges R, Eiden LE et al (2019) Chromaffin cells of the adrenal medulla: physiology, pharmacology, and disease. Compr Physiol 9:1443–1502. https://doi.org/10.1002/CPHY.C190003
4. Camacho M, Montesinos MS, Machado JD, Borges R (2003) Exocytosis as the mechanism for neural communication. A view from chromaffin cells. Rev Neurol 36:355–360. https://doi.org/10.33588/rn.3604.2003034
5. Sombers LA, Hanchar HJ, Colliver TL et al (2004) The effects of vesicular volume on secretion through the fusion pore in Exocytotic

release from PC12 cells. J Neurosci 24:303–309. https://doi.org/10.1523/JNEUROSCI.1119-03.2004

6. Mellander LJ, Trouillon R, Svensson MI, Ewing AG (2012) Amperometric post spike feet reveal most exocytosis is via extended kiss-and-run fusion. Sci Rep 2:907. https://doi.org/10.1038/SREP00907
7. Wightman RM, Schroeder TJ, Finnegan JM et al (1995) Time course of release of catecholamines from individual vesicles during exocytosis at adrenal medullary cells. Biophys J 68:383. https://doi.org/10.1016/S0006-3495(95)80199-2
8. Picollo F, Gatto Monticone D, Olivero P et al (2012) Fabrication and electrical characterization of three-dimensional graphitic microchannels in single crystal diamond. New J Phys 14:053011. https://doi.org/10.1088/1367-2630/14/5/053011
9. Picollo F, Battiato A, Bernardi E et al (2016) All-carbon multi-electrode array for real-time in vitro measurements of oxidizable neurotransmitters. Sci Rep 61(6):1–8. https://doi.org/10.1038/srep20682
10. Meunier A, Fulcrand R, Darchen F et al (2012) Indium tin oxide devices for amperometric detection of vesicular release by single cells. Biophys Chem 162:14–21. https://doi.org/10.1016/J.BPC.2011.12.002
11. Chen X, Gao Y, Hossain M et al (2007) Controlled on-chip stimulation of quantal catecholamine release from chromaffin cells using photolysis of caged Ca2+ on transparent indium-tin-oxide microchip electrodes. Lab Chip 8:161–169. https://doi.org/10.1039/B715308M
12. Kim BN, Herbst AD, Kim SJ et al (2013) Parallel recording of neurotransmitters release from chromaffin cells using a 10×10 CMOS IC potentiostat array with on-chip working electrodes. Biosens Bioelectron 41:736–744. https://doi.org/10.1016/J.BIOS.2012.09.058
13. White KA, Kim BN (2021) Quantifying neurotransmitter secretion at single-vesicle resolution using high-density complementary metal–oxide–semiconductor electrode array. Nat Commun 121(12):1–8. https://doi.org/10.1038/s41467-020-20267-0
14. Walsh TR, Wilson M, Sutton AP (2000) Hydrolysis of the amorphous silica surface. II. Calculation of activation barriers and mechanisms. J Chem Phys 113:9191. https://doi.org/10.1063/1.1320057
15. Lingle CJ, Martinez-Espinosa PL, Guarina L, Carbone E (2018) Roles of Na+, Ca2+, and K+ channels in the generation of repetitive firing and rhythmic bursting in adrenal chromaffin cells. Pflugers Arch Eur J Physiol 470:39–52. https://doi.org/10.1007/S00424-017-2048-1/FIGURES/3
16. Marcantoni A, Carabelli V, Vandael DH et al (2009) PDE type-4 inhibition increases L-type ca(2+) currents, action potential firing, and quantal size of exocytosis in mouse chromaffin cells. Pflugers Arch 457:1093–1110. https://doi.org/10.1007/S00424-008-0584-4
17. Carabelli V, Giancippoli A, Baldelli P et al (2003) Distinct potentiation of L-type currents and secretion by cAMP in rat chromaffin cells. Biophys J 85:1326–1337. https://doi.org/10.1016/S0006-3495(03)74567-6
18. Eiden LE, Emery AC, Zhang L, Smith CB (2018) PACAP signaling in stress: insights from the chromaffin cell. Pflugers Arch Eur J Physiol 470:79–88. https://doi.org/10.1007/S00424-017-2062-3/FIGURES/2
19. García AG, García-De-Diego AM, Gandía L et al (2006) Calcium signaling and exocytosis in adrenal chromaffin cells. Physiol Rev 86:1093–1131. https://doi.org/10.1152/PHYSREV.00039.2005/ASSET/IMAGES/LARGE/Z9J0040624130010.JPEG
20. Tomagra G, Picollo F, Battiato A et al (2019) Quantal release of dopamine and action potential firing detected in midbrain neurons by multifunctional diamond-based microarrays. Front Neurosci 13:288. https://doi.org/10.3389/fnins.2019.00288
21. Tomagra G, Aprà P, Battiato A et al (2019) Micro graphite-patterned diamond sensors: towards the simultaneous in vitro detection of molecular release and action potentials generation from excitable cells. Carbon N Y 152:424–433. https://doi.org/10.1016/j.carbon.2019.06.035
22. Kuhn B, Picollo F, Carabelli V, Rispoli G (2020) Advanced real-time recordings of neuronal activity with tailored patch pipettes, diamond multi-electrode arrays and electrochromic voltage-sensitive dyes. Pflügers Arch – Eur J Physiol 4731(473):15–36. https://doi.org/10.1007/S00424-020-02472-4
23. Picollo F, Battiato A, Bernardi E et al (2017) Microelectrode arrays of diamond-insulated graphitic channels for real-time detection of Exocytotic events from cultured chromaffin cells and slices of adrenal glands. Anal Chem 88:7493–7499. https://doi.org/10.1021/ACS.ANALCHEM.5B04449
24. Tomagra G, Battiato A, Bernardi E et al (2019) Diamond-based multi electrode arrays for monitoring neurotransmitter release. In:

Lecture notes in electrical engineering, vol 539. Springer, Cham, pp 125–134. https://doi.org/10.1007/978-3-030-04324-7_17

25. Picollo F, Gosso S, Vittone E et al (2013) A new diamond biosensor with integrated graphitic microchannels for detecting quantal exocytic events from chromaffin cells. Adv Mater 25:4696–4700. https://doi.org/10.1002/adma.201300710
26. Olivero P, Rubanov S, Reichart P et al (2016) Characterization of three-dimensional microstructures in single crystal diamond. Diam Relat Mater 15:1614–1621. https://doi.org/10.1016/j.diamond.2006.01.018
27. Uzan-Saguy C, Cytermann C, Brener R et al (1995) Damage threshold for ion-beam induced graphitization of diamond. Appl Phys Lett 67:1194. https://doi.org/10.1063/1.115004
28. Ziegler JF, Ziegler MD, Biersack JP (2010) SRIM – the stopping and range of ions in matter. Nucl Instr Methods Phys Res Sect B Beam Interact Mater Atoms 268:1818–1823. https://doi.org/10.1016/J.NIMB.2010.02.091
29. Tomagra G, Franchino C, Pasquarelli A et al (2019) Simultaneous multisite detection of quantal release from PC12 cells using micro graphitic-diamond multi electrode arrays. Biophys Chem 253:106241. https://doi.org/10.1016/j.bpc.2019.106241
30. Gosso S, Turturici M, Franchino C et al (2014) Heterogeneous distribution of exocytotic microdomains in adrenal chromaffin cells resolved by high-density diamond ultramicroelectrode arrays. J Physiol 592:3215–3230. https://doi.org/10.1113/JPHYSIOL.2014.274951
31. Moro M, López M, Gandía L et al (1990) Separation and culture of living adrenaline- and noradrenaline-containing cells from bovine adrenal medullae. Anal Biochem 185(2):243–248. https://doi.org/10.1016/0003-2697(90)90287-J

Chapter 16

Vesicle Collision Protocols for the Study of Quantum Size and Exocytotic Fraction Released

Soodabeh Majdi, Alex S. Lima, and Andrew G. Ewing

Abstract

We review the methods of vesicle impact electrochemical cytometry, intracellular impact electrochemical cytometry, and single cell amperometry and their application to measuring the storage of neurotransmitters in cellular vesicles. We provide protocols to measure vesicle content, the release of catecholamines, and from there the fraction of transmitter released in each exocytosis event. The focus here has been a combination of methods to evaluate factors related to neuronal function at the cellular level and implications in, for example, cognition.

Key words Vesicles, Electrochemistry, Electrochemical cytometry, Neurotransmitters, Exocytosis

1 Introduction

Neuronal communication occurs via released transmitters stored inside vesicles. This phenomenon is called exocytosis and involves several steps. Each vesicle is brought close to the presynaptic cellular membrane and docked at an active zone, a process called docking. Then the docked vesicle responds to calcium entry by an ATP-dependent process known as priming. In the last step, fusion between the lipid bilayers of the vesicle and the cellular membrane causes the release of neurotransmitters into the synaptic cleft.

PC12 is one of the most used cell lines to study the possible mechanism governing exocytosis. PC12 cells have a round or slightly oval shape and tend to form small clusters when grown in culture. The main neurotransmitter synthesized in PC12 cells and stored in vesicles is dopamine, but a small amount of norepinephrine is sometimes also present. PC12 cells were first isolated from a tumor in the rat adrenal gland in 1976 by Lloyd Greene and coworkers [1] and are now available commercially. Adrenal chromaffin cells are also widely used in research for amperometric detection of exocytosis. Chromaffin cells are located mainly in the medulla of

Ricardo Borges (ed.), *Chromaffin Cells: Methods and Protocols*,
Methods in Molecular Biology, vol. 2565, https://doi.org/10.1007/978-1-0716-2671-9_16,

the adrenal glands and receive signals from the splanchnic nerve of the sympathetic nervous system. They are commonly isolated from the adrenal glands and grown as primary cultures, which survive for a small interval of days. There are a variety of chromaffin cells depending on the animal, such as mouse, rat, and cow, and they exhibit distinct properties regarding the expression of specific receptors and ion channels. In chromaffin cells, norepinephrine and epinephrine are synthesized, stored, and released by large dense-core vesicles (LDCVs).

Vesicle impact electrochemistry cytometry (VIEC) and intracellular vesicle impact electrochemistry cytometry (IVIEC) stand out among the vesicle collision methods in the studies involving exocytosis of neurotransmitters in cells and animal models [2–4]. In general, these two methods are based on current measurements resulting from electrochemical reactions that occur when vesicles containing electroactive species, for example, catecholamines, hit the surface of an ultramicroelectrode or a nanoelectrode. Methods using this approach also are known as single-entity electrochemistry methods [5].

In VIEC, the measurements are carried out using a suspension of vesicles isolated from cells. In one form of these experiments, called adsorption VIEC, the procedure is to dip the electrode in a suspension of vesicles to allow the vesicles to adsorb on the electrode surface, and the measurements are conducted by moving the electrode to a separate buffer solution. Another way to perform VIEC is by placing the electrode in a suspension containing vesicles and to directly measure species as the vesicles impact and open on the electrode surface. This is called impact VIEC.

In IVIEC, the measurements are performed inside a cell where a nanotip electrode is pushed through the cell membrane. The signals obtained are related to single vesicles present in the cytoplasm opening after impacting/adsorbing the surface of the nanotip electrode. A possible mechanism of the vesicles opening on electrode surface in VIEC and IVIEC involves the movement of the proteins present to expose mainly a section of lipid bilayer on the vesicle membrane followed by electroporation [6].

In VIEC and IVIEC, the electroactive species are commonly catecholamines and the electrodes are made using carbon microfibers. However, some strategies have been developed using biosensors to measure non-electroactive species, for example, glutamate [7, 8]. Another example is the use of platinum microelectrodes on the detection of reactive oxygen species in stress granules [9]. Typical VIEC and IVIEC responses obtained during experiments are shown in Fig. 1. The signal in Fig. 1a is an example of transient current spikes where each spike is related to the oxidation of catecholamines from single vesicles opening at the electrode surface for IVIEC. Current trace for VIEC is similar. The analysis of

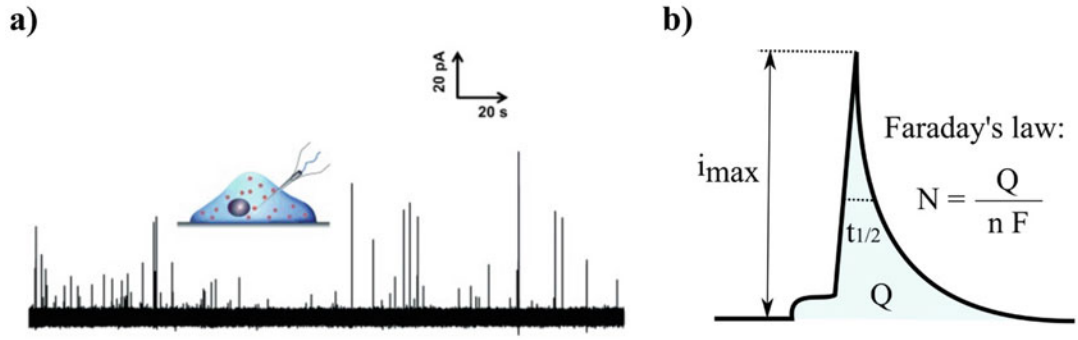

Fig. 1 (**a**) Representative peaks for an IVIEC experiment. (**b**) Schematic of a single peak from either VIEC or IVIEC. (Figures adapted from ref. 22)

the signals provides information about the dynamics of the opening process, and using Faraday's law, the number of molecules can be determined (Fig. 1b).

Dynamic parameters of vesicle opening can be used to understand the mechanism of how individual vesicles interact with electrodes and the number of molecules offers a piece of essential information related to the process of exocytosis. The number of molecules obtained using IVIEC can be compared with the number of molecules released during exocytosis to obtain the fraction of molecules released during exocytosis [10–14]. The number of molecules released during exocytosis is routinely obtained using single-cell amperometry (SCA). Briefly, in SCA, a polarized carbon ultramicroelectrode is positioned near the cell membrane from a target cell, and the current signal obtained is related to the electroactive species released and oxidized after cell stimulation [15]. Using this approach, Gu et al. studied the correlation between the fraction of release and plasticity by studying activity-induced plasticity. They showed that plasticity can occur at the level of a single vesicle by combining chemical analysis methods and a neuroendocrine cell line. They have shown that repetitive stimuli enhance the amount of transmitter release but decrease the number of exocytotic events and vesicular content, resulting in a higher fraction of release [16].

In another study, Zhu et al. [17] applied single-cell amperometry and IVIEC with nanotip electrodes to investigate the effects of cocaine and methylphenidate on exocytotic release and vesicle content in PC12 cells. Cocaine and methylphenidate have opposed influence on cognition even though both drugs block the dopamine transporter on the cell membrane to increase extracellular dopamine levels; however, they have opposite effects on the fraction of release that diminishes or increases after cocaine or methylphenidate exposure, respectively. They proposed that the fraction of release might be related to cognition.

SCA and IVIEC were used by Hatamie et al. [11] to reveal that insulin release from beta cells is also partial. They found out that the fraction of serotonin (as a proxy for insulin) released during exocytosis is only 34% of the stored content of serotonin in vesicles. They conclude that if this occurs for a small molecule like serotonin that will pass with relative ease through the partially open fusion pore, then it is likely that the release of insulin, which is a larger molecule than serotonin, will be impeded more strongly.

Utilizing the SCA and IVIEC methods to investigate the fraction released during exocytosis, Majdi and et al. [18] and Larsson et al. [14] monitored octopamine release and content in varicosities from neuromuscular junctions in *Drosophila* larvae. They have shown that the fraction of the vesicular octopamine content released from a living *Drosophila* larval neuromuscular neuron is very small. The percentage of released molecules was found to be 4.5% and 10.7% for single and complex events, respectively. The partial release in this neuronal system suggests the possibility that cells can regulate their chemical signaling strength via an open and closed fusion pore.

Glutamate biosensors have also been used to measure or show the fraction released of this transmitter is significantly less than full release. Although the published works to date do not suggest the same numbers of molecules in individual glutamate vesicles, they both suggest the fraction released is small [6, 7].

On the other end of the release fraction range, Wang et al. have shown the fractional vesicular 5-HT release in human carcinoid BON cells is 80% and can be increased to nearly full release with drugs [13]. These enterochromaffin cells, located in the gastrointestinal tract, use 5-HT signaling to modify normal gastrointestinal motility and inflammation. These cells are important for signaling from the gastrointestinal lumen to afferent nerve terminals as a pathway to directly transduce information to the nervous system [19, 20].

Experiments to probe vesicle content and opening dynamics have been carried out in several formats. These include VIEC, IVIEC, combined SCA and IVIEC on a single cell, VIEC with carbon nanopipettes, and combined VIEC and confocal microscopy. The detailed protocols for these experiments are given here.

2 Materials

2.1 Microelectrode Fabrication

The disk ultramicroelectrodes are fabricated in several steps (Fig. 2a):

2.1.1 Carbon Disk Electrodes

1. Insert a carbon microfiber into a borosilicate capillary tube (no filament, OD: 1.2 mm., ID: 0.69 mm) by vacuum aspiration. The microfiber used can be in different dimeter sizes, usually 5–33 μm.

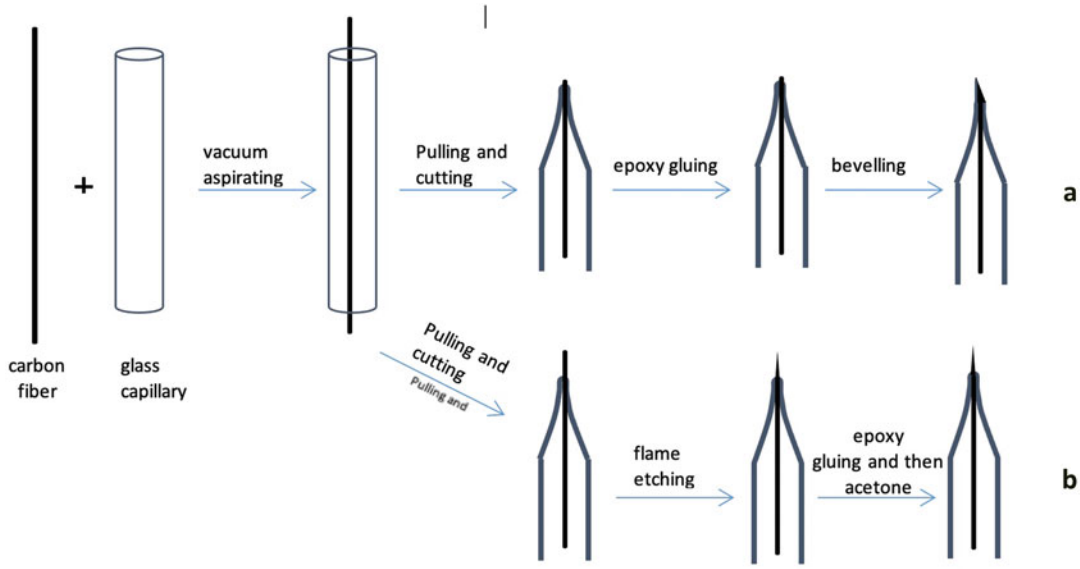

Fig. 2 Schematic representation of carbon disk ultramicroelectrodes (**a**) and carbon nanotip (**b**) electrodes fabrication. (Figure adapted from ref. 22)

2. Pull the capillaries containing the carbon microfibers using a micropipette puller (model PE-21, Narishige, Inc., Japan). The parameters used for pulling are the following: heat, 40; submagnet adjustment, 35; and main magnet adjustment, 30.
3. Using a microscope, localize the glass microfiber junction on the tip, and cut the excess of carbon microfiber present outside the tip of the microelectrode.
4. Seal the vacancy between microfiber and glass by dipping the ultramicroelectrode tip into low viscosity epoxy for 2–3 min. Proportion monomer/catalyst 2:1 (m/m).
5. Dry the epoxy inside of the electrode pipette tip in an oven at 100 °C overnight.
6. Bevel the ultramicroelectrodes at a 45° angle using a microgrinder. The final electrode should appear as in Fig. 2a (beveled disk) or Fig. 2b (nanotip; *see* below).
7. Test the electrode by cyclic voltammetry using a 100 mmol L^{-1} dopamine solution in 0.1 mol L^{-1} PBS (pH = 7.4). Potential window: −0.2 to 0.8 V vs. Ag/AgCl. Scan rate 100 mVs^{-1}. The electrodes should present a typical sigmoidal-shape voltammogram.

2.1.2 Carbon Nanotip Electrodes (CNEs) [21, 22]

The fabrication of CNEs involves the following steps (Fig. 2b):

Steps 1 and **2** are the same as for the carbon disk ultramicroelectrodes fabrication (Subheading 2.1.1).

3. Using a microscope, localize the glass microfiber junction on the tip, and cut the excess carbon microfiber present outside of the tip of the microelectrode, leaving around 100–200 μm length [2].
4. The carbon fiber is then flame etched by placing the end of the fiber in the blue part of a butane flame. When the end of the tip becomes red, the electrode is removed from the flame. All etched electrodes are checked under the microscope, and electrodes with a suitably sharp tip (diameter: 100–200 nm; length: 30–100 μm) are selected (*see* **Note 1**).
5. Seal the vacancy between microfiber and glass by dipping the ultramicroelectrodes tip into low-viscosity epoxy for 3 min and then 15 s in acetone to remove the epoxy from carbon fiber. Proportion epoxy monomer/catalyst 2:1 (m/m).
6. Dry the epoxy inside of the electrodes in an oven at 100 °C overnight.
7. Test the electrode by cyclic voltammetry using a 100 mmol L^{-1} dopamine solution in PBS (pH = 7.4). Potential window: −0.2 to 0.8 V vs. Ag/AgCl. Scan rate 100 mVs^{-1}. The electrodes should present a typical sigmoidal shape voltammogram. Figure 3a and b show an example of sigmoidal and non-sigmoidal voltammograms, respectively.

2.1.3 Carbon Nanopipette Electrodes

Nanopipettes with the tip radii from 50 to 600 nm are pulled from quartz capillaries (1.0 mm o.d., 0.5 mm i.d., with a filament) by the laser pipette puller. The parameters used for pulling using a pipette puller model P-2000 (Sutter instruments) are heat, 700; filament, 4; velocity, 30; delay, 130; and pull, 90. A layer of carbon is deposited on the inner wall of glass nanopipettes by chemical vapor deposition (CVD) at 900 °C for 30 min using a tube furnace. An Ar flow of 200 standard cubic centimeters per min is passed through the CVD reaction chamber during heating to protect the layer of carbon from oxidation. Once the furnace temperature reached 900 °C, a mixed flow of methane and Ar (3:5 methane to argon ratio) is passed through the reaction chamber (Fig. 4) [23].

2.1.4 ITO Microelectrode Arrays

There are different methods to fabricate ITO microelectrodes for application to cell and release applications. Indium tin oxide (In_2O_3/SnO_2)-coated glass slides (75 mm × 25 mm × 1 mm, film thickness∼150–300 A°) with a resistance of 70–100 Ω/square usually are prepared commercially from Sigma (St. Louis, MO). The ITO films are patterned, as per refs. 24 and 25, into 10- to 20-μm-wide stripes terminating in 1 by 1 mm squares at the edge of the slide by following a photolithographic and wet-etching procedure. The larger square pads allow connection to an amplifier, and the procedure is described in the literature [24, 25].

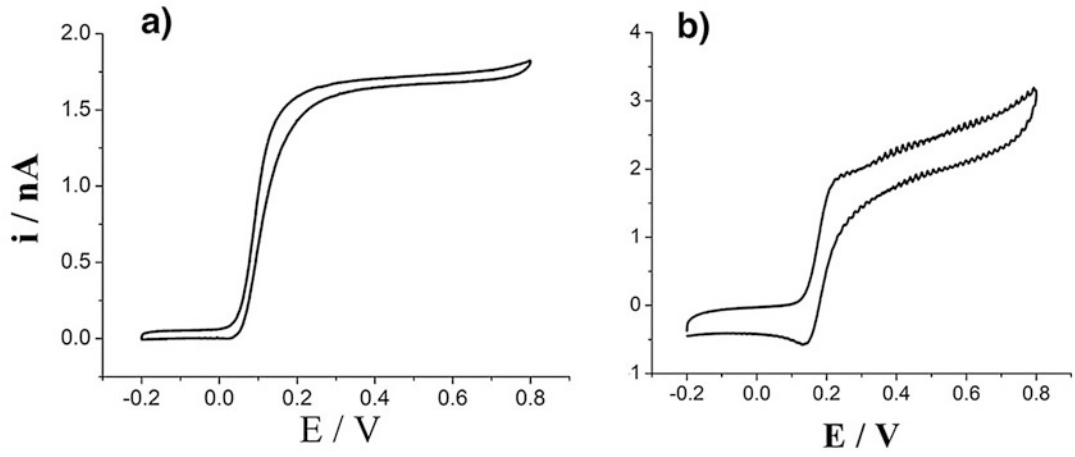

Fig. 3 (**a**) Representative sigmoidal and (**b**) non-sigmoidal voltammograms

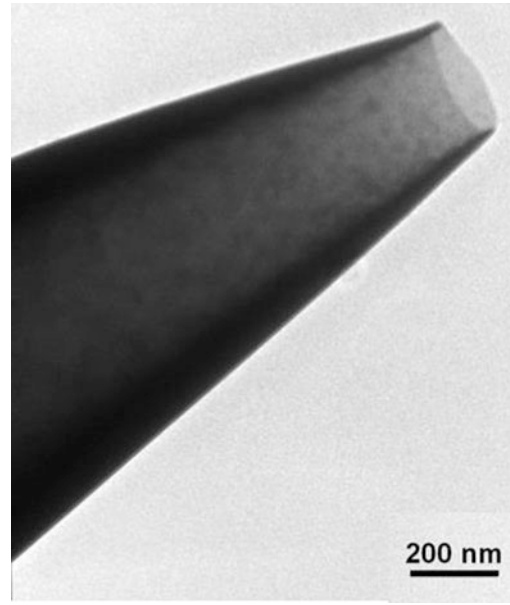

Fig. 4 Representative of carbon nanopipette electrodes. (Figure adapted from ref. 23)

In another method, a layer of 5-nm gold is first deposited on an ITO-coated coverslip (SPI Supplies) by e-beam thin-film evaporation from Lesker Company (Marlborough, United Kingdom). Then the surface is cleaned with isopropyl alcohol and blow-dried with nitrogen gas. A film with a thickness of about 1 μm is made by spin-coating the coverslip with a photoresist layer S1813 from SHIPLEY company (London, England) at 1792 × g for 30 s and is then baked at 115 °C for 1 min. A 20-channel microelectrode array (MEA) pattern is then developed and transferred to the

coverslip by UV lithography (KS MA6, Suss MicroTec) with a commercially available chrome mask of the 20-channel MEA design [26]. After UV exposure, the electrodes are developed with MF319 developer (SHIPLEY) for 1 min with mild shaking followed by hardening by baking at 115 °C for 5 min on a hot plate and finally dry etching using an argon plasma (for example, Oxford Ionfab 300 Reactive Ion Beam). The photoresist is removed by placement in a low- intensity ultrasonication bath with mr-Rem 400 (for example, from Micro Resist Technology) at 50 °C for 20 min after dry etching. Then the glass wafers with MEAs are spin-coated with the photoresist SU-83005 (MicroChem) at 1792 × g for 30 s. to produce a film of the SU-83005 with a thickness of about 5 μm, which leads to a layer of insulation covering most of the structure, except the probe area and the contact pad area. The wafer is then baked at 65 °C for 1 min and at 95 °C for 3 min on a hot plate. The pattern for the insulated area is defined on top of the MEAs by UV lithography (KS MA6, Suss MicroTec) with a second chrome mask showing the probe area and the contact pad design and is subsequently baked at 65 °C for 1 min and 95 °C for 3 min on a hot plate [26].

2.2 Cell Culture and Solutions

2.2.1 PC12 Cells

PC12 cells are maintained in phenol red-free RPMI-1640 media (PAA Laboratories, Inc., Australia) supplemented with 10% donor equine serum, 5% fetal bovine serum gold, and 0.4% penicillin streptomycin solution in a 7% CO_2, 100% humidity atmosphere at 37 °C. Cells are grown on mouse collagen-coated cell culture flasks (collagen type IV) and are subcultured every 7–9 days. Media are replaced every 2 days throughout the lifetime of all cultures. For single-cell experiments, PC12 cells are subcultured sparsely on mouse collagen-coated culture dishes (collagen type IV) 3–5 days before the experiment, and cell media is replaced every other day (*see* **Note 2**).

2.2.2 Chromaffin Cells and Vesicle

One of the most common chromaffin cells used is isolated from cow adrenal medulla by enzymatic digestion. To prepare bovine chromaffin cells, fresh glands are transported from a slaughterhouse in cold, sterile Locke's solution. Locke's solution contains NaCl (1540 mM), KCl (56 mM), $NaHCO_3$ (36 mM), glucose (56 mM), HEPES (50 mM), and 1% (v/v) penicillin, pH 7.4. This stock solution is diluted 10× with distilled water the day before the experiment and used for gland storage and to rinse the adrenal gland vein. After externally sterilizing the glands by spraying with a 70% solution of ethanol, fat and connective tissue are trimmed away. Adrenal veins are rinsed with Locke's solution previously thermostated at 37 °C to remove blood. The medulla is isolated after digesting the gland with introducing collagenase P (0.2%, Roche, Sweden) by syringe through the vein. Digested medulla is filtered over steel sieves and diluted with Locke's buffer to reduce

the activity of collagenase P through the adrenal vein by syringe injection and incubated for 20 min at 37 °C. The tissue suspension is then filtered over steel sieves and diluted with Locke's solution. The cells are pelleted at 300 g for 10 min at room temperature, and the pellet obtained is resuspended in Locke's buffer and filtered over a sterile, 100-μm nylon mesh. The chromaffin cell suspension is mixed with sterile Percoll/Locke's buffer (10:1) and centrifuged at 18,600 × g for 20 min at room temperature. The top layer of the density gradient is collected and filtered through a 100-μm nylon mesh. Again, the cell suspension is diluted with Locke's buffer and centrifuged at 300 g for 10 min at room temperature to exclude Percoll. The cells are seeded on collagen (IV)-coated plastic dishes and maintained in a humidified incubator at 37 °C, 5% CO_2 for a maximum of 5 days prior to experiments (*see* **Note 2**).

For vesicle isolation, the medulla was mechanically homogenized in homogenizing buffer, and the vesicles were purified using two series of centrifugation steps: (1) 1000 × g for 10 min to remove whole cells and (2) 10000 × g to pellet vesicles. All centrifugation was performed at 4 °C. The final pellet of vesicles was resuspended and diluted in homogenizing buffer and subsequently used for electrochemical measurements the same day.

2.2.3 β Cells

Pancreatic β cells are usually isolated from 5- to 12-month-old mice. Mice are anesthetized and sacrificed by cervical dislocation. Cannulation of the bile duct is performed with a 30 G needle, and a Liberase solution is injected in the pancreas. The pancreas is digested at 37 °C for 12 min in the presence of the Liberase solution. The digestion is stopped by addition of cold Hanks' balanced salts buffer (HBS), and islets are washed three times. HBS buffer contains 136.9 mM NaCl, 5.4 mM KCl, 1.3 mM $CaCl_2$, 0.8 mM $MgSO_4$, 0.44 mM KH_2PO_4, 0.34 mM Na_2HPO_4, 5.55 mM glucose, 4.2 mM $NaHCO_3$, and 0.1% (w/w) BSA. The islets are handpicked under a stereomicroscope in HBS supplemented with 5 mmol/L glucose. Isolated islets are cultured in RPMI 1640 culture medium containing 11.1 mM glucose, 10% fetal bovine serum (FBS), streptomycin (100 U/mL), and penicillin (100 U/mL) at 37 °C in an atmosphere of 5% CO_2. Islets are dispersed into single cells by gentle pipetting in cell dissociation buffer (Thermo Fisher Scientific) supplemented with trypsin (0.005%, Life Technologies) at a 9:1 ratio. Cells are washed and plated in serum-containing medium onto plates and allowed to settle.

2.2.4 Homogenizing Buffer

Homogenizing buffer contains 230 mM sucrose, 1 mM EDTA, 1 mM $MgSO_4$, 10 mM HEPES, 10 mM KCl, complete enzyme inhibitor (Roche), DNase I (10 μg/mL) (Roche), and 0.001 mM oligomycin, pH 7.4, ~310 mOsm (*see* **Note 3**).

2.2.5 Isotonic Solution It contains 150 mM NaCl, 5 mM KCl, 1.2 mM $MgCl_2$, 5 mM glucose, 10 mM HEPES, and 2 mM $CaCl_2$, pH 7.4.

2.3 Instruments

– Patch clamp amplifier capable to low-noise recording and capable to maintain at least +800 mV of holding potential.

*2.3.1 Amperometric Experiments (*See ***Note 4****)*

2.3.2 Positioning System

– Ultramicroelectrodes or stimulation pipette micromanipulators with piezoelectric or hydraulic translation along three axes (x, y, and z).

2.3.3 Microscopes

– Confocal microscope.
– Inverted microscope containing 10×, 20×, and 40× lens.

2.3.4 Temperature Control

– A planar Peltier stage coupled on the microscope. Temperature range −10 °C to 99 °C ± 0.1 °C.

2.3.5 Vibration and Electromagnetic Radiation Isolation

– Optical table.
– Faraday cage.

3 Methods

3.1 Vesicle Impact Electrochemistry Cytometry (VIEC)

3.1.1 Carbon Disk Electrodes

There are two modes to carry out VIEC: the adsorption mode where vesicles are allowed to adsorb on the electrode and then the electrode is transferred to a clean solution to carry out VIEC and the impact mode where vesicle opening is observed at an electrode in a solution of vesicles (*see* **Note 5**).

Adsorption-Based VIEC.

1. Adsorption of vesicles on ultramicroelectrode (UME) surface is carried out by placing a polished 33-μm disk UME in container with a concentrated suspension of vesicles for 10–20 min at 4 °C.
2. The UMEs are then transferred to an electrochemical cell containing homogenizing buffer at 37 °C.
3. The measurements are conducted inside of a Faraday cage, recording for 5 s at an applied potential of 0 mV vs. Ag/AgCl (baseline) and then switching the potential to 700 mV vs. Ag/AgCl for 5–20 min.
4. After each experiment, the UMEs can be cleaned by beveling and used again.

Impact-Based VIEC.

1. The polished 33-μm disk UME can be held with a simple microelectrode holder and is placed in the electrochemical cell containing 1 mL of homogenizing buffer at 37 °C.
2. A 100 μL of a vesicle suspension is added to the electrochemical cell consisting of a small glass vial. As the vesicles are in suspension, many contact the electrode surface.
3. The measurements are conducted by recording for 5 s at an applied potential of 0 mV vs. Ag/AgCl (baseline) and then switching the potential to 700 mV vs. Ag/AgCl for 5–20 min.
4. After each experiment, the UMEs are clean up by beveling, and it can be used again.

3.1.2 VIEC at Carbon Nanopipettes (CNPs)

1. The CNP is added to the electrochemical cell containing 1 mL of homogenizing buffer at 37 °C.
2. A 100 μL of vesicle suspensions is added to the electrochemical cell.
3. The measurements are conducted, recording for 5 s at an applied potential of 0 mV vs. Ag/AgCl (baseline) and then switching the potential to 700 mV vs. Ag/AgCl for 5–20 min.
4. After each experiment, the CNP is discarded.

3.2 Intracellular Impact Electrochemistry Cytometry (IVIEC)

3.2.1 Carbon Nanotip Electrodes and Carbon Nanopipettes

1. The cell medium is first replaced over the cultured cells using a pre-warmed isotonic solution (37 °C).
2. A 5 mL of pre-warmed isotonic solution (37 °C) is added to the cell culture dish, and it is maintained at 37 °C during the experiment.
3. Localize and target an attached cell in the dish bottom using inverted microscopy.
4. Using a manipulator, move the nanoelectrode (CNE or CNP) near the vicinity of the target cell (*see* **Note 6**).
5. Apply 700 mV vs. Ag/AgCl to the nanoelectrode selected to experiments.
6. Start recording the current.
7. Using the manipulator, slowly push the nanoelectrode inside the cell until about 2–5 μm penetration is achieved (Fig. 5a).
8. Stop the measurement when spikes are no longer observed.
9. Remove the nanoelectrode from inside of the cell, and replace it with a new one to start a new measurement.

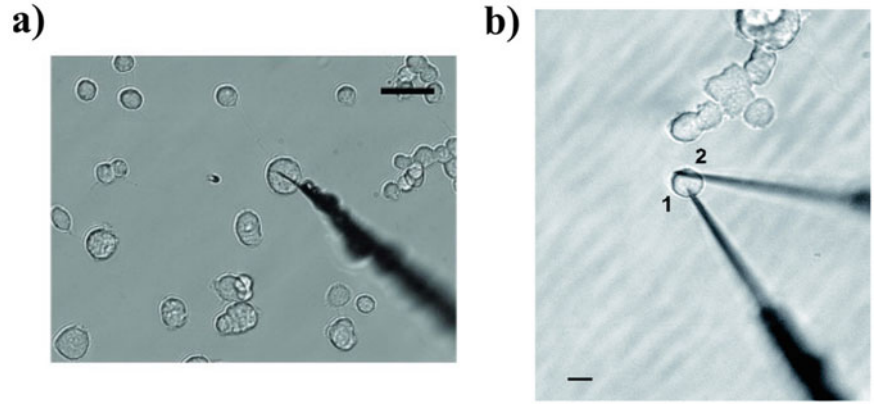

Fig. 5 (**a**) Intracellular measurement using a carbon nanotip electrode pushed inside of PC12 cell cytoplasm. (**b**) Dual electrode measurements (IVIEC-SCE). Scale bar 20 μm. (Figures adapted from ref. 22, 27)

3.3 Combined Techniques

3.3.1 Two Electrodes to Simultaneously Carry out SCA and IVIEC

Follow **Steps 1** to **3** from Subheading 3.2.1.

4. Using a manipulator, move the stimulation micropipette near the target cell. To make the stimulation micropipette, pull the capillary using a micropipette puller, and for the Sutter Puller, the following parameters are used: heat, 40; submagnet adjustment, 0; and main magnet adjustment, 75. Cut the tip under the microscope to expose an open capillary with diameter around 1–2 μm. The micropipette is coupled to a microinjection system and previously filled with a stimuli solution, for example, a solution containing high-potassium concentration.
5. Using manipulators, move two carbon nanotip electrodes near the target cell. Start by placing the CNE-1 used to perform the single-cell experiment (SCE) near the cell membrane and then the CNE-2 used to IVEC measurements.
6. Apply 700 mV vs. Ag/AgCl on both CNE.
7. Start recording the current.
8. Using the manipulator, slowly push the CNE-2 inside the cell to a distance of about 2–5 μm.
9. After obtaining the first spikes, move the CNE-1 onto the cell membrane (Fig. 5b).
10. After 5 s from **step 8**, start the chemical stimulation flushing the stimuli solution next to the cell for 5 s using a pressure of 20 psi.
11. Stop the measurements when spikes are no longer observed.

*3.3.2 VIEC with Combined Confocal Fluorescence Microscopy (See **Note 7**)*

Vesicle Labeling

1. Prepare a stock solution of FFN 511 using DMSO and final concentration to 10 $mmolL^{-1}$.
2. Label 10 mL of vesicle suspension by incubating for 40 min at 4 °C with 10 μL of 10 $mmolL^{-1}$ FFN 511 solution.
3. Change the incubation solution to 10 mL of the homogenizing buffer after centrifugation at 10,000 × g for 20 min.

4. Label 10 mL of resultant vesicle suspension by adding 142 μL of 18:1 Liss Rhod PE solution (1.5 mg/mL) and incubating at 4 °C for 15 min.
5. Change the incubation solution to 10 mL of the homogenizing buffer after centrifugation at 10,000 × g for 20 min.

Electrochemical Measurements

1. Position the MEA containing a polylactic acid (PLA) chamber on the microscopy stage, and add 1 mL of labeled vesicle suspension.
2. Using microscopy, localize the target microelectrode on the MEA.
3. After 5 min incubation with the labeled vesicle suspension to the MEA chamber, start the amperometric current measurements by applying 700 mV vs. Ag/AgCl.
4. Stop the measurements after 20 min.

3.3.3 Confocal Measurements

1. Scan the electrode zone using the XYT mode with an imaging area of 30–40 μm^2, a pixel size of 50–70 nm, and a time frame of 5 s.
2. Use 585 nm to excite the Rh-Pe and 575–650 nm to collect the fluorescence.
3. Use 405 nm to excite the FFN 511 and 460–550 nm to collect the fluorescence.

4 Notes

1. There is limited control of the flame etching process regarding the thickness and sharpness of the carbon tips. One might have to etch the electrodes couple of times to achieve the desired nanotip.
2. In PC12 cell and chromaffin cell experiments, one must always count the cells in the dishes, especially if they will be treated with another chemical. This is required to maintain consistency between results from different dishes. For chromaffin and PC12 cell experiments, ~500,000 and 200,000 cells are seeded on collagen (IV)-coated plastic dishes, respectively.
3. In preparing homogenizing buffer, EDTA dissolves quite slowly in water. A magnetic stir bar should be used in the beaker until all the EDTA is dissolved before adding other ingredients.
4. All amperometric measurements are carried out using a two-electrode configuration (working and reference electrodes).

5. In general, the tip of ultramicroelectrode and nanopipette electrodes are fragile. It is important to avoid hitting the tip of these devices on the wall or bottom of the electrochemical cell.
6. There might be different shapes of cells in the dishes, so one must be careful to choose round-shaped cells for collecting data. In chromaffin cell isolation, you might collect cortex cells from tissue with chromaffin cells. These cells look like chromaffin cells under the microscope but do not contain catecholamine. If no spikes are observed in IVIEC, it is possible this is due to analysis of a cortex cell instead of a chromaffin cell.
7. Electrochemical and confocal measurements are performed simultaneously.

References

1. Greene LA, Tischler AS (1976) Establishment of a noradrenergic clonal line of rat adrenal pheochromocytoma cells which respond to nerve growth factor. Proc Natl Acad Sci U S A 73(7):2424–2428
2. Lima A, Gu C, Hu K, Ewing A (2020) Electrochemistry at and in single cells. PennState, pp 125–160
3. Hu K, Nguyen TDK, Rabasco S et al (2021) Chemical analysis of single cells and organelles. Anal Chem 93:41–71. https://doi.org/10.1021/acs.analchem.0c04361
4. Wang Y, Ewing A (2021) Electrochemical quantification of neurotransmitters in single live cell vesicles shows exocytosis is predominantly partial. Chembiochem 22:807–813
5. Andreescu D, Kirk KA, Narouei FH, Andreescu S (2018) Electroanalytic aspects of single-entity collision methods for bioanalytical and environmental applications. ChemElectroChem 5:2920–2936. https://doi.org/10.1002/celc.201800722
6. Lovrić J, Najafinobar N, Dunevall J et al (2016) On the mechanism of electrochemical vesicle cytometry: chromaffin cell vesicles and liposomes. Faraday Discuss 193:65–79. https://doi.org/10.1039/c6fd00102e
7. Yang X-K, Zhang F-L, Wu W-T et al (2021) Quantitative nano-amperometric measurement of intravesicular glutamate content and its sub-quantal release by living neurons. Angew Chem Int Ed 60:15803–15808. https://doi.org/10.1002/anie.202100882
8. Wang YM, Fathali H, Mishra D et al (2019) Counting the number of glutamate molecules in single synaptic vesicles. J Am Chem Soc 141(44):17507–17511
9. Hu K, Relton E, Locker N et al (2021) Electrochemical measurements reveal reactive oxygen species in stress granules. Angew Chem Int Ed 60:15302–15306. https://doi.org/10.1002/anie.202104308
10. Wang Y, Gu C, Ewing AG (2021) A multimodal electrochemical approach to measure the effect of zinc on vesicular content and exocytosis in a single cell model of ischemia. QRB Discovery 2:e12. https://doi.org/10.1017/qrd.2021.10
11. Hatamie A, Ren L, Dou H et al (2021) Nanoscale amperometry reveals that only a fraction of vesicular serotonin content is released during exocytosis from beta cells. Angew Chem Int Ed 60:7593–7596. https://doi.org/10.1002/anie.202015902
12. Wang Z, He X, Long Le Vo K, Ewing AG (2021) Electrochemical and mass spectrometric measurement of enhanced intravesicular catecholamine content and exocytotic frequency at subanaesthetic ketamine doses. Anal Sens 1:166–170. https://doi.org/10.1002/anse.202100026
13. Wang Y, Gu C, Patel BA, Ewing AG (2021) Nano-analysis reveals high fraction of serotonin release during exocytosis from a gut epithelium model cell. Angew Chem Int Ed 60:23552–23556. https://doi.org/10.1002/anie.202108193
14. Larsson A, Majdi S, Oleinick A et al (2020) Intracellular electrochemical nanomeasurements reveal that exocytosis of molecules at living neurons is subquantal and complex. Angew Chem Int Ed 132(17):6777–6780
15. Chow RH, von Rüden L, Neher E (1992) Delay in vesicle fusion revealed by

electrochemical monitoring of single secretory events in adrenal chromaffin cells. Nature 356: 60–63. https://doi.org/10.1038/356060a0

16. Gu C, Philipsen MH, Ewing AG (2020) Mass spectrometric imaging of plasma membrane lipid alteration correlated with amperometrically measured activity-dependent plasticity in exocytosis. Int J Mol Sci 21:1–10. https://doi.org/10.3390/ijms21249519
17. Zhu W, Gu C, Dunevall J et al (2019) Combined amperometry and electrochemical cytometry reveal differential effects of cocaine and methylphenidate on exocytosis and the fraction of chemical release. Angew Chem Int Ed 131: 4282–4286. https://doi.org/10.1002/ange.201813717
18. Majdi S, Berglund EC, Dunevall J et al (2015) Electrochemical measurements of optogenetically stimulated quantal amine release from single nerve cell varicosities in drosophila larvae. Angew Chem Int Ed 54:13609–13612. https://doi.org/10.1002/anie.201506743
19. Bellono NW, Bayrer JR, Leitch DB et al (2017) Enterochromaffin cells are gut Chemosensors that couple to sensory neural pathways. Cell 170:185–198.e16. https://doi.org/10.1016/j.cell.2017.05.034
20. Liddle RA (2019) Neuropods. CMGH 7: 739–747
21. Strein TG, Ewing AG (1992) Characterization of submicron-sized carbon electrodes insulated with a phenol-allylphenol copolymer. Anal Chem 64:1368–1373. https://doi.org/10.1021/ac00037a012
22. Li X, Majdi S, Dunevall J et al (2015) Quantitative measurement of transmitters in individual vesicles in the cytoplasm of single cells with nanotip electrodes. Angew Chem Int Ed 54: 11978–11982. https://doi.org/10.1002/anie.201504839
23. Hu K, Wang Y, Cai H et al (2014) Open carbon nanopipettes as resistive-pulse sensors, rectification sensors, and electrochemical nanoprobes. Anal Chem 86:8897–8901. https://doi.org/10.1021/ac5022908
24. Sun X, Gillis KD (2006) On-chip amperometric neasurement of quantal catecholamine release using transparent indium tin oxide electrodes. Anal Chem 78(8):2521–2525. https://doi.org/10.1021/ac052037d
25. Gao C, Sun X, Gillis KD (2013) Fabrication of two-layer poly(dimethyl siloxane) devices for hydrodynamic cell trapping and exocytosis measurement with integrated indium tin oxide microelectrodes arrays. Biomed Microdevices 15(3):445–451. https://doi.org/10.1007/s10544-013-9744-1
26. Zheng Y-N, Nguyen TDK, Dunevall J et al (2021) Dynamic visualization and quantification of single vesicle opening and content by coupling vesicle impact electrochemical cytometry with confocal microscopy. ACS Meas Sci Au 1:131–138. https://doi.org/10.1021/acsmeasuresciau.1c00021
27. Gu C, Ewing AG (2021) Simultaneous detection of vesicular content and exocytotic release with two electrodes in and at a single cell. Chem Sci 12:7393–7400. https://doi.org/10.1039/d1sc01190a

Chapter 17

Patch Amperometry and Intracellular Patch Electrochemistry

Eugene V. Mosharov and Manfred Lindau

Abstract

Both patch amperometry (PA) and intracellular patch electrochemistry (IPE) take advantage of a recording configuration where an electrochemical detector—carbon fiber electrode (CFE)—is housed inside a patch pipette. PA, which is employed in cell-attached or excised inside-out patch clamp configuration, offers high-resolution patch capacitance measurements with simultaneous amperometric detection of catecholamines released during exocytosis. The method provides precise information on single-vesicle size and quantal content, fusion pore conductance, and permeability of the pore for catecholamines. IPE, on the other hand, measures cytosolic catecholamines that diffuse into the patch pipette following membrane rupture to achieve the whole-cell configuration. In amperometric mode, IPE detects total catechols, whereas in cyclic voltammetric mode, it provides more specific information on the nature of the detected molecules and may selectively quantify catecholamines, providing a direct approach to determine cytosolic concentrations of catecholaminergic transmitters and their metabolites. Here, we provide detailed instructions on setting up PA and IPE, performing experiments and analyzing the data.

Key words Patch amperometry, IPE, Cyclic voltammetry, Electrochemistry, Exocytosis, Synaptic vesicle, Fusion pore, Catecholamine, Cytosolic

1 Introduction

Release of neurotransmitters and neuropeptides from neurons and release of hormones from neuroendocrine cells occur by exocytosis: a specialized mechanism of secretion in which secretory vesicles fuse with the plasma membrane. Fusion of a single vesicle with the plasma membrane increases the plasma membrane area by the area of the vesicle membrane and produces a stepwise change in membrane capacitance. For large vesicles, these capacitance steps can be measured in whole-cell patch clamp capacitance measurements [1]. Vesicle fusion with the plasma membrane begins with the formation of a narrow fusion pore [2]. As for ion channels, the biophysical properties of fusion pores were initially characterized mainly by determining the pore conductance and its fluctuations.

Ricardo Borges (ed.), *Chromaffin Cells: Methods and Protocols*,
Methods in Molecular Biology, vol. 2565, https://doi.org/10.1007/978-1-0716-2671-9_17,

The first measurements of fusion pore conductance were performed with whole-cell patch clamp recordings from beige mouse mast cells with extremely large (>2 μm diameter) secretory vesicles [3].

When a vesicle fuses with the plasma membrane in a whole-cell patch clamp recording under voltage clamp, the added vesicle capacitance is charged rapidly to the voltage clamp potential. For very large vesicles, the associated charging current can be measured as a brief current transient, which can be analyzed to reveal the fusion pore conductance during the first ~100 μs of its existence [3–5]. Once the charging transient ceases, the fusion pore conductance can still be monitored by analyzing the currents generated by time-varying voltages applied to the cell in voltage clamp because the vesicle membrane is charged and discharged via the narrow fusion pore [3, 6]. These early studies showed that the average initial fusion pore conductance is ~200–300 pS and that the fusion pore conductance subsequently fluctuates until it either increases to an unmeasurably large value, indicating full fusion with the plasma membrane, or returns to zero, indicating fusion pore closure in a transient fusion event.

When a vesicle releases its contents, the release of oxidizable molecules can be detected with a CFE because the released molecules transfer electrons to the CFE when they make contact with its surface [7]. The resulting amperometric current indicates directly the rate at which the molecules arrive at the CFE surface [8]. To determine the relation between fusion pore conductance and flux of transmitter, experiments were performed using beige mouse mast cells loaded with serotonin. Whole-cell capacitance measurements were performed while a CFE recorded simultaneously the release of serotonin (Fig. 1a). These experiments revealed that in mast cells, the release flux was proportional to fusion pore conductance [9]. These pioneering and groundbreaking experiments could not be repeated in the same way to study fusion pore conductance and release from neurons or neuroendocrine cells because neurosecretory vesicles are very small. Even in bovine chromaffin cells, the dense core vesicles have a typical diameter of ~250 nm, corresponding to a vesicle membrane capacitance of only ~2 fF, which is difficult to resolve as a distinct capacitance step in whole-cell patch clamp capacitance measurements.

Such small capacitance steps can, however, be well resolved in cell-attached patch clamp capacitance measurements [10, 11], which have very low noise [12]. The low noise comes from the much smaller patch membrane conductance and capacitance compared to the whole cell membrane. Although analysis of the rapid initial charging currents to determine the initial fusion pore conductance as in [3] has so far not been possible in cell-attached mode (*see* **Note 1**), the determination of fusion pore conductance from the real and imaginary part of the currents in a capacitance

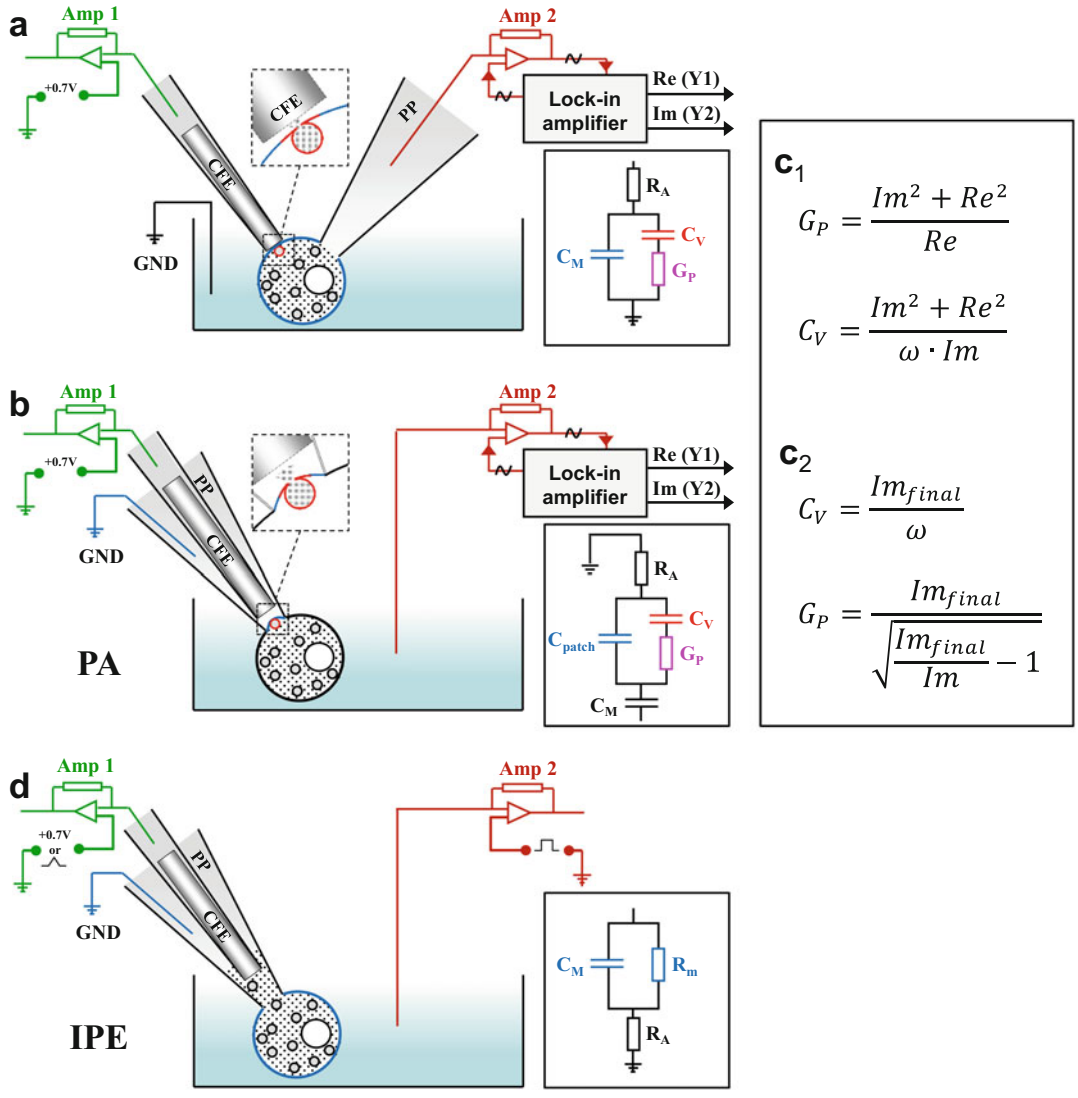

Fig. 1 Different modes of recordings. (**a**) Simultaneous whole-cell capacitance measurement and amperometric recording with a carbon fiber electrode (CFE). The equivalent circuit of the whole-cell patch clamp configuration with a fusing vesicle is shown in the box. (**b**) Patch amperometry (PA) in a cell-attached mode. The CFE and the ground electrode are both located inside the patch pipette. The sine wave for capacitance measurement is applied to the bath electrode. (**c_1**) Equations for calculating fusion pore conductance (G_P) and vesicle capacitance (C_V) from the changes in real (Re) and imaginary (Im) parts of the current output of the lock-in amplifier. Note that Re and Im denote the changes relative to the respective baselines for each individual fusion event. (**c_2**) Alternatively, the time course of G_P can be calculated from Im and the final value of the Im change after vesicle full fusion (Im_{final}). (**d**) Intracellular patch electrochemistry (IPE). After attaining a whole-cell mode, substances diffusing from the cytosol into the patch pipette are observed as a slow wave of oxidation current. CFE is used either in amperometric mode where it detects total catechols (a sum of catecholamines and their metabolites), or in cyclic voltammetric mode where it preferentially measures catecholamines

measurement using a lock-in amplifier is feasible [11], and the optimization of the recording parameters to determine fusion pore conductance has been analyzed [12].

Patch amperometry (PA) enables simultaneous measurements of vesicle fusion and transmitter release. The dense core vesicles of chromaffin cells release catecholamines, which are oxidizable molecules, and release from single vesicles can be well resolved using a CFE [7]. To combine cell-attached capacitance measurements with amperometric detection of release, the CFE needs to be mounted inside the patch pipette since release is now directed into the pipette tip. This led to the development of the patch amperometry technique (Fig. 1b), which has been described in considerable technical detail [13, 14]. PA recordings from bovine chromaffin cells revealed capacitance steps associated with amperometric spikes, demonstrating that these capacitance steps do indeed reflect exocytosis of single catecholaminergic dense core vesicles [15] (*see* example on Fig. 5a). Since the capacitance step size and the amperometric charge can be used to obtain the vesicle volume and the amount of catecholamines inside the same vesicle, correspondingly, the vesicular catecholamine concentration can be calculated for full fusion events [15, 16].

Amperometric spikes are frequently preceded by a so-called "foot signal" [17] and it was suspected that this foot signal or "pre spike feature" may reflect the slow leakage of transmitter through a narrow fusion pore. This hypothesis was confirmed using PA. It was found that the rate of catecholamine release fluctuates in parallel with the fusion pore conductance determined by sine wave-based admittance analysis (*see* example on Fig. 5b), indicating that during the foot signal, the rate of catecholamine release is controlled by the fusion pore [15, 18]. The initial fusion pore conductance is variable, as in other cell types, with a mean value of ~300 pS in cell-attached as well as excised inside-out patches [19]. Once the fusion pore opens, its conductance fluctuates until fusion goes to completion or until it closes again.

Intracellular patch electrochemistry (IPE) measures cytosolic oxidizable metabolites. As PA experiments often conclude with the rupture of the plasma membrane, it was noticed that attaining the whole cell is followed by a slow wave of amperometric current (*see* example on Fig. 6a). Further analysis demonstrated that in chromaffin cells [20], PC12 cells [21], and primary cultures of mouse dopaminergic neurons [22–24], this current mostly represents oxidation of cytosolic catechols—the sum of catecholaminergic transmitters, such as DA, NE, and Ep, and their metabolites, such as L-DOPA, DOPAC, DOPEG, etc. To provide specificity to the measurements of cytosolic molecules, CFE can also be used in cyclic voltammetric (CV) mode of detection, which has previously been employed to detect DA release kinetics from acute striatal slices [25]. As CFE in CV mode produces 10- to 20-fold higher

oxidation peaks for DA, EP, and NE than for other catechol metabolites [20], a combination of amperometric and CV measurements yields information about both the cytosolic pools of the transmitters that have been shown to be cytotoxic and about the rate of their turnover. Overall, to perform IPE recordings, the rig is modified, removing the lock-in amplifier and adding a capability to perform electrochemical recordings in the CV mode (Fig. 1d).

2 Materials

All solutions should be prepared using ultrapure water and analytical grade reagents; store all reagents at room temperature. Follow all waste disposal and animal welfare regulations.

2.1 Solutions and Small Parts

1. Cells to be studied need to be plated such that they are easily accessible on an inverted microscope (*see* **Note 2**).
2. Pipette and bath solutions for cell type and experimental conditions to be studied. For chromaffin cells and primary murine dopaminergic neurons:
   (a) Bath solution: 140 mM NaCl, 5 mM KCl, 2–5 mM $CaCl_2$, 1 mM $MgCl_2$, 10 mM HEPES/NaOH, 10 mM glucose, pH 7.3.
   (b) Pipette solution for PA: 50 mM NaCl, 100 mM TEA-Cl, 5 mM KCl, 10 mM $CaCl_2$, 1 mM $MgCl_2$, 10 mM HEPES/NaOH, pH 7.3.
   (c) Pipette solution for IP: 140 mM KGlu, 2 mM $MgCl_2$, 0.1 mM $CaCl_2$, 1 mM EGTA, 10 mM HEPES, 2 mM ATP, 0.1 mM GTP, pH 7.3.
3. Teflon-coated silver wire.
4. Borosilicate glass capillaries, outer diameter 2.0 mm, inner diameter 1.4 mm, and length 85 mm.
5. Carbon fibers (5 μm diameter).
6. Polyethylene (PE) tubing, outer diameter 0.8 mm and inner diameter 0.4 mm.
7. Patch pipette filling needle.
8. 1-ml plastic syringes and 0.22-μm syringe filters.
9. 3 M KCl.
10. 20-ml beaker with ethanol.
11. Two pairs of #5 fine forceps with tips protected by 0.5 cm of polyethylene tubing.
12. Sticky wax.
13. RG58C/U-type coaxial cables with 50 Ω impedance.

2.2 Equipment

1. Inverted microscope on a vibration-isolation table with micromanipulators and microscope-mounted video camera (*see* **Note 3**).
2. Patch clamp amplifier such as the HEKA EPC-7, EPC-10, or Axopatch 200B (*see* **Note 4**).
3. Electrochemistry amplifier with grounded headstage connector shield (*see* **Note 5**).
4. Analog-to-digital (A/D) converter (*see* **Note 6**).
5. Computer for controlling the A/D board and data recording (*see* **Note 7**).
6. Pipette puller.
7. CFE-pulling device (*see* Subheading 3.4, **step 2**).
8. Stereo microscope.
9. Patch amperometry pipette holder. Schematics and assembly instructions for a holder that fits the Axopatch 200B [20] are given below (*see* Subheading 3.5). STL files for printing the holder can be downloaded at https://github.com/DSulzerLab. We recommended using a stereolithography 3D printer such as FormLabs as it produces small electrode holder parts at sufficient accuracy and precision. *See* below for the assembly instructions.

2.3 Equipment for PA Only

10. Lock-in amplifier (SR 830; Stanford Research Instruments, Sunnyvale, CA, USA) with a 10 kΩ:100 kΩ 1:10 voltage divider at the signal input [12].
11. Computer-controlled analog signal adder. This device adds the sine wave from the lock-in to the holding potential and pulses as generated by the D/A converter. A TTL signal switches addition of the sine wave on and off (*see* **Note 4**).
12. Microforge for pipette tip conditioning (such as CPM-2; ALA Scientific Instruments Inc., Westbury, NY, USA) mounted on a suitable microscope.
13. Hot plate to melt sticky wax for pipette coating.

3 Method

3.1 Rig Setup for PA

1. Make connections on the rig as shown on Fig. 2a. Configure the data acquisition system to continuously record for at least 30 min five traces (Y1, Y2, I, V, A) at a sampling rate ≥1 kHz. The digital-to-analog (D/A) output controls the holding potential and provides pulses to monitor seal formation. A second D/A or TTL output provides a trigger signal to synchronize the oscilloscopes with the pulses. A third digital output provides a TTL signal to switch the sine wave adder.

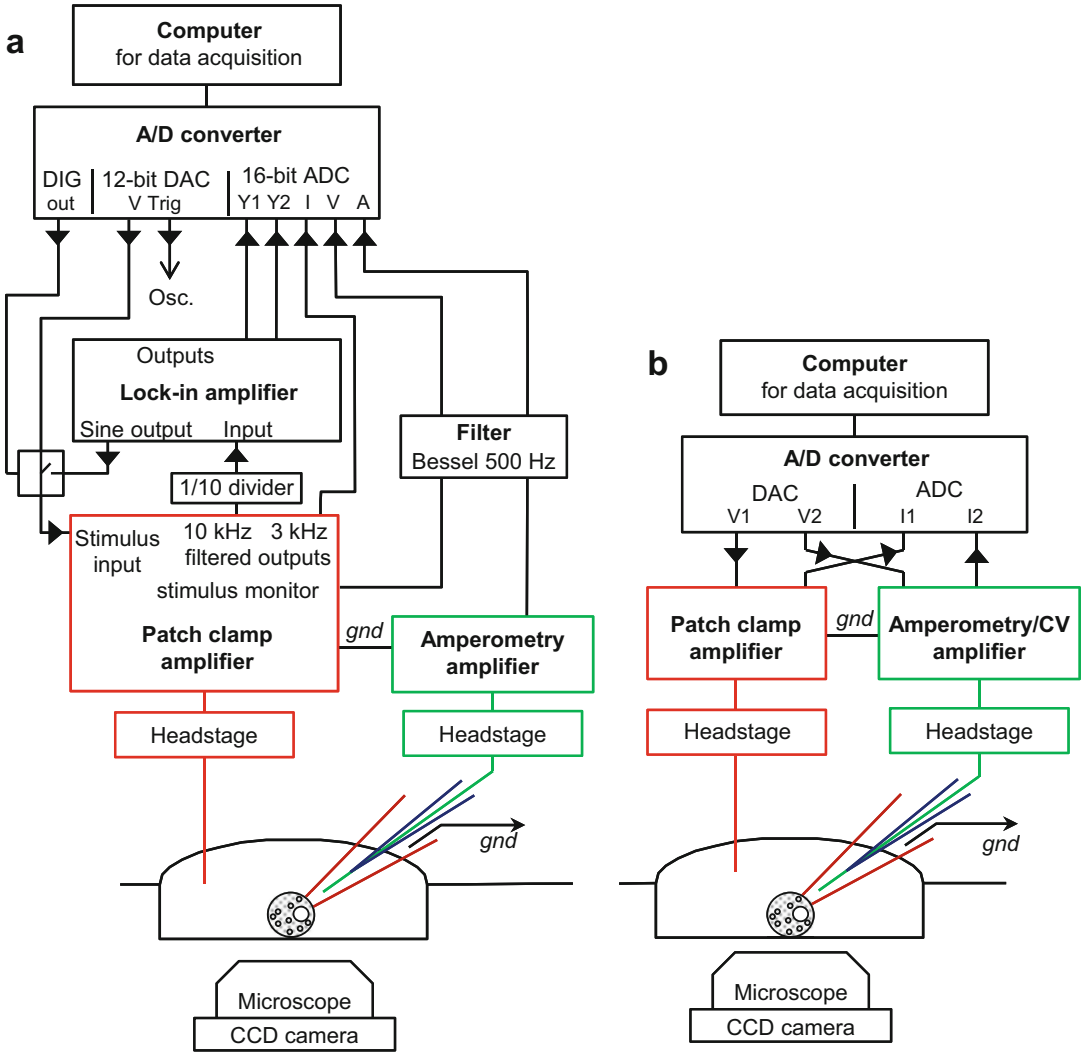

Fig. 2 Schematics for the connections between different electronic components for PA (**a**) and IPE (**b**)

2. The headstage of the amperometric amplifier is mounted on a micromanipulator to patch the cells, and the headstage of the patch clamp amplifier is mounted near the recording chamber. An Ag|AgCl wire immersed into the bath is connected to the input pin of the patch clamp amplifier headstage. Do not make any connections to the ground pin of the headstage of the patch clamp amplifier since the ground electrode will be connected to the amperometric amplifier shield.
3. Image acquisition capabilities are optional to store images of the pipette tip on the cell for later determination of the distance between the patch membrane and the tip of the CFE. An inexpensive USB or firewire camera is sufficient. Alternatively,

Table 1
SR830 lock-in amplifier settings

Time constant	1 ms, 24 dB
Signal input	Input: A, Couple: AC, Ground: FLOAT
Sensitivity	1 V
Reserve	LOW NOISE
Filters	LINE & 2×LINE
Channel 1	Output X, OFFSET Off, RATIO Off, Expand Off
Channel 2	Output Y, OFFSET Off, RATIO Off, Expand Off
Interface	RS232, 8, 9600, none
Reference	Phase +120[a], Freq 20 kHz, Ampl 0.5 V, Harm # 1, Trig SINE, Source INTERNAL

[a]The phase setting needs to be determined as described below

the distance can be measured and noted during the experiment with an eyepiece micrometer in the microscope.

4. Set the lock-in amplifier SR830 as indicated in Table 1. Set EPC-7 STIM SCALING to 0.1, which produces a 50-mV rms pipette voltage from the 0.5 V sine wave provided by the lock-in amplifier. Note that the scaling factors for the Axopatch 200B differ for the front panel and back panel switched inputs. If the front panel switched input is used, then the scaling factor is 0.02, and the lock-in output voltage must be set to 2.5 V to obtain a 50-mV rms pipette voltage signal. For the EPC-7, built-in FILTER 1 is set to 10 kHz to avoid clipping since a 20-kHz sine wave is used. The current monitor output is fed into the lock-in amplifier input via the 1:10 voltage divider because the output range of the EPC-7 is ±10 V whereas the maximum input range of the lock-in amplifier is only ±1 V. Since the whole-cell mode of the Axopatch employs a smaller feedback resistor, lower gain may be used.
5. At correct phase setting, the lock-in amplifier output Y1 is proportional to the membrane conductance and the output Y2 is proportional to the membrane capacitance [10]. The approximate phase setting for the lock-in amplifier can be found by slightly varying the C-slow compensation of the EPC-7. This may be done with open headstage. Set EPC-7 to voltage clamp mode, gain to 50 mV/pA; C-slow compensation to 10 pF range, C-slow to 0.2 pF, G-series to 0.2 μS, series resistance compensation off; filter 1–10 kHz, filter 2–3 kHz; stimulus scaling to 0.1, T_R to 2 μs. Apply sine wave to stimulus input and adjust C-fast and τ-fast to null the current. Now slightly vary C-slow, making sure the EPC-7 is not saturated (not "clipping"), and change the phase setting of the lock-in

amplifier. At the correct phase, changes in C-slow compensation appear only in the CH2 output (Y2, imaginary part of pipette current) with no change in CH1 output (Y1, real part). Note that an increase in C-slow compensation must produce a decrease in Y2 (capacitance decrease). This phase setting changes if any filters are changed or the gain is changed to the low-gain range. Always use 50 mV/pA gain for low noise recording. The procedure is analogous for the Axopach 200B in the "whole-cell $\beta = 1$ mode" choosing the corresponding settings for SERIES RESISTANCE and WHOLE-CELL CAP.

6. Using the calibrated C-slow compensation, a defined change such as 200 fF can be applied. However, this produces a large capacitive current saturating the amplifier. Thus, for calibration, the stimulus scaling must be switched from 0.1 to 0.01, giving a ten times smaller signal. This does not affect the phase setting. Now the change of the CH2 output is recorded for the 200 fF C-slow change. Since the actual recordings from cells will be done with stimulus scaling set to 0.1, this CH2 output change corresponds to a 20 fF change in a cell recording (*see* **Note 8**). In the PA_Acquire program (*see* **Note 7**), a calibration value is entered to convert the data into capacitance and conductance units.
7. The pipette current (I) is filtered with the built-in 3-kHz filter to suppress the 20 kHz sine wave and acquired by the A/D converter. An additional 500-Hz low-pass filter (optional) is recommended to filter the pipette current. The stimulus voltage (V) is filtered at 500 Hz and acquired to monitor holding potential changes. Set the voltage on the amperometric amplifier to +700 mV and gain to 10–40 mV/pA and acquire the amperometric current (A) filtered at 500 Hz.

3.2 Rig Setup for IPE

1. Make connections on the rig according to Fig. 2b. One D/A output controls the holding potential for the patch pipette and provides pulses for seal formation. Another D/A controls voltage applied to the CFE in amperometric and cyclic voltammetry (CV) modes. We used two Axopatch 200B amplifiers for the rig (*see* **Notes 9** and **10**).
2. A detailed description of CV can be found elsewhere [26]. Data acquisition and analysis for IPE in both CV and amperometric modes were performed using a subroutine locally written in Igor Pro (*see* **Note 7**).
3. Image acquisition is required for the calculation of the dilution of cytosolic transmitter inside the tip of the patch pipette. An inexpensive USB or firewire camera is sufficient.

3.3 Pipette Preparation and Assembly

1. Patch pipettes should have a tip diameter of 2–3 μm, a taper angle at the very tip of at least 20°, and a taper length of about 5 ± 0.5 mm. From 85-mm capillary, two pipettes of ~47 mm are yielded. A large opening angle is necessary to bring the tip of the CFE close to the pipette tip (*see* **Note 11**). Inspect each pipette after pulling for proper geometry.
2. *For PA only*: It is essential to coat pipettes with wax or Sylgard as previously described to reduce and stabilize pipette capacitance [27]. The coating must cover a sufficient part of the tip such that it protrudes well beyond the bath surface to minimize stray capacitance and bath-pipette capacitance fluctuations. Dipping the pipette tip in melted wax to reduce stray capacitance is the quicker method [13]. Right before use, fire polish pipettes with a microforge: Approach a heated wire with the pipettes tip such that the wax flows out and the tip narrows slightly.

3.4 Carbon Fiber Electrode (CFE) Fabrication

1. Cut an ~12-cm-long piece of polyethylene (PE) tubing, and immerse one end in a beaker with ethanol such that the entire tube fills by capillary action. Take a carbon fiber of at least 5 cm length with the PE tube-protected tweezers, and insert it into the PE tubing. Wick away ethanol by tapping tube on filter paper. Evaporate remaining ethanol at 50 °C for 30 min (*see* **Note 12**).
2. Bend a Pt/Ir wire of ~5 cm length and a diameter of 0.4 mm into a loop of ~6 mm diameter. Connect wire via a foot switch to a variable power supply (12 V, >3 A). Place loop vertically under a dissection microscope. Adjust the heat of the wire loop by holding a piece of PE tubing in the center of the wire loop (wire resistance of about 1 ohm, current about 2 A). After the heat is switched on, it should soften within 10–15 s and melt within 20–25 s.
3. With the loop placed horizontally, hold a carbon fiber-filled tube with both hands in the center of the heated wire loop, melt PE, and pull very gently. Pull on one side (about 1 cm) and push on the other side about half as much. This creates a tapered electrode that will fit easily in the patch pipette. Let PE melt around carbon fiber as a thin layer (*see* **Note 13**). Do not let both parts separate yet. Take a fresh scalpel blade and separate both parts on a clean glass surface.
4. Approach heated wire with carbon fiber tip such that the thin layer of PE melts back and forms a small bead. In a quick movement, switch off heat of wire, touch wire with the small PE bead, and pull CFE away from wire quickly. This forms an insulating layer of PE about 0.1 μm thickness around the carbon fiber (Fig. 3). A description on how to set up a

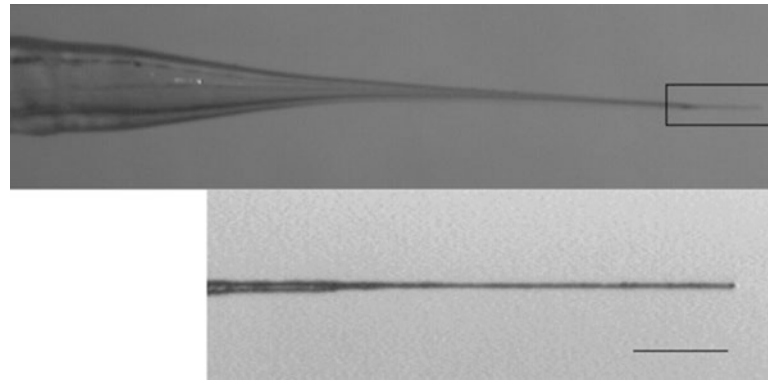

Fig. 3 Example of a carbon fiber electrode prepared by asymmetrical pulling. Lower image is a magnification of the box on the upper image. Note that the PE tubing tappers smoothly onto the CF and its tip lacks any beads of melted PE. Such a CFE can be easily inserted into the glass patch pipette and its tip can be moved very close to the pipette tip. Scale bar is 100 μm

programmable CFE puller is available as Supplementary Note 1 at https://www.nature.com/articles/nmeth0905-699.

5. Before use, recut tip to expose a freshly cut surface. Backfill CFE with 3 M KCl with a syringe via a pipette-filling needle. Cut CFE to a total length of ~90 mm.
6. Test CFE in amperometric and CV modes before electrode assembly.
   (a) In amperometric mode: Directly after applying the +700 mV, potentially, the amperometric current should decrease slowly, reaching a level that represents a CFE resistance of 35–140 GΩ within 1–2 min (20–5 pA at +700 mV stimulation voltage). The noise of the amperometric current should be below 1 pA rms.
   (b) In CV mode (*for IPE only*): Applying CV voltage ramps to the CFE produces large capacitive current the amplitude of which should stabilize within 10–20 min. Add 1 μM of dopamine to the bath solution, and you should see a clear increase of the current that corresponds to DA oxidation potential (typically 350–400 mV). At the same time, the difference voltammogram should show the typical DA oxidation profile [26].

3.5 Electrode and Holder Assembly

1. The close distance between the CFE and the patch membrane is important to reduce diffusional broadening of the amperometric spikes [8] and diffusional low-pass filtering of amperometric current fluctuations associated with fluctuations of fusion pore conductance. To achieve this, pipette holders were developed that contain the CFE in fixed position while

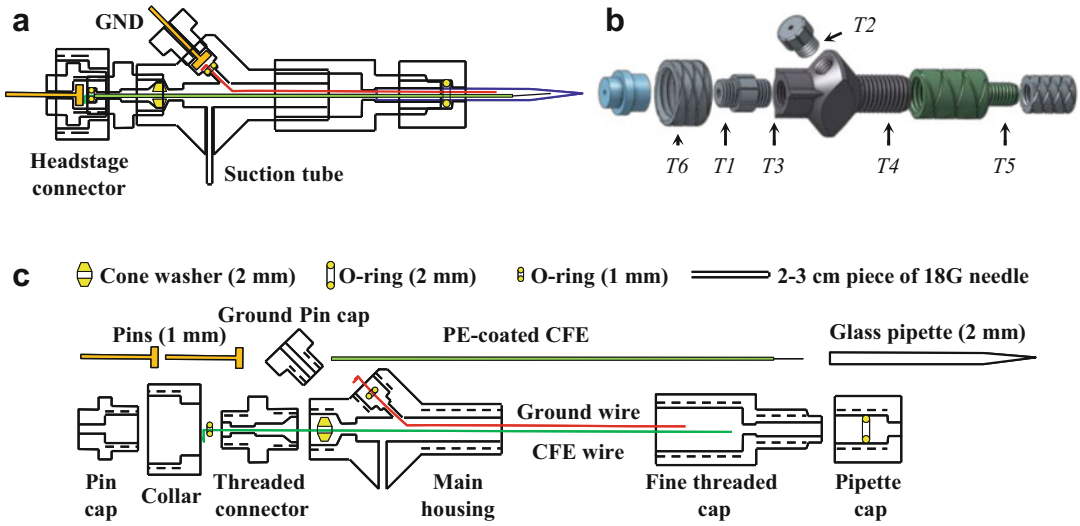

Fig. 4 PA/IPE Electrode holder design and assembly. Schematic of the assembled electrode holder (**a**), 3D model of its parts (**b**) and individual parts of the holder (**c**). Connecting threads (*T1–6*) are shown on **b**

the part that holds the pipette is connected to the part holding the CFE with an adjustable thread. With this design, the distance between pipette tip and CFE tip can be varied before the cell is actually patched. For the positioning, a compromise needs to be made such that the CFE tip is close enough to detect catecholamines released through the fusion pore with minimal diffusion time but far enough not to interfere with the seal formation.

2. An electrode holder design and assembly for the Axopatch 200B are shown in Fig. 4. There are two silver wires. The CFE wire is connected to the center pin of the BNC plug of the holder and will go inside the CFE tubing. The ground wire is connected to the side pin and will be inside the patch pipette but outside the CFE tubing. Make sure to clean off Teflon coating from silver wire ends.
3. Cut the ground wire to be shorter than the CFE wire so that the two will be distinguishable when the holder is assembled. Chlorinate both wires after cutting.
4. After assembly, only tighten threads *T1* and *T2* (Fig. 4b). Turn the fine threaded cap (*T4*) until about one-half to two-thirds of the thread is exposed. Housing and cap should not move or tilt significantly against each other; if this happens, apply vacuum grease to the thread.
5. Make sure thread *T3* is not tightened and slide the 3 M KCl-filled CFE all the way onto the longer silver wire, making sure the latter touches the KCl inside the PE tubing but is not

pushed all the way to the tip of it. After tightening *T3*, the CFE should be fixed inside the holder.

6. Make sure thread *T5* is not tightened and carefully insert the CFE tip into a glass pipette filled with pipette solution, preferably under a dissection microscope or a magnifying glass. Take care that the CFE does neither bend backward nor break nor poke through the pipette tip. Unscrew *T4* if CFE is too long and does not fit inside the pipette—if necessary, remove the CFE from the holder by loosening *T3*, cut it from the back, and start over from **step 4**.
7. Once the glass pipette is in place and the CFE is visible inside, tighten *T5*.
8. Under a stereomicroscope, turn the fine threaded cap (*T4*) to bring the tip of the CFE close to the tip of the pipette. Be careful not to push through the pipette tip with the fiber as this will not only destroy the pipette but also scrape off the PE insulation from the CFE. Don't try to push the CFE too far as it's optimal position will be determined later.
9. Attach the electrode holder to the headstage with *T6* on the collar. Use a crocodile clip to connect the ground pin of the holder to headstage's ground.
10. Add about 100 μl of bath solution and immerse the tip of the patch clamp electrode in the bath.
11. If the CFE is too close to the tip of the pipette, it's PE coating will start blocking the tip also acting as a resistor that will interfere with catecholamine detection and capacitance measurements. This can be monitored as a change in the height and the shape of the square test pulses applied to the patch clamp amplifier or CV current applied to the electrochemistry amplifier. Start test pulses and/or CV pulses, and carefully turn *T4* of the holder to approach the pipette tip with the CFE tip until they are 5–10 μm apart (1–2 times the CFE diameter). Again, be careful not to poke the CFE through the pipette tip as this might scratch off the thin insulation layer on the CFE. Continue moving the CFE closer, noting the change in the pulse current or CV current. If current transients decrease or changes shape, stop and unscrew *T4* (thus moving CFE away from the tip of the patch pipette) till currents are undistorted and look the same as before (*see* **Note 14**).
12. At final CFE position, acquire two images for further measurement of catecholamine diffusional distance (Y). Take one image focusing on the tip of the patch pipette and another one focusing on the tip of the CFE. Superimpose the two images and measure the distance h' of the vertical projection of h. As the holder is typically at 45° to the plane of the dish, h can be approximated as $1.41 \times h'$ (*see* Fig. 6).

3.6 Patching and Recording Exocytotic Events with PA

1. For general patch clamp instructions, follow the excellent description provided by Penner [28]. Use low patch clamp amplifier gain and give test pulses. Put slight positive pressure on the pipette and approach a cell using the micromanipulators. Upon touching a cell, the pipette resistance will slightly increase. Release positive pressure and apply suction until pipette resistance reaches several GΩ.
2. Increase gain of the EPC-7 to 50 mV/pA and set stimulus scaling to 0.1. Adjust C-fast and τ-fast compensation. Switch off test pulses, switch on sine wave, and start data acquisition. Readjust C-fast and τ-fast to compensate remaining capacitive currents until the sine wave current has minimal amplitude on the oscilloscope. Give some capacitance calibration pulses (if necessary, at reduced stimulus scaling; *see* Subheading 3.1, **step 5**). Try to complete these adjustments within a few seconds after achieving a gigaseal as cells release most releasable vesicles at the beginning of the recording due to mechanical stimulus of patching.
3. Exocytotic events can be identified by the synchronous appearance of an amperometric spike and a step in the Y2 trace proportional to membrane area increment, possibly associated with a transient increase in Y1 indicating a narrow fusion pore (Fig. 5a). Amperometric spikes without a change in Y2 trace indicate a transient breakage of the cell during sealing and freely floating vesicles outside the cell or clipping of the patch clamp amplifier. Observe the sine wave amplitude of the patch clamp current monitor during the experiment. Make sure it does not exceed ±10 V even if the clipping indicator might not be on. Readjust C-fast and τ-fast compensation to decrease the current amplitude. Steps in Y2 and a transient in Y1 without amperometric spike might indicate that the CFE is too far from the patch, the CFE is broken, or the vesicle was empty [29]. If capacitance steps are not confined to the Y2 trace but have a projection in Y1, either the EPC-7 is clipping (check!) or the phase of the patch is different from the preset phase. This may be corrected off-line (while clipping cannot be corrected for). To test the phase setting, gentle suction pulses may be applied that produce capacitance changes. They will likely have the same projection in Y1 as the capacitance steps from exocytotic events.
4. The end of an experiment is marked by either losing the seal or by the cell going to the whole-cell configuration. In the latter case, the cytosolic catecholamines diffuse out of the cell and cause a rather slow but fairly big wave in the oxidation current [20] (you are doing IPE now!).

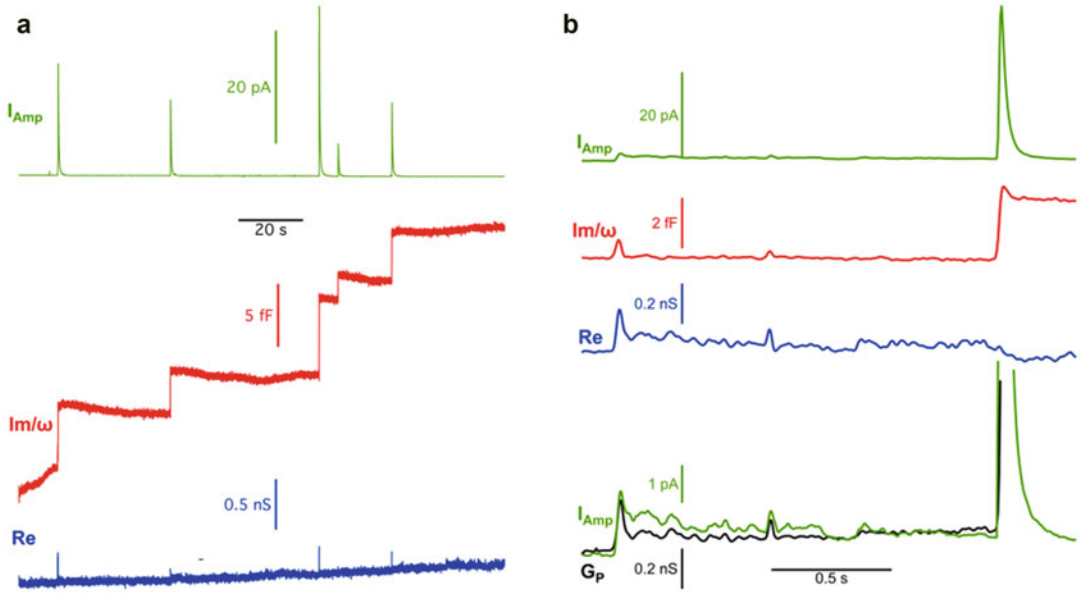

Fig. 5 Examples of PA recordings. (**a**) Exocytotic events can be identified by the synchronous appearance of an amperometric spike (green trace), and a step in the Im (Y2, red trace) proportional to membrane area of fused vesicles. A transient increase in Re (Y1, blue trace) associated with a capacitance step indicates formation and expansion of a narrow fusion pore. (Data from [18]) (**b**) Exocytotic event with exceptionally long foot signal. From top to bottom: Amperometric current (I_{Amp}, green trace), ΔCm (Im/ω, red trace), Re (blue trace), and fusion pore conductance G_P (black trace) with superimposed foot current on expanded scale (I_{Amp}, green trace). Note synchronous fluctuations in I_{Amp} and G_P. (Data from [5])

5. Event analysis addresses quantal analysis, vesicular concentrations, considerations for patch capacitance measurements, and fusion pore analysis [11, 12, 15, 16, 18, 19, 29, 30] as well amperometric spike analysis [8, 17, 31–35] and relationship between cell electrical activity and fusion. A detailed description of fusion pore analysis for cell-attached capacitance measurements and consideration for choosing the optimal sine wave frequency depending on vesicle size to be studied has been provided elsewhere [12].
6. Vesicle capacitance (C_V) and fusion pore conductance (G_P) can be calculated from the real and imaginary components of the lock-in amplifier current as shown in Fig. 1c (*see* **Note 15**). An Igor Pro experiment to view the recordings and to perform analysis can be downloaded as Supplementary Software from https://www.nature.com/articles/nmeth0905-699.

3.7 Measuring Cytosolic Catecholamines with IPE

1. Acquire images of the pipette (*see* Subheading 3.5, **step 11**) and the cell body. Make sure to record image scaling. These will be used during analysis to estimate dilution of cytosolic catecholamines inside the tip of the patch pipette.

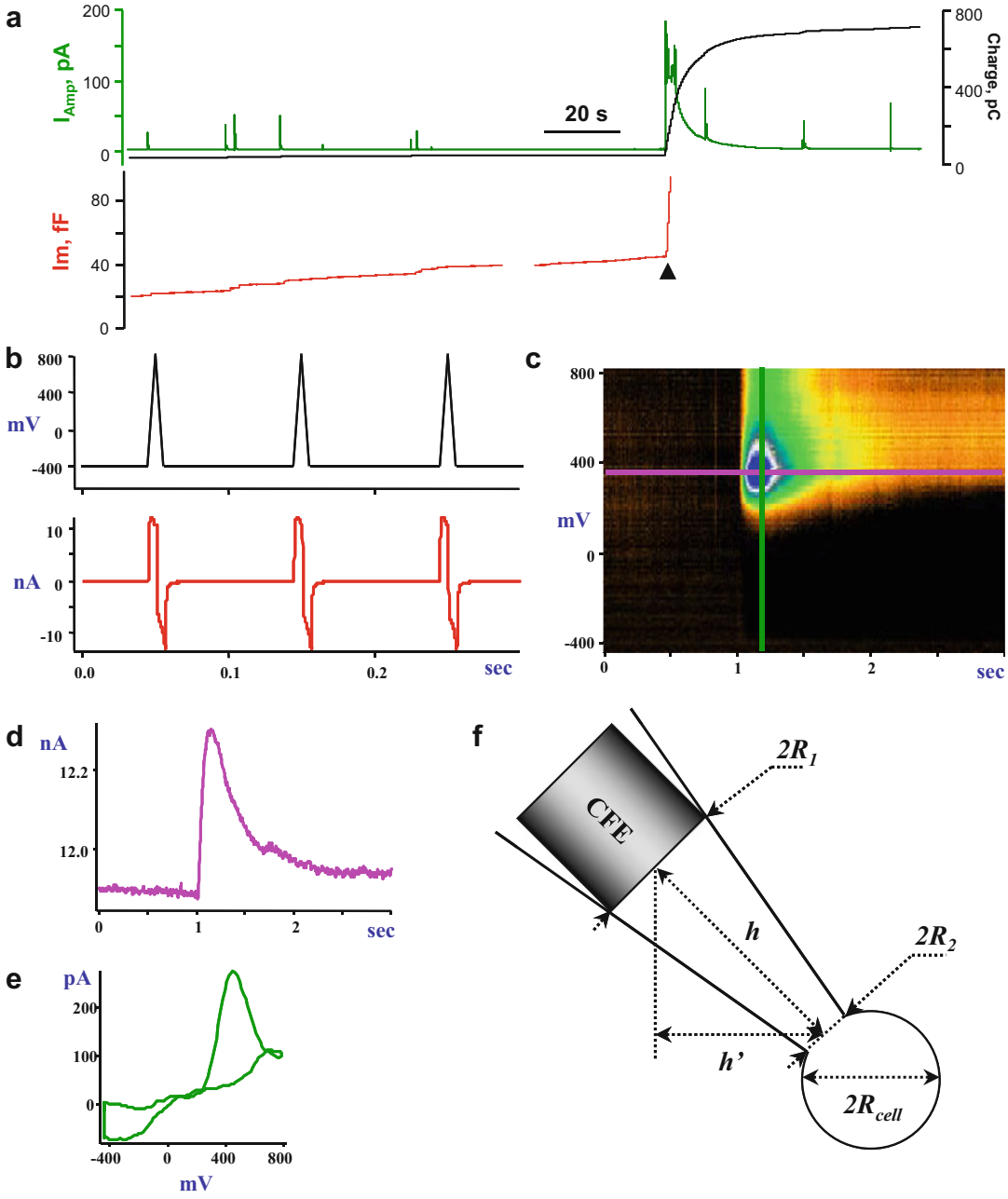

Fig. 6 Example of IPE recordings. (**a**) Example of IPE recording in an amperometric mode. Cell membrane rupture characterized by a large increase in membrane capacitance (arrowhead) is followed by a slow wave of amperometric current that represents oxidation of cytosolic metabolites. In the case of chromaffin cells and primary mouse neurons, IPE in amperometric mode detects the sum of catecholamines and their metabolites. Notice that vesicle fusion events can be observed both before and after attaining the whole-cell mode. (**b**) In the CV mode, triangular voltage ramps at of 250 mV/ms are applied at 100 ms intervals (top), producing capacitive and Faradic currents (bottom). (**c**) Faradic component of the CV current presented as a preudo-3D plot where the intensity of color indicates oxidative current at a given voltage and time. Horizontal cross-section of the plot at a fixed voltage (pink) produces the time course of catecholamine diffusion into the tip of the pipette (**d**), whereas vertical cross-section at fixed time (green) gives a voltammogram of catecholamines (**e**).

2. After attaining high-resistance seal (*see* Subheading 3.6, **step 1**), apply sharp suction to the patch pipette. When the plasma membrane is ruptured, substances diffusing from the cytosol into the patch pipette are observed as a slow wave of oxidation current. In amperometric mode, IPE detects total catechols (a sum of catecholamines and their metabolites), whereas in cyclic voltammetric mode, it preferentially measures catecholamines [20].
3. In the amperometric mode, the CFE potential is held at +700 mV. After baseline subtraction, the total area, the charge (Q), of the oxidation current wave is used to estimate cytosolic catechol concentration as $C = Q/(n \times F \times V)$, where $n = 2$ is the number of electrons transferred from one molecule to the CFE, $F = 96{,}485$ C/mol is Faraday's constant, and V_{cell} is the cytosolic volume (Fig. 6).
4. In CV mode, triangular voltage ramps from a holding −450 mV potential to +800 mV and then back to −450 mV over 10 ms (scan rate, 250 mV/ms) are applied at 100 ms intervals (Fig. 6). During the ramps, catecholamines produce a unique oxidation–reduction profile (voltammogram) allowing to differentiate them from other oxidizable cytosolic metabolites.
5. Start CV pulses with patch pipette submerged in the bath saline. Let pulses run till the amplitude of CV current transients (and current sampled at the oxidation potential for catecholamines; 300–450 mV) is stable.
6. After recording the wave of cytosolic transmitter entering the patch pipette, measure catecholamine-specific oxidation at the maximum of the current wave using subtraction voltammogram.
7. The height of the catecholamine oxidation peak can then be converted to catecholamine concentration using calibration curves. After accounting for differences in the active CFE area and the dilution of catecholamines inside the patch pipette (Fig. 6e), concentration in the cytosol can be calculated (*see* **Note 16**). This is described in detail in [20] and is incorporated into Igor Pro routine for the analysis of IPE data (*see* **Note 7**).

Fig. 6 (continued) (**f**) Dilution of cytosolic catecholamines at the tip of the patch pipette is calculated as $(V_{cell} + V_{PP})/V_{cell}$. Cell volume $V_{cell} = S \times 4/3 \times \pi \times (R_{cell})^3$, where S is 0.5, 0.75, or 1 depending on the shape of the cell under the microscope. Pipette volume $V_{PP} = \pi \times h/3 \times ({R_1}^2 + {R_2}^2 + R_1 \times R_2)$, where $h = \sqrt{2} \times h'$. (Adopted from [20])

4 Notes

1. Analysis of the rapidly charging transients to determine the initial fusion pore conductance has so far not been possible in cell attached mode because for a vesicle capacitance $C_V = 2$ fF, even for an extremely small fusion pore with a conductance G_P as low as 10 pS, the time constant to charge the vesicle $\tau = C_V/G_P$ would be as short as 200 μs. The total charge to change the vesicle membrane potential by 100 mV is 0.2 fC or about 1250 elementary charges. While this charge may in principle be detectable, so far it has not been possible to resolve the time course of such small transients in a cell-attached recording, which would be required to obtain a fusion pore conductance estimate.
2. Since the electrode configuration is reversed (the sine wave voltage is applied to the bath electrode), the stray capacitance between the bath solution and the microscope needs to be minimized to compensate most of it and to reduce noise. We use custom-made dishes in which a 10-mm hole is punched at the center of the tissue culture dishes and a 12-mm coverslip is glued underneath with Sylgard®. After poly-D-lysine and laminin coating, any type of cells can be plated. For the experiment, fill solution only into the inner well (typically <100 μL). Do not spill solution onto the surrounding plastic since overflowing and evaporation of solution give rise to cycles of large stray capacitance, making PA recordings extremely difficult.
3. It is important to use an objective with long working distance to minimize stray capacitance. We use a Zeiss 20×/0.5 or 40×/0.75 Plan-Neofluar objectives. An immersion objective on an upright microscope would produce a very high stray capacitance that cannot be compensated.
4. For PA, the headstage to which the pipette holder is connected must provide ground potential to the pipette holder shield. This is important to consider because some patch clamp amplifier headstages normally drive the headstage housing and pipette holder shield with the pipette potential to reduce stray capacitance. In this case, a modified headstage must be used where the housing is grounded. We obtained best results with the EPC-7. Similarly, the Axopatch 200B can be used in "whole-cell $\beta = 1$" mode for both PA and IPE. As the Axopatch 200B has two command signal inputs that are added internally—one being controlled by a front panel switch—the signal adder is not necessary although the sine wave must then be switched on and off manually.
5. Axopatch 200B can be used as the electrochemistry amplifier for both PA and IPE. Additionally, a modified version of VA10

(NPI Electronic) with grounded headstage shield can be employed. The HEKA EPC-10 is a dual amplifier that may be very practical. However, for the PA, a modified EPC-10 headstage must be used due to the fact that probe housing in the standard EPC-10 configuration is connected to "Vref." This standard headstage thus cannot be used since the reference electrode in the holder is connected to the shield. A modified headstage is available from HEKA where the housing and BNC connector shield are changed to "GND."

6. For PA, an A/D board with at least five channels and a sampling rate >1 kHz is required; for IPE, only two channels are needed. We used National Instruments PCI-MIO-16XE-10 board for PA and InstruTECH ITC-18 board for IPE.
7. For IPE data acquisition and analysis, we use home-written macros in Igor Pro (WaveMetrics) available for download at https://github.com/DSulzerLab. Igor Pro macros for PA acquisition and analysis are available from https://www.nature.com/articles/nmeth0905-699.
8. For convenience, we modified the patch clamp amplifier by inserting a switchable 20 Ω resistor in series with the C-slow potentiometer of the EPC-7. This capacitance dither applies capacitance compensation changes of 20 fF for calibration. In the Axopatch 200B, the built-in 100 fF capacitance dither may be used, but make sure to avoid saturation of the amplifier. It is possible to change the dithering circuit to provide a 10- or 20-fF signal following guidelines available upon request from Axon Instruments.
9. During CV, voltages up to 1 V are applied to the CFE. As Axopatch 200B amplifier has a 1/10 divider on its command input, a D/A converter capable of generating an output voltage up to 10 V is required. We used an ITC-18 D/A for this purpose, but there might be other options that we did not test.
10. Patch pipette command voltage is only needed for the control of seal formation between the plasma membrane and the glass pipette. We therefore do not routinely record the current output from the patch pipette amplifier and are using amplier's own controls to transition from cell-attached to whole-cell configurations.
11. Although puller settings need to be found experimentally, the following might serve as a guideline: The Sutter puller P-97 is set up with a box filament of 3 × 3 × 3 mm. *Air pressure* was set to 500, and the *air before pull* and the *air after pull* were 5 s each. The *ramp test* for the capillaries was 655. A single-line program looped four times and had the parameters *heat* 615, *pull* 0, *velocity* 50, and *time* 200. For larger taper angles, the velocity might be reduced slightly without increasing the

tip diameter substantially. Pipette resistance in the bath should be 1–3 MΩ.

12. An alternative method is to use vacuum to suck the CF inside the PE tubing. On a piece of white paper, separate exactly one CF fiber (>10 cm) from a fiber bundle (this can be done under a dissection microscope). Holding it with a finger on one side, approach the other side with a 12- to 15-cm piece of PE tubing connected to a vacuum line. Once the CF is sucked inside the tubing, disconnect from vacuum, and then carefully let go of the finger. Cut excess CF from both sides.
13. Pulling of PE tubing requires some practice. Pull just PE tubing without carbon fibers first until desired shape and taper are achieved. When pulling with a carbon fiber, make sure that PE melts around the fiber and does not just form a very thin tube.
14. A longer distance will broaden and flatten amperometric signals due to diffusion. It is difficult to record good amperometric signals at distances >30 μm. At too short a distance, besides possible interference with electrophysiological and electrochemical measurements, the CFE might interfere with seal formation as the patch of the cell is sucked into the pipette.
15. When a fusion pore is formed and if this is the only change during the respective time interval, C_V and G_P can be calculated for the time course of Im and Re using the equations of Fig. 1c$_1$. It is, however, possible that during the time interval of interest, ion channels open or close or the seal resistance fluctuates. These phenomena produce additional changes in the Re trace such that the equations of Fig. 1c$_1$ will not provide accurate results. In this case, the equations of Fig. 1c$_2$ may be used calculating G_P from Im and the final capacitance step size. With this method, the predicted and measured time courses should be compared to determine if the recording is consistent with the properties expected of a fusion pore opening.
16. As IPE in CV mode detects catecholamine concentration at the tip of the CFE, which is a few micrometers away from the cell, it is necessary to account for the dilution of molecules inside the patch pipette. A simple "geometric" approach can be used where cellular volume and the volume of the patch pipette are estimated from photographs taken before each recording, and the concentration of catecholamines at the CFE is multiplied by the calculated dilution factor (Fig. 6f). However, this method underestimates the true cytosolic catecholamine concentrations for two reasons: (1) There is a loss of molecules from the diffusion of catecholamines around the CFE into the shaft of the pipette, and (2) the actual free volume of the cytosol is smaller than the total cell volume as a portion of

the cytosol is occupied by vesicles and other organelles. Therefore, as an alternative approach, we used a random walk simulation [36] to fit experimentally recorded sampled current traces and calculate the initial concentration of catecholamines inside the cell. Based on the comparison of the two approaches, a simpler geometric method was employed and then multiplied by the factor of *1.65* for a more accurate representation of cytosolic transmitter concentration.

Acknowledgments

The preparation of this chapter was supported by NIH grant R35GM139608 to M.L. and a JPB grant (PI: D. Sulzer) for E.V.M.

References

1. Fernandez JM, Neher E, Gomperts BD (1984) Capacitance measurements reveal stepwise fusion events in degranulating mast cells. Nature 312:453–455
2. Sharma S, Lindau M (2018) The fusion pore, 60 years after the first cartoon. FEBS Lett 592: 3542–3562
3. Breckenridge LJ, Almers W (1987) Currents through the fusion pore that forms during exocytosis of a secretory vesicle. Nature 328:814–817
4. Spruce AE, Breckenridge LJ, Lee AK, Almers W (1990) Properties of the fusion pore that forms during exocytosis of a mast cell secretory vesicle. Neuron 4:643–654
5. Hartmann J, Lindau M (1995) A novel Ca (2+)-dependent step in exocytosis subsequent to vesicle fusion. FEBS Lett 363:217–220
6. Lindau M (1991) Time-resolved capacitance measurements: monitoring exocytosis in single cells. Q Rev Biophys 24:75–101
7. Wightman RM et al (1991) Temporally resolved catecholamine spikes correspond to single vesicle release from individual chromaffin cells. Proc Natl Acad Sci U S A 88:10754–10758
8. Schroeder TJ, Jankowski JA, Kawagoe KT, Wightman RM, Lefrou C, Amatore C (1992) Analysis of diffusional broadening of vesicular packets of catecholamines released from biological cells during exocytosis. Anal Chem 64:3077–3083
9. Alvarez de Toledo G, Fernández-Chacón R, Fernandez JM (1993) Release of secretory products during transient vesicle fusion. Nature 363:554–558
10. Neher E, Marty A (1982) Discrete changes of cell membrane capacitance observed under conditions of enhanced secretion in bovine adrenal chromaffin cells. Proc Natl Acad Sci U S A 79:6712–6716
11. Lollike K, Borregaard N, Lindau M (1995) The exocytotic fusion pore of small granules has a conductance similar to an ion channel. J Cell Biol 129:99–104
12. Debus K, Lindau M (2000) Resolution of patch capacitance recordings and of fusion pore conductances in small vesicles. Biophys J 78:2983–2997
13. Dernick G, de Toledo GA, Lindau M (2007) The patch amperometry technique: design of a method to study exocytosis of single vesicles. In: Michael AC, Borland LM (eds) Electrochemical methods for neuroscience. CRC Press, Boca Raton (FL), pp 315–336
14. Dernick G, Gong LW, Tabares L, Alvarez de Toledo G, Lindau M (2005) Patch amperometry: high-resolution measurements of single-vesicle fusion and release. Nat Methods 2: 699–708
15. Albillos A, Dernick G, Horstmann H, Almers W, Alvarez de Toledo G, Lindau M (1997) The exocytotic event in chromaffin cells revealed by patch amperometry. Nature 389:509–512
16. Gong LW, Alvarez De Toledo G, Lindau M (2003) Secretory vesicles membrane area is regulated in tandem with quantal size in chromaffin cells. J Neurosci 23:7917–7921
17. Chow RH, Rüden L, Neher E (1992) Delay in vesicle fusion revealed by electrochemical monitoring of single secretory events in adrenal chromaffin cells. Nature 356:60–63

18. Gong LW, de Toledo GA, Lindau M (2007) Exocytotic catecholamine release is not associated with cation flux through channels in the vesicle membrane but Na^+ influx through the fusion pore. Nat Cell Biol 9:915–922
19. Dernick G, Alvarez de Toledo G, Lindau M (2003) Exocytosis of single chromaffin granules in cell-free inside-out membrane patches. Nat Cell Biol 5:358–362
20. Mosharov EV, Gong LW, Khanna B, Sulzer D, Lindau M (2003) Intracellular patch electrochemistry: regulation of cytosolic catecholamines in chromaffin cells. J Neurosci 23: 5835–5845
21. Mosharov EV et al (2006) Alpha-synuclein overexpression increases cytosolic catecholamine concentration. J Neurosci 26:9304–9311
22. Mosharov EV et al (2009) Interplay between cytosolic dopamine, calcium, and alpha-synuclein causes selective death of substantia nigra neurons. Neuron 62:218–229
23. Choi SJ, Panhelainen A, Schmitz Y, Larsen KE, Kanter E, Wu M, Sulzer D, Mosharov EV (2015) Changes in neuronal dopamine homeostasis following 1-methyl-4-phenylpyridinium (MPP+) exposure. J Biol Chem 290: 6799–6809
24. Lieberman OJ et al (2017) alpha-synuclein-dependent calcium entry underlies differential sensitivity of cultured SN and VTA dopaminergic neurons to a parkinsonian neurotoxin. eNeuro 4:ENEURO.0167-17.2017. https://doi.org/10.1523/ENEURO.0167-17.2017
25. Michael DJ, Joseph JD, Kilpatrick MR, Travis ER, Wightman RM (1999) Improving data acquisition for fast-scan cyclic voltammetry. Anal Chem 71:3941–3947
26. Bucher ES, Wightman RM (2015) Electrochemical analysis of neurotransmitters. Annu Rev Anal Chem (Palo Alto Calif) 8:239–261
27. Hamill OP, Marty A, Neher E, Sakmann B, Sigworth FJ (1981) Improved patch-clamp technique for high-resolution current recording from cells and cell-free membrane patches. Pfluegers Arch/Eur J Physiol 391: 85–100
28. Penner R (1995) A practical guide to patch clamping. In: Sakmann B, Neher E (eds) Single channel recording. Plenum Press, New York, pp 3–30
29. Tabares L, Ales E, Lindau M, Alvarez De Toledo G (2001) Exocytosis of catecholamine-containing and catecholamine-free granules in chromaffin cells. J Biol Chem 276:39974–39979
30. Alés E, Tabares L, Poyato JM, Valero V, Lindau M, Alvarez de Toledo G (1999) High calcium concentrations shift the mode of exocytosis to the kiss-and-run mechanism. Nat Cell Biol 1:40–44
31. Jankowski JA, Schroeder TJ, Ciolkowski EL, Wightman RM (1993) Temporal characteristics of quantal secretion of catecholamines from adrenal medullary cells. JBC 268: 14694–14700
32. Jankowski JA, Finnegan JM, Wightman RM (1994) Extracellular ionic composition alters kinetics of vesicular release of catecholamines and quantal size during exocytosis at adrenal medullary cells. J Neurochem 63:1739–1747
33. Wightman RM, Schroeder TJ, Finnegan JM, Ciolkowski EL, Pihel K (1995) Time course of release of catecholamines from individual vesicles during exocytosis at adrenal medullary cells. Biophys J 68:383–390
34. Schroeder TJ, Borges R, Finnegan JM, Pihel K, Amatore C, Wightman RM (1996) Temporally resolved, independent stages of individual exocytotic secretion events. Biophys J 70:1061–1068
35. Segura F, Brioso MA, Gomez JF, Machado JD, Borges R (2000) Automatic analysis for amperometrical recordings of exocytosis. J Neurosci Methods 103:151–156
36. Sulzer D, Pothos EN (2000) Regulation of quantal size by presynaptic mechanisms. Rev Neurosci 11:159–212

Chapter 18

Artificial Cells for Dissecting Exocytosis

Yuanmo Wang and Ann-Sofie Cans

Abstract

The fusion of vesicles and exocytosis release of neurotransmitters into the extracellular space for detection and chemical signal decoding by neighboring cells is the key process in neuronal communication. It is important to understand what regulates exocytosis because the amount of neurotransmitters released into the synaptic cleft has a direct impact on brain function such as cognition learning and memory as well as on brain malfunctions. Much success in molecular biology can be credited for the existence of simplified model systems. Therefore, for gaining deeper insights into the details of exocytosis and what controls vesicle-mediated neurotransmission, functional artificial cells for exocytosis have been developed that can be used for studying various biophysical aspects and roles of molecules affecting exocytosis, which is difficult to study in living cells. Here, we describe the design and fabrication of specific artificial cell models and how chemical measurements at these cells can be implemented for probing dynamics of the exocytosis fusion pore and its effect on the regulation of neurochemical release. We introduce bottom-up synthetic methods for constructing model cells using protein-free giant unilamellar vesicles (GUV) as starting material, which allows further tuning of molecular complexity in a manner that is not possible in living cells and therefore can be used for dissecting the role of essential molecular components affecting the exocytosis process. The experimental setup uses microscopy video recording, micromanipulation and microelectroinjection techniques, and amperometry detection to study neurotransmitter release from these cells mimicking exocytosis.

Key words Fusion pore, Exocytosis, Vesicle, Secretion, Neurotransmitters, Artificial cell, Cell model, Giant unilamellar vesicles, Amperometry, Micromanipulation, Electroinjection, DNA-zipper

1 Introduction

Exocytosis is a cellular process that involves complex interactions of lipids and proteins such as the soluble N-ethylmaleimide-sensitive factor attachment protein receptor (SNARE) proteins and Ca^{2+} ions for fusing neurotransmitter-filled vesicles docked at the cell plasma membrane. Upon vesicle fusion, formation of a fusion pore allows neurotransmitters stored inside the vesicle to sieve through its opening and escape into the extracellular space where these molecules can transmit chemical signals to nearby target cells. What controls fusion pore dynamics determines the mode of

Ricardo Borges (ed.), *Chromaffin Cells: Methods and Protocols*,
Methods in Molecular Biology, vol. 2565, https://doi.org/10.1007/978-1-0716-2671-9_18,

exocytosis, and the amount of neurotransmitter released into synapses, which directly affects signaling strength. If the fusion pore expands its size and leads to that the vesicle membrane to fully collapse into the cell plasma membrane, the entire vesicular content will be expelled into the synaptic cleft and is referred to as "full exocytosis." However, if the fusion pore only remains open for a short period of time and then closes again, only a fraction of the vesicular contents will be released and refers to an exocytosis mode called "kiss-and-run," where the vesicle compartments are recaptured and reused for new rounds of exocytosis. Many studies on what controls different modes of exocytosis to be triggered have focused on the mechanisms for vesicle fusion and fusion pore dynamics. A great deal of knowledge has been gained by simplified lipid-based cell model systems, with or without proteins, that can mimic various stages of exocytosis. The cell models in comparison to live cell can easily be controlled in terms of the components and, for instance, allows membranes augmentation by various type of lipids and proteins and vesicle-encapsulating solutions [1–3].

Here, we introduce a bottom-up synthetic approach to create two types of simplified cell models for exocytosis that be used for studying the biophysics and molecular mechanisms affecting the dynamics of the exocytosis fusion pore and thereby mechanisms that affect the mode of exocytosis triggered [4–9]. The cell models presented are based on surface-immobilized GUVs that are connected to a multilamellar vesicle (MLV) protrusion, which makes these systems easy to manipulate by electroporation and microinjection techniques [10]. The GUV-MLVs are easy to synthesize using a modified method for dehydration–rehydration of small unilamellar vesicles (SUV), initially developed by Criado and Keller [11], and with the SUVs created from a soybean polar lipid extract (SPE) that contains a mixture of different phospholipids: 45.7% phosphatidylcholine, 22.1% phosphatidylethanolamine, 18.4% phosphatidylinositol, 6.9% phosphatidic acid, and 6.9% other mixed lipids. These GUV-MLV lipid-based systems that have previously been used for creating various vesicle nanotube networks can easily be tuned in terms of the molecular complexity of membranes and interior encapsulating solution in a way that is not possible in live cells [10, 12, 13]. The MLV function as a lipid reservoir for the model cell by supplying lipid membrane material to the GUV when performing micromanipulation and microinjection of solution inside the GUV compartment. In one of the two presented cell models, we show a method for inserting a glass pipette into a GUV to inflate neurotransmitter-filled vesicles on the inside of the GUV, creating a mimic of a neurotransmitter-filled secretory vesicle, that connect via an elongated fusion pore (lipid nanotube) to the model cell plasma membrane (GUV) where the fusion pore can be controlled to dilate lead to vesicle neurotransmitter release and thereby serve as a good model for studying

the later stages of exocytosis (Fig. 1) [4, 5]. In another cell model, we show how the SNARE–protein complexes that cells use to dock and fuse secretory vesicles were replaced by short complimentary DNA strands designed with a DNA sequence to hybridize in a zipper-like manner, like the coiled coil formation of SNAREs, and similar to the SNAREs can induce vesicle membrane fusion if complementary strands are placed in two different lipid bilayers, e.g., two different vesicle membrane, or in a vesicle membrane and a planar bilayer (Fig. 2) [9, 14]. The setup for these experiments uses phase-contrast, bright-field microscopy video recording to visualize the vesicle shape transitions during the exocytosis process in combination with sub-millisecond amperometry detection of neurotransmitter release, by the placement of a carbon fiber microelectrode in a synapse configuration near the membrane of these biomimetic cells performing exocytosis release. From these measurements, the kinetic and shape characteristics of individual amperometric spike can be used to reveal mechanistic details about the fusion pore dynamics at individual exocytosis events and be used to directly compare to exocytosis activity at live secretory cells.

2 Materials

2.1 Preparation of Small Unilamellar Vesicles (SUVs) from Soybean Lipid Extract

1. Prepare a solution of SPE lipids in chloroform (Avanti polar lipids # 541602) by placing 40 μL of SBE lipid solution (25 mg/mL dissolved in chloroform) into a cleaned round-bottom glass flask and add 100 μL of chloroform and a final lipid concentration of 1 mg/mL (*see* **Note 1**). The SUV preparation allows for additional augmentation of lipids by adding a fraction of other type of lipids to the SBL lipid mixture.
2. Place the glass container in a rotary evaporator for a minimum of 2 h while gently rotating the vial. This evaporates the chloroform results in forming a dry lipid film at the bottom of the glass container.
3. To rehydrate the lipid film and form vesicles, gently add 1 mL of potassium phosphate-buffered saline (KPi buffer): 5 mM Trizma base, 30 mM K_3PO_4, 30 mM KH_2PO_4, 1 mM $MgSO_4$, and 0.5 mM EDTA and pH = 7.4 on top of the dried lipid film. Also add 10 μL of glycerol to prevent complete hydration in the steps of dehydration–rehydration of SUVs to create GUV-MLVs (Subheading 3.1, **steps 1** and **2**). Seal the glass vial with parafilm, and place overnight in the fridge at 4 °C to allow the lipid film to gently swell.
4. The next day, place the glass vial into a sonication bath and sonicate for 10 min at room temperature. This should turn the clear sample solution into an opaque solution by the

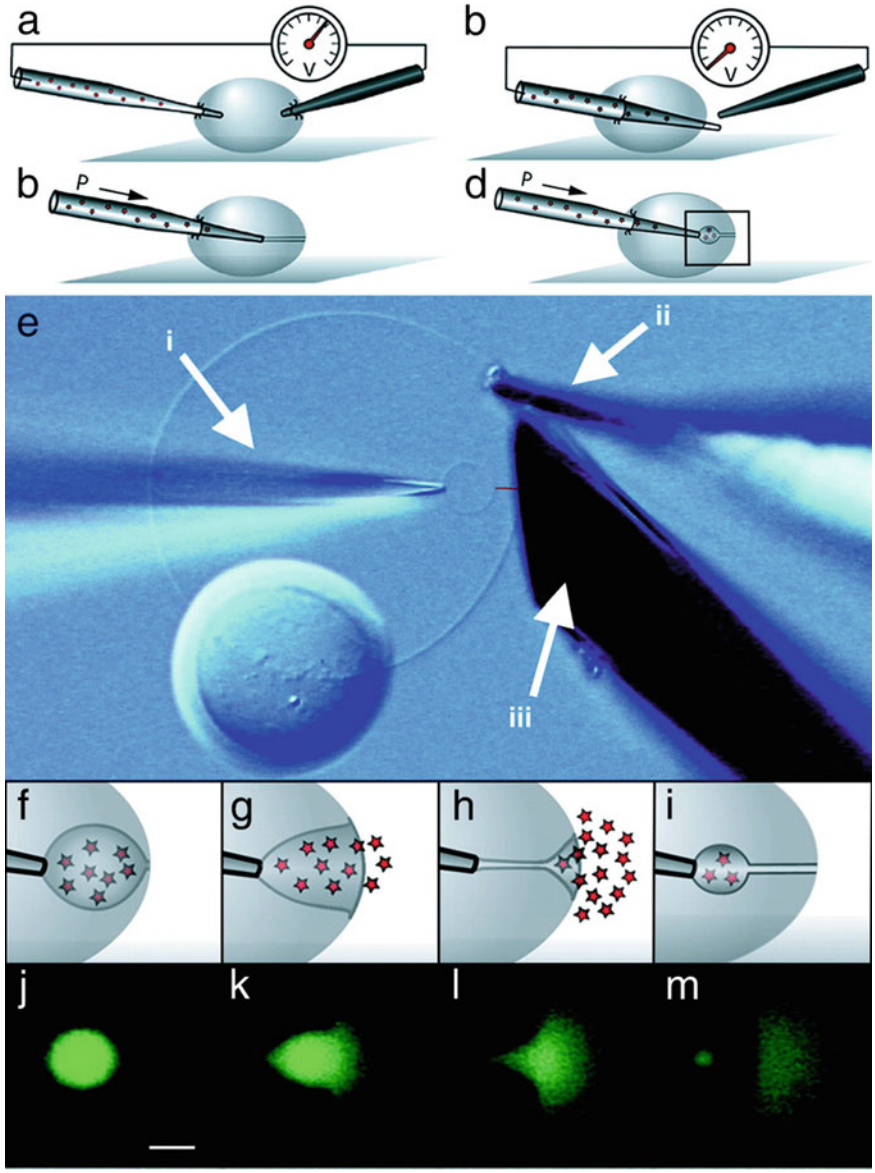

Fig. 1 Using a bottom-up approach to create an artificial cell for exocytosis. A schematic illustration of a neurotransmitter-filled microinjection pipette tip is inserted using electroporation (**a**) into the inside of a GUV and then (**b**) through the opposing wall of the GUV. (**c**) A lipid nanotube is pulled back into the center of the GUV, and (**d**) when microinjecting solution into the GUV, a neurotransmitter-filled vesicle is inflated. (**e**) A difference interference contrast, bright-field image of a GUV connected to an MLV with a micropipette (i) placed inside the GUV and inflates a vesicle and a red line that indicates the placement of the lipid nanotube connection to the GUV membrane, (ii) a counter electrode used for electroporation to facilitate insertion of the microinjection pipette tip, and (iii) a 30 μm in diameter carbon fiber microelectrode beveled to a 45° angle disc electrode. A schematic illustrates the steps of (**f**) inflating the inner secretory vesicle with neurotransmitter solution until only a toroidal pore remains of the lipid nanotube connection that (**g**) spontaneously burst open at a critical length of the nanopore and (**h**) cause the vesicle compartment to collapse into the GUV membrane and release its content. By maintaining the nanotube connection to the nanotip, a new inner vesicle can be inflated and refilled with neurotransmitter solution. Fluorescence microscopy imaging shows the vesicle growth and content release when inflating the vesicles with fluorescein solution, mimicking the later stages of exocytosis. Scale bar equals 10 μm. (Reproduced from ref. [5] with permission from [PNAS] with copyright (2003) National Academy of Sciences, USA)

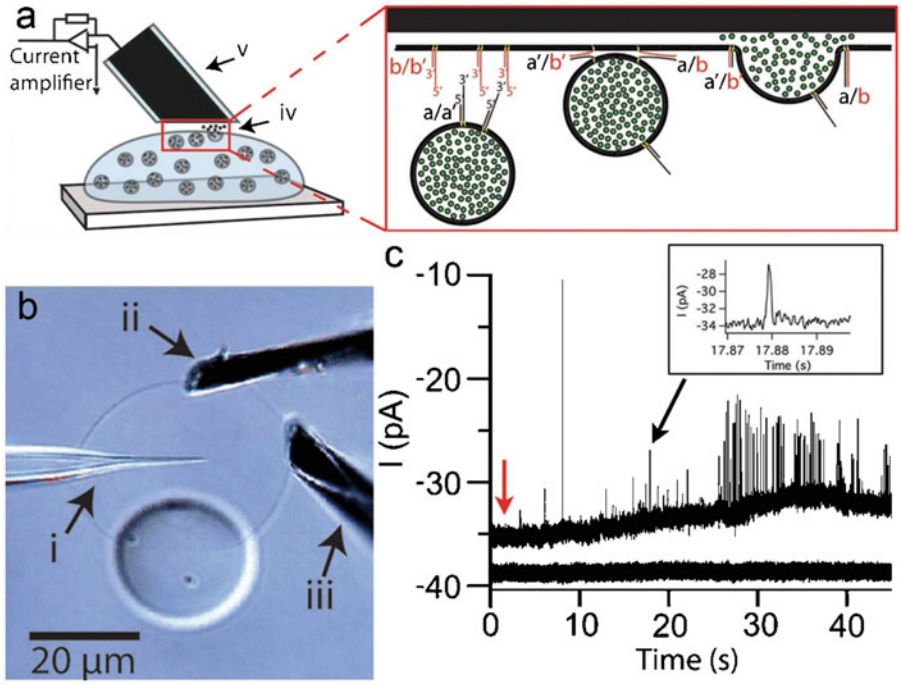

Fig. 2 (**a**) A schematic illustrating a GUV serving as cell model for exocytosis and filled inside with LUVs containing neurotransmitter molecules. The placement of an amperometric electrode at the surface of the GUV (v) is used to detect neurotransmitter release upon LUV fusion with the GUV membrane (iv). The expanded view shows the details of cholesterol-anchored DNA strands (b/b') indicated in red that are inserted into the inner leaflet of the GUV membrane bind and bind to complementary cholesterol-anchored DNA strands (a/a') placed in the outer leaflet of the LUV membrane, indicated in black, and hybridize in a zipper-like fashion and induce fusion of the LUV and GUV membranes, which result in the formation of a vesicle fusion pore and vesicle content release into the extracellular environment. (**b**) A phase contrast microscopy image of a GUV attached to an MLV acting as a lipid reservoir, a glass microinjection pipette that is electroinserted into the interior of a GUV (i), a counter electrode used for electroinsertion (ii), and a 5 μm in diameter amperometric carbon fiber microelectrode that has been beveled to a 45° angle (iii). (**c**) A current time trace of an amperometric recording of exocytosis release events at the secretory artificial cell (upper trace) with inset showing a single current spike from detection of a single vesicle exocytosis event. The lower trace shows a control experiment from inserting neurotransmitter-filled LUVs inside the GUV without cholesterol-DNA strand modification of the LUV membrane. (Reproduced from ref. [9] with permission from [Scientific Reports])

spontaneous formation of the SUVs. Vortex the glass vial (2–5 s) until a uniform solution is achieved.

5. Aliquot the SUV sample solution into smaller volumes (20- to 50-μL batches) into Eppendorf tubes, and store in the freezer at −20 °C for later use.

2.2 Preparation of Neurotransmitter-Filled Large Unilamellar Vesicles (LUV)

1. Prepare a solution of mixed lipids containing DOPC:DOPE: cholesterol and in a mass ratio of 39:21:40 by adding the lipids into clean round-bottom flask (*see* **Note 2**) and a 1:1 methanol: chloroform solution to a final lipid concentration of 0.5 mg/mL. Dry the lipids into a lipid film under a flow of nitrogen gas for 2 h.

2. To the rehydrate the lipid film, add 1 mL of 100 mM freshly made catecholamine solution, dissolved into a buffer containing 10 mM Tris(hydroxymethyl)-aminomethane hydrochloride (Tris), 100 mM NaCl, 1 mM EDTA and pH = 7.4. Incubate for 30 min to allow the lipid film to thoroughly swell.
3. To shake the lipid film off the wall of the sample vial, vortex the sample glass container to create a cloudy solution.
4. To promote a homogeneous concentration of the encapsulated neurotransmitter solution inside the LUVs, collect the LUV sample into a Falcon tube and subject the sample vial to five cycles of freeze/thawing by alternating the placement of the Falcon tube into liquid nitrogen solution and a warm water bath.
5. To unify the liposomes in size, use double 100-nm extrusion filter to extrude the LUV sample 11 times through the filters, which generates neurotransmitter-filled vesicles with an average size of 200 nm in diameter. Using an odd number of extrusions will collect the sample into the clean syringe.
6. To remove nonencapsulated neurotransmitters in the bulk LUV sample solution, place the extruded LUV sample (100 μL) on top of buffered size exclusion chromatography spin columns prefilled with packing material suitable for separation of small neurotransmitter molecules from the LUVs. Centrifuge the LUV sample for 2 min at 735 × *g*. Retain the eluate sample.
7. Purge the sample with nitrogen gas, cap tight, and store in the fridge at 4 °C until use.

2.3 Preparation of Carbon Fiber Microelectrodes for Amperometry Detection

1. Place carbon fibers of 5 or 33 μm in diameter on top of a white paper to enhance visualization of individual fibers. Connect one end of a borosilicate glass capillary (outer diameter of 1.2 mm and inner diameter of 0.69 mm) to an aspiration tube that ensures a tight seal around the glass capillary (*see* **Note 3**).
2. Place a finger at one end of a single carbon fiber, and hold the fiber down at the surface while positioning the open end of the glass capillary near one of the free ends of the carbon fiber while gently aspirating the carbon fiber into the glass capillary. Ensure that the carbon fiber goes through the entire length of the glass capillary, so when removing the aspiration source, the carbon fiber should stick out through both ends of the capillary.
3. Place the glass capillary with the inserted carbon fiber into the holder of a Sutter laser puller Model P-2000. Pull the glass capillary into two separate glass pipette tips (*see* **Note 4**).

4. Before removing the glass pipettes, use a pair of scissors to cut the carbon fiber that connects the two glass tips, which results in gaining two individual carbon fiber microelectrodes.
5. Place the carbon fiber on top of a thicker microscope slide at an inverted microscope. Use a sharp scalpel to manually cut the carbon fiber at the edge where the fiber extends from the edge of the capillary glass coating (*see* **Note 5**).
6. After manually cutting the carbon fiber microelectrode, insert the electrode tip into an epoxy solution for 10 min to allow the epoxy solution to move by capillary force into potentially existing open space between the carbon fiber and the surrounding capillary glass. Gently lift the electrodes out of the epoxy solution (*see* **Note 6**).
7. Gently place the microelectrodes side by side on a wooden holder modified with double-sided, heat-resistant tape. Place the wooden holder with the immobilized electrodes into an oven at 100 °C, and cure the epoxy seal at the electrodes overnight (*see* **Note 7**).
8. To prepare the microelectrode surface into flat 45°angle disc electrodes, place each electrode into the holder of a micropipette beveler. Set the holder at 45° beveling angle. To later facilitate the placement of the 45° angle electrode surface when performing the exocytosis measurement at the artificial cells, use a permanent marker to mark the topside of the glass capillary when the microelectrode is placed in the beveling holder (*see* **Note 8**).
9. Before use, test each electrode on the day of experiment by placing the electrode into a test solution, e.g., 0.1 mM freshly prepared dopamine solution in PBS buffer (pH = 7.4), and use cyclic voltammetry to monitor the steady-state current gained by the electrode. For a cyclic voltammetry scan using dopamine solution, apply a triangle waveform between 0.2 and 0.8 V versus an Ag/AgCl reference electrode at 100 mV/s, and verify that the voltammogram current amplitudes are in agreement with theoretical calculations for a 5- or 33-μm-diameter disc carbon fiber microelectrode, respectively [15].

2.4 Preparation of Glass Microinjection Pipette and Electroinjection of Pipette Solution

1. Place a borosilicate glass capillary (outer diameter of 1.00 mm and an inner diameter of 0.78 mm and with a filament inserted into the glass wall) into a glass capillary puller. Use instrumental settings of the capillary puller that create glass micropipette tips of approximately 0.5 μm in diameter.
2. Using a microcapillary pipette tip, backfill the glass pipette with solution of interest dissolved in 10 mM KPi buffer solution (pH = 7.4) (*see* **Note 9**).

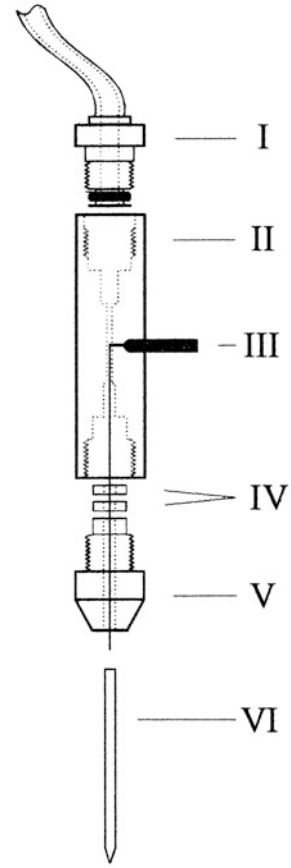

Fig. 3 A schematic illustrating the design of a glass micropipette holder that is used for microelectroinjection in these experiments. The glass capillary pipette (VI) is backfilled with a buffered solution and placed into the holder so that the platinum wire inside the holder inserts into the buffered solution of the micropipette, which ensures a conductive connection between the micropipette tip and the metal pin (III) at the outside of the holder. The micropipette tip when placed into the sample solution then creates a circuit by brass pin connection to a low-voltage pulse generator that is further connected to an Ag/AgCl reference electrode that is placed into the sample bulk solution. Voltage pulses applied through the pulse generator create an electric field at the tip of the micropipette and can be used for local electroporation when the pipette tip is placed near a lipid membrane that can be used for assisting insertion of the micropipette into liposome and cell membranes. The fitted holder (II) connects to a plastic tubing (I) that also connects to a microinjector pump, which can be used for simultaneous microinjection by the pipette. (Reproduced from ref. [16] with permission from [ACS Langmuir])

3. Place the solution-filled glass micropipette into a microelectropipette holder (Fig. 3) and connect to a micromanipulator [1]. Ensure the plastic tubing is connected at the back of the electroinjection holder and the microinjection pump (Eppendorf Femtojet or similar instrument).

4. Connect the metal pin connection from the platinum wire inserted inside of the solution-filled glass pipette to a voltage pulse generator and a carbon fiber counter electrode (Subheading 2.3, **items 1–7** without beveling) that is placed into the GUV-MLV sample solution at the microscope stage, creating a complete electrical circuit when also positioning the micropipette tip into the sample solution.
5. Set the injection pressure (Pi) at the microinjection pump to 20–40 hPa and the compensation pressure (Pc) to 5–10 hPa (*see* **Note 10**).
6. ConFig. the microscope for differential interference contrast (DIC) bright-field microscopy video imaging.
7. Start using a 10×/20× high NA (1.3) objectives to position the micropipette tip, the counter electrode, and the carbon fiber microelectrode tip above the sample containing the GUV-MLV, and use the micromanipulators to locate the tips at the center next to one another.
8. Focus the microscope objective to the focal plane of the surface-immobilized GUV-MLVs, and then move the focal point at 50–100 μm above the GUVs. Then use the micromanipulators to bring the micropipette and microelectrode tip straight down, and stop at the distance where the tips are in focus of the objective.
9. Focus the imaging plane at the middle section of the ultrathin edges of the GUV membrane (at the GUV widest point) using a 40× high NA (1.3) objectives. Use the fine mode of the micromanipulators to gently move the micropipette, counter electrode, and microelectrode tips into the same focus place as the middle height of the GUV.

3 Methods

3.1 Amperometry Measurement, an Artificial Cell of the Later Stages of Exocytosis (See Note 11)

1. Prepare surface-immobilized GUV-MLVs by adding 5 μL of freshly made or thawed SUV sample solution (from Subheading 2.1, **item 4**) onto the center of a regular glass coverslip (24 × 60 mm). Put the glass coverslip with the SUV sample in a vacuum desiccator for 20 min or until the droplet is fully dried, creating a thin lipid film.
2. Transfer the coverslip to the microscope stage, and place above the objective of a bright-field microscope equipped with difference interference contrast (DIC). Gently place a 50-μL droplet of KPi buffer solution on top of the dry lipid film. Wait 5 min to allow the lipid film to initiate the rehydration process while observing and ensuring the formation of GUV-MLV is initiated. Add additional 500 μL of KPi buffer and wait

20 min for the GUV-MLVs to firmly attach to the glass surface (*see* **Note 12**).

3. Turn on the microinjection pump. Bring a glass micropipette backfilled with 1 mM neurotransmitter (catechol or dopamine) solution (*see* Subheading 2.4, **item 2**) near the membrane surface of a GUV that is firmly attached to the surface by the connected MLV. Choose a GUV with a visible thin smooth membrane (indicates a GUV with unilamellar membrane) and diameter of ~25–50 μm. Position the glass pipette at the height of the GUV by the widest perimeter or at the vesicle (half height of the GUV from the glass coverslip). For initiating the micromanipulation methods that follows, it is important there is a lower net flow of solution coming out of the micropipette tip.
4. Therefore, focus the microscope image at the very tip of the pipette, and push the micropipette tip gently at the GUV membrane (~2–5 μm into the membrane). Ensure that a small dimple is formed at the membrane. Use the Pc at the microinjection pump to adjust the net solution flow out of the micropipette tip. If the net flow is too low and the GUV membrane is pulled into the pipette tip, increase the Pc until this stop. If the net flow is too high, which creates a significant distance between the pipette tip by the solution flow out of the pipette, then lower the Pc until the GUV membrane is almost in contact with the pipette tip (*see* **Note 13**).
5. To insert the micropipette into the interior of the GUV using electroporation, gently push the micropipette into the GUV membrane (~5–10 μm into the GUV membrane), creating a membrane indentation while placing the counter electrode at the other side of the GUV and applying a 3–5 of 4-ms pulses with a potential amplitude of ~ 20–40 V using a pulse generator (Digitimer Stimulator DS9A) as shown in Fig. 1a (*see* **Note 14**). This creates transient pores in the GUV membrane and helps for the micropipette to be inserted into the GUV.
6. A successful insertion of the micropipette tip to the inside of the GUV can be detected by watching the GUV membrane shape transform from an indentation to that the GUV membrane encloses at a higher point around the micropipette tip.
7. Verify the successful insertion of the micropipette by microinjecting solution from the pipette tip through applying a 2–5 s injection pulse ~50 hPa (Pi) at the microinjection pump. Verify that the microinjection leads to an increase in the GUV size (*see* **Note 15**).
8. Push the micropipette tip through the center interior of the GUV until reaching the opposing wall of the GUV. Gently push the pipette tip from the inside and out at the widest

GUV perimeter, creating an inverted dimple of the GUV membrane. Apply a few (three to five) 4-ms pulses of about 20–40 V between the micropipette tip and the counter electrode placed on the other side of the GUV membrane using a pulse generator. When the dimple shape formation at the micropipette tip disappears and the GUV membrane seals at a higher distance up at the micropipette tip, the glass pipette has been inserted through the second GUV wall, as shown in Fig. 1b.

9. Retract the micropipette horizontally to the interior and a distance between 1 and 2 μm from the GUV outer membrane to less than half the distance to the GUV center (*see* **Note 16**). Ensure the pipette is pulling in a spontaneously formed lipid nanotube that connects the micropipette tip and the GUV membrane (Fig. 1c). If no lipid nanotube is visible, redo Subheading 3.1, **step 5**. until succeeding (*see* **Note 16**).
10. With a nanotube connection at the micropipette tip, microinject neurotransmitter solution from the glass pipette and into the lipid nanotube by increasing the Pc at the microinjection pump until it causes a net flow of solution out of the micropipette tip that is high enough (about 40–50 hPa, for a 0.5-μm pipette tip) to start inflating a neurotransmitter-filled vesicle by the lipid nanotube (Fig. 1d).
11. Allow the newly formed vesicle to continuously grow while the lipid nanotube shortens and until the lipid nanotube is so short that there is only a toroidal-shaped pore remaining. Because of the high-energy state of the toroidal-shaped pore, membrane energetics will spontaneously open to a larger pore size and cause the vesicle membrane to collapse into the GUV membrane, and thereby release the vesicle neurotransmitter content, as illustrated in Fig. 1f–h.
12. After the vesicle release and a new nanotube has formed between the pipette tip and the GUV membrane (Fig. 2i), maintain the same Pc pressure and allow a new neurotransmitter-filled vesicle to be formed (Fig. 1i) (*see* **Note 17**). This configuration and **steps 10** and **11** in Subheading 3.1 mimic steps of the later stages of exocytosis as illustrated in Fig. 2j–m by inflating the inner vesicle with a solution mixture of dopamine and fluorescent dye that is subsequently released by the dilated fusion pore.
13. To perform amperometry recording of the later stages of exocytosis at the artificial cells, place a freshly 45° angle beveled and tested disc carbon fiber microelectrode in close contact to the GUV membrane where the lipid nanotube opening is located (Fig. 2e). The ideal distance is to create a thin liquid film of a hundred nanometers that separate the electrode and

GUV-MLV surface, which are similar conditions for postsynaptic detection of chemical release at the synapse.

14. Use a low-noise potentiostat and apply a constant potential of +700 mV at the working electrode versus an Ag/AgCl reference electrode that is positioned into the GUV-MLV sample solution at a good distance away from the working electrode to record the current versus time trace of the continuous exocytosis release from the artificial cells as described from Subheading 3.1, **steps 10–12**. Digitalize the signal at 10 kHz and filter the recorded signal by applying an internal low-pass Bessel filter at 2 kHz.
15. To collect simultaneous information on vesicle secretory size and dynamic shape transitions, start the video recording of the exocytosis release from these cells ensuring DIC imaging mode. Repeat Subheading 3.1, **steps 10–12** while recording the simulated neurotransmitter release events using amperometry detection and in parallel video recording of the vesicle fusion events. Each exocytosis release event recorded as an individual amperometric spikes can be used to extract the kinetics and amount of neurotransmitter released at each exocytosis event and be correlated to the vesicle size and alteration in fusion pore shape changes using image analysis from the video recording (*see* **Note 18**).

3.2 Monitoring Exocytosis Vesicle Fusion and Release from an Artificial Cell

1. Prepare surface-immobilized GUV-MLVs according to the steps described in Subheading 3.1, **steps 1** and **2**.
2. Backfill a glass microinjection pipette with a solution containing 1.25 μM of target cholesterol-DNA strands (b/b′) (mimicking the function of the target-SNARE syntaxin and SNAP-25 in cells) with a DNA sequence of 5′-ACC-TGT-AGT-CTT-TAT-TCC-GTG-GTC-CCT-cholesterol-3′(b) and 5′-cholesterol-aGC-CAG-CAC-GGA-3′(b′).
3. Electroinsert the micropipette into the GUV and microinject the target cholesterol-DNA strand (b/b′) solution into the interior of the GUV. To allow the cholesterol moieties to self-insert into the GUV membrane, incubate for 20 min. This anchors the target DNA strands at the inner leaflet of the GUV membrane.
4. Prior to each experiment, functionalize the neurotransmitter-filled LUVs (*see* Subheading 2.2) with complementary vesicle-cholesterol-DNA strands (a/a′) in the LUV membrane and serve to mimic the vesicle-SNARES in cells, in a buffer solution containing 10 mM Tris–HCl, 100 mM NaCl, 1 mM EDTA and pH = 7.4, and add cholesterol-tagged nucleotides with a DNA sequence of 5′-TGG-ACA-TCA-GAA-AATA-AGG-CACA-GAC-GGA-cholesterol-3′ (a) and 5′-ACC-TGT-AGT-

CTT-TAT-TCC-GTG-GTC-CCT-cholesterol-3′(a′) in a 1:20–1:40 molar ratio of LUV-to-DNA and a total lipid concentration of 50 μg/mL. Incubate for 15 min to allow the cholesterol moiety of the vesicle-DNA strand to self-insert into the outer leaflet of the LUV membrane. This will decorate the LUV outer membrane leaflet with complementary DNA strands to those inserted into the inner leaflet of the GUV membrane.

5. Backfill a glass microinjection pipette with the solution of neurotransmitter-filled LUVs decorated with vesicle-DNA strands. Electroinsert the micropipette into the GUV membrane and microinject the LUV solution into the interior of the GUV. Incubate for 30 min to allow the LUV to dock at the GUV inner membrane by binding to complementary DNA strands at the GUV membrane.
6. Backfill a micropipette with 2 mM $CaCl_2$ solution. Electroinsert into the GUV membrane and microinject into the interior of the GUV. This will result in the complementary DNA strands to hybridize in a zipper-like fashion and bring about the fusion of the LUV and GUV membranes. Upon formation of a fusion pore between the two membranes, the neurotransmitters encapsulated inside the LUV interior will be released through the fusion pore formed and into the extracellular space.
7. To study the full exocytosis process from the DNA-zipper-catalyzed exocytosis process, after injection of the calcium solution into the GUV, position a carbon fiber microelectrode in close contact to the GUV surface. Apply a constant +700 mv potential at the carbon fiber electrode surface versus an Ag/AgCl reference electrode to record spontaneous events of vesicle fusion and neurotransmitter release from these biomimetic cells for exocytosis.

3.3 Data Analysis of the Amperometry Recordings

1. To analyze the recorded amperometry data of exocytosis, use a software program that allows analysis of the current transients in the current versus time trace so that the integrated total charge for individual current peaks and dynamic current spike parameters can be determined. A useful software for exocytosis current time trace analysis was developed in the Sulzer lab and has been written for the data analysis program Igor [17].
2. When analyzing the amperometric spikes, select a threshold limit for peaks of three times the root-mean square (RMS) standard deviation of the noise for each recording.
3. Analyze the amperometric spikes from each cell, recording manually to prevent false spikes that do not show Gaussian shape or overlapping current spikes that can be a result from simultaneously detected exocytosis event. Therefore, only

accept Gaussian-shaped spikes with a threshold of minimum three times the RMS noise.

4. Use the dynamic current spike parameters to extract kinetic and dynamic information of the exocytosis process such as peak rise time, amplitude, and fall time that gives information on the fusion pore dilation process and vesicle content release but also can provide information of pre-spike features that correspond to the formation of the fusion pore and leakage of neurotransmitter before the pore expands. The presence or absence of the pre-spikes will be an important feature to monitor in the artificial cell model, as this is a phenomenon that is highly debated in cell-based experiments, and therefore of great importance if able to discern these features from the simplified artificial models and gain information about what controls the kinetics and stability and dynamics fusion pore opening and flickering before vesicle dilation.

4 Notes

1. When preparing the lipid solutions, use glass syringes that have been thoroughly cleaned by filling and rinsing the syringe with chloroform solution at least five times before use. When handling chloroform, avoid using plastic materials, perform all the experimental steps in a fume hood, and wear appropriate gloves and eye protection gear.
2. Clean the round-bottom glassware before use by immersing the glassware in Deconnex 2% for 15 min, followed by thorough rinse using Milli-Q water and dry the glass. Alternatively, in a 500-mL beaker, add 300 mL of Milli-Q water and 60 mL of NH_4Cl. Raise the solution temperature to 80 °C. Add 60 mL of H_2O_2. Place the round-bottom flasks into the beaker solution for 20 min. Rinse the glassware thoroughly in Milli-Q solution and dry the glass. Cover the clean glassware using parafilm and store until use.
3. Since the manual fabrication of microelectrodes often produces a fraction ofelectrodes that might be damaged due to broken glass or crack formation in the glass, it is good to prepare a stock of 50–100 electrodes for a set of upcoming experiments.
4. Although settings can vary between instruments and depend on the capillary dimensions and material used, the puller settings therefore need to be optimized in the lab before use. However, as an indication, the following settings have been used previously in our lab when using borosilicate glass capillary with outer diameter of 1.2 mm and inner diameter of

0.69 mm and the Sutter capillary puller P-2000: heat = 400, filament = 4, velocity = 35, delay = 180, and pull = 100.

5. By placing a 5-mm cylinder-shaped sticky tack at the one end of the glass slide allows to place the glass capillary back end of the microelectrode on top of the sticky tack and tilting the microelectrode tip down and to the center of the microscope objective. This is to facilitate visualization and manually cutting the microelectrode tip using a scalpel.
6. To move the electrodes at slow pace can prevent bulky glue drops from forming at the tip of the electrode.
7. It is important to remember that placing the electrodes at sticky tape and with the electrode tips sticking out at one side of the holder, any physical contact with the electrodes may result in electrodes easy to break. Therefore, ensure that the electrodes are handled with great care and always stored safely. Ideal is, after baking, to move the electrodes over to a holder where the electrodes are fixed in place and protected from physical damage.
8. Since the disc electrode needs to be placed with the flat side in proximity at the surface of the artificial cells and with a 90° angle to the microscope slide for obtaining optical imaging capabilities during the experiments, it is very helpful to be guided by mark at the glass capillary when placing the microelectrode into the head stage at the right angle for positioning. To ensure a fresh and clean electrode during experiment, ideally save the electrode beveling to the day of experiments.
9. Sometimes when backfilling the glass micropipette with solution, tiny air bubbles can get stuck at the very tip of the glass pipette, which prevents microinjection to function properly. To remove air bubbles, hold the glass capillary by hand with the glass tip positioned down and gently flick the side of the glass pipette. Observe liberation of potential air bubbles from the micropipette tip.
10. It is important to initially set the Pc to low enough pressure to only create a net minimal outflow of the backfilled neurotransmitter solution. If Pc is set to low, the capillary force of the micropipette tip will pull solution into the pipette. If Pc is set too high, the net Poiseuille flow out may be too high and impair the initial steps of micromanipulation of the GUV (Subheading 3.1, **steps 4** and **5**).
11. The methodology in Subheading 3.2 that describes the measurements of studying the later stages of exocytosis applies similar of using a GUV-MLV system and to a cell bleb membrane as the starting material for creating an artificial cell for

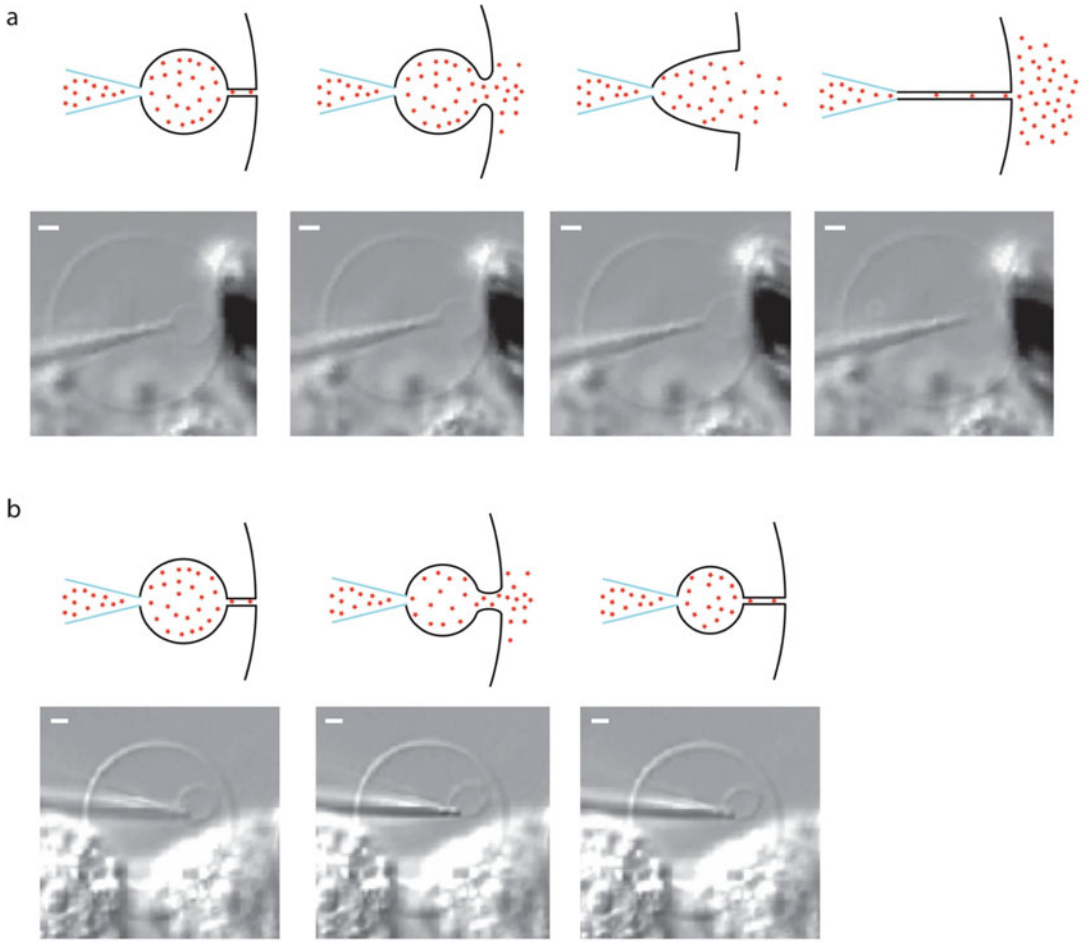

Fig. 4 Schematic and microscopy images of artificial cells with an inflated neurotransmitter-filled vesicle created from a cell plasma membrane bleb display two different modes of exocytosis: (**a**) full exocytosis release where the vesicle fusion pore dilates to the extent that the inflated vesicle membrane collapses into the plasma membrane of the cell model (the bleb) and (**b**) a mode of exocytosis where the fusion pore only briefly increases its size before it shrinks in size again and leads to that only a part of the vesicle content is released into the extracellular space. Scale bars are 1 μm. (Reproduced from ref. [7] with permission from [Sci Rep])

exocytosis, which provides a cell model membrane containing both lipids and proteins in the membrane [7, 8]. The protocol is the same apart from that the manipulation of the GUV membrane is altered by placement of micropipettes and electrodes close to the membrane of the cell plasma membrane bleb that protrudes from a cell body and with the bleb having similar size and shape as a GUV-MLV as shown in Fig. 4, where the artificial cell based on a cell bleb has been used to study two modes of exocytosis.

12. This method requires the spontaneous formation of unilamellar vesicles that connect to MLVs. For easy micromanipulation and high-quality video recording of the vesicle shape transitions of the GUV membrane during artificial exocytosis, a difference interfering contrast (DIC) filter microscope is needed to visualize the thin unilamellar vesicle membrane. Also to succeed in manipulation of the vesicle membrane, it is important that the GUV-MLV formed adhere well to the glass coverslip surface. Use fresh SUV solutions or freshly thawed SUV solution that has been stored in the −20 °C freezer. Upon thawing, the sample might need 1–2 s of vortexing to achieve a homogeneous solution before use.
13. If no dimple is visible, the Pc might be too low, which creates zero or negative flow out of the pipette tip. Then increase the Pc. Alternatively, the lack of net flow out of the micropipette tip might be due to lipid material clogging the tip or that air bubbles are stuck at the tip. If so, increase the Pc at the microinjection pump in step increments of 5–10 hPa until a dimple at the GUV membrane is observed. If increasing the Pc too much, a larger net flow of solution will create, creating a flow that pushes the GUV membrane away from the pipette tip, and will impair micromanipulation of the GUV if close-enough contact cannot be achieved. If so, then lower the Pc until only a small dimple by the pipette tip is visible. If lowering the Pc does not produce a membrane dimple, a large indentation might be a sign of a broken glass micropipette tip and needs to be exchanged by a new solution-filled glass micropipette. Also, if elevating the Pc and there is no sign of flow from the micropipette tip, move the pipette tip at safe distance away from the GUV surface (at least 100 μm) and apply the cleaning flush function at microinjection pump. This can help pushing lipid material out that is clogging the micropipette tip or pushing air bubbles out that has been stuck at the tip. After a cleaning flush, move the micropipette tip back to near the GUV membrane and redo the dimple test. If a dimple is still not achieved, exchange to a new solution-filled micropipette tip and reposition next to the GUV.
14. Keep the length of pulses short (1–4 ms). The voltage amplitude often needs to be adjusted. Start at lower potentials (20 V), and if electroporation is not successful, increase the voltage amplitude in steps of 5 V at a time and up to 40–50 V. To minimize GUV movement at this step, aim to keep the needle pushing at the membrane by the widest perimeter of the GUV, which corresponds to the half height of the GUV from the bottom of the surface of the glass slide.

15. If the GUV that is targeted already has a large volume, it might be difficult to judge if the microinjection leads to an increase in GUV volume. Another way to determine if the micropipette is inserted into the GUV is to observe the surface of the MLV when microinjecting solution. If the MLV smooth surface is altering its surface appearance and, for instance, that hexagonal patterns start forming at the surface, it is a sign that the GUV is pulling lipid material from the MLV in response to microinjection of solution into the GUV interior.
16. Since the lipid nanotube due to the membrane energetics will always seek its shortest distance to the GUV membrane, it is important to not pull the lipid nanotube past the center of the GUV, or it will move to the side of the GUV where the micropipette is inserted. If this happens, redo Subheading 3.1, **step 4**.
17. If the vesicle growth is impaired, the net flow of neurotransmitter solution might be too low. This can be adjusted by increasing the Pc until the vesicle growth is maintained.
18. Due to the very small currents (pA) being measured, it is important to eliminate electronic noise during the amperometry recording, and therefore, the experimental setup needs to be shielded with a Faraday cage.

References

1. Vance JA, Devaraj NK (2021) Membrane mimetic chemistry in artificial cells. J Am Chem Soc 143:8223–8231
2. Salehi-Reyhani A, Ces O, Elani Y (2017) Artificial cell mimics as simplified models for the study of cell biology. Exp Biol Med 242: 1309–1317
3. Xu C, Hu S, Chen X (2016) Artificial cells: from basic science to applications. Mater Today 19:516–532
4. Cans AS, Wittenberg N, Eves D et al (2003) Amperometric detection of exocytosis in an artificial synapse. Anal Chem 75:4168–4175
5. Cans AS, Wittenberg N, Karlsson R et al (2003) Artificial cells: unique insights into exocytosis using liposomes and lipid nanotubes. Proc Natl Acad Sci 100:400–404
6. Keighron JD, Wigström Kurczy ME et al (2015) Amperometric detection of single vesicle acetylcholine release events from an artificial cell. ACS Chem Neurosci 6:181–188
7. Mellander LJ, Kurczy ME, Najafinobar N et al (2014) Two modes of exocytosis in an artificial cell. Sci Rep 4:3847
8. Najafinobar N, Mellander LJ, Kurczy ME et al (2016) Cholesterol alters the dynamics of release in protein independent cell models for exocytosis. Sci Rep 6:33702
9. Simonsson L, Kurczy ME, Trouillon R et al (2012) A functioning artificial secretory cell. Sci Rep 2:824
10. Jesorka A, Stepanyants N, Zhang H et al (2011) Generation of phospholipid vesicle-nanotube networks and transport of molecules therein. Nat Protoc 6:791–805
11. Criado M, Keeller BU (1987) A membrane fusion strategy for single-channel recordings of membranes usually non-accessible to patch-clamp pipette electrodes. FEBS Lett 224: 172–176
12. Karlsson A, Karlsson R, Karlsson M et al (2001) Networks of nanotubes and containers. Nature 409:150–152
13. Karlsson M, Sott K, Davidsson M et al (2002) Formation of geometrically complex lipid nanotube-vesicle networks of higher-order topologies. Proc Natl Acad Sci 99: 11573–11578

14. Stengel G, Zahn R, Höök F (2007) DNA-induced programmable fusion of phospholipid vesicles. J Am Chem Soc 129: 9584–9585
15. Bath BD, Michael DJ, Trafton BJ et al (2000) Subsecond adsorption and desorption of dopamine at carbon-fiber microelectrodes. Anal Chem 72:5994–6002
16. Karlsson M, Nolkranz K, Davidsson MJ et al (2000) Electroinjection of colloid particles and biopolymers into single unilamellar liposomes and cells for bioanalytical applications. Anal Chem 72:5857–5862
17. Mosharov EV, Sulzer D (2005) Analysis of exocytotic events recorded by amperometry. Nat Methods 2:651–658

Part III

Chromaffin Granules and Membrane Traffic

Chapter 19

Isolation and Purification of Chromaffin Granules from Adrenal Glands and Cultured Neuroendocrine Cells

Arlek González-Jamett, María Constanza Maldifassi, and Ana María Cárdenas

Abstract

Chromaffin granules isolated from adrenal glands constitute a powerful experimental tool to the study of secretory vesicle components and their participation in fusion and docking processes, vesicle aggregation, and interactions with cytosolic components. Although it is possible to isolate and purify chromaffin granules from adrenal glands of different species, bovine adrenal glands are the most used tissue source due to its easy handling and the large amount of granules that can be obtained from this tissue. In this chapter, we describe an easy-to-use and short-term protocol for efficiently obtaining highly purified chromaffin granules from bovine adrenal medulla. We additionally include protocols to isolate granules from cultured bovine chromaffin cells and PC12 cells, as well as a section to obtain chromaffin granules from mouse adrenal glands.

Key words Chromaffin cells, Chromaffin granules, Dense core secretory vesicles, Adrenal glands, Adrenal medulla, Granule isolation, PC12 cells

1 Introduction

Adrenaline, the main hormone released during the acute systemic response to stress, is stored in chromaffin granules, which are a type of large dense core vesicles present in adrenal chromaffin cells (Fig. 1). These granules that have a size between 100 and 500 nm [1, 2] store a cocktail of proteins, neuropeptides, nucleotides, catecholamines, and ions, among other molecules [3]. The most abundant intraluminal protein inside chromaffin granules is chromogranin A, a type of acidic secretory glycoprotein that binds catecholamines, ATP and Ca^{2+}, and therefore contributes to the high intragranular concentrations of these molecules [4]. These secretory vesicles also store diverse neuropeptides, among them enkephalin, galanin, and neuropeptide-Y [5, 6]. All these intraluminal molecules are released during exocytosis although the amount

Ricardo Borges (ed.), *Chromaffin Cells: Methods and Protocols*,
Methods in Molecular Biology, vol. 2565, https://doi.org/10.1007/978-1-0716-2671-9_19,

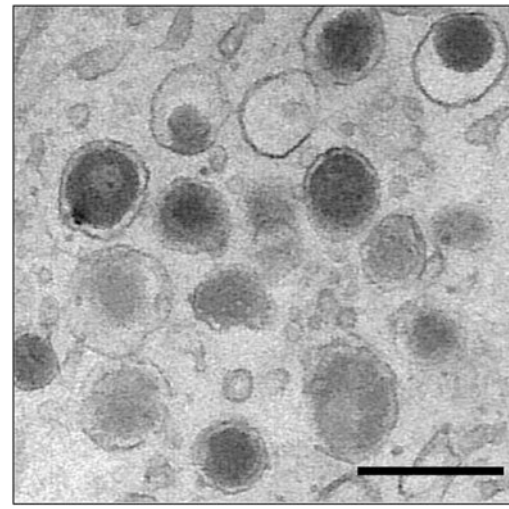

Fig. 1 Electron microscopy photography of chromaffin granules in a primary culture of bovine adrenal chromaffin cells. Note the diversity in the size of the electro-dense core and halo of chromaffin granules. Scale bar = 500 nm

and type of transmitters secreted seem to depend on the intensity of the stimulus [7, 8].

Proteomic analyses of chromaffin granules have allowed the identification of over 300 different proteins in both soluble and membrane fractions [9]. As expected, in the soluble fraction were found proteins involved in the synthesis and processing of hormones, neuropeptides, and neurotransmitters, whereas transporters and proteins involved in vesicle trafficking and exocytosis localized in the membrane fraction [9, 10]. Proteins of the chromaffin granule membrane, such as synaptobrevin, synaptotagmin, and synaptophysin, play critical roles in Ca^{+2}-regulated exocytosis [11]. In this process, synaptotagmin acts as a Ca^{2+} sensor that catalyzes a complex formed by synaptobrevin and the plasma membrane proteins SNAP-25 and syntaxin [12]. Synaptophysin regulates the dynamics of the fusion pore, an intermediate channel that connects the vesicle lumen with the extracellular space upon vesicle–plasma membrane fusion [13], defining the mode of exocytosis [14, 15]. Intraluminal proteins in chromaffin granules, such as chromogranin A and the tissue plasminogen activator (tPA) play important roles in controlling the fusion pore expansion and thereby modulate their own release during exocytosis [16, 17]. Other proteins that associate to the cytosolic side of the chromaffin granule membrane further modulate exocytosis. Among them myosin V [18] and dynamin-2 [19] contribute to the interaction between chromaffin granules and the actin cytoskeleton, modulating the amount and kinetics with which transmitters are released during exocytosis [20, 21].

For decades, isolated chromaffin granules have been a useful tool for the characterization of vesicle membrane proteins and their intraluminal composition [3, 22, 23]. These intact chromaffin granules and their purified membranes have constituted suitable preparations to analyze molecular mechanisms that govern vesicle transmembrane potential [24], proton transport across the V-ATPase [25–27], ATP transport [28, 29], catecholamine loading [25, 30–33], Ca^{2+} accumulation in the granule lumen [34, 35], Ca^{2+}-dependent vesicle aggregation and fusion [36–40], and F-actin interaction [41, 42], among others.

Here, we describe a detailed protocol to isolate and purify chromaffin granules from bovine adrenal gland medulla modified from a former procedure described in 1967 by Smith and Winkler [43]. This protocol yields intact chromaffin granules useful for experimentation with the complete organelle in vitro. Alternatively, the same protocol may provide "ghosts" of granules, a membrane-enriched fraction useful to study membrane components and interactions. In addition, protocols to isolate and purify granules from previously cultured chromaffin cells or from the PC12 cell line, as well as a section to obtain chromaffin granules from mouse adrenal glands, are included.

2 Materials

2.1 Tissue Samples

1. Five to twenty freshly collected bovine adrenal glands obtained from the slaughterhouse (*see* **Notes 1** and **2**).
2. Cultured bovine chromaffin cells.
3. Cultured PC12 cells.
4. Six to eight weeks old C57BL/6 J mice.

2.2 Reagents and Solutions

1. Locke's solution: 154 mM NaCl, 5.6 mM KCl, 3.6 mM $NaHCO_3$, 10 mM HEPES, 5.6 mM glucose, 100 I.U/mL penicillin, 80 mg/mL gentamicin, adjusted to pH 7.4.
2. Bovine serum albumin (BSA) solution: 3 mg/mL BSA in Locke's solution.
3. Collagenase solution: 250–350 IU/mL collagenase type I, 3 mg/mL BSA, 0.15 mg/mL DNAase I, and 0.15 mg/mL in Locke's solution.
4. 0.3 M sucrose solution (in Milli-Q water), store at 4 °C.
5. 1.6 M sucrose solution (in Milli-Q water), store at 4 °C.
6. Hypotonic solution: 1 mM HEPES containing a protease inhibitor cocktail and adjusted to pH 7.0.
7. Intracellular solution: 140 mM potassium aspartate, 5 mM $MgCI_2$, 5 mM ATP, 5 mM glucose, 0.5 mM EGTA, and

20 mM PIPES, adjusted to pH 6.8 and containing a protease inhibitor cocktail.

8. 70% ethanol.
9. Percoll®.
10. Dulbecco's Modified Eagle Medium: Nutrient Mixture F-12 (DMEM/F-12) containing 10% fetal bovine serum, 10,000 units penicillin, and 50 mg/mL gentamicin sulfate.

2.3 Glass and Plastic Supplies

1. Rubber or nitrile gloves.
2. Sterile glass Pasteur pipettes.
3. Sterile plastic Pasteur pipettes.
4. Surgical gauze.
5. Rubber band.
6. Cell scraper.
7. 150-mm Petri dishes.
8. 50-, 100-, or 500-mL beakers.
9. 20-mL syringes.
10. 0.2-μm syringe filters.
11. 15-mL Dounce homogenizer with loose-fitting (type B) pestle.
12. 50-mL centrifuge tubes (for Sorvall rotor SS-34 or equivalent).
13. 4-mL polycarbonate ultracentrifuge tubes.
14. 60-mm culture dishes.

2.4 Equipment and Instruments

1. Surgical scissors.
2. Scalpels.
3. Stainless steel spatula.
4. Sorvall SS34 fixed angle rotor or an equivalent rotor.
5. Refrigerated benchtop centrifuge.
6. Type 45 Ti rotor or equivalent.
7. Refrigerated ultracentrifuge with (Sw60Ti) rotor.
8. Tissue Tearor Homogenizer (probe diameter 4.5 mm and length 4.8 cm).
9. Magnifying glass.

3 Methods

The schemes in Figs. 2 and 3 summarize the protocol detailed below.

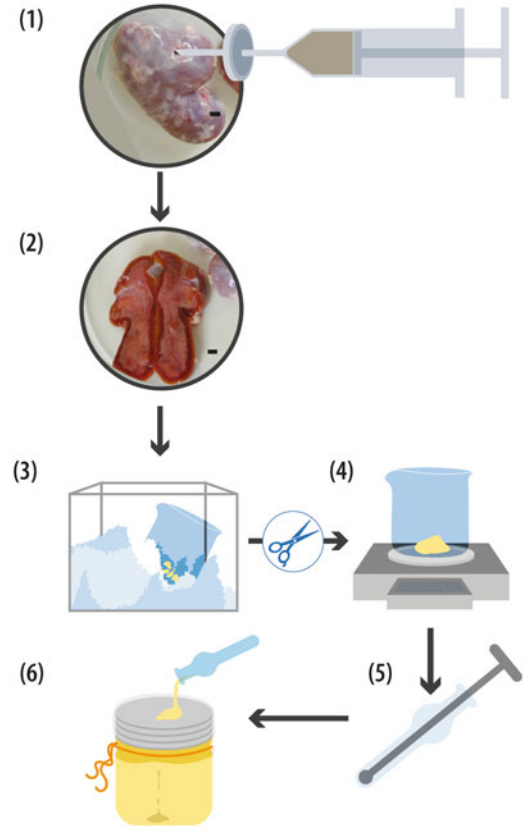

Fig. 2 Bovine adrenal medulla homogenization. (1) Bovine adrenal glands are perfused with collagenase in Locke/glucose/BSA solution using a syringe and then incubated for 25 min at 37 °C. (2) Glands are opened, and medulla (distinguished for its pinkish-orange color) is dissected using a scalpel. Scale bars in (1) and (2) are 3 mm. (3) The medullas are placed in a beaker on ice and chopped with scissors into small pieces. (4) The chopped medullas are placed in a previously weighted beaker to determine the tissue weight. (5) A 0.3 M cold sucrose solution is added (5 mL/1 g of medulla), and the mix is transferred into a Douncer homogenizer. (6) The resulting homogenate is filtered through four layers of gauze. *Protocol continues in* Fig. 3

3.1 Adrenal Medulla Dissection

1. Immediately after arriving from the slaughterhouse (*see* **Note 2**), place the glands in sterile glass Petri dishes and remove most of the fat tissue using surgical scissors.
2. Wash the glands in cold Locke's solution and put them in another sterile Petri glass.
3. Introduce collagenase in Locke/glucose/BSA (5 mL per gland) through the adrenal vein orifice using a syringe and a 0.2-μm syringe filter until the gland is completely inflated. Place the glands in a beaker and incubate for 25 min at 37 °C (*see* **Note 3**).

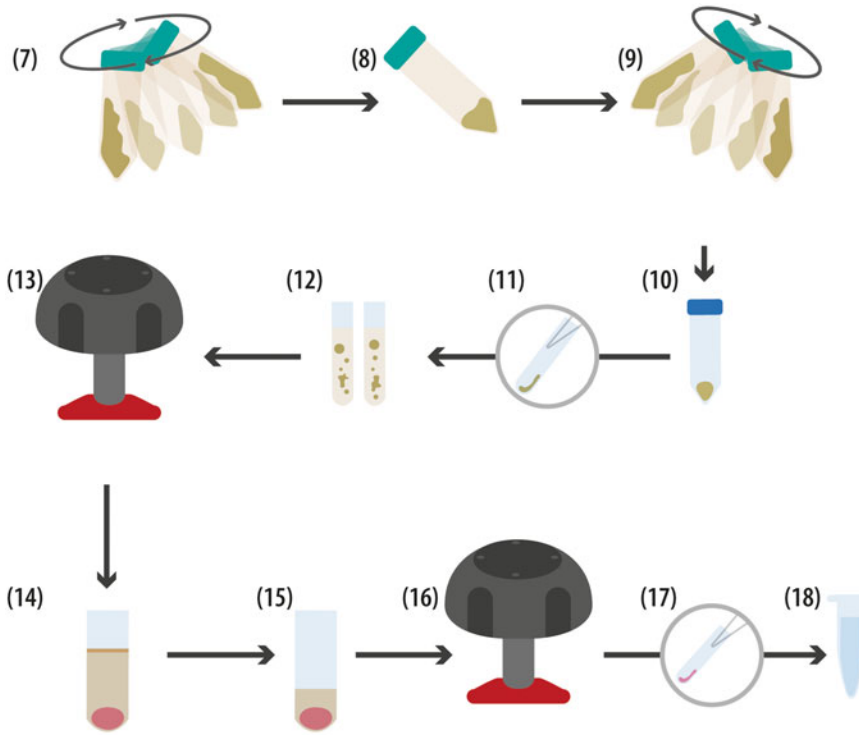

Fig. 3 Chromaffin granule isolation and purification. *Continuation of the protocol in* Fig. 2. (7) Filtered homogenate is transferred to centrifuge tubes and centrifuged at 2000 g for 10 min at 4 °C. (8) Supernatants are collected, transferred to new centrifuge tubes, and (9) centrifuged at 20,000 × *g* for 30 min at 4 °C. (10 and 11) Pellets are gently resuspended in 0.3 M cold sucrose solution. (12) Resuspended pellets are transferred to polycarbonate ultracentrifuge tubes containing cold 1.6 M sucrose solution. (13) Centrifugation at 100,000 g for 60 min at 4 °C is performed. (14) Resulting pink pellets are enriched in intact chromaffin granules. The brown band at the 0.3 M/1.6 M sucrose interface contains mitochondria and other organelles. (15) Pink pellets can be resuspended in cold hypotonic buffer solution containing protease inhibitors and (16) centrifugated at 100,000 g for 1 h at 4 °C. (17) Pellets are enriched in chromaffin granule membranes. (18) Pellets can be resuspended in intracellular solution and stored at −80 °C

4. Place the glands in a sterile Petri dish, and with the help of surgical scissors, cut along the longest circumference of the gland going through the capsule but taking care of not touching the medulla (*see* **Note 4**). Discard cortical tissue.
5. With the help of a scalpel, proceed to dissect the medulla, which is easily distinguished for its pinkish-orange color, different from the reddish-brown color of the cortex.
6. Chop the medullae into small pieces using surgical scissors, and collect the tissue in a sterile beaker previously weighted. Determine the weight of adrenal medulla recovered (*see* **Note 5**).

It is possible to isolate intact chromaffin granules starting from cultured bovine chromaffin cells (skip to alternative protocols in Subheading 3.5 of this section).

3.2 Adrenal Medulla Homogenization

1. Add 0.32 M of cold sucrose solution (5 mL per 1 g of medulla) and transfer it to a Douncer tissue homogenizer.
2. Gently homogenize medulla tissue, keeping it on ice.
3. Filter the homogenized fractions through a four-layer gauze. The piece of gauze must be attached with a rubber band to the top of a 50-mL baker (*see* **Note 6**).
4. Once all fractions have been filtered, remove the piece of gauze (*see* **Note 7**) and transfer the homogenate to 50-mL centrifuge tubes previously cooled to 4 °C. Centrifuge at 2000 g for 10 min at 4 °C.
5. Collect supernatants and discard pellets that contain nuclei and broken cells.

3.3 Chromaffin Granule Isolation and Purification

1. Transfer the supernatant to new 50-mL tubes and centrifuge at 20,000 × *g* for 30 min at 4 °C. The obtained pellet is enriched in chromaffin granules but also has a little fraction of mitochondria and lysosomes.
2. Discard supernatants and gently remove the brownish part of the pellets with the help of a sterile glass Pasteur pipette.
3. Gently resuspend the pellets in 0.3 M cold sucrose solution (4 mL per each gland) using a Pasteur pipette (*see* **Note 8**).
4. Per each gland, prepare two 4-mL polycarbonate ultracentrifuge tubes, previously cooled to 4 °C, and add 2 mL of 1.6 M of cold sucrose solution to each one.
5. Gently add to each tube 2 mL of the pellet resuspended in 0.3 M sucrose, taking care of not disturbing the interface between both sucrose solutions (let the suspension slide slowly down the tube wall).
6. Carefully place the tubes on the buckets of the ultracentrifuge rotor and centrifuge at 100,000 g for 60 min at 4 °C (e.g., 49.000 rpm in the sw60Ti Beckman type rotor).
7. Remove supernatants, and save the pink color pellet, which corresponds to purified chromaffin granules, whereas the brown band at the interface between the 0.3 M and 1.6 M sucrose fractions corresponds to mitochondria and other organelles (*see* **Note 9**).
8. High purity of isolated chromaffin granules can be verified by electron microscopy and/or Western blot using antibodies against intragranular proteins such as chromogranin A [44].

3.4 Chromaffin Granule Membrane Enrichment

1. Chromaffin granule membranes-enriched fractions or chromaffin granules "ghosts" can be obtained by osmotic lysis of the purified intact granules by resuspending the pellet in 4 mL

of cold hypotonic buffer solution containing protease inhibitors.

2. Homogenize using Pasteur pipettes.
3. Centrifugate the suspension at 100,000 g for 1 h at 4 °C.
4. Remove the supernatant and resuspend the pellet (chromaffin granule membranes) in 1 mL of cold hypotonic buffer or your experimental solution (*see* **Note 10**).
5. The purification efficiency of chromaffin granule membranes can be confirmed by Western blot using antibodies against diverse markers such as mitochondria (e.g., cytochrome C oxidase or succinate dehydrogenase) and endoplasmic reticulum (e.g., calnexin) [40, 44].
6. Purified chromaffin granule membranes constitute a useful tool for biochemical analysis of the machinery implicated in secretion (*see* **Note 11**).

3.5 Obtention of Granules from Other Sources

Despite the great utility of chromaffin granules isolated from bovine adrenal medulla, some experimental strategies that require chronic pharmacological treatments or the knockout of a particular protein become difficult to approach using bovine tissue. Two feasible alternatives are (A) to isolate intact chromaffin granules starting from cultured bovine chromaffin cells or PC12 cells and (B) to isolate chromaffin granules from mouse adrenal glands.

3.5.1 Primary Culture of Chromaffin Cells from Bovine Adrenal Glands

1. Perfuse bovine glands with collagenase in LOCKE/glucose/BSA solution two times at 37 °C for 20 min each time, and after digestion, separate medulla from adrenal cortex, and crumble and filter the medulla tissue through one layer of surgical gauze.
2. Centrifuge the resulting cell suspension at 1000 g for 10 min at room temperature, wash the obtained pellet, and then subject it to a Percoll gradient at 20,000 g for 20 min to separate chromaffin cells from erythrocytes and endothelial cells.
3. Resuspend the obtained chromaffin cell-enriched fraction in a LOCKE/glucose/BSA solution, and centrifuge twice at 1000 g for 10 min at room temperature.
4. Resuspend the resulting precipitate in DMEM/F-12 (Invitrogen) with 10% of fetal bovine serum (GIBCO), penicillin, and gentamicin, and filter through a double layer of surgical gauze. The cell suspension must be cultured at a density of 2–three million cells per plate in 60-mm culture dishes. Any treatment to be performed in cultured cells should be carried out between 2 and 5 days of culture.
5. After treatment, remove the culture medium using plastic Pasteur pipettes, add 2 mL of cold 0.3 M sucrose, and detach the

cells using a cell scraper. Transfer the suspension to a 15-mL tube previously cooled on ice. Add another 2 mL of cold 0.3 M sucrose to the plate to collect any remaining cells, and transfer it to the 15-mL tube.

6. Homogenize the cell suspension using a Tissue Tearor Homogenizer at medium power for 30–40 s.
7. Transfer the suspension to a 50-mL centrifuge tube kept on ice, add cold 0.3 M of sucrose to make up to 30 mL, and centrifuge at 1000 g for 10 min at 4 °C.
8. Discard the pellet that corresponds to nuclei and cellular debris, and transfer the supernatant to a new 50-mL tube previously cooled. Make up to 30 mL with cold 0.3 M sucrose, and centrifuge at 10,000 g for 20 min.
9. Discard the supernatant and carefully resuspend the precipitates in 1.63 mL of cold 0.3 M sucrose. Once resuspended, it should be kept on ice. The precipitate contains chromaffin granules, mitochondria, and lysosomes.
10. To obtain chromaffin granule membrane-enriched fractions, refer to Subheading 3.4.

3.5.2 Mouse Chromaffin Granule Isolation

1. All protocols involving animals must be approved by the local authorities and ethics committees. Animal sacrifice must be accomplished ensuring that no pain will be induced to the animal. We recommend animal sacrifice with decapitation by means of a guillotine under isoflurane anesthesia. In our laboratory, we usually use 4–5% during anesthesia induction and 1.5–3% during anesthesia maintenance [45]. The number of animals to be employed in this protocol will depend on the downstream technique for investigating different aspects of chromaffin granules, their membranes, or their contents. Please see examples in Pardo et al. [46] and Díaz-Vera et al. [44].
2. In order to dissect the mice adrenal gland, the animal must be set supine.
3. With 70% ethanol, sterilize the incision area of the abdomen. Sometimes, it is preferred to previously remove the animal's hair by using scissors in that area in order to avoid contamination.
4. With formerly sterilized tweezers, hold the animal's skin upright, cut open the skin of the abdomen using sterilized scissors, and locate the adrenal glands (these ovaloid-shaped organs are situated above each kidney).
5. Remove glands and place them on a sterile Petri dish. Using a surgical scalpel, remove all fat. This step should be done avoiding dehydration of the organ using cold Locke's solution.

6. Carefully isolate the medulla from the darker surrounding cortex using a scalpel. It is recommended to perform this step under a magnifying glass.
7. Cut the medulla in pieces and weight
8. Homogenize medulla following Subheading 3.2 from above
9. To obtain isolated chromaffin granules using the method based on Smith and Winkler [43], as in Díaz-Vera et al. [44] or Sakamoto et al. [29], please follow Subheading 3.3, and to attain enriched granule membranes, refer to Subheading 3.4. Alternatively, a different protocol based on gradient fractionation using a radiocontrast solution has been published by Pardo et al. [46] (*see* **Note 12**).

4 Notes

1. Most of the reported preparations of chromaffin granules use bovine adrenal glands in consideration to the amount of tissue obtained. However, chromaffin granule can be also obtained from mouse adrenal glands (for details, *see* Subheading 3.5).
2. Bovine adrenal glands should be transported to the laboratory as early as possible after their removal in sterile conditions and kept on ice containers.
3. This step is not described in other chromaffin granule isolation protocols [47–49], but it is very helpful for cell disaggregation.
4. This step and the following ones should be performed at 0–5 °C, keeping all containers on ice and using cold solutions. Centrifugations should be carried out at 4 °C.
5. You will get approximately 1–2 g of medulla tissue per each bovine adrenal gland [49].
6. Use a spatula to spread the homogenate across the surface of the gauze. This facilitates the filtering process.
7. Squeeze the liquid that remains in the gauze and add it to the filtered homogenate.
8. Take care to leave away any dark brown waste or red blood cells that may appear at the bottom of the pellet.
9. At this point, intact purified granules can be resuspended in 1.6 M sucrose and stored at 4 °C for a few days. Alternatively, purified intact granules can be resuspended in a standard intracellular solution and stored at −80 °C for weeks to months. For granule aggregation assays, chromaffin granules can be suspended in an isotonic solution, typically containing 240–300 mM sucrose, a buffer (HEPES o PIPES) to keep

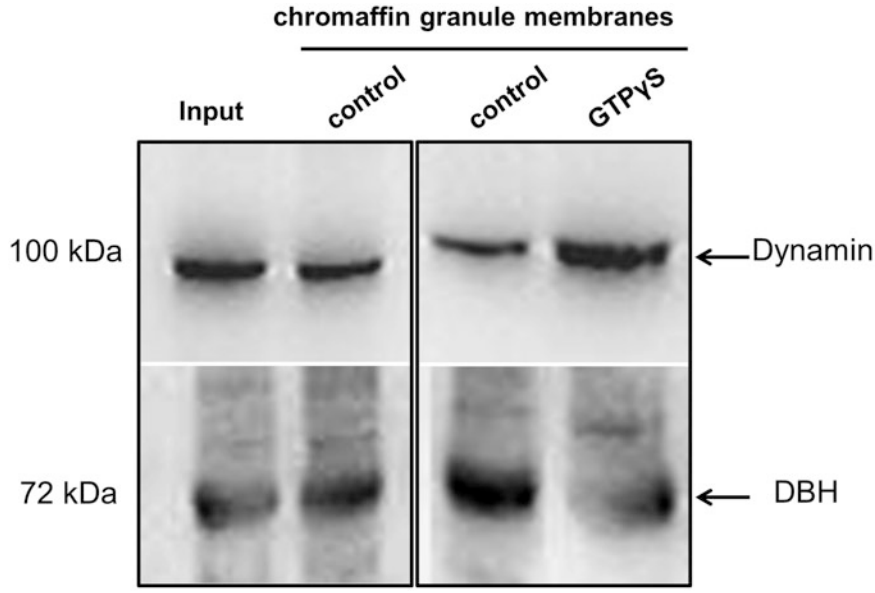

Fig. 4 Representative Western blot showing the expression of the large GTP-ase dynamin (a 100-kDa band) in purified bovine chromaffin granule membranes (following the protocol described in Fig. 2). Note that the presence of GTPγS seems to increase the association of dynamin to chromaffin granule membranes. Input: Cultured chromaffin cell extract. DBH: Dopamine-β-hydroxylase. Refer to **Note 11**

the pH in the range of 6.8–7.0, and variable concentrations of $CaCl_2$ and KCl depending on the aim of the study [50–52].

10. Purified chromaffin granule membranes resuspended in hypotonic buffer solution can be stored at −80 °C for months.
11. To exemplify the usefulness of purified granule membranes for biochemical analysis of molecules involved in exocytosis, we performed a Western blot assay to estimate the association of the large GTP-ase dynamin to chromaffin granule membranes [14]. When chromaffin granule membranes are resuspended in hypotonic buffer containing 1 mM GTPγS, a non-hydrolyzable analogue of GTP [53], the association of dynamin to granule membranes seems to be enhanced (Fig. 4), suggesting that the dynamin's GTP-ase activity is required for dynamin dissociation from secretory granules.
12. Recently, another protocol using a continuous density gradient with iodixanol has been proposed [46]. The protocol consists of two steps. In the first step, isolation of a crude vesicle fraction takes place where the resulting preparation possesses sufficient vesicles for downstream applications. In the second step, continuous gradient fractionation of the crude fraction using iodixanol occurs. At this point, different purified fractions are attained, and each can be used for diverse measurements. For a purification comparison using Western blot

between sucrose gradient fractions and iodixanol-obtained fractions, please refer to the supplementary Figure 2 in the manuscript of Pardo et al. [46].

Acknowledgments

We thank Ms. María José Guerra and Daniela M. Ponce for providing images of adrenal glands. This work was supported by ACE210014 from ICM-ANID and FONDECYT 1220825 (to A.M.C.), Chile.

References

1. Grabner CP, Price SD, Lysakowski A, Fox AP (2005) Mouse chromaffin cells have two populations of dense core vesicles. J Neurophysiol 94:2093–2104
2. Ardiles AO, Maripillán J, Lagos VL, Toro R, Mora IG, Villarroel L, Alés E, Borges R, Cárdenas AM (2006) A rapid exocytosis mode in chromaffin cells with a neuronal phenotype. J Neurochem 99:29–41
3. Crivellato E, Nico B, Ribatti D (2008) The chromaffin vesicle: advances in understanding the composition of a versatile, multifunctional secretory organelle. Anat Rec (Hoboken) 291: 1587–1602
4. Borges R, Díaz-Vera J, Domínguez N, Arnau MR, Machado JD (2010) Chromogranins as regulators of exocytosis. J Neurochem 114rie:335–343
5. Bastiaensen E, De Block J, De Potter WP (1988) Neuropeptide Y is localized together with enkephalins in adrenergic granules of bovine adrenal medulla. Neuroscience 25: 679–686
6. Fried G, Wikström LM, Franck J, Rökaeus A (1991) Galanin and neuropeptide Y in chromaffin granules from the guinea-pig. Acta Physiol Scand 142:487–493
7. Fulop T, Radabaugh S, Smith C (2005) Activity-dependent differential transmitter release in mouse adrenal chromaffin cells. J Neurosci 25:7324–7332
8. Perrais D, Kleppe IC, Taraska JW, Almers W (2004) Recapture after exocytosis causes differential retention of protein in granules of bovine chromaffin cells. J Physiol 560:413–428
9. Wegrzyn JL, Bark SJ, Funkelstein L, Mosier C, Yap A, Kazemi-Esfarjani P, La Spada AR, Sigurdson C, O'Connor DT, Hook V (2010) Proteomics of dense core secretory vesicles reveal distinct protein categories for secretion of neuroeffectors for cell-cell communication. J Proteome Res 9:5002–5024
10. Wegrzyn J, Lee J, Neveu JM, Lane WS, Hook V (2007) Proteomics of neuroendocrine secretory vesicles reveal distinct functional systems for biosynthesis and exocytosis of peptide hormones and neurotransmitters. J Proteome Res 6:1652–1665
11. Cárdenas AM, Marengo FD (2016) How the stimulus defines the dynamics of vesicle pool recruitment, fusion mode, and vesicle recycling in neuroendocrine cells. J Neurochem 137: 867–879
12. Marengo FD, Cárdenas AM (2018) How does the stimulus define exocytosis in adrenal chromaffin cells? Pflugers Arch 470:155–167
13. Álvarez de Toledo G, Montes MÁ, Montenegro P, Borges R (2018) Phases of the exocytotic fusion pore. FEBS Lett 592:3532–3541
14. González-Jamett AM, Báez-Matus X, Hevia MA, Guerra MJ, Olivares MJ, Martínez AD, Neely A, Cárdenas AM (2010) The association of dynamin with synaptophysin regulates quantal size and duration of exocytotic events in chromaffin cells. J Neurosci 30:10683–10691
15. Chang CW, Hsiao YT, Jackson MB (2021) Synaptophysin regulates fusion pores and exocytosis mode in chromaffin cells. J Neurosci 41: 3563–3578
16. Weiss AN, Anantharam A, Bittner MA, Axelrod D, Holz RW (2014) Lumenal protein within secretory granules affects fusion pore expansion. Biophys J 107:26–33
17. Abbineni PS, Bittner MA, Axelrod D, Holz RW (2019) Chromogranin A, the major lumenal protein in chromaffin granules, controls fusion pore expansion. J Gen Physiol 151: 118–130

18. Rosé SD, Lejen T, Casaletti L, Larson RE, Pene TD, Trifaró JM (2003) Myosins II and V in chromaffin cells: myosin V is a chromaffin vesicle molecular motor involved in secretion. J Neurochem 85:287–298
19. González-Jamett AM, Momboisse F, Guerra MJ, Ory S, Báez-Matus X, Barraza N, Calco V, Houy S, Couve E, Neely A, Martínez AD, Gasman S, Cárdenas AM (2013) Dynamin-2 regulates fusion pore expansion and quantal release through a mechanism that involves actin dynamics in neuroendocrine chromaffin cells. PLoS One 8:e70638
20. Olivares MJ, González-Jamett AM, Guerra MJ, Baez-Matus X, Haro-Acuña V, Martínez-Quiles N, Cárdenas AM (2014) Src kinases regulate de novo actin polymerization during exocytosis in neuroendocrine chromaffin cells. PLoS One 9:e99001
21. González-Jamett AM, Guerra MJ, Olivares MJ, Haro-Acuña V, Baéz-Matus X, Vásquez-Navarrete J, Momboisse F, Martinez-Quiles N, Cárdenas AM (2017) The F-actin binding protein cortactin regulates the dynamics of the exocytotic fusion pore through its SH3 domain. Front Cell Neurosci 11:130
22. Winkler H, Westhead E (1980) The molecular organization of adrenal chromaffin granule. Neuroscience 5:1803–1823
23. Malosio M, Giordano T, Laslop A, Meldolesi J (2004) Dense-core granules: a specific hallmark of the neuronal/neurosecretory cell phenotype. J Cell Sci 117:743–749
24. Pollard HB, Zinder O, Hoffman PG, Nikodejevic O (1976) Regulation of the transmembrane potential of isolated chromaffin granules by ATP, ATP analogs, and external pH. J Biol Chem 251:4544–4550
25. Akeson MA, Deamer DW (1989) Steady-state catecholamine distribution in chromaffin granule preparations: a test of the pump-leak hypothesis of general anesthesia. Biochemistry 28:5120–5127
26. Ludwig J, Kerscher S, Brandt U, Pfeiffer K, Getlawi F, Apps DK, Schägger H (1998) Identification and characterization of a novel 9.2-kDa membrane sector-associated protein of vacuolar proton-ATPase from chromaffin granules. J Biol Chem 273:10939–10947
27. Zhou Z, Peng SB, Crider BP, Andersen P, Xie XS, Stone DK (1999) Recombinant SFD isoforms activate vacuolar proton pumps. J Biol Chem 274(22):15913–15919. https://doi.org/10.1074/jbc.274.22.15913
28. Bankston LA, Guidotti G (1996) Characterization of ATP transport into chromaffin granule ghosts. Synergy of ATP and serotonin accumulation in chromaffin granule ghosts. J Biol Chem 271:17132–17138
29. Sakamoto S, Miyaji T, Hiasa M, Ichikawa R, Uematsu A, Iwatsuki K, Shibata A, Uneyama H, Takayanagi R, Yamamoto A, Omote H, Nomura M, Moriyama Y (2014) Impairment of vesicular ATP release affects glucose metabolism and increases insulin sensitivity. Sci Rep 4:6689
30. Taugner G (1972) The effects of univalent anions on catecholamine fluxes and adenosine triphosphatase activity in storage vesicles from the adrenal medulla. Biochem J 130:969–973
31. Ramu A, Pazoles CJ, Creutz CE, Pollard HB (1981) Catecholamine transport by isolated chromaffin granules. Influence of MgATP and a disulfonic stilbene on (R)-norepinephrine/epinephrine exchange and spontaneous epinephrine efflux. J Biol Chem 256:1229–1234
32. Deupree JD, Weaver JA (1984) Identification and characterization of the catecholamine transporter in bovine chromaffin granules using [3H] reserpine. J Biol Chem 259:10907–10912
33. Terland O, Grønberg M, Flatmark T (1991) The effect of calcium channel blockers on the H(+)-ATPase and bioenergetics of catecholamine storage vesicles. Eur J Pharmacol 207:37–41
34. Krieger-Brauer H, Gratzl M (1982) Uptake of Ca2+ by isolated secretory vesicles from adrenal medulla. Biochim Biophys Acta 691(1):61–70. https://doi.org/10.1016/0005-2736(82)90214-0
35. Bulenda D, Gratzl M (1985) Matrix free Ca2+ in isolated chromaffin vesicles. Biochemistry 24:7760–7765
36. Creutz CE, Scott JH, Pazoles CJ, Pollard HB (1982) Further characterization of the aggregation and fusion of chromaffin granules by synexin as a model for compound exocytosis. J Cell Biochem 18:87–97
37. Nir S, Stutzin A, Pollard HB (1987) Effect of synexin on aggregation and fusion of chromaffin granule ghosts at pH 6. Biochim Biophys Acta 903:309–318
38. Drust DS, Creutz CE (1988) Aggregation of chromaffin granules by calpactin at micromolar levels of calcium. Nature 331:88–91
39. Wang W, Creutz CE (1992) Regulation of the chromaffin granule aggregating activity of annexin I by phosphorylation. Biochemistry 31:9934–9939
40. Kreutzberger AJB, Kiessling V, Liang B, Seelheim P, Jakhanwal S, Jahn R, Castle JD, Tamm LK (2017) Reconstitution of calcium-

mediated exocytosis of dense-core vesicles. Sci Adv 3:e1603208
41. Fowler VM, Pollard HB (1982) Chromaffin granule membrane-F-actin interactions are calcium sensitive. Nature 295:336–339
42. Morita K, Pollard HB (1985) Chromaffin granule-cytoskeleton interaction. Stabilization by F-actin of ATPase in purified chromaffin granule membranes. FEBS Lett 181:195–198
43. Smith AD, Winkler H (1967) A simple method for the isolation of adrenal chromaffin granules on a large scale. Biochem J 103:480–482
44. Díaz-Vera J, Morales YG, Hernández-Fernaud JR, Camacho M, Montesinos MS, Calegari F, Huttner WB, Borges R, Machado JD (2010) Chromogranin B gene ablation reduces the catecholamine cargo and decelerates exocytosis in chromaffin secretory vesicles. J Neurosci 30: 950–957
45. García-Campos P, Báez-Matus X, Jara-Gutiérrez C, Paz-Araos M, Astorga C, Cea LA, Rodríguez V, Bevilacqua JA, Caviedes P, Cárdenas AM (2020) N-acetylcysteine reduces skeletal muscles oxidative stress and improves grip strength in dysferlin-deficient Bla/J mice. Int J Mol Sci 21:4293
46. Pardo MR, Estévez-Herrera J, Castañeyra L, Borges R, Machado JD (2017) Isolation of mouse chromaffin secretory vesicles and their division into 12 fractions. Anal Biochem 536: 1–7
47. Cidon S, Nelson N (1983) A novel ATPase in the chromaffin granule membrane. J Biol Chem 258:2892–2898
48. Creutz CE (2010) Isolation of chromaffin granules. Curr Protoc Cell Biol Chapter 3: Unit 3.39.1-10
49. Birinci Y, Preobraschenski J, Ganzella M, Jahn R, Park Y (2020) Isolation of large dense-core vesicles from bovine adrenal medulla for functional studies. Sci Rep 10: 7540
50. Morita K, Tomares SM, Pollard HB (1996) Enhancement by F-actin of MgATP-dependent dopamine uptake into isolated chromaffin granules. Biochem Mol Biol Int 40:61–66
51. Damer CK, Creutz CE (1996) Calcium-dependent self-association of synaptotagmin I. J Neurochem 67:1661–1668
52. Brownawell AM, Creutz CE (1997) Calcium-dependent binding of sorcin to the N-terminal domain of synexin (annexin VII). J Biol Chem 272:22182–22190
53. Shumilina EV, Khaitlina SY, Morachevskaya EA, Negulyaev YA (2003) Non-hydrolyzable analog of GTP induces activity of Na+ channels via disassembly of cortical actin cytoskeleton. FEBS Lett 547:27–31

Chapter 20

Confocal Microscopy Studies of F-Actin Cytoskeleton Distribution and Dynamics Using Fluorescent LifeAct Constructs in Bovine Adrenal Chromaffin Cells

José Villanueva, Yolanda Giménez-Molina, and Luis M. Gutiérrez

Abstract

Cultured bovine chromaffin cells have been characterized as a successful model to study changes in the cytoskeleton during the secretory process. In this sense, the distribution and dynamics of the F-actin cytoskeleton can be studied by confocal microscopy using appropriate molecular tools such as LifeAct, a peptide that stains the structures of F-actin. In this work, we describe some methodological protocols making possible to study, under controlled stimulus conditions, the local dynamic changes of F-actin in the cortical zone and also to detect the simultaneous displacements of chromaffin granules and organelles in active zones.

Key words LifeAct, F-actin cytoskeleton, Confocal microscopy, Chromaffin cells

1 Introduction

The transport of neurosecretory dense core vesicles is governed by filamentous actin (F-actin), a part of the cell cytoskeleton. The study of F-actin structural and dynamic changes requires microscopic techniques with a good signal/noise ratio like confocal fluorescence techniques [1]. Initial tools to study live images of the F-actin cytoskeleton, such as the expression of Actin-GFP fusion proteins, allowed to advance in the knowledge of F-actin structural dynamics although with some limitations. In this sense, the simultaneous use of transmitted light scanning and confocal fluorescent microscopy techniques demonstrated the relationship between the dynamics of the F-actin cytoskeleton and the movement of the granules in cultured bovine chromaffin cells depending on the state of rest or cellular stimulation, respectively [2].

Fortunately, a new functional tool called LifeAct was successfully tested to address limitations with previous fluorescent GFP-F-actin fusion proteins. LifeAct is a 17-amino-acid peptide that

Ricardo Borges (ed.), *Chromaffin Cells: Methods and Protocols*,
Methods in Molecular Biology, vol. 2565, https://doi.org/10.1007/978-1-0716-2671-9_20,

stained F-actin structures in eukaryotic cells without interfering with actin dynamics in vivo [3]. Using this tool, we were able to study not only the fine displacements of F-actin fibers at specific subplasmalemal points but the effects on cortical chromaffin granules and organelles motion under these cytoskeletal local changes using the appropriate specific markers (*see* Subheading 2.3) [4–6].

This article describes some methodological approaches to study mainly local dynamic events in the F-actin cortical network in bovine chromaffin cells but also the additional possibility of analyzing the effect in cortical chromaffin granule and organelle motion that underlie F-actin these cytoskeletal changes.

2 Materials

All solutions have to be prepared using purifying deionized water (sensitivity of 18 MΩ-cm at 25 °C) and analytical grade reagents. Prepare and store all reagents at 4 °C (unless indicated otherwise).

2.1 Adrenal Glands

Adrenal glands were obtained from an industrial slaughterhouse that is subject to strict regulations in accordance with European community guidelines. Glands were quickly transported in cold (4 °C) Locke buffer 1× to our laboratory.

2.2 Chromaffin Cells Reagents, Solutions, and Fungibles

1. Locke buffer 1×: 154 mM NaCl, 5.58 mM KCl, 3.6 mM $NaHCO_3$, 5.6 mM glucose, 5 mM HEPES, sterilized, adjusted to pH 7.4 and stored at 4 °C. It can be used up to 2 weeks.
2. Type A Collagenase Solution: Cold Locke buffer 1×, 0.25% Type A Collagenase, 0.5% BSA. Should be prepared immediately before use.
3. Diluted Percoll Continuous Gradient: Mix fresh 36 mL of Percoll Continuous Gradient with 4 mL of Locke buffer 1×. It should preferably be prepared 15 min before use and kept at 37 °C.
4. Dulbecco's Modified Eagle Medium (DMEM), stored at 4 °C.
5. Supplemented DMEM: DMEN supplemented with 10% fetal calf serum, 10 μM cytosine arabinoside, 10 μM 5-fluoro-2-′-deoxyuridine, 50 IU/mL penicillin, and 50 μg/mL streptomycin, stored at 4 °C. It can be used up to 2 weeks.
6. Petri dishes 35 mm in diameter.

2.3 Basal and Depolarizing Solutions

1. Krebs/HEPES (K/H) basal solution: 134 mM NaCl, 4.7 mM KCl, 1.2 mM KH_2PO_4, 1.2 mM $MgCl_2$, 2.5 mM $CaCl_2$, 11 mM glucose, 0.56 mM ascorbic acid, and 15 mM HEPES, pH 7.4.

2. Krebs/HEPES (high K) depolarizing solution: 80 mM NaCl, 59 mM KCl, 1.2 mM KH_2PO_4, 1.2 mM $MgCl_2$, 2.5 mM $CaCl_2$, 11 mM glucose, 0.56 mM ascorbic acid, and 15 mM HEPES, pH 7.4.

2.4 Fluorescent Protein Expression and Fluorochrome Dyes

1. eGFP-LifeAct (commercial plasmid: pCMV LifeAct-TagGFP2), like an example to analyze F-actin behavior [2].
2. NPY–mRFP (plasmid provided by Professor Dr. Takashi Tsuboi, Department of Life Sciences, University of Tokyo) as described elsewhere [7, 8].
3. Mitotracker-Red CMXRos [9].

2.5 DNA Electroporation Kit

Electroporation kit served to visualize the F-actin cytoskeleton and chromaffin granules in living primary mammalian neurons.

2.6 Perfusion System

One special support parallel to the stage of the confocal microscope with up to six 10-to 25-mL syringes suspended to ensure an appropriate gravimetric flow of the solutions contained in them (Fig. 1a).

Each syringe has a connected downstream duct whose flow would be regulated by a system of switched valves electronically operated to be opened alternately in a controlled manner ensuring a sustained flow of the solutions.

Both ducts flow into a mixer (Fig. 1b), which ends in a single final duct that flows into the perfusion tip (Fig. 1b). This entire system is regulated exactly by micrometric screws that ensure the correct positioning of the perfusion tip on the cells of the sample well (Fig. 1c).

2.7 Confocal Microscopy

Confocal laser system mounted on an inverted microscope incorporating a 100× PLAN-Apochromatic oil immersion objective with 1.45 NA. Excitation was achieved using a 488-nm argon laser 40 mW to excite eGFP or with a 543 nm He/Ne 10 mW to excite mRFP or Mitotracker Red FM.

We used single register mode for one fluorescent signal experiments or the sequential register mode for different fluorescent signals.

2.8 Data Analysis

All microscopy images were analyzed with Image J software using integrated measurements and plug-ins to measure the variations in distance and intensity (software downloaded from https://imagej.nih.gov/ij/).

Graphs were obtained with appropriate statistical and graphing software. Two-way ANOVA test was used to establish the significance of the experimental data. The data were expressed as the mean ± SEM values from experiments performed on single expansion and retraction events (n events), from at least three different cultures.

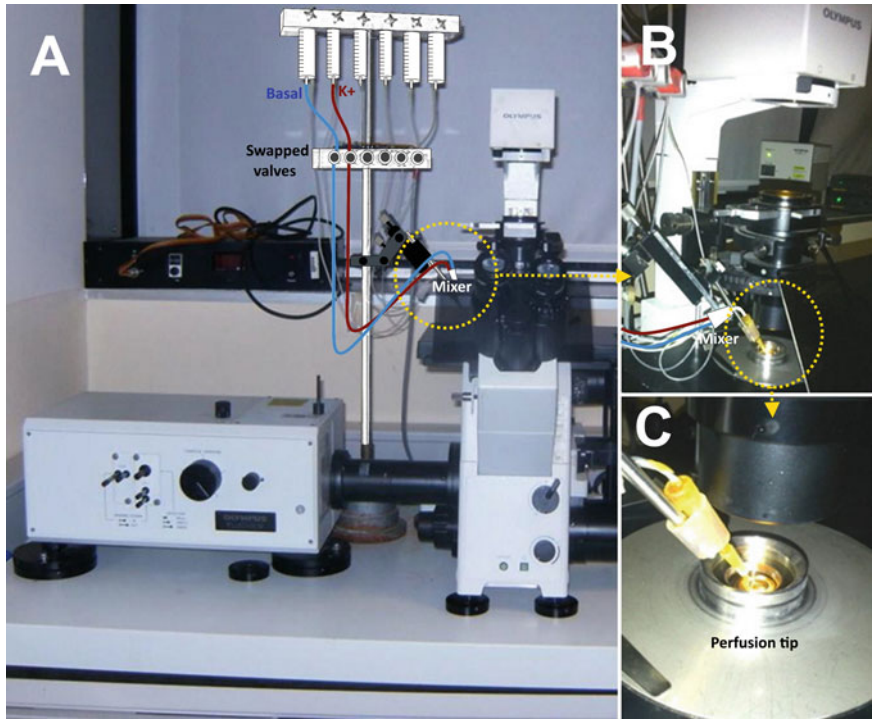

Fig. 1 Confocal microscope and perfusion system. Panel **a** shows the perfusion system that is parallel to the stage of the confocal microscope (Panel **a**). The mechanism has the ability to precisely change the position of the perfusion tip close to the sample without actually touching it (Panel **c**). The system offers the possibility of managing up to six different solutions that come together in a tube mixer collector (Panel **b**). In our experiments, we used only two solutions: basal (Panel **a**, blue line) and depolarizing (Panel **a**, brown line). Both solutions can be perfused in a swapped mode using a set of electronically controlled valves to activate and deactivate the release of each solution without affecting the perfusion flow. Thus, it is possible to maintain a constant flow during the selected time and regulate both the beginning and the end of each treatment at the same time that we define the beginning and the end of the recording of fluorescence images with the confocal in each experiment. This makes it possible to develop a sustained stimulation between 10 and 50 s of the recordings, that is, a stimulation of 40 s (stimulation protocol 10-40-10)

3 Methods

3.1 Isolation, Culture, and Transfection of Bovine Chromaffin Cells

1. Chromaffin cells are isolated from bovine adrenal glands using collagenase digestion and finally separated from debris and blood cells using a centrifugation in Percoll gradients as have been described before [10, 11].
2. Briefly, each gland should be trimmed of fat and perfused, using a syringe, via adrenal vein with 3–5 mL of Type A Collagenase Solution over a period of 15 min at 37 °C. This perfusion protocol should be repeated up to three times.

3. Each gland should be dissected using scissors and the exposed medulla scraped and disaggregated mechanically to obtain a cell homogenate.
4. The resulting solution should be resuspended with Locke buffer 1× (37 °C) and successively filtered using first a sieve of 217 micrometers diameter and a second one of 82 micrometer diameter.
5. The resulting filtered cell suspension should be added to a Locke buffer 1× to a final volume of 200 mL and centrifuged once (100 × g for 5 min) in Locke buffer 1× at room temperature to wash out collagenase.
6. Cell pellets obtained should be then resuspended using Locke buffer 1× up to a final volume of 42 mL and mixed with 38 mL of Diluted Percoll Continuous Gradient.
7. The last mixed suspension should be centrifuged for 22 min at 37 °C in an appropriate rotor at 21,000 × g.
8. After centrifugation, cells equilibrating between densities of 1.045 and 1.075 g/mL must be collected. This gradient fraction contained chromaffin cells without blood cells and debris.
9. The isolated chromaffin cells should be washed twice by centrifugation (100 × g for 5 min) in Locke buffer 1× at room temperature.
10. Isolated cells should be harvested and resuspended with 10 mL of Dulbecco's Modified Eagle Medium (DMEM) and counted in a Neubauer chamber to estimate cell number and concentration.
11. To obtain transfected cells, aliquots containing 5 million of isolated chromaffin cells (from **step 3**) must be transfected with appropriate DNA.
12. When we wanted to perform dynamic studies of the F-actin cytoskeleton only, we should perform a simple transfection using 1–3 μg of eGFP-LifeAct DNA expression plasmid alone.
13. When we wanted to include in the study not only the dynamic changes of the F-actin cytoskeleton but also the dynamic effects of these changes on the chromaffin granules, we should perform a double transfection using both 1.5 μg of eGFP-LifeAct and 1.5 μg NPY–mRFP DNAs (*see* **Note 2**).
14. The transfection protocol should be performed using the Amaxa Basic Nucleofector kit for primary mammalian neuronal cells according to the manufacturer's instructions (Program O-005, Amaxa).
15. Transfected cells should be plated in 35-mm Petri dishes as monolayer cultures with Dulbecco's Modified Eagle Medium (DMEM) supplemented (150,000 cells/cm^2) and transferred

to a culture incubator 37 °C 5% CO_2. Transfected cells could be used between the second and fourth day after plating.

3.2 Fluorochrome Mitochondrial Labeling

1. To be able to study the underlying behavior of organelles such as mitochondria linked to dynamic changes of the F-actin cytoskeleton, we must use cells expressing eGFP-LifeAct, after 2 or 4 days from transfection (from Subheading 3.1, **step 15**), and then they should be incubated with Mitotracker-Red CMXRos, following the procedure advised by the manufacturer (*see* **Note 3**).
2. Briefly, in each 35-mm Petri dish containing eGFP-LifeAct-expressing cells, culture media should be replaced with Krebs/HEPES (K/H) basal solution.
3. To stain a population of mitochondria for dynamic experiments, we must incubate 15 min at room temperature under darkness with Mitotracker-Red CMXRos. Working solution (1 μM).
4. After incubation, samples should be washed twice with Krebs/HEPES (K/H) basal solution to washout marker excess [12].

3.3 Dynamic Confocal Experiments-1: Expansions and Retractions

1. Petri dishes containing cells expressing eGFP-LifeAct alone, eGFP-LifeAct/NPY-mRFP or eGFP-LifeAct/Mitotracker-Red CMXRos labeled, must be mounted into a sample plate using Krebs/HEPES (K/H) basal solution.
2. The sample plate should be placed on the support of the confocal microscope and the perfusion system adjusted for optimal control of basal or stimulating conditions in a sustained way (Fig. 1).
3. Our stimulation protocol, called 10-40-10, must be as follows: 10 s under perfusion with Krebs/HEPES (K/H) basal solution (control conditions), change to perfusion for 40 s with Krebs/HEPES (High K) depolarizing solution (stimulating conditions), and finally 10 s again with Krebs/HEPES (K/H) basal solution (return to control condition). Our perfusion system must be able to maintain a steady flow throughout the protocol. All tests must be performed at 30 °C to evoke the highest effect [6]. This protocol could be modified using other stimulation mechanisms to complement our studies on F-actin cytoskeletal dynamics (*see* **Note 1**).
4. After locating appropriate cells (emission in green for eGFP-LifeAct only, or emission both in green and red for eGFP-LifeAct/NPY-mRFP or eGFP-LifeAct/Mitotracker-Red CMXRos; *see* Subheading 2.6), we must proceed to focus them on a cellular equatorial Z plane to observe in detail at the same time the cortical boundaries of the F-actin cytoskeleton that surround the cell, the cytoplasm, and the cell nucleus

(this lasts as a reference point). To improve the acquisition, the magnification should be increased up to 5×.

5. The stimulation 10-40-10 protocol should be initiated in each type of experiment obtaining image recordings of every second during the 60 s lasting the experimental procedure.

3.4 Data Analysis of Expansions and Retractions

1. Time-lapse records should be analyzed using Image J software to identify, measure, and classify local events at the cortical part of these cells.
2. If we analyzed the test with eGFP-LifeAct alone, we could observe basically two large groups of behaviors of F-actin fibers during these dynamic processes. One group would be characterized by an outstanding movement of the fibers as a local type pushing mechanism toward the extracellular medium (Fig. 2a). The other group could be defined by processes of fiber retraction at specific points of the cortical network, as a mechanism of internalization or displacement to a more internal point in the cellular cytoplasm (Fig. 2c).
3. The first of these events could be defined as expansions, while the s could be classified under the term retractions.
4. Displacements should be quantified by means of total distance values between an internal static point (defined in the nuclear profile, not shown) and the profile line (Fig. 2d, e, yellow dot line) of the F-actin cortical network in the active zones for both types of events at the different study periods of the 10-40-10 stimulus protocol: first 10 s, next 40 s, and last 10 s. Subsequently, these total distance data between two points could be converted into distance variations in the time of the network profile line to observe the net displacement of the fibers in each event in response to stimulus. For this conversion, we should perform a subtraction of each of the distances obtained in time with respect to the corresponding one for first 10 s (before stimulus). Results from distance variations should be analyzed independently according to the type of event (expansions and retractions) and averaged separately.
5. The average of data obtained can demonstrate the existence of a local displacement of the network outward (expansion), or inward (retraction), in response to the depolarizing stimulus. The distance from the initial position of the fibers (at 5 s after start of the 10-40-10 protocol) would reach gradually a maximum or minimum value around 20 s after the start of the stimulus (30 s from the start). Interestingly, when the stimulus ceased (last 10 s, 55 s from the start), the fibers began to return to their original position proving the transitory nature of these local dynamics (Fig. 2d, e) [6].

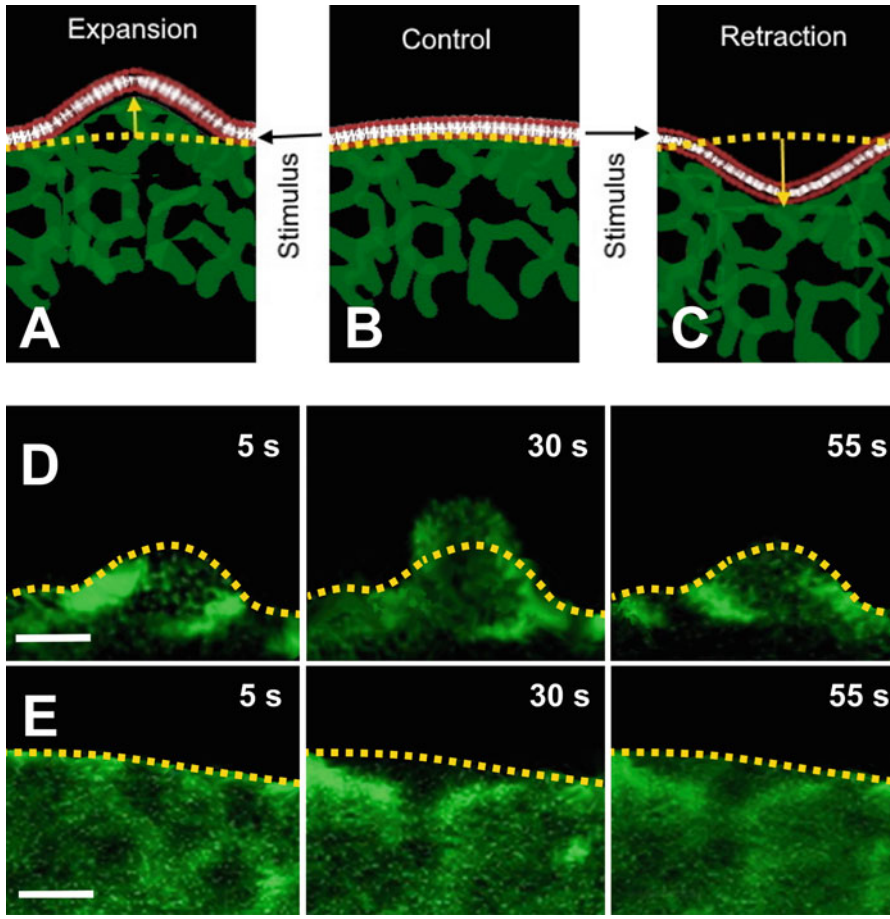

Fig. 2 Net displacements of the F-actin cortical network during expansions and retractions events during stimulation of bovine chromaffin cells. Model of expansions (**a**) and retractions (**c**) of cortical cytoskeleton after a high-potassium stimulus. Yellow dotted lines show the initial position of cortical F-actin before stimulus (**b**). Confocal fluorescence microscopy images of a temporal sequence at 5 s (prior to stimulation), 30 s (during stimulation), and 55 s (after stimulation) for an expansion (panel **d**) and a retraction (panel **e**) of an isolated cell with double eGFP-LifeAct transfection (green) using 10-40-10 stimulation protocol (*see* Subheading 3.2, **step 3**). The yellow dotted lines represent the position of the F-actin profile at 5 s (prior to stimulation). Bars represent 1 μm

6. If we analyzed the test with both eGFP-LifeAct and NPY-mRFP using the same protocol showed before (*see* **step 3**), to also estimate dense granules displacements (*see* **Note 2**), we could also observe two large groups of behavior in chromaffin granules subsequent to expansion (Fig. 3a), or retraction events (Fig. 3b), of F-actin fibers.
7. Similar assays could be obtained using eGFP-LifeAct and Mitotracker-Red CMXRos and quantifying mitochondrial displacement (*see* **Note 3**) associated with cytoskeletal expansion or retraction events (not shown).

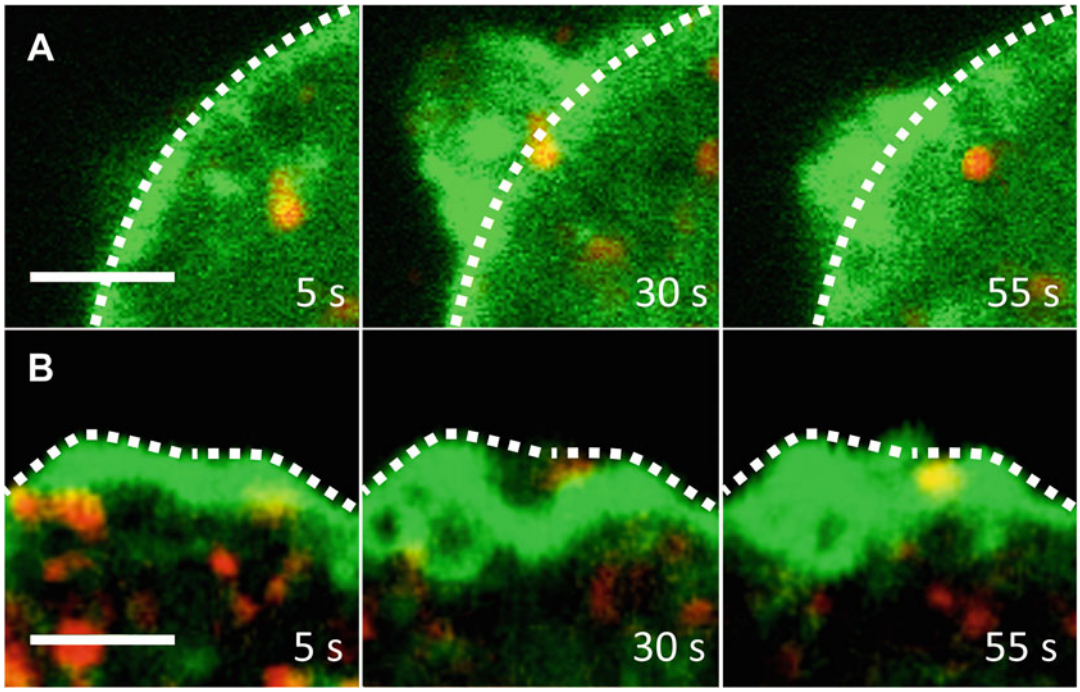

Fig. 3 F-actin and vesicular displacements in areas of expansions and retractions in bovine chromaffin cells. (**a** and **b**) Confocal fluorescence microscopy images of a model temporal sequence at 5 s (prior to stimulation), 30 s (during stimulation), and 55 s (after stimulation) for an expansion (**a**) and a retraction (**b**) of an isolated cell with double eGFP-LifeAct transfection (green) and NPY-mRFP (red) using 10-40-10 stimulation protocol (*see* Subheading 3.2, **step 3**). The white dotted lines represent the position of the F-actin profile at 5 s (prior to stimulation). Bars represent 1 μm

3.5 Dynamic Confocal Experiments-2: F-Actin Tail Comets

1. F-actin tail comets have been morphologically characterized in multiple cell systems as structures with a high degree of fiber alignment at their peripheries [13] and a high density in internal F-actin microfilaments crisscrossed within them [14]. Functionally, they were proposed as authentic cellular propulsion systems of organelles [15, 16]. Recently, our research group managed to observe and analyze some examples of these F-actin tail comets in isolated chromaffin cells [6]. Next, we will describe a methodology that could be used to analyze the dynamics of these special F-actin structures.
2. Bovine chromaffin cells doubly transfected with the eGFP-LifeAct and NPY-mRFP vectors (*see* Subheading 3.1) should be subjected to a 10-40-10 stimulation protocol at 30 °C as we described above.
3. After locating appropriate cells (emission both in green and red for eGFP-LifeAct/NPY-mRFP or eGFP-LifeAct/Mitotracker-Red CMXRos; *see* Subheading 2.6), we could proceed to focus them on two possible planes: first a cellular equatorial Z plane

to observe in detail at the same time the cortical boundaries of the F-actin cytoskeleton that surround the cell, the cytoplasm, and the cell nucleus (this lasts as a reference point) and second, a cellular polar Z plane (top) to observe the upper boundaries of the F-actin cytoskeleton and the immediately adjacent sub-plasmalemmal space. To improve the acquisition, the magnification was increased up to 5×.

4. We should use a 10-40-10 stimulation protocol (*see* Subheading 3.3). Data should be acquired in a sequential mode for two fluorescent signals (eGFP-LifeAct and NPY-mRFP) in order to avoid channel cross talk. Records must be obtained using time lapse every second during the 60 s of the procedure.

3.6 Data Analysis of F-Actin Tail Comets

1. During our investigations, we could detect some F-actin tail comets moving in the cellular equatorial Z plane. These comets showed two structural components: F-actin comet tails (tagged with eGFP-LifeAct) and the vesicular head of the comet (tagged with NPY-mRFP). To analyze each XY path, fluorescent image thresholds must be established to determine spatial position of each particle centroid in time-lapse studies (Fig. 4a). The XY trajectories should be analyzed to calculate vectors, the displacement vectors, and the mean speeds under the conditions of each test. In our experience, the measured displacements of both structural components usually show similar orientation and shared sections (colocation), which seems to be the consequent of a joint movement of both (Fig. 4c) [6].
2. This joint movement could also be observed for the XY trajectories of comets located in cellular polar Z planes (top) (Fig. 4b). In a special way, it is possible to perform a space-time reconstruction XYT of an F-actin tail comet model and its joined vesicular head (Fig. 4d). In our experience, this XYT reconstructions could show that this joint motion of F-actin and vesicles developed in a spiralized and nonlinear way [6]. The observed spiralization could be the result of the physical properties of thrust by polymerization of F-actin.
3. The results obtained could link the F-actin tail comets like a special phenomenon of vesicular propulsion but in this case linked to the transport of chromaffin granules [15, 16].

4 Notes

1. To complement these studies, we could analyze other stimulation mechanism like acetylcholine using Krebs/HEPES Ach-stimulating solution: 10 μM acetylcholine, 134 mM NaCl, 4.7 mM KCl, 1.2 mM KH_2PO_4, 1.5 mM $MgCl_2$,

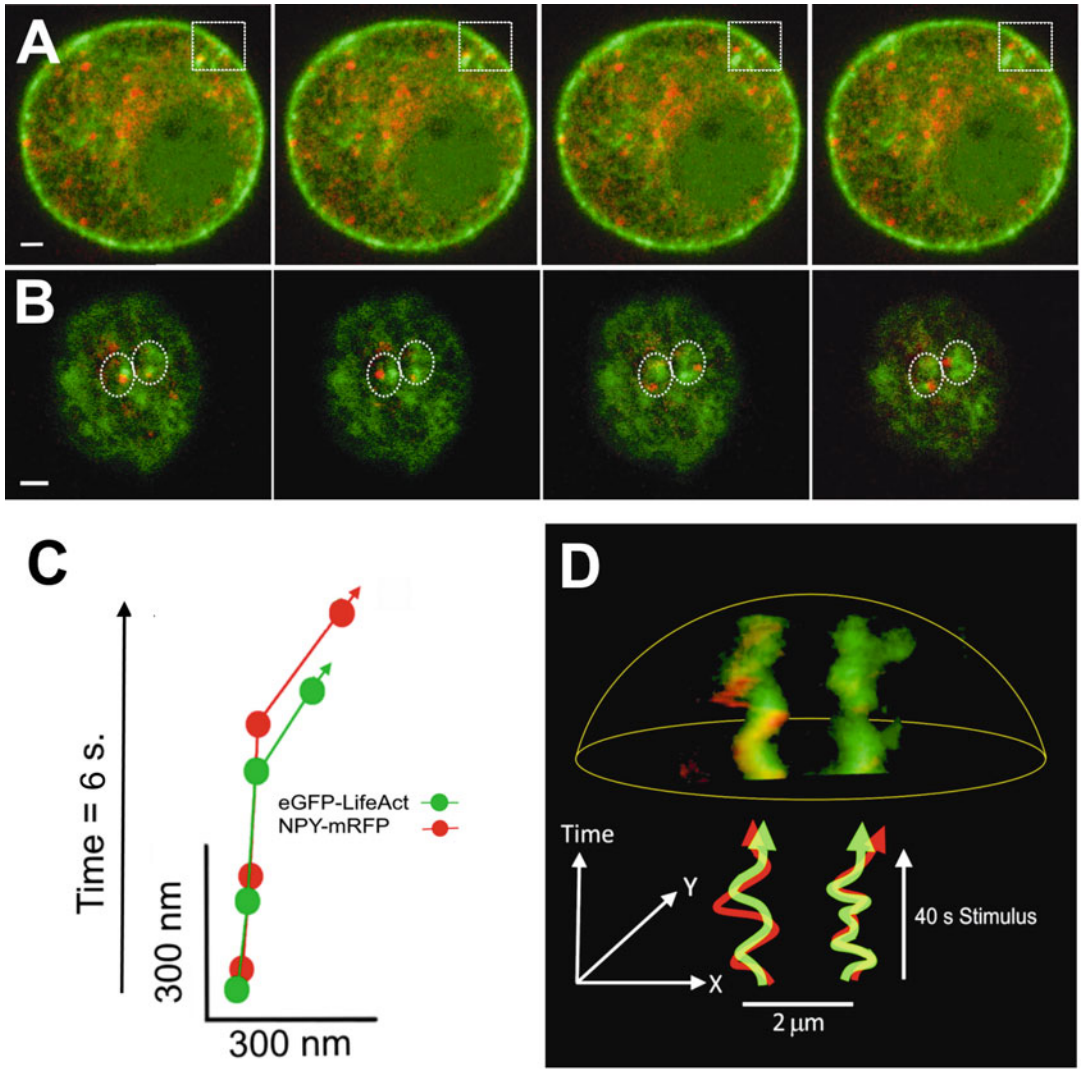

Fig. 4 Evolution, trajectory, and displacement model for F-actin tail comets in a bovine chromaffin cell. Panel **a**, temporal sequence of fluorescence confocal microscopy images of an equatorial plane of an isolated cell transfected with the vector eGFP-LifeAct (green) and NPY-mRFP (red) stimulated with Krebs/HEPES (High K) depolarizing solution at 30 °C. The images correspond to a time interval of 2.2 s. The white square identifies the region of comet event. Panel **b**, confocal microscopy image of fluorescence in polar plane "top" of an isolated cell with double transfection of the vector eGFP-LifeAct (green) and NPY-mRFP (red) stimulated with Krebs/HEPES (high K) depolarizing solution at 30 °C. The white circles mark two model comets. Panel **c**, XY trajectories of F-actin (green) and vesicle (red) for the comet detected in cellular equatorial plane (Panel **a**) during stimulation time. Time jumps of 2.2 s for a total represented distance of 700 nm (6.6 s). Panel **d**, XYT reconstruction of F-actin (green) and vesicle (red) for the two comets detected in the polar cellular plane (Panel **b**) during the stimulation time. Bars represent 1 μm

2.5 mM $CaCl_2$, 11 mM glucose, 0.56 mM ascorbic acid, and 15 mM Na-HEPES, pH 7.4. The perfusion and stimulating protocol could be the same named 10-40-10 except for the

replacement of depolarizing solution by Ach-stimulating solution.

2. If we need to correlate both cytoskeleton and chromaffin vesicle dynamics in this cellular model, dense core vesicles can be labeled by NPY–mRFP plasmid transfection (plasmid provided by Professor Dr. Takashi Tsuboi, Department of Life Sciences, University of Tokyo) as described elsewhere [7, 8]. We should perform a double DNA transfection using the AMAXA protocol with 2 micrograms of eGFP-LifeAct and 2 micrograms of mRFP-NPY. Assay protocol could be like that described in 2.9 except for a sequential acquisition using a 488 nm argon ion 40 mW to excite eGFP and a 543 nm He/Ne 10 mW for RF. Finally, the analysis of the data would involve an additional analysis of the displacement of the centroid of the vesicles marked with mRFP-NPY with respect to the reference of the cytoskeleton in the area of the expansion or retraction events (not shown) [6].
3. In the case that we need to visualize the behavior of organelles such as mitochondria, we can use specific markers such as Mitotracker-Red CMXRos. This procedure would require prior marking with Mitotracker-Red CMXRos following the procedure advised by the manufacturer. The procedure of stimulation and subsequent analysis of results would be the same as described in Point 2 of this section [12].

Acknowledgments

This work was supported by grants from the Spanish Ministerio de Ciencia e Innovación (PID2020-114824GB-I00, MINECO, FEDER, UE) to LMG.

References

1. Trifaro JM, Gasman S, Gutiérrez LM (2008) Cytoskeletal control of vesicle transport and exocytosis in chromaffin cells. Acta Physiol 192:165–172. https://doi.org/10.1111/j.1748-1716.2007.01808.x
2. Giner D et al (2005) Real-time dynamics of the F-actin cytoskeleton during secretion from chromaffin cells. J Cell Sci 118(Pt 13): 2871–2880
3. Riedl J et al (2008) Lifeact: a versatile marker to visualize F-actin. Nat Methods 5(7): 605–607. https://doi.org/10.1038/nmeth.1220
4. Meunier FA, Gutiérrez LM (2016) Captivating new roles of F-actin cortex in exocytosis and bulk endocytosis in neurosecretory cells. Trends Neurosci 39:605–613. https://doi.org/10.1016/j.tins.2016.07.003
5. Villanueva J, Giménez-Molina Y, Viniegra S, Gutiérrez LM (2016) F-actin cytoskeleton and the fate of organelles in chromaffin cells. J Neurochem 137:860–866. https://doi.org/10.1111/jnc.13560
6. Giménez-Molina Y, Villanueva J, Francés MDM, Viniegra S, Gutiérrez LM (2018) Multiple mechanisms driving F-actin-dependent transport of organelles to and from secretory sites in bovine chromaffin cells. Front Cell Neurosci 12:344

7. Taraska JW, Perrais D, Ohara-Imaizumi M, Nagamatsu S, Almers W (2003) Secretory granules are recaptured largely intact after stimulated exocytosis in cultured endocrine cells. PNAS 100(4):2070–2075. https://doi.org/10.1073/pnas.0337526100
8. Aoki R, Kitaguchi T, Oya M, Yanagihara Y, Sato M, Miyawaki A et al (2010) Duration of fusion pore opening and the amount of hormone released are regulated by myosin II during kiss-and-run exocytosis. Biochem J 429: 497–504. https://doi.org/10.1042/BJ20091839
9. Poot M, Pierce RH (1999) Detection of changes in mitochondrial function during apoptosis by simultaneous staining with multiple fluorescent dyes and correlated multiparameter flow cytometry. Cytometry 38:311–317
10. Gil A, Gutiérrez LM, Carrasco-Serrano C, Alonso MT, Viniegra S, Criado M (2002) Modifications in the C terminus of the synaptosome-associated protein of 25 kDa (SNAP-25) and in the complementary region of synaptobrevin affect the final steps of exocytosis. J Biol Chem 277:9904–9910
11. Almazan G, Aunis D, Garcia AG et al (1984) Effects of collagenase on the release of [3H]-noradrenaline from bovine cultured adrenal chromaffin cells. Br J Pharmacol 81: 599–610
12. Villanueva J, Viniegra S, Giménez-Molina Y, García-Martinez V, Expósito-Romero G, del Mar FM, García-Sancho J, Gutiérrez LM (2014) The position of mitochondria and ER in relation to that of the secretory sites in chromaffin cells. J Cell Sci 127(Pt 23):5105–5114. https://doi.org/10.1242/jcs.160242
13. Zhukarev V, Ashton F, Sanger JM, Sanger JW, Shuman H (1995) Organization and structure of actin filament bundles in Listeria-infected cells. Cell Motil Cytoskeleton 30:229–246
14. Cameron LA, Svitkina TM, Vignjevic D, Theriot JA, Borisy GG (2001) Dendritic organization of actin comet tails. Curr Biol 11:130–135
15. Taunton J, Rowning BA, Coughlin ML, Wu M, Moon RT, Mitchison TJ, Larabell CA (2000) Actin-dependent propulsion of endosomes and lysosomes by recruitment of N-WASP. J Cell Biol 148:519–530
16. Temm-Grove CJ, Jockusch BM, Rohde M, Niebuhr K, Chakraborty T, Wehland J (1994) Exploitation of microfilament proteins by listeria monocytogenes: microvillus-like composition of the comet tails and vectorial spreading in polarized epithelial sheets. J Cell Sci 107 (Pt 10):2951–2960

Chapter 21

Unveiling the Nanoscale Dynamics of the Exocytic Machinery in Chromaffin Cells with Single-Molecule Imaging

Adekunle T. Bademosi and Frédéric A. Meunier

Abstract

Neuronal and hormonal communication relies on the exocytic fusion of vesicles containing neurotransmitters and hormones with the plasma membrane. This process is tightly regulated by key protein–protein and protein–lipid interactions and culminates in the soluble *N*-ethylmaleimide-sensitive factor attachment protein receptor (SNARE) complex formation and zippering that promotes vesicular fusion. Located on both sides of the vesicle and the plasma membrane, the zippering of the SNARE complex acts to overcome the energy barrier afforded by the repulsive electrostatic force stemming from apposing two negatively charged phospholipid membranes. Another component opposing the timely organization of the fusion machinery is thermal Brownian energy that tends to homogenize all cellular molecules by constantly switching their motions and directions through short-lived molecular interactions. Much less is known of the mechanisms counteracting these chaotic forces, allowing seamless cellular functions such as exocytic fusion. Super-resolution microscopy techniques such as single-molecule imaging have proven useful to start uncovering these nanoscale mechanisms. Here, we used single-particle tracking photoactivatable localization microscopy (sptPALM) to track syntaxin-1-mEos, a SNARE protein located on the plasma membrane of cultured bovine chromaffin cells. We demonstrate that syntaxin-1-mEos undergoes dramatic change in its mobility in response to secretagogue stimulation leading to increased nanoclustering. These nanoclusters are transient in nature and likely to provide docked vesicles with a molecular environment conducive to exocytic fusion.

Key words sptPALM, Nanoclusters, Syntaxin-1, SNARE, Chromaffin cells

1 Introduction

Single-molecule imaging (*also termed single-particle tracking* (spt)) has become an established method of choice to unravel the molecular dynamics that guide and regulate cellular homeostatic functions such as exocytosis [1–3], endocytosis [4–6], autophagy [7–10], and synaptic plasticity [11]. The earliest applications of spt investigated the soluble N-ethylmaleimide-sensitive factor attachment receptor (SNARE) proteins as well as their regulators. Using

Ricardo Borges (ed.), *Chromaffin Cells: Methods and Protocols*,
Methods in Molecular Biology, vol. 2565, https://doi.org/10.1007/978-1-0716-2671-9_21,

quantum dots, the Triller laboratory revealed by spt that the SNARE protein syntaxin-1 exhibits compartment-specific mobility, which is decreased within synapses compared to extra-synaptic areas [12]. Earlier studies carried out in fixed cells demonstrated that syntaxin-1 is organized into nanoscale-sized clusters (hereafter termed nanodomains) and that interactions mediated by the SNARE motif of syntaxin-1 were essential for this clustering [13, 14]. To provide a more detailed organization of single SNARE proteins, the Ashery group used the super-resolution imaging method, direct stochastic optical reconstruction microscopy (*d*STORM), to unveil the localization and the organization of syntaxin-1 and its partner SNARE protein-synaptosomal-associated protein, 25 kDa (SNAP-25) in PC12 cells [15]. This study highlighted in detail the organization of these SNARE proteins into nanodomains, their shape, the varying size distribution, and the density gradient of packed molecules within them.

To further probe into the dynamics of these proteins at nanoscale resolution, the Duncan group used photoactivatable localization microscopy (PALM) as well as single-particle tracking PALM (sptPALM) by tagging photoactivatable mCherry to syntaxin-1 and its cognate protein Munc18-1. They revealed a heterogeneous distribution and diffusional behaviors of these proteins on the plasma membrane [1]. Further, they indicated that Munc18-1 molecules exhibit two distinct dynamic movement: a slower population indicative of its binding to membrane-bound syntaxin-1 and a faster unbound population. A work that applied fluorescence nanoscopy with photon-limited spatial resolution in neurons showed that preassembled SNARE complexes containing "zippered" syntaxin-1 and SNAP-25 (needed to overcome the energy barrier between the vesicle's membrane and the plasma membrane) also had Munc18-1 associated [16].

By using sptPALM with the photoconvertible fluorescent protein mEos2 [17] to image wild-type Munc18-1 as well as priming-deficient Munc18-1 mutant (Munc18-1$^{\Delta 317\text{-}333}$) and using universal point accumulation in nanoscale topography (uPAINT) to image syntaxin-1-GFP in PC12 cells engineered to knockdown Munc18-1/2 (DKD-PC12 cells), we examined the exocytosis-induced changes in the organization and dynamics of these proteins [18]. We showed that syntaxin-1 is recruited into nanodomains, and Munc18-1 exits similar overlapping nanodomains in an activity-dependent manner. This engagement of syntaxin-1 into the nanodomains is dependent on the priming role of the Munc18 domain 3a loop region (residues 317-333) [18–21]. We further showed that botulinum neurotoxin type E light chain (BoNT/E-LC), which cleaves SNAP-25 thereby preventing SNARE complex assembly [22], blocks the activity-dependent decrease in syntaxin-1 mobility associated with the onset of exocytosis. This immobilization, therefore, most likely results from

syntaxin-1 recruitment during SNARE complex assembly. Hence, by applying spt techniques, we highlight how critical change in syntaxin-1 nanoscale dynamics is associated with its main function in neurosecretory cells, which is to mediate SNARE complex formation and promote the fusion of secretory vesicles underpinning neurotransmitter release [23].

A caveat to all these studies is that they were carried out either in neurosecretory cells (whose large dense core vesicles (LDCV) release does not necessarily reflect the mechanistic nature of synaptic vesicle release in neuronal synapses) or in cultured neurons (that are not necessarily fully representative of neuronal synapses in a live animals). To address this deficiency, we examined the nanoscale organization and dynamics of syntaxin-1 in the neuromuscular junction (NMJ) of transgenic syntaxin-1-mEos2 expressing live third instar *Drosophila* larva [3, 24]. By using sptPALM in oblique illumination of the sample in combination with either thermogenetic or optogenetic induction of presynaptic activity, we showed that syntaxin-1 is also organized in nanodomains in live NMJs and that neuronal stimulation increases its mobility driving syntaxin-1 molecules out of these clusters. Our use of the *Drosophila* N-ethylmaleimide-sensitive factor (NSF) mutant (comatose), to prevent disassembly of the SNARE complex after vesicular fusion, and the tetanus toxin light chain (TeTx/LC) expression, to cleave VAMP2 and prevent SNARE complex formation, further indicated that at least some of these clusters were present at the interface between the plasma membrane and docked synaptic vesicles. Interestingly, we observed that upon inhibition of the SNARE complex formation by TeTx/LC, the mobility of syntaxin-1 in live synapses was similar to that found in neurosecretory cells [3]. This strengthens our earlier observation that the level of mobility of single syntaxin-1 molecules is indicative of its function as well as its association with other proteins in the exocytic machinery.

Despite these unique insights provided by investigating the vesicle-release machinery at single-molecule resolution in live neuronal synapses, neurosecretory cells still provide an easily accessible interface to perturb the exocytic proteins crucial in investigating neuronal transmission. For example, we have identified the cortical actin meshwork in chromaffin cells as a dynamic "casting net" that undergoes activity-dependent relaxation that is crucial for delivering secretory vesicles to the plasma membrane [25]. We showed that actin polymerization under the control of phosphatidylinositol (4,5)bisphosphate mediates the translocation of secretory vesicles to the plasma membrane of chromaffin cells [26]. Interestingly, transmembrane proteins such as syntaxin-1 have been proposed to be bound within "pickets" and "fences" created by this cortical actin meshwork and to undergo hop diffusion between compartments created by these "pickets" [27, 28]. The expectation, therefore, is that the increased fusion of vesicles during secretagogue

stimulation of chromaffin cells will elicit increased confinement of syntaxin-1 at the plasma membrane due to increased formation of SNARE complexes and due to increased enclosure within the pickets of the now relaxed cortical actin network.

In this chapter, we describe our methods to culture bovine chromaffin cells, to transfect the cells with mEos2-tagged syntaxin-1, and to examine how inhibition of actin polymerization affects the mobility of syntaxin-1. Since the inhibition of actin polymerization (by cytochalasin D) is associated with decreased vesicular translocation to the plasma membrane and slower fusion of secretory vesicles in chromaffin cells [26, 29], we anticipate that the vesicle docking and priming-mediated confinement of syntaxin-1 during elevated activity will be attenuated in cells treated with cytochalasin D. In addition, we describe our methods to image single-molecules of syntaxin-1-mEos2 in the plasma membrane of these cells and our analytical methods using PALMTracer a customized software plugin written in the environment of Metamorph (Molecular Devices) [30, 31] to quantify the dynamic movement of the proteins at nanoscale resolution. Further, we describe our use of a recently developed in-house analytical tool that allows for in-depth spatiotemporal analysis of nanodomains [32].

2 Materials

2.1 Chromaffin Cell Culture

Reagents to be used for chromaffin cells dissociation include:

1. Buffer A: 145 mM NaCl, 5 mM KCl, 1.2 mM Na_2HPO_4, 20 mM HEPES-NaOH, pH 7.4.
2. Protease solution buffer A: 10 mM glucose, 0.2% protease.
3. Collagenase solution buffer A: 10 mM glucose, 12.5 mM collagenase.
4. Glucose solution buffer A: 6 mM glucose.
5. Dulbecco's Modified Eagle Medium (DMEM) supplemented with 10% serum supreme, 2.5 μg/mL fungizone, 50 μg/mL gentamycin, and 10 mM HEPES.
6. 2-mL syringe.
7. 29-mm glass-bottom imaging dishes (Cell Vis, D29-14-1.5-N).
8. Water bath.
9. Surgical instruments scissors and scalpel.
10. 250-mL flask.
11. 50-mL falcon tube.
12. Muslin filter (250 μm).

13. A hemacytometer.
14. Centrifuge machine.

2.2 Transfection (Electroporation)

Cells can be transfected by electroporation using:

1. Amaxa Nucleofector Kits (Lonza) that includes the Nucleofector solution (Lonza) and the Nucleofector device (Lonza).
2. Cuvettes (Sigma-Aldrich-Z706086, 0.2 cm gap).
3. Eppendorf tubes.
4. The plasmid to be transfected.

2.3 Imaging Buffer

1. Buffer A: 145 mM NaCl, 5 mM KCl, 1.2 mM Na_2HPO_4, 20 mM HEPES-NaOH, pH 7.4, and 10 mM glucose.
2. Water bath (37 °C).
3. Sterile filter unit (0.22 μM, Millex).
4. Cytochalasin D (4 μM): Dissolved in dimethyl sulfoxide (DMSO).

2.4 Microscope Setup for Imaging

For live-cell super-resolution microscopy imaging:

1. Transfected chromaffin cells plated on glass-bottom imaging dishes are imaged at 37 °C in total internal reflection fluorescence (TIRF) mode of illumination. This can be done using a custom-built TIRF microscope.
2. We recommend use of a Roper Scientific iLas^2 Ring-TIRF microscope fitted with:
3. A CFI Apo 100×/1.49 numerical aperture oil-immersion objective (Nikon Instruments).
4. An Evolve 512 delta electron-multiplying charge-coupled device (EMCCD) camera (Photometrics).
5. A Perfect Focus System (PFS (Nikon Instruments)).
6. An iLas^2 double-laser illuminator for 360° TIRF illumination (Roper Scientific).
7. A laser dichroic QUAD Beam-splitter (LF405/488/561/635 (Semrock)).
8. The appropriate laser set, namely, 405 nm, 488 nm, and 561 nm lasers (100 mW).
9. A Oko Touch (Okolab) controller to regulate the temperature and CO_2 access of the imaging dishes.
10. A desktop computer installed with Metamorph software (Molecular Devices) for image acquisition.
11. Tetraspeck™ microspheres (Thermo Fisher) for TIRF angle calibration.

12. Alternately, the ELYRA PS.1 microscope (Zeiss) with a α Plan-Apochromat 100×/1.49 numerical aperture oil-immersion objective and a sensitive EMCCD camera can be used. Image acquisition can be done using the Zen Black acquisition software (Carl Zeiss).
13. Polyethylene tubing (Microtube Extrusions) and 1250-μL syringe (GILSON) to help deliver chemical stimulant unto the imaging dish during data acquisition.

2.5 Software for Data Analysis

1. Acquired single-molecule imaging data can be analyzed with suitable single-molecule tracking analytical software [24, 33, 34].
2. PALMTracer 2 (version 2.0.4.17780) customized for use on Metamorph software (Molecular Devices) is suitable to analyze the acquired data [33, 35].
3. Nanoscale spatiotemporal indexing clustering (NASTIC) [32] implemented on Python graphic user interface is suitable to provide in-depth spatiotemporal analysis of the acquired data.

3 Methods

3.1 Chromaffin Cell Preparation

In a laminar flow hood, the chromaffin cells can be isolated through protease digestion of bovine adrenal glands irrespective of gender of the cattle as previously described [36, 37]. The different solutions that help isolate the cells are to be filter-sterilized on the day of the procedure prior to commencing cell dissociation.

1. Keep the excised bovine adrenal glands collected from bovine abattoir on ice-cold buffer A supplemented with fungizone.
2. Remove the excess exterior fat, arteries, veins, and connective tissue from the adrenal glands using large scissors.
3. Perfuse the adrenal vein with 3 mL of protease solution using a 10-mL syringe until the gland is free of blood, and then place the gland in a sterile 250-mL beaker.
4. Once all the glands are perfused, cover the beaker with foil and place it in a water bath at 37 °C for 15–17 min.
5. Using a sterile scissor, cut the adrenal glands longitudinally along the axis of the gland from the adrenal vein.
6. Use a sterile scalpel to remove the lower portion of the medulla from the cortex of the gland, and place it in a sterile 250-mL spinner flask that contains collagenase solution.
7. Once all the medullar portion has been removed, seal the cap of the flask with parafilm, and place the flask on a shaker (speed 250, duration 25 min, and temperature 37 °C).

8. Filter the extracted collagenase–medulla solution mixture through a sterile muslin filter (250 μm) into a sterile 250-mL beaker.
9. Transfer the filtrate into a sterile 50-mL falcon tube and centrifuge at 1200 rpm for 9 min.
10. Resuspend and centrifuge (without filtering) until the supernatant is very clear. We recommend repeating this step at least two or more times.
11. Remove and discard the supernatant, and then resuspend the cell pellet initially in 1 mL of DMEM solution. After getting an even distribution of chromaffin cells, DMEM solution, add an extra 9 mL of DMEM.
12. Filter this solution through a single layer of muslin and count the cells in a clean hemacytometer. Add additional DMEM media as needed and transfect the cells with plasmid of choice.

3.2 Transfection of Chromaffin Cells

Select the appropriate electroporation program on the Nucleofector device. Label two Eppendorf tubes (1.5 mL) for each transfection. The first is to be used for the chromaffin cells, while the second is to be used of the Nucleofector solution.

1. Introduce 2.5 million cells into the first tube (ideally less than 1 mL in volume).
2. Add 100 μL of Nucleofector solution into the second Eppendorf tube, and add 2–4 μg of the plasmid of choice as well into the same tube. We recommend adjusting the concentration of the plasmid if you are doing a double or triple transfection into the same cells (total DNA concentration should not exceed 4 μg).
3. Spin the cells at 1000 rpm for 1 min, and aspirate the supernatant carefully without displacing the cell pellet.
4. To ensure all DMEM is removed, resuspend the cell pellet in Opti-MEM, then spin again at 1000 rpm, and discard the supernatant without displacing the cell pellet.
5. Resuspend the cell pellet in the Nucleofector plasmid solution (about 100 μL) from the second Eppendorf tube. Avoid bubbles during this step.
6. Transfer the mixture into electroporation cuvette. Insert the cuvette into the Nucleofector device, and electroporate using the preselected program called X-001.
7. Add warm (37 °C) and fresh DMEM into the cuvette, and then transfer the entire solution onto the glass-bottom culture imaging dishes using Pasteur pipette. Avoid using normal pipette tips as they will shear the cells. One transfection can be divided onto three to five imaging dishes depending on your

requirements. To increase the concentration of cells in the glass well of the imaging dish, initially plate cells (200–400 μL) only within this well, and then incubate the dishes at 37 °C for 60 min.

8. Thereafter, add fresh DMEM to the dishes, and incubate them at 37 °C for 24–48 h before commencement of single-molecule imaging.

3.3 Single-Molecule Imaging Preparation

1. Imaging media: On the imaging day, prior to the commencement of imaging on the TIRF microscope, prepare fresh imaging media—buffer A (pH 7.4) supplemented with glucose (10 mM).
2. Secretagogue stimulation: To induce exocytosis by chemical agents [38] such as $BaCl_2$ (2 mM) or nicotine (100 μM) plus $CaCl_2$ (2 mM), prepare buffer A—chemical stimulant mixture.
3. TIRF angle calibration: Couple an imaging dish plated with Tetraspeck™ microspheres unto the 100× objective (Nikon Instruments) using the proper index-matching liquid (Immersol™ 518/37 °C, Zeiss). Ensure the perfect focus system (PFS) is switched on to correct for focus drift. On the desktop computer, open the Metamorph software and access the iLas^2 graphic user interface to ensure an annular illumination pattern of the observed field of view of the microspheres. Make use of the defined coordinates (four key arrows respectively pointing north, east, south, and west) to calibrate the TIRF angle for each laser filter cube.
4. Temperature of the TIRF microscope: Switch on the Oko Touch controller to fix the stage temperature at 37 °C and the CO_2 at 5%. This ensures the well-being of chromaffin cells on the dishes during image acquisition.
5. Imaging dish preparation: Discard DMEM from the dishes plated with transfected chromaffin cells. Wash the dishes once with 1 mL of warm imaging buffer. Fill the imaging dishes with 1.5 mL of imaging media. Gently replace the media without displacing the attached cells on the imaging dishes. Add the index-matching liquid unto the 100× objective prior to placing the imaging dish.
6. Inhibiting actin polymerization: Dilute cytochalasin D in buffer A solution and DMSO in buffer A as well. To inhibit actin polymerization in chromaffin cells expressing syntaxin-1-mEos2, incubate the cells in 4 μM of cytochalasin D-buffer A solution for 20 min. For the control experiments, incubate cells in DMSO buffer solution for 20 min.

3.4 Single-Molecule Data Acquisition (sptPALM)

1. Localize transfected chromaffin cells (for example, syntaxin-1-mEos2-transfected cells can be located using 491 nm excitation) (Fig. 1a, b). Choose moderately large cells >8 μm in diameter. Take a snapshot of the cell in the green spectra fluorescence emission and save it.
2. For consistency of the size of view on the Metamorph data acquisition software, place cells within an acquisition view that is 256 by 256 pixels in size. Switch on the 405 and 561 nm lasers. Keep the 405 nm laser at low power (<4%) to ensure a relatively low and stochastic photoconversion rate of mEos2 fluorophores from the green-emitting to the red-emitting species. Place the 561 nm laser at moderately high-power levels (~70%) to maintain the excitation of the photoconverted fluorophores. Together, these laser settings help with imaging of single protein mobility.
3. Begin data acquisition using a 50-Hz imaging capture frame rate and acquire 16,000 frames or more (Fig. 1c). Save the acquired movie after imaging.
4. To induce secretagogue stimulation, locate the cell to be stimulated using the 491-nm laser. Add 500 μl of warm imaging media–chemical stimulant (for example, 2 mM $BaCl_2$) solution mixture unto the imaging dish using the polyethylene tubing and 1250-μL syringe. Commence data acquisition using the same settings as above.
5. Image a minimum of 8 cells each in both non-stimulated and stimulated conditions.

3.5 Data Processing

1. Single molecules can be localized using a wavelet-based segmentation analysis that produces super-resolved trajectory, intensity, and diffusion coefficient maps (Fig. 1di–iii) using a simulated annealing-based tracking algorithm in PALMTracer2, a program written to operate in the Metamorph software [33, 35]. PALMTracer ensures a high-precision localization of the photoactivated fluorophores by use of a Gaussian fitting of each molecule.
2. Place the movie to be analyzed and its corresponding green emission spectra image within the Metamorph software. Draw the bounding limit of the cell with the snapshot image. This created region of interest (ROI) is essential to analyze molecule movement only within the cell of interest to be analyzed.
3. Set the appropriate spatial resolution limit (0.106 μm) and the frame rate of capture (50 Hz).
4. Initiate processing of the movies and tracking of single molecules. Trajectories lasting more than eight frames are constructed by the software. The diffusion characteristics of each trajectory is extracted as mean square displacement (MSD) and

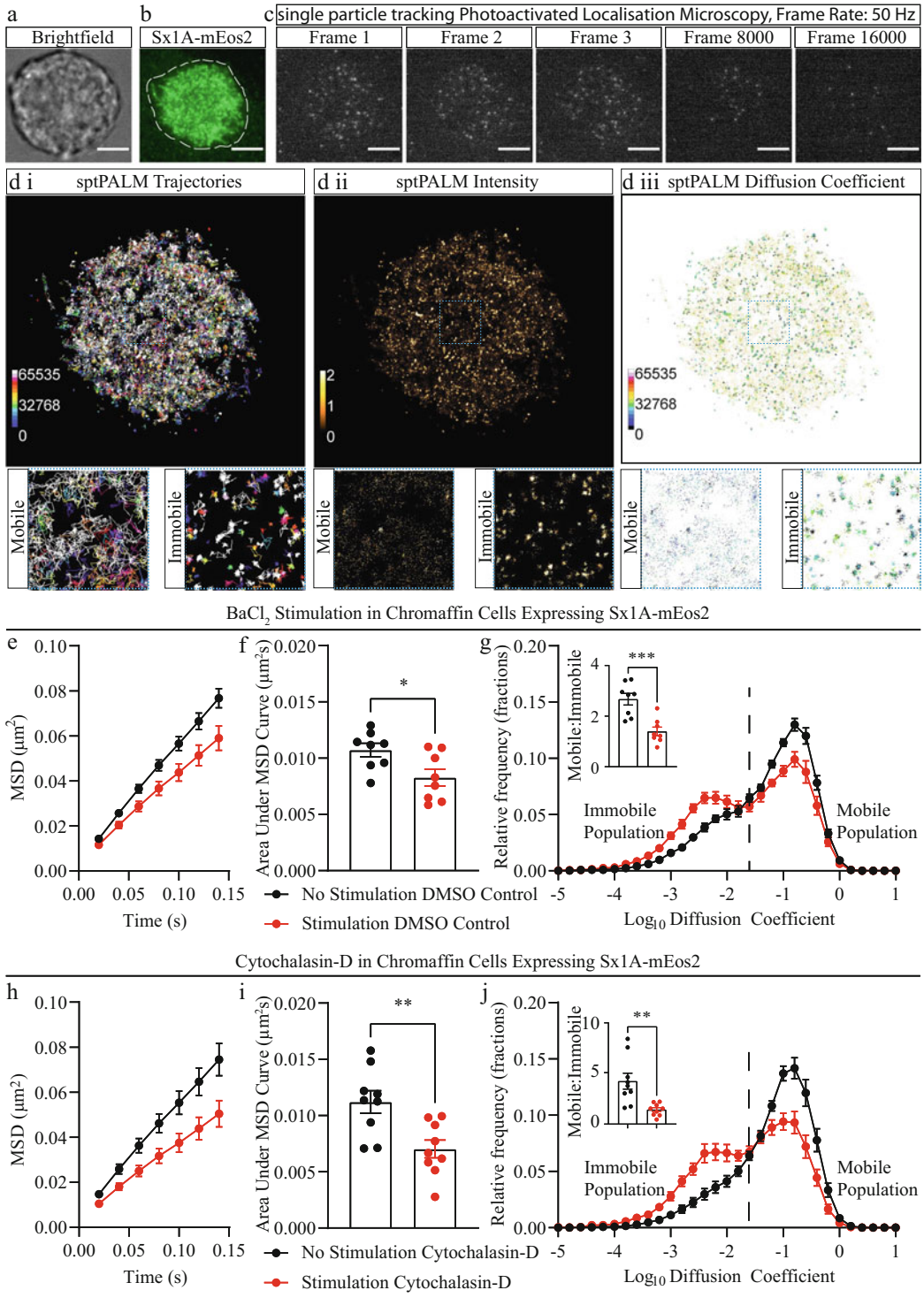

Fig. 1 Single-molecule imaging of syntaxin-1 in cytochalasin D-treated chromaffin cells. (**a**) Bright-field image of chromaffin cell capture with the 100× objective. (**b**) TIRF image of the same cell when illuminated with 488 nm laser shows expression of syntaxin-1-mEos2 (Sx1A-mEos2). (**c**) Single-particle tracking photoactivated localization microscopy (sptPALM) imaging of Sx1A-mEos2 in the same cell illuminated with 405-nm and 561-nm lasers using a frame capture rate of 50 Hz and with 16,000 frames (320 s) acquired. Scale bar 5 μm.

diffusion coefficient (D). These are also computed and generated as Microsoft Excel files by the software. For a trajectory of N data points (coordinates $x(t)$, $y(t)$ at times $t = 0$ to $(N - 1) \times \Delta t$ (this is the inverse of the acquisition rate, for example, with 50 Hz, $\Delta t = 20$ ms)), the MSD for time intervals $\tau = n \times \Delta t$ is calculated using the formulae:

$$\mathrm{MSD}(n \times \Delta t) = \sum_{i=1}^{N-n} [x((i+n) \times \Delta t) - x(i \times \Delta t)]^2 + [y((i+n) \times \Delta t) - y(i \times \Delta t)]^2 / (N - n)$$

Further, for each MSD, the diffusion coefficient (D) is calculated from the linear fits of the first four points by the equation $\mathrm{MSD}(t) = a + 4Dt$, where a is the y-intercept. The MSD measures the area (μm^2) covered by each molecule over time (20 ms) between frame of the acquired movie. The diffusion coefficient is presented as a relative frequency distribution histogram (Log_{10} of $\mu m^2\ s^{-1}$) (Fig. 1g, j).

5. Analyze all movies acquired for all physiological conditions being studied (non-stimulated as well as stimulated). Plot the average MSD and diffusion coefficient for the trajectories in all the cells in each physiological condition (Fig. 1e–j).

3.6 In-Depth Data Analysis

1. The proteins that guide the precise mechanisms of the neurosecretory vesicle release machinery also cluster together within nanodomains, and this is mediated by different parameters including homodimerization, heterodimerization, and lipid interaction [14, 23, 39]. These nanodomains are highly dynamic in that they assemble and disassemble with time, and this can be quantified from sptPALM data with appropriate analytical tools [23]. A recently developed spatial indexing algorithm called nanoscale spatiotemporal indexing clustering (NASTIC) [32] can be applied to the single-molecule data to quantify the dynamic nature of occurrence of these nanodomains on a timescale (Fig. 2a–l).
2. The averaging of MSD has the caveat of not providing an outlook of the transitional changes in the diffusion of the molecules as they might switch from "free" to "confined" and vice versa within the same trajectory. We recommend the application of hidden Markov modelling (HMM), which

Fig. 1 (continued) (**d**) Analysis of the acquired movie using PALMtracer produces super-resolved trajectories (i), localization intensity (ii), and diffusion coefficient (iii) maps. Zoomed images: Analysis of the single molecules yielded two populations of moving proteins, a mobile and an immobile fraction. (**e**, **h**) Analysis of single-particle tracking expressed as mean square displacement (MSD) curve as a function of time (**f**, **i**), the corresponding area under the MSD curves (AUC) (**g**, **j**), and the relative frequency distribution of diffusion coefficients of syntaxin-1 in chromaffin cells (*inset*: ratio of mobile to immobile populations). Statistical comparisons were performed using Student's *t*-test (*$p < 0.05$, **$p < 0.01$, ***$p < 0.001$)

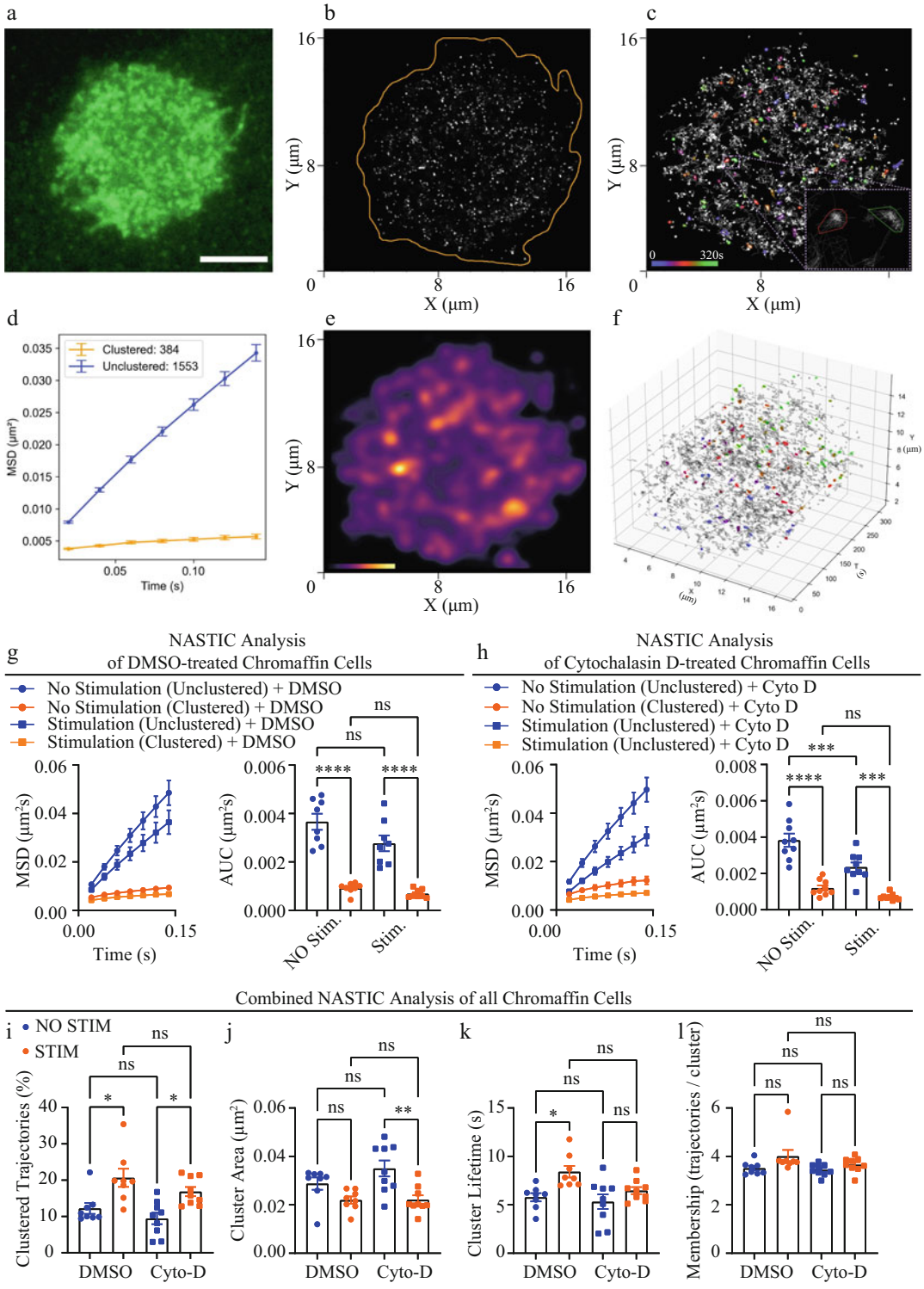

Fig. 2 Application of nanoscale spatiotemporal indexing clustering (NASTIC) analysis to sptPALM data acquired in chromaffin cells. (**a**) Sx1A-mEos2-expressing chromaffin cell (this is the same representative cell used in Fig. 1). (**b**) NASTIC plot of every single molecule detected during sptPALM data acquisition. (**c**) Bounding box radius and time window used by NASTIC to characterize clustered trajectories (in color) over the duration of

reveals the different transitory states of mobility that the trajectories exhibit as well as their occupancy within each state [3, 40, 41].

4 Notes

1. Imaging after transfection: For the best expression of the transfected plasmids, we recommend waiting for at least 24 h before commencement of single-molecule imaging. This is to ensure sufficient translation of fluorescently tagged proteins in the cells to be imaged.
2. Loss of some frames during data acquisition: When the displayed preview image is set to show all frames captured (that is, set at one) during data acquisition, some frames might be lost when saving your data. To avoid this, we recommend displaying only one frame for every 100 that is captured (that is, set at 100).
3. Batch processing: If analyzing multiple files where all data acquisition parameters (such as laser bleaching power) have been kept constant, then the batch processing feature on the PALMTracer can be used to bulk process and analyze all such single-molecule movies.
4. Filtering single-molecule data during analysis: Due to the rapid bleaching time of most photoactivatable and photoconvertible fluorophores, the length of the observed trajectories could be very short. Therefore, molecules that do not appear in eight consecutive frames (160 ms) are discarded during analysis as the MSD is best calculated from trajectories that meet this criterion. Further, on the PALMTracer, allow for a maximum movement of each localization between each frame to be 0.318 μm (for transmembrane proteins, for example, Syntaxin-1) and 0.53 μm (for membrane-associated proteins, for example, Munc18-1).
5. Number of trajectories per cell criteria: The diffusion coefficient range of the acquired data from 0.00001 to 1 $\mu m^2\ s^{-1}$ is

Fig. 2 (continued) acquire data, 320 s. *Inset*: Displays a zoomed view of two clustered trajectories at different time points against the background of unclustered trajectories. (**d**) MSD curves of clustered and unclustered detections in the analyzed data. Error bars indicate standard error of mean (SEM). (**e**) Two-dimensional kernel density estimation of all detections. (**f**) Three-dimensional [*x*, *y*, *t*] projection of spatiotemporal Sx1A-mEos2 clusters resolved in space and time. (**g**, **h**) MSD curves and AUC of Sx1A-mEos2 in non-stimulated and $BaCl_2$-stimulated cells treated with either DMSO or cytochalasin D. Comparison of cluster metrics that analyzed for percentage of clustered trajectories (**i**), the cluster area (**j**), cluster lifetime (**k**), and membership (that is, number of trajectories per cluster) (**l**). Comparisons were performed using one-way ANOVA with Tukey's multiple comparison test (ns = no significance, *$p < 0.05$, **$p < 0.01$, ***$p < 0.001$, ****$p < 0.0001$)

plotted as a relative frequency distribution histogram with bins from −5 to 1. Cells with few trajectories will have no data in some bins of the analyzed data. Adding this data from such cells to others with sufficient trajectories will skew the observed mean data and may lead to erroneous conclusions. We therefore recommend discarding data from cells with less than 1000 trajectories.

6. Number of cells to image: For paired experiments, we recommend imaging a minimum of 15 cells from three independent experiments.
7. Interpreting the data: The significance of the differences in the plotted MSD curves can be calculated from the analysis of the Area Under each MSD Curve (AUC) (Fig. 1f, i). Our data indicates that the effect of secretagogue stimulation on syntaxin-1 is to decrease the distance covered by the single molecules with time. Further, the inhibition of actin polymerization by cytochalasin D did not alter the effect of vesicle fusion in decreasing syntaxin-1 mobility, indicating that SNARE complex-mediated trapping of syntaxin-1 might be solely responsible for altering the dynamics of syntaxin-1 during neurotransmitter release.

Analysis of the diffusion coefficient curves reveals a distribution of two populations, a mobile and an immobile one (Fig. 1e, f), and a ratio of these populations is used to perform statistical analysis. In our data, the mobile population of syntaxin-1 is decreased with a corresponding increase in the immobile population upon secretagogue stimulation, and this is unchanged by cytochalasin D treatment.

Further spatiotemporal characterization and analysis of individual trajectories of each syntaxin-1 molecule can be obtained from NASTIC, which is available on the free and open-source Python graphic user interface [32]. Our data when analyzed by NASTIC (Fig. 2a–f) produced clustered and unclustered trajectories that were either distinct or overlapping on the timescale. NASTIC analysis revealed that the inhibition of actin polymerization by cytochalasin D did not alter the clustering of syntaxin-1 molecules (Fig. 2g, h, I, and l). However, it altered the size of the clusters formed and their lifetime (Fig. 2j, k). NASTIC analysis provides unique spatiotemporal insight into single-molecule data acquired in chromaffin cells.

Acknowledgments

The single-molecule super-resolution imaging was carried out at the Advanced Microscopy Facility within the Queensland Brain Institute (QBI). The authors would like to thank Dr. Tristan Wallis for his help with the nanoclustering NASTIC analysis. A.T.B. was supported by Race Against Dementia (RAD)–Dementia Australia Research Foundation (DARF) postdoctoral fellowship. This work is supported by Australian Research Council (ARC) Discovery Project Grant (DP190100674) and an ARC Linkage Infrastructure, Equipment, and Facilities Grant (LE130100078) to F.A.M. F.A.M. is an NHMRC Senior Research Fellow (APP1155794).

References

1. Smyth AM, Yang L, Martin KJ, Hamilton C, Lu W, Cousin MA et al (2013) Munc18-1 protein molecules move between membrane molecular depots distinct from vesicle docking sites. J Biol Chem 288(7):5102–5113
2. Kavanagh DM, Smyth AM, Martin KJ, Dun A, Brown ER, Gordon S et al (2014) A molecular toggle after exocytosis sequesters the presynaptic syntaxin1a molecules involved in prior vesicle fusion. Nat Commun 5:5774
3. Bademosi AT, Lauwers E, Padmanabhan P, Odierna L, Chai YJ, Papadopulos A et al (2017) In vivo single-molecule imaging of syntaxin1A reveals polyphosphoinositide- and activity-dependent trapping in presynaptic nanoclusters. Nat Commun 8:13660
4. Baranov MV, Olea RA, van den Bogaart G (2019) Chasing uptake: super-resolution microscopy in endocytosis and phagocytosis. Trends Cell Biol 29(9):727–739
5. Li D, Shao L, Chen BC, Zhang X, Zhang M, Moses B et al (2015) ADVANCED IMAGING. Extended-resolution structured illumination imaging of endocytic and cytoskeletal dynamics. Science 349(6251):aab3500
6. Nosov G, Kahms M, Klingauf J (2020) The decade of super-resolution microscopy of the presynapse. Front Synaptic Neurosci 12:32
7. Karanasios E (2019) Correlative live-cell imaging and super-resolution microscopy of autophagy. Methods Mol Biol 1880:231–242
8. Kenny SJ, Chen XS, Ge L, Xu K (2019) Super-resolution microscopy unveils FIP200-scaffolded, cup-shaped organization of mammalian autophagic initiation machinery. bioRxiv. https://doi.org/10.1101/712828
9. Klionsky DJ, Abdel-Aziz AK, Abdelfatah S, Abdellatif M, Abdoli A, Abel S et al (2021) Guidelines for the use and interpretation of assays for monitoring autophagy (4th edition) (1). Autophagy 17(1):1–382
10. Vanhauwaert R, Kuenen S, Masius R, Bademosi A, Manetsberger J, Schoovaerts N et al (2017) The SAC1 domain in synaptojanin is required for autophagosome maturation at presynaptic terminals. EMBO J 36(10):1392–1411
11. Kneussel M, Triller A, Choquet D (2014) SnapShot: receptor dynamics at plastic synapses. Cell 157(7):1738, e1
12. Ribrault C, Reingruber J, Petković M, Galli T, Ziv NE, Holcman D et al (2011) Syntaxin1A lateral diffusion reveals transient and local SNARE interactions. J Neurosci 31(48):17590–17602
13. Sieber JJ, Willig KI, Heintzmann R, Hell SW, Lang T (2006) The SNARE motif is essential for the formation of syntaxin clusters in the plasma membrane. Biophys J 90(8):2843–2851
14. Sieber JJ, Willig KI, Kutzner C, Gerding-Reimers C, Harke B, Donnert G et al (2007) Anatomy and dynamics of a supramolecular membrane protein cluster. Science 317(5841):1072–1076
15. Bar-On D, Wolter S, van de Linde S, Heilemann M, Nudelman G, Nachliel E et al (2012) Super-resolution imaging reveals the internal architecture of nano-sized syntaxin clusters. J Biol Chem 287(32):27158–27167
16. Pertsinidis A, Mukherjee K, Sharma M, Pang ZP, Park SR, Zhang Y et al (2013) Ultrahigh-resolution imaging reveals formation of neuronal SNARE/Munc18 complexes in situ. Proc Natl Acad Sci U S A 110(30):E2812–E2820

17. McKinney SA, Murphy CS, Hazelwood KL, Davidson MW, Looger LL (2009) A bright and photostable photoconvertible fluorescent protein. Nat Methods 6(2):131–133
18. Kasula R, Chai YJ, Bademosi AT, Harper CB, Gormal RS, Morrow IC et al (2016) The Munc18-1 domain 3a hinge-loop controls syntaxin-1A nanodomain assembly and engagement with the SNARE complex during secretory vesicle priming. J Cell Biol 214(7):847–858
19. Han GA, Malintan NT, Collins BM, Meunier FA, Sugita S (2010) Munc18-1 as a key regulator of neurosecretion. J Neurochem 115(1):1–10
20. Malintan NT, Nguyen TH, Han L, Latham CF, Osborne SL, Wen PJ et al (2009) Abrogating Munc18-1-SNARE complex interaction has limited impact on exocytosis in PC12 cells. J Biol Chem 284(32):21637–21646
21. Martin S, Tomatis VM, Papadopulos A, Christie MP, Malintan NT, Gormal RS et al (2013) The Munc18-1 domain 3a loop is essential for neuroexocytosis but not for syntaxin-1A transport to the plasma membrane. J Cell Sci 126 (Pt 11):2353–2360
22. Hayashi T, McMahon H, Yamasaki S, Binz T, Hata Y, Südhof TC et al (1994) Synaptic vesicle membrane fusion complex: action of clostridial neurotoxins on assembly. EMBO J 13(21):5051–5061
23. Padmanabhan P, Bademosi AT, Kasula R, Lauwers E, Verstreken P, Meunier FA (2020) Need for speed: super-resolving the dynamic nanoclustering of syntaxin-1 at exocytic fusion sites. Neuropharmacology 169:107554
24. Bademosi AT, Lauwers E, Amor R, Verstreken P, van Swinderen B, Meunier FA (2018) In vivo single-molecule tracking at the drosophila presynaptic motor nerve terminal. J Vis Exp 131:56952
25. Papadopulos A, Gomez GA, Martin S, Jackson J, Gormal RS, Keating DJ et al (2015) Activity-driven relaxation of the cortical actomyosin II network synchronizes Munc18-1-dependent neurosecretory vesicle docking. Nat Commun 6:6297
26. Wen PJ, Osborne SL, Zanin M, Low PC, Wang HT, Schoenwaelder SM et al (2011) Phosphatidylinositol(4,5)bisphosphate coordinates actin-mediated mobilization and translocation of secretory vesicles to the plasma membrane of chromaffin cells. Nat Commun 2:491
27. Kusumi A, Fujiwara TK, Chadda R, Xie M, Tsunoyama TA, Kalay Z et al (2012) Dynamic organizing principles of the plasma membrane that regulate signal transduction: commemorating the fortieth anniversary of Singer and Nicolson's fluid-mosaic model. Annu Rev Cell Dev Biol 28:215–250
28. Kusumi A, Tsunoyama TA, Hirosawa KM, Kasai RS, Fujiwara TK (2014) Tracking single molecules at work in living cells. Nat Chem Biol 10(7):524–532
29. Berberian K, Torres AJ, Fang Q, Kisler K, Lindau M (2009) F-actin and myosin II accelerate catecholamine release from chromaffin granules. J Neurosci 29(3):863–870
30. Giannone G, Hosy E, Sibarita JB, Choquet D, Cognet L (2013) High-content super-resolution imaging of live cell by uPAINT. Methods Mol Biol 950:95–110
31. Sibarita JB (2014) High-density single-particle tracking: quantifying molecule organization and dynamics at the nanoscale. Histochem Cell Biol 141(6):587–595
32. Wallis TP, Jiang A, Hou H, Gormal RS, Durisic N, Balistreri G et al (2021) Molecular videogaming: super-resolved trajectory-based nanoclustering analysis using spatio-temporal indexing. bioRxiv. https://doi.org/10.1101/2021.09.08.459552
33. Nair D, Hosy E, Petersen JD, Constals A, Giannone G, Choquet D et al (2013) Super-resolution imaging reveals that AMPA receptors inside synapses are dynamically organized in nanodomains regulated by PSD95. J Neurosci 33(32):13204–13224
34. Sage D, Pham TA, Babcock H, Lukes T, Pengo T, Chao J et al (2019) Super-resolution fight club: assessment of 2D and 3D single-molecule localization microscopy software. Nat Methods 16(5):387–395
35. Kechkar A, Nair D, Heilemann M, Choquet D, Sibarita JB (2013) Real-time analysis and visualization for single-molecule based super-resolution microscopy. PLoS One 8(4):e62918
36. Gormal RS, Nguyen TH, Martin S, Papadopulos A, Meunier FA (2015) An actomyosin II constricting ring initiates the fission of activity-dependent bulk endosomes in neurosecretory cells. J Neurosci 35(4):1380–1389
37. Meunier FA, Feng ZP, Molgó J, Zamponi GW, Schiavo G (2002) Glycerotoxin from Glycera convoluta stimulates neurosecretion by up-regulating N-type Ca2+ channel activity. EMBO J 21(24):6733–6743
38. Papadopulos A, Martin S, Tomatis VM, Gormal RS, Meunier FA (2013) Secretagogue stimulation of neurosecretory cells elicits filopodial extensions uncovering new functional release sites. J Neurosci 33(49):19143–19153
39. Bar-On D, Gutman M, Mezer A, Ashery U, Lang T, Nachliel E (2009) Evaluation of the

heterogeneous reactivity of the syntaxin molecules on the inner leaflet of the plasma membrane. J Neurosci 29(39):12292–12301

40. Joensuu M, Martínez-Mármol R, Padmanabhan P, Glass NR, Durisic N, Pelekanos M et al (2017) Visualizing endocytic recycling and trafficking in live neurons by subdiffractional tracking of internalized molecules. Nat Protoc 12(12):2590–2622
41. Joensuu M, Padmanabhan P, Durisic N, Bademosi AT, Cooper-Williams E, Morrow IC et al (2016) Subdiffractional tracking of internalized molecules reveals heterogeneous motion states of synaptic vesicles. J Cell Biol 215(2):277–292

Part IV

Miscellanea

Chapter 22

Determination of Catecholamines in a Small Volume (25 μL) of Plasma from Conscious Mouse Tail Vein

Kechun Tang and Sushil K. Mahata

Abstract

The determination of plasma catecholamine levels is commonly used as a measure of the sympathetic nervous system's response to stress and is highly important for diagnosis, therapy, and prognosis of cardiovascular diseases, catecholamine-secreting tumors arising from the chromaffin cells of the sympathoadrenal system, and affective disorders. Diseases in which catecholamines are significantly elevated include pheochromocytoma, Parkinson's disease, Alzheimer's disease, neuroblastoma, ganglioneuroblastoma, von Hippel–Lindau disease, baroreflex failure, chemodectina (nonchromaffin paraganglioma), and multiple endocrine neoplasia. Plasma norepinephrine levels provide a guide to prognosis in patients with stable, chronic, and congestive heart diseases. The method described here for the determination of plasma catecholamines is based on the principle that plasma catecholamines are selectively adsorbed on acid-washed alumina at pH 8.7 and then eluted at a pH between 1.0 and 2.0. Upon injection, catecholamines in elutes were separated by a reversed phase C-18 column. After separation, the catecholamines present within the mobile phase enter the electrochemical detector. Electrochemical detection occurs because electroactive compounds oxidize at a certain potential and thereby liberate electrons that create measurable current. Catecholamines readily form quinones under these conditions, get oxidized, release two electrons, and create current. The electrochemical detector detects this electrical current that linearly correlates to the catecholamine concentration loaded into the ultra-performance liquid chromatography instrument. A 15-min mixing time during the adsorption and desorption steps was found to be optimal. If the washing step was omitted, the catecholamines could not be eluted from the acid-washed alumina. To prevent dilution, the alumina had to be centrifuged and not aspirated to dryness after the washing step. We report here that by changing the range in the electrochemical detector, plasma catecholamines were measured with only 12.5 μL of plasma and more reliably with 25 μL of plasma. The detection limit was 1 ng/mL. This assay method is very useful as blood can be collected from the tail vein in a conscious mouse and the same mouse can be used for time-dependent or age-dependent studies.

Key words Dopamine, Norepinephrine, Epinephrine, Catecholamine, Plasma, Chromatography, Electrochemical detection

1 Introduction

Catecholamines are important natural molecules containing a catechol ring, which act as neurotransmitters or hormones at central

Ricardo Borges (ed.), *Chromaffin Cells: Methods and Protocols*,
Methods in Molecular Biology, vol. 2565, https://doi.org/10.1007/978-1-0716-2671-9_22,

and peripheral levels [1]. The main endogenous catecholamines are norepinephrine (NE), epinephrine (EPI), and dopamine (DA). Liquid chromatography with electrochemical detection is a reliable technique for catecholamine assay [2]. The electrochemical detection of NE and EPI in plasma after separation by liquid chromatography was first described by Watson in 1981 [3], based on previous work by Keller et al. [4]. This procedure is unsurpassed by any other method for the determination of catecholamines, e.g., liquid chromatography with fluorometric or electrochemical detection [5–7], gas liquid chromatography with electron capture detection [8], and mass fragmentography [9, 10], or by radioenzymatic assays [11–13].

We have documented a reliable, reproducible, simple-to-perform, and adequately sensitive method for determination of plasma catecholamines in 25 μL of plasma. This method can be used to detect plasma catecholamines in response to the following conditions: (i) determining stress-induced catecholamine secretion at different time points from the same mouse, (ii) determining age-dependent catecholamine secretion from the same mouse, (iii) finding a correlation between glucose-stimulated insulin and catecholamine secretion from the same mouse, (iv) correlating glycogenolysis with catecholamine secretion from the same mouse, and (v) correlating age-associated development of Alzheimer's disease (dementia), hypertension (high blood pressure), diabetes (high blood glucose), and sarcopenia (loss of muscle function).

The present study reveals comparable plasma catecholamine levels when blood is drawn from conscious mouse and from deeply anesthetized (with isoflurane) mouse. This contrasts with the findings reported earlier where the authors reported much higher plasma catecholamine levels between blood drawn from catheterized mice, decapitated mice, and CO_2-inhaled mice [14]. Therefore, isoflurane-induced anesthesia is a better choice if blood must be drawn in anesthetized mice.

2 Materials

2.1 Standard Curve

DL-norepinephrine hydrochloride, (±)-epinephrine hydrochloride, 3,4-dihydroxybenzylamine hydrochloride (DHBA), and dopamine hydrochloride) were used for making the standard curve.

2.2 Tris Buffer

Trizma® base (2-amino-2-(hydroxymethyl)-1,3-propanediol)) and ethylenediaminetetraacetic acid (EDTA) disodium salt dihydrate were used to make Tris buffer.

2.3 Phosphate--Citrate Buffer

NaH_2PO_4, Na_2EDTA, sodium citrate, diethylamine hydrochloride, 1-octanosulfonic acid, phosphoric acid, and N, N-dimethylacetamide were used to prepare the phosphate-citrate buffer.

2.4 Mobile Phase

Phosphate-citrate buffer and acetonitrile.

2.5 Adsorption and Desorption of Catecholamines

Aluminum oxide (Al_2O_3), laboratory tube mixer, centrifuge tube filters (0.22 μm pore size), and hydrochloric acid (HCl).

2.6 Instrument

Ultra-performance liquid chromatography (UPLC), reverse-phase dC18 column (2.1 × 150 mm; 3 μm particle size, 100 A), polypropylene tube, and an electrochemical detector.

2.7 Software

Empower-3 (Waters Corporation, MA).

3 Methods

3.1 Mouse Tail Vein Plasma Collection

Mouse was held in a mouse holder, and tail was cut about 1 mm. Blood was collected with EDTA-coated Micro-Hematocrit Capillary Tubes until it is four-fifth full, then transferred to a 500-μL Eppendorf tube with 2 μL of 0.5 M EDTA, and kept on ice. Blood samples were spun at 8400 × g, 4 °C, for 5 min. 25 μL of plasma was transferred to a 2-mL Eppendorf tube and kept on −80 °C for future assay.

3.2 Preparation of Plasma Samples

1. 25 μL of plasma was thawed, and DHBA (1 ng/sample) in 200 μL of Tris buffer (0.1 M tris, 0.05 M EDTA, pH 8.7) as internal control was added to thawed plasma sample (*see* **Note 1**).
2. 10–15 mg of Al_2O_3 was added to each sample for adsorption of catecholamines at pH of 8.7, and tubes were rotated on a laboratory tube mixer for 10–15 min at room temperature.
3. The aluminum beads were spun down after completion of rotation, the supernatant was removed, 500 μL of water was added to the beads, and the mixture was transferred to a centrifuge tube filter (0.22 μm pore size). At this point, the filter cartridge was moved to a 2-mL collection tube. After first spin (8400 × g 1 min), another 500 μL of water was added and spun again until the aluminum beads are dry.
4. The filter cartridge was moved back to its original filter tube, and 50 μL of 0.1 N HCl was added for desorption of catecholamines. The lid was closed, and the tube was "vortexed" for 5 s (*see* **Note 2**). Sample was spun down and the eluted sample used for UPLC assay.

3.3 Electrochemical Detection of Catecholamines

1. Eluted samples were transferred to polypropylene tube and placed on the sample plate. The running speed was set at 0.3 mL/min, and column temperature was set at 30 °C. Chromatographic separation was achieved on a universal, silica-based, reversed-phase C-18 column, which was equilibrated with the mobile phase at least 6 h before use (*see* **Note 3**).
2. The software Empower-3 was used to control the performance and data analysis.
3. Catecholamines were detected by an electrochemical detector in DC mode. The electrochemical detector was set up with the following parameters: temperature = 28 °C, EC = +0.50 V, filter = 0.1 s, range = 100 pA (*see* **Note 4**).
4. Phosphate-citrate buffer was used for the mobile phase [15, 16]. Simply, 3.45 g NaH_2PO_4 (final conc. 25 mM), 100 mg Na_2EDTA (final concentration 268 μM), 14.7 g sodium citrate (final concentration 50 mM), 1.1 g diethylamine hydrochloride (final concentration 10 mM), and 0.72 g 1-octanosulfonic acid (final concentration 0.072%) were added in about 900 mL HPLC grade water in a beaker, and the solution was mixed with a stir bar. After adjusting pH to 3.1 with phosphoric acid, water was added to make 1000-mL solution, which was filtered (0.22 μm pore size) in a 500-mL tissue culture bottle. 21 mL of N,N-dimethylacetamide (final concentration 2.2%) was added to the phosphate-citrate buffer followed by addition of 5% acetonitrile (V/V), and then 5% (V/V) acetonitrile was added as isocratic mode. The concentration of the mobile phase was kept constant throughout the chromatographic process (*see* **Note 5**).

3.4 Standard Curve

1. 5 mg of NE, EPI, DHBA, and DA were dissolved in 2.5 mL of 0.1 N HCl to make a stock solution of 2 mg/mL.
2. Stock solutions were thawed and diluted to different concentrations for different RANGE of electrochemical detector. The standard mixture that was used for 100 pA RANGE included the following: NE (50 pg/μL), EPI and DHBA (75 pg/μL), and DA (12.5 pg/μL). The following ratios were used to make the standard curve: NE:EPI:DHBA:DA = 4:6:6:1 (*see* **Note 6**).
3. Serial dilution was made four times to obtain five different concentrations that gave five different points in the standard curve.
4. The following concentrations of NE were used to generate its standard curve: 31.25, 62.5, 125, 250, and 500 pg/μL (Fig. 1a and b). The standard curve went through every point and generated an R^2 value of 0.992 (Fig. 1c) (*see* **Note 7**).

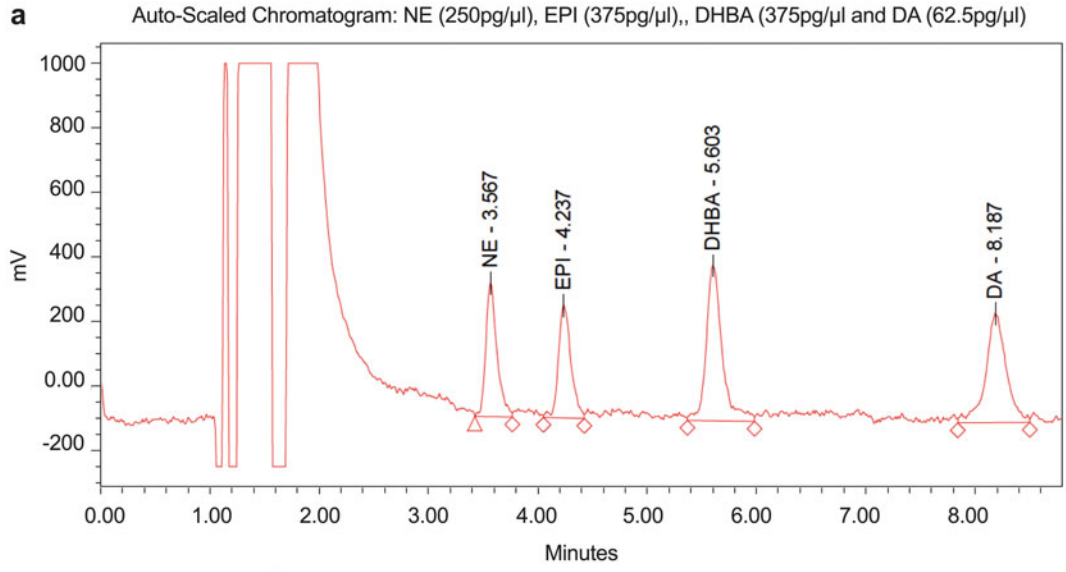

b

Peak Results						
#	Name	RT	Area	Height	Amount	Units
1	NE	3.567	2934405	413545	250	pg/µl
2	EPI	4.237	2782383	349407	375	pg/µl
3	DHBA	5.603	4860862	480696	375	pg/µl
4	DA	8.187	4449916	337148	62.5	pg/µl

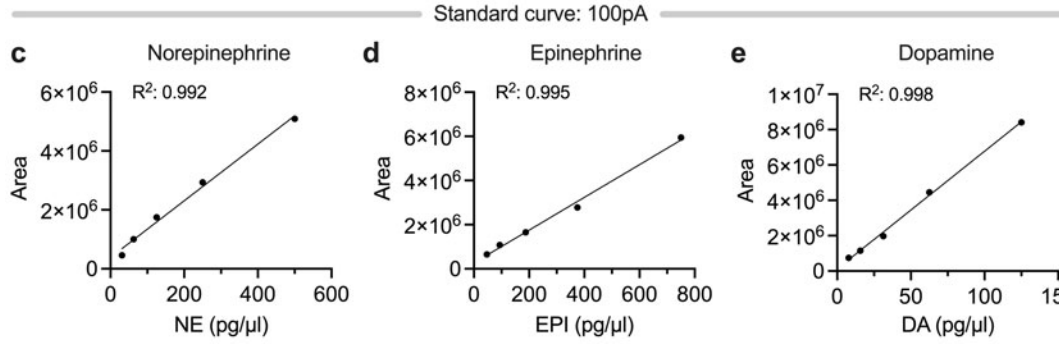

Fig. 1 Determination of standard curve of catecholamines at 100 pA current. (**a**) The following concentration of the standards was used to generate the chromatogram shown here: norepinephrine (NE: 250 pg/µL), epinephrine (EPI: 375 pg/µL), 3,4-didroxybenzylamine (DHBA: 375 pg/µL), and dopamine (DA: 62.5 pg/µL). (**b**) Peak results showing retention time (RT), area, height, amount, and the unit (pg/µL). (**c**) NE standard curve: The following concentrations of NE were used to generate its standard curve: 31.25, 62.5, 125, 250, and 500 pg/µL. (**d**) EPI standard curve: The following concentrations of EPI were used to generate its standard curve: 46.875, 93.75, 187.5, 375, and 750 pg/µL. (**e**) DA standard curve: The following concentrations of DA were used to generate its standard curve: 7.813, 15.625, 31.25, 62.5, and 125 pg/µL

5. The following concentrations of EPI were used to generate its standard curve: 46.875, 93.75, 187.5, 375, and 750 pg/μL (Fig. 1a and b). Like NE, the standard curve went through every point and produced an R^2 value of 0.995 (Fig. 1d).
6. The following concentrations of DA were used to generate its standard curve: 7.813, 15.625, 31.25, 62.5, and 125 pg/μL (Fig. 1a and b). Like NE and EPI, the standard curve went through every point and produced an R^2 value of 0.998 (Fig. 1e).

3.5 Detection of Catecholamines in Different Plasma Volumes

1. *12.5 μL plasma*: The lowest volume of plasma that was used to measure catecholamines was 12.5 μL (Fig. 2a and b). We found 16.842 ng/mL of NE and 5.919 ng/mL of EPI when catecholamines in 12.5 μL of plasma was adsorbed in 200 μL of Tris-buffer with ~10 mg Al_2O_3, desorbed in 50 μL of 0.1 N HCl, and 40 μL was injected into the system.
2. *25 μL plasma*: Although plasma catecholamines were detected in 12.5 μL of plasma, the volume that gave consistent and reliable plasma catecholamines was 25 μL. We detected 29.439 ng/mL of NE and 14.523 ng/mL of EPI when catecholamines in 25 μL of plasma was adsorbed in 200 μL of Tris buffer with ~10 mg Al_2O_3, desorbed in 50 μL of 0.1 N HCl, and 40 μL was injected into the system (Fig. 2c and d).
3. *50 μL plasma*: The following values were detected: 15.117 ng/mL of NE and 11.898 ng/mL of EPI when 50 μL of plasma was eluted with 50 μL of 0.1 N HCl and injected 20 μL of eluent (Fig. 3a and b).
4. *100 μL plasma*: The following values were detected: 14.949 ng/mL of NE and 14.140 ng/mL of EPI when 100 μL of plasma was eluted with 100 μL of 0.1 N HCl and injected 20 μL of eluent (Fig. 3c and d).
5. *200 μL plasma*: The following values were detected: 10.603 ng/mL of NE and 14.747 ng/mL of EPI when 200 μL of plasma was eluted with 100 μL of 0.1 N HCl and injected 10 μL of eluent (Fig. 4a and b) (*see* **Note 8**).

3.6 Comparable Plasma Catecholamine Levels When Blood Was Collected from the Tail Vein in Conscious Mice and from the Heart in Deeply Anesthetized Mice

1. *Blood collected from the tail vein*: To ascertain whether plasma catecholamines vary when blood is drawn from the tail vein in a conscious mouse versus from the heart in deeply anesthetized mouse, blood was collected from the tail vein and the heart and determined plasma catecholamines in 25 μL of plasma. In tail vein plasma (25 μL), 14.063 ng/mL of NE and 26.487 ng/mL of EPI were found (Fig. 5a and b).
2. *Blood collected from the heart*: 13.491 ng/mL of NE and 30.215 ng/mL of EPI were detected in plasma extracted from the blood drawn from the heart (Fig. 5c and d).

a

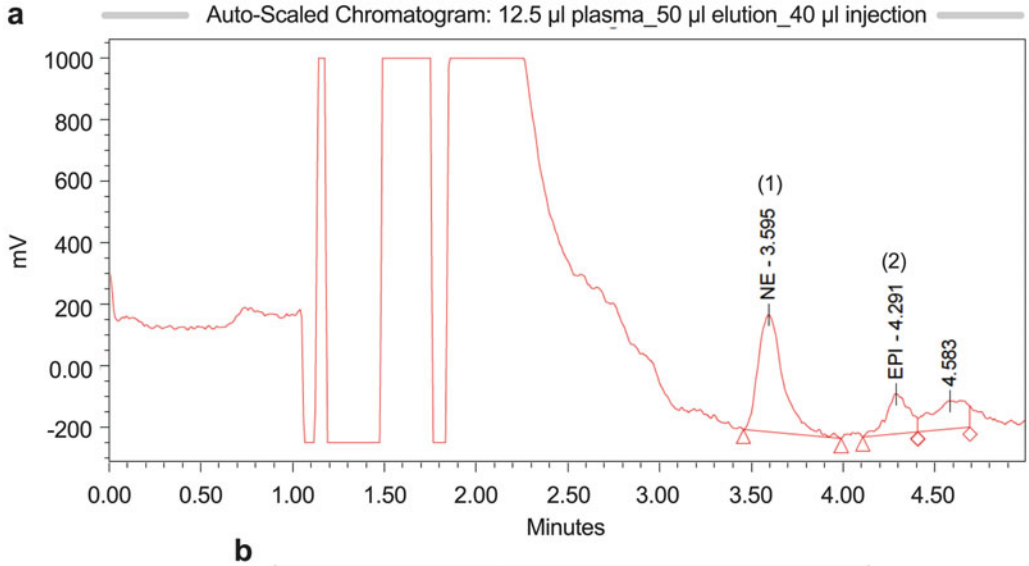

b

Peak Results						
#	Name	RT	Area	Height	Amount	Units
1	NE	3.595	3638203	381057	16.842	pg/µl
2	EPI	4.291	1127242	131697	5.919	pg/µl

c

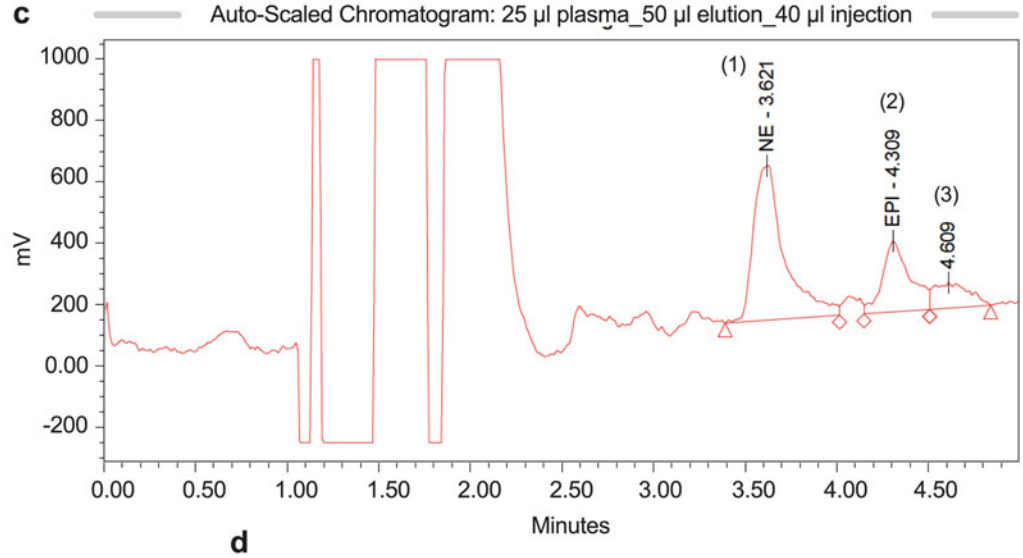

d

Peak Results						
#	Name	RT	Area	Height	Amount	Units
1	NE	3.621	5958410	506637	29.439	pg/µl
2	EPI	4.309	2410755	229800	14.523	pg/µl

Fig. 2 Estimation of catecholamines in 12.5 and 25 µL of plasma. (**a**) Chromatogram showing NE and EPI concentrations in 12.5 µL of plasma. The catecholamines were adsorbed in activated aluminum oxide, extracted with 50 µL of 0.1 N HCl, and 40 µL of eluted solution was injected to determine the catecholamine concentration. (**b**) Peak results showing retention time (RT), area, height, and amount (pg/µL). (**c**) Chromatogram showing NE and EPI concentrations in 25 µL of plasma. Elution volume was 50 µL and injection volume was 40 µL. (**d**) Peak results showing retention time (RT), area, height, and amount (pg/µL)

a

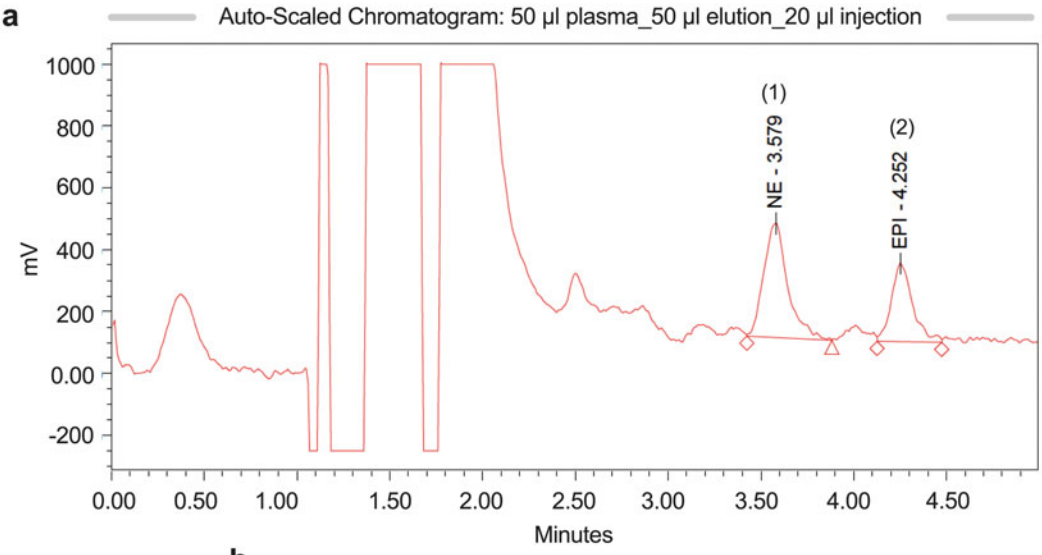

b

Peak Results						
#	Name	RT	Area	Height	Amount	Units
1	NE	3.579	3320541	371874	15.117	pg/µl
2	EPI	4.252	2019199	251972	11.898	pg/µl

c

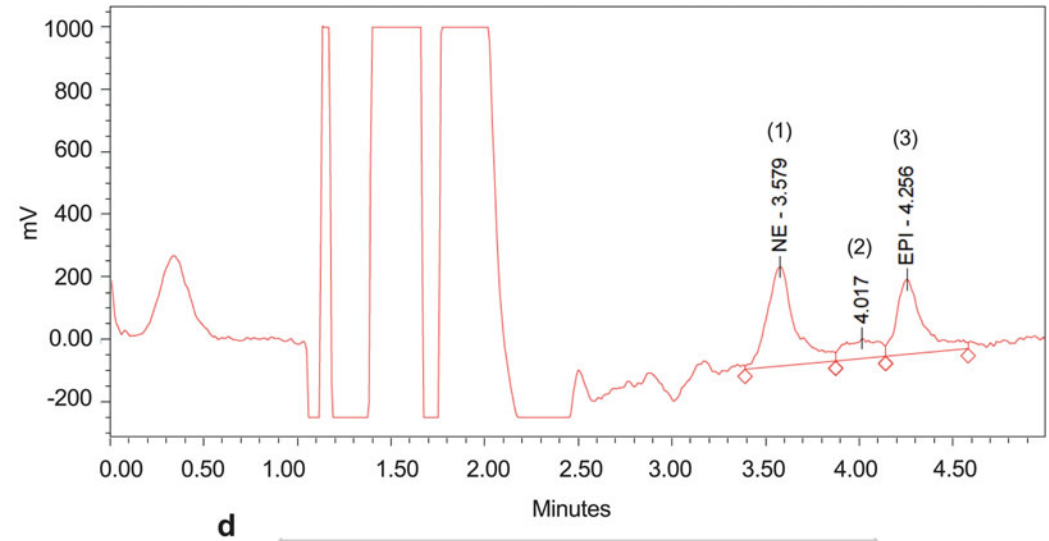

d

Peak Results						
#	Name	RT	Area	Height	Amount	Units
1	NE	3.579	3289582	319747	14.949	pg/µl
2	EPI	4.256	2353737	241132	14.140	pg/µl

Fig. 3 Assessment of catecholamines in 50 and 100 µL of plasma. (**a**) Chromatogram showing NE and EPI concentrations in 50 µL of plasma. The catecholamines were adsorbed in activated aluminum oxide, eluted with 50 µL of 0.1 N HCl, and 20 µL of eluted solution was injected to determine the catecholamine concentration. (**b**) Peak results showing retention time (RT), area, height, and amount (pg/µL). (**c**) Chromatogram showing NE and EPI concentrations in 100 µL of plasma. Elution volume was 100 µL and injection volume was 20 µL. (**d**) Peak results showing retention time (RT), area, height, and amount (pg/µL)

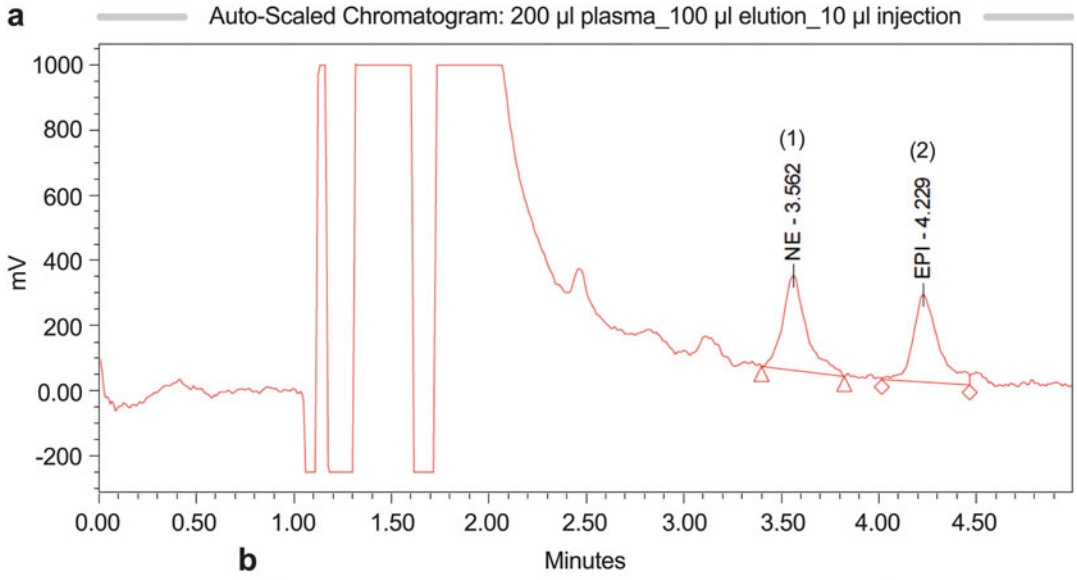

Peak Results

#	Name	RT	Area	Height	Amount	Units
1	NE	3.562	2489080	292026	10.603	pg/µl
2	EPI	4.229	2444204	269640	14.747	pg/µl

Fig. 4 Measurement of catecholamines in 200 µL of plasma. (**a**) Chromatogram showing NE and EPI concentrations in 200 µL of plasma. The catecholamines were adsorbed in activated aluminum oxide, eluted with 100 µL of 0.1 N HCl, and 10 µL of eluted solution was injected to determine the catecholamine concentration. (**b**) Peak results showing retention time (RT), area, height, and amount (pg/µL)

4 Notes

1. Changes in sensitivity of the assay on the electrochemical detector were essential to detect low (increased sensitivity by decreasing range) and high (decreased sensitivity by increasing range) levels of catecholamines in plasma samples. Changes in sensitivity mandated changes in DHBA concentration.
2. Vortexing was crucial for desorption of catecholamines from Al_2O_3.
3. Equilibration with the mobile phase was essential to obtain a stable baseline.
4. 5 nA to 100 pA RANGE were used to reliably detect catecholamines from different tissues including adrenal gland, PC12 cells, heart, kidney, spleen, white adipose tissue, brain (hypothalamus, thalamus, hippocampus, striatum, cortex, cerebellum, brainstem, spinal cord), gut regions (esophagus, fundus, body, pylorus, duodenum, jejunum, ileum, and colon), as well

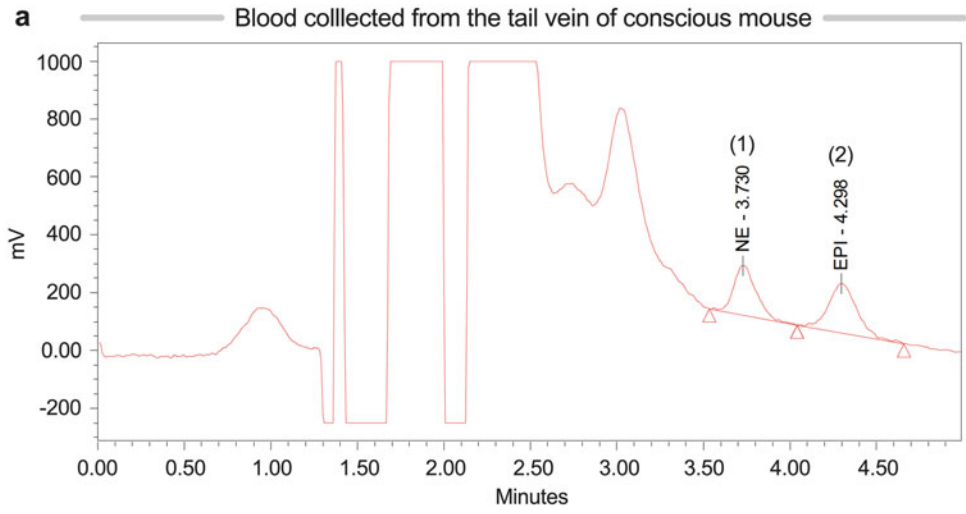

b 25 µl plasma_50 µl elution_20 µl injection

Peak Results						
#	Name	RT	Area	Height	Amount	Units
1	NE	3.730	1572021	172295	14.063	pg/µl
2	EPI	4.298	1984423	171500	26.487	pg/µl

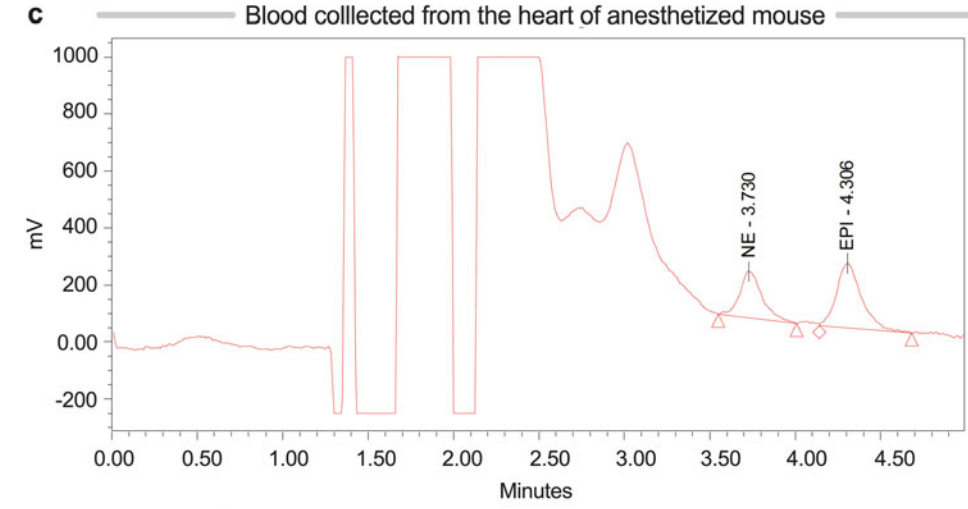

d 25 µl plasma_50 µl elution_20 µl injection

Peak Results						
#	Name	RT	Area	Height	Amount	Units
1	NE	3.730	1509865	165111	13.491	pg/µl
2	EPI	4.306	2290981	225400	30.215	pg/µl

Fig. 5 Evaluation of catecholamines in 25 µL of plasma drawn from tail vein and heart. (**a**) Chromatogram showing NE and EPI concentrations in 25 µL of plasma. Blood was collected from the tail vein of conscious mouse; plasma catecholamines were adsorbed in activated aluminum oxide, eluted with 50 µL of 0.1 N HCl; and 20 µL of eluted solution was injected to determine the catecholamine concentration. (**b**) Peak results showing retention time (RT), area, height, and amount (pg/µL). (**c**) Blood was collected from the heart of deeply anesthetized (isoflurane) mouse. Chromatogram showing NE and EPI concentrations in 25 µL of plasma. Elution volume was 50 µL and injection volume was 20 µL. (**d**) Peak results showing retention time (RT), area, height, and amount (pg/µL)

as plasma. Since plasma concentration of catecholamines is low, 100 pA RANGE was used.

5. Degassing of the mobile phase was not required and was kept in room temperature for a week.
6. Different concentrations of catecholamines for the standard curve were used to get the comparable maximal peaks in the same run.
7. Although 31.25 pg/μL of NE was used as the lowest dose in the standard curve, 1 ng/mL of NE was detected in plasma when the original plasma volume (dilution in Empower-3) and the injection volume (weight in Empower-3) were adjusted in 100 pA RANGE. Less than 1 ng/mL was detected when sensitivity was increased by decreasing RANGE such as 50 pA. However, detection at 50 pA RANGE was coupled with unstable baseline and increased signal to noise ratio.
8. Plasma catecholamines were determined using 12.5, 25, 50, 100, and 200 μL of plasma volumes where the elution and/or injection volumes were changed so that the detected catecholamine values from the different plasma volumes are similar.

References

1. Rozet E, Morello R, Lecomte F et al (2006) Performances of a multidimensional on-line SPE-LC-ECD method for the determination of three major catecholamines in native human urine: validation, risk and uncertainty assessments. J Chromatogr B Analyt Technol Biomed Life Sci 844:251–260
2. Kagedal B, Goldstein DS (1988) Catecholamines and their metabolites. J Chromatogr 429:177–233
3. Watson E (1981) Liquid chromatography with electrochemical detection for plasma norepinephrine and epinephrine. Life Sci 28:493–497
4. Keller R, Oke A, Mefford I, Adams RN (1976) Liquid chromatographic analysis of catecholamines routine assay for regional brain mapping. Life Sci 19:995–1003
5. Anton AH, Sayre DF (1962) A study of the factors affecting the aluminum oxide-trihydroxyindole procedure for the analysis of catecholamines. J Pharmacol Exp Ther 138: 360–375
6. Laverty R, Taylor KM (1968) The fluorometric assay of catecholamines and related compounds: improvements and extensions to the hydroxyindole technique. Anal Biochem 22: 269–279
7. Yui Y, Fujita T, Yamamoto T, Itokawa Y, Kawai C (1980) Liquid-chromatographic determination of norepinephrine and epinephrine in human plasma. Clin Chem 26:194–196
8. Imai K, Wang MT, Yoshiue S, Tamura Z (1973) Determination of catecholamines in the plasma of patients with essential hypertension and of normal persons. Clin Chim Acta 43:145–149
9. Wang MT, Imai K, Yoshioka M, Tamura Z (1975) Gas-liquid chromatographic and mass fragmentographic determination of catecholamines in human plasma. Clin Chim Acta 63: 13–19
10. Jacob K, Vogt W, Knedel M, Schwertfeger G (1978) Quantitation of adrenaline and noradrenaline from human plasma by combined gas chromatography–high-resolution mass fragmentography. J Chromatogr 146:221–226
11. Passon PG, Peuler JD (1973) A simplified radiometric assay for plasma norepinephrine and epinephrine. Anal Biochem 51:618–631
12. Weise VK, Kopin IJ (1976) Assay of cathecholamines in human plasma: studies of a single isotope radioenzymatic procedure. Life Sci 19: 1673–1685
13. Da Prada M, Zürcher G (1976) Simultaneous radioenzymatic determination of plasma and tissue adrenaline, noradrenaline and dopamine within the femtomole range. Life Sci 19(8): 1161–1174

14. Lucot JB, Jackson N, Bernatova I, Morris M (2005) Measurement of plasma catecholamines in small samples from mice. J Pharmacol Toxicol Methods 52:274–277
15. Gayen JR, Gu Y, O'Connor DT, Mahata SK (2009) Global disturbances in autonomic function yield cardiovascular instability and hypertension in the chromogranin A null mouse. Endocrinology 150:5027–5035
16. Ying W, Tang K, Avolio E et al (2021) Immunosuppression of macrophages underlies the cardioprotective effects of CST (Catestatin). Hypertension 77:1670–1682

Chapter 23

Quantification of Chromogranin A and Its Fragments in Biological Fluids

Flavio Curnis, Barbara Colombo, and Angelo Corti

Abstract

Human chromogranin A (CgA), a 439-residue long neurosecretory protein, can serve as a circulating biomarker for a wide range of neuroendocrine tumors. Increased levels of immunoreactive CgA are also present in the blood of patients with cardiovascular, gastrointestinal, or inflammatory diseases with, in certain cases, important diagnostic and prognostic implications. A growing body of evidence suggest that CgA and various CgA-derived fragments have complex roles in the regulation of cardiovascular system, metabolism, innate immunity, angiogenesis, and tissue repair, sometime with opposite biological effects. For example, while full-length CgA ($CgA_{1\text{-}439}$) inhibits angiogenesis, the $CgA_{1\text{-}373}$ fragment, at certain doses, is proangiogenic. Thus, the selective quantification of CgA and its fragments in the blood of patients (and in other biological fluids) is of great experimental and clinical interest. Here, we describe methods to produce $CgA_{1\text{-}439}$ and $CgA_{1\text{-}373}$ and to develop ELISAs capable of detecting these polypeptides in a very selective manner. The same approach can be used, in principle, also for developing assays for other fragments.

Key words Chromogranin A, $CgA_{1\text{-}373}$, Expression, Purification, Antibody, Assay, ELISA

1 Introduction

Human chromogranin A (CgA), an acidic protein belonging to the "*granins*" family, is a 439-residue long polypeptide present in the secretory granules of many neuroendocrine cells and neurons [1–6]. In different tissues, CgA can undergo differential posttranslational modifications, including glycosylation, phosphorylation, sulfation, and proteolytic cleavage [5, 7, 8]. Upon exocytosis, this protein and its fragments are released in the extracellular environment, together with the co-stored hormones, and then in circulation. Structural studies have shown that circulating CgA in healthy subject consists of a mixture of full-length CgA ($CgA_{1\text{-}439}$) and CgA-derived fragments of different size, including large polypeptides lacking part or the entire C-terminal region and shorter fragments [9]. Abnormal plasma levels of immunoreactive CgA have

Ricardo Borges (ed.), *Chromaffin Cells: Methods and Protocols*,
Methods in Molecular Biology, vol. 2565, https://doi.org/10.1007/978-1-0716-2671-9_23,

been detected in patients with neuroendocrine tumors, consequent to the fact that CgA and its fragments can be abnormally released in the blood by neoplastic neuroendocrine cells. Thus, plasma levels of CgA and its fragments, for example, the N-terminal fragment called vasostatin-1, can serve as a biomarker for the follow-up of a wide range of neuroendocrine tumors [10]. Elevated levels of CgA immunoreactivity have been detected also in the blood of patients with gastrointestinal, inflammatory, renal, metabolic, or cardiovascular diseases, with, in certain cases, important diagnostic and prognostic implications [5, 11].

A large body of experimental evidence suggests that $Cg_{A1\text{-}439}$ and its fragments contribute to regulate the cardiovascular system, innate immunity, metabolism, angiogenesis, tissue repair, and tumor growth in a very complex (and sometime opposite) manner [12]. For example, while full-length $CgA_{1\text{-}439}$ can exert antiangiogenic effects at physiological concentrations, cleavage of R_{373}–R_{374} site in the C-terminal region generates the $CgA_{1\text{-}373}$ fragment capable of promoting angiogenesis with a bell-shaped dose–response curve [13–15]. Upon cleavage, the exposed $PGPQLR_{373}$ site of $CgA_{1\text{-}373}$ can bind neuropilin-1 (NRP-1), an important co-receptor of vascular endothelial growth factor (VEGF); antibodies against this site (cryptic in $CgA_{1\text{-}439}$) reduce angiogenesis and tumor growth in various animal models of solid tumors [15]. Further proteolytic processing of $CgA_{1\text{-}373}$ to $CgA_{1\text{-}372}$, which can be triggered by plasma carboxypeptidases, causes loss of NRP-1 binding and proangiogenic activity [15]. Thus, cleavage of circulating CgA in tumors and then in the blood may represent mechanisms for regulating tumor angiogenesis and vascular biology in a very localized manner. Accordingly, a significant correlation between CgA fragmentation at the R_{373}–R_{374} site and tumor microvessel density has been observed in the bone marrow of patients with multiple myeloma [9]. Furthermore, cleavage of circulating CgA C-terminal region predicts progression-free and overall survival in patients with pancreatic ductal adenocarcinoma [16].

Given the complexity of the CgA system, which consists of full-length molecules and various fragments, it is desirable to have at hand specific assays capable of detecting these polypeptides in a very selective manner. The purpose of this article is to describe methods for developing ELISAs selective for full-length CgA and for its fragments. As an example, we describe the methods for (a) the production and purification of full-length CgA ($CgA_{1\text{-}439}$) and $CgA_{1\text{-}373}$ fragment (for assay standardization), (b) antibody production, and (c) ELISA development.

2 Materials

2.1 Reagents

1. Ampicillin.
2. Agar.
3. Isopropyl-β-D-thio-galactopyranoside (IPTG).
4. Protease Inhibitor Cocktail Set III, EDTA-Free (Calbiochem).
5. Benzonase® Nuclease (Novagen).
6. Synthetic peptides: CPGPQLR (Cys-$CgA_{368\text{-}373}$), ($CgA_{367\text{-}372}$) GPGPQL, GPGPQLR ($CgA_{367\text{-}373}$), SSMKLSFRARAYGFR GPGPQLR ($CgA_{352\text{-}373}$), CQALRRG (Cys-$CgA_{434\text{-}439}$), QALRRG ($CgA_{434\text{-}439}$), and RPEDQELESLSAIEAELEKVA HQLQALRRG ($CgA_{410\text{-}439}$).
7. Mouse antihuman CgA N-terminal region monoclonal antibody (mAb) B4E11 (*see* **Note 1**).
8. Bovine serum albumin (BSA) and human serum albumin (HSA).
9. Tween 20.
10. Normal goat serum (NGS).
11. Goat anti-rabbit IgG polyclonal antibody–horseradish peroxidase conjugate.
12. Hydrogen peroxide (30% w/v).
13. *O*-phenylenediamine tablets (OPD; 5 mg/tablet).
14. Normal human plasma (NHS).

2.2 Cells and Plasmids

1. SK-N-BE cells (CRL-2271, ATCC).
2. *E. coli* strain Rosetta™(DE3) (Novagen).
3. *E. coli* strain DH5α-competent cells.
4. pET11b expression plasmid (Novagen).
5. Champion™ pET Directional TOPO® Expression Kits (K100-01, Novagen).

2.3 Chromatographic Resins and Columns

1. Ion-exchange chromatography resins: Q-Sepharose Fast Flow and SOURCE 15 Q (Cytiva).
2. Affinity chromatography resin: calmodulin-agarose (SIGMA).
3. Detoxi-Gel™ Endotoxin Removing Gel (PIERCE).
4. Immobilized metal affinity chromatography resin: Ni-Sepharose 6 Fast Flow (Cytiva).
5. N-hydroxysuccinimide-activated Sepharose 4 Fast Flow (Cytiva).

6. Empty chromatographic columns: C-10/20 column, XK-16/20 columns (Cytiva), and Econo-Pac® Chromatography Columns (BIO-RAD).
7. Protein-A Sepharose 4 Fast Flow (Cytiva).

3 Methods

The methods described below outline (1) the construction of plasmids for the expression of full-length CgA ($CgA_{1\text{-}439}$) and $CgA_{1\text{-}373}$, the latter fused with a His-tag, (2) the expression of both proteins in *E. coli* cells and their purification, (3) the production of anti-CgA antibodies, and (4) the development of ELISAs for detecting mixtures of full-length CgA and fragments (*Total-CgA ELISA*), full-length $CgA_{1\text{-}439}$ (CgA_{439}*-ELISA*), and $CgA_{1\text{-}373}$ (CgA_{373}*-ELISA*) in plasma and other biological fluids.

3.1 Preparation of $CgA_{1\text{-}439}$ Expression Plasmid

This paragraph describes a cloning strategy that can be exploited for the preparation of a pET11 expression vector useful to produce $CgA_{1\text{-}439}$.

1. Prepare the cDNA coding for human $CgA_{1\text{-}439}$ starting from total RNA extracted from SK-N-BE following standard techniques [17].
2. Amplify the cDNA by PCR using the following primers:
   5′ GAACATATGCTCCCTGTGAACAGCCCTATG (*5′ NdeI primer*)
   3′ TCAGGATCCTCATCAGCCCCGCCGTAGTGC (*3′* BamHI primer) (*see* **Note 2**)
3. Digest the PCR product with NdeI/SacI and SacI/BamHI to generate two fragments of 183 bp and 1146 bp, respectively.
4. Ligate these fragments with an NdeI/BamHI-digested pET11b vector.
5. Transform DH5α-competent cells, and screen the resulting colonies by PCR using T7 promoter and T7 terminator primers.
6. Select positive clones and confirm their identity by plasmid DNA sequencing. The selected plasmid is called CgA-pET11.

3.2 Production of Recombinant Human $CgA_{1\text{-}439}$

The methods described below outline the expression and the purification process of CgA. The protocol refers to 2 L of cell culture. The flowchart of the fermentation and purification steps is shown in Fig. 1. The entire procedure takes 10 days. The steps described in Subheadings 3.2.1, 3.2.2, and 3.2.3. outline the procedure for extracting CgA from *E. coli* cells as a soluble protein. The steps described in Subheadings 3.2.4, 3.2.5, 3.2.6, 3.2.7, and 3.2.8.

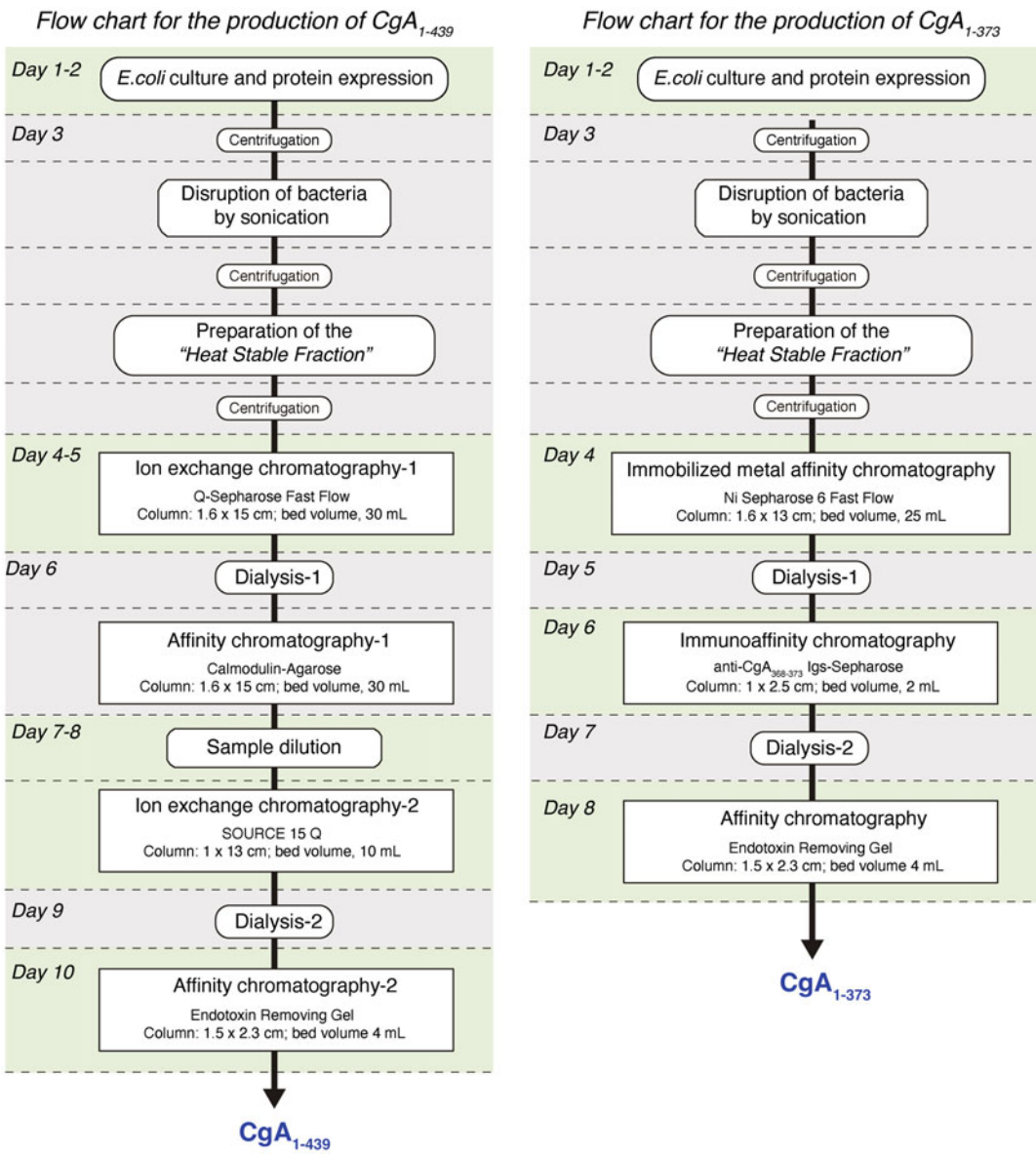

Fig. 1 Flowchart of human $CgA_{1\text{-}439}$ and $CgA_{1\text{-}373}$ production and purification. Types of chromatographic resin and column geometry (diameter and length) are reported in each panel

outline the procedure for the purification of CgA from heat stable extract. The steps described in Subheadings 3.2.9 outline the procedure to reduce endotoxin levels in the CgA product.

3.2.1 Preparation of Pre-inoculum

1. Freshly prepare autoclaved Luria Broth (LB) by mixing 1% tryptone, 0.5% yeast extract, and 1% NaCl, pH 7.0.
2. Transform Rosetta™(DE3)-competent cells with CgA-pET11 plasmid using standard protocols [17].

3. Plate cells on LB–agar plates (1.5% w/v agar in LB) containing ampicillin (100 μg/mL) and incubate overnight at 37 °C.
4. Select single colonies and transfer them in 100 mL of LB containing ampicillin (100 μg/mL) using a 500-mL flask. Incubate overnight at 37 °C under shaking (200 rpm) (*see* **Note 3**).

3.2.2 Cell Culture and Protein Expression

1. Fill four flasks (void volume, 2.5 L) with 500 mL of LB containing 100 μg/mL ampicillin, and add to each flask 10 mL of the pre-inoculum.
2. Incubate at 37°C under vigorous shaking (200 rpm) until the O.D. at 600 nm is about 4–5 units, and induce protein expression by adding IPTG (final concentration, 0.5 mM). Let the cells to grow for 1.5 h (*see* **Note 4**).
3. Centrifuge the culture (6000 × g, 10 min, 4°C).
4. Discard the supernatant and recover the bacterial pellet (*see* **Note 5**).

3.2.3 Disruption of Bacteria by Sonication and Preparation of the "Heat Stable" Fraction

1. Resuspend the bacterial pellets with 100 mL of 20 mM Tris–HCl, pH 8.0, containing 1 mM EDTA, 1% Protease Inhibitor Cocktail Set III, and 0.1% Benzonase® Nuclease.
2. Transfer the resuspended cells into four 50-mL tubes (25 mL/tube). Lyse the bacterial suspension by sonication (*see* **Note 6**).
3. Centrifuge the sonicated material (14,000 × g, 20 min, 4 °C), recover the soluble fraction, and discard the pellet.
4. Heat the soluble fraction in boiling water for 6 min.
5. Cool the tubes on ice for 15 min and centrifuge (14,000 × g, 20 min, 4 °C).
6. Recover the soluble fraction (*heat stable fraction, HSF*), store it at −80 °C, and discard the pellet.

3.2.4 Ion Exchange Chromatography-1

1. Load the *HSF* product (flow rate 1 mL/min) onto an XK-16/20 column filled with 30 mL of Q-Sepharose Fast Flow resin, pre-equilibrated with 90 mL of 1 mM EDTA, 20 mM Tris–HCl buffer, pH 8.0 (*Buffer A*) (*see* **Note 7**).
2. Wash the column overnight with 500 mL of *Buffer A* (flow rate 0.5 mL/min), and elute the bound proteins with 1 mM EDTA, 0.6 M NaCl, 20 mM Tris–HCl buffer, pH 8.0 (*Buffer B*) using the following gradient: 30–100% *Buffer B* (300 mL), 100% *Buffer B* (30 mL), and flow rate 2 mL/min.
3. Collect 5-mL fractions and analyze them by SDS-PAGE. Pool fractions with the highest putative $CgA_{1\text{-}439}$ content and purity, as judged from the observed bands, and store the product at −80 °C until the next step.

3.2.5 Dialysis-1

1. Add $CaCl_2$ (1 mM, final concentration) to the product.
2. Dialyze the product (cutoff: 12,000 Da) against 2 L of 1 mM $CaCl_2$, 100 mM KCl, 20 mM Tris–HCl buffer, pH 7.5 (*Buffer C*) (30 min, 4 °C); then discard the dialysis buffer.
3. Repeat this step for four additional times. The final product is called *QS-d*.

3.2.6 Affinity Chromatography-1

1. Fill an XK-16/20 column with 30 mL of calmodulin–agarose resin, and equilibrate the column with 90 mL of 0.2 mM $CaCl_2$, 100 mM KCl, 20 mM Tris–HCl buffer, pH 7.5 (*Buffer D*).
2. Load the *QS-d* product and wash the column with the following buffers: (a) *Buffer D;* (b) 0.2 mM $CaCl_2$, 500 mM KCl, 20 mM Tris–HCl buffer, pH 7.5; and (c) *Buffer D* (300 mL of each buffer*;* flow rate 2 mL/min).
3. Elute the bound protein with 1 mM EGTA, 100 mM KCl, 20 mM Tris–HCl buffer, pH 7.5 (90 mL); collect the product (called *CAL*) and analyze it by SDS-PAGE. Store at −80 °C until the next step.

3.2.7 Ion Exchange Chromatography-2

1. Fill a C-10/20 column filled with 10 mL of SOURCE 15 Q resin and equilibrate the column with *Buffer A* (flow rate 0.5 mL/min).
2. Dilute the *CAL* product twofold with *Buffer A* and load the product onto the column.
3. Wash the column overnight with *Buffer A* (100 mL; flow rate 0.1 mL/min), and elute the bound proteins using the following salt gradient: 47–60% *Buffer B* (100 mL; flow rate 0.5 mL/min) and 100% *Buffer B* (30 mL; flow rate 0.5 mL/min).
4. Collect fractions of 2 mL and analyze them by SDS-PAGE. Pool fractions with the highest putative $CgA_{1\text{-}439}$ content and purity, as judged from the observed bands, and store the product at −80 °C.

3.2.8 Dialysis-2

1. Dialyze the product (cutoff: 3500 Da) against 53 volumes of 0.9% NaCl (60 min, 4 °C).
2. Repeat this step for four additional times.
3. Store the product at −80 °C.

3.2.9 Affinity Chromatography-2 (Endotoxin Removal)

1. Fill an Econo-Pac column with 4 mL of Detoxi-Gel™ Endotoxin Removing Gel, and wash the column with 20 mL of 1% sodium deoxycholate and with 100 mL of 0.9% NaCl (flow rate 4 mL/min) (*see* **Note 8**).
2. Load the product on the column, and collect the flow-through in a 50-mL tube (flow rate 0.5 mL/min).

3. Wash the column with 0.9% NaCl (4 mL; flow rate 0.5 mL/min), and collect the flow-through into the same 50-mL tube.
4. Regenerate the column as described above, and reload the flow-through onto the column; collect again the flow-through in a new 50-mL tube.
5. Aliquot the final product, which corresponds to purified $CgA_{1\text{-}439}$, and store aliquots at −80 °C (*see* **Note 9**).

3.3 Preparation of $CgA_{1\text{-}373}$ Expression Plasmid

This paragraph describes a cloning strategy that can be exploited for the preparation of a pET100D/TOPO expression vector useful to produce $CgA_{1\text{-}373}$ fused to a His-tag (*see* **Note 10**).

1. Prepare the cDNA coding for $CgA_{1\text{-}373}$ by PCR using the CgA-pET11 plasmid (*see* above) and the following primers:
   5′-CACCCTCCCTGTGAACAGCCCTATG (*5′ $CgA_{1\text{-}7}$ primer*)
   5′-**TCA**TCGCAGCTGCGGCCCAGG (*3′ $CgA_{368\text{-}373}$ primer*) (*see* **Note 11**)
2. Ligate the PCR product into a pET100/D-TOPO plasmid according to the Champion™ pET Directional TOPO® Expression Kits manual.
3. Follow the kit's instruction for the next steps of cloning. The selected plasmid is called $CgA_{1\text{-}373}$-pET100D/TOPO.

3.4 Production of $CgA_{1\text{-}373}$

The methods described below outline the expression and the purification process of His-tagged $CgA_{1\text{-}373}$. The protocol refers to 2 L of cell culture. The flowchart of the fermentation and purification steps is shown in Fig. 1. The entire procedure takes 8 days.

3.4.1 Fermentation and Preparation of the Heat Stable Fraction

Fermentation of transformed *E. coli* cell and preparation of crude extract containing the $CgA_{1\text{-}373}$ (heat stable fraction, HSF) can be performed as described above for the expression of $CgA_{1\text{-}439}$, except that $CgA_{1\text{-}373}$-pET100/D plasmid is used.

3.4.2 Immobilized Metal Chelate Affinity chromatography (IMAC)

1. Fill an XK-16/20 columns with 25 mL of Ni Sepharose 6 Fast Flow column, and equilibrate the column with 500 mM NaCl, 20 mM imidazole, 20 mM sodium phosphate buffer, pH 7.4 (*Buffer I*) (flow rate 2 mL/min).
2. Load the crude extract, prepared as described above (*HSF*), onto the column and collect the flow-through.
3. Wash the column with 250 mL of *Buffer I,* and elute the bound proteins with 260 mM imidazole, 500 mM NaCl, 20 mM sodium phosphate buffer, pH 7.4.
4. Collect 5-mL fractions and store them on ice.

5. Remove an aliquot from fractions for SDS-PAGE analysis, and store them at 80 °C. Pool fractions with the highest $CgA_{1\text{-}373}$ content and purity, as judged from the observed bands.

3.4.3 Dialysis-1

1. Dialyze the product (cutoff: 3500 Da) against 28 volumes of 150 mM NaCl, 50 mM sodium phosphate buffer, pH 7.3 (PBS) (1 h, 4 °C).
2. Repeat this step for four additional times.
3. Store the product at −80 °C until the next step.

3.4.4 Immunoaffinity Chromatography

1. Fill a C-10/20 column with of anti-$CgA_{368\text{-}373}$ Igs-Sepharose resin (prepared using anti-$CgA_{368\text{-}373}$ immunoglobulins described below), and equilibrate the column with PBS (flow rate 1 mL/min) (*see* **Note 12**).
2. Load the product onto the column, and collect the flow-through.
3. Wash the column with PBS, and elute the bound proteins with 500 mM NaCl, 200 mM glycine-HCl buffer, pH 2.5.
4. Collect 0.5-mL fractions, and add 50 μL of 1 M Tris (*see* **Note 13**).
5. Analyze fractions by SDS-PAGE analysis, and pool fractions with the highest $CgA_{1\text{-}373}$ content and purity, as judged from the observed bands. Store the product at −80 °C.

3.4.5 Dialysis-2

1. Dialyze the product (cutoff: 3500 Da) against 28 volumes of 0.9% NaCl (1 h, 4 °C).
2. Repeat this step for four additional times.

3.4.6 Affinity Chromatography (Endotoxin Removal)

1. Load the product on a Detoxi-Gel™ Endotoxin Removing Gel column and proceed as described for $CgA_{1\text{-}439}$.

3.5 Biochemical Characterization of $CgA_{1\text{-}439}$ and $CgA_{1\text{-}373}$

Protein purity and identity. The purity and the identity of $CgA_{1\text{-}439}$ and $CgA_{1\text{-}373}$ can be estimated using several different analytical procedures, including SDS-PAGE, mass spectrometry, ELISA, and Western blot.

Figure 2a and b shows a representative SDS-PAGE analysis of purified $CgA_{1\text{-}439}$ and $CgA_{1\text{-}373}$ under reducing and nonreducing condition. Purified $CgA_{1\text{-}439}$ and $CgA_{1\text{-}373}$ typically show single bands of about 70 KDa and 65 KDa, respectively. A faint band of higher molecular weight can be also observed under not reducing condition, presumably corresponding to disulfide-bridged protein aggregates. Both proteins typically show a purity of about 95%, as can be determined by densitometric analysis of the SDS-PAGE gel.

The amount of lipopolysaccharide in our preparations is typically lower than 0.01 U/μg of purified protein, as measured by

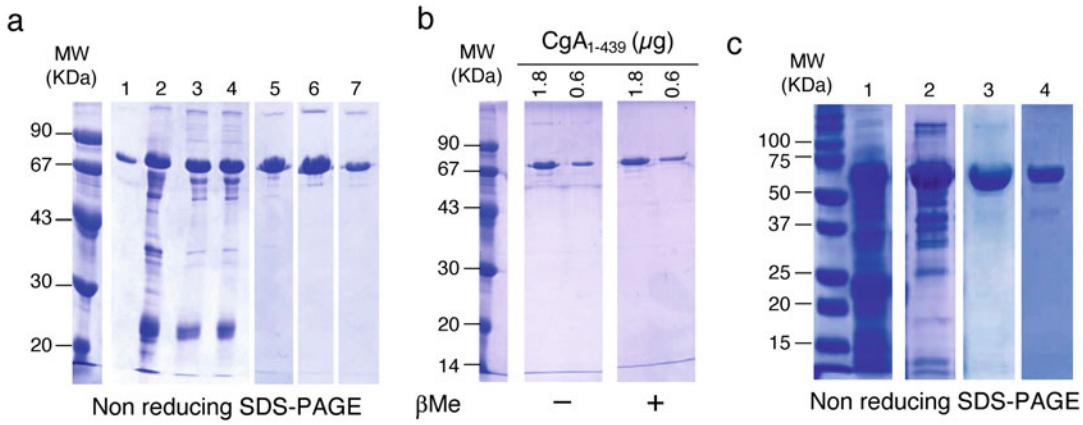

Fig. 2 SDS-PAGE analysis of $CgA_{1\text{-}439}$ and $CgA_{1\text{-}373}$. (**a**) Nonreducing SDS-PAGE of the products obtained after the various purification steps of $CgA_{1\text{-}439}$ (*see* the flowchart in Fig. 1, *left*). (*Lane 1*) CgA reference standard; (*Lane 2*) heat stable fraction; (*Lane 3*) ion exchange chromatography-1; (*Lane 4*) dialysis-1; (*Lane* 5) affinity chromatography-1; (*Lane 6*) ion exchange chromatography-2; (*Lane 7*) affinity chromatography-2. (**b**) SDS-PAGE analysis of purified $CgA_{1\text{-}439}$ under reducing (βMe +) and nonreducing conditions (βMe −). The amount of $CgA_{1\text{-}439}$ loaded are indicated. (**c**) Nonreducing SDS-PAGE of the products obtained after the various purification steps of $CgA_{1\text{-}373}$ (*see* the flowchart of Fig. 1, *right*). (*Lane 1*) heat stable fraction; (*Lane 2*) immobilized metal affinity chromatography; (*Lane 3*) immunoaffinity chromatography; (*Lane 4*) affinity chromatography. MW: molecular markers. Gels: 12.5% polyacrylamide; staining: Coomassie Brilliant Blue R250

quantitative chromogenic limulus amebocyte lysate (LAL) test. Mass spectrometry analysis of $CgA_{1\text{-}439}$ shows a molecular weight of 49,061 Da, in good agreement with the expected molecular mass 49,045 Da.

Yields. About 5–15 mg of $CgA_{1\text{-}439}$ and 0.1–1 mg of His-tagged $CgA_{1\text{-}373}$ can be recovered from 1 L of fermentation, as measured by ELISA.

3.6 Preparation of Antibodies

These paragraphs describe the methods for the preparation of the antibodies necessary for $CgA_{1\text{-}373}$ purification and ELISAs development.

3.6.1 Preparation and Purification of Anti-$CgA_{368\text{-}373}$ Antibodies

1. Immunize two New Zealand rabbits with the Cys-$CgA_{368\text{-}373}$ peptide (CPGPQLR) coupled to keyhole-limpet hemocyanin (KLH) via succinimidyl 4-[N-maleimidomethyl]cyclohexane-1-carboxylate (SMCC) (*see* **Note 14**).
2. Boost rabbits with the immunogen at day 0, 21 28, 35, and 42, bleed the animals at day 44, and prepare the sera (*see* **Note 15**).
3. Analyze the levels of the raised antibodies by direct ELISA using microtiter plates coated with the immunogen (KLH-$CgA_{368\text{-}373}$) or with $CgA_{352\text{-}373}$.

4. Prepare a $CgA_{367\text{-}373}$-Sepharose affinity column by coupling 25 mg of peptide GPGPQLR ($CgA_{367\text{-}373}$) to 10 mL of N-hydroxysuccinimide (NHS)-activated Sepharose 4 Fast Flow resin (*see* **Note 12**).
5. Dilute 1:2 the antisera prepared above with PBS, filter on 0.45-μm filter, and load the product onto a C-10/20 column containing 10 mL of $CgA_{367\text{-}373}$-Sepharose (flow rate 1 mL/min); wash the column with 50 mL of PBS, and elute the bound antibodies with 40 mL of 500 mM NaCl, 200 mM glycine–HCl buffer, pH 2.5 (flow rate 1 mL/min, fraction size 2 mL).
6. Add 0.2 mL of 1 M Tris to each fraction, and remove an aliquot for UV analysis (A_{280} nm).
7. Dialyze the product (cutoff: 12.5 KDa) against 150 mM NaCl (overnight, 4 °C).
8. To remove the anti-$CgA_{368\text{-}372}$ antibodies, load the product onto a $CgA_{367\text{-}372}$-Sepharose affinity column (prepared as described above using the GPGPQL ($CgA_{367\text{-}372}$) peptide in place of $CgA_{367\text{-}373}$), collect the flow-through, and then concentrate it by ultrafiltration (*see* **Note 16**). The final product, consisting of anti-$CgA_{368\text{-}373}$ immunoglobulins, is used for $CgA_{1\text{-}373}$ purification and *CgA_{373}-ELISA* development.

3.6.2 Preparation and Purification of Anti-$CgA_{434\text{-}439}$ Antibodies

1. Preparation and purification of anti-$CgA_{434\text{-}439}$ polyclonal antibodies can be performed using the same procedure described above for anti-$CgA_{368\text{-}373}$ using the Cys-$CgA_{434\text{-}439}$ peptide coupled to KLH (KLH-$CgA_{434\text{-}439}$) as immunogen (*see* **Notes 14** and **15**).
2. Analyze the levels of raised antibodies by ELISA using microtiter plates coated with the immunogen (KLH-$CgA_{434\text{-}439}$) or with the $CgA_{410\text{-}439}$ peptide.
3. Purify the antisera on 4 mL of Protein-A Sepharose 4 Fast Flow column using standard procedures. Aliquot the final product and store it at −80 °C.

3.6.3 Preparation and Purification of Anti-$CgA_{1\text{-}439}$ Antibodies

Antihuman recombinant $CgA_{1\text{-}439}$ IgGs can be raised in New Zealand rabbits by intradermal injection of 200 μg of recombinant $CgA_{1\text{-}439}$ with complete Freund's adjuvant as described previously [18]. Anti-$CgA_{1\text{-}439}$ polyclonal antibodies can be further purified from the animal sera by affinity chromatographic on Protein-A Sepharose using standard procedures. Aliquot the final product and store it at −80 °C.

3.7 Characterization of Antibody Specificity

The specificity of anti-$CgA_{1\text{-}439}$, anti-$CgA_{434\text{-}439}$, and anti-$CgA_{368\text{-}373}$ antibodies can be checked by direct ELISA using microtiter plates coated with or without $CgA_{1\text{-}439}$ and $CgA_{1\text{-}373}$. Representative results of these assays are reported in Fig. 3a, showing that the

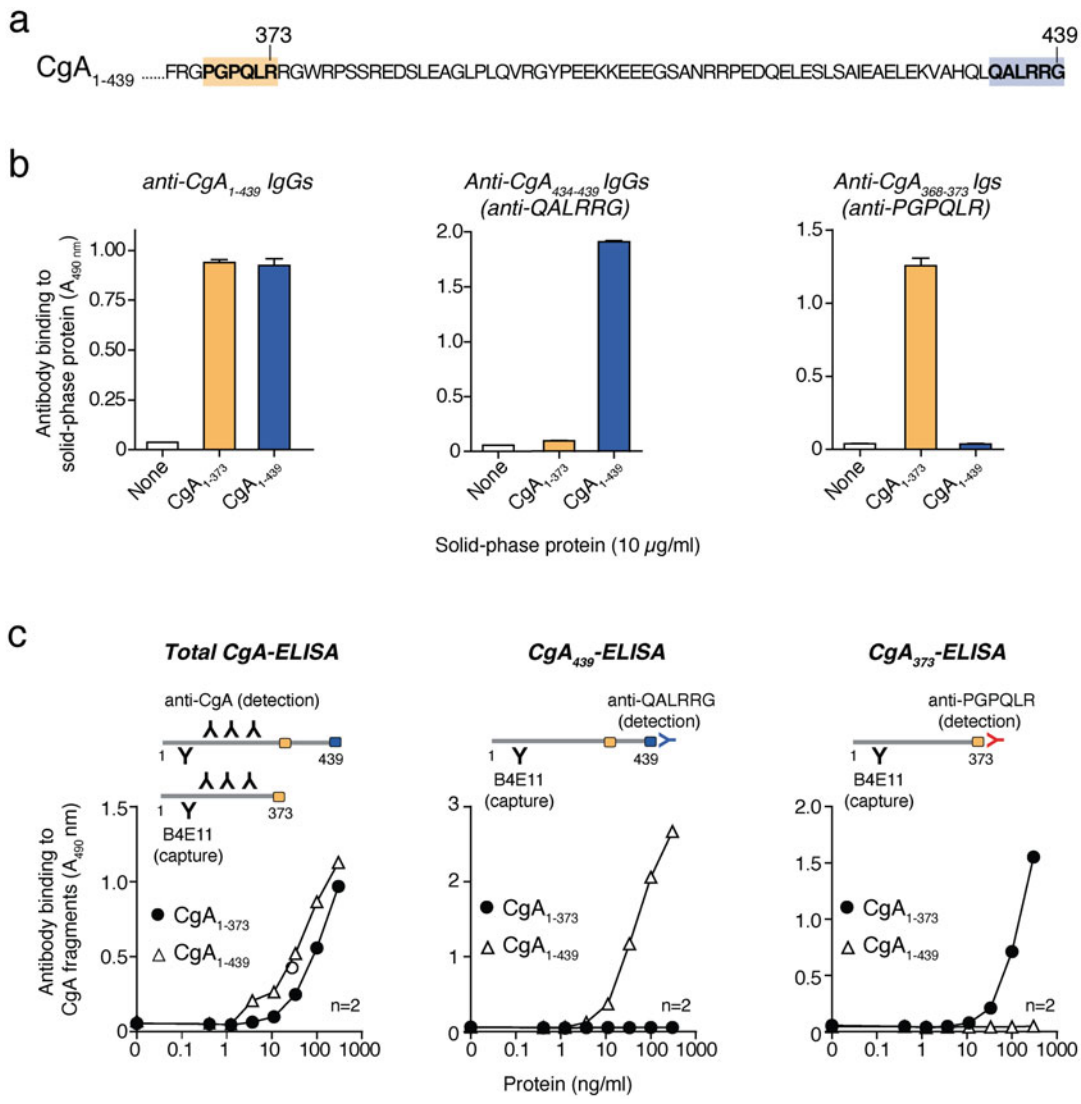

Fig. 3 Development of antibodies and sandwich ELISAs for detecting total CgA, full-length CgA, and fragmented CgA. (**a**) Amino acid sequence of human $CgA_{365-439}$ region. The sequence QALRRG (blue box) corresponds to the epitope recognized by antibodies against the C-terminal residues of $CgA_{434-439}$. The sequence PGPQLR (yellow box) corresponds to a cryptic site of the full-length CgA exposed after cleavage at R373; this site is recognized by anti-$CgA_{368-373}$ antibodies in the cleaved CgA_{1-373} fragment but not the full-length molecule. (**b**) Binding of rabbit anti-CgA_{1-439}, anti-$CgA_{434-439}$ (QALRRG), and anti-$CgA_{368-373}$ (PGPQLR) antibodies to microtiter plates coated with or without human CgA_{1-439} or CgA_{1-373}, as detected by ELISA with a goat anti-rabbit IgGs-peroxidase conjugate. Note that the anti-QALRRG antibodies can selectively detect the full-length molecule but not the fragment, and vice versa in the case of anti-PGPQLR antibodies. (**c**) Schematic representation of *Total CgA*-, *CgA_{439}*-, and *CgA_{373}-ELISA* (based on mAb B4E11 in the capture step and the indicated rabbit antiserum in the detection steps) and binding curves obtained with these ELISAs. Note that CgA_{439}- and CgA_{373}-ELISAs, but not the Total CgA-ELISA, can specifically detect CgA_{1-439} and CgA_{1-373}, respectively [15]

anti-$CgA_{1\text{-}439}$ antibodies recognizes both proteins, while the anti-$CgA_{434\text{-}439}$ or anti-$CgA_{368\text{-}373}$ antibodies selectively recognize $CgA_{1\text{-}439}$ or $CgA_{1\text{-}373}$, respectively.

3.8 ELISAs

The methods described below outline three sandwich ELISAs for detecting (1) total CgA (i.e., full-length CgA and large fragments lacking part or the entire C-terminal region and containing the N-terminal and central region (*Total CgA-ELISA*)), (2) full-length $CgA_{1\text{-}439}$ (*CgA_{439}-ELISA*), and (3) $CgA_{1\text{-}373}$ (*CgA_{373}-ELISA*). All these assays are based on the use of mAb B4E11 (epitope: human $CgA_{68\text{-}71}$) in the capture step and anti-$CgA_{1\text{-}439}$ antibodies (epitope located in the central part of the molecule) or anti-$CgA_{434\text{-}439}$ antibodies (epitope: $CgA_{434\text{-}439}$) or anti-$CgA_{368\text{-}373}$ antibodies (epitope $CgA_{368\text{-}373}$) in the detection steps. A schematic representation of the ELISAs is reported in Fig. 3b.

3.8.1 Total CgA-ELISA

1. Coat 96-well PVC microtiter plates (Carlo Erba, cod. FA5280100, Italy) with mAb B4E11 (10 μg/mL in PBS, 50 μL/well), and incubate overnight at 4 °C (*see* **Note 1**).
2. Wash the plate three times by emptying and filling with PBS.
3. Fill the wells with 3% BSA in PBS (200 μL/well), incubate 2 h at room temperature, and then wash again three times with PBS.
4. Fill the wells with 50 μL of *recombinant CgA standard* solutions (range 4.6–300 ng/mL; *see* **Note 17**) or samples diluted in PBS containing 0.5% BSA, 2.5% NGS, 0.05% Tween 20, 1:5000 Protease Inhibitor Cocktail Set III, 2 mM EDTA (*Assay Buffer*), and incubate for 1.5 h at 37 °C (*see* **Note 18**).
5. Wash the plate eight times by emptying and filling with PBS containing 0.05% Tween 20 (PBS-T).
6. Add to each well 50 μL of anti-$CgA_{1\text{-}439}$ antibodies diluted in *Assay Buffer* (final concentration 10 μg/mL), and incubate for 1.5 h at 37 °C.
7. After washing eight times with PBS-T, add to each well 50 μL of goat anti-rabbit IgG-HRP diluted 1:1000 in *Assay Buffer*, and incubate for 1 h at room temperature.
8. Wash again with PBS-T and fill each well with 70 μL of *o*-phenylenediamine solution (1 tablet in 7.5 mL of distilled water containing 10 μL of 30% hydrogen peroxide) and incubate for 10–20 min.
9. Block the chromogenic reaction by adding 10% sulfuric acid (70 μL/well).
10. Measure the absorbance at 490 nm of each well using an ELISA plate reader.

3.8.2 CgA_{439}-ELISA

1. Coat the plate with mAb B4E11, and block it with BSA as described above for the *Total CgA-ELISA*.
2. Fill the wells with 50 μL of recombinant $CgA_{1\text{-}439}$ standard solutions (range 4.6–300 ng/mL), or samples, diluted in *Assay Buffer* containing 50% CgA-depleted NHS; incubate for 1.5 h at 37 °C (*see* **Note 19**).
3. Wash the plate eight times by emptying and filling with PBS containing 0.05% Tween 20 (*PBS-T*).
4. Add to each well 50 μL of anti-$CgA_{1\text{-}439}$ antibodies diluted in *Assay Buffer* (final concentration 10 μg/mL); incubate for 1.5 h at 37 °C.
5. Wash the plate eight times with PBS-T, and detect antibody binding with goat anti-rabbit IgG-HRP as described above for *Total CgA-ELISA*.

3.8.3 CgA_{373}-ELISA

The *CgA_{373}-ELISA* can be performed using the same procedure described above for *CgA_{439}-ELISA*, except that $CgA_{1\text{-}373}$ is used for the preparation of standard solutions and that anti-$CgA_{368\text{-}373}$ antibodies are used in the detection step.

4 Notes

1. Mouse monoclonal antibody B4E11 (epitope: human $CgA_{68\text{-}71}$) was prepared by standard hybridoma procedures, as described [18]. In principle, other mouse monoclonal antibodies against the N-terminal or central region of CgA could be used, in place of mAb B4E11, if they have good affinity for full-length CgA and CgA fragments (*Kd* in the subnanomolar range).
2. These primers contain the NdeI and BamHI restriction sites (*underlined*), necessary for cloning procedure, and the ATG translation starting codon and TCA stop codons (*bold*).
3. Do not prepare glycerol stocks of Rosetta™(DE3) cells transformed with CgA-coding plasmid because we have observed a progressive loss of protein expression.
4. Remove 1-mL aliquot of non-induced and induced cell culture for SDS-PAGE analysis.
5. Do not store the cellular pellet for later purification since massive CgA degradation may occur, even if the pellet is stored at −80 °C.
6. During the sonication process, store the sample on ice to avoid overheating. To assess bacterial lysis, remove 10 μL of the sonicated sample, centrifuge for 5 min at 13,000 g, dilute the supernatant 1:100 with extraction buffer, and measure the

absorbance at 280 nm. Repeat the sonication step until the absorbance at 280 nm does not further increase. Typically, few cycles of sonication are sufficient to obtain a final absorbance at 280 nm of about 100 units.

7. All chromatographic buffers should be prepared with sterile endotoxin-free water and vacuum-filtered on 0.45 μm of cellulose nitrate filters. The purification steps should be carried out in a cold room. All chromatographic products are kept on ice unless otherwise indicated.
8. Carefully read and follow the technical data sheet of Detoxi-Gel™ Endotoxin Removing Gel before proceeding with purification.
9. Purified $CgA_{1\text{-}439}$ and $CgA_{1\text{-}373}$ can be stored at −80 °C for few years; the storage of diluted products should be avoided.
10. Carefully read and follow the manual of Champion™ pET Directional TOPO® Expression Kit. This plasmid allows the production of $CgA_{1\text{-}373}$ with a His-tag and the Xpress™ epitope fused with the N-terminus of $CgA_{1\text{-}373}$ (a detailed map of the pET100/D plasmid and the resulting fusion product is shown in the manual).
11. The $CgA_{1\text{-}7}$ primer contains the CACC sequence (*underlined*), necessary for the directional cloning of the PCR product, whereas the $CgA_{368\text{-}373}$ primer contains the TCA translation stop codon (***bold***).
12. Peptide/antibody coupling to NHS-activated Sepharose is performed according to the manufacturer's instructions.
13. Purification yield can be increased by reloading the flow-through.
14. Rabbit polyclonal antibody production can be also done by companies that provide this service (e.g., Proteogenix, France).
15. Test the sera of immunized rabbit by ELISA after the fourth administration of the antigen. If the antiserum titer is low, an additional boost of immunogen can be done.
16. Ultrafiltration can be carried out using an Amicon® Stirred Cell equipped with 10 KDa cutoff filter (Millipore cat. PLGC04310).
17. These ELISAs use, as reference standards, recombinant proteins produced in *E. coli*, thus lacking posttranslational modifications that may occur in natural CgA. Moreover, they cannot detect CgA fragments lacking the N-terminal region of CgA as the mAb B4E11 used in the capture step is against the $CgA_{68\text{-}71}$ epitope. These assays can be used for the detection of natural CgA in plasma. Serum samples cannot be used

as full-length CgA is cleaved by thrombin CgA during blood coagulation [13].

18. The CgA_{1-439} standard solutions must be prepared in PBS containing 0.1% HSA, 0.05% Tween 20, 2 mM EDTA, and 1:200 Protease Inhibitor Cocktail Set III, EDTA-Free (30 μg/mL final protein concentration, in single-use aliquots of 20 μL). Test serum or plasma samples in duplicate using serial dilution (e.g., 1:3, 1:9, or 1:27 dilution).
19. The reference standard solutions of these assays are prepared as described above for CgA_{1-439} reference standards, except that the dilution buffer should contain 50% of CgA-depleted normal human plasma (NHP). CgA-depleted NHP can be prepared by loading NHP (1:2 in PBS) onto a mAb B4E11-Sepharose column and collecting the flow-through. Serial dilution (e.g., 1:2, 1:4, 1:8) of plasma samples should be tested in duplicate.

Acknowledgments

The research leading to these results has received funding from AIRC under IG 2019 – ID. 23470 project – P.I. Corti Angelo.

References

1. Banks P, Helle KB (1965) The release of protein from the stimulated adrenal medulla. Biochem J 97:40C–41C
2. Deftos LJ (1991) Chromogranin A: its role in endocrine function and as an endocrine and neuroendocrine tumor marker. Endocr Rev 12(2):181–187
3. Janson ET, Holmberg L, Stridsberg M, Eriksson B, Theodorsson E, Wilander E, Oberg K (1997) Carcinoid tumors: analysis of prognostic factors and survival in 301 patients from a referral center. Ann Oncol 8(7):685–690
4. Taupenot L, Harper KL, O'Connor DT (2003) The chromogranin-secretogranin family. N Engl J Med 348(12):1134–1149
5. Helle KB, Corti A, Metz-Boutigue MH, Tota B (2007) The endocrine role for chromogranin A: a prohormone for peptides with regulatory properties. Cell Mol Life Sci 64(22):2863–2886. https://doi.org/10.1007/s00018-007-7254-0
6. Portela-Gomes GM, Grimelius L, Wilander E, Stridsberg M (2010) Granins and granin-related peptides in neuroendocrine tumours. Regul Pept 165(1):12–20
7. Gadroy P, Stridsberg M, Capon C, Michalski JC, Strub JM, Van Dorsselaer A, Aunis D, Metz-Boutigue MH (1998) Phosphorylation and O-glycosylation sites of human chromogranin A (CGA79-439) from urine of patients with carcinoid tumors. J Biol Chem 273(51):34087–34097
8. Sanduleanu S, De Bruine A, Stridsberg M, Jonkers D, Biemond I, Hameeteman W, Lundqvist G, Stockbrugger RW (2001) Serum chromogranin A as a screening test for gastric enterochromaffin-like cell hyperplasia during acid-suppressive therapy. Eur J Clin Investig 31(9):802–811
9. Bianco M, Gasparri AM, Colombo B, Curnis F, Girlanda S, Ponzoni M, Bertilaccio MT, Calcinotto A, Sacchi A, Ferrero E, Ferrarini M, Chesi M, Bergsagel PL, Bellone M, Tonon G, Ciceri F, Marcatti M, Caligaris Cappio F, Corti A (2016) Chromogranin A is preferentially cleaved into pro-angiogenic peptides in the bone marrow of multiple myeloma patients. Cancer Res 76:1781–1179. https://doi.org/10.1158/0008-5472.CAN-15-1637
10. O'Connor DT, Bernstein KN (1984) Radioimmunoassay of chromogranin A in plasma as a

measure of exocytotic sympathoadrenal activity in normal subjects and patients with pheochromocytoma. N Engl J Med 311(12):764–770

11. Loh YP, Cheng Y, Mahata SK, Corti A, Tota B (2012) Chromogranin A and derived peptides in health and disease. J Mol Neurosci 48(2):347–356. https://doi.org/10.1007/s12031-012-9728-2
12. Mahata SK, Corti A (2019) Chromogranin A and its fragments in cardiovascular, immunometabolic, and cancer regulation. Ann N Y Acad Sci 1455(1):34–58. https://doi.org/10.1111/nyas.14249
13. Crippa L, Bianco M, Colombo B, Gasparri AM, Ferrero E, Loh YP, Curnis F, Corti A (2013) A new chromogranin A-dependent angiogenic switch activated by thrombin. Blood 121(2):392–402. https://doi.org/10.1182/blood-2012-05-430314
14. Theurl M, Schgoer W, Albrecht K, Jeschke J, Egger M, Beer AG, Vasiljevic D, Rong S, Wolf AM, Bahlmann FH, Patsch JR, Wolf D, Schratzberger P, Mahata SK, Kirchmair R (2010) The neuropeptide catestatin acts as a novel angiogenic cytokine via a basic fibroblast growth factor-dependent mechanism. Circ Res 107(11):1326–1335. https://doi.org/10.1161/CIRCRESAHA.110.219493
15. Dallatomasina A, Gasparri AM, Colombo B, Sacchi A, Bianco M, Daniele T, Esposito A, Pastorino F, Ponzoni M, Marcucci F, Curnis F, Corti A (2019) Spatiotemporal regulation of tumor angiogenesis by circulating chromogranin A cleavage and neuropilin-1 engagement. Cancer Res 79(8):1925–1937. https://doi.org/10.1158/0008-5472.CAN-18-0289
16. Reni M, Andreasi V, Gasparri AM, Dugnani E, Colombo B, Macchini M, Bianco M, Dallatomasina A, Citro A, Assi E, Protti MP, Esposito A, Falconi M, Curnis F, Piemonti L, Corti A (2020) Circulating chromogranin A is cleaved into vasoregulatory fragments in patients with pancreatic ductal adenocarcinoma. Front Oncol 10:613582. https://doi.org/10.3389/fonc.2020.613582
17. Sambrook J, Fritsch EF, Maniatis T (eds) (1989) Molecular cloning a laboratory manual. Cold Spring Harbor Laboratory, Cold Spring Harbor, NY
18. Corti A, Longhi R, Gasparri A, Chen F, Pelagi M, Siccardi AG (1996) Antigenic regions of human chromogranin A and their topographic relationships with structural/functional domains. Eur J Biochem 235(1–2):275–280

Chapter 24

Cytotoxicity Models in Chromaffin Cells to Evaluate Neuroprotective Compounds

María F. Cano-Abad and Manuela G. López

Abstract

Primary cultures of bovine chromaffin cells are considered a good model to evaluate potential neuroprotective compounds for two major reasons: (i) they share many common features to neurons as they synthesize, store, and release neurotransmitters; they are excitable cells that express voltage-dependent calcium, potassium, and sodium channels; they express different neuronal receptor subtypes; and (ii) they can be easily cultured in high quantities from adult animals; as adult para-neurons, they can be used to reproduce different neurodegenerative-like cytotoxicity models. In this chapter, we describe protocols to mimic calcium overload (veratridine and thapsigargin) and oxidative stress (rotenone plus oligomycin-A and 6-hydroxydopamine) to evaluate potential neuroprotective compounds.

Key words Chromaffin cells, Cytotoxicity, Calcium overload, Free radicals, Drug screening, Neuroprotection, LDH, Veratridine, 6-Hydroxydopamine

1 Introduction

Chromaffin cells are considered neuronal-like cells as they share many common features to neurons such as (i) they synthesize, store, and release neurotransmitters; (ii) they are excitable cells that express voltage-dependent calcium, potassium, and sodium channels; (iii) they express different neuronal receptor subtypes; and (iv) they contain regulated intracellular calcium stores. Contrary to primary neuronal cultures that are obtained from prenatal mice or rats, bovine chromaffin cells (BCC) have the advantage that they can be easily isolated and cultured from adult animals in large quantities. For all these reasons, BCCs have been used to reproduce different pathological mechanisms described in acute and chronic neurodegenerative diseases such as calcium overload and oxidative stress to screen new drugs with putative neuroprotective properties.

Ricardo Borges (ed.), *Chromaffin Cells: Methods and Protocols*,
Methods in Molecular Biology, vol. 2565, https://doi.org/10.1007/978-1-0716-2671-9_24,

1.1 Calcium Overload Models

Dysregulation of Ca^{2+} is decisive for brain cell death and neurodegeneration after ischemic stroke, Alzheimer's disease, Parkinson's disease, Huntington's disease, or multiple sclerosis [1]. Therefore, establishing in vitro models that reproduce intracellular Ca^{2+} deregulation is useful to evaluate potential compounds for the diseases mentioned above. In this case, veratridine and thapsigargin have been widely used in BCCs to achieve this purpose.

- *Veratridine* is an alkaloid that acts on voltage-dependent Na^+ channels that causes membrane depolarization–repolarization cycles, mimicking repeated action potentials followed by large oscillations of the cytosolic Ca^{2+} concentration ($[Ca^{2+}]_c$) [2, 3]; these continuous Ca^{2+} oscillations lead to calcium overload and cell death [3–5]. The characteristic mechanism of action of this alkaloid has been used to mimic brain ischemia [6], epileptic seizures [7], or migraine [8, 9]. The use of veratridine, as a model of Ca^{2+} overload, has been widely used to evaluate new compounds for these diseases.
- *Thapsigargin* is a sesquiterpene lactone and a potent cytotoxin that induces apoptosis by inhibiting the sarcoplasmic/endoplasmic reticulum Ca^{2+} ATPase (SERCA) pump, which is necessary for cellular viability. In Alzheimer's disease, the ER Ca^{2+} store is regulated upon presenilins; actually, there is evidence that indicate that those proteins are the Ca^{2+} regulators of the ER. For this reason, thapsigargin can mimic the presenilin like disease described for Alzheimer's disease [10, 11].

1.2 Oxidative Stress Models

Mitochondrial dysfunction leads to oxidative stress, and oxidative stress is considered as one of the main drivers in neurodegeneration [12]. Therefore, evaluation of effective therapeutic agents that target redox homeostasis in neurodegenerative disease requires models that reproduce these features. In this context, we describe the following two models:

- *Mitochondrial dysfunction*. One of the most widely used models to induce mitochondrial disruption is the simultaneous blockade of mitochondrial complexes I and V by using the combination of rotenone plus oligomycin-A, respectively. This cytotoxic model causes mitochondrial depolarization, oxidative stress, and apoptotic cell death measured as an increase in cleaved caspase 3 [13, 14].
- *6-Hydroxydopamine (6-OHDA)*. 6-OHDA uses the same catecholamine transport system as dopamine, and it accumulates in the cytosol, inducing neurotoxicity of dopaminergic neurons; for this reason [15], it has been widely used in vitro and in vivo as a Parkinson's model. It causes reactive oxygen species by the autooxidation of 6-OHDA and by inhibiting the mitochondrial

respiratory chain complex I [16]. Chromaffin cells are also susceptible to 6-OHDA cytotoxicity, which causes cell death by a mechanism that implicates the production of free radicals [17].

2 Materials

Equipment: Incubator with temperature and CO_2 control, laminar flow cabinet, centrifuge, and spectrophotometer microplate reader.

Solutions: Krebs-HEPES solution (pH 7.4) containing 145 mM NaCl, 5.9 mM KCl, 1.2 mM $MgCl_2$, 2 mM $CaCl_2$, 10 mM sodium HEPES, and 10 mM glucose.

Reagents: Culture medium: Dulbecco's Modified Eagle Medium (DMEM), penicillin/streptomycin, and fetal calf serum. Veratridine, thapsigargin, and 6-hydroxydopamine (6-OHDA), rotenone, oligomycin A, and poly-L-lysine. Lactate dehydrogenase (LDH) kit (*see* **Note 1**).

3 Methods

3.1 Preparation and Plating of BCC

1. Bovine adrenal medullary chromaffin are isolated as described in Moro et al. [18].
2. Pre-plate cells in a 150-mm-diameter Petri dish and leave them in the incubator for 30 min [3] (*see* **Note 2**).
3. Gently tilt the plate and collect the supernatant into a sterile beaker, avoiding dragging cells attached to the plate.
4. Add 5% fetal calf serum, 50 IU mL^{-1} penicillin, and 50 μg/mL^{-1} streptomycin.
5. Stir gently the cells with the media to evenly distribute the cells in the culture media before plating.
6. Plate cells in 24-well pates at a density of 5×10^5 cells/well (1 mL per well) (*see* **Note 3**).
7. Maintain cultures at 37 °C in a water-saturated atmosphere with 5% CO_2. After 24–48 h, the neuroprotection studies can be initiated.

3.2 Evaluation of Neuroprotectants in Different Cytotoxicity Models

Design experiments with the following conditions: (i) basal, (ii) toxic per se, and (iii) evaluation of the neuroprotectant compound in the presence of the toxic (*see* **Note 4**). Each variable is normally performed in triplicate (*see* **Note 5**). Depending on the selected cytotoxicity model, the most frequently used experimental conditions to evaluate neuroprotective compounds are those described below (*see* **Note 6** for other considerations on protocols):

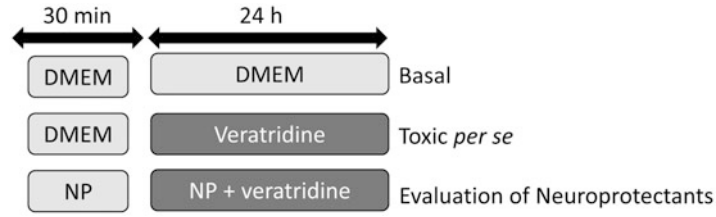

Fig. 1 Schematic representation of veratridine calcium overload model (*NP,* neuroprotectant)

3.2.1 Veratridine Model (Fig. 1)

1. *Basal*:
   (a) Add 500 μL of serum-free DMEM to each well and maintain for 30 min.
   (b) Remove and add 500 μL of serum-free DMEM and maintain for 24 h.
2. *Veratridine toxicity* per se:
   (c) Add 500 μL of serum-free DMEM to each well and maintain for 30 min.
   (d) Remove and add 500 μL of veratridine at 30 μM in serum-free DMEM, and maintain for 24 h.
3. *Evaluation of neuroprotectants*:
   (e) Add 500 μL of the neuroprotectant compound at the selected concentration dissolved in serum-free DMEM for 30 min.
   (f) Then remove the neuroprotectant compound and add 500 μL of the neuroprotectant compound in the presence of veratridine 30 μM for 24 h.

3.2.2 Thapsigargin Model (Fig. 2)

1. *Basal*: Add 500 μL of serum-free DMEM to each well and maintain for 24 h.
2. *Thapsigargin toxicity* per se:
   (a) Add 500 μL of serum-free DMEM containing 3 μM of thapsigargin for 2 h.
   (b) Remove media and add 500 μL of serum-free DMEM for 24 h.
3. *Evaluation of neuroprotectants*:
   (c) Add 500 μL of the neuroprotectant compound at the selected concentration dissolved in serum-free DMEM for 24 h.
   (d) Remove neuroprotectant compound and add thapsigargin (3 μM) with the neuroprotectant compound for 2 h.
   (e) Remove thapsigargin from the wells and add neuroprotectant compound alone in DMEM for another 24 h.

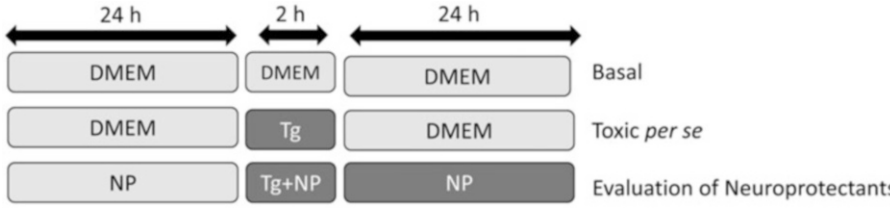

Fig. 2 Schematic representation of thapsigargin RE calcium release model (*Tg* thapsigargin, *NP* neuroprotectant)

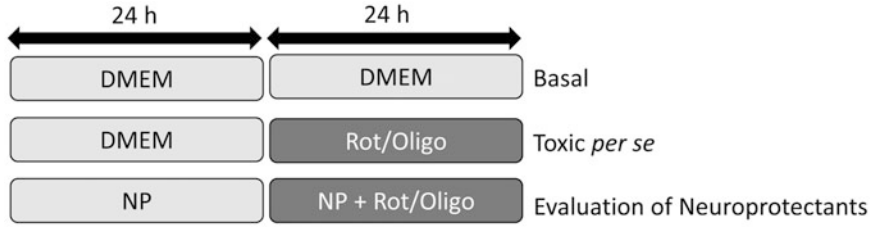

Fig. 3 Schematic representation of Rot/Oligo mitochondrial dysfunction model (*NP* neuroprotectant, *Rot* rotenone, *Oligo* oligomycin A)

3.2.3 Rotenone Plus Oligomycin A Model (Fig. 3)

1. *Basal*: Add 500 μL of serum-free DMEM to each well and change every 24 h.
2. *Rot/Oligo toxicity* per se:
   (a) Add 500 μL of serum-free DMEM for 24 h.
   (b) Remove media and add 500 μL of serum-free DMEM containing oligomycin (10 μM) plus rotenone (30 μM) for 24 h.
3. *Evaluation of neuroprotectants (NP)*:
   (c) Add 500 μL of the neuroprotectant compound at the selected concentration dissolved in serum-free DMEM for 24 h.
   (d) Remove neuroprotectant compound and add 500 μL of serum-free DMEM containing the neuroprotectant compound with oligomycin (10 μM) plus rotenone (30 μ M) for 24 h.

3.2.4 6-OHDA Model (Fig. 4)

1. Just before the experiment: Prepare 6-OHDA at 30 μM in Krebs-HEPES solution containing 0.3 mg/mL^{-1} of ascorbic acid (6-OHDA-ascorbic) (*see* **Note 7**).
2. *Basal*:
   (a) Add 500 μL of DMEM to each well for 30 min.
   (b) Remove and add 500 μL of Krebs-HEPES with ascorbic acid (0.3 mg/mL^{-1}) for 30 min.
   (c) Remove and add 500 μL of DMEM for 24 h.

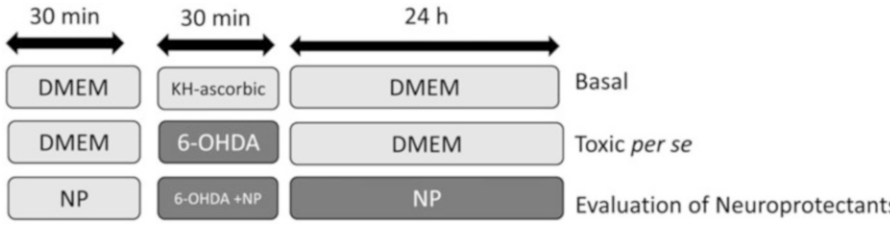

Fig. 4 Schematic representation of 6-OHDA oxidative stress model, also used as a Parkinson's model (*NP* neuroprotectant, *KH* Krebs-HEPES solution)

3. *6-OHDA* per se:
   (d) Add 500 μL of DMEM to each well for 30 min.
   (e) Remove and add 500 μL of 30 μM 6-OHDA-ascorbic solution for 30 min.
   (f) Remove and add 500 μL of DMEM medium, and maintain for 24 h.
4. *Evaluation of neuroprotectants*:
   (g) Add 500 μL of DMEM medium containing the neuroprotectant compounds for 30 min.
   (h) Remove and add 500 μL of the neuroprotectant compound plus 6-OHDA (30 μM ascorbic) for 30 min.
   (i) Remove the media and add 500 μL of DMEM medium containing only the neuroprotectant compound for 24 h.

3.3 Evaluation of Cell Viability: Lactate Dehydrogenase (LDH) Assay (See Note 8)

1. At the end of the experiment, remove 100 μL from the supernatant and take it to a 96-well clean plate.
2. Remove completely the rest of the media carefully (*see* **Note 9**).
3. Add 1 mL of DMEM containing 1% Triton ×100 (for LDH_i determination) to lysate the cells attached to the bottom of the well.
4. Remove 100 μL from each well and take it to a 96-well clean plate.
5. In the 96-well plate: Add 100 μL of reagent mix from the commercial LDH kit (*see* **Note 10**) to each well containing the extracellular medium (100 μL taken in Point 1) or intracellular one (100 μL taken in Point 4).
6. Incubate the plate in a dark space for 30 min at 37 °C.
7. Introduce the 96-well plate in a spectrophotometer to measure their absorbance at a wavelength of 492 nm; this value will provide the extracellular (LDH_e) and intracellular (LDH_i) values.

8. Calculations: Total LDH activity is calculated as the sum of the intracellular plus the extracellular LDH. Released LDH_e is defined as the percentage of extracellularcompared to total LDH_{total} activity, which correlates with the amount of cell death (% $LDH_e = LDH_e \times 100/LDH_{total.}$); the higher this %, the higher the cell death) [19] (*see* **Note 11**).

4 Notes

1. Concentrated solutions of veratridine, thapsigargin, and oligomycin-A are prepared in dimethylsulfoxide. Concentrations below 0.1% DMSO do not interfere with viability measurements. For neuroprotection studies, appropriate dilutions for the toxics and neuroprotectants are made in DMEM serum-free or Krebs-HEPES.
2. Pre-plating just after isolation of cells achieves reduction of contamination with endothelial cells. Alternatively, proliferation inhibitors (10 μM cytosine arabinoside and 10 μM fluorodeoxyuridine) can also be considered.
3. If BCCs have difficulty to attach, coating the plates with of 0.01 mg mL^{-1} of poly-L-lysine can improve their attachment. The protocol consists in preparing a stock solution of poly-L-lysine at 0.1 mg mL^{-1}. Before treating the plates, poly-L-lysine is diluted in sterile water to a final concentration of 0.01 mg mL^{-1}; 1 mL of diluted poly-L-lysine is added to each well for 30 min. Thereafter, wash three times with sterile distilled water. At the end, completely remove all the water, and let the plates dry well (they can be kept in the hood under UV light overnight) before seeding.
4. Neuroprotectants can be potentially neurotoxic per se. In this case, a viability study can be run with the compounds alone; usually, a high concentration is tested (i.e., 100 μM).
5. In Fig. 5, you can find a typical 24-well plate distribution to evaluate up to six different concentrations of a given neuroprotectant in triplicates.
6. Each of these experiments is normally repeated in three to five different cell cultures to achieve statistics. Note that in each plate, a basal (considered 100% viability) and toxic per se (considered maximum toxicity) condition is included as these values will be considered to determine if the compounds have afforded a protective effect or not.

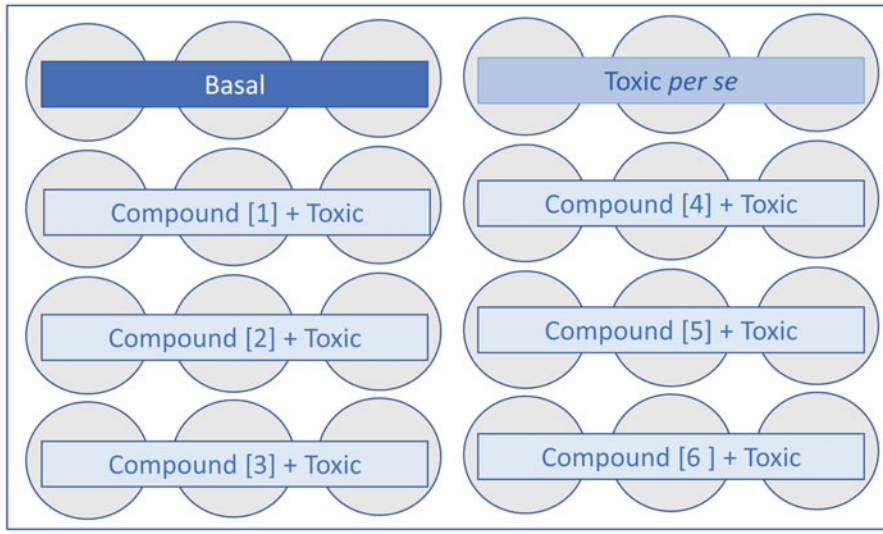

Fig. 5 Distribution of a 24-well plate to perform a neuroprotection concentration–response curve in triplicate

7. The neuroprotectant (NP) can be incubated at different time points. Selecting one or another protocol can be determined by different factors. Here are some suggestions: (1) *Pre-incubation protocol (NP is incubated previous to the toxic)*: It is the standard protocol when evaluating for the first time a new compound. It is also selected if the mechanism of action of the compound requires activation of a transcription factor or protein synthesis to induce neuroprotective proteins or activating neuroprotective pathways. (2) *Co-incubation protocol (NP and toxic are incubated at the same time)*: If the compound is expected to block, modulate, or activate voltage channels, the co-incubation protocol is an excellent model to discover the effect of novel compounds over the voltage-dependent channels. (3) *Post-incubation protocol (NP is incubated after the toxic)*: In human diseases, a neuroprotective effect is desired once the pathology is installed. This protocol in usually used after the NP has proven neuroprotection in the pre-incubation protocol. Using a post-incubation protocol, the NP can be added at different time points after the toxic to evaluate the time window for neuroprotection.
8. The solution must be prepared freshly just before performing the experiment and protected from light since 6-OHDA oxidizes upon light exposition and loses its cytotoxic effect. Addition of ascorbic acid maintains an acidic pH that contributes to prevent oxidation of 6-OHDA.
9. When measuring LDH, all culture media should be devoid of serum as it interacts with LDH and readout will not be feasible. If some serum is required, this can be reduced to 1% maximum.

10. The supernatant must be withdrawn very carefully, well by well with the manual micropipette, to prevent detaching the cells from the bottom of the plate; if these are detached, the readout of the extracellular LDH will not be reliable.
11. There are several commercially available kits to measure LDH; in this protocol, we have used the Colorimetric Boehringer Mannheim LDH cytotoxicity detection kit. If you use one from another manufacturer, you will have to follow their instructions.
12. A good basal viability rate should be around 10%; if this value is very high, over 20%, the culture is not in optimal conditions for the experiment.

Acknowledgments

We thank the Spanish Ministry of Science, Innovation and Universities grant Ref. RTI2018-095793-B-I00 to M.G.L, the General Council for Research and Innovation of the Community of Madrid and European Structural Funds grant Ref. B2017/BMD-3827, and the European Union for COST Action Ref. CA20121.

References

1. Zündorf G, Reiser G (2011) Calcium dysregulation and homeostasis of neural calcium in the molecular mechanisms of neurodegenerative diseases provide multiple targets for neuroprotection. Antioxid Redox Signal 14:1275–1288. https://doi.org/10.1089/ars.2010.3359
2. López MG, Artalejo AR, García AG, Neher E, García-Sancho J (1995) Veratridine-induced oscillations of cytosolic calcium and membrane potential in bovine chromaffin cells. J Physiol 482:15–27. https://doi.org/10.1113/jphysiol.1995.sp020496
3. Cano-Abad MF, López MG, Hernández-Guijo JM et al (1998) Effects of the neuroprotectant lubeluzole on the cytotoxic actions of veratridine, barium, ouabain and 6-hydroxydopamine in chromaffin cells. Br J Pharmacol 124:1187–1196. https://doi.org/10.1038/sj.bjp.0701955
4. Maroto R, De la Fuente MT, Artalejo AR, Abad F, López MG, García-Sancho J, García AG (1994) Effects of Ca^{2+} channel antagonists on chromaffin cell death and cytosolic Ca^{2+} oscillations induced by veratridine. Eur J Pharmacol 270:331–339. https://doi.org/10.1016/0926-6917(94)90009-4
5. Maroto R, de la Fuente MT, Zapater P, Abad F, Esquerro E, García AG (1996) Effects of omega-conotoxin MVIIC on veratridine-induced cytotoxicity and cytosolic Ca^{2+} oscillations. Brain Res 714:209–214. https://doi.org/10.1016/0006-8993(95)01543-4
6. Wermelskirchen D, Wilffert B, Peters T (1992) Veratridine-induced intoxication: an in vitro model for the characterization of anti-ischemic compounds? J Basic Clin Physiol Pharmacol 3:293–321. https://doi.org/10.1515/jbcpp.1992.3.4.293
7. Otoom SA, Hasan Z. (2004) Propofol exhibits antiepileptic activity in hippocampal pyramidal neurons. Pharmacol Biochem Behav. 77:595-599. https://doi.org/10.1016/j.pbb.2003.12.021
8. Pauwels PJ, Leysen JE, Janssen PA (1998) Ca^{2+} and Na^{+} channels involved in neuronal cell death. Protection by flunarizine. Life Sci 48:1881–1893. https://doi.org/10.1016/0024-3205(91)90220-6
9. Novalbos J, Abad-Santos F, Zapater P, Cano-Abad MF, Moradiellos J, Sánchez-García P, García AG (1999) Effects of dotarizine and flunarizine on chromaffin cell viability and cytosolic Ca^{2+}. Eur J Pharmacol 366:309–317. https://doi.org/10.1016/s0014-2999(98)00916-9

10. Giacomello M, Barbiero L, Zatti G, Squitti R, Binetti G, Pozzan T, Fasolato C, Ghidoni R, Pizzo P (2005) Reduction of Ca^{2+} stores and capacitative Ca^{2+} entry is associated with the familial Alzheimer's disease presenilin-2 T122R mutation and anticipates the onset of dementia. Neurobiol Dis 18:638–648. https://doi.org/10.1016/j.nbd.2004.10.016
11. Arias E, Alés E, Gabilan NH, Cano-Abad MF, Villarroya M, García AG, López MG (2004) Galantamine prevents apoptosis induced by beta-amyloid and thapsigargin: involvement of nicotinic acetylcholine receptors. Neuropharmacology 46:103–114. https://doi.org/10.1016/s0028-3908(03)00317-4
12. Yaribeygi H, Panahi Y, Javadi B, Sahebkar A (2018) The underlying role of oxidative stress in neurodegeneration: a mechanistic review. CNS Neurol Disord Drug Targets 17:207–215. https://doi.org/10.2174/1871527317666180425122557
13. Egea J, Rosa AO, Cuadrado A, García AG, López MG (2007) Nicotinic receptor activation by epibatidine induces heme oxygenase-1 and protects chromaffin cells against oxidative stress. J Neurochem 102:1842–1852. https://doi.org/10.1111/j.1471-4159.2007.04665.x
14. Moreno-Ortega AJ, Al-Achbili LM, Alonso E, de Los RC, García AG, Ruiz-Nuño A, Cano-Abad MF (2016) Neuroprotective effect of the novel compound ITH33/IQM9.21 against oxidative stress and Na^{+} and Ca^{2+} overload in motor neuron-like NSC-34 cells. Neurotox Res 30:380–391. https://doi.org/10.1007/s12640-016-9623-7
15. Luthman J, Fredriksson A, Sundström E, Jonsson G, Archer T (1989) Selective lesion of central dopamine or noradrenaline neuron systems in the neonatal rat: motor behavior and monoamine alterations at adult stage. Behav Brain Res 33:267–277. https://doi.org/10.1016/s0166-4328(89)80121-4
16. Kumar R, Agarwal AK, Seth PK (1995) Free radical-generated neurotoxicity of 6-hydroxydopamine. J Neurochem 64:1703–1707. https://doi.org/10.1046/j.1471-4159.1995.64041703.x
17. Abad F, Maroto R, López MG, Sánchez-García P, García AG (1995) Pharmacological protection against the cytotoxicity induced by 6-hydroxydopamine and H_2O_2 in chromaffin cells. Eur J Pharmacol 293:55–64. https://doi.org/10.1016/0926-6917(95)90018-7
18. Moro MA, López MG, Gandía L, Michelena P, García AG (1990) Separation and culture of living adrenaline- and noradrenaline-containing cells from bovine adrenal medullae. Anal Biochem 185:243–248. https://doi.org/10.1016/0003-2697(90)90287-j
19. Cano-Abad MF, Villarroya M, García AG, Gabilan NH, López MG (2001) Calcium entry through L-type calcium channels causes mitochondrial disruption and chromaffin cell death. J Biol Chem 276:39695–39704. https://doi.org/10.1074/jbc.M102334200

INDEX

Ricardo Borges (ed.), *Chromaffin Cells: Methods and Protocols*,
Methods in Molecular Biology, vol. 2565, https://doi.org/10.1007/978-1-0716-2671-9,

R

S

T

U

V

W